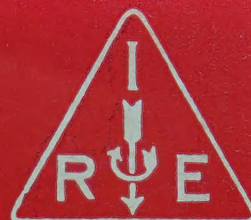


IRE Transactions



on Microwave Theory and Techniques

PERIODICAL

UNIVERSITY OF HAWAII

LIBRARY

Longman

Volume MTT-8

MARCH, 1960

Number 2

In This Issue

Broad-Band Coaxial Choked Coupling Design

A Study of Multielement Transmission Lines

Measurement of Relative Phase Shift at Microwave Frequencies

Resonant Modes in Waveguide Windows

Temperature Compensation of Coaxial Cavities

A Graphical Method for Measuring Dielectric Constants at Microwave Frequencies

Wide-Band Strip-Line Magic-T

A General Theorem on an Optimum Stepped Impedance Transformer

Minimal Positive Polynomials

Complementarity in the Study of Transmission Lines

High Resolution Millimeter Wave Fabry-Perot Interferometer

Boundary Conditions and Ohmic Losses in Conducting Wedges

On the Theory of the Ferrite Resonance Isolator

Analysis of Microwave Measurement Techniques by Means of Signal Flow Graphs

Stepped Transformers for Partially Filled Transmission Lines

Parametric Diodes in a Maser Phase-Locked Frequency Divider

Parametric Devices and Masers: An Annotated Bibliography

7800
3

PUBLISHED BY THE

Professional Group on Microwave Theory and Techniques

IRE PROFESSIONAL GROUP ON MICROWAVE THEORY AND TECHNIQUES

The Professional Group on Microwave Theory and Techniques is an association of IRE members with professional interest in the field of Microwave Theory and Techniques. All IRE members are eligible for membership and will receive all Group publications upon payment of the prescribed annual fee of \$3.00. Members of the American Physical Society and the Institution of Electrical Engineers of Great Britain may become affiliated with PGMTT and receive all Group publications upon payment of the Affiliate fee of \$7.50 per year.

Administrative Committee

Chairman

A. A. OLINER

Vice-Chairman

K. TOMIYASU

Secretary-Treasurer

H. M. ALTSCHULER

T. N. ANDERSON

R. C. HANSEN

G. SHAPIRO

R. E. BEAM

W. W. MUMFORD

G. SINCLAIR

A. C. BECK

W. L. PRITCHARD

P. D. STRUM

A. G. CLAVIER

S. W. ROSENTHAL

M. C. THOMPSON

S. B. COHN

T. S. SAAD

R. D. WENGENROTH

R. F. SCHWARTZ

Ex-Officio

H. F. ENGELMANN

Honorary Life Member

GEORGE C. SOUTHWORTH

Editor

DONALD D. KING

PGMTT Chapters

Albuquerque-Los Alamos
Baltimore
Boston
Buffalo-Niagara
Chicago
Columbus
Denver-Boulder
Long Island
Los Angeles

Leland J. Allen
Marvin Cohn
Robert Rivers
R. E. Kell
Robert Hargis
B. Querido
H. E. Bussey
H. L. Backman
George Underberger

New York
Northern N.J.
Omaha-Lincoln
Philadelphia
San Diego
San Francisco
Schenectady
Syracuse
Tokyo, Japan
Washington, D.C.

D. J. Stock
R. M. Foley
C. M. Hyde
J. T. Beardwood
B. I. Small
Theodore Moreno
V. W. Amoth
E. B. Mullen
Kiyoshi Morita

R. O. Stone

IRE TRANSACTIONS®

on Microwave Theory and Techniques

Published by the Institute of Radio Engineers, Inc., for the Professional Group on Microwave Theory and Techniques, at 1 East 79th Street, New York 21, New York. Responsibility for the contents rests upon the authors, and not upon the IRE, the Group, or its members. Price per copy: IRE PGMTT members, \$2.50; IRE members, \$3.75, nonmembers, \$7.50. Annual subscription price: IRE members, \$8.50; colleges and public libraries, \$12.75; nonmembers, \$17.00.

Address all manuscripts to Donald D. King, PGMTT Editor, Electronic Communications, Inc., 1830 York Road, Timonium, Md. Submission of three copies of manuscripts, including figures, will expedite the review.

COPYRIGHT ©1960—THE INSTITUTE OF RADIO ENGINEERS, INC.

Printed in U.S.A.

All rights, including translations, are reserved by the IRE. Requests for republication privileges should be addressed to the Institute of Radio Engineers, 1 E. 79th St., New York 21, N.Y.

IRE Transactions

on

Microwave Theory and Techniques

Volume MTT-8

MARCH, 1960

Number 2

EDITORIAL BOARD

Editor

Donald D. King

Advertising Editor

Tore N. Anderson

D. J. Angelakos
W. P. Ayres
R. W. Beatty
A. D. Berk
A. D. Bresler
J. C. Cachieris
S. B. Cohn
R. E. Collin
I. Goldstein
R. C. Hansen
H. Heffner
E. M. T. Jones
R. W. Klopfenstein
P. A. Loth
R. V. Lowman
T. Moreno
S. P. Morgan
K. S. Packard, Jr.
M. C. Pease
J. Reed
J. M. Richardson
P. A. Rizzi
S. D. Robertson
N. G. Sakiotis
R. F. Schwartz
W. Sichak
D. C. Stinson
P. D. Strum
E. Strumwasser
L. Swern
E. N. Torgow
P. H. Vartanian, Jr.
M. T. Weiss
G. J. Wheeler
R. F. Whitmer
J. C. Wiltse
F. J. Zucker

TABLE OF CONTENTS

Editorial.....	Harold M. Barlow	131
----------------	------------------	-----

CONTRIBUTIONS

Broad-Band Coaxial Choked Coupling Design.....	Howard E. King	132
A Study of Multielement Transmission Lines.....	Hiroshi Kogō	136
Measurement of Relative Phase Shift at Microwave Frequencies.....	C. A. Finnila, L. A. Roberts and C. Süsskind	143
Resonant Modes in Waveguide Windows.....	M. P. Forrer and E. T. Jaynes	147
Temperature Compensation of Coaxial Cavities.....	J. R. Cogdell, A. P. Deam and A. W. Straiton	151
A Graphical Method for Measuring Dielectric Constants at Microwave Frequencies.....	Charles B. Sharpe	155
Wide-Band Strip-Line Magic-T.....	E. M. T. Jones	160
A General Theorem on an Optimum Stepped Impedance Transformer.....	Henry J. Riblet	169
Minimal Positive Polynomials.....	James E. Eaton	171
Complementarity in the Study of Transmission Lines.....	G. H. Owyang and R. King	172
High Resolution Millimeter Wave Fabry-Perot Interferometer.....	William Culshaw	182
Boundary Conditions and Ohmic Losses in Conducting Wedges.....	Robin M. Chisholm	189
On the Theory of the Ferrite Resonance Isolator.....	E. Schlömann	199
Analysis of Microwave Measurement Techniques by Means of Signal Flow Graphs.....	J. K. Hunton	206
Stepped Transformers for Partially Filled Transmission Lines.....	D. J. Sullivan and D. A. Parkes	212
Parametric Diodes in a Maser Phase-Locked Frequency Divider.....	M. L. Stitch, N. O. Robinson and W. Silvey	218
Parametric Devices and Masers: An Annotated Bibliography.....	E. Mount and B. Begg	222
Correction to "Tables for Cascaded Homogeneous Quarter-Wave Transformers".....	Leo Young	243

CORRESPONDENCE

Analysis of Split Coaxial Line Type Balun.....	Hiroshi Kogō	245
Nonreciprocal Attenuation of Ferrite in Single-Ridge Waveguide.....	T. S. Chen	247
A New Automatic Frequency Regulation System.....	J. R. Singer	249
On Some Problems in Designing Microwave Faraday-Rotation Devices.....	S. J. Lewandowski and J. Konopka	249
Equivalence of 0 and -1 Space Harmonics in Helical Antenna Operation.....	T. S. MacLean and D. A. Watkins	251
Application of Perturbation Theory to the Calculation of ω - β Characteristics for Periodic Structures.....	Murray D. Sirkis	251
Ice as a Bending Medium for Waveguide and Tubing.....	Franklin S. Coale	252
On Higher-Order Hybrid Modes of Dielectric Cylinders.....	S. P. Schlesinger, P. Diamant, and A. Viganis	252
A Property of Symmetric Hybrid Waveguide Junctions.....	J. M. Smith	253
Attenuation in a Resonant Ring Circuit.....	K. Tomiyasu	253
Reciprocal Ferrite Phase Shifters.....	Alvin Clavin	254
Contributors.....		255
PGMTT National Symposium Program.....		260
PGMTT Roster.....		261



Harold M. Barlow

Harold M. Barlow was born on November 15, 1899, in London, England. After graduating in engineering at University College, London, in 1922, he received the Ph.D. degree in physics in 1924, from the same school.

His first academic appointment was as a lecturer in the design of electrical machinery at University College. Since World War II, he has specialized more particularly in high-frequency work. As Superintendent of the Radio Department at the Royal Aircraft Establishment, England, during the war years, he worked with radar, and it was largely as a result of that experience that he became so interested in microwaves. He still tries to maintain contact with the power side of electrical engineering, and as a teacher, discourages specialization except to a limited extent in the final year of the degree course.

Professor Barlow is a member of the Council of the British IEE, the British Broadcasting Corporation's Scientific Advisory Committee, and the Radio Research Board.

Editorial

H. M. BARLOW†

ELECTRICAL engineering as a technology necessarily embodies applications of physics, and in the microwave branch, a particularly close link exists between the two subjects of study. The phenomenal progress in microwave work has come about as a result of physicist and engineer working side by side, each making his own kind of contribution, much to the benefit of both. Cross fertilization of ideas is always profitable, and in microwaves, perhaps more than in many other things, this has had exceedingly valuable results. The engineers have discovered the need to broaden their approach to problems of the electromagnetic field and to delve much more deeply into matters concerning the behavior of electrical materials in such fields. The high frequencies involved have naturally been a dominant factor in the new work they had to do.

Prior to the advent of microwaves, which for practical purposes only really came on the scene during World War II, most electrical engineers were content to examine their guided-wave problems in terms of circuit theory, and even in the VHF part of the spectrum, that treatment sufficed for most purposes. In the microwave band, equivalent circuits still play their part, but more often field theory is required to give an intimate and precise picture of the situation. The behavior of the field at a boundary between two different media is almost always of special interest, and much of our microwave work centers around that aspect of the subject. This is not surprising when we recall that air, as the pervading medium of the space in which we live, has many excellent properties for electromagnetic wave propagation, and most of the limitations we have to accept are imposed by the various forms of guide and supporting structure introduced for the purpose of directing energy along a particular route. The commission demanded by the guide for this service is often an important consideration, and so are the losses in any associated solid dielectric. It is a salutary thought that even at low frequency, the permissible electric stress in a high-power cable is limited primarily by voids in the insulation, tending to reduce the performance to that attainable with a gas dielectric, while at high frequency, we generally try to use as little solid dielectric as possible in order to keep down the power absorbed.

Microwaves, in teaching us to think and study more particularly in terms of the electromagnetic field rather than the electric circuit, have encouraged a more unified approach to our problems, and this is perhaps the most important need today in the science of electrical

engineering. The power engineer often reasons and acts from a point of view which is very different from his colleague in the radio field. Both have something of value to offer, but it is nevertheless true that the younger science tends to be more progressive and to give wider scope for challenging ideas.

How many engineers realize that the basic mechanism of the mechanical force on the conductors of the armature of a motor carrying current is the same as that of radiation pressure, and moreover, that its counterpart, the Hall effect, arises in a way which is the precise equivalent of the EMF generated in the armature? How many engineers have ever thought of the equalizer rings on a wave-wound dc machine as performing the same function as the strapping of a multicavity magnetron, or of the rotating magnetic field of a polyphase induction motor as a surface wave? How often do power engineers use, or indeed think of, the Poynting vector in relation to their calculations for power transmission, and how many of them are still inclined to visualize the power as passing through the conductors themselves? What proportion of our colleagues dealing with the design of ac machines consider the problem of the distribution of current over the cross section of conductors in terms of wave propagation and recognize that even at 50 cps the wavelength in copper is only about 5 cm? It might justly be argued that there is little of immediate practical value to be gained from any broader approach to these and similar matters, but this is a short-term view and, in the long run, one generally finds that it is from the wider horizon that the most important developments emerge. To that end, it is particularly important that teachers should do all they can to bring together in the minds of their students basic scientific ideas that are closely allied. This may encourage wider attempts at generalization, which is always difficult to achieve without losing some of the detail—detail that is sometimes of vital importance in an engineering problem. In spite of all the difficulties, the fact remains that without some further measure of unification in the teaching of electrical engineering, the growth of the subject will force the tendency toward narrow specialization to become still more pronounced. The close contact between physicist and engineer in the microwave field has broadened the outlook of both. Let us do our best to insure that the same kind of interchange is not lost between the power and the radio engineer. The great ideas on which our future so largely depends will surely come from the closest possible collaboration, and particularly from those who have the gift of a broad scientific understanding of the problems presented to them.

† Elec. Engrg. Dept., University College, London, England.

Broad-Band Coaxial Choked Coupling Design*

H. E. KING†

Summary—Equations and curves are presented to predict the frequency bandwidth of coaxial choke couplings in terms of the choke parameters. Choke couplings discussed are those applicable to rotary joints and dc isolation units.

INTRODUCTION

COAXIAL choke-type rotary joint designs have been discussed by Ragan,¹ and many joints have been built following his presentation. Recently, Muehe² discussed a method to widen the bandwidth of coaxial choke-type rotary joints by reducing the characteristic admittance of the transmission line for a quarter wavelength on each side of the chokes. Muehe's discussion was based on the analogous case of broadbanding short-circuited quarter wavelength stubs in parallel with the transmission line, by changing the characteristic impedance of the line on each side of the stub for a distance of one-quarter wavelength.

The broadbanding of coaxial choke couplings under the present discussion is not based on a change in transmission line impedance, but is based on an extension of the conventional methods. As outlined by Ragan, broadbanding of choke couplings may be accomplished by displacing the outer and inner conductor chokes along the transmission line by one-quarter wavelength. The purpose of this paper is to present general equations and curves relating to the VSWR, to the characteristic impedance of the choke sections, and to the spacing of the two chokes. From these curves, one can predict the bandwidth of a rotary joint design.

EQUATIONS FOR CHOKE COUPLING

A conventional coaxial rotary joint is shown in Fig. 1. To prevent radiation losses due to the outer conductor choke and to provide a means of placing a bearing at a low current point, the external choke section of characteristic impedance Z_{03} , is added. In most practical cases, the characteristic impedance Z_{03} is made as high as possible and is usually much greater than the characteristic impedance Z_{02} of the outer conductor choke.

For simplification in this analysis, Z_{03} is assumed to be infinite. Also, both the choke sections are $\lambda/4$ long at the center frequency, and their characteristic impedances Z_{01} and Z_{02} are assumed to be equal; thus, the choke input impedances are equal, or $Z_1 = Z_2$. The characteristic impedance, Z_0 , of the transmission line is normalized to 1.

The $ABCD$ matrix of the two chokes displaced by the length l along a lossless transmission line is

$$\begin{bmatrix} 1 & -jZ_{01} \cot \beta l_1 \\ 0 & 1 \end{bmatrix} \begin{bmatrix} \cot \beta l & j \sin \beta l \\ j \sin \beta l & \cos \beta l \end{bmatrix} \cdot \begin{bmatrix} 1 & -jZ_{01} \cot \beta l_1 \\ 0 & 1 \end{bmatrix}, \quad (1)$$

where βl_1 is the electrical length of the choke sections and βl is the electrical spacing between the two chokes. The final matrix when multiplied through is

$$\begin{bmatrix} \cos \beta l + Z_{01} \cot \beta l_1 \sin \beta l & -2jZ_{01} \cot \beta l_1 \cos \beta l - jZ_{01}^2 \cot^2 \beta l_1 \sin \beta l + j \sin \beta l \\ j \sin \beta l & \cos \beta l + Z_{01} \cot \beta l_1 \sin \beta l \end{bmatrix}. \quad (2)$$

In addition to facilitating the design of rotary joints, the information presented here can be utilized to build wideband dc isolation units. Wideband dc isolation units have been developed³ using the design described; dc isolation units are required whenever blocking of dc on both the inner and outer conductors is desired.

The insertion loss is given by⁴

$$\begin{aligned} L &= 10 \log_{10} \{ 1 + 1/4[(A - D)^2 - (B - C)^2] \}, \\ &= 10 \log_{10} \{ 1 - 1/4[-j(2Z_{01} \cot \beta l_1 \cos \beta l \\ &\quad + Z_{01}^2 \cot^2 \beta l_1 \sin \beta l)]^2 \}, \\ &= 10 \log_{10} \left\{ 1 + \frac{|K|^2}{4} \right\}. \end{aligned} \quad (3)$$

Next, let

$$\beta l_1 = \frac{\pi}{2} + \phi \quad \text{and} \quad \beta l = n\beta l_1 = n\left(\frac{\pi}{2} + \phi\right).$$

* Manuscript received by the PGMTT, July 29, 1959; revised manuscript received September 17, 1959.

† Space Technology Labs., Inc., Los Angeles, Calif.
¹ G. L. Ragan, "Microwave Transmission Circuits," M.I.T. Rad. Lab. Ser., McGraw-Hill Book Co., Inc., New York, N. Y., vol. 9, p. 407; 1948.

² C. E. Muehe, "Quarter-wave compensation of resonant discontinuities," IRE TRANS. ON MICROWAVE THEORY AND TECHNIQUES, vol. MTT-7, pp. 296-297; April, 1959.

³ By Ramo-Wooldridge, a division of Thompson Ramo Woolridge Inc., Los Angeles, Calif.

⁴ R. M. Fano and A. W. Lawson, "Microwave Transmission Circuits," M.I.T. Rad. Lab. Ser., McGraw-Hill Book Co., Inc., New York, N. Y., vol. 9, p. 551; 1948.

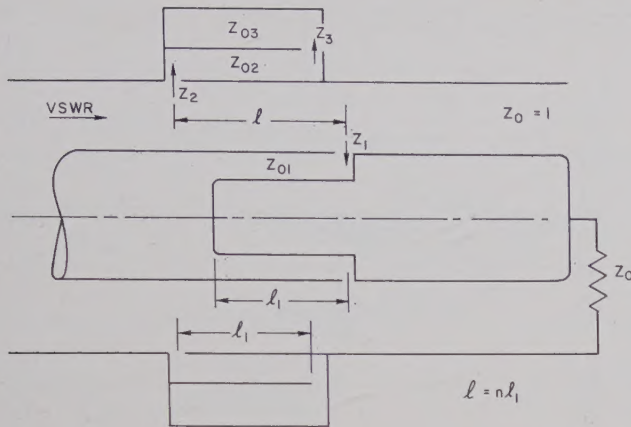


Fig. 1—Coaxial transmission line with choke couplings used as a rotary joint.

Then $|K|$ is written as

$$|K| = 2Z_{01} \tan \phi \cos n \left(\frac{\pi}{2} + \phi \right) - Z_{01}^2 \tan^2 \phi \sin n \left(\frac{\pi}{2} + \phi \right), \quad (4)$$

where ϕ = the difference in electrical length from the center frequency choke length of $\pi/2$. The relation of $|K|$ to the coaxial transmission line voltage-standing-wave ratio, VSWR, is

$$|K| = \frac{\text{VSWR} - 1}{\sqrt{\text{VSWR}}}. \quad (5)$$

Bandwidth is arbitrarily defined as the ratio of the two frequencies for which the transmission line VSWR is 1.1:1 (insertion loss less than 0.01 db) or in symbolic form, the bandwidth is

$$\frac{f_2}{f_1} = \frac{90 + |\phi_2|}{90 - |\phi_1|}. \quad (6)$$

DISCUSSION OF CURVES

A graph of the input VSWR to the transmission line is shown in Fig. 2 for the case when $Z_{01} = 0.0324$ for various conditions of n . When $n=0$, the input terminals of the chokes are located on the same transverse plane. The VSWR is calculated from

$$|K|_{n=0} = 2Z_{01} \tan \phi. \quad (7)$$

When the chokes are displaced by $\lambda/4$ at the center frequency, then $n=1$, or (4) is reduced to

$$|K|_{n=1} = (2Z_{01} + Z_{01}^2) \tan \phi \sin \phi. \quad (8)$$

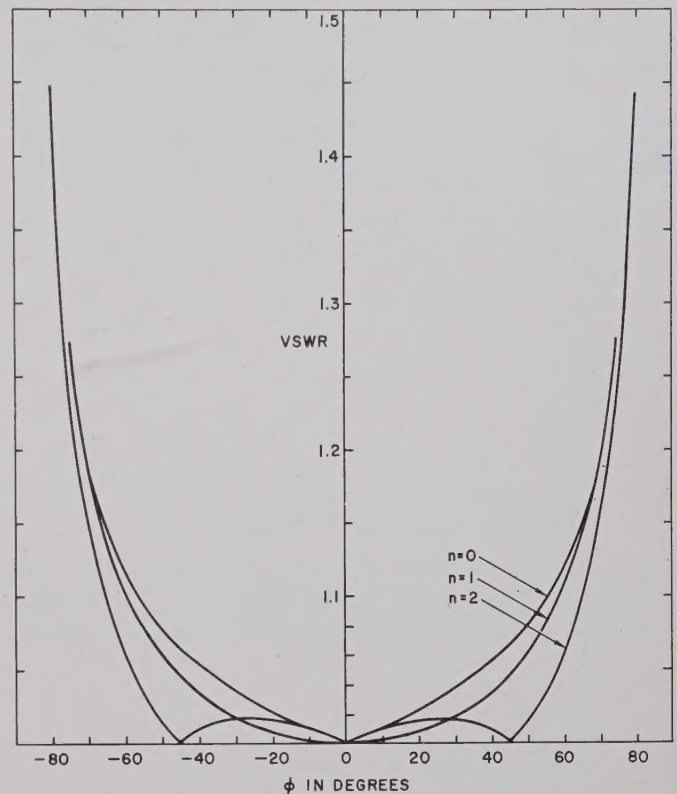


Fig. 2—Input VSWR to coaxial transmission line with choke couplings for various values of n . Choke impedance, $Z_{01} = 0.0324$ (normalized to unity). Characteristic impedance Z_{03} is assumed to be infinite.

When $n=1$, a zero derivative exists at the origin, a condition considered to be the maximally flat case.

When the input choke terminals are separated by $\lambda/2$ at the center frequency ($n=2$), the $n=2$ curve shows a wider bandwidth compared to the $n=1$ condition. For the $n=2$ condition, $|K|$ is written as

$$|K|_{n=2} = 2Z_{01} \tan \phi \cos^2 \phi - 2(Z_{01} + Z_{01}^2) \tan \phi \sin^2 \phi. \quad (9)$$

When the chokes are separated by $\lambda/4$ at the center frequency, or $n=1$, the frequency bandwidth ratio vs Z_{01} is plotted in Fig. 3, where the band edge limits were determined by a voltage-standing-wave ratio of 1.1:1. Fig. 4(a) is a curve of frequency bandwidth ratio vs Z_{01} for $n=2$. The peak voltage-standing-wave-ratio within the band limits is plotted in Fig. 4(b).

Where $Z_{01} = 0.0324$ and $n=2$, the bandwidth for a VSWR of less than 1.1:1 is 6.2:1. With the same choke impedance except that $n=2.67$ ($\beta l = 240^\circ$ at the center frequency), a still wider frequency bandwidth of 8.15:1 is theoretically feasible as illustrated by the solid line curve of Fig. 5. Note that the curve is unsymmetrical and the peak within the band is slightly higher than for the case when $n=2$. In actual experience, the slightly higher peak should not produce any detrimental ef-

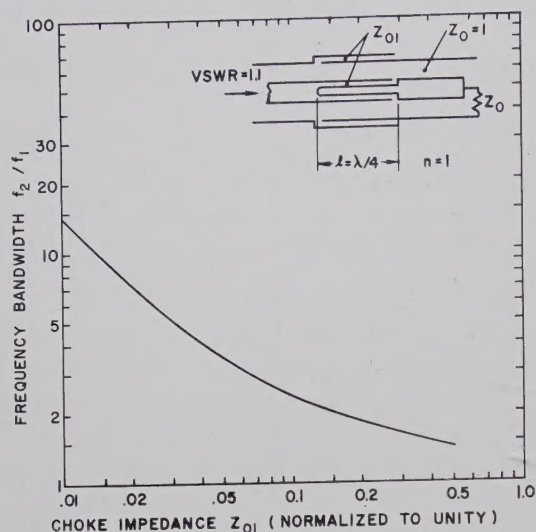
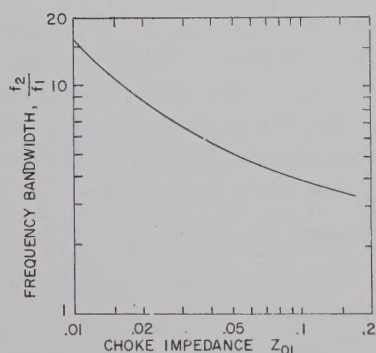
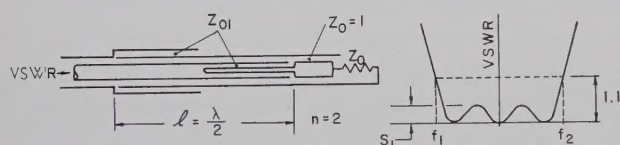
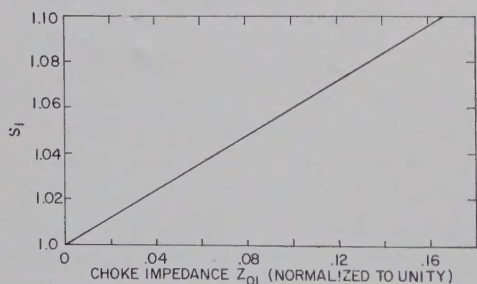


Fig. 3—Frequency bandwidth curve of coaxial transmission line with choke couplings when chokes are spaced $\lambda/4$ at the center frequency. Bandwidth determined by the transmission line VSWR of 1.1:1. Characteristic impedance Z_{03} is assumed to be infinite.



(a)



(b)

Fig. 4—Response curves for coaxial transmission line with choke couplings when chokes are spaced $\lambda/2$ apart at the center frequency. (a) Frequency bandwidth determined by the transmission line VSWR of 1.1:1. (b) The value of the peak VSWR within the band limits. Characteristic impedance Z_{03} is assumed to be infinite.

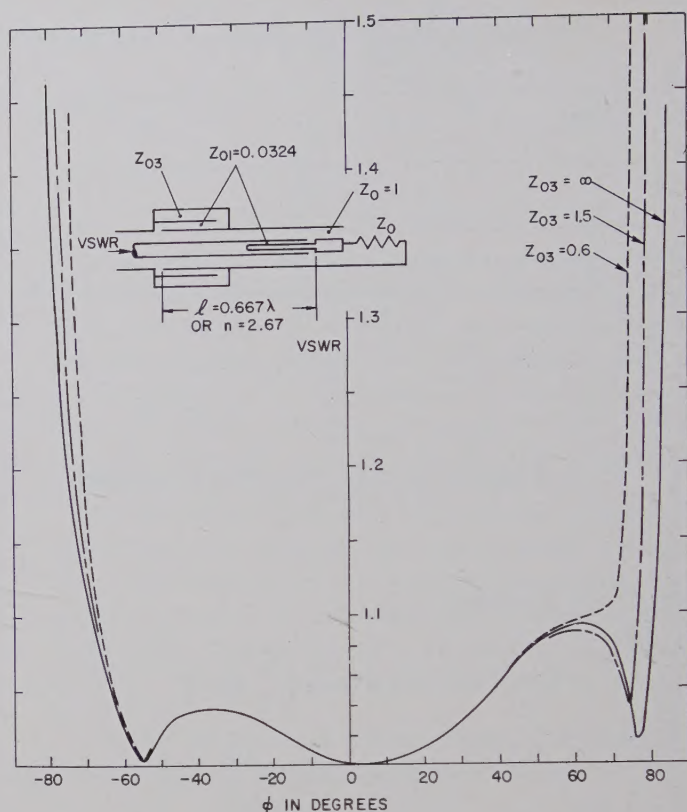


Fig. 5—Input VSWR curve of coaxial transmission line with choke couplings when chokes are spaced 0.667λ apart for $Z_{01} = 0.0324$ (normalized to unity).

fects. With any given value of Z_{01} an optimum spacing between chokes can be determined to give the widest frequency bandwidth.

OTHER CONSIDERATIONS

For extremely wide bandwidth choke couplings, the finite value of Z_{03} should be considered. The solid line curve of Fig. 5 represents the condition when the external choke impedance Z_{03} is infinite while the broken line curves represent two finite values of Z_{03} .

The dashed line curve of Fig. 5 shows the reduction in bandwidth if the normalized characteristic impedance of Z_{03} is 0.6. For a normalized characteristic impedance Z_{03} of 1.5, the dash-dot curve indicates an improvement in the VSWR response. Note that there is no major increase in VSWR due to the finite value of Z_{03} provided $|\phi| < 70^\circ$. Usually only for extremely wide bandwidth choke coupling designs (when $|\phi| > 70^\circ$) is it necessary to calculate the effects of Z_{03} on the VSWR response.

If the external diameter is a limiting factor that prevents a large value of Z_{03} from being selected, an effective increase in the external choke impedance can be obtained by making it $\lambda/2$ long at the midfrequency as illustrated in Fig. 6. Now the impedance $Z_3 + Z_4$ terminates the outer conductor choke Z_{02} , instead of only Z_3 .

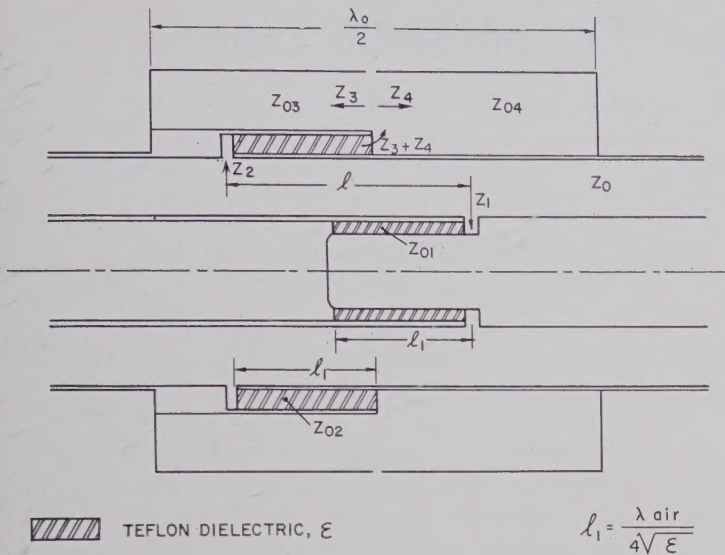


Fig. 6—Broadband coaxial rotary joint of dc isolation unit design using choke couplings.

In a practical design, the slight reduction in bandwidth due to the finite impedance of the external choke can be compensated by lowering the characteristic impedance Z_{02} . In a practical case, Z_{02} can be made smaller than Z_{01} .

Basically, the wide bandwidth of choke couplings is obtained by the use of low values of the choke's characteristic impedances, Z_{01} and Z_{02} . By the use of teflon insulation, choke characteristic impedance of less than 1.5 ohm is readily obtained. The increase in dissipation losses because of the use of teflon dielectric is compensated for by the shorter physical length⁵ of the choke that is required.

Fig. 7 is a photograph of a dc isolation unit built³ for a frequency range of 70 mc to 850 mc (VSWR less than 1.5) using the design described herewith. Performance data of the dc isolation unit is illustrated in Fig. 8, showing both the calculated and measured VSWR response. The measured insertion loss was found equal to the mismatch loss.

CONCLUSION

The curves (Figs. 3 and 4) and the analysis should be helpful for the design of wide-band coaxial rotary joints or dc isolation units. Prediction of the final performance for various choices of parameters is possible.

APPENDIX

CHOKE LOSSES DUE TO TEFLON DIELECTRIC

To demonstrate the effects of the choke losses due to the use of teflon dielectric, the following relations are presented. The input resistance to a resonant transmission line with a relative dielectric constant of unity, is

⁵ See Appendix.

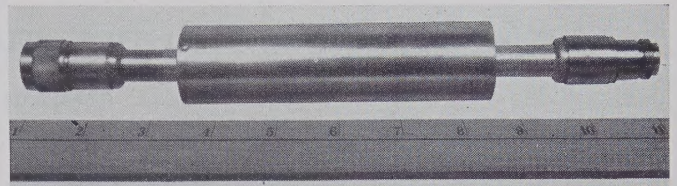


Fig. 7—DC isolation unit built for 70 mc to 850 mc operation (VSWR less than 1.5) using the choke coupling design described.

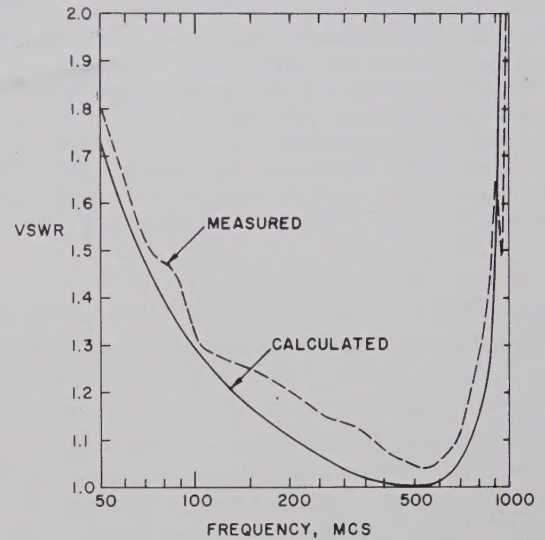


Fig. 8—Measured and calculated VSWR curves of the dc isolation unit of Fig. 7.

expressed as

$$R_{in\epsilon=1} = Z_0 \alpha l = \frac{Rl}{2} + \frac{GZ_0^2 l}{2}, \quad (10)$$

where

$$\alpha = \frac{R}{2Z_0} + \frac{GZ_0}{2}.$$

Assuming that the dielectric constant is increased to ϵ_r , the characteristic impedance Z_0 and length l , are both reduced by $1/\sqrt{\epsilon_r}$. A dielectric-filled resonant line, assuming the same dielectric dissipation factor of equation (10) will have the input resistance

$$R_{in\epsilon=\epsilon_r} = \frac{Rl}{2\sqrt{\epsilon_r}} + \frac{GZ_0^2 l}{2\epsilon_r^{3/2}}. \quad (11)$$

Note that the copper loss term is reduced by $1/\sqrt{\epsilon_r}$. Furthermore, the dielectric loss term is reduced by a factor of $1/\epsilon_r^{3/2}$.

In actuality, the dielectric loss is increased from zero to a finite value when converting an air dielectric filled choke to a teflon dielectric filled choke. However, the loss tangent of teflon is very small, Z_0 is small, and the dielectric loss term is also reduced by $1/\epsilon_r^{3/2}$. Thus, in a practical case, instead of increased dissipation losses due to the use of teflon dielectric, the losses are reduced.

A Study of Multielement Transmission Lines*

HIROSHI KOGŌ†

Summary—Although many papers have been published on the subject of multielement transmission lines, the application to practical problems seems rather inconvenient. The author proposes a solution to the general equations which relate the voltage difference between the lines and the mesh current. Under particular conditions, it is shown that only a single type of propagating mode exists. In this case, the solution has been obtained by the so called "decomposition method," i.e., assuming several virtual two element transmission lines in lieu of the existing multielement transmission line. The problem has been solved by means of the resolved superposed virtual lines taking into account the existing boundary condition.

INTRODUCTION

PAPERS concerning multielement transmission lines have been proposed by many authors.¹⁻¹²

However, the majority refers strictly to the general theory^{3,4} and involve complicated matrix problems; the application of these results to simple practical problems is inconvenient. There are some simple problems as, for instance, the coupling theory between two wave guides,⁵⁻⁷ three parallel conducting lines,^{8,9} which is treated by balanced and longitudinal or by the right hand polarized, left hand polarized and longitudinal modes. However, there appears to be no paper concerning the practical calculations for the problem of more than four element transmission lines.

We shall now propose another form of the multielement transmission line problem; in a particular case it can be easily solved by use of the "decomposition method," i.e., by first assuming several virtual two element transmission lines concerned with the existing multielement transmission line. The problem has been solved by means of the resolved superposed virtual lines, taking

into account the existing boundary conditions.

The following results were obtained:

- 1) Generally, n -lines have $(n-1)$ propagation modes, but in particular conditions they have only one. It is then possible to analyze most multielement transmission lines.
- 2) The majority of multielement line problems generally start from the fundamental linear differential equations. However, the definition of the propagation mode derived from these has not been explained in terms of the Maxwell equations.
- 3) As the propagation mode of the multiple line system, it may be questioned whether the TEM wave (perfect transverse wave) exists, and if it exists, whether the propagation mode can be TEM. Moreover, in such a case, it is necessary to examine the relationship of the line constants.

A STUDY BASED ON ELECTROMAGNETIC WAVE THEORY

For this analysis, a perfect conductor of uniform cross section shall exist parallel in the homogeneous dielectric medium; the distance between each conductor is assumed to be extremely shortened compared to the wavelength. On the uniform line of arbitrary cross section with the axis in the z direction, an electromagnetic wave will exist in the form, $\exp j(\omega t - \beta z)$. If all the conductors are perfect conductors, the electromagnetic field E_x , H_x must satisfy $E_x = 0$, $\partial H_x / \partial n = 0$ on these conductors.

Accordingly $E_x \neq 0$, $H_x = 0$ (TM mode), $E_x = 0$, $H_x \neq 0$ (TE mode) and $E_x = H_x = 0$ (TEM mode) waves on the multiline, propagate in the general shielding line; the number of these modes has no direct relation to any line numbers. It is also evident that all modes are propagated independently due to their orthogonal properties. Furthermore, when the distance between these lines can be neglected compared with the wavelength, TEM waves alone will exist, as TE and TM waves will be cut off. Under these conditions alone can the relation between the multiline equation and the Maxwell equations be found.

The general equations of multilines are given as follows:

$$\frac{dV_r}{dx} = \sum_m z_{rm} I_m, \quad \frac{dI_r}{dx} = \sum_n y_{rn} V_n \quad (1)$$

where V_r is the potential of line r , I_r is its current and x its directional distance for its transmission line. When this system transmits the TEM wave, the field can be derived from $\exp j(\omega t \pm \beta z)$, where $\beta = \omega \sqrt{\mu \epsilon}$.

If L_{rm} is the inductance per unit length and C_{rn} is the

* Manuscript received by the PGMTT, March 13, 1959; revised manuscript received, September 22, 1959.

† Faculty on Engrg., Chiba Univ., Chiba, Japan.

¹ J. R. Carson, and R. S. Hoyt, "Propagation of periodic currents over a system of parallel wires," *Bell Sys. Tech. J.*, vol. 6, pp. 495-545; July, 1927.

² Schelkunoff, "Electromagnetic Waves," pp. 235-236, D. Van Nostrand Co., Inc., New York, N. Y.; 1956.

³ L. A. Pipes, "Matrix theory of multi-conductor transmission lines," *Phil. Mag.*, vol. 24, pp. 97-100; July, 1937.

⁴ S. O. Rice, "Steady state solution of transmission line equations," *Bell Sys. Tech. J.*, vol. 20, pp. 131-178; April, 1941.

⁵ S. E. Miller, "Coupled wave theory and wave guide applications," *Bell Sys. Tech. J.*, vol. 33, pp. 662-719; May, 1954.

⁶ W. H. Louisell, "Analysis of the single tapered mode coupler," *Bell Sys. Tech. J.*, vol. 34, pp. 853-870; July, 1955.

⁷ A. G. Fox, "Wave coupling by warped normal mode," *Bell Sys. Tech. J.*, vol. 34, pp. 823-852; July, 1955.

⁸ W. L. Firestone, "Analysis of transmission line directional couplers," *Proc. IRE*, vol. 42, pp. 1529-1538; October, 1954.

⁹ R. C. Kenschli, "Further analysis of transmission line directional couplers," *Proc. IRE*, vol. 43, pp. 867-869; July, 1955.

¹⁰ L. V. Bewley, "Traveling Waves on Transmission System," John Wiley and Sons, Inc., New York, N. Y.; 1951.

¹¹ Raisbeck and Maulsy, "Transmission characteristics of a three-wire coaxial line," *Bell Sys. Tech. J.*, vol. 37, pp. 835-876; July, 1958.

¹² H. Kogō, "Research on the split coaxial type balun," Antenna Research Committee of E.C.C. of Japan; October, 1955.

capacitance z_{rm} , y_{rn} will be given by the following equations:

$$z_{rm} = j\omega L_{rm}, \quad y_{rn} = j\omega C_{rn}.$$

Accordingly, from (1)

$$V_r = \pm \frac{\omega}{\beta} \sum_m L_{rm} I_m, \quad I_r = \pm \frac{\omega}{\beta} \sum_n C_{rn} V_n. \quad (2)$$

Then, from (2)

$$V_r = \sum_m L_{rm} \sum_n C_{mn} V_n.$$

The left term in the above mentioned equation is a function for r alone. Therefore,

$$\sum_m L_{rm} C_{mr} = 1, \quad \sum_m L_{rm} C_{mn} = 0 \quad (r \neq n)$$

or

$$\sum_m z_{rm} y_{mr} = \frac{-\omega^2}{c^2}, \quad \sum_m z_{rm} y_{mn} = 0 \quad (r \neq n) \quad (3)$$

where c is the light velocity. As a simple example, the three-line is considered:

$$\begin{aligned} \frac{dV_1}{dx} &= z_{11}I_1 + z_{m1}I_2, & \frac{dV_2}{dx} &= z_m I_1 + z_2 I_2 \\ \frac{dI_1}{dx} &= y_1 V_1 + y_m V_2, & \frac{dI_2}{dx} &= y_m V_1 + y_2 V_2. \end{aligned} \quad (4)$$

From the above equation, the following equation can be obtained.

$$\begin{aligned} \frac{d^4 V_1}{dx^4} - (Z_1 Y_1 + 2z_m y_m + z_2 y_2) \frac{d^2 V_1}{dx^2} \\ + (z_1 z_2 - z_m^2)(y_1 y_2 - y_m^2) V_1 = 0. \end{aligned} \quad (5)$$

Putting $V_1 = \exp \gamma x$, the solution can be obtained by calculating γ .

$$\gamma = \pm [\gamma_0^2 \pm \sqrt{4\gamma_0^4 - 4(z_1 z_2 - z_m^2)(y_1 y_2 - y_m^2)}]^{1/2} \quad (6)$$

where

$$\gamma_0^2 = \frac{1}{2}(z_1 y_1 + 2z_m y_m + z_2 y_2).$$

Substituting the relation of (3), we will obtain

$$\begin{aligned} z_1 y_1 + z_m y_m &= z_2 y_2 + z_m y_m = -\frac{\omega^2}{c^2} \\ z_1 y_m + z_m y_2 &= z_m y_1 + z_2 y_m = 0, \end{aligned} \quad (7)$$

$$\gamma = \pm \gamma_0 = \pm \frac{j\omega}{c}. \quad (8)$$

In general multiple-element transmission lines, the matrix of the constant is written as follows:

$$[\gamma] = \begin{bmatrix} \gamma_{11} & \gamma_{12} & \cdots \\ \gamma_{21} & \gamma_{22} & \cdots \\ \vdots & \vdots & \ddots \end{bmatrix} \cdots = \quad (9)$$

The diagonal terms become $\gamma_{11} = \gamma_{22} = \cdots = \gamma_0$ and the excess terms will be $\gamma_{12} = \gamma_{21} = \gamma_{13} = \cdots = 0$.

GENERAL SOLUTION

Eq. (1) in the previous section relates the voltage and current of each line. The voltage difference of the lines is used instead of the line voltage, because it is more convenient in connection with the intrinsic transmission mode and also for handling this problem. Now, if V_{ik} is the voltage difference between the arbitrary lines i and k , as shown in Fig. 1, then

$$\frac{dV_{ik}}{dx} = \frac{dV_i}{dx} - \frac{dV_k}{dx} = \sum_{s=1}^n Z_{is} I_s - \sum_{s=1}^n Z_{ks} I_s \quad (10)$$

and the current I_s flowing on the line S is

$$\frac{dI_s}{dx} = \sum_{j=1}^n Y_{sj} V_{sj} \quad (11)$$

where Z_{ik} is the series impedance per unit length and Y_{ik} is the parallel admittance per unit length.

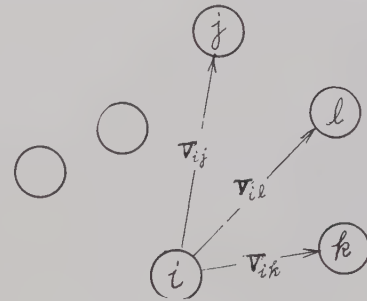


Fig. 1—Voltage difference between arbitrary lines.

From (10) and (11)

$$\frac{d^2 V_{ik}}{dx^2} = \sum_{s=1}^n \Gamma_{ks}^i V_{is} \quad (12)$$

where

$$\Gamma_{ks}^i = \sum_{j=1}^n (Z_{ij} + Z_{ks} - Z_{kj} - Z_{is}) Y_{js}. \quad (13)$$

Note: z and y in the previous section have the following relations:

$$z_{ij} = Z_{ij}, \quad y_{jk} = -Y_{jk} \quad (j \neq k), \quad y_{jj} = \sum_k' Y_{jk}.$$

Now, in (12), we will consider the k, j component H_{kj}^{-1i} of H^{-1i} based on the specific i to set up the diagonal matrix from the similar transformation of $H^{-1} \Gamma H$:

$$V_k^i = \sum_j H_{kj}^{-1i} V_{ij}. \quad (14)$$

From the above transformation, we obtain

$$\frac{d^2 V_k^i}{dx^2} = \sum_m \left\{ \sum_{sj} H_{kj}^{-1i} \Gamma_{js}^i H_{sm}^i \right\} = D_k^i V_k^i, \quad (15)$$

$$\therefore V_k^i = A_k \exp \sqrt{D_k^i} x + B_k \exp (-\sqrt{D_k^i} x), \quad (16)$$

$$\frac{dI_k}{dx} = \sum_k \frac{dI_{ik}}{dx} = \sum_k Y_{ik} V_{ik} \quad (17)$$

$$I_{ik} = Y_{ik} \int V_{ik} dx = \sum_{j=1}^n H_{kj}^i \frac{Y_{ik}}{\sqrt{D_k^i}} \tilde{V}_j^i, \quad (18)$$

where

$$\tilde{V}_j^i = A_j \exp \sqrt{D_j^i} x - B \exp (-\sqrt{D_j^i} x).$$

Thus, if we adopt a pair of V_j^i, I_j^i , the actual current I_{ik} will be shown by the intrinsic transmission mode. And the calculation of the diagonal matrix will be obtained by a similar transformation as follows.

$$|\Gamma^i - XU| = 0. \quad (19)$$

The eigenvalue D of transmission constant Γ^i based on the line i is shown by the unit matrix U and the unknown X . The K -component of characteristic column vector ϕ^{im} belonging to this root D_m is shown as follows:

$$\phi_k^{im} = C_m |(\Gamma^i - D_m U)^{ik}|^{\dagger} \quad (20)$$

where C_m is an arbitrary constant and $(\Gamma^i - D_m U)^{ik}$ is the cofactor of k -component in $(\Gamma^i - D_m U)$.

SYMMETRICAL LINE

Using the above mentioned theory, we shall now carry out a simple exercise. There are three transmission lines placed parallel inside the shielding line number 4, as shown in Fig. 2.

At first, the line equation is obtained as follows from (12) and (13):

$$\frac{d^2}{dx^2} \begin{bmatrix} V_{41} \\ V_{42} \\ V_{43} \end{bmatrix} = \begin{bmatrix} \Gamma_{11}^4 & \Gamma_{12}^4 & \Gamma_{13}^4 \\ \Gamma_{21}^4 & \Gamma_{22}^4 & \Gamma_{23}^4 \\ \Gamma_{31}^4 & \Gamma_{32}^4 & \Gamma_{33}^4 \end{bmatrix} \begin{bmatrix} V_{41} \\ V_{42} \\ V_{43} \end{bmatrix} = [\Gamma][V]. \quad (21)$$

Each element in Γ is obtained from (13). For instance,

$$\begin{aligned} \Gamma_{11}^4 &= \sum_{j=1}^4 {}^{(1)}(Z_{4j} + Z_{11} - Z_{ij} - Z_{41}) Y_{j1} \\ &= (Z_{42} + Z_{11} - Z_{12} - Z_{41}) Y_{21} \\ &\quad + (Z_{43} + Z_{11} + Z_{13} - Z_{41}) Y_{31} \\ &\quad + (Z_{44} + Z_{11} - Z_{14} - Z_{41}) Y_{41}. \end{aligned} \quad (22)$$

Other Γ_{ks}^i can be acquired similarly. In a particular case, as when we consider the symmetrical line where the diagonal terms are equal and the excess terms are also equal, we obtain the following equations:

$$\begin{aligned} Z_{11} &= Z_{22} = Z_{33} = Z_0, & Z_{12} &= Z_{23} = Z_{31} = Z_m, \\ Y_{41} &= Y_{42} = Y_{43} = Y_0, & Y_{12} &= Y_{23} = Y_{31} = Y_m. \end{aligned}$$

And, if we assume that the current flows only in the inner surface of the shielding line,

$$Z_{44} = 0.$$

Substituting these relations into Γ_{ks}^i

$$\Gamma_{11}^4 = \Gamma_{22}^4 = \Gamma_{33}^4 = Z_0 Y_0 + 2(Z_0 - Z_m) Y_m$$

$$\Gamma_{12}^4 = \Gamma_{32}^4 = \Gamma_{31}^4 = Z_m Y_0 + (Z_m - Z_0) Y_0.$$

Substituting the above mentioned equation into $[\Gamma]$ of (12),

$$[\Gamma] = \begin{bmatrix} \alpha & \beta & \beta \\ \beta & \alpha & \beta \\ \beta & \beta & \alpha \end{bmatrix} \quad (23)$$

where

$$\alpha = Z_0 Y_0 + 2(Z_0 - Z_m) Y_m,$$

and

$$\beta = Z_m Y_0 + (Z_m + Z_0) Y_m.$$

This transmission wave has α and β mode, and because of its mutual coupling, it has complicated propagation characteristics.

We now calculate the eigenvalue of the transmission line,

$$\begin{vmatrix} \alpha - \lambda & \beta & \beta \\ \beta & \alpha - \lambda & \beta \\ \beta & \beta & \alpha - \lambda \end{vmatrix} = 0$$

and obtain the root $\alpha + 2\beta$ and the two degenerating roots $\alpha - \beta$ as follows:

$$\lambda_1 = \alpha + 2\beta = (Z_0 + 2Z_m) Y_0$$

$$\lambda_2 = \alpha - \beta = (Z_0 - Z_m)(Y_0 + 3Y_m). \quad (24)$$

It is difficult to find the line propagating the modes λ_1 and λ_2 as in the above mentioned equations, but in a particular case when it forms a symmetry, the roots can be acquired by the following method:

1) The transmission line is chosen from a pair of lines 4 and 1, 2, 3 combined as shown in Fig. 3. In this case, the admittance of a pair per unit length is $3Y_0$, the self-impedance per unit length of each line is Z_0 , and the mutual impedance is $2Z_m$. The series impedance per unit length of each line is $Z_0 + 2Z_m$ as the current flows in both lines in the same direction. Therefore, the series impedance of three lines become $(Z_0 + 2Z_m/3)$ and the parallel admittance is $3Y$. Accordingly,

$$\lambda_1 = \frac{Z_0 + 2Z_m}{3} 3Y = (Z_0 + 2Z_m) Y_0.$$

This coincides with λ_1 of (24).

2) A pair of lines 2 and 3 is chosen for the transmission line, as shown in Fig. 4. In this case, lines 1 and 4 are fixed by the symmetry, and no current flows through the lines. The series impedance of lines 2 and 3 per unit length becomes $2(Z_0 - Z_m)$ as the current flows in the opposite direction.

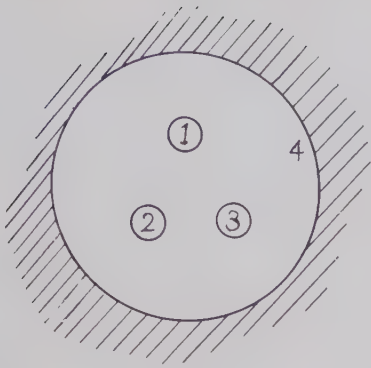


Fig. 2—Three transmission lines placed in parallel inside the shielding line number 4.

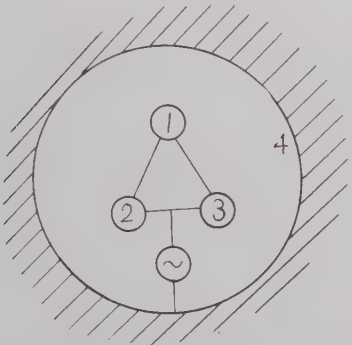


Fig. 3—A pair of lines 4 and 1, 2, 3 in a lump.

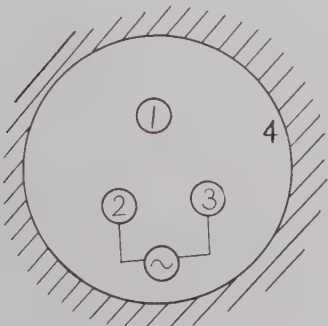


Fig. 4—A pair of lines 2 and 3.

As the parallel admittance between lines 2 and 3 is

$$Y_m + \frac{Y_0 + Y_m}{2}$$

$$\lambda_2 = 2(Z_0 - Z_m) \left(Y_m + \frac{Y_0 + Y_m}{2} \right)$$

$$= (Z_0 - Z_m)(Y_0 + 3Y_m).$$

This coincides with λ_2 in (24). As a result, the actual line can be composed by choosing two lines, 1) and 2). Now, consider the result we obtain if the arbitrary line is adopted.

3) A pair of lines 1 and 2, 3, 4 combined is chosen for the transmission line. In this case, λ_3 is calculated as follows from the same consideration:

$$\lambda_3 = \left(Z_0 - Z_m \frac{2Y_m}{Y_0 + Y_m} \right) (Y_0 + 2Y_m).$$

This value is not equal to both λ_1 and λ_2 . Therefore, it is clear that finding the particular line is necessary for the intrinsic propagation. The solution of lines can be acquired from the above mentioned relations, and as these lines consist of four numbers, three equations must be prepared. For the case of 1), the voltage between line 1, 2, 3 and 4 is calculated for V_{123-4} , and for the case of 2), the voltage between line 2 and 3 is calculated for V_{2-3} , and V_{1-2} is calculated similarly.

$$V_{123-4} = A_1 \exp \sqrt{\lambda_1} x + B_1 \exp (-\sqrt{\lambda_1} x),$$

$$V_{2-3} = A_2 \exp \sqrt{\lambda_2} x + B_2 \exp (-\sqrt{\lambda_2} x),$$

$$V_{1-2} = A_3 \exp \sqrt{\lambda_2} x + B_3 \exp (-\sqrt{\lambda_2} x). \quad (25)$$

The line equations can be solved when arbitrary constants are determined by using the boundary condition of the actual lines derived from the above mentioned equations. The relation between the actual possible transmission lines 1) and 2) and the intrinsic propagation can obviously be obtained, as 1) and 2) are known in this example, but if the lines are unknown, the following method can be adopted.

First, we shall obtain the following equations from (20) with regard to λ_1 and λ_2 .

$$\begin{bmatrix} \phi_1^{4(\lambda_1)} \\ \phi_2^{4(\lambda_1)} \\ \phi_3^{4(\lambda_1)} \end{bmatrix} = c(\lambda_1) \begin{bmatrix} \alpha - \lambda_1 & \beta \\ \beta & \alpha - \lambda_1 \\ \beta & \beta \\ \beta & \alpha - \lambda_1 \\ \beta & \beta \\ \alpha - \lambda_1 & \beta \end{bmatrix}$$

$$= 3\beta^2 c(\lambda_1) \begin{bmatrix} 1 \\ 1 \\ 1 \end{bmatrix} \quad (26)$$

$$\begin{bmatrix} \phi_1^{4(\lambda_2)} \\ \phi_2^{4(\lambda_2)} \\ \phi_3^{4(\lambda_2)} \end{bmatrix} = 3\beta^2 c(\lambda_2) \begin{bmatrix} 0 \\ -1 \\ 1 \end{bmatrix} \text{ or } 3\beta^2 c(\lambda_2) \begin{bmatrix} 1 \\ -1 \\ 0 \end{bmatrix}. \quad (27)$$

Accordingly, we find the following relation between the voltages v_1, v_2, v_3 acting as the intrinsic propagation and the actual voltages V_{41}, V_{42}, V_{43} :

$$\begin{bmatrix} V_{41} \\ V_{42} \\ V_{43} \end{bmatrix} = \begin{bmatrix} 1 & 0 & 1 \\ 1 & -1 & -1 \\ 1 & 1 & 0 \end{bmatrix} \begin{bmatrix} v_1 \\ v_2 \\ v_3 \end{bmatrix} \quad (28)$$

where

$$v_1 = A_1 \exp \sqrt{\lambda_1} x + B_1 \exp (-\sqrt{\lambda_1} x)$$

$$v_2 = A_2 \exp \sqrt{\lambda_2} x + B_2 \exp (-\sqrt{\lambda_2} x)$$

$$v_3 = A_3 \exp \sqrt{\lambda_2} x + B_3 \exp (-\sqrt{\lambda_2} x).$$

Thus, each actual voltage is shown as a function of v_1 , v_2 and v_3 , but when each equation is written only by one intrinsic propagation mode, the voltage is chosen as follows:

$$\begin{bmatrix} V_1 \\ V_1 \\ V_1 \end{bmatrix} = \begin{bmatrix} 1 & 0 & 1 \\ 1 & -0 & -1 \\ 1 & 1 & 0 \end{bmatrix} \begin{bmatrix} v_1 \\ 0 \\ 0 \end{bmatrix} \quad (29)$$

$$\begin{bmatrix} 0 \\ -V_2 \\ V_2 \end{bmatrix} = \begin{bmatrix} 1 & 0 & 1 \\ 1 & -1 & -1 \\ 1 & 1 & 0 \end{bmatrix} \begin{bmatrix} 0 \\ v_2 \\ 0 \end{bmatrix} \quad (30)$$

$$\begin{bmatrix} V_3 \\ -V_3 \\ 0 \end{bmatrix} = \begin{bmatrix} 1 & 0 & 1 \\ 1 & -1 & -1 \\ 1 & 1 & 0 \end{bmatrix} \begin{bmatrix} 0 \\ 0 \\ v_3 \end{bmatrix} \quad (31)$$

In this case, $V_1=v_1$, $V_2=v_2$ and $V_3=v_3$. The above mentioned equations were arranged to relate them to the existing line, and (29) becomes the function to only λ_1 and (30) and (31) are the functions to only λ_2 . Namely, (29) and V_{123-4} of (25) are the same and they correspond to line 1). Similarly, (30) and V_{2-3} are the same and (31) and V_{1-2} are the same, and both equations correspond to line 2).

DECOMPOSITION METHOD

The analysis on symmetrical lines has been described in the previous section. Thus, if we analyze the actual voltage as the decomposite voltage V_{123-4} , V_{2-3} , V_{1-2} and so on, these will cause intrinsic propagation.

In a specific case where the transmission mode is single, a similar consideration can be applied to the usual transmission line by developing the above theory. In general, the actual voltage V_i will be given by the following equation as the linear combination of the voltage v_{ik} where the particular lines i, k are chosen for the transmission line and the line current is ceased except for the lines i, k :

$$\begin{aligned} V_i &= A_i \exp \sqrt{\lambda_0} x + B_i \exp (-\sqrt{\lambda_0} x) = \sum_k v_{ik} \\ &= \sum_k [a_{ik} \exp \sqrt{\lambda_0} x + b_{ik} \exp (-\sqrt{\lambda_0} x)]. \end{aligned} \quad (32)$$

But a_{ik} and b_{ik} should be determined by the boundary condition in the multilayer and not by i, k lines independently. The current in this case is shown as follows:

$$i_{ik} = Y_{0ik} [a_{ik} \exp \sqrt{\lambda_0} x - b_{ik} \exp (-\sqrt{\lambda_0} x)]. \quad (33)$$

Where Y_{0ik} is the characteristic admittance between i and k , it can be calculated by the following equation:

$$Y_{0ik} = c C_{ik} \quad (34)$$

where C_{ik} is the electrostatic capacity per unit length between i and k and c is the light velocity.

We can now consider the ideal equation of the n transmission line which satisfies the condition as follows. Let

us first take the condition in which the current flows only in two arbitrary lines, namely the i, k elements, with no current flowing in the other elements. Since the number of independent components of voltage or current is $n-1$, we will be able to find the other if we know the $n-1$ terminal voltage or line-current.

$$\begin{aligned} v_{ik} &= a_{ik} \exp \sqrt{\lambda_0} x + b_{ik} \exp (-\sqrt{\lambda_0} x) \\ i_{ik} &= Y_{0ik} [a_{ik} \exp \sqrt{\lambda_0} x - b_{ik} \exp (-\sqrt{\lambda_0} x)] \\ &= Y_{0ik} \bar{v}_{ik}. \end{aligned} \quad (35)$$

In Fig. 5, the condition in which the current flows only between i and k is

$$\begin{aligned} i_j &= \sum_l Y_{0jl} v_{jl} = \sum_l Y_{0jl} (v_{ji} + v_{il}) \\ &= \sum_l Y_{0jl} (x_l \bar{v}_{ik} - x_j \bar{v}_{ik}) = 0. \end{aligned}$$

Therefore,

$$\sum_l Y_{0jl} (x_l - x_j) = 0 \quad (36)$$

where \sum' shows the total summation ($1, 2, 3 \dots, n$) except j , assuming $x_i=0$ and $x_k=1$. Eq. (36) is $(n-2)$ linear equation concerning $(n-2)$ of the unknown numbers, x_1, x_2, \dots, x_n (except $n=i, k$). That is

$$\begin{bmatrix} -\sum_l Y_{01l} & Y_{012} & \dots & Y_{01n} \\ Y_{021} - \sum_l Y_{02l} & & & \\ \vdots & & & \\ Y_{0n1} \dots - \sum_l Y_{0nl} & & & \end{bmatrix} \begin{bmatrix} x_1 \\ x_2 \\ \vdots \\ x_n \end{bmatrix} = \begin{bmatrix} -Y_{01k} \\ -Y_{02k} \\ \vdots \\ -Y_{0nk} \end{bmatrix} \quad (37)$$

Solving the above mentioned equation, if we add a voltage x_j times the i, k voltage between i and l lines, to all the l lines with the exception of i, k , the line current except i, j becomes zero. And the i th line current becomes

$$i_i = \sum_l Y_{0il} \bar{v}_{il} = \left(\sum_l Y_{0il} x_l \right) \bar{v}_{ik}. \quad (38)$$

We call such a line the "fundamental transmission line" with respect to the line element i, k . We now divide the n -line into m groups which are called line bundle L ($1, 2, \dots, q$) and those bundles preserve the same potential as shown in Fig. 6. Namely, they are to be jointed to each line with a perfect conductor line of infinitesimal small diameter. Thus, we can deal with the m th transmission line. The characteristic admittance between B ($1, 2, \dots, p$) and L ($1, 2, \dots, q$) of the arbitrary line bundle is as follows:

$$i_{Bb} = \sum_{b=1}^p \sum_{l=1}^q i_{BbDd} = \sum_{b=1}^p \sum_{l=1}^q Y_{0BbLl} \bar{v}_{BL} \quad (39)$$

$$Y_{0BL} = \sum_{b=1}^p \sum_{l=1}^q Y_{0BbLl} \quad (40)$$

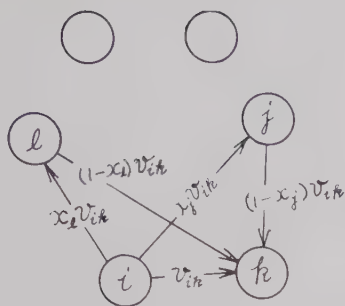
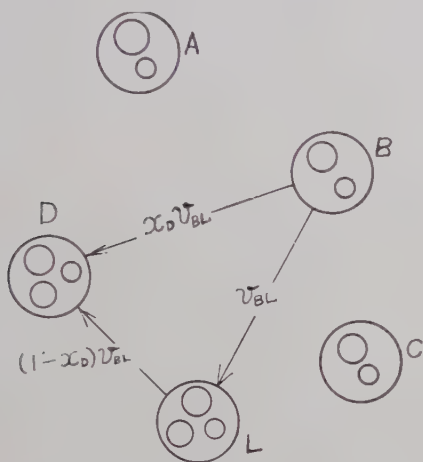
Fig. 5—Condition in which current flows only between i and k .

Fig. 6—Transmission line dividing some groups.

The current i_{Bb} which runs into each element Bb in the line bundle B and the current distributed factor α will be

$$i_{Bb} = \sum_D' \sum_d i_{BbDd} = \sum_D' \sum_d Y_{0BbDd} x_D \bar{v}_{BL} \quad (41)$$

$$= \frac{\sum_D' \sum_d Y_{0BbDd} x_D}{\sum_D' Y_{0BD} x_D} i_{BL} = \frac{\sum_D' \sum_d Y_{0BbDd} x_D}{\sum_D' \sum_b \sum_d Y_{0BbDd} x_D} i_{BL}$$

$$i_{Bb} = \alpha i_{BL}. \quad (42)$$

Also, the current i_{Aa} which runs into each element a in the arbitrary bundle A except BL , is derived as follows:

$$i_{Aa} = \sum_D' \sum_d i_{AaDd} = \frac{\sum_D' \sum_d Y_{0AaDd} (x_D - x_A)}{\sum_D' \sum_b \sum_d Y_{0BbDd} x_D} i_{BL}. \quad (43)$$

When the given n transmission line is considered as a line bundle $A, B \cdots M$ divided properly into m numbers, it can be regarded as a two-transmission line; the characteristic admittance is derived by $\sum_D' Y_{0BD} x_D$ for any two-line BL . It may be called the fundamental transmission line on line element i, k . In n transmission line, many fundamental lines are found by various arrangements. Any n transmission line can be formed by superposition of v_{ik}, i_{ik} for a suitable fundamental transmission line $(n-1)$, as the degree of freedom of an n -line is $(n-1)$.

In this case, every line element must be used as an element of the fundamental line at least once. What $(n-1)$ fundamental transmission line should be adopted is easily decided by analyzing it properly according to the given problem.

EXAMPLE: "SPLIT COAXIAL-TYPE BALUN" AS A THREE-TRANSMISSION LINE

Fig. 7(a) shows the equivalent circuit of the split coaxial-type balun terminating with Y_{12}, Y_{23}, Y_{31} , neglecting the earth effect. This circuit can be decomposed from two types of transmission lines, as shown in Fig. 7(b) and (c).

By (40) and (42) in the previous section, the characteristic admittance and the current distributed factor α are shown as follows:

$$Y_{013-2} = Y_{021} + Y_{023}$$

$$\alpha = \frac{Y_{012}}{Y_{012} + Y_{023}}.$$

Also, the voltage divider factor x_2 from (37) is shown as follows:

$$-\sum_S Y_{02S} x_2 = -Y_{021}$$

$$x_2 = \frac{Y_{012}}{Y_{012} + Y_{023}}.$$

Relations between the voltage and the current in Fig. 7(a) are derived by superposition in (b) and (c).

$$I_1 = -\frac{Y_{012}}{Y_{012} + Y_{023}} i_1 - i_2$$

$$I_2 = i_1$$

$$V_{23} = v_1 - \frac{Y_{012}}{Y_{012} + Y_{023}} v_2$$

$$V_{31} = v_2.$$

Applying the boundary condition at the termination $l=0$, voltage and current at this surface are shown as follows:

$$I_1 = Y_{12} V_{23} - (Y_{12} + Y_{31}) V_{31}$$

$$I_2 = (Y_{13} + Y_{23}) V_{23} + Y_{12} V_{31}$$

$$-i_2 = -j \left(Y_{031} + \frac{Y_{032} Y_{012}}{Y_{031} + Y_{023}} \right) \cot \beta l_0 v_2 = Y_{s13} v_2$$

$$i_1 = (Y_{12} + Y_{23}) v_1$$

$$+ \left(Y_{12} \frac{Y_{023}}{Y_{012} + Y_{023}} - \frac{Y_{012}}{Y_{012} + Y_{023}} Y_{23} \right) v_2.$$

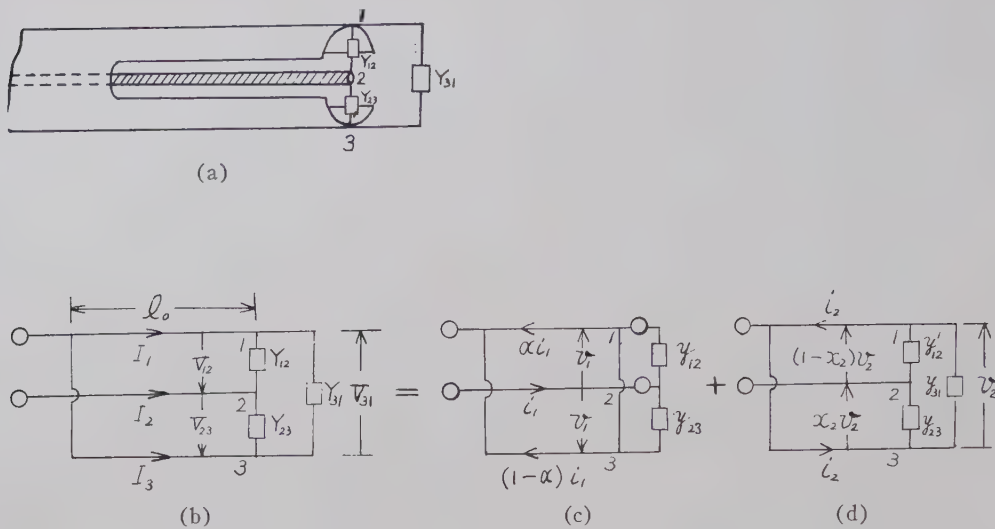


Fig. 7—Split coaxial type balun. (a) Construction. (b) Equivalent circuit. (c), (d) Decomposite circuit.

Input admittance Y_{in} is shown as follows:

$$Y_{in} = \frac{i_1}{v_1} = \frac{(Y_{12} + Y_{23})(Y_{31} + Y_{s13}) + Y_{23}Y_{12}}{Y_{31} + Y_{s13} + Y_{12} \frac{Y_{023}^2}{(Y_{012} + Y_{023})^2} + Y_{23} \frac{Y_{012}^2}{(Y_{012} + Y_{023})^2}}$$

In the case of symmetrical split, $Y_{012} = Y_{023}$, then

$$Y_{in} = \frac{4(Z_1 + Z_2 + Z_R)}{4Z_1Z_2 + Z_1Z_R + Z_2Z_R}$$

where

$$Z_1 = \frac{1}{Y_{12}}, \quad Z_2 = \frac{1}{Y_{23}}, \quad Z_R = \frac{1}{Y_{31} + Y_{s13}}$$

When a segment of the outer split cylinder is shorted to the central conductor,

$$Y_{12} = \infty, \quad \text{then} \quad Y_{in} = 4(Y_{23} + Y_{31} + Y_{s13}),$$

putting

$$Y_{23} + Y_{31} = Y_R$$

$$Y_{in} = 4(Y_R + Y_{s13}).$$

In other words, the input admittance is equal to four times the load Y_R and slot admittance Y_{s13} .

CONCLUSION

The main object of this paper is to discuss transmission modes and, under particular conditions where there is only one mode in the line, the adoption of the specific solution: the decomposition method.

This analysis based on the decomposition method can be used to produce useful solutions for many complex practical problems, *i.e.*, balun, diplexer, etc.

ACKNOWLEDGMENT

The author is grateful to Dr. Kiyoshi Morita, Professor of Tokyo Institute of Technology, for his guidance in the course of this work, and to T. Sawaguri for helpful discussions.

Measurement of Relative Phase Shift at Microwave Frequencies*

C. A. FINNILA†, L. A. ROBERTS‡, AND C. SÜSSKIND§

Summary—A method is described for measuring the relative phase shift of microwave devices, such as traveling-wave tubes, which utilizes the serrodyne technique to transfer the measurements into the audio-frequency range. The method is used to measure the phase shift incidental to the variation of the dc potentials applied to the several electrodes of a 2- to 4-kmc traveling-wave tube. This method is particularly useful in coaxial systems, where accurately calibrated phase shifters (and attenuators without phase shift) are not available.

INTRODUCTION

A PROBLEM often encountered, when making relative phase-shift measurements at microwave frequencies through active devices, is the determination of the phase shift between two signals whose relative amplitudes may vary over some dynamic range. In such cases, the common method of comparing the two signals by a measurement in the shift of the null of a standing-wave pattern created by the two signals traveling in opposite direction through a transmission line cannot be conveniently used, because in such cases the minima may not be very well defined. If the relative amplitudes of the two signals differ by 10 db or more, it becomes extremely difficult even to observe a minimum. The system to be described below avoids this difficulty by shifting the measurement to audio frequencies at which such large dynamic ranges can be readily handled with existing instruments. A similar technique has also been used for the measurement of the phase-shift characteristics of ferrites as a function of the applied magnetic field,¹ and although complex, proves to be quite workable and speedy.

In the present instance, the method was (independently) developed in an effort to measure changes in RF phase shift through traveling-wave tubes with changes in the several tube dc-supply potentials. Measurement of over-all phase shift was not necessary; only relative phase-shift measurements were needed.

Phase characteristics of traveling-wave tubes must be known in the design of many systems: keeping incidental phase modulation within specified limits is often an important requirement. For instance, the phase char-

acteristics of a tube can be used to specify stability and hum level for its power supplies. In some cases traveling-wave tubes may be used for phase or frequency modulation, and phase shift must be accurately known.

For the series of phase measurements reported here, the requirements on the phase-measurement system (see Fig. 1) were rather severe; a wide range of phase shifts had to be measured accurately. Because of the number of measurements needed, they had to be taken quickly to make useful results available in a reasonable time. Since the gain of a traveling-wave tube varies greatly for some changes in its supply potentials, it was essential that the phase-measurement system should not be affected by large changes in signal amplitude.

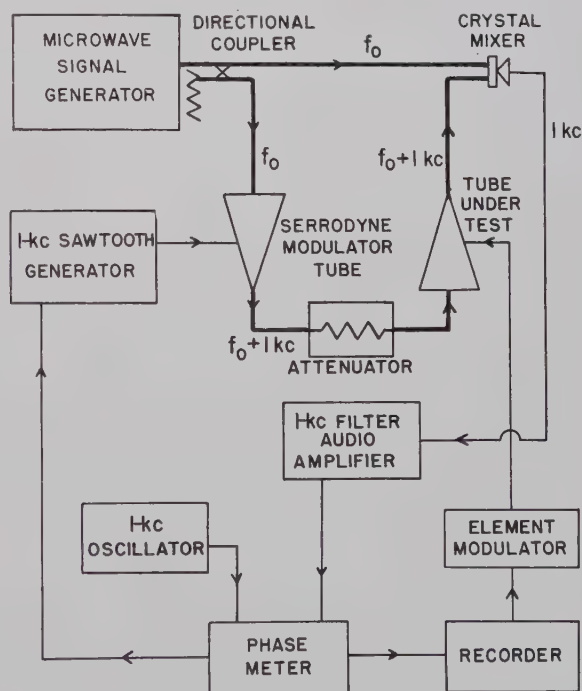


Fig. 1—Phase-measurement system.

PHASE-MEASUREMENT SYSTEM

The key component in the phase-measurement system is a serrodyne frequency translator.² This device yields two stable microwave frequencies, f_0 and $f_0 + 1$ kc, as shown in Fig. 1. The latter signal is passed through the tube under test and mixed with f_0 ; the difference

* Manuscript received by the PGMTT, July 27, 1959.

† Electronics Res. Lab., University of California, Berkeley, Calif. Formerly at Huggins Labs., Inc., Sunnyvale, Calif.

‡ Watkins-Johnson Co., Palo Alto, Calif. Formerly at Huggins Labs., Inc., Sunnyvale, Calif.

§ Dept. of Elec. Engrg., University of California, Berkeley, Calif.

¹ J. B. Linker, Jr., and H. H. Grimm, "Automatic microwave transmission measuring equipment," *Rev. Sci. Instr.*, vol. 28, pp. 559-563; July, 1957.

² R. C. Cumming, "The Serrodyne frequency translator," *Proc. IRE*, vol. 45, pp. 175-186; February, 1957.

frequency of 1 kc exhibits the same phase shift as the microwave signal $f_0 + 1$ kc. In this way, the measurement of phase shift can be carried out at the audio frequency by a simple comparison with a standard 1-kc oscillator. The principal advantage of the serrodyne technique is that it allows the generation of a phase-stable 1-kc intermediate frequency. A traveling-wave tube of the same frequency capabilities as the one under test can be used for the serrodyne. Serrodyne operation can be best visualized as an approximation to continually increasing phase modulation. If the phase of a signal is increased or decreased at a constant rate, a constant shift in frequency is produced. No known electronic device can continue to increase its amount of phase shift indefinitely, but if phase shift is increased steadily until 2π radians of phase shift has been produced, the instantaneous-signal values will be the same as at 0° phase shift.³ A quick return to zero at this point produces only a minor disturbance, and phase shift may be continued. Phase shift through many traveling-wave tubes is approximately proportional to helix voltage for phase shifts of well over 2π radians. Moreover, the necessary change in helix voltage does not appreciably change the tube's gain, especially if the tube has more than the customary amount of attenuation between input and output. The serrodyne used here produces a shift of 1 kc in the signal passing through it when its helix is modulated by a 1-kc sawtooth wave of sufficient amplitude to produce 2π radians of phase modulation. All spurious-modulation components are lower by at least 20 db than the shifted signal.

The path of microwave signals is shown by the thick line in Fig. 1. A conventional signal generator covering the frequency range of the tube under test is used. It is adjusted to give a proper signal input to the crystal mixer to produce linear mixing (1 mw for the crystal used). A directional coupler taps a small part of this signal and sends it through the serrodyne modulator tube. After being shifted in frequency in the serrodyne tube, the signal goes to an attenuator. Enough attenuation is used to insure that the signal at the mixer from this branch of the circuit does not reach a level sufficient to cause nonlinear mixing at any time during a test. For the crystal used, this signal has to be lower by at least 20 db than that from the signal generator. Too much attenuation must also be avoided, since it results in the 1-kc IF signal being too close to noise.

After the attenuator, the signal passes through the tube under test, and then through a directional coupler to the crystal mixer, where a 1-kc sine wave is produced. The 1-kc signal passes through a narrow-band 1-kc filter (to remove spurious harmonic components) and is then

amplified and applied to the phase meter. Since the signal often varies in amplitude owing to changes in the gain of the tube during a test, an amplifier with high output capability and low noise level is used. Since the phase meter can operate with signal-input amplitudes changing by ratios as high as 100:1, it is generally not necessary to change gain during a measurement series. The amplifier also has an adjustable phase-shift network which is convenient for setting initial readings.

The phase meter measures difference in phase between the signals at its two inputs. Within the meter, several limiters are used to convert each input signal to a square wave. The metering circuit measures the ratio of the time during which one square wave is positive and the other negative to the total time of the cycle. The meter is calibrated directly in degrees of phase angle between the two inputs. It can be read to within $\pm 0.5^\circ$ for any amount of total phase shift. With this phase-metering method the input signals can have any waveforms, provided the waveforms are such that they produce square waves with equal positive and negative portions after passage through the limiters. One way to insure that this condition is met is to make the input signals low-distortion sinusoids.

In order to measure relative phase shift, it is necessary to supply a phase reference to the phase meter. This reference is provided by a stabilized 1-kc oscillator. The oscillator has to be quite stable, because any change in its frequency would be converted to a change in phase by the 1-kc filter used in the system. The oscillator output goes directly to the phase meter. As a by-product, the phase meter converts the 1-kc oscillator signal to a square wave. Part of this square wave is used to synchronize the sawtooth generator of the serrodyne frequency-conversion system. By this method, phase reference information is put into the microwave part of the system.

The remainder of the required system is the unit labeled Element Modulator. This is a special dc power supply that can be placed in series with any of the elements of the tube under test. It is used to vary element voltages to the tube under test by known amounts while relative phase shift is recorded.

TUBE MEASUREMENT

As an example of the operation of this phase-measurement system, consider the results of measurements made on Huggins Laboratories Type HA-1 traveling-wave tubes. These are 10-mw, magnetically focused, general-purpose traveling-wave tubes capable of operation between 2 and 4 kmc. Five of these tubes were tested to obtain average results.

Relative phase shift as a function of 1) helix voltage, 2) "grid" (actually a gridless beam-forming electrode) voltage, 3) anode voltage, and 4) collector voltage was measured. In addition, changes in phase shift caused by

³ To be sure, a mechanical phase shifter *can* be used to increase phase shift indefinitely, but owing to mechanical limitations can only do so at a rate of a few radians per second, which is not a convenient intermediate frequency.

changes in solenoid voltage (causing changes in the magnetic focusing field) were measured. Measurements were made at 2, 3, and 4 kmc. The measurements, which covered a large over-all phase shift, were generally taken twice. The phase-shift control was shifted 90° between the two tests. The average of these two curves tended to cancel out some error from the phase meter as well as errors arising from short-range drift.

Some of the details of the measurement procedure can be illustrated by a brief outline of a typical test. After a sufficient warm-up time, the signal generator is set at the proper frequency and its output to the correct value (1 mw). The proper attenuator is attached. The element modulator is next set for the range of voltages to be used and put in series with the tube element to be tested.

Adjustments of the phase-measurement system are then made, partly with an oscilloscope that is also used to monitor system operation. First, the sawtooth generator is set to 1 kc and synchronized with the 1-kc oscillator. Second, the sawtooth amplitude to the serrodyne tube is set. The oscilloscope is connected to the crystal output before the 1-kc filter. Starting from zero, the amplitude control is slowly increased and the development of the 1-kc sine wave is observed. The amplitude is set for minimum discontinuity in the detected waveform. Next, the 1-kc amplifier gain is set to produce maximum output without distortion when the traveling-wave tube under test is also at maximum gain. (Gain often changes when the voltage to one of the tube elements is changed.) Phase readings are then recorded for different values of voltage on the tube element under consideration.

EXPERIMENTAL RESULTS

The average curves summarize the data best. For the range of grid voltages covered, the change in gain was considerable and signal-to-noise ratios were poor for high values of negative grid voltage. Fig. 2 shows the fair agreement between several tubes as *helix* voltage is varied. Fig. 3 shows the same result, averaged over five tubes, but showing curves at three frequencies.

The data for changes in *collector* and *solenoid* voltages resulted in phase shifts that were small, and showed relatively large variations between tubes, although the general trends were the same.

Phase shifts resulting from changes in *anode* voltage and in *grid* voltage are shown in Figs. 4 and 5, respectively, again for the average of five tubes and at three frequencies. These curves are of considerable practical interest, as variations in either anode or grid voltage are, of course, the common methods of amplitude-modulating the tube. (Phase changes have also been observed as a result of changes in RF drive level, when the dc electrode voltages were fixed. These phase changes were observed not only near the saturation level of the

traveling-wave tube, where the effect is well known and is commonly ascribed to nonlinear beam behavior, but also 20 to 30 db below saturation. This observation is an extremely interesting by-product of the present measurement technique.)

EFFECTIVENESS AND POTENTIALITIES OF THE MEASUREMENT SYSTEM

The relative complexity of the phase-measurement system leads to some problems. The system is very sensitive. One-half degree of phase shift is noticeable. Poor operation of any component of the system leads to noticeable error, especially in the power supplies of both the traveling-wave tube under test and the serrodyne tube. These were electronically regulated power supplies supplied from a regulated ac power source. Despite this precaution, short-term system drift often amounted to 3° . The drift seemed to be related to the power supplies.

The phase meter itself contributed to error. It was rated for ± 2 per cent accuracy, which often amounted to $\pm 3^\circ$. The sign of the error often changed rapidly when crossing 0° or 180° meter readings. This type of error could not be reduced except by extensive alterations of the phase-meter circuits. The error did, however, tend to average out when data were averaged for two phase-measurement tests with 90° of fixed phase shift inserted between them.

Unfortunately, this system could not be checked for accuracy by comparison with a standard, since no standard of sufficient accuracy was readily available. Many of the individual components of the system were checked and corrected. They were thought unlikely to cause noticeable error. On the basis of constancy of results, it is estimated that most of the phase measurements were within $\pm 3^\circ$. While this accuracy is sufficient for many purposes, greater accuracy would be needed for some uses, particularly in attempts to use phase data for a better understanding of the operation of the tube itself. If higher accuracy of phase measurements were necessary, a phase measurement system of this type could probably be constructed to give data accurate to within $\pm 0.5^\circ$. This accuracy would require a different type of audio phase meter and better power supplies.

The primary advantage of this system is its speed of measurement. With manual meter readings, a tube can be completely tested in one day. In addition, the system can be readily adapted to mechanized data collecting. The phase meter could drive a data recorder, with its paper feed driving a potentiometer wired to the element modulator. Thus a phase curve could be recorded directly. The only reason why mechanized data recording was not used in the measurements described above was that the equipment had not yet been completed.

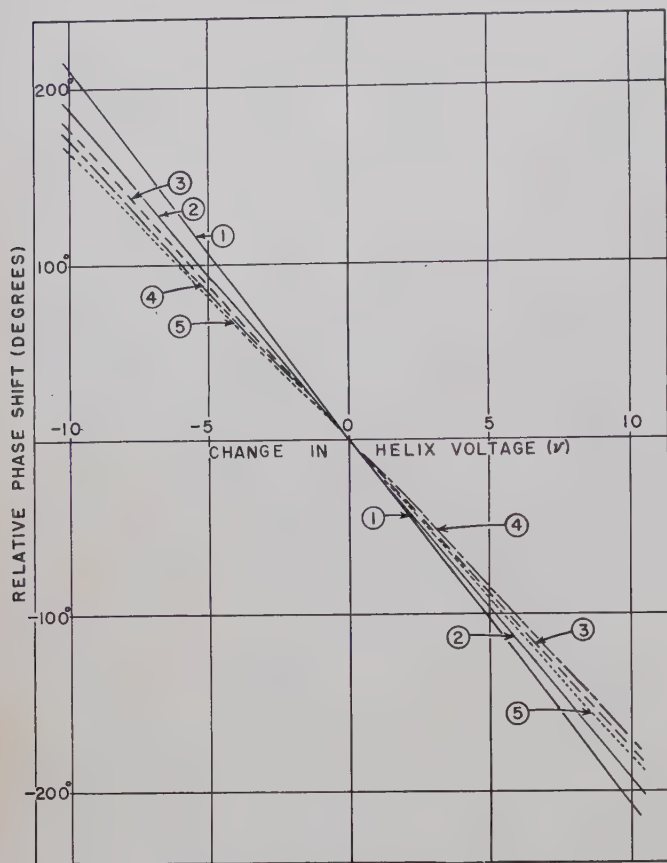


Fig. 2—Phase change for five tubes as a function of helix voltage, at a single frequency (3 kmc).

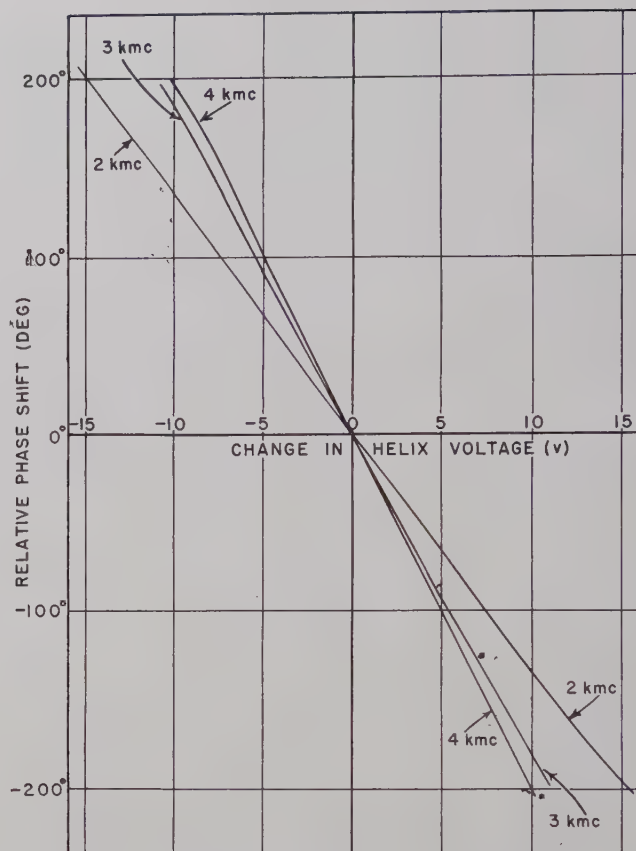


Fig. 3—Phase change for five tubes (average values) as a function of helix voltage, at three frequencies.

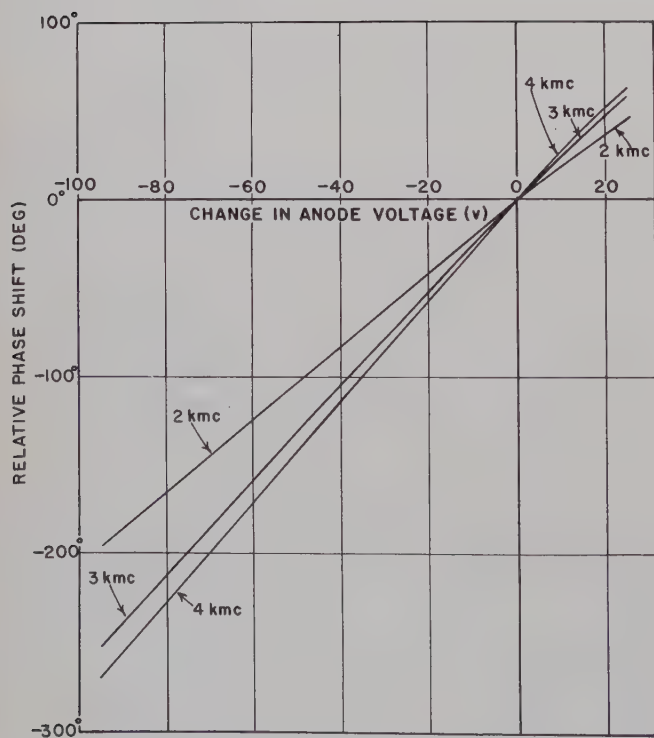


Fig. 4—Phase change for five tubes (average values) as a function of anode voltage, at three frequencies.

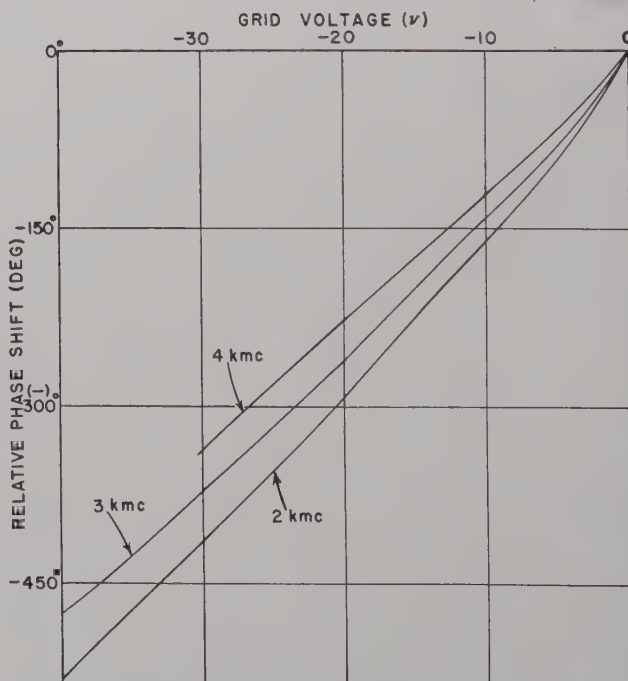


Fig. 5—Phase change for five tubes (average values) as a function of grid voltage, at three frequencies.

CONCLUSIONS

A system of making relative phase measurements at microwave frequencies has been described. It is capable of making these measurements even if the signals to be compared differ widely in amplitude. Although the system is complicated, it can yield data quickly. Many of the components of the system are in rather general use in a microwave laboratory. The audio-frequency phase meter is probably the largest piece of special equipment needed. This system would thus seem to warrant consideration whenever a large number of phase measurements are needed. The system is especially worthy of

consideration where traveling-wave or klystron tubes are available for the frequencies of interest.

Examples of phase characteristics of Huggins Laboratories HA-1 traveling-wave tubes have also been given. This tube is typical of many traveling-wave tubes now in use. The curves show that fairly good filtering of traveling-wave-tube power supplies is needed to prevent spurious phase modulation.

ACKNOWLEDGMENT

The aid of R. A. Huggins, who made available the equipment and experimental facilities, is gratefully acknowledged.

Resonant Modes in Waveguide Windows*

M. P. FORRER† AND E. T. JAYNES‡

Summary—Analysis and experimental verification of a class of resonant fields, called ghost-modes, occurring in waveguide dielectric windows are presented. Numerical solutions for a simple geometry are given through universal curves. Knowledge about ghost-modes has importance to designers of high-power windows. It also leads to a measuring technique for dielectric constants through a frequency measurement.

INTRODUCTION

THE general phenomenon of ghost-modes in imperfect waveguides, special cases of which have been noted before, was predicted by one of the authors.¹ The present paper presents a quantitative analysis and confirming experiments of a class of ghost-mode resonances occurring in a particularly simple waveguide window, where exact analysis, using transmission-line theory, is applicable. A ghost-mode is a

resonant electromagnetic field configuration, existing in the vicinity of certain waveguide obstacles, such as dielectric windows. Its transverse field configuration is that of an ordinary waveguide mode and its resonant frequency lies below the cutoff frequency of the particular mode in the unperturbed guide. Thus, the ghost-mode fields decay exponentially on either side of the waveguide obstacle and no energy travels away. Within the region of the obstacle the z -variation of the fields must have oscillatory character.

ANALYSIS

A window configuration simple enough to allow exact analysis is shown in Fig. 1. The dielectric slab shall be homogeneous and isotropic; the surrounding waveguide shall be straight and lossless, but its cross-sectional shape may be arbitrary. Under these assumptions the window does not introduce modal conversions, and analysis may proceed using conventional transmission-line theory.

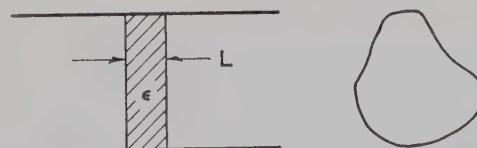


Fig. 1—Transverse dielectric slab window.

* Manuscript received by the PGMTT, August 31, 1959.

The research reported in this paper was supported jointly by the U. S. Army Signal Corps, the U. S. Air Force, and the U. S. Navy (Office of Naval Research).

† General Electric Microwave Lab., Palo Alto, Calif.

‡ Microwave Lab., W. W. Hansen Labs. of Physics, Stanford University, Stanford, Calif.

¹ E. T. Jaynes, "Ghost modes in imperfect waveguides," *PROC. IRE*, vol. 46, pp. 415-418; February, 1958. (Note that Fig. 2 in this reference was incorrectly drawn; the curves should be rotated 180° in the plane of the paper, about an axis passing through the center of the diagram.)

In the air-filled guide, the n th waveguide mode has a wave impedance

$$Z_{wn} = Z_0 \left\{ \frac{k/k_{3n}}{k_{3n}/k} \right\}, \quad (1)$$

where the upper and lower expressions within curly brackets relate to TE and TM modes, respectively. The quantities Z_0 and k are the free-space impedance and the free-space propagation constant. The waveguide propagation constant of the n th mode is $k_{3n} = \sqrt{k^2 - k_{cn}^2}$. We shall be interested in frequencies below waveguide cutoff. Here it is convenient to replace jk_{3n} by the real, positive quantity $k_{3n}' = \sqrt{k_{cn}^2 - k^2}$ in all expressions. The wave impedance, for example, becomes

$$Z_{wn} = jZ_0 \left\{ \frac{k/k_{3n}'}{-k_{3n}'/k} \right\}. \quad (2)$$

In the guide completely filled with material of dielectric constant ϵ , one has

$$Z_{wn}^{(\epsilon)} = Z_0 \left\{ \frac{k/\beta_n}{\beta_n/\epsilon k} \right\}, \quad (3)$$

where $\beta_n = \sqrt{\epsilon k^2 - k_{cn}^2}$ is the propagation constant of the n th mode in the dielectric filled guide.

The geometrical configuration (Fig. 1) has a symmetry plane $z=0$. Any resonant fields, therefore, have symmetry properties with respect to $z=0$, which may be of an even or odd character. Analytically, advantage is taken of this fact by considering only the region $z>0$ under the condition of an electric or magnetic short circuit at $z=0$.

Electric Short at $z=0$: $Z_{wn}(0)=0$

Under this condition, the impedance at the dielectric-air interface ($z=L/2$) is

$$Z_{wn}(L/2) = -jZ_{wn}^{(\epsilon)} \tan \beta_n L/2. \quad (4)$$

Continuity of tangential field components at the dielectric-air interface requires continuity of wave impedance,

$$Z_{wn}(L/2) = Z_{wn}. \quad (5)$$

Substituting (2)–(4) into (5) yields

$$\tan \beta_n L/2 = \left\{ \frac{-\beta_n/k_{3n}'}{\epsilon k_{3n}'/\beta_n} \right\}. \quad (6a)$$

$$(6b)$$

Frequencies that satisfy this equation are the ghost-mode resonant frequencies.

Magnetic Short at $z=0$: $Z_{wn}(0)=\infty$

The impedance at the dielectric-air interface becomes

$$Z_{wn}(L/2) = jZ_{wn}^{(\epsilon)} \cot \beta_n L/2, \quad (7)$$

and the continuity condition of tangential fields at $z=L/2$ leads to

$$\cot \beta_n L/2 = \left\{ \frac{\beta_n/k_{3n}'}{-\epsilon k_{3n}'/\beta_n} \right\}. \quad (8a)$$

$$(8b)$$

Eqs. (6b) and (8a) always have at least one real solution. A field analysis shows that these solutions are characterized by *even* symmetry of their longitudinal field component. They will be called even modes, and the number N_e of such solutions is determined by

$$N_e - 1 < \sqrt{\epsilon - 1} \frac{k_{cn} L}{2\pi} < N_e. \quad (9)$$

On the other hand, (6a) and (8b) have real solutions only when ϵ and L exceed certain minimum values. Solutions obtained in such cases exhibit *odd* symmetry of their longitudinal field component, and will be called odd modes. In general, there exist N_o odd modes, if

$$N_o < \sqrt{\epsilon - 1} \frac{k_{cn} L}{\pi} < N_o + 1. \quad (10)$$

Resonant field patterns corresponding to the lowest frequency solutions for some simple waveguide modes are sketched in Fig. 2. The upper-right and lower-left hand patterns correspond to (6), the others correspond to (8).

Eqs. (6) and (8) may be solved graphically by our plotting both sides of the equations as functions of frequency, k/k_{cn} , and determining the points of intersection. Such solutions, obtained for various values of ϵ and $k_{cn}L$, are shown in Figs. 3 and 4. Typically, the TE resonant frequencies decrease faster than the TM resonant frequencies, as $k_{cn}L$ is increased. All curves approach the value $(k/k_{cn})_{\text{res}} = \epsilon^{-1/2}$ for very large $k_{cn}L$. This is true for both TE and TM resonant modes and is plausible from the fact that for very large $k_{cn}L$ practically the entire field is confined to the inside of the dielectric, and resonances occur, in a well-known manner, when the dielectric is an integral number of half wavelengths long.

EXPERIMENTAL VERIFICATION OF GHOST-MODES

The ghost-mode resonances derived above are experimentally verified by an arrangement shown in Fig. 5. A window sample was placed into the center of a three-inch ID circular waveguide section. Both ends of the approximately two-foot long section were left open, since the modes of interest are below waveguide cutoff and have substantially decayed when reaching the open

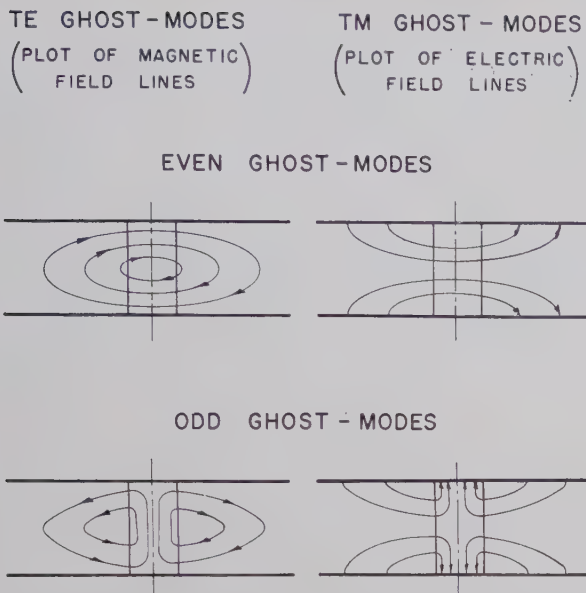


Fig. 2—Sketch of the lowest TE and TM ghost-mode field patterns of an even and an odd symmetry. (The transverse field variations shown apply to TE₁₀ and TM₁₁ in rectangular guide or TE₁₁ and TM₀₁ in circular guide.)

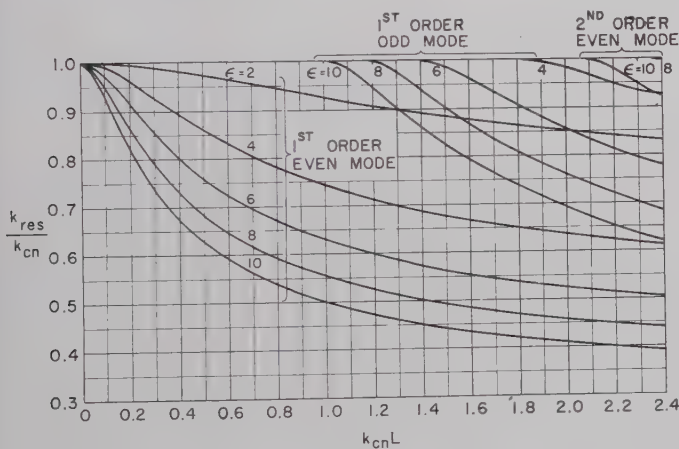


Fig. 3—Universal curves showing TE ghost-mode resonant frequencies of a transverse dielectric slab.

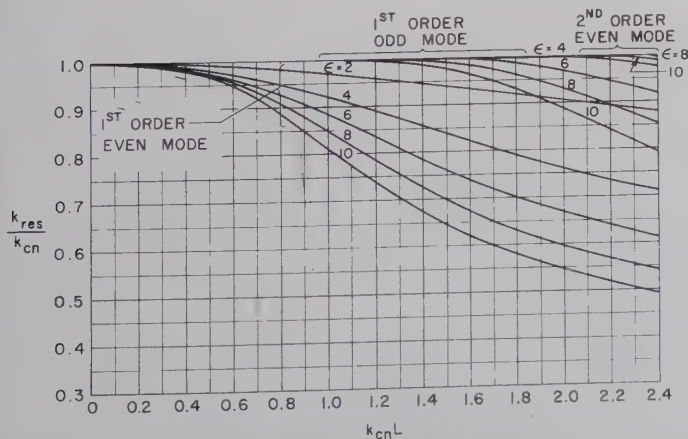


Fig. 4—Universal curves showing TM ghost-mode resonant frequencies of a transverse dielectric slab.

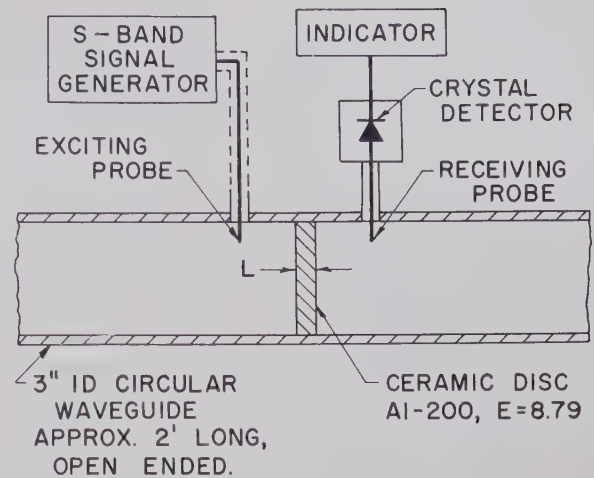


Fig. 5—Ghost-mode experiment.

ends. Microwave energy was loosely coupled to the guide through an electric probe at the guide wall, approximately four inches away from the dielectric. A similar probe, located on the opposite side of the dielectric, was connected to a crystal rectifier and an indicator. The coupling between the probes is small, so that strong indicator deflections occur only at resonance conditions in the guide. Such resonances, observed below 3 kmc, were identified as TE₁₁ and TM₀₁ ghost-modes, by observing the transverse symmetries of the residual fields at the open guide ends with a small perturbation rod. To vary the slab thickness L , one or more ceramic discs ($\epsilon=8.79$) of $\frac{1}{8}$ -inch thickness were stacked up. The observed ghost-mode frequencies are marked on Fig. 6, which also contains the theoretical curves for the particular arrangement as a comparison.

The approximate Q factors indicated were determined from the half-power bandwidth of the resonances. The Q factors generally decrease for larger slab thickness because the resonant fields become more and more confined to the volume of the relatively lossy dielectric.

The good agreement between theoretical and experimental data in Fig. 6 may be taken as a confirmation of the fact that the dielectric constant is known to good accuracy. Conversely, one might well make use of the described experiment to determine unknown dielectric constants of slabs by measuring a ghost-mode resonant frequency. Error analysis applied to the lowest TE₁₁ ghost-mode in our experiment yields

$$\frac{\Delta\epsilon}{\epsilon} = -15.5 \left(\frac{\Delta f}{f} \right)_{\text{res}}$$

for a slab of $\frac{1}{8}$ -inch thickness (neglecting geometrical errors). Considering the precision attainable in frequency measurements, this appears encouraging. If the dielectric constant of the slab is large, a possible air gap δ between the dielectric and the waveguide wall may be

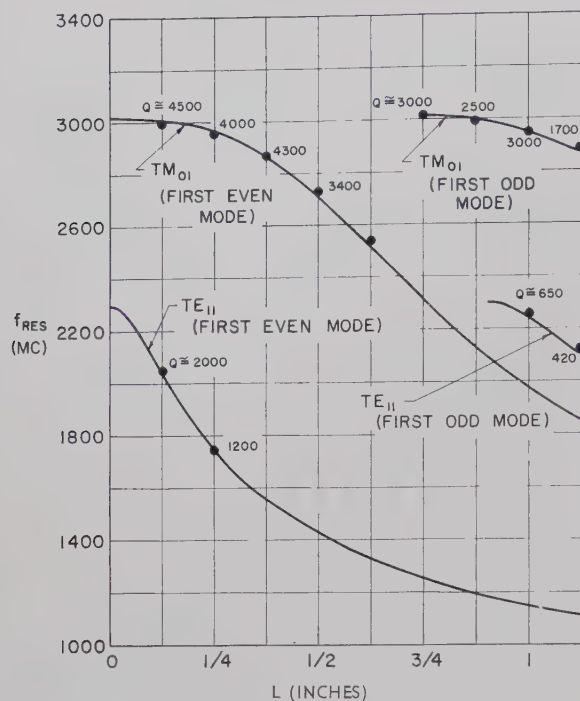


Fig. 6—Ghost-mode resonant frequencies of ceramic discs ($\epsilon=8.79$) of various thickness L . Curves are computed, dots are measured.

come troublesome. It may introduce an error of the following order of magnitude:

$$\left(\frac{\Delta f}{f}\right)_{\text{res}} = \frac{1}{2} \frac{\epsilon(\delta/a)}{1 + \epsilon(\delta/a)},$$

where a is a transverse waveguide dimension, *e.g.*, waveguide radius.

CONCLUSION

The phenomenon of resonant ghost-modes existing in the vicinity of a dielectric window has been discussed both theoretically and experimentally for the simplest geometry available. In practice, the ghost-mode resonances of some higher-order waveguide modes may coincide with the operating frequency of the dominant waveguide mode. Since these modes are orthogonal, no coupling would be expected under ideal conditions. However, imperfections, such as a slight tilt of the window, uneven thickness, or inhomogeneous dielectric may provide the modal coupling.

Waveguide discontinuities (irises, couplers, bends, etc.) located in the vicinity of the window may also provide this function. Since the ghost-mode resonances have high Q , only a small amount of coupling is required to produce appreciable resonant fields.

High-power microwave signals are very likely accompanied by harmonics. These harmonic frequencies may coincide with ghost-mode resonances, and coupling may be provided by imperfections or discontinuities.

Appreciable excitation of ghost-modes may considerably lower the breakdown power of a waveguide window.

Rather than minimizing the coupling to these modes by close tolerances, the window designer may find the information of Figs. 3 and 4 useful to avoid the existence of ghost-modes within the operating frequency range.

Ghost-mode resonances may exist in dielectric windows of more complicated geometry than that discussed above. Examples include slanted dielectric plates and ceramic cones. Analysis of such configurations becomes complicated. Transmission-line theory is no longer useful, but the mathematical tool of a normal-mode expansion may be employed and yields approximate results.² Such windows of increased complexity generally couple many waveguide modes together. A ghost-mode is, therefore, no longer a pure waveguide mode in its transverse field configuration. Moreover, if such a ghost-mode is strongly coupled to the propagating dominant waveguide mode, its external Q factor may become rather small, so that the resonance is less pronounced.

The existence of ghost-modes in dielectric obstacles of arbitrary shape may be made plausible by the following: the insertion of dielectric material ($\epsilon > 1$) into the guide effects an increase in "electrical cross section" of the guide, so that a wave may have propagating character (*i.e.*, oscillatory z -variation) within the length L of the obstacle, while it decays outside. The frequencies at which the impedance boundary conditions on both sides of the obstacle can be met are the ghost-mode resonances.

Analysis of ghost-modes for any given window geometry makes it possible to determine the dielectric constant of the material through a frequency measurement. Even without analysis, a ghost-mode resonance measurement may be useful as a uniformity test of dielectric samples.

It is of interest to note the behavior of two windows (of the kind shown in Fig. 1) placed in the same waveguide. If the distance between them is such that the ghost-mode fields overlap, there appear two resonant frequencies, one being slightly higher, the other slightly lower than the original ghost-mode resonance. The situation is analogous to coupled resonant tanks. It may be analyzed by use of the same methods as were employed analyzed using the same methods as were employed above. Such analysis and corresponding experiments have been performed and show good agreement. This experiment is particularly interesting as it represents one of the rare cases where the coupling between resonant circuits may be found easily and accurately through analysis.

Finally, it might be noted that the location of ghost-mode resonances represents a simple but unusually interesting laboratory experiment by which several aspects of waveguide theory can be demonstrated in the teaching of microwave techniques.

² M. P. Forrer, "On the Boundary Value Problem of Waveguide Windows," W. W. Hansen Labs. of Physics, Stanford University, Stanford, Calif., Microwave Lab. Rept. No. 575; March, 1959.

Temperature Compensation of Coaxial Cavities*

J. R. COGDELL†, A. P. DEAM‡ AND A. W. STRAITON‡

Summary—This paper describes a technique for temperature compensation of coaxial cavities by controlling the capacitance between the end of the center conductor and an end plate across the outer conductor. A formula is derived for this capacitance which is verified experimentally. Supplemental design data are also obtained experimentally.

INTRODUCTION

A DROP-TYPE atmospheric refractometer operating at 403 mc has recently been reported by A. P. Deam.^{1,2} The sensing element for this unit is a coaxial cavity whose resonant frequency controls a Pound stabilized oscillator.³ In this cavity application a cavity which is tunable in the normal sense, over a wide bandwidth, is not necessary. Instead, the cavity is effectively tuned by the atmospheric dielectric constant which is purposely vented into the cavity. Montgomery⁴ has described the construction and compensation of coaxial cavities for tuning over a relatively large bandwidth. In the case of the frequency standard cavity, as the desired cavity might be considered, simpler bimetallic techniques may be employed to effectively utilize the capacitance discontinuity for compensation.

In the design process, leading to cavity development, calculation of the absolute resonant frequency was desired with as great an accuracy as possible since no manual tuning would be allowed. Approximations⁵ to the discontinuity at the open end of a $\lambda/4$ cavity have been derived. However, none of these yields the accuracy desired, and an effort was made to represent the discontinuity more accurately. This discontinuity expression is included as part of the cavity design.

The cavity chosen to be compensated is designated by Ramo and Whinnery⁶ as a "foreshortened coaxial line." The cavity, as shown in Fig. 1, is very similar to an ordinary quarter wavelength coaxial cavity and differs only in that its outer conductor is extended past the

inner conductor for a short distance and closed with a conducting plane. When the gap between the center conductor and the endplate is small compared with a wavelength, it acts as a simple capacitance. The equivalent circuit which approximately represents the electrical properties of the cavity is that of a transmission line of length L_p terminated with a capacitance. This circuit is shown in Fig. 2. The resonant frequency of the cavity is a function of the length of the center conductor and the length of the end gap. Compensation requires that thermally-caused changes in the dimensions of the center conductor and gap produce opposing changes of equal magnitude in the cavity's frequency.

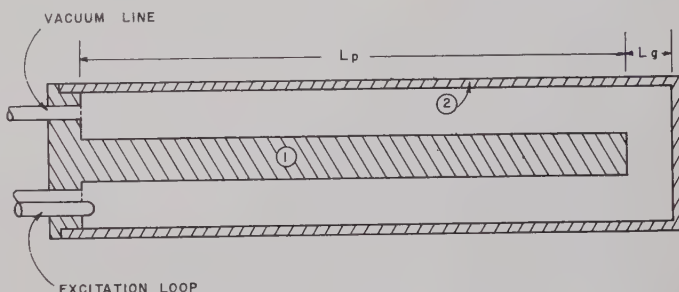


Fig. 1—Section of temperature-compensated cavity.

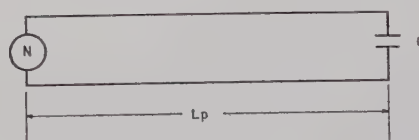


Fig. 2—Equivalent circuit of type II cavity.

DESIGN

When the cavity is resonant, in any plane, susceptances looking in opposite directions will be equal in magnitude and opposite in sign. At the plane of the end of the center conductor, the susceptance looking into the line will be that of a shorted transmission line of length L_p , and the susceptance looking into the gap will be that of a simple capacitance. Equating these susceptances gives

$$Y_0 \cot \frac{2\pi L_p f_r}{c} = 2\pi f_r C \quad (1)$$

where

C = capacitance of end space in farads,
 Y_0 = characteristic admittance of coaxial line in mhos,
 c = velocity of light.

* Manuscript received by the PGMTT, July 27, 1959; revised manuscript received, October 5, 1959.

† Lincoln Labs., Mass. Inst. Tech., Cambridge, Mass. Formerly at Elec. Engrg. Res. Lab., University of Texas, Austin, Tex.

‡ Elec. Engrg. Res. Lab., University of Texas, Austin, Tex.

¹ A. P. Deam, "An Expendable Atmospheric Radio Refractometer," Elec. Engrg. Res. Lab., Rept. No. 108; University of Texas, Austin, Tex.; May, 1959.

² A. P. Deam, "An Expendable Atmospheric Refractometer," presented at URSI Convention, Washington, D. C.; May, 1959.

³ R. V. Pound, "Frequency stabilization of microwave oscillators," PROC. IRE, vol. 35, pp. 1405-1415; December, 1947.

⁴ C. G. Montgomery, "Techniques of Microwave Measurements," M.I.T. Rad. Lab. Ser., McGraw-Hill Book Co., Inc., New York, N. Y., vol. 11; 1947.

⁵ N. Marcuvitz, "Waveguide Handbook," M.I.T. Rad. Lab. Ser., vol. 10; 1951.

⁶ S. Ramo and J. R. Whinnery, "Waves and Fields in Modern Radio," John Wiley and Sons, Inc., New York, N. Y., p. 415; 1953.

The end capacitance is kept small in these cavities and does not have a great effect on the frequency of the cavity. The length of the center conductor is, therefore, nearly one-fourth of a wavelength, and the following is a good approximation:

$$\text{ctn} \frac{2\pi L_p f_r}{c} = \frac{\pi}{2} - \frac{2L_p f_r}{c}. \quad (2)$$

Substitution of (2) into (1) and rearrangement produces

$$f_r = \frac{c}{4 \left[L_p + \frac{cC}{V_0} \right]}. \quad (3)$$

The capacitance of the end configuration as shown in Fig. 3 will now be considered. A potential difference between the plates is assumed, the fields in the enclosed space are determined, the surface charges are calculated, and the capacitance is evaluated by the familiar formula, $C = q/V_0$.

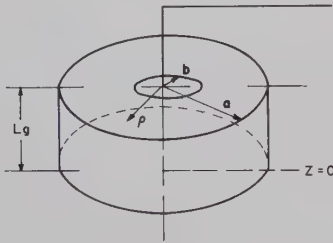


Fig. 3—End capacitance configuration.

A solution to Laplace's equation suitable for the boundary conditions is

$$V = \Sigma (A_n \cosh \lambda_n z + B_n \sinh \lambda_n z) J_0(\lambda_n \rho), \quad (4)$$

where A_n , B_n , and λ_n , the separation constant, may take on any value. The boundary conditions are

$$z = 0 \quad V = 0 \quad (5)$$

$$\rho = a \quad V = 0 \quad (6)$$

$$z = L_g \quad V = V_0 \quad 0 < \rho < b$$

$$= V_0 \frac{\ln a/\rho}{\ln a/b} \quad b < \rho < a. \quad (7)$$

A logarithmic potential distribution was chosen for (7) because this is the normal distribution in a coaxial line. Boundary conditions (5) and (6) can be satisfied if

$$A_n = 0, \quad J_0(a\lambda_n) = 0,$$

and boundary condition (7) can be satisfied if $B_n \sinh \lambda_n L_g$ are made the Fourier coefficients of an expansion of (7) in Bessel functions.

$$B_n \sinh \lambda_n L_g = \frac{2}{a^2 J_1^2(\lambda_n a)} \left[\int_0^b V_0 \rho J_0(\lambda_n \rho) d\rho + \int_b^a \frac{V_0 \ln a/\rho}{\ln a/b} \rho J_0(\lambda_n \rho) d\rho \right], \quad (8)$$

$$B_n = \frac{2V_0 J_0(\lambda_n b)}{a^2 \ln a/b \lambda_n^2 \sinh \lambda_n L_g J_1^2(\lambda_n a)}. \quad (8a)$$

The potential in the space is therefore

$$V = \sum_{n=1}^{\infty} \frac{2V_0 J_0(\lambda_n b) \sinh \lambda_n z J_0(\lambda_n \rho)}{a^2 \ln a/b \lambda_n^2 J_1^2(\lambda_n b) \sinh \lambda_n L_g}. \quad (9)$$

The known potential defines the charge density on the surfaces, and the total charge on either plate can be found readily. The capacitance can be found by dividing the total charge on either plate by the total voltage, V_0 . In an ordinary capacitor, the total charge on both surfaces will be equal. This is not necessarily true in this case, since a potential distribution was assumed at the plane of $z = L_g$. The total charges, in fact, are different and lead to different values for the capacitance. Considering the charges on the smaller surface, the capacitance is calculated to be

$$C = \sum_{n=1}^{\infty} \frac{4\pi \epsilon b J_0(\lambda_n b) J_1(\lambda_n b) \coth \lambda_n L_g}{a^2 \ln a/b \lambda_n^2 J_1^2(\lambda_n a)}, \quad (10)$$

and the capacitance following from the charge on the larger surface is

$$C = \sum_{n=1}^{\infty} \frac{4\pi \epsilon a J_0(\lambda_n b) J_1(\lambda_n b) \coth \lambda_n L_g}{a^2 \ln a/b \lambda_n^2 J_1^2(\lambda_n a)}. \quad (11)$$

The two values differ by a factor of a/b with (11) giving the larger value. It might be expected that the proper value for the capacitance lies somewhere between those given by (10) and (11). Let the proper value be expressed by

$$C = \sum_{n=1}^{\infty} \frac{4\pi \epsilon \delta J_0(\lambda_n b) J_1(\lambda_n b) \coth \lambda_n L_g}{a^2 \ln a/b \lambda_n^2 J_1^2(\lambda_n a)} \quad (12)$$

where δ is an effective radius. The correct value for δ can be found by referring to (3) which shows that the cavity will have the same resonant frequency as an open circuited line of length $L_p + cC/V$. A coaxial line which is terminated in a circular waveguide operating beyond cutoff will have an effective length, $L_p + d$. The apparent lengthening of the center conductor, given by the term d , expresses the effect of the discontinuity which is produced at the plane where the coaxial line is terminated in the circular waveguide.

As the gap length, L_g , is increased, the term cC/V_0 should approach the value of d produced by the discontinuity mentioned. This value of d may be determined from formulas or tables and used to evaluate δ .

As an example, consider an application to a specific cavity with inner and outer radii of 0.250 inch and 0.84 inch, respectively. Previous experience of this laboratory shows that d is approximately 0.290 inch for cavities of this type. This value fixes the value of δ at 0.651 inch and gives a value of capacitance which is between those of (10) and (11). With these values, the resonant frequency of the cavity under consideration is

the outer conductor be made of cold-rolled steel ($\alpha_2 \approx 12 \times 10^{-6}/C^\circ$), and L_p be slightly less than a quarter wavelength, 7.05 inches, for instance. The solution of (17), using these values is shown in Fig. 4, and the correct value for L_g can be seen to be 0.63 inch. This dimension, when substituted into (13a), shows that $L_p = 7.025$ inches will give the correct frequency of 403 mc.

$$f_r = \frac{c}{4 \left[L_p + \frac{4\pi\epsilon(0.651)c}{Y_0(0.80)^2 l_n} \sum_{n=1}^{\infty} \frac{J_0(0.250\lambda_n)J_1(0.250\lambda_n)}{\lambda_n^2 J_1^2(0.840\lambda_n)} \right]}, \quad (13)$$

which reduces to

$$f_r = \frac{c}{4L_p + \frac{2(0.651)}{(0.84)^2} \sum_{n=1}^{\infty} \frac{J_0(0.250\lambda_n)J_1(0.250\lambda_n)}{\lambda_n^2 J_1^2(0.840\lambda_n)}}. \quad (13a)$$

Temperature compensation will now be considered. The rate of change of resonant frequency, f_r , with temperature θ , is given by

$$\frac{df_r}{d\theta} = \frac{\partial f_r}{\partial L_g} \frac{dL_g}{d\theta} + \frac{\partial f_r}{\partial L_p} \frac{dL_p}{d\theta} = 0. \quad (14)$$

The solution to (14) is of interest in the region of the resonant frequency, 403 mc, and the value of L_p (and therefore of $\partial f_r / \partial L_p$) does not vary widely even when L_g is varied over a wide range. This justifies the fact that a constant, evaluated for (13a), can be used for $\partial f_r / \partial L_p$ in (14).

The derivatives of the two dimensions with respect to temperature can be evaluated easily enough. If the expansion coefficients of the inner and outer conductors are denoted by α_1 and α_2 , respectively, then

$$\frac{dL_p}{d\theta} = \alpha_1 L_p \quad (15)$$

and

$$\frac{dL_g}{d\theta} = \alpha_2(L_p + L_g) - \alpha_1 L_p. \quad (16)$$

Substitution of these into (14) and rearrangement produces

$$\frac{\partial f_r}{\partial L_g} = \frac{-\alpha_1 L_p}{L_p(\alpha_2 - \alpha_1) + L_g(\alpha_2)} \frac{\partial f_r}{\partial L_p}. \quad (17)$$

Eq. (17) can be solved graphically for L_g by evaluating $\partial f_r / \partial L_g$ as a function of L_g from (13a), and plotting both sides of (17) against L_g . As a further special case, let the inner conductor be made of invar ($\alpha_1 \approx 1 \times 10^{-6}/C^\circ$),

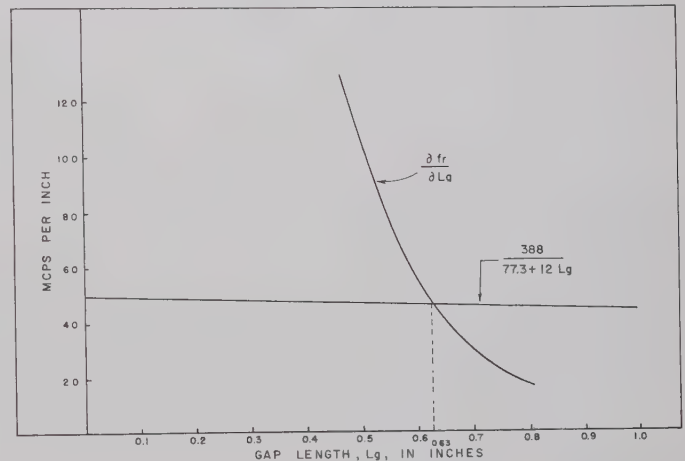


Fig. 4—Graphical solution of (9).

EXPERIMENTAL WORK

Eq. (13a) was verified by making a cavity with a movable end-plate as shown in Fig. 5, and varying L_g while noting its effects on the resonant frequency. A Pound stabilized oscillator was coupled to the cavity by a loop which was adjusted for critical coupling, and the frequency of the oscillator was monitored with a Gertsch FM-3 frequency meter as the gap distance was varied. Fig. 6 shows the result of such a test. Although the theoretical curve gives slightly lower values (of the order of 0.2 per cent) than the experimental curve, the shapes of the curves are similar; thus, the dimensions calculated from (13a) should produce compensation since only the slope of the curve is used in that calculation.

Two aspects of the cavity which could not be approached analytically were investigated with the cavity which was constructed to verify (13). These were 1) the effect of venting the endplate, and 2) the effect of boring holes in the center conductor. A cavity used to sense the atmospheric refractive index might have both these features. The results of such tests are shown in Figs. 7 and 8. From these it can be seen that the shape of the fre-

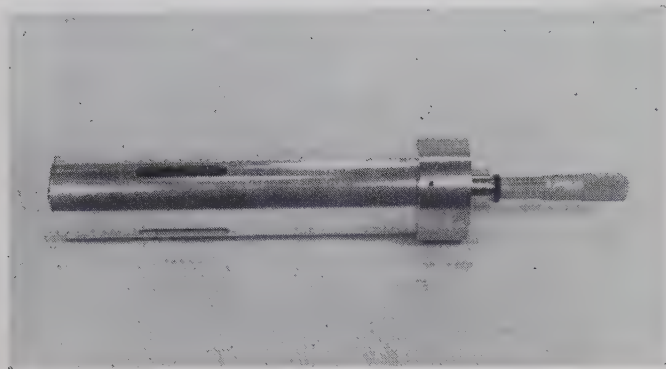


Fig. 5—Cavity with variable endplate in place.

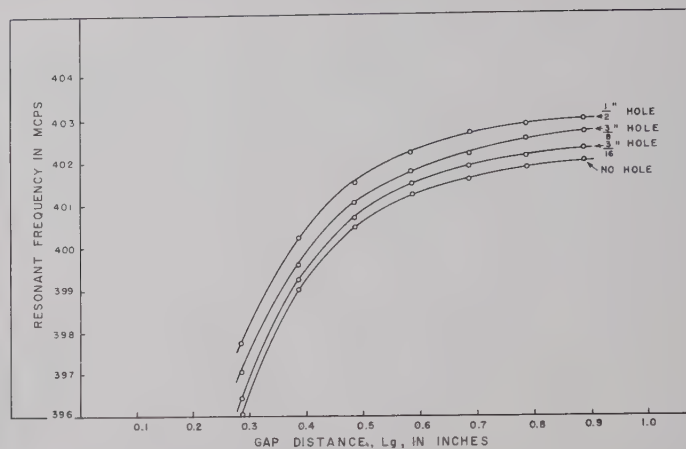


Fig. 8—Resonant frequency vs gap distance showing effect of boring holes in center conductor.

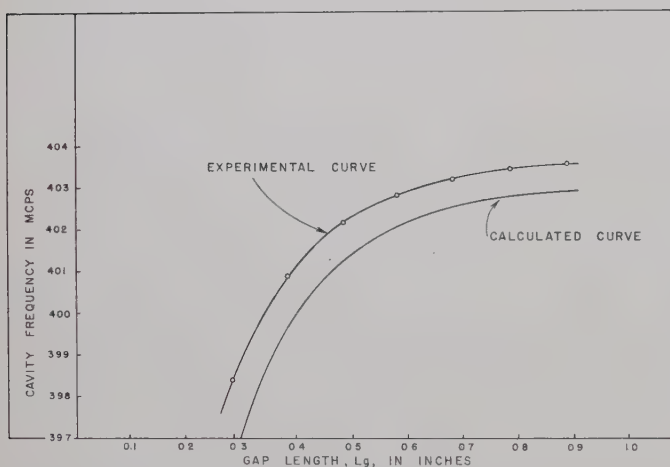


Fig. 6—Resonant frequency vs gap distance.

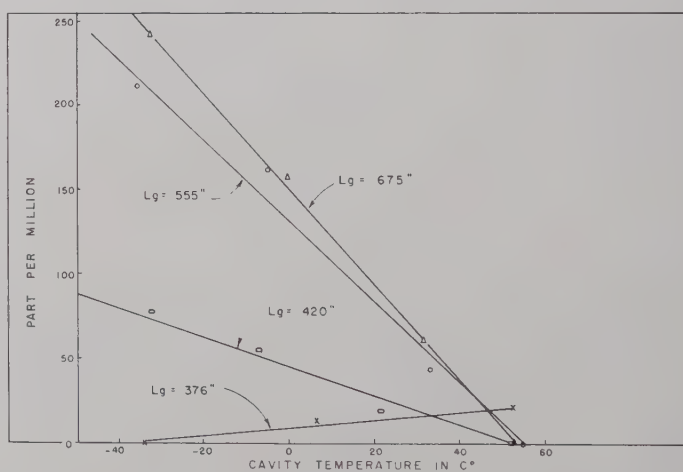


Fig. 9—Cavity compensation with different size gap lengths.

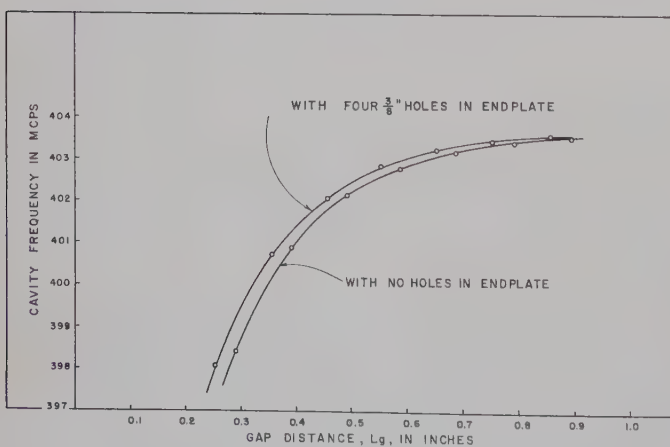


Fig. 7—Resonant frequency vs gap distance showing effect of venting endplate.

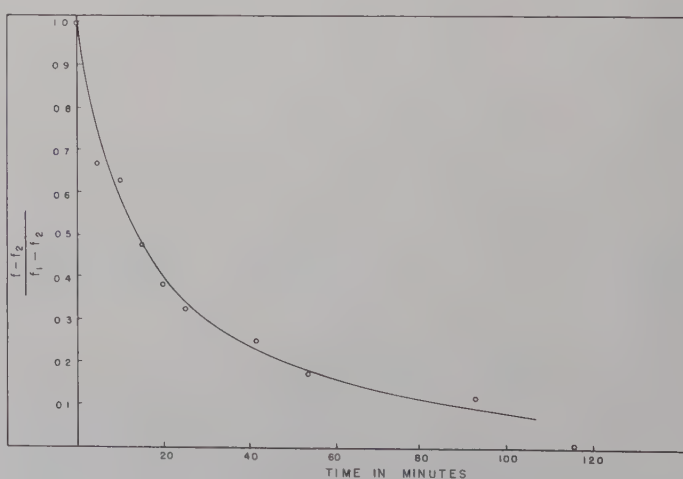


Fig. 10—Long-time transient response.

quency vs gap-distance curve is not affected greatly by boring holes in the endplate and center conductor; thus, the compensation would not be affected markedly by these modifications.

RESULTS

Temperature Compensation

A cavity was constructed with the following dimensions: $b = 0.250$, $a = 0.840$, $L_g = 0.675$, and $L_p = 7.025$ (all dimensions in inches). The cavity had a resonant frequency of 403.5 mc, 0.2 per cent higher than (13a) would indicate, and an unloaded Q of 2280.

The temperature compensation of the cavity was measured by placing it in a constant-temperature bath and measuring its resonant frequency as a function of temperature. The cavity temperature was varied from -32°C to 53°C , and the temperature coefficient of the cavity was found to be 2.62 parts/million/ $^\circ\text{C}$ undercompensation; *i.e.*, the cavity frequency was lowered as the temperature was raised. This was a rather surprising result since an uncompensated invar cavity would be expected to exhibit a temperature coefficient of $1 \times 10^{-6}/^\circ\text{C}$ undercompensation. The high coefficient indicated one of two things: either 1) the invar center conductor had a higher expansion coefficient than advertised, or 2) some unexpected effect (such as eccentricity of the center conductor, for example) was present. Whatever the cause of the undercompensation, the gap length had to be shortened to compensate

for it. This was done in steps until a final gap length of 0.376 inch produced a temperature coefficient of $0.25 \times 10^{-6}/^\circ\text{C}$ overcompensation, which was considered satisfactory. Fig. 9 shows the effects of the various gap lengths on the compensation of the cavity.

Transient Response

During the temperature tests some data on the transient response of the cavity were obtained. The cavity experienced a rise in temperature when it was inserted into the temperature bath. The response of the cavity showed two time constants, one associated with the transfer of heat to the outer conductor and the other associated with the transfer of heat to the center conductor. These time constants were measured to be 1.1 minute and 29 minutes, respectively. These results agree fairly well with the response determined analytically. As shown in Fig. 10, the cavity reached thermal equilibrium in about 2 hours after it experienced a change in temperature.

It should be mentioned that these figures for the transient response are not those which would be experienced in actual use. When employed in atmospheric soundings, the rate of transfer of heat from the air to the cavity would be very slow so that it would be expected that the cavity would have essentially the same temperature throughout the center post and the body at a given time. Hence, the temperature compensation techniques described in this paper would be effective.

A Graphical Method for Measuring Dielectric Constants at Microwave Frequencies*

CHARLES B. SHARPE†

Summary—This paper describes a graphical method for measuring the real and imaginary parts of the dielectric constant $\epsilon/\epsilon_0 = \epsilon' - j\epsilon''$ of materials at microwave frequencies. The method is based on the network approach to dielectric measurements proposed by Oliner and Altschuler in which the dielectric sample fills a section of transmission line or waveguide. In contrast to their method, the network representing the dielectric sample is analyzed in terms of the bilinear transformation

$$\Gamma' = \frac{a\Gamma + b}{c\Gamma + d}; \quad ad - bc = 4.$$

The analysis proceeds from the geometric properties of the image circle in the Γ plane obtained by terminating the output line in a calibrated sliding short.

The technique described retains the desirable features of the network approach but avoids the necessity of measuring both scattering coefficients. As a result the procedure is more direct and, in the case of the TEM configuration, leads to an entirely graphical solution in which the complex dielectric constant can be read from a Smith chart overlay.

INTRODUCTION

THERE are many techniques for making dielectric measurements at microwave frequencies.¹ One of the more interesting methods proposed in recent years is that due to Oliner and Altschuler,² in which the

* Manuscript received by the PGM-TT, August 7, 1959; revised manuscript received October 9, 1959. This work was sponsored by the U. S. Army Signal Res. and Dev. Lab., Fort Monmouth, N. J.
† The University of Michigan Res. Inst., Ann Arbor, Mich.

¹ A. von Hippel, ed., "Dielectric Materials and Applications," J. Wiley and Sons, Inc., New York, N. Y., ch. 2; 1954.

² A. Oliner and H. Altschuler, "Methods of measuring dielectric constants based upon a microwave network viewpoint," *J. Appl. Phys.*, vol. 26, pp. 214-219; February, 1955.

dielectric sample filling a section of waveguide is represented by a two-port microwave network as illustrated in Fig. 1. In their method the scattering matrix of the network is determined at reference planes T_1 and T_2 by Deschamps³ procedure or, when the network can be regarded as lossless, by alternative so-called precision techniques. The complex relative dielectric constant $\epsilon/\epsilon_0 = \epsilon' - j\epsilon''$ is then obtained from either

$$\epsilon/\epsilon_0 = (Y/Y_0)^2 \text{ (TEM modes)} \quad (1a)$$

or

$$\epsilon/\epsilon_0 = \frac{(Y/Y_0)^2 + (\lambda_{0g}/\lambda_c)^2}{1 + (\lambda_{0g}/\lambda_c)^2} \text{ (H modes)}, \quad (1b)$$

where the wave admittance Y in the dielectric relative to the wave admittance of the empty guide Y_0 is given in terms of the scattering coefficients by

$$(Y/Y_0)^2 = \frac{(1 - S_{11})^2 - S_{12}^2}{(1 + S_{11})^2 - S_{12}^2}, \quad (2)$$

and λ_{0g} and λ_c refer to the guide wavelength and the cutoff wavelength, respectively, in the air-filled guide.

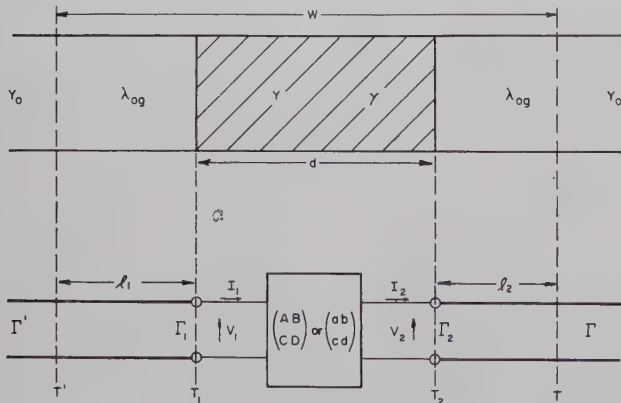


Fig. 1.—Dielectric sample in a waveguide and its equivalent circuit.

Oliner and Altschuler point out that the introduction of the network point of view to dielectric measurements results in two major advantages over earlier methods. First, it becomes possible to employ precision techniques in the determination of the network parameters. For example, in Deschamps' geometrical method, the image circle, representing the locus of points in the input reflection coefficient plane as a sliding short is moved in the output waveguide, is determined by graphical averaging. Therefore, the center of the image circle and its radius, as well as quantities derived from them, can be determined to a higher degree of precision than that of a single data point. The second feature of the network method which can be exploited to advantage in dielectric measurements concerns the concept of invariance.

³ G. A. Deschamps, "Determination of reflection coefficients and insertion loss of a waveguide junction," *J. Appl. Phys.*, vol. 24, pp. 1046-1050; August, 1953.

Briefly stated, invariance in the present case refers to the method of microwave network representation or measurement which calls for a minimum number of physical length measurements. Thus, for the configuration illustrated in Fig. 1 it is possible to take advantage of the known symmetry of the network to reduce to one the number of required distance measurements. The single measurement required may be either the length of the sample, d (location invariant) or the location of the one of the sample faces, T_1 or T_2 (length invariant). The desirability of employing a distance invariant method lies in the fact that errors arising from physical distance measurements are generally greater than those resulting from the electrical distance measurements, assuming that corrections have been made for errors in the location of the voltage minimum caused by spurious discontinuities if they exist.

The purpose of the present paper is to describe a technique for measuring dielectric constants which retains the desirable features of the network approach but which can be accomplished more directly and with a minimum of computation. In the case of the TEM configuration, the dielectric constant can be obtained by a purely graphical procedure in which the desired complex constant is read directly from a Smith Chart.

THEORY

The dielectric-filled section of line or waveguide can be represented at reference planes T_1 and T_2 by the $(ABCD)$ circuit parameters which relate the input and output voltages and currents, as defined in Fig. 1, by the matrix equation

$$\begin{bmatrix} V_1 \\ I_1 \end{bmatrix} = \begin{bmatrix} A & B \\ C & D \end{bmatrix} \begin{bmatrix} V_2 \\ I_2 \end{bmatrix}, \quad (3)$$

where $AD - BC = 1$. If we take

$$Z_1 = V_1/I_1, \quad Z_2 = V_2/I_2, \quad (4)$$

then a bilinear relationship is obtained between the impedances Z_1 and Z_2 :

$$Z_1 = \frac{AZ_2 + B}{CZ_2 + D}. \quad (5)$$

This transformation has often been used in analyzing the properties of linear two-port networks. However, it will be more convenient in the present case to consider the network representing the dielectric sample in terms of a bilinear transformation in the reflection coefficient or Γ plane. Thus, if the input and output reflection coefficients are defined, respectively, by

$$\Gamma_1 = \frac{Y_0 - Y_1}{Y_0 + Y_1}, \quad \Gamma_2 = \frac{Y_0 - Y_2}{Y_0 + Y_2}, \quad (6)$$

it can be shown that

$$\Gamma_1 = \frac{a\Gamma_2 + b}{c\Gamma_2 + d}, \quad (7)$$

where

$$\begin{aligned} a &= A - BY_0 - C/Y_0 + D, \\ b &= A + BY_0 - C/Y_0 - D, \\ c &= A - BY_0 + C/Y_0 - D, \\ d &= A + BY_0 + C/Y_0 + D. \end{aligned} \quad (8)$$

Reciprocity is assured if $ad - bc = 4$. If the network is symmetrical, as in the present case, then $b = -c$. Eq. (7) is sometimes called the direct transformation to distinguish it from the inverse transformation

$$\Gamma_2 = \frac{-d\Gamma_1 + b}{c\Gamma_1 - a}. \quad (9)$$

The matrix composed of the $(abcd)$ parameters might be termed the reflection matrix of the network. Although the transformation (7) has been used by Mathis⁴ and also by Bolinder,⁵ employing a different normalization, it has not enjoyed widespread use as a tool in network analysis. As would be expected, the reflection matrix bears a close connection to the scattering matrix. It can be shown that, in general,

$$S = \begin{bmatrix} S_{11} & S_{12} \\ S_{21} & S_{22} \end{bmatrix} = \begin{bmatrix} b/d & 2/d \\ (ad - bc)/2d & -c/d \end{bmatrix}. \quad (10)$$

An obvious application of (10) is suggested in the Appendix. The components of the reflection matrix transform in a manner very similar to the manner in which the scattering coefficients transform as a result of a shift in reference planes. Referring to Fig. 1, the reflection matrix at reference planes T' and T is given by

$$\begin{bmatrix} a' & b' \\ c' & d' \end{bmatrix} = \begin{bmatrix} e^{-j\phi_1} & 0 \\ 0 & e^{j\phi_1} \end{bmatrix} \begin{bmatrix} a & b \\ c & d \end{bmatrix} \begin{bmatrix} e^{-j\phi_2} & 0 \\ 0 & e^{j\phi_2} \end{bmatrix}, \quad (11)$$

where $\phi_1 = 2\pi l_1/\lambda_{0g}$, $\phi_2 = 2\pi l_2/\lambda_{0g}$, and the primed coefficients are defined by

$$\Gamma' = \frac{a'\Gamma + b'}{c'\Gamma + d'}. \quad (12)$$

Returning to the problem at hand the $(ABCD)$ matrix of the dielectric-filled section at reference planes T_1 and T_2 is

$$\begin{bmatrix} A & B \\ C & D \end{bmatrix} = \begin{bmatrix} \cosh \gamma d & \frac{\sinh \gamma d}{Y} \\ Y \sinh \gamma d & \cosh \gamma d \end{bmatrix} \quad (13)$$

from which (8) yields,

$$\begin{aligned} a &= 2 \cosh \gamma d - (Y/Y_0 + Y_0/Y) \sinh \gamma d, \\ b &= -c = -(Y/Y_0 - Y_0/Y) \sinh \gamma d, \\ d &= 2 \cosh \gamma d + (Y/Y_0 + Y_0/Y) \sinh \gamma d, \end{aligned} \quad (14)$$

where $\gamma = \alpha + j\beta$ is the propagation constant in the dielectric. A purely algebraic relation between Y/Y_0 and the $(abcd)$ parameters can be obtained by forming

$$\Gamma_E \equiv \frac{a - d}{2c} = \frac{1 + (Y/Y_0)^2}{1 - (Y/Y_0)^2}. \quad (15)$$

This expression is entirely equivalent to (2) involving the scattering coefficients. The merit of the reflection parameter representation lies in the simplicity of (15), as well as in the facility it provides in the geometric interpretation of the problem. Thus, it will be shown that Γ_E can be determined through a series of simple geometric constructions based on the image circle diagram. The desired dielectric constant then follows from (1a) or (1b).

In the interest of generality we will proceed from the initial assumption that reference planes T and T' are located arbitrarily with respect to the sample. Eq. (12) is first rewritten in the form⁴

$$\Gamma' = \frac{a\bar{c}|\Gamma|^2 - b\bar{d}}{c\bar{c}|\Gamma|^2 - d\bar{d}} - \frac{[\bar{c}\bar{\Gamma} + \bar{d}]}{[c\bar{c}\Gamma + d]} \left[\frac{ad - bc}{c\bar{c}|\Gamma|^2 - d\bar{d}} \right] \Gamma, \quad (16)$$

where the bar over a quantity designates the complex conjugate and the primes have been omitted. One can determine the center of the image circle and its radius from (16) by inspection. Thus, when $|\Gamma| = 1$, corresponding to a reactive termination in the output waveguide, the first term in (16) will be a complex constant and the magnitude of the second term will be a constant for all values of reactance. Referring to Fig. 2, the center of the image circle in the Γ' plane is

$$\Gamma_{c'} = \frac{a\bar{c} - b\bar{d}}{c\bar{c} - d\bar{d}} \quad (17)$$

and the radius is

$$R = \frac{4}{|c\bar{c} - d\bar{d}|}. \quad (18)$$

There are three points in the reflection plane which are of special interest. The iconocenter $\Gamma_{o'} = S_{11} = b/d$ is the map or image of $\Gamma = 0$ in the Γ' plane. There are a number of geometric constructions which can be used to obtain the iconocenter once the image circle, and its center are known.^{3,6-8} All of these methods make use of

⁴ J. E. Storer, L. S. Sheingold, and S. Stein, "A simple graphical analysis of a two-port waveguide junction," *Proc. IRE*, vol. 41, pp. 1004-1013; August, 1953.

⁷ F. L. Wentworth and D. R. Barthel, "A simplified calibration of two-port transmission line devices," *IRE TRANS. ON MICROWAVE THEORY AND TECHNIQUES*, vol. MTT-4, pp. 173-175; July, 1956.

⁸ G. A. Deschamps, "A variant in the measurement of two-port junctions," *IRE TRANS. ON MICROWAVE THEORY AND TECHNIQUES*, vol. MTT-5, pp. 159-161; April, 1957.

⁴ H. F. Mathis, "Some properties of image circles," *IRE TRANS. ON MICROWAVE THEORY AND TECHNIQUES*, vol. MTT-4, pp. 48-50; January, 1956.

⁵ E. F. Bolinder, "Impedance and Power Transformations by the Isometric Circle Method and Non-Euclidean Hyperbolic Geometry, M.I.T. Res. Lab. of Electronics, Cambridge, Mass., Tech. Rept. 312; June 14, 1957.

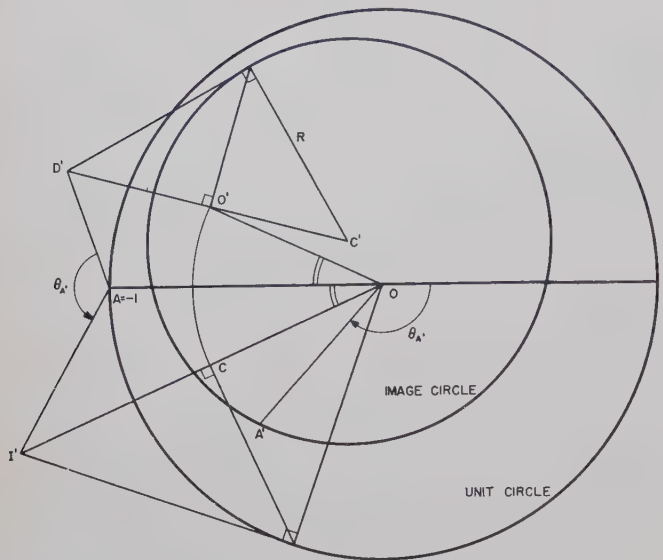


Fig. 2—Construction of $\Gamma_{D'}$ and $\Gamma_{I'}$, and determination of reference angle $\theta_{A'}$.

a calibrated short behind the network, and all but the last method referenced depend on a knowledge of the wavelength in the output waveguide. The other two points of interest in the reflection plane are $\Gamma_{D'} = a/c$ and $\Gamma_{I'} = -d/c$. These points have a special significance in the theory of the bilinear transformation and can be shown to mark the center of the isometric circles for the direct and inverse transformations, respectively.⁹

GRAPHICAL ANALYSIS

Once $\Gamma_{O'}$ and $\Gamma_{C'}$ are determined, $\Gamma_{D'}$ can be readily constructed by inverting $\Gamma_{O'}$ with respect to the image circle as illustrated in Fig. 2. The proof of this statement is contained in

$$(\Gamma_{D'} - \Gamma_{C'}) (\bar{\Gamma}_{O'} - \bar{\Gamma}_{C'}) = R^2, \quad (19)$$

which follows from (17), (18), and the condition, $ad - bc = 4$. The construction of the point $\Gamma_{I'}$ follows in an analogous way, although in contrast to the previous case, the angle of $\Gamma_{I'}$ will depend on the choice of the output reference plane T . It is convenient at this point to locate T symmetrically with respect to T' so that $l_1 = l_2$. Assuming for the moment that T has been so located, the symmetry of the network representing the dielectric then guarantees that $b = -c$, and $\Gamma_{I'}$ can be determined graphically by constructing the reciprocal of $\Gamma_{O'}$. This construction is also illustrated in Fig. 2. It is interesting to note that $\Gamma_{I'}$ is also the inverse with respect to the unit circle of $\Gamma_C = -\bar{c}/\bar{d}$, which is the map in the output Γ plane of the center of the image circle, $\Gamma_{C'}$, via the inverse transformation (9).

⁹ E. F. Bolinder, "Impedance and polarization-ratio transformations by a graphical method using the isometric circles," IRE TRANS. ON MICROWAVE THEORY AND TECHNIQUES, vol. MTT-4, pp. 176-180; July, 1956.

The location of T is accomplished by noting that when $b = -c$, the point $A = -1$ maps into A' at

$$\Gamma_{A'} = \frac{1 + \Gamma_{D'}}{1 + \Gamma_{I'}}. \quad (20)$$

The reference point A' on the image circle is determined by the angle $\theta_{A'} = \arg \Gamma_{A'}$, which can be constructed from $\Gamma_{D'}$ and $\Gamma_{I'}$, as shown in Fig. 2. Thus, in order to guarantee symmetry one locates T at that position of the short in the output waveguide which establishes a voltage minimum at a distance $l = (\pi - \theta_{A'})\lambda_{0g}/4\pi$ from T' toward the generator in the input waveguide. It should be noted that this procedure establishes T only to within a multiple of half a wavelength. However, an approximate knowledge of the location of the sample suffices to remove any ambiguity.

At this point it is desirable to distinguish between the location invariant and the length invariant procedures. In the location invariant procedure, T' is located at an arbitrary point in the input waveguide, and T is determined from symmetry considerations as described above. The distance to the sample faces is calculated from $l_1 = l_2 = (w - d)/2$, where w and d are defined in Fig. 1 and are assumed to be known. It then remains to transform $\Gamma_{D'}$ and $\Gamma_{I'}$ to reference planes T_1 and T_2 at the sample faces. If $\Gamma_{D'}$ and $\Gamma_{I'}$ denote the isometric centers relative to planes T' and T , and Γ_D and Γ_I the corresponding quantities relative to planes T_1 and T_2 , then it follows from (11) that

$$\Gamma_D = e^{2j\phi} \Gamma_{D'}, \quad \Gamma_I = e^{-2j\phi} \Gamma_{I'}, \quad (21)$$

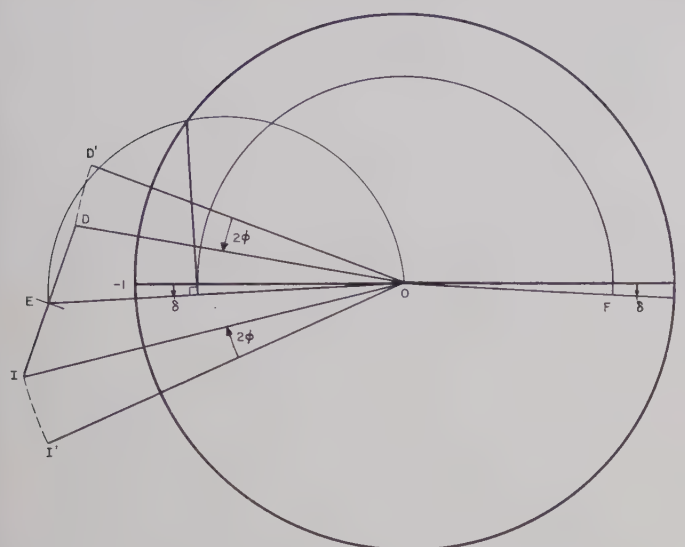
where $\phi = (w - d)\pi/\lambda_g$. The transformation of reference planes and the construction of Γ_E , which is the average of Γ and Γ_I , is apparent from Fig. 3. In the case of a TEM structure, the desired dielectric constant can be read directly from a Smith Chart overlay, in view of (1a) and (15), by constructing the point

$$\Gamma_F \equiv -1/\Gamma_E = \frac{\epsilon/\epsilon_0 - 1}{\epsilon/\epsilon_0 + 1}. \quad (22)$$

This construction is also shown in Fig. 3.

In the length invariant procedure one makes the initial assumption that the front face of the sample can be located accurately by physical means, thus making $T' = T_1$. This amounts to a trivial distance determination, which, in rectangular waveguides, can be readily accomplished by mounting the sample in a shorting switch. Since the analysis proceeds from the assumption of symmetry, no distance measurement is required in the length invariant case and the actual location of reference plane T is of no interest. The points Γ_E and Γ_F are derived directly from $\Gamma_{D'}$ and $\Gamma_{I'}$ as determined in Fig. 2 without shifting reference planes.

When the loss tangent of the dielectric is relatively small, the graphical method will give rather poor per-

Fig. 3—Shift of reference planes and construction of Γ_F .

centage accuracy in the determination of ϵ'' . In this case it is advisable to determine ϵ'' independently. This can be done most simply by using the already determined image circle to calculate the intrinsic insertion loss of the dielectric.¹⁰ The necessary formulas are listed below for the convenience of the reader. If $\rho = |\Gamma_c|$ is the distance of the center of the image circle from the origin of the reflection plane, it can be shown that

$$2\alpha d = \ln \left[\frac{\sqrt{(1+R)^2 - \rho^2} + \sqrt{(1-R)^2 - \rho^2}}{\sqrt{(1+R)^2 - \rho^2} - \sqrt{(1-R)^2 - \rho^2}} \right]. \quad (23)$$

Knowing ϵ' , the desired ϵ'' is then obtained from either

$$\epsilon'' = 2 \left(\frac{\alpha\lambda}{2\pi} \right)^2 \sqrt{1 + \left(\frac{2\pi}{\alpha\lambda} \right)^2 \epsilon'} \quad (\text{TEM modes}), \quad (24)$$

where λ is the free-space wavelength or

$$\epsilon'' \cong \frac{\alpha\lambda_{0g}}{\pi} \frac{\sqrt{[1 + (\lambda_{0g}/\lambda_c)^2]\epsilon' - (\lambda_{0g}/\lambda_c)^2}}{1 + (\lambda_{0g}/\lambda_c)^2} \quad (\text{H modes}), \quad (25)$$

¹⁰ K. Tomiyasu, "Intrinsic insertion loss of a mismatched network," IRE TRANS. ON MICROWAVE THEORY AND TECHNIQUES, vol. MTT-3, pp. 40-44; January, 1955.

if

$$\epsilon'' \ll \epsilon' - \frac{1}{1 + (\lambda_c/\lambda_{0g})^2}. \quad (26)$$

APPENDIX

It is well known that repeated bilinear transformations can be expressed in terms of a matrix product. Thus, if n linear networks are connected in cascade as shown in Fig. 4, the reflection matrix of the combination is given by

$$\begin{bmatrix} 2^{n-1}a & 2^{n-1}b \\ 2^{n-1}c & 2^{n-1}d \end{bmatrix} = \begin{bmatrix} a_1 & b_1 \\ c_1 & d_1 \end{bmatrix} \begin{bmatrix} a_2 & b_2 \\ c_2 & d_2 \end{bmatrix} \cdots \begin{bmatrix} a_n & b_n \\ c_n & d_n \end{bmatrix}. \quad (27)$$

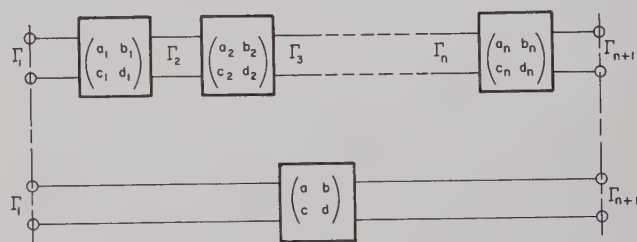


Fig. 4—Cascade connection of linear, bilateral two-port networks.

The factor of 2^{n-1} guarantees that $ad - bc = 4$ if $a_i d_i - b_i c_i = 4$, $i = 1, 2, 3, \dots, n$. The problem of determining the scattering matrix of a cascade connection of networks is, therefore, reduced to a systematic and relatively direct procedure through the use of (27) and (10). In this application the reflection matrix bears a close resemblance to the transmission or T matrix,¹¹ as might have been anticipated from

$$T = \begin{bmatrix} a/2 & -c/2 \\ -b/2 & d/2 \end{bmatrix}. \quad (28)$$

¹¹ C. G. Montgomery, R. H. Dicke, and E. M. Purcell, "Principles of Microwave Circuits," M.I.T. Rad. Lab. Ser., McGraw-Hill Book Co., Inc., New York, N. Y., vol. 8, p. 150; 1948.

Wide-Band Strip-Line Magic-T*

E. M. T. JONES†

Summary—This paper presents theoretical performance calculations of a novel form of wide-band strip-line Magic-T that uses two dual strip-line band-pass filters. When all four ports are terminated in the same impedance, the VSWR at each port is less than 1.47 over a 2:1 frequency band, while the isolation between opposite ports is greater than 20 db over this frequency band.

INTRODUCTION

THE fundamental characteristics of distributed-circuit hybrids, which function as Magic-T's, were described by Tyrell¹ in 1947. Since that time, a number of workers have described the performance of practical wide-band realizations constructed in coaxial line²⁻⁵ and strip line.⁵ The best reported performance of these Magic-T's was obtained by Alford and Watts,⁵ who quote for their coaxial-line model, operating from 100 to 200 mc, isolations of greater than 45 db and VSWR's of less than 1.4 at any port.

This paper contains a theoretical analysis of a new type of wide-band strip-line Magic-T. A schematic diagram of this device is shown in Fig. 1. It is seen that ports 4 and 3 and ports 4 and 2 are connected by means of transmission lines of characteristic impedance Z and electrical length θ . Port 1 is connected to port 2 by means of a band-pass filter⁶ having image impedance Z_o ⁷ and image phase shift β , while port 1 is connected to port 3 by a band-pass filter which is the dual of that connecting ports 1 and 2. It has image impedance Z_s and an image phase shift $\beta+180$ degrees. The definitions⁶ of these quantities are

$$Z_s = \frac{2Z_{oe}Z_{oo} \sin \theta}{[(Z_{oe}-Z_{oo})^2 - (Z_{oe}+Z_{oo})^2 \cos^2 \theta]^{1/2}}, \text{ or, the}$$

image impedance of the filter with the pair of shorted strips.

* Manuscript received by the PGMTT, September 2, 1959. The work described in this paper was sponsored by the USASRD under Contract DA 36-039 SC-74862.

† Stanford Research Institute, Menlo Park, Calif.

¹ W. A. Tyrell, "Hybrid circuits for microwaves," *PROC. IRE*, vol. 35, pp. 1294-1306; November, 1947.

² T. Morita and L. S. Sheingold, "A coaxial Magic-T," *IRE TRANS. ON MICROWAVE THEORY AND TECHNIQUES*, vol. 1, pp. 17-23; November, 1953.

³ V. I. Albanese and W. P. Peyser, "An analysis of a broad-band coaxial hybrid ring," *IRE TRANS. ON MICROWAVE THEORY AND TECHNIQUES*, vol. 6, pp. 369-373; October, 1958.

⁴ W. V. Tyminski and A. E. Hylas, "A wide-band hybrid ring for UHF," *PROC. IRE*, vol. 41, pp. 81-87; January, 1953.

⁵ A. Alford and C. B. Watts, "A wide-band coaxial hybrid," 1956 IRE NATIONAL CONVENTION RECORD, Pt. 1, pp. 171-179.

⁶ E. M. T. Jones and J. T. Bolljahn, "Coupled-strip-transmission-line filters and directional coupler," *IRE TRANS. ON MICROWAVE THEORY AND TECHNIQUES*, vol. 4, pp. 75-81; April, 1956.

⁷ The subscript s applies to the filter with the pair of short-circuited strips, while the subscript o applies to the filter with the pair of open-circuited strips.

Z_{oe} = Characteristic impedance of one coupled strip, measured with respect to ground, with equal currents flowing in the same direction.

Z_{oo} = Characteristic impedance of one coupled strip, measured with respect to ground, with equal currents flowing in opposite directions.

$Z_o = Z_{oe}Z_{oo}/Z_s$, or, the image impedance of the filter with the pair of open-circuited strips.

θ = Electrical length of each band-pass filter and each line of characteristic impedance Z .

$$\beta = \cos^{-1} \left[\frac{(Z_{oe} + Z_{oo})}{(Z_{oe} - Z_{oo})} \cos \theta \right] \text{ image phase shift of}$$

the filter with the pair of open-circuited strips.

$\beta+180^\circ$ = Image phase shift of the filter with the pair of short-circuited strips.

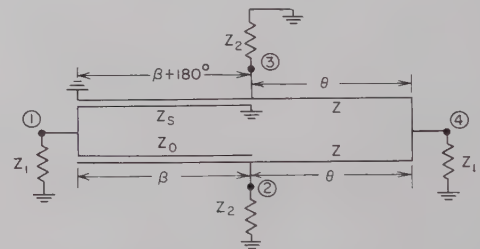


Fig. 1—Schematic diagram of a wide-band strip-line magic-T.

At midband, where $\theta=90^\circ$, it is seen that β is always equal to 90° for arbitrary values of Z_{oe} and Z_{oo} . If one chooses Z_{oe} and Z_{oo} as

$$\begin{aligned} Z_{oe} &= Z(\sqrt{2} + 1) \\ Z_{oo} &= Z(\sqrt{2} - 1) \end{aligned} \quad (1)$$

then, $Z_o = Z_s = Z$ at midband. If, in addition, the values of the four terminating impedances satisfy the relation

$$2Z_1 = Z_2 = Z \quad (2)$$


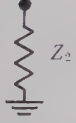
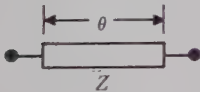
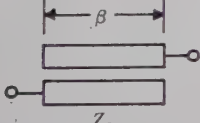
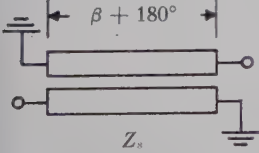
then the Magic-T is perfectly matched at midband at all ports and, hence, has perfect midband isolation between ports 1 and 4, and ports 2 and 3. Inspection of Fig. 1 shows that ports 2 and 3 are equivalent to the through arms of a waveguide Magic-T while ports 1 and 4 are equivalent to the ports on the series and shunt arms, respectively, of a waveguide Magic-T. At frequencies other than the midband frequency, the various ports will not be perfectly matched and the isolation

between opposite ports will not be infinite. Nevertheless, as will be shown later, the calculated performance of this Magic-T is quite good over a 2:1 frequency band. Calculations are also presented for cases when the various impedances are different from those defined by (1) and (2). It is shown that optimum performance over the 2:1 frequency band is obtained when $Z_1/Z = Z_2/Z = 0.8024$ and $Z_o/Z = 1.0785$ at midband.

The performance of these Magic-T's as a function of frequency is analyzed here in terms of the well-known $ABCD$ matrices of the individual networks within a particular Magic-T. These matrices are listed in Table I for reference.

TABLE I

 $ABCD$ MATRICES OF THE INDIVIDUAL NETWORKS IN THE MAGIC-T

Network	Matrix
	$\begin{vmatrix} 1 & 0 \\ \frac{1}{Z_1} & 1 \end{vmatrix} = M_1 $
	$\begin{vmatrix} 1 & 0 \\ \frac{1}{Z_2} & 1 \end{vmatrix} = M_2 $
	$\begin{vmatrix} \cos \theta & jZ \sin \theta \\ j \frac{\sin \theta}{Z} & \cos \theta \end{vmatrix} = M_3 $
	$\begin{vmatrix} \cos \beta & +jZ_o \sin \beta \\ j \frac{\sin \beta}{Z_o} & \cos \beta \end{vmatrix} = M_4 $
	$\begin{vmatrix} -\cos \beta & -jZ_o \sin \beta \\ -j \frac{\sin \beta}{Z_o} & -\cos \beta \end{vmatrix} = M_5 $

The techniques used to compute the input impedance of any port and the output voltages at the other ports will now be illustrated for the case when port 1 is energized. Fig. 2 shows the Magic-T of Fig. 1 redrawn in a convenient form for computation of the input impedance of port 1 and the isolation between ports 1 and 4.

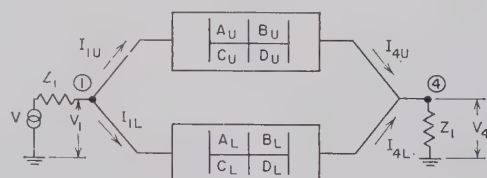


Fig. 2—Magic-T equivalent circuit used in computing voltages at ports 1 and 4.

Here the matrix elements of the upper network are given by

$$\begin{vmatrix} A_U & B_U \\ C_U & D_U \end{vmatrix} = |M_5| \times |M_2| \times |M_3|, \quad (3)$$

while those in the lower network are given by

$$\begin{vmatrix} A_L & B_L \\ C_L & D_L \end{vmatrix} = |M_4| \times |M_2| \times |M_3|. \quad (4)$$

The voltages and currents at the two ports are related by

$$\begin{aligned} V_1 &= A_U V_4 + B_U I_{4U} \\ I_{1U} &= C_U V_4 + D_U I_{4U} \end{aligned} \quad (5)$$

and

$$\begin{aligned} V_1 &= A_L V_4 + B_L I_{4L} \\ I_{1L} &= C_L V_4 + D_L I_{4L}. \end{aligned} \quad (6)$$

The currents I_{4U} and I_{4L} are related as

$$(I_{4U} + I_{4L})Z_1 = V_4. \quad (7)$$

When (7) is substituted into (6) and (5), one finds that the input impedance $Z_{in(1)}$ at port 1 is

$$Z_{in(1)} = \frac{V_1}{I_{1U} + I_{1L}} = \frac{A_U B_L + B_U A_L + \frac{B_U B_L}{Z_1}}{-2 + B_U C_L + B_L C_U + D_U A_L + D_L A_U + \frac{B_U D_L + D_U B_L}{Z_1}}. \quad (8)$$

The input impedance at port 4 when port 1 is terminated in Z_1 is easily determined by replacing, in (8), A_U by D_U , D_U by A_U , A_L by D_L , and D_L by A_L .

It is easy to show that the ratio of V_1/V_4 when port 1 is energized is given as

$$\frac{V_1}{V_4} = \frac{\frac{B_U B_L}{Z_1} + A_U B_L + A_L B_U}{B_L + B_U} \quad (9)$$

The ratio V_4/V_1 when port 4 is energized is determined by replacing, in (9), A_U by D_U and A_L by D_L , which shows that in general these ratios are slightly different. The actual insertion loss, $I.L.$, between ports 1 and 4, is independent of the direction of propagation through the network and is given by

$$I.L. = \left[\frac{1}{|1 + \Gamma_{in(1)}|} \frac{\frac{B_U B_L}{Z_1} + A_U B_L + A_L B_U}{B_L + B_U} \right]^2 \quad (10)$$

or

$$I.L. = \left[\frac{1}{|1 + \Gamma_{in(4)}|} \frac{\frac{B_U B_L}{Z_1} + D_U B_L + D_L B_U}{B_L + B_U} \right]^2,$$

where

$$\Gamma_{in(1)} = \frac{Z_{in(1)} - Z_1}{Z_{in(1)} + Z_1}$$

$$\Gamma_{in(4)} = \frac{Z_{in(4)} - Z_1}{Z_{in(4)} + Z_1}.$$

Eq. (10) predicts that the insertion loss between ports 1 and 4 is infinite only when $Z_e = Z_o = Z$.

The voltage at port 3 when port 1 is energized is determined with the aid of the circuit in Fig. 3. The matrices in this circuit have the values

$$\begin{vmatrix} A' & B' \\ C' & D' \end{vmatrix} = |M_4| \times |M_2| \times |M_3| \times |M_1| \times |M_3| \quad (11)$$

and

$$\begin{vmatrix} A_5 & B_5 \\ C_5 & D_5 \end{vmatrix} = M_5.$$

The voltage ratio V_3/V_1 is

$$\frac{V_3}{V_1} = \frac{B' + B_5}{\frac{B' B_5}{Z_2} + A' B_5 + A_5 B'} \quad (12)$$

The voltage at port 2 when port 1 is energized is determined with the aid of Fig. 4. The matrices in this circuit have the values

$$\begin{vmatrix} A'' & B'' \\ C'' & D'' \end{vmatrix} = |M_5| \times |M_2| \times |M_3| \times |M_1| \times |M_3|, \quad (13)$$

and

$$\begin{vmatrix} A_4 & B_4 \\ C_4 & D_4 \end{vmatrix} = |M_4|.$$

The voltage ratio V_2/V_1 is

$$\frac{V_2}{V_1} = \frac{B'' + B_4}{\frac{B' B_4}{Z_2} + A'' B_4 + A_4 B''} \quad (14)$$

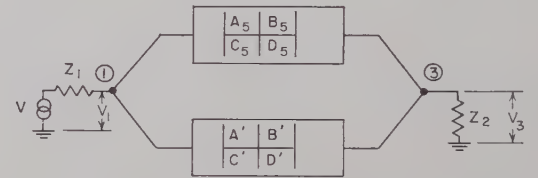


Fig. 3—Magic-T equivalent circuit used in computing voltages at ports 1 and 3.

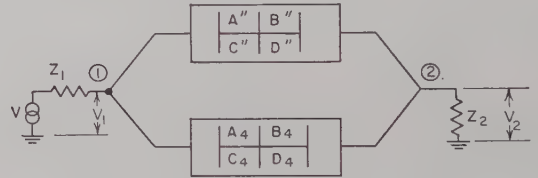


Fig. 4—Magic-T equivalent circuit used in computing voltages at ports 1 and 2.

The input impedance of the other ports and the voltage transfer coefficients between the various ports when a particular port is energized may be written by inspection using the above technique. One interesting result of such a procedure is the fact that the insertion loss between ports 2 and 3 is infinite only when $Z_e Z_o = Z^2$ and $\theta = \beta = 90^\circ$. This condition is satisfied at midband for all the Magic-T's discussed here.

The electrical performances of five Magic-T's have been computed on a high-speed digital computer using the above formulas. The important electrical parameters of these structures are listed in Table II. The input impedance at the four ports of these Magic-T's are plotted in Figs. 5 through 9. It is observed that in all cases the real part of the input impedance of a port is a symmetrical function of frequency while the imaginary part is an antisymmetrical function of frequency. Furthermore, the input impedance at each of the various ports of any one Magic-T has a different variation with fre-

TABLE II
ELECTRICAL PARAMETERS OF VARIOUS STRIP-LINE MAGIC-T's

	Magic-T Number 1	Magic-T Number 2	Magic-T Number 3	Magic-T Number 4	Magic-T Number 5
Z_{0e}/Z	2.414	2.550	2.550	2.550	2.550
Z_{0o}/Z	0.414	0.392	0.392	0.392	0.392
Z_1/Z	0.500	0.500	0.6350	0.7407	0.8024
Z_2/Z	1.000	1.000	1.000	0.8696	0.8024
Z_o/Z (Midband)	1	1.0785	1.0785	1.0785	1.0785
Z_s/Z (Midband)	1	0.9272	0.9272	0.9272	0.9272
β (when $Z_s/Z = Z_o/Z$)	90°	$90^\circ \pm 30.7^\circ$	$90^\circ \pm 30.7^\circ$	$90^\circ \pm 30.7^\circ$	$90^\circ \pm 30.7^\circ$
θ (when $Z_s/Z = Z_o/Z$)	90°	$90^\circ \pm 22^\circ$	$90^\circ \pm 22^\circ$	$90^\circ \pm 22^\circ$	$90^\circ \pm 22^\circ$

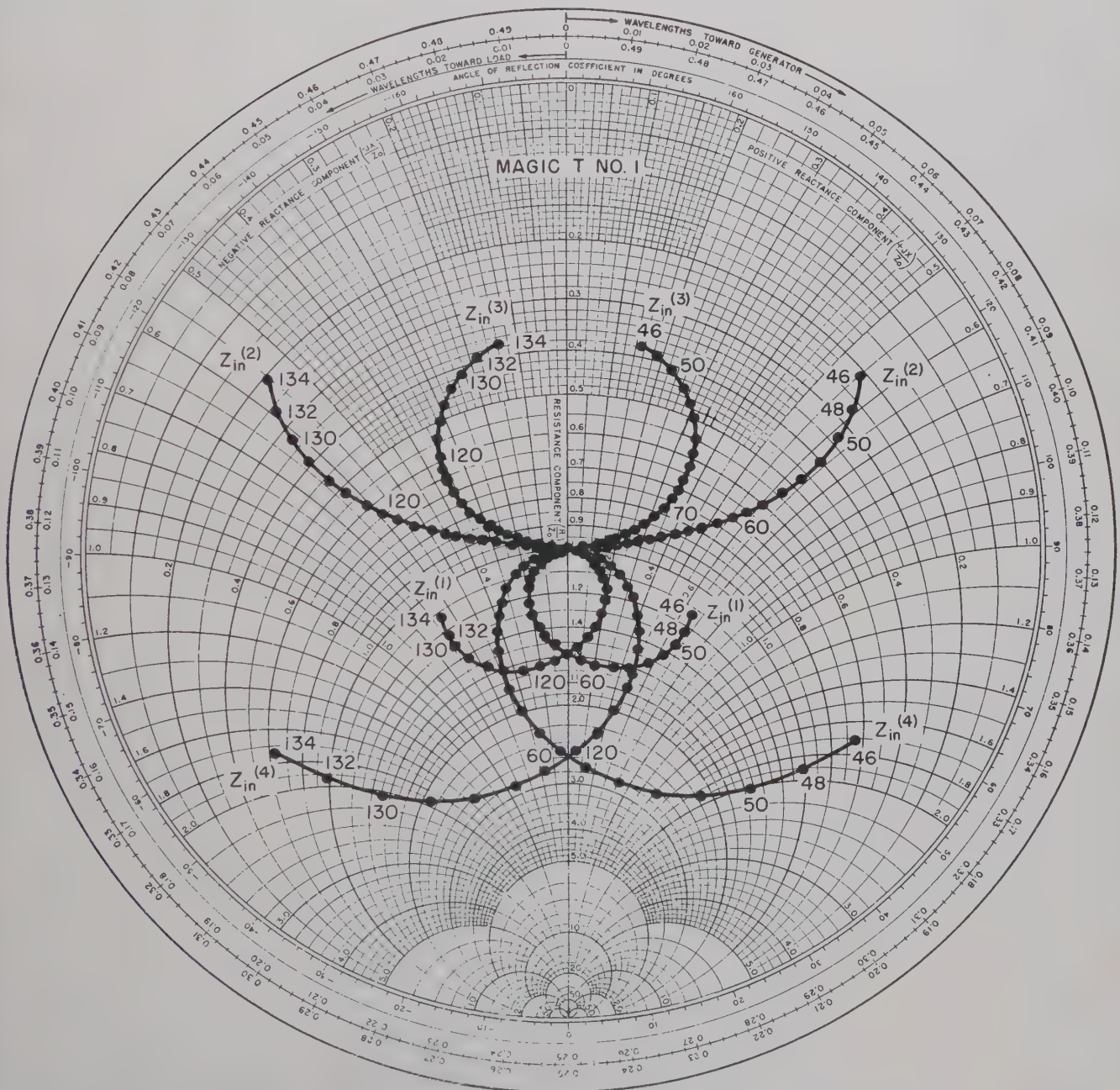


Fig. 5—Input impedance of Magic-T 1.

quency since this device has no electrical plane of symmetry.

Magic-T 1 is designed to be matched at all ports at midband. It also has infinite isolation between ports 1 and 4 and ports 2 and 3 at midband. The input match at the various ports deteriorates at frequencies above and below midband. At the edges of a 2:1 frequency band the VSWR at port 4 rises to 2.55.

Magic-T 2 was designed to have perfect isolation between ports 1 and 4 at $\theta = 90^\circ \pm 22^\circ$ and approximately equal isolation between these ports at the center and at

the edges of a 2:1 frequency band. As mentioned before, it also has perfect isolation between ports 2 and 3 at $\theta = 90^\circ$. The frequency variation of the isolation between these pairs of ports is shown in Fig. 10. It is observed that over a 2:1 frequency band the isolation between ports 1 and 4 is always greater than 24.8 db, while the isolation between ports 2 and 3 drops to 22.2 db at the edges of such a band. The input impedance of the various ports is quite similar to that of Magic-T 1, and at the edges of a 2:1 frequency band the VSWR at port 4 rises to 2.45.

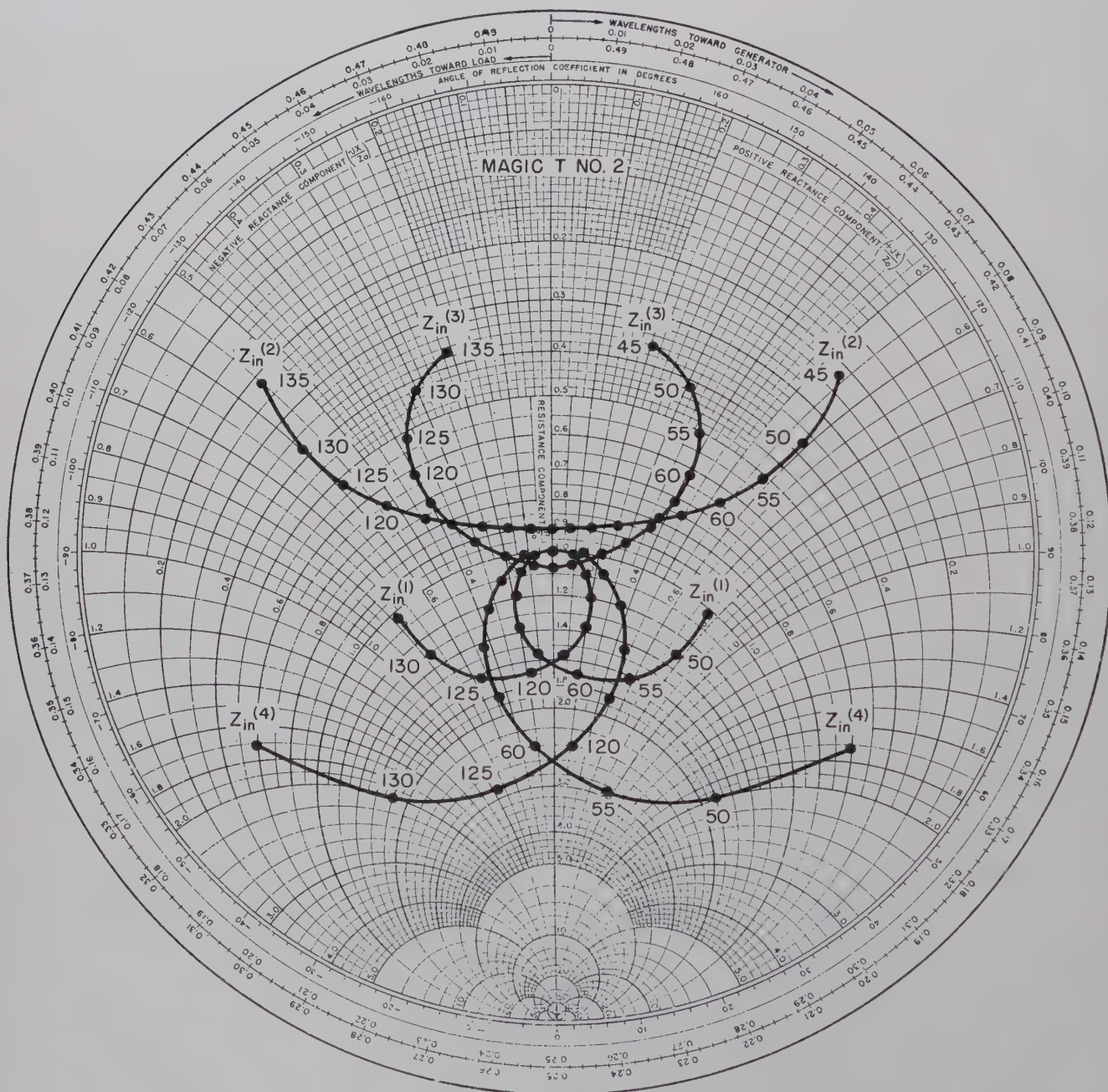


Fig. 6—Input impedance of Magic-T 2.

Fig. 7—Input impedance of Magic-T 3.

frequency is quite similar over a 2:1 frequency band. Hence, it is believed that the parameters of Magic-T 5 are essentially optimum for a 2:1 frequency band of operation. The isolation between diagonally opposite ports is plotted in Fig. 10. It is seen that the isolation is quite similar to that of Magic-T 2.

In many applications the most pertinent parameters of a Magic-T are the input impedance of the various ports and the isolation between opposite ports (*i.e.*, between ports 1 and 4 and ports 2 and 3). However, it is sometimes desirable to know approximately the ratio,

R , of wanted to unwanted voltages at ports 2 and 3 when port 1 or 4 is energized, or the ratio of wanted to unwanted voltages at ports 1 and 4 when port 2 or 3 is energized. This ratio R is V_b/V_U when port 1 or 3 is energized and V_U/V_b when port 4 or 2 is energized. Here V_b is the balanced voltage and V_U the unbalanced voltage.⁸ An approximation to R can be obtained by the

⁸ When port 1 or port 4 is energized, $V_b = |V_3 - V_2|/2$ and $V_U = |V_3 + V_2|/2$. When port 2 or port 3 is energized $V_b = |V_1 - V_4|/2$ and $V_U = |V_1 + V_4|/2$.

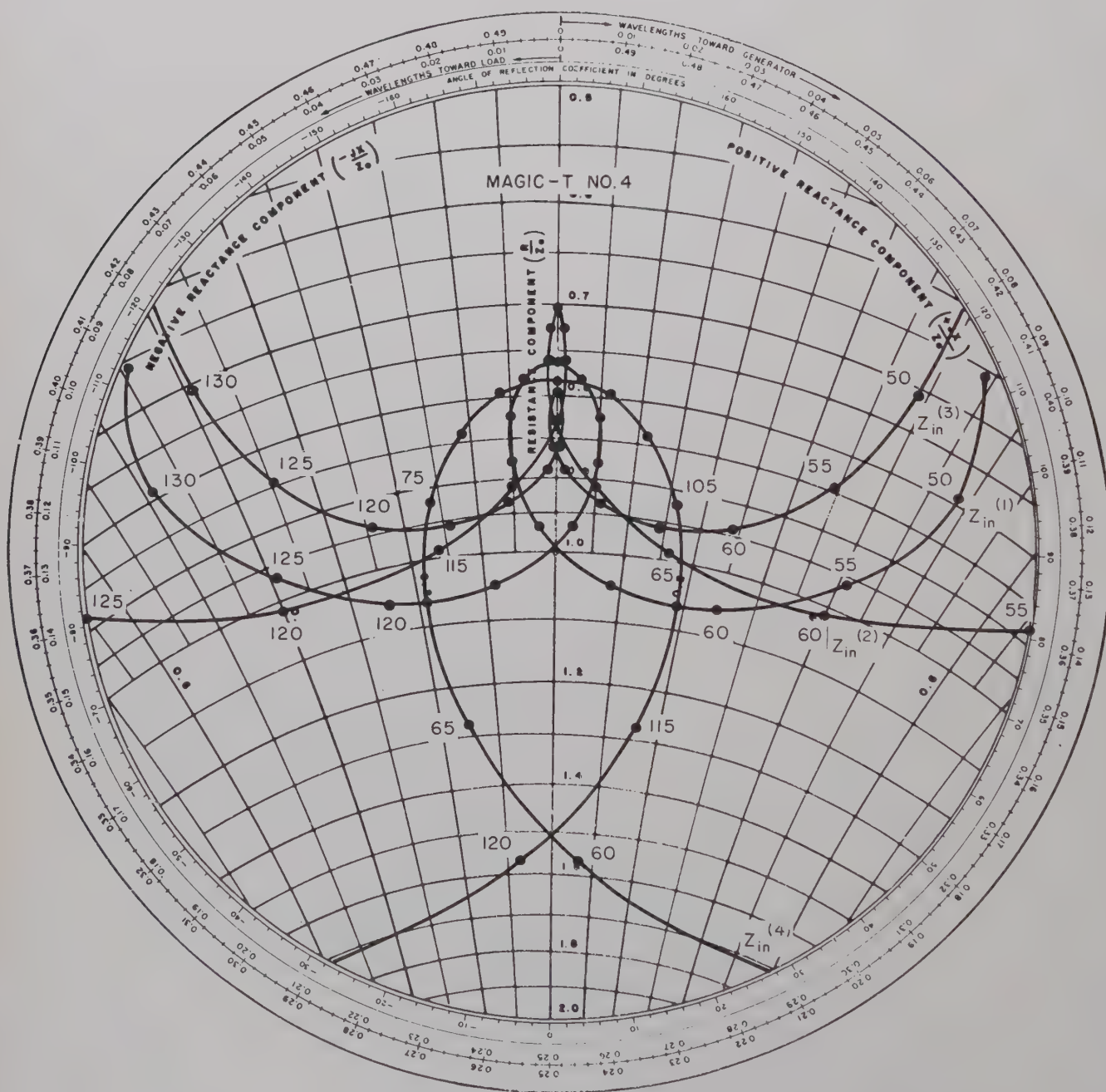


Fig. 8—Input impedance of Magic-T 4.

simple procedure outlined below. Inspection of Fig. 1 shows that when port 1 is energized

$$\frac{V_1^2}{Z_1} \approx \frac{V_2^2}{Z_2} + \frac{V_3^2}{Z_2} + \frac{V_4^2}{Z_1} \quad (15)$$

or

$$\frac{V_1^2}{Z_1} \approx \frac{2V_b^2}{Z_2} + \frac{2V_u^2}{Z_2} + \frac{4Z_1}{Z^2} V_u^2 \quad (16)$$

In deriving (16), use has been made of the fact that

$$V_2^2 + V_3^2 \equiv 2V_u^2 + 2V_b^2$$

and it is assumed that $\theta \approx \beta = \pi/2$ and $Z_s \approx Z_0 \approx Z$ over the operating band. Recalling that the insertion loss (*I.L.*) is approximately V_1^2/V_4^2 it is seen that

$$\frac{V_1^2}{V_4^2} \approx I.L. \approx \frac{V_b^2 Z^2}{2V_u^2 Z_1 Z_2} + \frac{1}{2Z_1 Z_2} + 1 \approx \frac{V_b^2 Z^2}{2V_u^2 Z_1 Z_2} \quad (17)$$

and

$$R^2 \approx I.L. \left(\frac{2Z_1 Z_2}{Z^2} \right). \quad (18)$$

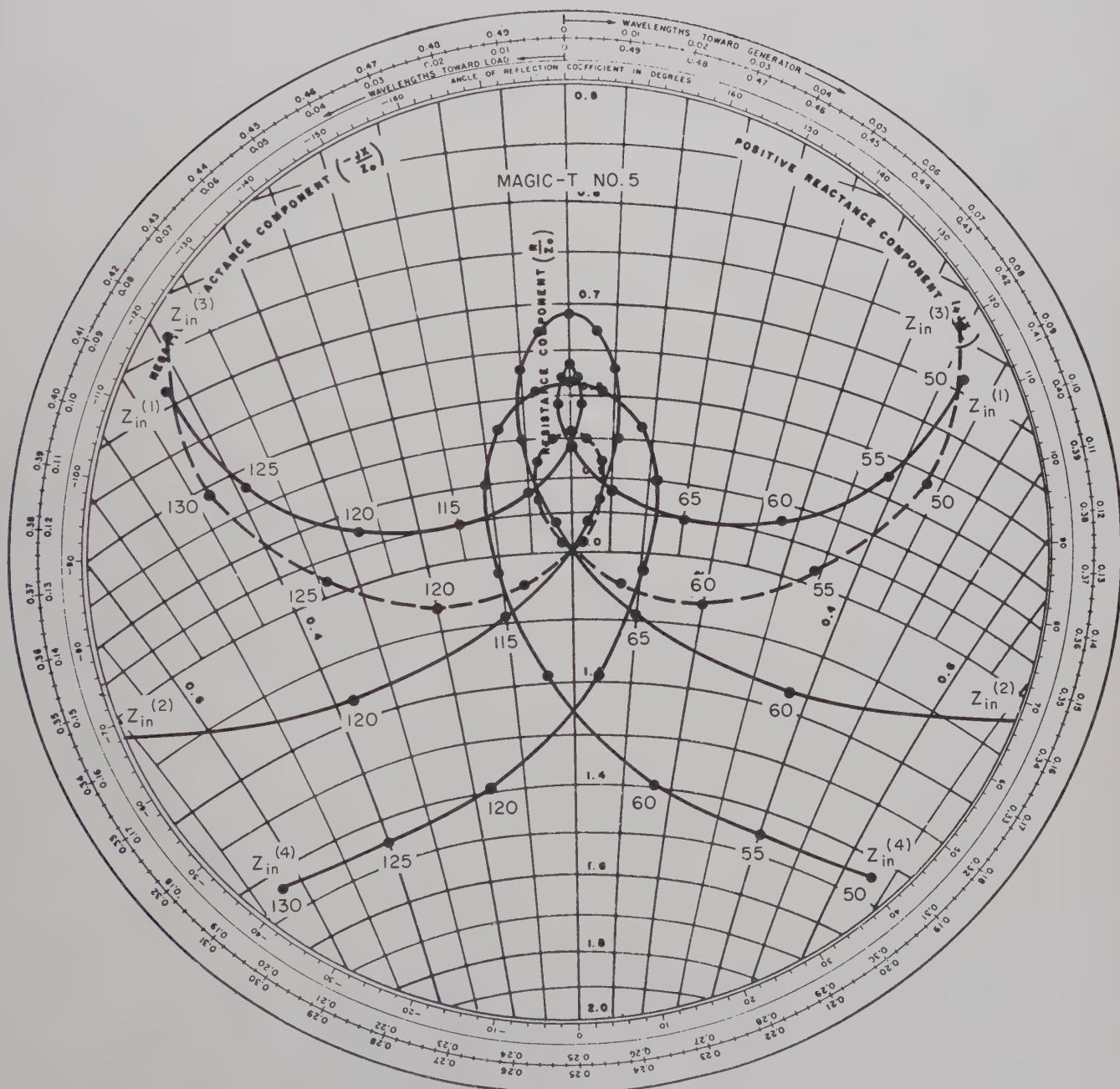


Fig. 9—Input impedance of Magic-T 5.

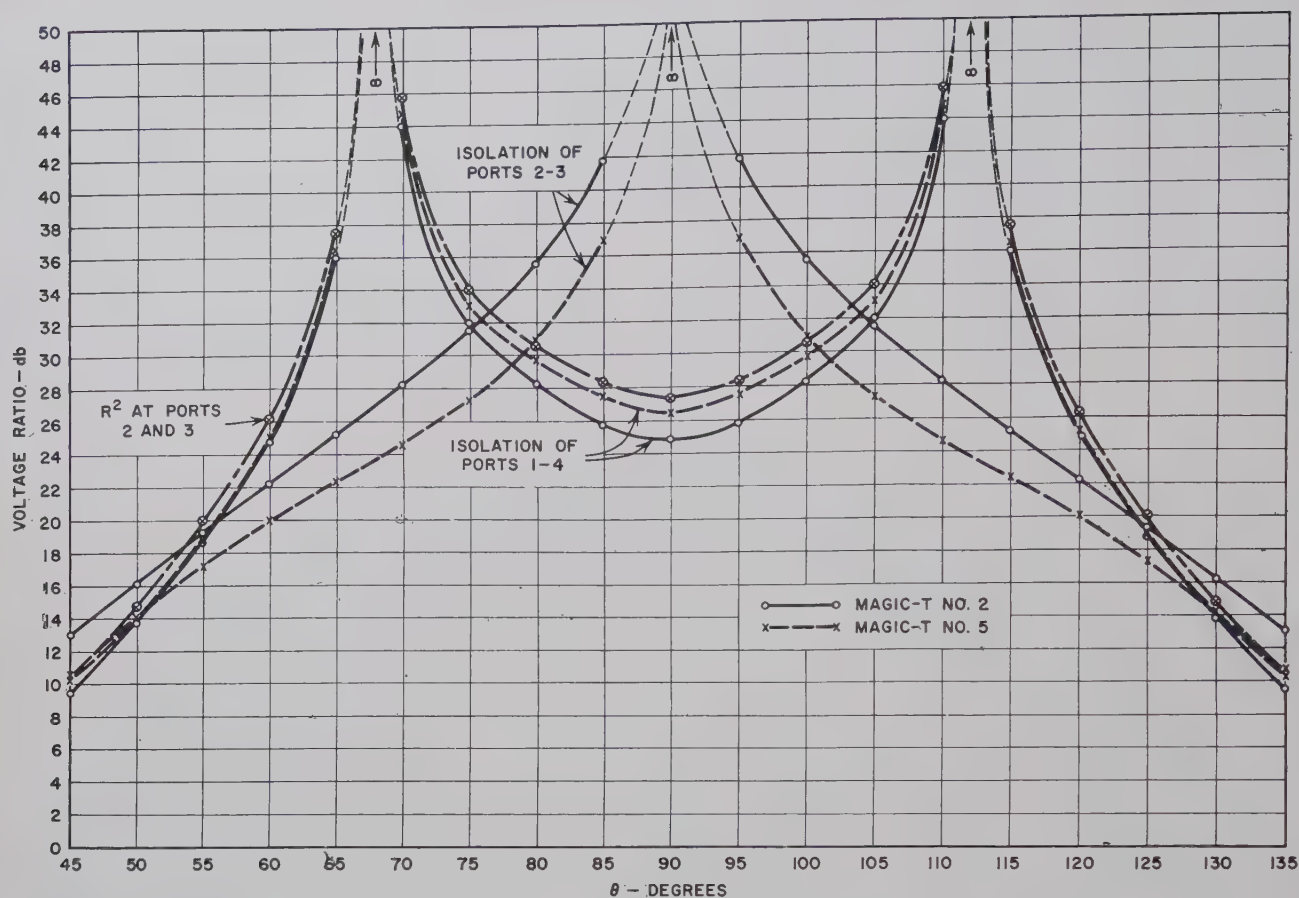


Fig. 10—Isolation between ports 1 and 4 and between ports 2 and 3 for Magic-T's 2 and 5.

It is easy to show that (18) also applies to ports 2 and 3 when port 4 is energized, and to ports 1 and 4 when either port 2 or port 3 is energized.

Application of (18) to Magic-T 2 shows that the insertion loss between opposite ports is numerically equal to R^2 at the other two ports. In Fig. 10 is plotted the correct value of R^2 , calculated from (12) and (14) at ports 2 and 3 when port 1 is energized. It is seen to agree very

closely with the approximate value of R^2 computed by (18). In Magic-T 5, (18) predicts that R^2 is about 1 db greater than the insertion loss between opposite ports.

ACKNOWLEDGMENT

The author wishes to acknowledge the help of J. K. Shimizu in carrying through some of the theoretical calculations presented here.

A General Theorem on an Optimum Stepped Impedance Transformer*

HENRY J. RIBLET†

Summary—With the assistance of a mathematical theorem demonstrated by Eaton in a companion paper, it is shown rigorously, in the limit of small impedance transformation, that the familiar binomial impedance transformer, consisting of equal quarter-wave steps, is the shortest, monotonic, maximally-flat, stepped, transmission-line transformer having steps commensurate in length with the midband guide-wavelength, and coincident zeros at the midband frequency.

It is shown how this theorem places very severe limitations on any effort to improve on the performance of a quarter-wave transformer by increasing the number of its impedance steps without a corresponding increase in its length.

INTRODUCTION

L SOLYMAR¹ has, in a recent paper, considered the problem of the optimum design of monotonic, stepped, transmission-line transformers. He has made the simplifying assumption that multiple reflections from the impedance discontinuities can be neglected, and has introduced the requirement of monotonicity to avoid the problem of "supermatch" which can otherwise appear, even when multiple reflections are considered. He employs the even polynomials proposed by Riblet,² to construct examples which show the interesting fact that, for given relative bandwidth, the quarter-wave transformer does not give the smallest pass-band reflection coefficient if additional length is available. He observes that, with transformers less than one-eighth wavelength long, this procedure results in nonmonotonic solutions.

Solymar's problem involves the length of the transformer, its bandwidth, and the ratio of tolerable reflection coefficient in the pass band to the reflection coefficient to be transformed. Any general discussion of the optimum design is exceedingly involved, and the results will certainly depend on the constraints placed on these three variables.

Several years ago, the writer considered the same general problem and was forced by its analytical difficulty to limit his investigation to the maximally-flat transformer. This restriction, however, permits a major simplification in the statement of the problem, since the

variables of bandwidth and tolerable reflection coefficient may then be simultaneously specified, while the number of coincident zeros at the "resonant" frequency precisely determines the length of the transformer.

Even for an impedance transformer of finite bandwidth, of course, its tolerable VSWR is closely related to the number of zeros occurring in the operating band. Consideration of Solymar's examples will show that the number of zeros in the band of his "optimum" transformers does not exceed the number available from the longest quarter-wave transformer which can be fitted into the available length. When he improves on the performance that a quarter-wave transformer will yield, it is the spacing of the zeros which is adjusted. His efforts to introduce additional zeros leads to nonmonotonic solutions. In fact, it may be conjectured, in general, that additional zeros in the operating band of the impedance transformer will result in a nonmonotonic design.

THE PROBLEM

Consider the stepped, transmission-line transformer shown schematically in Fig. 1, operating between input

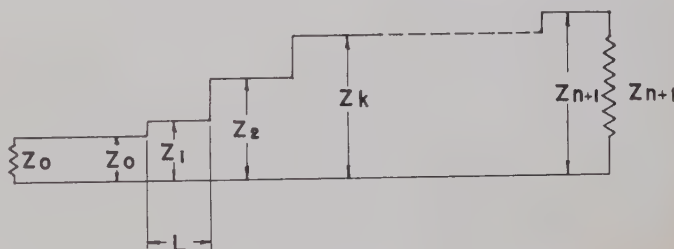


Fig. 1—Schematic of n -section transformer.

and output impedances Z_0 and Z_{n+1} , respectively. Γ_i is the reflection coefficient at the i th step. For a monotonic transformer all of the Γ_i have the same sign. The input reflection coefficient ρ neglecting multiple reflections, is known to be

$$\rho = \Gamma_1 + \Gamma_2 x + \Gamma_3 x^2 + \cdots + \Gamma_{n+1} x^n,$$

where $x = \exp \{i4\pi l/\lambda_0\}$.

If we require that ρ have n zeros at the particular frequency, where $\lambda_0 = \bar{\lambda}_0$, we immediately find a solution of the problem in the form

$$\rho = C(x + 1)^n, \quad (1)$$

if we select $l = \bar{\lambda}_0/4$, since then $x = \exp \{i\pi \bar{\lambda}_0/\lambda_0\}$ which equals -1 at the particular frequency. This is, of course, the familiar binomial, maximally-flat, transformer consisting of n , equal-length quarter-wave sections in which

* Manuscript received by the PGM-TT, July 23, 1959; revised manuscript received, October 19, 1959. The problem and proof were presented before the URSI meeting, Washington, D. C., May, 1953. The discussion of Solymar's paper has been added as a result of the renewed interest in the problem.

† Microwave Development Labs., Inc., Wellesley, Mass.

¹ L. Solymar, "Some notes on the optimum design of stepped transmission-line transformers," IRE TRANS. ON MICROWAVE THEORY AND TECHNIQUES, vol. MTT-6, pp. 374-378; October, 1958.

² H. J. Riblet, "Discussion on 'A current distribution for broad-side arrays which optimizes the relationships between beamwidth and side-lobe level,'" PROC. IRE, vol. 35, pp. 489-492; May, 1947.

the Γ_i 's have the ratios of the binomial coefficients. For engineering purposes, (1) may be rewritten as

$$|\rho| = \Gamma \{ \cos (\pi \bar{\lambda}_g / 2\lambda_g) \}^n, \quad (2)$$

where Γ is the reflection coefficient to be matched by the transformer. Eq. (2) defines, in terms of n , the bandwidth over which a given $|\rho|/\Gamma$ will not be exceeded.

It is the object of this paper to indicate how the binomial, quarter-wave transformer is optimum in the sense that no shorter stepped, monotonic transformer can have additional zeros at the chosen frequency. For this purpose, consider a transformer consisting of sections each $\bar{\lambda}_g/4r$ in length, where r is an integer. If a shorter, monotonic transformer could be designed using sections of this length, still having n coincident zeros, it would mean that a polynomial of degree less than nr in $x = \exp \{ i\pi \bar{\lambda}_g / r\lambda_g \}$ could be constructed having positive real coefficients, with n coincident roots for $\lambda_g = \bar{\lambda}_g$. The condition on the degree follows from the fact that the over-all length of an impedance transformer is equal to the degree of the polynomial representing the input reflection coefficient multiplied by the length of the individual transformer sections. That this is impossible follows immediately from the purely mathematical theorem.³

Theorem: The real polynomial of minimum degree with positive coefficients having n roots at $e^{i\pi/r}$ is $(x^r + 1)^n$.

Moreover since the solution $\rho = C(x^r + 1)^n$ for the shorter steps is identical to (1) for the quarter-wave steps, we see that our efforts to improve on the quarter-wave transformer have brought us back to the starting point. We can thus prove the following theorem on an optimum impedance transformer.

Theorem A: The shortest, monotonic, stepped impedance transformer, all of whose steps are commensurate in length with $\bar{\lambda}$ having n coincident zeros for $\lambda_g = \bar{\lambda}_g$, is the binomial, quarter-wave transformer having n steps.

Proof: The requirement that the steps be commensurate with $\bar{\lambda}_g$ permits the selection of an r sufficiently large so that any shorter transformer meeting the conditions of the theorem can be thought to consist of steps each $\bar{\lambda}_g/4r$ in length. The theorem proved by Eaton is then applicable and a contradiction results.

³ This theorem was conjectured by the writer, but its truth was in doubt for over a year before the ingenious proof given in the companion paper was found by J. E. Eaton. During that year, a careful search of the literature and inquiry of experts in the related branch of analysis failed to reveal any previous interest in this type of problem.

ENGINEERING APPLICATIONS

This theorem cannot restrict the performance of practical transformers without additional arguments involving "continuity" and "limits" since there is no way of determining when the conditions requiring commensurate lengths and coincident zeros have been met.⁴ Accordingly its rigorous application is limited to purely theoretical design procedures. For example, it may be applied to the problem of Solymar, as follows.

Theorem B: No design procedure, which is independent of bandwidth, can yield a monotonic, stepped, impedance transformer having n zeros in its pass band, consisting of a fixed number of sections of fixed length, each commensurate with $\bar{\lambda}_g$, which is shorter in over-all length than $n\bar{\lambda}_g/4$.

Proof: The existence of such a design procedure would imply the existence of an infinite sequence of polynomials of fixed degree having the property that n of their roots approach some limiting value $e^{i\pi/r}$. The coefficients of these polynomials each then constitute a finite number of infinite sequences of bounded, positive real numbers. By a fundamental theorem, these sequences have limit points which are non-negative and bounded, and, thus, define a positive, real polynomial with n coincident zeros. This polynomial must at least be of degree nr , and so the design procedure cannot yield transformers shorter than $n\bar{\lambda}_g/4$.

CONCLUSION

Two theorems are demonstrated showing that the quarter-wave transformer is optimum under certain idealized conditions. Although these conditions are implicit in present design procedures, a deficiency exists in the theory which has the result that it is not applicable to an actual transformer. This limitation is not essential to the theory, however, and one may hope that it will be removed ultimately.

In the meantime the theorems give mathematical reality to the demarcation between monotonic design and "supermatch" and will serve as beacons pointing to certain obstacles which will have to be faced in any effort to put more zeros in the pass band of a monotonic transformer than are contained in the quarter-wave transformer of optimum design.

⁴ Although some progress has been made in this direction, the problem is complicated by its delicate algebraic nature. For example, a quarter-wave transformer when imagined to consist of shorter length steps is certainly on the verge of nonmonotonicity.

Minimal Positive Polynomials*

JAMES E. EATON†

Summary—A proof is given of a purely mathematical theorem on the polynomial of lowest degree with positive coefficients having a prescribed root of unity as a multiple root.

H. J. Riblet has conjectured the theorem below. In the preceding paper,¹ he applies his theorem to optimum impedance transformer design.

THEOREM

THE polynomial $(x^r+1)^n$ is the unique monic polynomial of lowest degree with non-negative coefficients that has $e^{i\pi/r}$ as an n -fold root.

The degree of the minimal positive polynomial is at most nr . Let the polynomial be

$$f(x) = a_{nr}x^{nr} + a_{nr-1}x^{nr-1} + \cdots + a_0.$$

If $n=1$, the imaginary part of $f(e^{i\pi/r})$, of necessity zero, may be written as

$$a_{r-1} \sin(r-1)\pi/r + \cdots + a_1 \sin \pi/r.$$

Therefore, $a_k=0$, $0 < k < r$, for in this range $0 < \sin k\pi/r$. The real part, also zero, now reduces to $-a_r + a_0$. Hence, $f(x) = a_r(x^r+1)$.

For larger n , note that if $e^{i\pi/r}$ is an n -fold root of $f(x)$ it is also a root of the first $n-1$ derivatives of $f(x)$. It is then a root of

$$F(x) = b_0 f(x) + b_1 x f'(x) + \cdots + b_{n-1} x^{n-1} f^{(n-1)}(x)$$

for any choice of the constants b_i . $F(x)$ may be rewritten as

$$F(x) = a_{nr}g(nr)x^{nr} + a_{nr-1}g(nr-1)x^{nr-1} + \cdots + a_0g(0) \quad (1)$$

where

$$g(k) = b_0 + b_1k + b_2k(k-1) + \cdots + b_{n-1}k(k-1) \cdots (k-n+2). \quad (2)$$

Although, in so far as $g(k)$ appears in (1), k is restricted to certain integral values. Eq. (2) defines $g(k)$ as a polynomial in k of degree $n-1$.

In (1) replace x by $e^{i\pi/r}$ and compute the imaginary part of $F(x)$ to obtain

$$a_{nr}g(nr) \sin nr\pi/r + a_{nr-1}g(nr-1) \sin (nr-1)\pi/r + \cdots + a_1g(1) \sin \pi/r = 0. \quad (3)$$

The constants b_i in (2) may be chosen so that $g(k)$ has the same sign as $\sin k\pi/r$, $0 < k < nr$. Since a_k is not negative, this will imply that $a_k g(k) \sin k\pi/r$ also is not negative and hence, by (3), zero.

The proper behavior of $g(k)$ is readily obtained by requiring that $g(k)=0$, $k=r, 2r, \cdots, (n-1)r$. This leads to a system of $n-1$ linear homogeneous equations in the n quantities $b_0, b_1, \cdots, b_{n-1}$. The system has non-trivial solutions and one may be selected for which $g(1)$ is positive. Since $g(k)$ is of degree $n-1$, it has no other roots and $g(k) \sin k\pi/r \geq 0$. Therefore, $a_k=0$ if k is not divisible by r . Thus, $f(x)$ is a polynomial in x^r : $f(x) = h(x^r)$. It has the n -fold root $e^{i\pi/r}$ and $h(x)$ accordingly has the n -fold root $e^{i\pi}$. This shows that $h(x) = a_{nr}(x+1)^n$ and $f(x) = a_{nr}(x^r+1)^n$.

* Manuscript received by the PGMTT, August 23, 1959; revised manuscript received, October 19, 1959.

† Queens College, Flushing, N. Y.

¹ H. J. Riblet, "A general theorem on an optimum stepped impedance transformer," IRE TRANS. ON MICROWAVE THEORY AND TECHNIQUES, this issue, pp. 169-170.

Complementarity in the Study of Transmission Lines*

G. H. OWYANG† AND RONOLD KING‡

Summary—The principle of complementarity is applied to the slot transmission line. The properties of a dual circuit are investigated. The pairs of several possible duals for a given configuration are correlated and new quantities are defined for use with different types of circuits. A complete parallelism between the two-wire line and the two-slot line is established for the ideal cases and is extended by approximation to include the practical cases.

Measurements were made with a two-slot transmission line and its associated probing system. The method of testing the line for balance is discussed. The transverse distribution of the longitudinal current and the attenuation constant were measured.

The analogy between the steady-state field in a conducting medium and the electrostatic field in a dielectric is investigated. The expressions for the constants of a two-slot line are given in a form that permits a ready evaluation from experimental data obtained with the electrolytic tank. The measured results are compared with theoretical values.

I. THE PRINCIPLE OF COMPLEMENTARITY

A. Introduction

IF two physically different phenomena, A and B , are described by the same mathematical formulation, quantitative conclusions may be drawn about A from a study of B . This is true of complementary problems in electromagnetic theory, in which the field about a configuration A of slots in a perfectly conducting infinite plane of zero thickness is related to the field about a configuration B of conducting strips arranged in free space to correspond exactly to the slots in A .

B. Duality Between the Electromagnetic Field of an Electric and a Magnetic Source

Consider groups of perfect electric and perfect magnetic conductors in a homogeneous medium characterized by the complex permittivity $\epsilon = \epsilon_e - j\sigma_e/\omega$, and the permeability μ (see Fig. 1). S_1, S_2, \dots are the surfaces of the electric conductors, S_1^*, S_2^*, \dots of the magnetic conductors. The appropriately generalized field and continuity equations are

$$\text{curl } \mathbf{E} = -\mathbf{J}^* - j\omega\mu\mathbf{H}, \quad \text{div } \mathbf{E} = \rho/\epsilon; \quad (1a)$$

$$\text{curl } \mathbf{H} = \mathbf{J} + j\omega\epsilon\mathbf{E}, \quad \text{div } \mathbf{H} = \rho^*/\mu; \quad (1b)$$

$$\text{div } \mathbf{J} + j\omega\rho = 0 \quad \text{div } \mathbf{J}^* + j\omega\rho^* = 0. \quad (1c)$$

(The symbols are defined in Fig. 4.) The boundary conditions on the surfaces of the conductors are

$$\hat{n} \times \mathbf{E} = \hat{n} \cdot \mathbf{H} = 0 \quad (2a)$$

on the electric conductors S_1, S_2, \dots , and

$$\hat{n} \times \mathbf{H} = \hat{n} \cdot \mathbf{E} = 0 \quad (2b)$$

* Manuscript received by the PGM-TT, June 4, 1959; revised manuscript received, October 20, 1959. This research was supported jointly by the Navy Department (ONR), the Signal Corps of the U. S. Army, and the U. S. Air Force, under contract Nonr. 1866(32.)
† Rad. Lab., University of Michigan, Ann Arbor, Mich. Formerly at Gordon McKay Lab., Harvard University, Cambridge, Mass.
‡ Gordon McKay Lab., Harvard University, Cambridge, Mass.

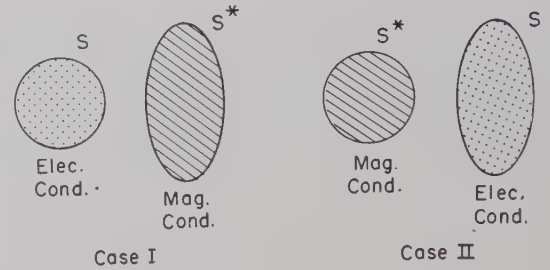


Fig. 1

on the magnetic conductors S_1^*, S_2^*, \dots , where n is a unit outward normal.

It can be shown that an interchange of the electric and magnetic sources and conductors in a given system results in an interchange of the E - and H -fields. In particular, if

$$\mathbf{J}_2 = -\eta_e \mathbf{J}_1^*, \quad \mathbf{J}_2^* = \zeta_e \mathbf{J}_1, \quad (3a)$$

$$\rho_2 = -\eta_e \rho_1, \quad \rho_2^* = \zeta_e \rho_1, \quad (3b)$$

where $\zeta_e^2 = 1/\eta_e^2 = \mu/\epsilon$, the field vectors are given by

$$\mathbf{E}_2 = -\zeta_e \mathbf{H}_1, \quad \mathbf{H}_2 = \eta_e \mathbf{E}_1. \quad (4)$$

The subscripts 1 and 2 refer to cases I and II (Fig. 1), respectively.

C. Fields with E -symmetry and H -symmetry.

In rectangular coordinates the field vectors \mathbf{E} and \mathbf{H} are E -symmetric (or H -antisymmetric) with respect to the plane $x=0$ if

$$\begin{aligned} E_u(x) &= \begin{cases} -E_u(-x), & u = x \\ E_u(-x), & u = y \text{ or } z \end{cases} \\ H_u(x) &= \begin{cases} H_u(-x), & u = x \\ -H_u(-x), & u = y \text{ or } z. \end{cases} \end{aligned} \quad (5)$$

The shorthand notations $F(x)$ and $F(-x)$ are used for $F(x, y, z)$ and $F(-x, y, z)$. The corresponding field vectors with H -symmetry (or E -antisymmetry) are

$$\begin{aligned} E_u(x) &= \begin{cases} E_u(-x), & u = x \\ -E_u(-x), & u = y \text{ or } z, \end{cases} \\ H_u(x) &= \begin{cases} -H_u(-x), & u = x \\ H_u(-x), & u = y \text{ or } z. \end{cases} \end{aligned} \quad (6)$$

With these definitions, any function $F(x)$ may be expressed as the sum of symmetric and antisymmetric components in the form $F(x) = F_s(x) + F_a(x)$ where

$$F_i(x) = \frac{1}{2} \{ \hat{x}[F_x(x) \mp F_x(-x)] + \hat{y}[F_y(x) \pm F_y(-x)] + \hat{z}[F_z(x) \pm F_z(-x)] \}. \quad (7)$$

$i=s$ for the upper signs, $i=a$ for the lower signs.

With (5)–(7) it follows directly that for a structure in space that is symmetric, the field equations are independent of the sign of x and may be separated into E -symmetric and H -symmetric parts. These are, for H -symmetry,

$$\text{curl } \mathbf{E}_a(x) + j\omega\mu\mathbf{H}_s(x) = -\mathbf{J}_s^*(x), \quad (8a)$$

$$\text{curl } \mathbf{H}_s(x) - j\omega\epsilon\mathbf{E}_a(x) = \mathbf{J}_a^*(x); \quad (8b)$$

for E -symmetry,

$$\text{curl } \mathbf{E}_s(x) + j\omega\mu\mathbf{H}_a(x) = -\mathbf{J}_a^*(x), \quad (8c)$$

$$\text{curl } \mathbf{H}_a(x) - j\omega\epsilon\mathbf{E}_s(x) = \mathbf{J}_s(x). \quad (8d)$$

It follows from (5) that at $x=0$,

$$E_{sx}(0) = H_{ay}(0) = H_{az}(0) = 0 \quad (9)$$

so that in a homogeneous medium the E -symmetric field satisfies the boundary conditions (2) of a perfect magnetic conductor at $x=0$, and is not disturbed by the insertion of a plane sheet of perfect magnetic conductor of arbitrary shape and size in the plane of symmetry. Similarly, from (6)

$$E_{ay}(0) = E_{az}(0) = H_{sx}(0) = 0, \quad (10)$$

so that the H -symmetric field satisfies the boundary conditions (2) of a perfect electric conductor at $x=0$ and is undisturbed by the insertion of a plane sheet of perfect electric conductor in the plane of symmetry.

D. Duality Between a Thin Disk and a Hole in a Thin Sheet

Let a thin disk made of a perfect electric conductor be placed in the plane of symmetry ($x=0$) in a homogeneous medium as shown in Fig. 2(a). In this medium there exists an electromagnetic field maintained by a symmetric distribution of electric currents $\mathbf{J}_s(x)$. It follows from (8) that the field is E -symmetric so that it behaves just as if a magnetic conductor were located in the plane of symmetry outside the disk as shown in Fig. 2(b).

If the electric and magnetic conductors are interchanged, Fig. 2(d) is obtained. Since the regions $x>0$ and $x<0$ are separated by the sheets of conductor, (3) may be used with opposite signs in these two regions. That is, the distribution of magnetic current is anti-symmetric for the new system, so that it satisfies the following relations:

$$\mathbf{J}_{a4}^*(x) = \zeta_e \mathbf{J}_{s3}(x), \quad \mathbf{J}_{a4}^*(-x) = -\zeta_e \mathbf{J}_{s3}(-x), \quad (11)$$

where the subscripts 3 and 4 refer to the systems before and after the change. Since the excitation is by anti-symmetric magnetic currents, the field has E -symmetry and it is immaterial whether the sheet of magnetic conductor is present or not. Therefore, Figs. 2(c) and 2(d) represent equivalent configurations and the formulas shown in the figure follow directly from (3) and (4)

The following situations have been shown to be duals: a thin disk of perfect electric conductor in the plane of

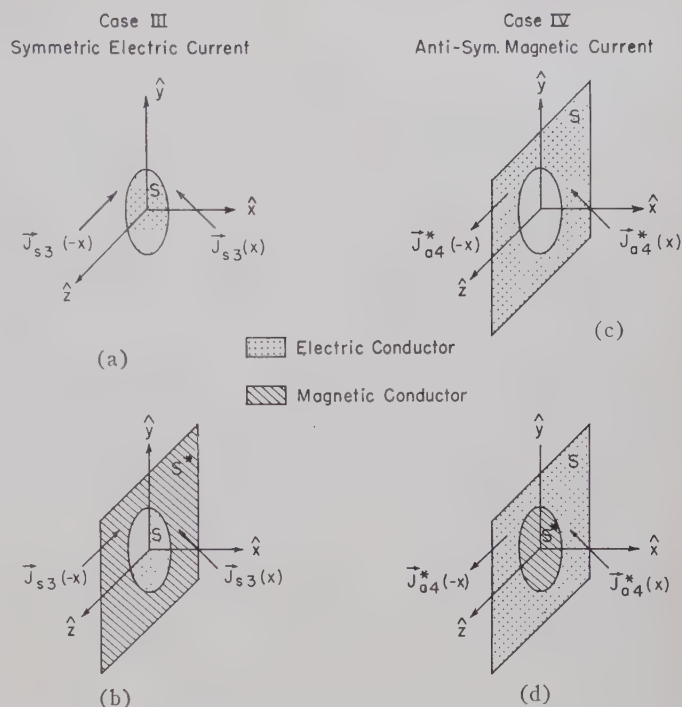


Fig. 2—Duality between metallic disk and hole in metallic screen.

Field: E -symmetry with respect to $x=0$ plane

$$E_x(x) = -E_x(-x) \quad H_x(x) = H_x(-x)$$

$$E_y(x) = E_y(-x) \quad H_y(x) = -H_y(-x)$$

$$E_z(x) = E_z(-x) \quad H_z(x) = -H_z(-x)$$

$x > 0$

$x < 0$

$$\mathbf{J}_{a4}^*(x) = \zeta_e \mathbf{J}_{s3}(x) \quad v/m^2$$

$$\mathbf{J}_{a4}^*(x) = -\zeta_e \mathbf{J}_{s3}(x) \quad v/m^2$$

$$\mathbf{E}_4(x) = -\zeta_e \mathbf{H}_3(x) \quad v/m$$

$$\mathbf{E}_4(x) = \zeta_e \mathbf{H}_3(x) \quad v/m^2$$

$$\mathbf{H}_4(x) = \eta_e \mathbf{E}_3(x) \quad a/m$$

$$\mathbf{H}_4(x) = -\eta_e \mathbf{E}_3(x) \quad a/m$$

$$\eta_e^2 = \frac{1}{\zeta_e^2} = \frac{\epsilon}{\eta^2} = \frac{1}{\mu} \left(\epsilon_e + \frac{\sigma_e}{j\omega} \right) \text{ mho}^2$$

symmetry of an E -symmetric field that is excited by a symmetrical distribution of electric currents; an infinite sheet of electric conductor with a hole that has the same size and shape as the disk if the sheet is placed in the plane of symmetry of an E -symmetric field that is excited by an antisymmetric distribution of magnetic currents.

In a similar manner, it can be shown that a magnetic conducting disk in an electromagnetic field that is excited by symmetric magnetic currents is the dual of a similar hole in a magnetic conducting sheet located in a field that is generated by an antisymmetric distribution of electric currents. The arrangements for these two cases are shown in Fig. 3.

E. Terminology

Since several dual configurations may be defined for a given structure, it is desirable to label each type of network unambiguously. The circuit made of ordinary electrically conducting strips is the *actual electric circuit* or the *electric strip circuit*, the complementary circuit made of fictitious magnetic strips is the *fictitious magnetic circuit* or the *magnetic strip circuit*, and the complementary circuit obtained by cutting slots in a metallic

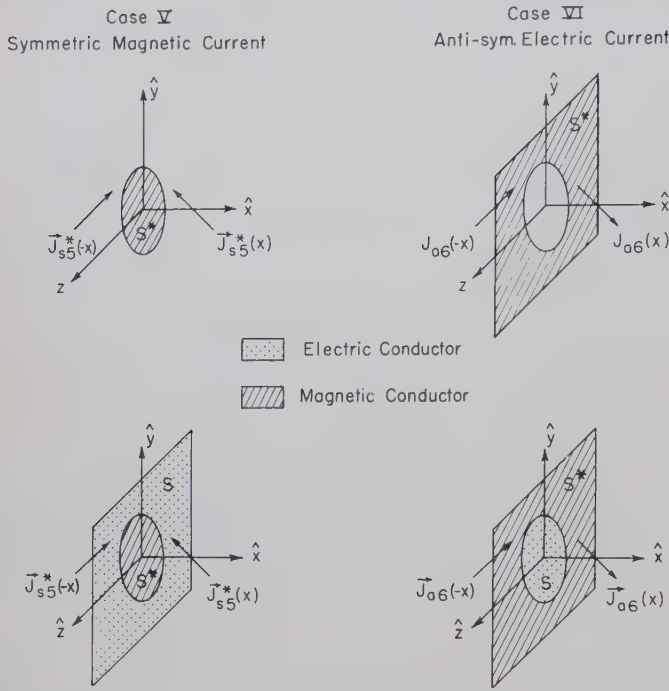


Fig. 3—Duality between magnetic disk and hole in magnetic screen.

Field: H -symmetry with respect to $x=0$ plane

$$E_x(x) = E_x(-x) \quad H_x(x) = -H_x(-x)$$

$$E_y(x) = -E_y(-x) \quad H_y(x) = H_y(-x)$$

$$E_z(x) = -E_z(-x) \quad H_z(x) = H_z(-x)$$

$$\begin{array}{ll} x > 0 \quad J_{as}(x) = -\eta_e J_{s5}^*(x) \quad a/m^2 & x < 0 \quad J_{as}(x) = \eta_e J_{s5}^*(x) \quad a/m^2 \\ E_s(x) = -\zeta_e H_s(x) \quad v/m & E_s(x) = \zeta_e H_s(x) \quad v/m \\ H_s(x) = \eta_e E_s(x) \quad a/m & H_s(x) = -\eta_e E_s(x) \quad a/m \end{array}$$

$$\eta_e^2 = \frac{1}{\zeta_e^2} = \frac{\epsilon}{\mu} = \frac{1}{\mu} \left(\epsilon_e + \frac{\sigma_e}{j\omega} \right) \text{ mho}^2$$

surface is the *slot circuit*. The dual obtained by replacing a given original configuration of conductors by its complement is called the *physical dual*. For example, a metallic disk is the physical dual of a hole of similar shape in a metallic screen and vice versa. A system of electric conductors and a similar system of magnetic conductors are *ideal* or *fictitious duals*. A magnetic strip is the ideal dual of a geometrically identical electric strip. A new set of quantities is needed for use in fictitious duals. These are given conventional names preceded by the word "magnetic." An asterisk is attached to the symbol for such a magnetic quantity for identification, as shown in Fig. 4.

The quantities used to describe a slot circuit are preceded by the word "complementary" and their symbols are primed to distinguish them from those for electric circuits. The complementary currents and charges are, of course, those maintained on the complementary conducting surfaces. Complementary quantities are listed in Fig. 4.

The duality between pairs of circuits and associated equations is illustrated in Fig. 4. Note that the quantities listed for the electric and magnetic strip circuits are duals. Corresponding quantities for the slot and the

magnetic strip circuits are not duals, but some of them are equivalent as indicated in parentheses.

F. Generalized Two-Slot Transmission-Line Theory

An ideal two-slot transmission line consists of two parallel slots that are cut in an infinitely thin, perfectly conducting sheet of infinite size (see Fig. 5). The ideal (although physically fictitious) dual consists of two parallel thin strips, made of a perfect magnetic conductor, that lie in the xy -plane, symmetrically located with respect to the x -axis and with their centers separated by a distance b . If the width a of the strip satisfies the inequalities, $\beta_0 a \ll 1$, $b^2 \gg a^2$, it is proper to define a total axial magnetic current and a total magnetic charge per unit length and to assume that their transverse distributions are approximately symmetrical with respect to the center of each strip. In order to make radiation negligible, the condition $(\beta_0 b)^2 \ll 1$ is imposed.

At distances from both ends of the transmission line that are large compared with the separation b of the strips, the following relations¹ are obtained for the magnetic scalar and vector potential differences $V^*(w)$ and $W_x^*(w)$. The same formulas apply to the electric potentials if the asterisks are omitted.

$$\frac{\partial^2}{\partial w^2} V^*(w) - \gamma_0^{*2} V^*(w) = 0, \quad (12a)$$

$$\frac{\partial^2}{\partial w^2} W_x^*(w) - \gamma_0^{*2} W_x^*(w) = 0, \quad (12b)$$

$$I_x^*(w) = \frac{1}{\gamma_0^*} \frac{\partial}{\partial w} V^*(w) \quad (13)$$

where $\gamma_0^{*2} = \gamma_0^* \gamma_0^*$. The magnetic line constants (with asterisk) and their electric duals are summarized as follows:

$$\begin{aligned} z_0^* &= r_0^* + j\omega l_0^* = (j\omega\epsilon/\pi) \ln(b/a), \\ z_0 &= (j\omega\mu/\pi) \ln(b/a); \end{aligned} \quad (14a)$$

$$\begin{aligned} y_0^* &= j\omega c_0^* = (j\omega\mu\pi)/\ln(b/a), \\ y_0 &= g_0 + j\omega c_0 = (j\omega\pi\epsilon)/\ln(b/a). \end{aligned} \quad (14b)$$

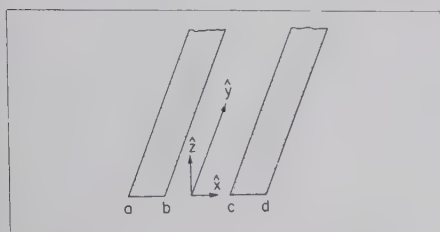
Note that $\epsilon = \epsilon_e - j\sigma_e/\omega$. The magnetic potentials $V^*(w)$ and $W_x^*(w)$ for the ideal dual of the two-slot line satisfy the conventional transmission-line equations just as do the potentials $V(w)$ and $W_x(w)$ for the two-wire line. The line constants for the magnetic strips are similar to those for electric strips. The approximate solution for the magnetic current and scalar potential difference may be obtained with a corrective terminal-zone network as for a two-wire line.²

Equivalent circuits of the magnetic strip line and the slot line are shown in Fig. 6.

¹ R. W. P. King, "Transmission-Line Theory," McGraw-Hill Book Co., Inc., New York, N. Y., p. 13; 1955.

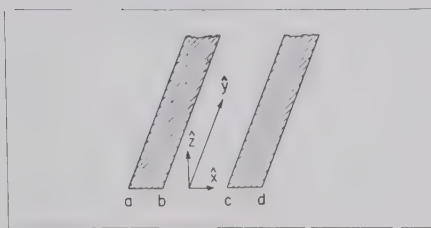
² *Ibid.*, p. 58.

Electric Circuit or Electric Strip Circuit



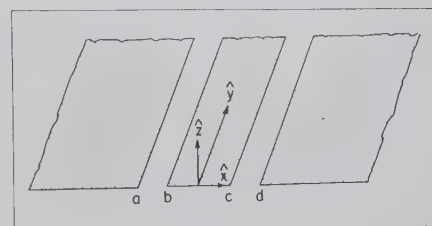
Original (or Physical Dual)

Fictitious Magnetic Circuit or Magnetic Strip Circuit



Ideal or Fictitious Dual

Slot Circuit



Physical Dual (or Original)

Field: E -symmetry with respect to $z=0$ plane E -field \mathbf{E} v/m H -field \mathbf{H} a/m Current Density (Volume) \mathbf{J} a/m^2 Current Density (Surface) \mathbf{K} a/m Charge Density (Volume) ρ as/m^3 Charge Density (Surface) η as/m^2

Potential Difference

$$V = \int_b^c \mathbf{E} \cdot d\mathbf{x} \quad v$$

Current

$$I_y = \int_c^d \hat{n} \times \mathbf{H} \cdot d\mathbf{x} = - \int_c^d K_y dx \quad a$$

Impedance

$$z = \frac{V}{I} \quad \text{ohm}$$

Capacitance per unit length

$$c \quad f/m$$

Inductance per unit length

$$l \quad h/m$$

Field Equations: Boundary Conditions:

$$\nabla \times \mathbf{H} = \mathbf{J} + j\omega\epsilon\mathbf{E} \quad \hat{n} \times \mathbf{H} = -\mathbf{K}$$

$$\nabla \times \mathbf{E} = -j\omega\mu\mathbf{H} \quad \hat{n} \times \mathbf{E} = 0$$

$$\nabla \cdot \mathbf{H} = 0 \quad \hat{n} \cdot \mathbf{H} = 0$$

$$\nabla \cdot \mathbf{E} = \frac{1}{\epsilon} \rho \quad \hat{n} \cdot \mathbf{E} = \frac{-1}{\epsilon} \eta$$

Potential Functions:

$$\mathbf{H} = \frac{1}{\mu} \nabla \times \mathbf{A}$$

$$\mathbf{A} = \frac{\mu}{4\pi} \int_v \mathbf{J} K_0 d\tau'$$

$$\mathbf{E} = -\nabla\phi - j\omega\mathbf{A}$$

$$\phi = \frac{1}{4\pi\epsilon} \int_v \rho K_0 d\tau'$$

$$\text{where } \epsilon = \epsilon_0 + \frac{\sigma_0}{j\omega}, \quad K_0 = \frac{1}{R} e^{-j\beta_0 R}, \quad R^2 = (x-x')^2 + (y-y')^2 + (z-z')^2$$

Field: H -symmetry with respect to $z=0$ planeMagnetic E -field $\mathbf{E}^*(=\mathbf{H}')$ a/m Magnetic H -field $\mathbf{H}^*(=\mathbf{E}')$ v/m Magnetic Current Density (Volume) \mathbf{J}^* v/m^2 Magnetic Current Density (Surface) \mathbf{K}^* v/m Magnetic Charge Density (Volume) ρ^* vs/m^3 Magnetic Charge Density (Surface) η^* vs/m^2

Magnetic Potential Difference

$$V^* = \int_b^c \mathbf{E}^* \cdot d\mathbf{x} (=I') \quad a$$

Magnetic Current

$$I_y^* = \int_c^d \hat{n} \times \mathbf{H}^* \cdot d\mathbf{x} = \int_c^d K_y^* dx (=V') \quad v$$

Magnetic Impedance

$$z^* = \frac{V^*}{I^*} (=y') \quad \text{mho}$$

Magnetic Capacitance per unit length

$$c^*(=l') \quad h/m$$

Magnetic Inductance per unit length

$$l^*(=c') \quad f/m$$

Field Equations: Boundary Conditions:

$$\times = -\mathbf{J}^* - j\omega\mu\mathbf{E}^* \quad \hat{n} \times \mathbf{H}^* = \mathbf{K}^*$$

$$\nabla \times \mathbf{E}^* = j\omega\epsilon\mathbf{H}^* \quad \hat{n} \times \mathbf{E}^* = 0$$

$$\nabla \cdot \mathbf{H}^* = 0 \quad \hat{n} \cdot \mathbf{H}^* = 0$$

$$\nabla \cdot \mathbf{E}^* = \frac{1}{\mu} \rho^* \quad \hat{n} \cdot \mathbf{E}^* = \frac{-1}{\mu} \eta^*$$

Magnetic Potential Functions:

$$\mathbf{H}^* = \frac{-1}{\epsilon} \nabla \times \mathbf{A}^*$$

$$\mathbf{A}^* = \frac{\epsilon}{4\pi} \int_v \mathbf{J}^* K_0 d\tau'$$

$$\mathbf{E}^* = -\nabla\phi^* - j\omega\mathbf{A}^*$$

$$\phi^* = \frac{1}{4\pi\mu} \int_v \rho^* K_0 d\tau'$$

Field: E -symmetry with respect to $z=0$ planeComplementary H -field $\mathbf{H}'(=\mathbf{E}^*)$ a/m Complementary E -field $\mathbf{E}'(=\mathbf{H}^*)$ v/m Complementary Current Density (Volume) \mathbf{J}' a/m^2 Complementary Current Density (Surface) \mathbf{K}' a/m Complementary Charge Density (Volume) ρ' as/m^3 Complementary Charge Density (Surface) η' as/m^2

Complementary Current

$$I_y' = \int_b^c \hat{n} \times \mathbf{H}' \cdot d\mathbf{x} = - \int_b^c K_y' dx (=V^*) \quad a$$

Complementary Potential Difference

$$V' = \int_c^d \mathbf{E}' \cdot d\mathbf{x} (=I^*) \quad v$$

Complementary Transverse Admittance

$$y' = \frac{I'}{V'} (=z^*) \quad \text{mho}$$

Complementary Inductance per unit length

$$l' (=c^*) \quad h/m$$

Complementary Transverse Capacitance per unit length

$$c' (=l^*) \quad f/m$$

Field Equations: Boundary Conditions:

$$\nabla \times \mathbf{H}' = \mathbf{J}' + j\omega\epsilon\mathbf{E}' \quad \hat{n} \times \mathbf{H}' = -\mathbf{K}'$$

$$\nabla \times \mathbf{E}' = j\omega\mu\mathbf{H}' \quad \hat{n} \times \mathbf{E}' = 0$$

$$\nabla \cdot \mathbf{H}' = 0 \quad \hat{n} \cdot \mathbf{H}' = 0$$

$$\nabla \cdot \mathbf{E}' = \frac{1}{\epsilon} \rho' \quad \hat{n} \cdot \mathbf{E}' = \frac{-1}{\epsilon} \eta'$$

Complementary Potential Functions:

$$\mathbf{H}' = \frac{1}{\mu} \nabla \times \mathbf{A}'$$

$$\mathbf{A}' = \frac{\mu}{4\pi} \int_v \mathbf{J}' K_0 d\tau'$$

$$\mathbf{E}' = -\nabla\phi' - j\omega\mathbf{A}'$$

$$\phi' = \frac{1}{4\pi\epsilon} \int_v \rho' K_0 d\tau'$$

Fig. 4—Complementarity between strip and slot circuits.

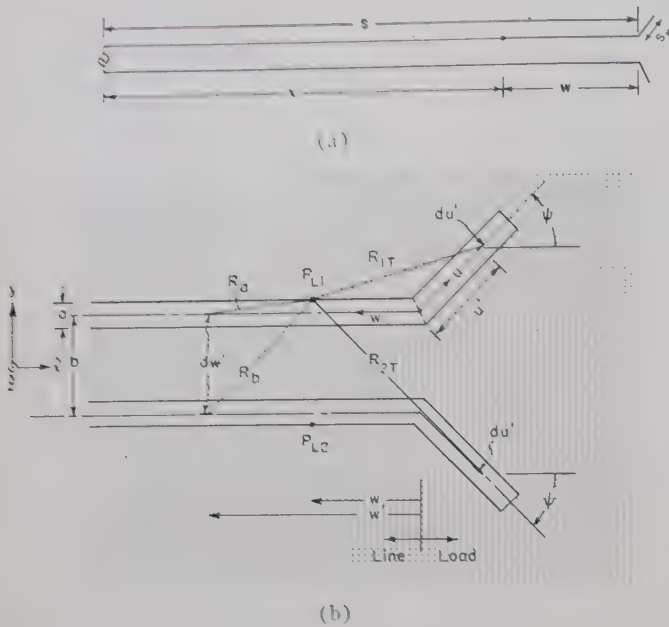


Fig. 5—Arrangement of a two-slot line.

where $K(k)$ is the complete elliptic integral of the first kind, $k = a_0/b_0$ is the modulus, $k'^2 = 1 - k^2$, $2a_0$ is the distance between the inner edges of the strips, and $2b_0$ is the distance between the outer edges of the strips. Subject to the condition that the width of the strips is very small compared to the distance between centers so that $a_0 \approx b_0$, the characteristic impedance is approximately

$$Z_{1c} \approx (\mu_0/\epsilon_0)^{1/2} \pi^{-1} \ln (4\Delta/\delta), \quad (16)$$

where $\delta = b_0 - a_0$ is the width of the strip and $\Delta = b_0 + a_0$ is the distance between their centers. From transmission-line theory, the characteristic impedance of a two-wire line of circular conductors is

$$Z_{2c} = (\mu_0/\epsilon_0)^{1/2} \pi^{-1} \ln (b/a) \quad (17)$$

where b is the distance between the centers of the wires and a is the radius of each. The two strip line evidently behaves like a two-wire line with the same distances between the centers of the conductors and with wires of radius equal to one-quarter the width of the strips.

II. EXPERIMENTAL STUDY OF THE TWO-SLOT TRANSMISSION LINE

A. The Equipment

The two-slot transmission line is bounded by three pieces of aluminum sheet and an aluminum strip. The ground plane has the over-all dimensions of 6 feet 2 inches by 12 feet 1 inch; it is supported horizontally by a wooden framework at a height about halfway between the floor and the ceiling. The thickness of the aluminum is $\frac{1}{4}$ inch; the center strip is $\frac{1}{2}$ inch by $\frac{1}{4}$ inch in cross section, $7\frac{1}{2}$ feet in length, and supported by a tapered strip of polystyrene that rests on a wooden support.

Several driving devices for the two-slot line were tested. A two-wire line drive [see Fig. 7(a)] was found to be unsatisfactory since the slotted ground plane is an unsymmetrical load that unbalances the two-wire line and causes undesirable radiation. A microstrip drive [see Fig. 7(b)] has the advantage of simplicity in construction and compactness. It consists of a conductor separated from the ground plane by a thin sheet of dielectric. The conductor can be either a flat strip or a wire of small diameter. This conductor is connected to the center-strip of the two-slot line. A coaxial-line drive [see Fig. 7(c)] consists of a piece of coaxial line with its outer conductor deformed into a rectangular shape so that it will fit smoothly onto the ground plane. A $\frac{1}{2}$ -inch by $\frac{1}{4}$ -inch waveguide was found to be suitable for the outer conductor; a $\frac{3}{8}$ -inch diameter brass rod was used as the inner conductor. Two short-circuiting plungers, one on each side of the point of feeding, were provided for matching.

Two different probing systems were employed in the research: the surface-probe system and the enclosed probe system. The surface-probe system consists of a carrier mounted on and movable along a cross-beam,

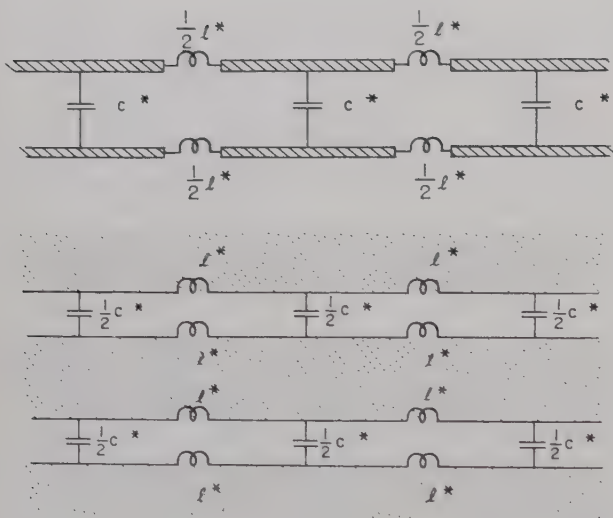


Fig. 6—Equivalent circuits of a two-slot line; diagonal shading indicates magnetic conductors, dots indicate electric conductors.

G. Conclusion

A parallelism between the two-slot line and the two-strip line has been established. Consequently, the well-known solution of the two-wire line equations, as well as complementary measuring techniques, may be applied to the two-slot line. The line parameters that have been derived are true for infinitely thin slots. However, it can be shown⁸ that the characteristic impedance Z_{1c} of a very thin two-strip line is given by

$$Z_{1c} = (l/c)^{1/2} = (\mu_0/\epsilon_0)^{1/2} K(k)/K(k'), \quad (15)$$

⁸ G. H. Owyang and T. T. Wu, "The approximate parameters of slot lines and their complements," IRE TRANS. ON ANTENNAS AND PROPAGATION, vol. AP-6, pp. 49-55; January, 1958.

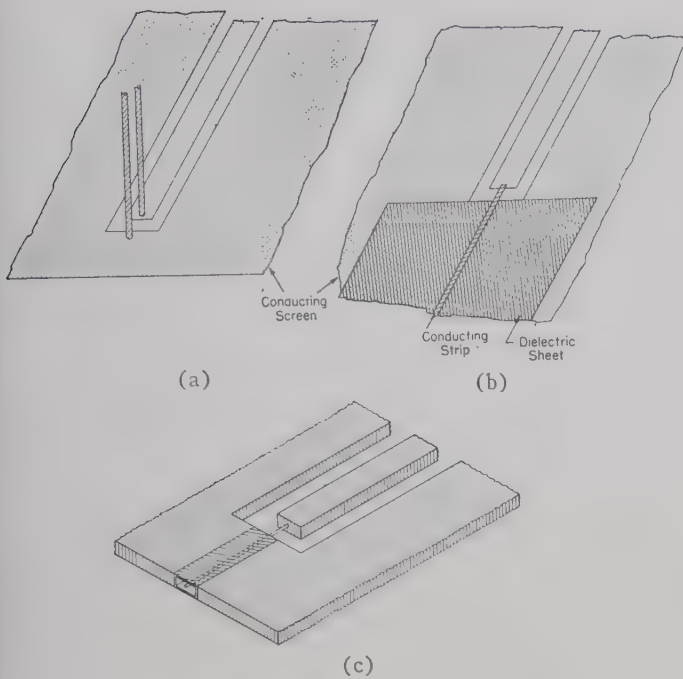


Fig. 7—Methods of driving a two-slot line.

the supporting structure of which rolls on circular steel tracks which are mounted along the sides of the wooden framework. The connection from the probe carrier to the probe is made by a section of stiff transmission line which consists of a piece of a $\frac{1}{4}$ -inch O.D. brass tubing slipped over a RG-58 coaxial cable. This brass tubing is threaded and slotted at the upper end to provide a height adjustment.

The enclosed-probe system consists of a movable probe that projects through a slot in a waveguide ($\frac{1}{2}$ inch by $\frac{1}{4}$ inch) which forms the edge of the aluminum sheet. In this system, only the probe itself is exposed to the field to be measured; the connection to the probe and the driving mechanism are either shielded or far away from the point where the measurement is being made. Thus the disturbance caused by the presence of the probing system is minimized and, in addition, the degree of flatness of the metallic sheets has little effect on the signal picked up by the probe.

B. Balancing the Two-Slot Transmission Line

An efficient transmission line should radiate little power. It is well known in two-wire line theory that unbalanced currents radiate. This is also true of a two-slot line in which the currents on the two side plates are unequal at corresponding points. A simple method to determine whether a two-slot line is balanced or not is to record the response of the detector while the probe is moved perpendicularly across the line. The response curve should be symmetrical with respect to the line if a balanced condition is maintained. However, the symmetry of the measured response curve may be affected by the slight variation in the flatness of the ground screen so that an alternative method is desirable.

It is very difficult, if not impossible, to obtain two exactly identical probes; therefore, the direct comparison of the signals picked up by two probes in the two slots will give little information about the condition of balance of the line. With two probes which have slightly different gains, the symmetry of the line current may be determined by the method of cancellation. This is accomplished by adjusting the phases of the signals from the two probes so that the transmission-line modes are opposite in phase while the radiation modes, if they exist, are in phase. Thus a constant resultant signal along the line means that the line is balanced, and the existence of a standing wave in the resultant signal along the line indicates the presence of an unbalanced current in a radiation mode. The probes used are those enclosed in the edges of the two sideplates. These probes are placed at a cross section where the field is strong and are tuned for maximum signal separately by adjusting the tuning stubs. The reading on the variable standard attenuator is recorded. The two circuits are then joined together through a tee with a line stretcher inserted in one probe-circuit. The line stretcher is adjusted for minimum signal and the attenuation of the standard attenuator is reduced to increase the sensitivity of the detector. One of the double-stub tuners may also be adjusted if it helps to decrease the signal. This procedure may be repeated until a true minimum is obtained. The probes are then moved simultaneously along the entire line and the detected signal is noted. Negligible variations in the minimum signal were observed and this minimum signal was more than fifty decibels below (almost noise level) the signal level of either one of the probes. A short piece of lossy cable is inserted in each probe circuit to reduce the possible coupling between the probes.

C. The Transverse Distribution of the Longitudinal Current on a Two-Slot Line

The transverse distribution of the longitudinal current on the metallic surface bounding the two-slot line is measured by moving a surface probe in the direction perpendicular to the slots. The probe is of the shielded-loop type and is oriented with the normal to the plane of the loop parallel to the direction of its movement. Owing to the fact that a loop probe measures the average flux encircled by it, a rectangular loop with round, curved, short sides is used. A loop of such shape has an advantage over a circular loop in being able to measure the average field of a point closer to the metal surface with the same clearance between the probe and the surface. Both the amplitude and the phase of the current are shown in Fig. 8.

The current in the center strip is opposite in phase to that in the side plates and the currents in the two side plates are in phase. The measurements show the current to be concentrated near the edges as expected. The measured apparent decrease in current toward the axis of the center strip is very sensitive to the height of the

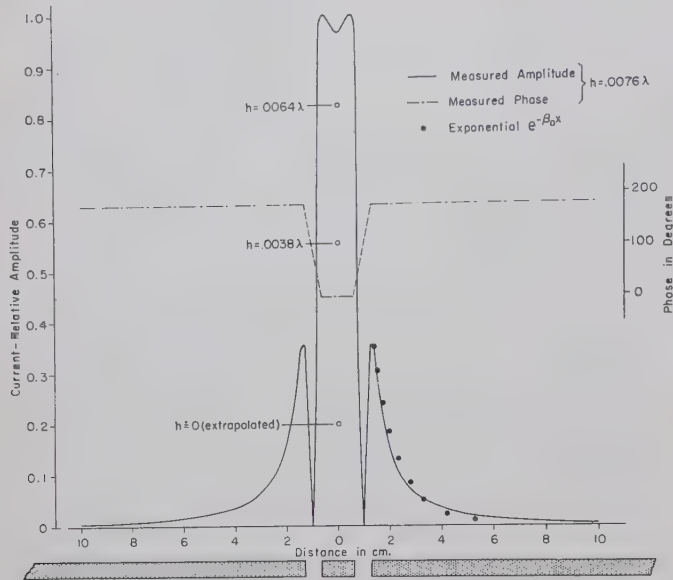


Fig. 8—Distribution of longitudinal current in a two-slot line

probe. If the maximum amplitude of the longitudinal current is denoted by I_m , the amplitude of the current along the center line of the center strip by I_c , and the distance between the center of the loop probe to the conducting surface by h , then the observed results are as follows:

h	0.0038λ	0.0064λ	0.0076λ
$\frac{I_c}{I_m}$	0.55	0.82	0.98

At $h=0.0038 \lambda$, the loop is almost in contact with the conducting surface. If these current ratios are plotted against the distance h and the curve so obtained is extrapolated to the point $h=0$, it is found that the ratio I_c/I_m of the surface current density in the center strip is approximately 0.20. From the distribution of the electromagnetic field it is expected that I_c/I_m has a minimum at the center of the strip and the measurements do verify this fact. Qualitatively, one could imagine the two-slot line to be roughly equivalent to a coplanar four-conductor transmission line. The four conductors are located near the edges of the conducting sheets and the strip. The total currents in the inner two conductors are equal in amplitude and phase; they are equal in amplitude as those in the outer two conductors, but opposite in phase. The current on the side plates decays very rapidly as the distance from the slot increases. This current drops below one-half of one per cent of the peak value within one-quarter of a wavelength from the center of the center strip. It is interesting to note that this decay is almost exponential with distance.

Owing to the nonuniformity in the amplitude of the field configuration, it is not possible to measure the transverse distribution of the transverse current by simply rotating the loop-probe ninety degrees from the position used for measuring the longitudinal current. In this position the loop may respond in its transverse di-

pole mode to the large E -field in addition to the usual response to the magnetic (or differential electric) field. This was verified by repeating the measurement with a dipole probe with the axis of the dipole perpendicular to the slot; a curve similar to that obtained with the loop probe was obtained.

D. The Measurement of the Attenuation Constant

It is usually very difficult to measure the attenuation constant of a low-loss transmission line. However, if the location of the probe can be measured very accurately along the line, then the method based upon the width of the distribution curve near its minimum is applicable. This method involves the determination of the width Δw_n of the distribution curve at a convenient power level p (usually $p^2=2$ is chosen) above the minimum point at two different locations, w_n and w_{n+m} . The value of the attenuation constant α is given by⁴

$$\alpha = \frac{\beta}{2(p^2 - 1)^{1/2}} \frac{\Delta w_n - \Delta w_{n+m}}{w_n - w_{n+m}} \text{ nepers per meter.} \quad (18)$$

In the evaluation of the attenuation constant, the portion of the distribution curve near the minimum point is plotted out completely and then extended to locate the minimum. The width of the curve is measured at a power level $p^2=2$ above this minimum. The relative probe position Δw_n is determined by means of two dial-indicators. These dial-indicators are provided with 0.001-inch graduation. The actual location of the point of minimum is not very critical since the value of $(w_n - w_{n+m})$ is of the order of meters.

The measured value of the attenuation constant of the two-slot transmission line is 3.41×10^{-3} nepers per meter which is of the same order of magnitude as that of a two-wire transmission line.

III. MEASUREMENT OF THE PARAMETERS OF THE TWO-SLOT LINE BY THE METHOD OF ANALOGY

A. Introduction

As a substitute for the mathematical analysis of a field problem, the method of field mapping by analogy is useful when the particular field in question is too complicated for rigorous mathematical treatment. It is based upon the correspondence between the steady current field maintained by two oppositely charged electrodes immersed in a homogeneous conducting medium and the electromagnetic field surrounding two similar conductors of infinite length carrying equal and opposite currents.

Since the potential functions ϕ_c in a conductor and ϕ_d in a dielectric both satisfy Laplace's equation, and since the normal components of the electric fields E_c at the boundary between two conductors and E_d at the boundary between two dielectrics satisfy conditions that differ only by a constant factor, it follows that these two cases are analogous. By taking the ratio of the total

⁴ King, *op. cit.*, p. 275.

current passing through a volume in a conducting medium, which is bounded by lines of the electric field and two equipotential surfaces at arbitrary points, and the total dielectric flux in a similarly-bounded volume in a dielectric medium, the total capacitance C_d between the equipotential surfaces in the dielectric may be related to the total resistance R_c between the equipotential surfaces in the conducting medium as follows:

$$\frac{\epsilon_d}{\sigma_c} = C_d R_c. \quad (19)$$

It is assumed that the potential differences between the equipotential surfaces in the two cases are equal. ϵ_d is the complex permittivity of the dielectric, σ_c is the conductivity of the conducting medium.

One method of utilizing the analogy between the electric field in a conductor and the electric field in a dielectric is by means of the current distribution in an electrolytic tank filled with a conducting liquid. The electrodes to be investigated are immersed in the liquid and a probe and a bridge-circuit are used to locate the equipotential lines. The orthogonal stream lines are drawn in afterwards to complete the field map. The capacitance C between two electrodes in vacuum may be evaluated from the following formula:

$$C = \epsilon_0 \frac{Q}{V} = \frac{\epsilon_0 \oint_{1c} E_n(s) ds}{\int_{bc} \mathbf{E} \cdot d\mathbf{s}}, \quad (20)$$

where ϵ_0 is the dielectric constant in vacuum, Q is the total charge on one conductor, V is the potential difference between the conductors, E_n is the normal component of the E -field on the surface of the conductor, \oint_{1c} is the contour-integral taken around the surface of one conductor, and \int_{bc} is the line-integral taken between the two conductors.

The magnitude of the electric field \mathbf{E} at any point may be determined from a field plot by drawing a stream line through the point in question, and dividing the potential difference between two equipotential lines lying equal distances from each side of the point by the length of the stream line between them. This method gives good results if the equipotential lines are closely spaced. The normal components of the electric field E_n on the surfaces of the conductor may be obtained by first determining in this manner the value of the E -field along a stream line at several points at different distances from the surface. These values are then plotted against their respective distances from the surface and the curve through them extrapolated to zero distance. Since the electric lines terminate perpendicularly at the conducting surface, the values so obtained are the desired normal components of the electric field. It is usually unnecessary to evaluate the line integral in the denominator of (20), since the potential difference between the electrodes can easily be normalized to unity. Thus, the

capacitance between two electrodes may be obtained from the distribution of the field and (20) by numerical integration.

The substitution of (19) into $LC = \mu_0 \epsilon_0$ leads to the following relation:

$$L = \mu_0 R_c \sigma_c. \quad (21)$$

Thus, the inductance of two conductors immersed in a dielectric may be obtained from the resistance between the same conductors immersed in another conducting medium.

The attenuation constant of a system of two conductors may be computed from the field distribution in the following manner. If δI is the current carried by an element of surface of width δs on a conductor and of unit length in the direction of propagation, then the total ohmic loss per unit length in both conductors is given by

$$P_L = \frac{R^s}{\zeta_0^2} \oint_{c1} E_n^2 ds + \frac{R^s}{\zeta_0^2} \oint_{c2} E_n^2 ds, \quad (22)$$

where the surface resistance

$$R^s = \left(\frac{\pi f \mu}{\sigma} \right)^{1/2}, \quad \zeta_0^2 = \frac{\mu_0}{\epsilon_0}$$

is the free-space wave impedance and $\mathbf{E} = \zeta_0 \mathbf{H}$ is used. The contour integrals \oint_{c1} and \oint_{c2} are to be taken around the surfaces of the two conductors, no. 1 and no. 2, respectively. If V is the potential difference between the conductors, then the power transmitted is given by

$$P = VI = \frac{V}{\zeta_0} \oint_{1c} E_n ds. \quad (23)$$

The attenuation constant caused by the ohmic loss in the conductors is, therefore, given by

$$\alpha = \frac{1}{2} \frac{P_L}{P} = \frac{R^s}{2V} \frac{\oint_{c1} E_n^2 ds + \oint_{c2} E_n^2 ds}{\zeta_0 \oint_{1c} E_n ds}. \quad (24)$$

Thus, the attenuation constant is expressed in a form which can be evaluated from the distribution of the field in the conductors. The integrals involved are similar to those in (20) and (21).

B. Measurements in the Electrolytic Tank

The analogous electromagnetic field of the two-slot line was measured in the Harvard Electrolytic Tank, which has been described in detail.⁵

In order to determine the field of the two-slot line with the electrolytic tank, it was necessary to construct a model electrode that had the same cross-sectional view as the two-slot line. Since there is no current crossing the vertical plane of symmetry of the structure, either the

⁵ P. A. Kennedy and G. Kent, "The Electrolytic Tank," Harvard University, Cambridge, Mass., Cruft Lab. Tech. Rept. No. 214; 1956.

right or the left half may be removed if an insulating wall is placed along the vertical plane of symmetry. For the same reason, the lower half of the transmission line may be omitted when an insulating wall is placed along the horizontal plane of symmetry, that is, in the slot at a distance one-half the thickness of the conductor from the surface. Thus, only one-fourth of the cross section of the actual two-slot line is required. The model [see Fig. 9(d)] was used to obtain the distribution of the H' -field of a two-slot line.

It was also desired to obtain the distribution of the E -field of the complementary two-strip line. This could be constructed from the distribution of the H -field of a model which had the same cross-sectional view as the actual two-strip line [see Fig. 9(a)]. However, the distribution of the E -field could also be obtained directly from the electrolytic tank by using conjugate electrodes.

The conjugate electrodes are obtained from the original electrodes [see Fig. 9(a)] by using insulators in place of conductors.⁶ These are joined together by a thin insulating wall along the horizontal plane of symmetry [see Fig. 9(b)]. A thin conducting surface is placed on each side of this insulating wall where the excitation is applied. Evidently the lines of the current maintained by the conjugate electrodes are orthogonal to those of the original electrodes.

It can be shown that the magnetic field H_1 maintained with two conducting electrodes immersed in an electrolyte and the electric field E_2 of the conjugate electrodes immersed in the same electrolyte satisfy the same field equation and boundary conditions. Therefore, these two fields are analogous to each other and, consequently, the conjugate electrodes may be used to obtain the distribution of the conjugate field of the original electrodes in the electrolytic tank.

By symmetry, the right half of the conjugate electrode [see Fig. 9(b)] may be removed if an insulating wall is erected along the vertical plane of symmetry. Similarly, the lower half may be removed if a conducting surface is placed at the horizontal plane of symmetry. A conducting surface is required here because the stream lines are normal to this plane. The conjugate model is reduced to its final form as shown in Fig. 9(c).

It is interesting to note that the two models, one for measuring the complementary H' -field of the two-slot line [Fig. 9(d)] and the other for measuring the electric field of the two-strip line [Fig. 9(c)], differ only to the extent in which the insulator protrudes out of the conducting surface. In the cases when the conductors are infinitely thin, these two models become identical. Therefore, the same model may be used to measure either the distribution of H' -field of a two-slot line or the distribution of the E -field of a complementary two-strip line by using different insulating inserts.

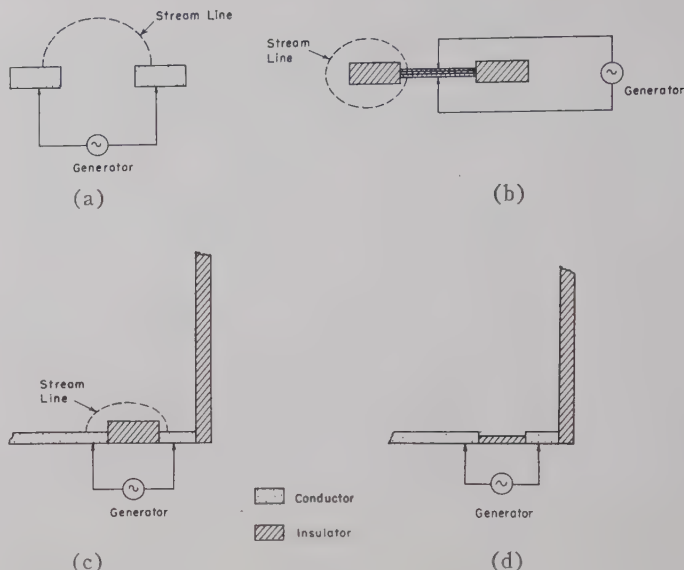


Fig. 9. Two-strip line model and its conjugate model.

In carrying out the measurements in the electrolytic tank, the equipotential lines are plotted directly and the stream lines are then drawn in. An easy way of constructing the orthogonal curves is to construct auxiliary circles⁷ (see Fig. 10) between the equipotential lines first, and then to draw curves tangent to those circles and perpendicular to the equipotential lines. Circle-templates are found to be very helpful for this purpose and a reasonably good curvilinear graph usually may be obtained the second trial. A typical example of such a graph is shown in Fig. 10.

The distribution of the field around the two-slot line was obtained by the method mentioned above. The normal component of the electric field at the surface of the electrode was evaluated according to the method described in Section III-A. The capacitance per unit length, the inductance per unit length and the attenuation constant of the two-slot line were computed from (20), (21), and (24) by numerical integrations. These values are listed in Table I.

The capacitance per unit length and the inductance per unit length of the two-slot line were also determined by measuring the resistance between the corresponding electrodes [see (19) and (20)].

The conductivity of the electrolyte may be determined from the measured resistance between the inner and the outer conductor of a model of a coaxial line filled with a known quantity of electrolyte. The leakage conductance per unit length g of a coaxial cable is given by⁸

$$g = \frac{2\pi\sigma}{\ln \frac{a_2}{a_1}}, \quad (25)$$

⁶ E. Weber, "Electromagnetic Fields," John Wiley and Sons, Inc., New York, N. Y., vol. 1, p. 186; 1950.

⁷ John F. H. Douglass, "Electric, Magnetic, and Thermal Field," vol. 1; and "Experimental Graphical Methods: Mapping," published by the author, ch. 3, p. 3-1, 1953.

⁸ King, *op. cit.*, p. 22.

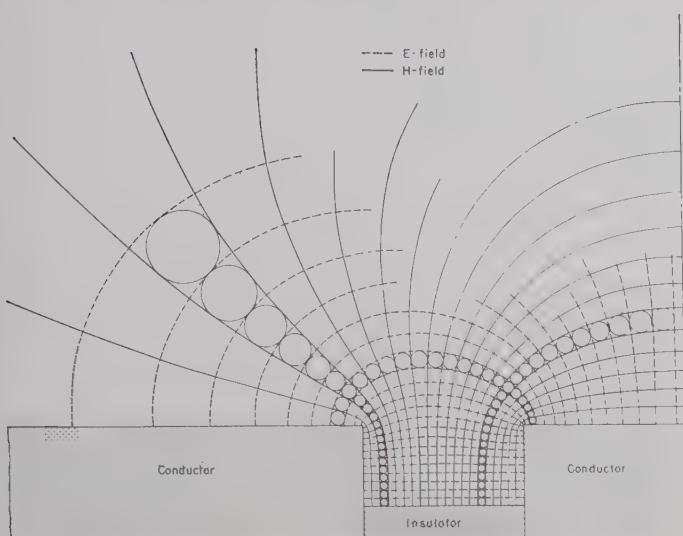


Fig. 10—A typical distribution of the field around a two-slot line.

TABLE I
LINE CONSTANTS OF TWO-SLOT LINE

	$\alpha \cdot 10^{-3}$ nepers/m	c $\mu\text{mf}/\text{m}$	l $\mu\text{h}/\text{m}$
<i>Thin Metal Model:</i>			
Theoretical—Analogy from King, "Transmission-line Theory"	—	20.2	0.55
Theoretical—Wu and Owyang*	1.28	27.75	0.402
Electrolytic Tank—Flux Plot	—	26.7	0.416
Electrolytic Tank—Resistance Measurement	—	29.8	0.373
<i>Thick Metal Model:</i>			
Theoretical—Corrected for Thickness (King)†	—	37.9	0.293
Theoretical—Corrected for Thickness (Wu and Owyang*)	—	44.45	0.246
Measurement at 750 mc	3.14	—	—
Electrolytic Tank—Flux Plot	4.21	49.4	0.227
Electrolytic Tank—Resistance Measurement	—	53.5	0.208

* T. T. Wu, and G. H. Owyang "The approximate parameters of slot lines and their complements, IRE TRANS. ON ANTENNAS AND PROPAGATION, vol. AP-6, pp. 49-55; January, 1958.

† The correction for the width of the slot is not included.

where a_2 and a_1 are the radii of the outer and the inner conductors, respectively, and σ is the conductivity of the material between these conductors. By rearranging (25) and multiplying the numerator and the denominator by the factor $(a_2^2 - a_1^2)$, the conductivity σ of the medium can be expressed as

$$\sigma = \frac{1}{RV_0} (a_2^2 - a_1^2) \ln \frac{a_2}{a_1}, \quad (26)$$

where R is the resistance between the inner and the outer conductors and V_0 is the volume occupied by the medium between these conductors. The volume V_0 is introduced in (26) because it is easier to fill the coaxial-line model with a definite amount of electrolyte than to measure the depth of the liquid inside the model.

With the conductivity of the electrolyte and the resistance between the electrodes of the two-slot line

model determined, the capacitance per unit length and the inductance per unit length may be computed from (19) and (21). These values are listed in Table I.

C. Conclusion

Both the theoretical and the experimental values of the two-slot line parameters are tabulated in Table I. Despite the fact that none of the conditions required by the theoretical analysis is fulfilled exactly by the actual model under consideration, the two sets of values are not too far apart. The discrepancies are caused both by the degree in which the ideal theoretical model is approximated and by the experimental errors. In the theoretical analysis it is required that the width of the slot be very small compared with the separation and that the metal sheet be relatively thin. The actual line has a separation of only three times the width of the slot which is the same as the thickness of the metal sheet.

The theoretical capacitance per unit length for a thin conducting sheet may be corrected for the case of a thick plate, since the total capacitance consists of the contribution from the top and the bottom surface of the conductor and from the surfaces inside the slots. This involves adding twice the capacitance of two parallel surfaces of unit length with a width equal to the thickness of the plate and a separation equal to the width of the slot. It follows from (20) and (21) that the corrected inductance per unit length may be obtained by multiplying the theoretical value by the ratio of the capacitance due to the surfaces inside the slots and the total capacitance. These values are also tabulated in Table I.

In the evaluation of the line parameters by the method of field mapping, errors may be introduced in the process of measurement, construction of orthogonal curves, evaluation of the E -field (this involves both graphical errors and errors in the approximation), extrapolation of the curves, and the numerical integration of the formulas. If only 1.5 per cent of error is introduced in each of the above possible sources, 9 per cent of error is possible in the final result. By using a larger model, a larger tank, a larger map, and a greater amount of labor, the accuracy of this method may be improved.

The distribution of the electric field about a two-strip line has also been measured by means of conjugate electrodes. This was found to coincide with the distribution of the H -field of the physical dual at distances that are greater than approximately one-half the width of the conductor away from the strip. This indicates that the principle of complementarity^{9,10} may be applicable without appreciable error even when the metallic screen has a finite thickness, if a small region near the strip or the complementary slot is excluded.

⁹ H. G. Booker, "Slot aerials and their relation to complementary wire aerials—Babinet's principle," *J.I.E.E. (London)*, vol. 93, pt. III A, no. 4, pp. 620-625; 1946.

¹⁰ S. Uda and Y. Mushiaki, "The input impedances of slit antennas," *The Technology Reports of the Tohoku University*, vol. 14, no. 1, p. 46; 1949.

High Resolution Millimeter Wave Fabry-Perot Interferometer*

WILLIAM CULSHAW†

Summary—The design and operation of a microwave Fabry-Perot interferometer at wavelengths around 6 mm is described. This uses reflectors which are simple, easy to make, and which are capable of scaling for operation at short wavelengths in the ultramicrowave region. With power reflection coefficients around 0.999, very sharp fringes and Q values around 100,000 were obtained on the interferometer. Effects of diffraction in the interferometer are considered, and wavelength measurements with this particular interferometer indicate that accuracies of 0.04 per cent are obtained without any diffraction correction. Advantages of such an interferometer for ultramicrowaves are that the component parts are large compared with the wavelength, the effects of diffraction decrease with the wavelength, and the problem of maintaining a high Q with a single mode of propagation and a structure of adequate size is made much easier. Such an interferometer forms the cavity resonator for ultramicrowaves. It can thus be used for such conventional purposes as wavelength measurements, wavelength spectral analysis, dielectric constant, and loss measurements, or as the cavity resonator for frequency stabilization, or as the cavity resonator for a millimeter- or submillimeter-wavelength maser.

I. INTRODUCTION

BECAUSE of its low loss and high frequency selectivity the resonant cavity forms an almost indispensable component in the fields of microwave techniques and microwave measurements. In general, however, the dimensions of each cavity must be comparable with the wavelength in order to avoid undue trouble from higher order modes; and at shorter wavelengths, say around 1 mm, such cavities would become difficult to make, and difficult to use for many of the conventional purposes and measurements. In addition, for cavities of the same material, shape, and mode of operation, the Q values are proportional to the square root of the resonant wavelength. This leads to a reduced precision in measurements, and to an increased effect of losses in such resonant structures at short wavelengths.

In what may be called the ultramicrowave region of wavelengths,¹ there is thus a definite need for some replacement of the conventional cavity resonator. Since cavities operate on the principle of multiple reflections and interference, it is natural to consider the use of an ultramicrowave form of an optical interferometer to replace the cavity in this region. Thus, the use of a microwave interferometer based on the optical Fabry-Perot interferometer² is indicated; the main problem for ultramicrowaves being the design of suitable reflectors with

low loss and adequate reflectivity, to give a large number of multiple reflections and hence sharp fringes. This problem has been considered in a previous paper.³

The advantages of such an interferometer or cavity resonator for ultramicrowaves are that the reflectors and component parts are large compared with the wavelength. In fact the larger they are the less are the effects of diffraction on the measurements, and instead of becoming more difficult, the problem of maintaining a high Q with a single mode of propagation and a structure of adequate size, becomes easier the smaller the wavelength.

Such an interferometer forms the cavity resonator for ultramicrowaves and can be used for wavelength measurements, wavelength spectral analysis, dielectric constant and loss measurements, and also as a cavity resonator for frequency stabilization, millimeter-wave maser work, or for any other purpose for which microwave resonant cavities are used.

In this paper the results of a pilot investigation on an interferometer employing new reflector designs are presented. The theory of the interferometer, including diffraction effects, is given, and the particular reflector designs used are discussed. This interferometer was operated at a wavelength of 6.28 mm. Values of the reflectivity obtained are given together with the results of wavelength measurements with the interferometer. Fringe sharpness and Q values were also measured, the fringes obtained being extremely sharp in agreement with theory. Some computations on the effects of diffraction for various reflectivities and aperture sizes were also made, the reflectors being assumed infinite in extent.

The results obtained substantiate the great potential use of this interferometer in the ultramicrowave region, and in addition show its use as regards precision measurements of wavelength, and hence the velocity of electromagnetic waves.

II. THEORY AND DIFFRACTION EFFECTS

Fig. 1 shows the symmetrical reflector or multiple interference section of the interferometer. Here r_v is the voltage amplitude reflection coefficient, and t is the amplitude transmission coefficient of a single reflector. Methods for computing these for various reflector designs have been considered in a previous paper.³ A

* Manuscript received by the PGMTT, September 28, 1959; revised manuscript received, October 26, 1959.

† National Bureau of Standards, Boulder Labs., Boulder, Colo.
¹ I. Kaufman, "The band between microwave and infrared regions," *PROC. IRE*, vol. 47, pp. 381-396; March, 1959.

² F. A. Jenkins and H. E. White, "Fundamentals of Optics," McGraw-Hill Book Co., Inc., New York, N. Y., pp. 269-276; 1950.

³ W. Culshaw, "Reflectors for a microwave Fabry-Perot interferometer," *IRE TRANS. ON MICROWAVE AND THEORY TECHNIQUES*, vol. MTT-7, pp. 221-228; April, 1959.

plane wave of amplitude E_0 incident on the reflectors as shown gives rise to waves of amplitudes E_1 , E_2 , E_3 , and E_4 as indicated. The electric and magnetic fields at any point z between the reflectors may then be found by applying boundary conditions, or by the use of multiple reflections,⁴ and are given by

$$E = \frac{E_0 t \exp(-jkz) \{1 + r_v \exp[-2jk(d-z)]\}}{1 - r_v^2 \exp(-2jkd)},$$

$$H = \frac{E_0 t \exp(-jkz) \{1 - r_v \exp[-2jk(d-z)]\}}{Z_0 [1 - r_v^2 \exp(-2jkd)]}, \quad (1)$$

where $k = 2\pi/\lambda$ for a lossless medium between the reflectors, d is the distance between the reflectors, and $Z_0 = (\mu/\epsilon)^{1/2}$ is the intrinsic impedance for the TEM mode of propagation between them. The impedance at any point z between the reflectors is then

$$Z = E/H. \quad (2)$$

The transmission coefficient t gives the attenuation and phase shift in passing through a reflector, and without loss in generality we may neglect any phase changes which occur on reflection, *i.e.*, put $r_v = r$. The reflector separation d for optimum transmission is then given by

$$2kd = n\pi, \quad n = 1, 2, 3, \text{ etc.}, \quad (3)$$

where n is the order of interference. The fields between the reflectors for this separation then follow from (1), and the Q value of the reflector system may then be determined from

$$Q = \omega \frac{\text{Energy stored in reflector system}}{\text{Mean dissipation of power in reflector system}}. \quad (4)$$

Since the energy stored is given by $(1/2)\epsilon \int \mathbf{E} \cdot \mathbf{E}^* dv$, and the mean energy dissipated per unit area is given by $(1/2)(1 - |r|^2) \text{Re}(\mathbf{E} \times \mathbf{H}^*)$, where the Poynting vector flux is evaluated at the reflector surface, then assuming no loss in the medium between the reflectors, we obtain

$$Q = [n\pi(1 + |r|^2)]/[2(1 - |r|^2)] \quad (5)$$

which is independent of any transmission losses occurring in the reflectors, and depends only on the reflectivity.

Similarly from (1) and (3), maximum and minimum values of the electric field between the reflectors at resonance, *viz.* $2kd = n\pi$, are given by

$$|E|_{\max}^2 = E_0^2 |t|^2 (1 + |r|)^2 / (1 - |r|^2)^2; \quad (6)$$

$$|E|_{\min}^2 = E_0^2 |t|^2 (1 - |r|)^2 / (1 - |r|^2)^2. \quad (7)$$

If there are no losses in the reflectors, $|t|^2 = 1 - |r|^2$ and (6) and (7) reduce to simpler forms involving only the reflectivity again. Similar equations hold for maximum and minimum values of the magnetic field.

⁴ C. G. Montgomery, *et al.*, "Technique of Microwave Measurements," M.I.T. Rad. Lab. Ser., McGraw-Hill Book Co., Inc., New York, N. Y., pp. 561-564; 1957.

To consider the effects of diffraction in the complete interferometer we require the reflection and transmission coefficients r_I and t_I of the interferometer section shown in Fig. 1. These may be deduced from (1) and are given by

$$r_I = \frac{E_1}{E_0} = \frac{r_v [1 + (t^2 - r_v^2) \exp(-2jk_z d)]}{1 - r_v^2 \exp(-2jk_z d)}, \quad (8)$$

$$t_I = \frac{E_4}{E_0} = \frac{t^2 \exp(-jk_z d)}{1 - r_v^2 \exp(-2jk_z d)}, \quad (9)$$

where $k_z = k \cos \theta$ is the propagation constant for a wave incident obliquely on the reflector, θ being the angle between z -axis and the propagation vector k .

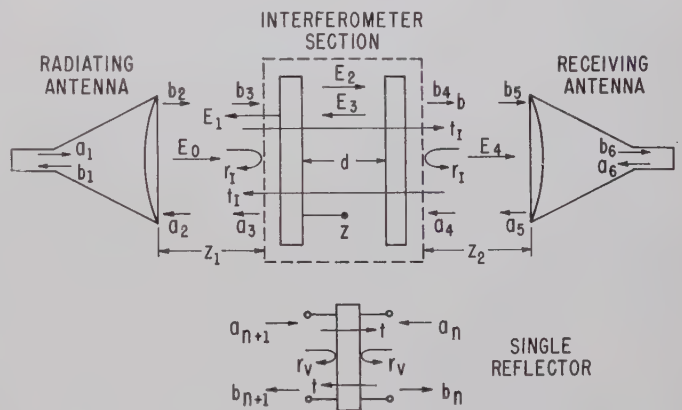


Fig. 1—Diagram for millimeter wave Fabry-Perot interferometer.

The T matrix⁵ of the interferometer section shown in Fig. 1, relating the incident and reflected waves, is then given by

$$\begin{bmatrix} b_4 \\ a_4 \end{bmatrix} = \begin{bmatrix} T_{11}^I & T_{12}^I \\ T_{21}^I & T_{22}^I \end{bmatrix} \begin{bmatrix} a_3 \\ b_3 \end{bmatrix} \quad (10)$$

where

$$T_{11}^I = (t_I^2 - r_I^2)/t_I, \quad T_{12}^I = r_I/t_I = -T_{21}^I,$$

and

$$T_{22}^I = 1/t_I.$$

We may now deduce the reflection and transmission for the complete microwave interferometer, including the radiating and receiving apertures, and the various distances involved. The theory given here is based on the scalar diffraction treatment of the problem instead of on the more precise vector treatment.⁶ Some computations of the diffraction correction in a Michelson interferometer⁷ showed that the agreement between the sca-

⁵ C. G. Montgomery, R. H. Dicke, and E. M. Purcell, "Principles of Microwave Circuits," M.I.T. Rad Lab. Ser., McGraw-Hill Book Co., Inc., New York, N. Y., pp. 150-151; 1948.

⁶ D. M. Kerns and E. S. Dayhoff, "Theory of Diffraction in Microwave Interferometry." (Paper to be submitted for publication.)

⁷ W. Culshaw, J. M. Richardson, and D. M. Kerns, "Precision Millimeter Wave Interferometry at the U. S. National Bureau of Standards," *Proc. Symp. on Interferometry*, National Physical Lab., Teddington, Eng.; June 9-11, 1959.

lar and vector results is better than one part in 10^8 , when the radiating aperture is some 50 wavelengths in extent. It is thus believed that the use of scalar diffraction theory in the Fabry-Perot interferometer is adequate for such aperture sizes, when the reflectors are very large compared with the wavelength, and have a high reflectivity.

The field at any point in front of the radiating or horn apertures used in the interferometer is due to the superposition of waves in the plane-wave spectrum radiated. This is given by

$$g(k_x, k_y) = \frac{1}{2\pi} \iint E(x, y) \exp[j(k_x x + k_y y) dx dy], \quad (11)$$

where $E(x, y)$ represents the aperture field in phase and amplitude, $g(k_x, k_y)$ is the radiated plane-wave spectrum or spectral density function, and k_x, k_y, k_z are the rectangular components of the propagation vector. Considering now only radiation from the waveguide-horn transducer along a particular direction \mathbf{k} , and reception back along this same direction, the reciprocity relation between the radiated and received waves may be found. Representing the scattering matrix of the four terminal thus singled out by $[S]$, and its impedance matrix by $[Z]$, we have⁸

$$[Z] = ([I] - [S])^{-1}([I] + [S])[Z_0] \quad (12)$$

where $[I]$ is the unit matrix, and $[Z_0]$ the diagonal matrix of elements Z_1 , the waveguide characteristic impedance, and Z_2 , which might be $k_z/\omega\epsilon$ or $\omega\mu/k_z$ depending on the polarization, is the impedance along the z axis of the plane wave considered. Since $Z_{12} = Z_{21}$, *i.e.*, the impedance matrix is symmetric, from (12) we obtain

$$S_{12}Z_2 = S_{21}Z_1. \quad (13)$$

In the scalar approximation the polar angle θ is assumed small and Z_2 is taken as constant, and hence $S_{12} = CS_{21}$ where C is a constant. S_{21} corresponds to the radiated spectral density function $g(k_x, k_y)$, and we may write the scattering matrix of the radiating antenna for the particular direction \mathbf{k} considered as

$$\begin{bmatrix} b_1 \\ b_k \end{bmatrix} = \begin{bmatrix} S_{11} & Cg(k_x, k_y) \\ g(k_x, k_y)dk_xdk_y & S_{22} \end{bmatrix} \begin{bmatrix} a_1 \\ a_k \end{bmatrix}. \quad (14)$$

Here a wave of amplitude $g(k_x, k_y)dk_xdk_y$ is radiated, reception for a wave returning along this same direction also being governed by the function $g(k_x, k_y)$. Amplitudes a_1, b_1 and a_k, b_k , respectively, correspond to incident and reflected waves at arbitrary terminals in the waveguide, and at an arbitrary plane $z=0$, which is taken as the plane of the radiating aperture.

The factor S_{22} represents the portion of the returning plane wave which is scattered by the antenna into a radiation pattern depending on the particular antenna,

but which differs greatly from its usual radiation pattern or polar diagram. There will of course be contributions to this scattered radiation from all the other plane waves in the spectrum which is received by the antenna, and this leads to an extremely complicated S_{22} term, and to multiple reflections between any antenna and a reflector. Practically it is necessary to reduce the effect of S_{22} by attention to antenna design, and if necessary to insert additional attenuation between antennas and reflectors to reduce effects of any multiple reflections. In what follows this term is assumed to be small, and it is put into (14) to indicate that these effects can occur.

With this clarification of the S_{22} term, an equivalent T matrix, similar to (10), for the waveguide-radiating antenna transducer may be written down appropriately for the cascading of elements in the complete interferometer. Similar matrices may be written for the receiving aperture-waveguide transducer, and for the line lengths z_1 , and z_2 , shown in Fig. 1, between the antennas and reflectors. From these together with (10), the equation for reflection and transmission through the complete interferometer is obtained in matrix form. As expected the S_{22} term gives rise to multiple reflections and transits in the interferometer. Neglecting these, and with $S_{11}=0$, *i.e.*, the antennas are matched to the waveguides, the resultant amplitude reflection and transmission coefficients are obtained by integration over the radiated plane-wave spectrum, *viz.*,

$$\begin{aligned} r_f &= C_1 \iint [g(k_x, k_y)]^2 \exp(-j2k_z z_1) r_I dk_x dk_y, \\ t_f &= C_2 \iint [g(k_x, k_y)]^2 \exp[-jk_z(z_1 + z_2)] t_I dk_x dk_y. \end{aligned} \quad (15)$$

Where C_1, C_2 are constants, $g(k_x, k_y)$ is assumed the same for both radiating and receiving apertures and is symmetrical about the normal to the aperture.

The reflectors are considered infinite in extent so that there is no modification, by multiple reflections, of the plane-wave spectrum radiated by the horn aperture, this spectrum then being the one effective in the complete interferometer. The diffraction correction in this case arises from the summation of those plane waves which are passed by the reflector system to give the observed transmission maxima. From (15) we can compute the reflector and transmitted fringe shapes for any radiation pattern $g(k_x, k_y)$, and reflectivity $|r|^2$; deviations from the position of optimum transmission given by (3) then represent the corrections due to diffraction in a wavelength measurement with the interferometer.

Consider the transmission coefficient t_f ; the factor t_I due to the reflectors becomes a sharp function for high values of reflectivity, and the reflector system then acts like a plane-wave filter, passing various portions of the radiated spectrum as d is optimized for each plane wave in the spectrum, *i.e.*, when

$$2k_z d = n\pi, \quad n = 1, 2, 3, \text{ etc.} \quad (16)$$

⁸ H. J. Carlin, "An Introduction to the Use of the Scattering Matrix in Network Theory," Microwave Res. Inst., Polytechnic Inst. of Brooklyn, Brooklyn, N. Y., Rept. R-366-54; June 1954.

This is illustrated in Figs. 2 and 3 where the radiation pattern $g(k_x, k_y)$, and the expression $[g(k_x, k_y)]^2 \times |t_I|$ are plotted for a uniformly illuminated slot 24λ wide, with $n=50$ and 400 , and a reflectivity $|r|^2=0.999$. The sharp peaks show how the antenna pattern is scanned by the selective reflector system as the distance d is continuously optimized for various angles θ , since $k_x = k \cos \theta$. In the method of operation considered here we vary d to get the transmitted maximum signal amplitude. Figs. 2 and 3 show how the "fringe" builds up as we scan across the antenna pattern. We have not included phase variations in these considerations, but the results indicate that the position of maximum response will occur when the interferometer is optimized for plane waves close to the axis, *i.e.*, around the $\theta=0$ position. A similar phenomenon occurs in the optical Fabry-Perot² interferometer where a circular fringe system appears, the rings getting sharper as we move out from the center. Since this result would give an accurate measure of the free space wavelength, or propagation constant k , it may be expected that errors due to diffraction will be small for high reflectivities and large reflectors.

This is substantiated by some provisional computations made using (15). Fig. 4 shows the computed fringes obtained for d varying around values corresponding to orders of $n=160$ and 478 , assuming a reflectivity $|r|^2$ of 0.99 . The wavelength used in the computations was 6.27817 mm, and the function $g(k_x, k_y)$ used corresponded to that radiated by a 60 -cm square aperture with an H_{10} rectangular waveguide mode field distribution. Wavelengths of 6.278183 mm and 6.271877 mm were obtained from the positions of the computed transmission maxima at the above orders of interference. These results indicate that even at the relatively low values of reflectivity used here, wavelength measurements with very large reflectors are quite accurate. Since a measure of the insertion loss of the interferometer is given for infinite reflectors by the ratio of the areas under the antenna pattern and the curves of $|t_I| [g(k_x, k_y)]^2$, it is apparent from Figs. 2 and 3 that the insertion loss in the interferometer will depend on the reflectivity and order of interference used. It will also depend on the width of the radiated angular spectrum. The magnitude of the diffraction correction and the insertion loss can be made smaller with decreasing wavelengths, since apertures and reflectors larger in terms of the wavelength can then be used.

III. REFLECTOR DESIGNS AND REFLECTIVITY MEASUREMENTS

In the microwave region reflectors can be designed using metallic rods, irises, dielectric sheets, etc., suitably positioned on an equivalent transmission line, and for which an equivalent circuit representation may be found. Such methods have been considered previously by the author,³ where the reflectors consist of capacitive or inductive rod gratings, or perforated hole gratings stacked behind each other. Optimization of the designs

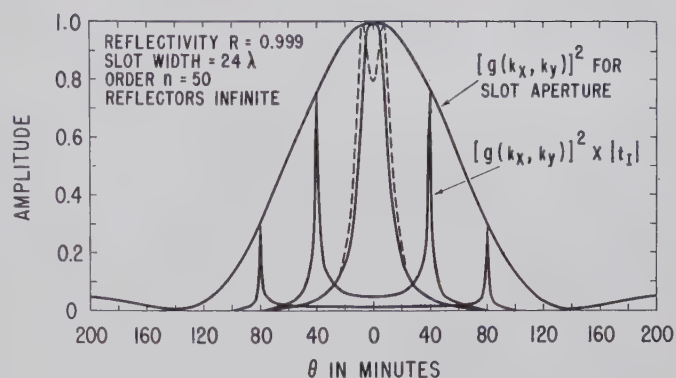


Fig. 2—Scanning of antenna pattern by reflector system, and buildup of fringe in microwave Fabry-Perot interferometer.

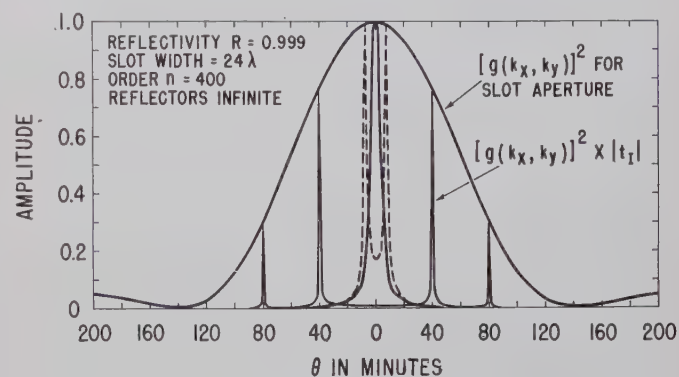


Fig. 3—Scanning of antenna pattern by reflector system and buildup of fringe in microwave Fabry-Perot interferometer.

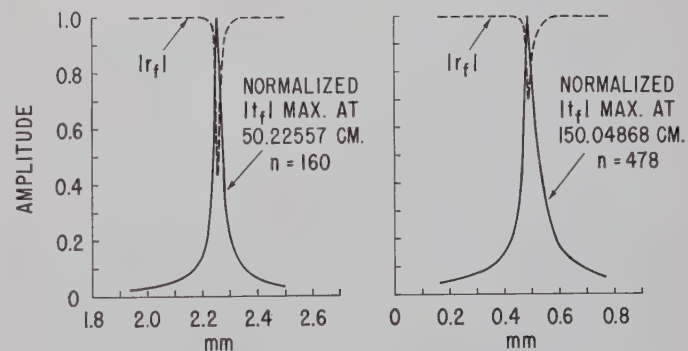


Fig. 4—Computed responses of Fabry-Perot interferometer for infinite reflectors, $|r|^2=0.99$, apertures 60 cm square, $\lambda=6.27817$ mm.

and the bandwidth of such structures are also considered. Fig. 5 shows two types of reflectors which have been used on the microwave Fabry-Perot interferometer described here. The rod structure shown is a capacitive type grating, with the electric vector perpendicular to the rods. A number of such gratings are stacked behind each other at the spacing for optimum reflectivity. The rods were made from steel "drill-rod," the diameter of which is held to fairly close tolerance, and which is fairly straight. Different numbers of layers or gratings could be used and the change in reflectivity studied. In this design the rods were $\frac{1}{16}$ inch in diameter, the spacing between the rods in a grating was

0.103 inch, the spacing between gratings was $\lambda/2$, the apertures were 7.5 inches square, and the wavelength was 6.28 mm.

The other reflector shown in Fig. 5 consists of a single brass plate $\frac{3}{8}$ inch thick with holes $\frac{1}{16}$ inch in diameter. The holes were drilled in it at a $\frac{1}{8}$ -inch spacing. A number of these could be stacked behind each other, but calculations show that the reflectivity from one such sheet is quite high. This is found by using the approximate rule for the transmission coefficient of a small hole in a thick plate,⁹ which gives a value of $|r|^2 = 0.9993$ for the single perforated brass plate.

In Fig. 6, which shows the complete interferometer, the reflectivity was measured by observing the transmission coefficients of the reflectors. Two horn-lens apertures were used as shown, and the insertion loss due to placing a carefully aligned reflector between them was measured. There were multiple reflection effects between the reflector and the horn antennas, and a mean value of insertion loss was used. The measured reflectivity of the plate was 0.9993; this high value clearly indicating the potentialities of this structure for obtaining sharp fringes on the interferometer. Table I shows the reflectivity from various layers of rods in the capacitive grating; the agreement with calculated values is quite reasonable. These extremely high reflectivities clearly indicate the advantages of a microwave Fabry-Perot interferometer, as regards fringe sharpness, over its optical counterpart.

IV. THE INTERFEROMETER AND RESULTS

Fig. 6 shows a photograph of the interferometer with the 6-inch-square radiating horn-lens aperture on the left and a similar receiving horn on the right. Radiation at a wavelength around 6.278 mm is obtained by multiplying up from a quartz-crystal-controlled oscillator at 5.525 mc, which gives a source stable in frequency to a few parts in 10^8 , and with a reasonably steady power output of 1 mw or so at 47,736 mc. By adjustment of a small capacitance in the 5.525-mc oscillator circuit, the frequency can be changed over a range of 12 mc around 47,736 mc. The radiation is then incident on the reflector system, the reflectors being supported on the large aluminum blocks which contain ball bushings and which slide on the supporting steel rods shown. Superheterodyne detection is used at the receiver, a QK294 klystron, frequency stabilized to a high Q resonant cavity after the method of Pound¹⁰ and acting as a local oscillator at 47,706 mc. This is followed by an IF amplifier, a dc amplifier, and the Esterline-Angus recorder. One of the reflectors can be moved slowly by a lead screw and motor drive, and the fringes can be recorded. In addition, there are micrometers for accurate setting of the reflector, and also provision for measuring the change in reflector

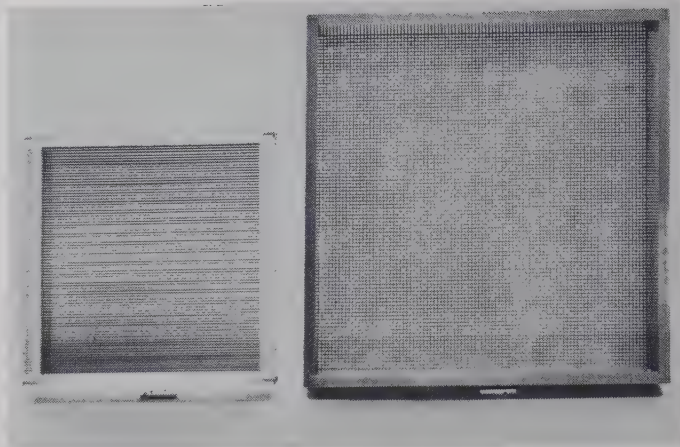


Fig. 5—Capacitive rod gratings and perforated plate reflectors for millimeter wave Fabry-Perot interferometer.

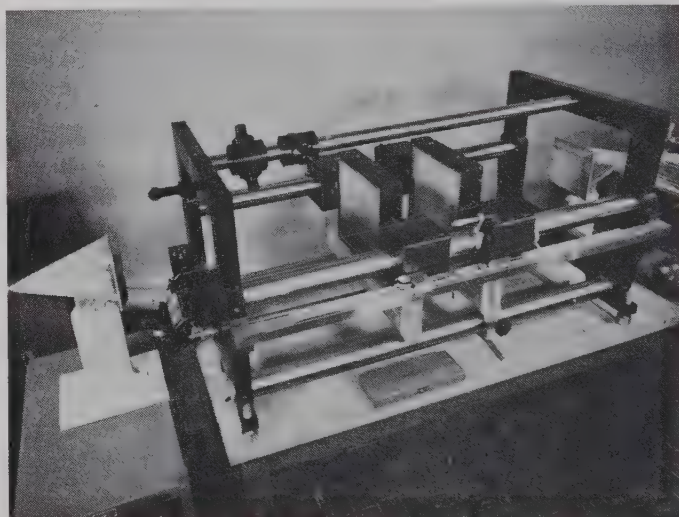


Fig. 6—Millimeter wave Fabry-Perot interferometer.

TABLE I
CALCULATED AND MEASURED VALUES OF REFLECTIVITY FROM A
NUMBER n OF STACKED CAPACITIVE ROD GRATINGS

n	1	2	3	4	5
$ r_n ^2$ measured	0.4635	0.9000	0.98415	0.999	0.99976
$ r_n ^2$ calculated	0.4854	0.8796	0.97699	0.99683	0.99925

separation by length gauges, and hence for determining the number of fringes in a given displacement of the moveable reflector.

To set up the interferometer, the horn apertures are aligned along the axis of the reflector carriage, and adjusted for optimum signal without the reflectors. The reflectors are then inserted in their mounts, which have various screw adjustments for setting the reflector surfaces parallel and perpendicular to the axis. Some adjustments of these are made until a transmitted fringe is seen when moving the reflectors apart. These reflector adjustments are rather critical at the high reflectivities involved here, and they are continued until the cleanest and sharpest possible fringe is obtained. Maladjustment of the reflectors can lead to various fringe shapes; each

⁹ C. G. Montgomery, R. H. Dicke, and E. M. Purcell, *op. cit.*, p. 201.

¹⁰ R. V. Pound, "Electronic frequency stabilization of microwave oscillators," *Rev. Sci. Inst.*, vol. 17, pp. 490-505; November, 1946.

fringe may consist of two separate sharp maxima, or there may be a number of smaller fringes associated with the main maximum. This reflector adjustment is critical and tedious, and the use of optical collimation methods would probably lead to a more satisfactory procedure.

Fig. 7 shows the increase in sharpness of the fringes for 1, 2, and 3 layers of the capacitive rod gratings discussed in Section III. In addition to the sharpening of the fringes, the signal at the minimum between the fringes decreases towards the noise level. Further layers were added but no additional sharpening of the fringes was observed. This is without doubt due to the relatively small reflector area used here, *viz.* 7.5 inches square, since the multiple reflections between the finite reflectors will modify the angular spectrum of radiation between them, and this becomes the dominant effect at relatively high reflectivities. For large reflectors the fringe sharpness for 4 layers would increase over that obtained for 3 layers.

Fig. 8 shows the very sharp transmitted fringes obtained with the 12-inch-square perforated plate reflector at a reflector-separation of 7 inches. The spacing between the fringes corresponds to $\lambda/2$ or 3.14 mm, and the complete fringe occupies a length of about 5×10^{-4} inches. Similar fringes were obtained for a reflector-separation of 30 inches, except that the fringes became somewhat wider. This effect is mainly due to the finite size of reflectors used, but it also depends on the radiating aperture size used, and could be reduced by the use of larger (in terms of the wavelength) apertures and reflectors. Even so, these fringes are the sharpest ever obtained on a Fabry-Perot interferometer, and the importance and use of this interferometer as the cavity resonator for ultramicrowaves is clearly indicated.

Another measure of fringe sharpness may be defined by

$$Q_d = \lambda / 2\Delta d, \quad (17)$$

where Δd is the displacement from the maximum- to the half-intensity points on the fringe. Since $^3Q_d = nQ/2$ it follows from (5) that

$$Q_d = \pi(1 + |r|^2)/(1 - |r|^2) \quad (18)$$

and for $|r|^2 = 0.999$ this gives $Q_d = 6280$. With the perforated plate reflectors Q_d , values of 2000 and 530 have been measured at reflector-separations of 25 cm and 75 cm, respectively. The theoretical value of Q_d given by (5) assumes a single plane wave in the interferometer, whereas the antenna radiates a whole spectrum of these of a width dependent on its dimensions and field distribution. Apertures 6 inches square were used here, the beamwidth or plane-wave spectrum extending at least some 2° either side of the central maximum. In addition the effects of the finite reflector size, particularly at the larger reflector-separations, and the scanning of the antenna pattern at the larger reflector-separations, all contribute to an increase in the measured fringe width.

Fig. 9 shows the increase in fringe width with reflec-

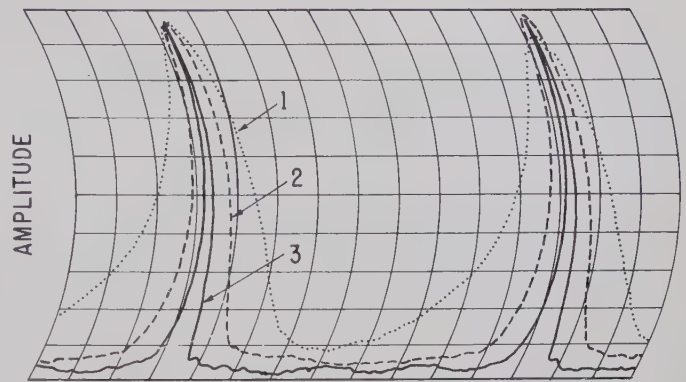


Fig. 7—Fringes for 1, 2, and 3 layers of capacitive rod gratings. $\lambda = 6.28$ mm, reflectors 7.5 inches square and 10 inches apart.

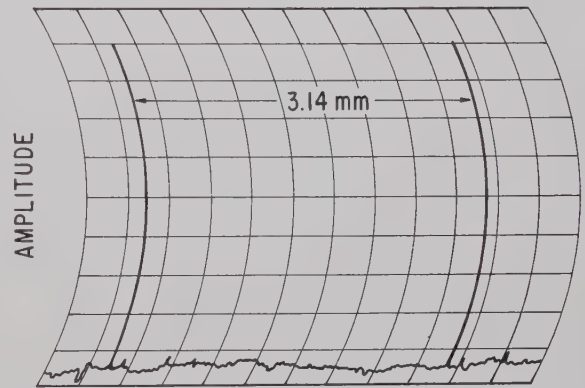


Fig. 8—Fringes on interferometer with perforated sheet reflectors. Reflectors 12 inches square, 7 inches apart, $\lambda = 6.28$ mm.

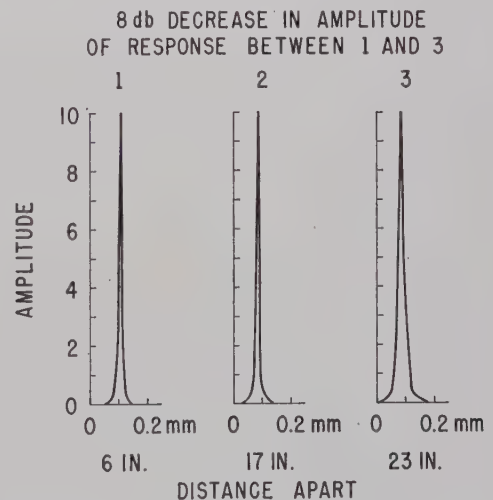


Fig. 9—Showing increasing fringe width with reflector separation. 12-inches-square perforated sheet reflectors.

tor separation for the 6-inch-square apertures and 12-inch-square reflectors. In addition there is a falling off in the intensity of the fringes as the reflector-separation is increased. At a reflector spacing of 6 inches, the insertion loss of the reflector system is around 15 db. This is due to the selectivity of the reflector system, as is evident from Figs. 2 and 3. For a larger order of interference the selectivity increases, assuming infinite reflec-

tors, and the insertion loss will increase. There will also be, in this case, effects due to the finite reflector size used, and in the present experiment an increase in insertion loss of some 8 db occurs when the reflector separation increases from 6 inches to 23 inches.

Frequency selectivity measurements were made on the 12-inch-square perforated sheet-reflectors by changing the frequency of the quartz-crystal oscillator in the frequency multiplier chain. Results were obtained for reflector separations of 6 inches and 17 inches, and gave values of 87,000 and 116,000, respectively, for Q . The frequency selectivity is thus extremely high for the wavelength used, *viz.* 6.28 mm, and could probably be made higher. Similar results can be obtained at still shorter wavelengths and the interferometer has great potential use for measurements and devices in the ultramicrowave region.

Variations in the width of the same fringe for various reflector dimensions are shown in Fig. 10 for a reflector spacing of 25 cm. The increase in fringe width for the smaller reflectors is evident, and there is also a reduction in the intensity of the fringes with the smaller reflectors. Similar results were obtained at reflector spacings of 75 cm, the fringes being some 4 or 5 times wider than those shown in Fig. 10. At a 25-cm spacing the difference between fringes for 12-inch- and 10-inch-square reflectors is not very great. Here the antenna pattern is beginning to be the dominant thing as regards fringe width. At the larger spacing the difference between 12-inch- and 10-inch-square reflectors is more pronounced, and the use of larger reflectors would reduce the fringe width. As already indicated the fringes are quite sharp, since one large division on the abscissa of the chart corresponds to 1.75×10^{-3} inches.

The wavelength of the radiation was measured on the interferometer by starting with an initial reflector separation and counting the number of fringes in a given displacement. For this initial work the displacement was measured with Pratt & Whitney end gauges mounted in the V groove shown in Fig. 6; the results are shown in Table II. For these measurements, the distance between the radiating and receiving horns was 72 inches, and the distance to the first reflector from the radiator was 26.5 inches; this reflector was fixed in position. Taking the velocity of light as $c = 299,792.5$ km/second,¹¹ and the known frequency of 47,736 mc, the following values of wavelength are obtained. For n , the refractive index of the air surrounding the interferometer, equal to 1.0003, $\lambda_{\text{air}} = 6.27835$ mm, and for $n = 1.0002$, $\lambda_{\text{air}} = 6.27896$. The refractive index n was not measured, but is expected to be within the above range. For the present purposes of comparison it is sufficient to use the mean values of Table II, and the mean of the calculated wavelength in air; then the discrepancy amounts to

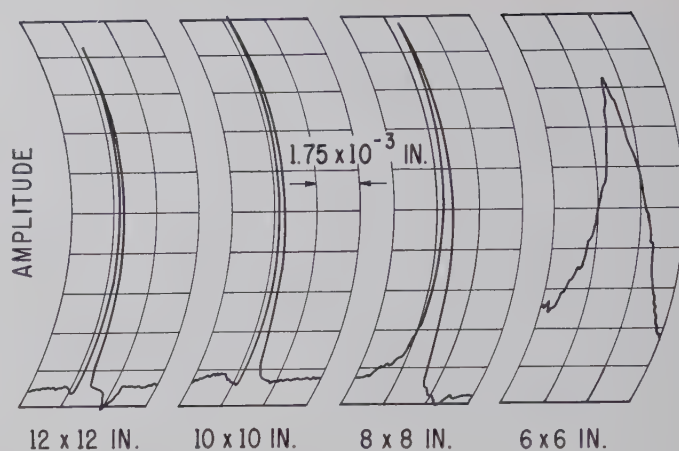


Fig. 10—Variation in fringe shape with reflector size. Perforated sheet reflector, dimensions shown. Spacing $d = 25$ cm.

TABLE II
RESULTS OF WAVELENGTH MEASUREMENTS WITH THE
MICROWAVE FABRY-PEROT INTERFEROMETER

Initial reflector separation, in inches	Number of fringes	Reflector size, in inches	Measured wavelength, in millimeters
7	97	12×12	6.28102
7	97	10×10	6.28108
7	97	8×8	6.28108
7	146	12×12	6.28142
7	146	10×10	6.28146
20	97	12×12	6.28138
23	146	12×12	6.28100
23	146	10×10	6.28118

0.04 per cent, the measured values being too high. For precision measurements a diffraction correction must be applied to the measured values based on (15), and the effect of a finite reflector size on the measurements investigated further. The displacements would also have to be measured more accurately than in this case. Nevertheless, the present agreement between measured and computed wavelengths is good enough for many purposes, even without any diffraction or other corrections, the error being around 0.04 per cent for this particular interferometer. This accuracy is better than that of most commercial resonant cavity wavemeters at this frequency, and the superiority of the interferometer would be much more evident at shorter wavelengths.

V. CONCLUSIONS

The results obtained here on the microwave Fabry-Perot interferometer are very significant, and indicate its great potential use at millimeter and submillimeter wavelengths. The microwave reflector designs used here at 6-mm wavelengths give the required high values of reflectivity, are relatively simple and easy to make, and thus permit the use of reasonable scaling factors for operation with ultramicrowaves. A high value of wavelength resolution has been obtained with the present interferometer, and this would be useful in the wave-

¹¹ K. D. Froome, "A new determination of the free-space velocity of electromagnetic waves," *Proc. Roy. Soc. (London) A*, vol. 247, pp. 109-122; September, 1958.

length analysis of millimeter wavelength sources too high in frequency to be measured conventionally.

Operating in the TEM mode the interferometer represents the ideal form of cavity resonator, permitting the use of relatively large structures at very small wavelengths with complete freedom from troubles due to higher order modes. The Q values obtained here are higher than can readily be attained by a conventional cavity resonator at these frequencies, and the indications are that still higher Q values can be obtained for apertures and reflectors larger in terms of the wavelength. As the cavity resonator for ultramicrowaves, the use of the interferometer for dielectric constant and loss measurements on both solids and gases is clearly indicated, and in the ultramicrowave region of the spectrum such a method becomes most advantageous. Its use in all other microwave devices employing a cavity is also possible, and in particular it would appear that the interferometer can be used with facility as the cavity resonator for masers designed to operate at millimeter and submillimeter wavelengths.

Aperture and reflector dimensions of 24λ and 50λ , respectively, in extent were used here, and the insertion loss at optimum transmission is around 15 db. Consequently,

the reflected power is quite high so that the fringes are best observed in transmission. For smaller wavelengths the problem of adequate aperture and reflector dimensions in terms of the wavelength becomes easier, and interferometers for specific purposes such as maser cavities become easier to accommodate and use with the associated apparatus. Also with apertures and reflectors which are large in terms of the wavelength, the problem of the diffraction correction becomes less severe and important, and the ease with which the interferometer can be used for precision measurements such as the velocity of light, and as a microwave standard of length, will improve with the use of shorter wavelengths.

VI. ACKNOWLEDGMENT

The author would like to thank Dr. D. M. Kerns and Dr. J. M. Richardson for valuable discussions on the work; Dr. P. F. Wacker and W. T. Grandy Jr. for the numerical analysis and programming required in computing values of the diffraction integrals; M. G. Humpal for his careful work in the construction of the interferometer; and H. E. Bussey for his helpful comments on the paper.

Boundary Conditions and Ohmic Losses in Conducting Wedges*

ROBIN M. CHISHOLM†

Summary—The present work is concerned with the boundary conditions required to calculate the ohmic losses occurring in metallic wedges under the influence of electromagnetic waves which are sinusoidal in time. The validity of the surface impedance condition used in calculating waveguide wall losses is examined carefully, and a "modified" surface impedance condition, which can be applied to wedge problems in which the perfectly conducting solution is known, is developed. A simple waveguide having a circular cross section, a sector of which is occupied by a metal wedge, is used as an example. The tangential magnetic field variations along the surface of the wedge are shown graphically, demonstrating, near the tip of the wedge, a large deviation from the tangential magnetic field of the perfectly conducting solution.

* Manuscript received by the PGMTT, July 20, 1959; revised manuscript received November 5, 1959. This work was supported by a grant extended to the Dept. of Electrical Engrg., University of Toronto, Toronto, Can., by the Defence Res. Board of Canada under Extramural Res. Grant DRB 5540-02.

† Dept. of Electrical Engrg., Queen's University, Kingston, Ontario, Canada.

I. INTRODUCTION

THE heat losses within any conducting object caused by the presence of an electromagnetic field, can be calculated by calculating the average flow of power into the object as a result of the tangential fields on its surface. The boundary conditions which must be imposed on the surface of a metallic wedge in order to calculate this power flow must be considered very carefully. The standard surface impedance condition used in the calculation of waveguide wall losses relates the tangential electric field at a conducting boundary to the known tangential magnetic field which would exist at the boundary if it were perfectly conducting. This condition, when applied to wedge problems, often leads to fields which do not satisfy the Meixner edge condition [1] and to infinite power losses in the region of the tip.

Wedge problems have received considerable attention in the past because of the possibility of infinite field strengths at the tip of any wedge-shaped boundary. Because of this, the common technique of discarding wave functions which possess singularities cannot be used, and many boundary value problems involving wedges appear at a first glance to lack uniqueness. In 1949 Meixner published his classical paper [1] on the "edge condition," which added a further "boundary condition" to wedge problems, making their solution, in any situation, unique. Since then, the formulation of problems involving perfectly conducting wedges has been quite straightforward, although the subsequent solutions to many such problems are very complex. In recent years, the problem of diffraction by an imperfectly conducting wedge has been treated [2], [3] and the surface impedance boundary condition used. Although some doubt was expressed about the validity of the condition in the neighborhood of the wedge tip, it was assumed to hold for the entire wedge face and no apparent difficulties resulted.

Difficulties do arise, however, when the surface impedance condition is used to modify solutions to perfectly conducting wedge problems for the purpose of calculating ohmic losses, and, for this reason, the general problem of field behavior near conducting wedges is studied in the present work. In Section II, the exact field behavior within a few skin depths of the wedge tip is examined. In Section III, the surface impedance condition is derived using a wedge-shaped boundary and is expressed in an integral form which reduces to the well known surface impedance condition [4] except within a few skin depths of the tip of the wedge. In Section IV, the coupled modes in a wedge or septate waveguide (Fig. 2) are developed and the reason for the apparent breakdown in the surface impedance condition at the tip of the wedge is illustrated. An approximate solution to the problem is developed which agrees with the analyses of Sections II and III and a numerical example, using the wedge waveguide, is presented graphically in Fig. 3.

II. FIELD BEHAVIOR NEAR THE TIP

In treating the behavior of the fields near the tip of the wedge, the cylindrical coordinates r , ϕ , and z are used. The z axis is taken along the axis of the wedge which is shown in cross section in Fig. 1. The wedge has been symmetrically placed with respect to the x axis and, in the region outside of the wedge, the coordinate angle ϕ is measured from the positive x axis. The fields within the metal wedge are represented in terms of another cylindrical coordinate system \bar{r} , $\bar{\phi}$, and \bar{z} in which the coordinate angle $\bar{\phi}$ is measured from the negative x axis, as shown. The two faces of the wedge are given by

$$\phi = +\phi_1, \quad \bar{\phi} = -\phi_2$$

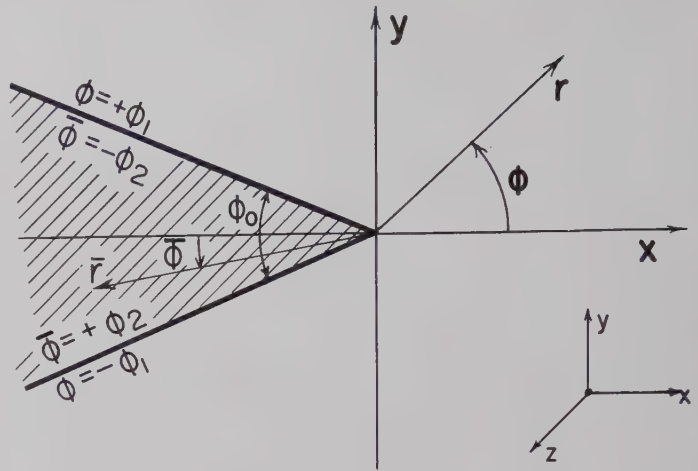


Fig. 1—The coordinate system used.

and

$$\phi = -\phi_1, \quad \bar{\phi} = +\phi_2,$$

and the total wedge angle ϕ_0 is given by

$$\phi_0 = 2\phi_2.$$

The fields are assumed to vary as $\exp(j\omega t)$ and the electric properties of the wedge are designated by a complex permittivity,

$$\bar{\epsilon} = \epsilon_0 - j\sigma/\omega,$$

where $j = \sqrt{-1}$, and σ is the electrical conductivity in mhos per meter. The wedge is assumed to have a magnetic permeability, $\bar{\mu}$, which is very close to μ_0 . Variation in the z direction is assumed to be of the form $\exp(-j\beta z)$, as it would be in a wedge waveguide.

The other four field components can be expressed in terms of E_z and H_z by the following relationships [5]:

$$E_r = -(j\beta/\alpha^2) \frac{\partial E_z}{\partial r} - (j\omega\mu/\alpha^2 r) \frac{\partial H_z}{\partial \phi}, \quad (1)$$

$$E_\phi = -(j\beta/\alpha^2 r) \frac{\partial E_z}{\partial \phi} + (j\omega\mu/\alpha^2) \frac{\partial H_z}{\partial r}, \quad (2)$$

$$H_r = (j\omega\epsilon/\alpha^2 r) \frac{\partial E_z}{\partial \phi} - (j\beta/\alpha^2) \frac{\partial H_z}{\partial r}, \quad (3)$$

$$H_\phi = -(j\omega\epsilon/\alpha^2) \frac{\partial E_z}{\partial r} - (j\beta/\alpha^2 r) \frac{\partial H_z}{\partial \phi}, \quad (4)$$

where β , in the case of the wedge waveguide, is the axial propagation constant $2\pi/\lambda_g$ and α is related to the free-space propagation constant $k = 2\pi/\lambda_0$, by the relation,

$$\alpha^2 = k^2 - \beta^2.$$

Representations of the form (1) to (4) are valid both inside and outside of the wedge when the appropriate ϵ and μ are used. The constant β must be the same for both regions, but $\bar{\alpha}$ in the interior region is many times larger than α in the exterior region. In both regions,

both E_z and H_z must satisfy the two-dimensional wave equation,

$$r \frac{\partial}{\partial r} \left(r \frac{\partial \psi}{\partial r} \right) + \frac{\partial^2 \psi}{\partial \phi^2} + (\alpha r)^2 \psi = 0, \quad (5)$$

where $\psi = E_z$ or H_z and $\bar{\alpha}$ replaces α in the interior region.

Following a procedure similar to that used by Meixner [6], the fields E_z and H_z can be expanded in a power series in r about the origin, $r=0$.

$$E_z = \sum_n c_n r^{t+n-1} \quad (6)$$

and

$$H_z = \sum_n \gamma_n r^{t+n-1}, \quad (7)$$

where the c_n 's and γ_n 's are functions of the angle ϕ and $0 < \text{Re}(t) < 1$. Using (1) to (4), similar series can be derived in terms of the c_n 's and γ_n 's for the four transverse field components. The Meixner edge condition [1], which requires that the energy density in the fields be integrable at the wedge tip, limits the behavior of the six field components for small values of r . It is a simple matter to show that finite energy requires the two field components parallel to the wedge axis to remain finite as r approaches zero. This, in turn, means that, if $0 < \text{Re}(t) \leq 1$, c_1 and γ_1 are the smallest nonzero coefficients in the series for E_z and H_z . The transverse field components, however, may behave as r^{t-1} as long as the real part of t is greater than zero.

Substituting (6) and (7) into the wave equation (5), yields simple, ordinary differential equations for the coefficients c_n and γ_n , and in particular,

$$\frac{d^2 c_1}{d\phi^2} + t^2 c_1 = 0 \quad (8)$$

with similar equations for γ_1 , \bar{c}_1 , and $\bar{\gamma}_1$, where the bar indicates fields within the wedge. This means that

$$c_1 = l_1 \cos(t\phi) + l_2 \sin(t\phi), \quad (9)$$

and

$$\gamma_1 = \lambda_1 \cos(t\phi) + \lambda_2 \sin(t\phi). \quad (10)$$

Within the metal wedge, \bar{E}_z and \bar{H}_z can be expressed in the same form, and in both regions the behavior of the transverse field components as r approaches zero can be found using (1) to (4) together with (9) and (10). In the outside region,

$$E_r = [L_1 \cos(t\phi) + L_2 \sin(t\phi)] r^{t-1} \quad (11)$$

$$E_\phi = [L_2 \cos(t\phi) - L_1 \sin(t\phi)] r^{t-1}, \quad (12)$$

$$H_r = [\Lambda_1 \cos(t\phi) + \Lambda_2 \sin(t\phi)] r^{t-1}, \quad (13)$$

$$H_\phi = [\Lambda_2 \cos(t\phi) - \Lambda_1 \sin(t\phi)] r^{t-1}, \quad (14)$$

with a similar representation within the wedge. In terms of c_1 and γ_1 ,

$$L_1 = -(jt/\alpha^2) \{ \beta l_1 + \omega \mu \lambda_2 \}, \quad (15)$$

$$L_2 = -(jt/\alpha^2) \{ \beta l_2 - \omega \mu \lambda_1 \}, \quad (16)$$

$$\Lambda_1 = -(jt/\alpha^2) \{ \beta \lambda_1 - \omega \epsilon l_2 \}, \quad (17)$$

$$\Lambda_2 = -(jt/\alpha^2) \{ \beta \lambda_2 + \omega \epsilon l_1 \}. \quad (18)$$

An identical set of relationships holds for the barred quantities which represent the fields within the wedge. Continuity conditions at the wedge faces can then be used to determine the L 's and Λ 's in terms of a single amplitude factor. An estimate of how small r must be before the first term is predominant in all of the series involved, can be made by studying (5). This equation can be written in terms of the dimensionless variable (αr) and power series solutions appropriate to each region would involve either (αr) or $(\bar{\alpha} r)$. Since, within the metal, $\bar{\alpha} \simeq (-j\omega\mu\sigma)^{1/2}$, the condition that the first term of the series *within the wedge* be predominant is that $(r/\delta) \ll 1$ where $\delta = (2/\omega\mu\sigma)^{1/2}$ is the skin depth of the metal.

The continuity of E_r , ϵE_ϕ , H_r and μH_ϕ at the two wedge faces yields eight homogeneous, linear equations in the eight unknown coefficients which determine the field behavior near the tip of the wedge. Because of symmetry with respect to the angle ϕ , these equations can be separated into two sets of four equations each. For fields which are even in E_z and odd in H_z with respect to ϕ ($l_2 = \bar{l}_2 = \lambda_1 = \bar{\lambda}_1 = 0$),

$$L_1 \cos(t\phi_1) - \bar{L}_1 \cos(t\phi_2) = 0, \quad (19)$$

$$\epsilon_0 L_1 \sin(t\phi_1) + \bar{\epsilon} \bar{L}_1 \sin(t\phi_2) = 0, \quad (20)$$

$$\Lambda_2 \sin(t\phi_1) + \bar{\Lambda}_2 \sin(t\phi_2) = 0, \quad (21)$$

$$\mu_0 \Lambda_2 \cos(t\phi_1) - \bar{\mu} \bar{\Lambda}_2 \cos(t\phi_2) = 0. \quad (22)$$

A nontrivial solution to this set of equations exists if, and only if,

$$\begin{vmatrix} \cos(t\phi_1) & -\cos(t\phi_2) \\ \sin(t\phi_1) & g \sin(t\phi_2) \end{vmatrix} \begin{vmatrix} \sin(t\phi_1) & \sin(t\phi_2) \\ \cos(t\phi_1) & -q \cos(t\phi_2) \end{vmatrix} = 0, \quad (23)$$

where

$$g = \bar{\epsilon}/\epsilon_0 \quad \text{and} \quad q = \bar{\mu}/\mu_0.$$

Eq. (23) yields two sets of discrete *eigenvalues* for the exponent t . One set, which depends only on g , makes the first factor in (23) vanish. The other set, which depends only on q , makes the second factor vanish.

A similar set of equations results from fields which are odd in E_z and even in H_z with respect to the angle ϕ in Fig. 1. In general, four sets of eigenvalues for t occur. Two sets depend only on the electric properties of the wedge and are given by the roots of

$$1 - g = \frac{\sin(t\pi)}{\cos(t\phi_1) \sin(t\phi_2)}, \quad (24)$$

and

$$1 - g = \frac{\sin(t\pi)}{\cos(t\phi_2) \sin(t\phi_1)} \quad (25)$$

The first of these is associated with fields which are even in E_z and the second with fields which are odd in E_z with respect to the coordinate angle ϕ . Replacing g by q in (24) and (25), two other sets of eigenvalues occur which depend only on the magnetic properties of the wedge.

Solutions associated with values of t , determined by the electric properties of the wedge, yield nonzero values for L_1 and \bar{L}_1 in (19) to (22), but admit only the trivial solution, $\Lambda_2 = \bar{\Lambda}_2 = 0$, for the coefficients associated with H_r and H_ϕ in (13) and (14). Solutions associated with values of t determined by the magnetic properties of the wedge, on the other hand, yield nonzero values for the Λ 's and admit only the trivial solution for the L 's. It can be seen, from (11) to (14), that a field component can become infinite at the tip of the wedge *only* if an eigenvalue of t which is less than unity admits a non-zero value for the L 's or Λ 's associated with that component. This, in turn, means that any singularities in the transverse components of the magnetic field at the tip of the wedge depend only on the magnetic properties of the wedge. Singularities in the transverse components of the electric field, moreover, depend only on the electric properties of the wedge. If the wedge has a magnetic permeability μ equal to μ_0 and a conductivity of σ mhos per meter, then

$$1 - g = (j\sigma/\omega\epsilon_0)$$

and

$$1 - q = 0.$$

The "magnetic eigenvalues" are determined by the roots

$$0 = \frac{\sin(t\pi)}{\cos(t\phi_1) \sin(t\phi_2)} \quad (26)$$

and

$$0 = \frac{\sin(t\pi)}{\cos(t\phi_2) \sin(t\phi_1)} \quad (27)$$

which yield only integral, nonzero values for t . This means that no singularity can occur in either H_r or H_ϕ at the tip of the wedge. If μ is close to μ_0 , moreover, t will lie very close to a positive integer and any singularity in H_r or H_ϕ will be of a very low order.

The "electric eigenvalues," on the other hand, are determined by the roots of

$$(j\sigma/\omega\epsilon_0) = \frac{\sin(t\pi)}{\cos(t\phi_1) \sin(t\phi_2)} \quad (28)$$

and

$$(j\sigma/\omega\epsilon_0) = \frac{\sin(t\pi)}{\cos(t\phi_2) \sin(t\phi_1)} \quad (29)$$

For large values of $(\sigma/\omega\epsilon_0)$, these eigenvalues lie close to the zeros of $\sin(t\phi_1)$, $\sin(t\phi_2)$, $\cos(t\phi_1)$, and $\cos(t\phi_2)$, which are given by

$$t_{1,n} = (n+1)\pi/(2\phi_1) \quad (30)$$

and

$$t_{2,n} = (n+1)\pi/(2\phi_2) \quad (31)$$

where n is a positive integer or zero. Eigenvalues which are even multiples of $\pi/2\phi_1$ or odd multiples of $\pi/2\phi_2$ are associated with solutions for E_z which are odd with respect to the angle ϕ . The others are associated with fields which are even in E_z .

If ϕ_2 lies between 0 and $\pi/2$, then the only eigenvalue less than unity in either (30) or (31) is

$$t_{1,0} = \pi/2\phi_1. \quad (32)$$

For finite but large σ , moreover, the lowest eigenvalue for the metallic wedge is approximately given by

$$t_E = t_{1,0} - \frac{j\omega\epsilon_0 \tan(t_{1,0}\pi)}{\sigma\phi_1} \quad (33)$$

As σ becomes infinite, t_E approaches $t_{1,0}$, the eigenvalue for the perfectly conducting wedge, as $1/\sigma$ or as δ^2 , where δ is the *skin depth*. This "perturbation" in t caused by the finite wall conductivity, therefore, is a second order effect compared to the "coupled modes" discussed in Section III.

The axial fields associated with this lowest eigenvalue are given, near the tip of the wedge, by

$$E_z = l_1 \cos(t_E\phi) r^{t_E} \quad (34)$$

and

$$H_z = \lambda_2 \sin(t_E\phi) r^{t_E}, \quad (35)$$

where l_1 and λ_2 are related to each other from (18) by

$$l_1 = (-\beta/\omega\epsilon_0)\lambda_2 \quad (36)$$

since $\Lambda_2 = 0$. Eq. (36) shows a fixed coupling between E_z and H_z which is independent of the conductivity σ of the wedge. The two magnetic field components which are perpendicular to the axis of the wedge, moreover, cannot have a singularity of an order greater than r^{t_H-1} where t_H is the lowest eigenvalue associated with the magnetic properties of the wedge. This eigenvalue in practice is very close to unity. Using (3) and (4), these conditions can be expressed mathematically in terms of the two tip equations:

$$\frac{\partial E_z}{\partial \phi} - \frac{\beta}{\omega\epsilon_0} r \frac{\partial H_z}{\partial r} \rightarrow 0 \quad \text{faster than } r^{t_H} \quad (37)$$

and

$$\frac{\partial H_z}{\partial \phi} + \frac{\omega\epsilon_0}{\beta} r \frac{\partial E_z}{\partial r} \rightarrow 0 \quad \text{faster than } r^{t_H} \quad (38)$$

These equations do not, of course, restrict the behavior of E_z and H_z unless these field components individually approach zero more slowly than r^{t_H} . It can be shown, however, that (37) implies (38) and is a necessary and sufficient condition for finding the coupled E_z near the tip of an imperfectly conducting wedge if H_z is a given wave function which approaches zero as r^t where $t < t_H$ [and indeed t can be as low as t_E in (33)].

III. FIELD BEHAVIOR AWAY FROM THE TIP

In Appendix I an expression is derived for the relationship between E_z and H_r on the surface of a metal wedge where the coordinates used are shown in Fig. 1. The expression is in integral form and holds everywhere on the faces of the wedge. For highly conducting wedges the expression reduces to

$$E_z(r, \phi_1) = \frac{\omega\mu}{2} \int_{-\infty}^r H_r H_0^{(2)}(\bar{\alpha}|x|) dx \quad (39)$$

in which E_z is the axial electric field on the surface $\phi = +\phi_1$, a distance r from the tip of the wedge. H_r is the radial magnetic field a distance x from the point at which E_z is being evaluated. $H_0^{(2)}(\bar{\alpha}|x|)$ is a Hankel function of the second kind [7] which behaves as $(\frac{1}{2}\pi\bar{\alpha}|x|)^{-1/2} \exp(-j\bar{\alpha}|x| - \frac{1}{4}\pi)$ for large values of $|x|$. If $\bar{\alpha}$ has a negative imaginary part $H_0^{(2)}(\bar{\alpha}|x|)$ vanishes rapidly as $|x|$ increases and, for r more than a few skin depths, the upper limit in (39) can be taken as $+\infty$. Furthermore, if H_r is continuous and slowly varying near the point $x=0$, it can be replaced by its value at $x=0$, in which case (39) becomes

$$E_z(r, \phi_1) = \frac{\omega\mu}{2} H_r(r, \phi_1) \int_{-\infty}^{\infty} H_0^{(2)}(\bar{\alpha}|x|) dx. \quad (40)$$

This integral can readily be evaluated by using tables of Laplace transforms [8] to yield

$$E_z(r, \phi_1) = \frac{\omega\mu}{2} H_r(r, \phi_1) \frac{2}{(\bar{\alpha})} = Z_s H_r(r, \phi_1) \quad (41)$$

for large values of wedge conductivity. Z_s is called the surface impedance of the metal and is related to the skin depth δ by

$$Z_s = \frac{\omega\mu\delta(1+j)}{2}. \quad (42)$$

The same analysis can be used to relate E_r at the wedge face $\phi = \phi_1$ to H_z yielding the result,

$$E_r(r, \phi_1) = -Z_s H_z(r, \phi_1). \quad (43)$$

Relationships on the other wedge face $\phi = -\phi_1$ are identical except for sign.

This *surface impedance condition* relates the tangential electric field at the surface of the wedge to the *total* tangential magnetic field existing at the same point.

This relationship is valid to within a few skin depths of the wedge tip, and the error introduced by assuming that it holds over the entire wedge face does not appear to be too large. This assumption has been used successfully in diffraction problems [2] and the integral expression (39) does not indicate any violent breakdown in the relationship. If the actual H_r , however, is assumed to be the same as it would be if the wedge were perfectly conducting, this field becomes infinite at the wedge tip in many problems. Applying the surface impedance condition in this case would yield an axial electric field which would become infinite at the wedge tip in violation of the edge condition. This difficulty, however, can be resolved by considering a simple example.

The lowest propagating mode of the wedge waveguide shown in cross section in Fig. 2, when perfectly conducting walls are assumed, is governed by the axial magnetic field,

$$H_z^0 = J_t(\alpha r) \sin(t\phi) \quad (44)$$

where $t = t_{1,0} = \pi/2\phi_1$, and $J_t(\alpha r)$ is a Bessel function of the first kind. The constant α is defined in Section II following (4). The radial magnetic field associated with this mode is given by (3), namely,

$$H_r^0 = \frac{-j\beta}{\alpha} J_t'(\alpha r) \sin(t\phi). \quad (45)$$

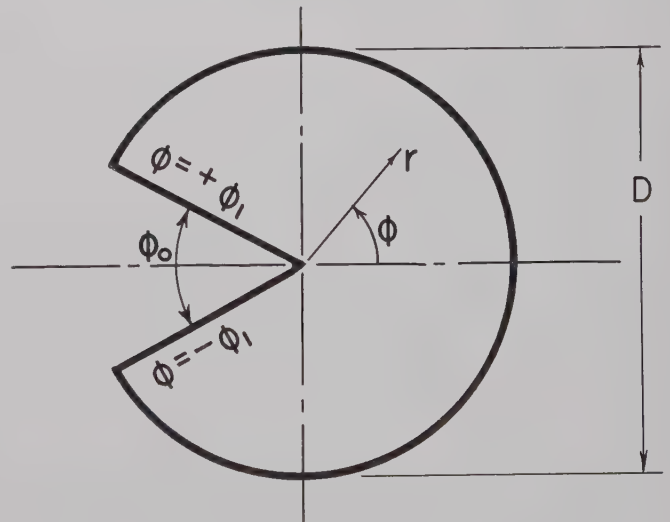


Fig. 2—The wedge waveguide.

The finite conductivity of the walls will introduce an axial electric field proportional to Z_s or to the skin depth δ . This perturbation cannot be taken care of by the small perturbation in the eigenvalue t , which by (33) is proportional to δ^2 , and a coupled mode must be introduced. By using a well known relationship for Bessel functions [9] a wave function E_z^e can be found which, on both wedge faces, satisfies the condition,

$$E_z^e = \pm Z_s H_r^0, \quad (46)$$

and which has the form,

$$E_z^e = -\frac{Z_s j \beta}{2\alpha} \left[\frac{J_{t-1}(\alpha r) \cos[(t-1)\phi]}{\cos[(t-1)\phi_1]} - \frac{J_{t+1}(\alpha r) \cos[(t+1)\phi]}{\cos[(t+1)\phi_1]} \right]. \quad (47)$$

This "coupled" mode, moreover, carries with it a radial magnetic field which is related to E_z^e by (3). Calling this coupled magnetic field H_r^e , it is given by

$$H_r^e = \frac{j\omega\epsilon}{\alpha^2 r} \frac{\partial E_z^e}{\partial \phi}. \quad (48)$$

Since, for any fixed position on the surface of the wedge, E_z^e is proportional to $Z_s H_r^0$, H_r^e is also proportional to $Z_s H_r^0$ and vanishes as the wall conductivity becomes infinite. One is therefore tempted to assume that H_r^e is negligibly small compared to H_r^0 in problems involving metal wedges. The r in the denominator of (48), however, makes H_r^e become arbitrarily large for small values of r , and the ratio of H_r^e to H_r^0 on the wedge surface is given by

$$\frac{H_r^e}{H_r^0} = \frac{-b Z_s}{r} \cot(\phi_1) \left[\frac{t^2 J_t(\alpha r)}{(\alpha r) J_t'(\alpha r)} - 1 \right] \quad (49)$$

where $b = (j\omega\epsilon/\alpha^2)$ and $Z_s = \omega\mu\delta(1+j)/2$, where δ is the skin-depth. This ratio is small if r/δ is large but, for finite values of δ , this ratio becomes infinite as r approaches zero.

This result suggests a modified surface impedance condition in which H_r^0 is replaced by $(H_r^0 + H_r^e)$. The surface impedance condition then becomes

$$E_z^e = Z_s [H_r^0 + (j\omega\epsilon/\alpha^2 r) \partial E_z^e / \partial \phi]. \quad (50)$$

For points more than a few skin depths away from the tip of the wedge, (50) is just (46), the surface impedance condition used in all waveguide problems. As r approaches zero, however, (50), which can be rewritten in the form,

$$\frac{r}{b Z_s} E_z^e = \frac{-\beta}{\omega\epsilon} r \frac{\partial H_z^0}{\partial r} + \frac{\partial E_z^e}{\partial \phi}, \quad (51)$$

using (45), approaches the tip equation (37) provided that E_z^e and H_z^0 both approach zero as r^t where $t+1$ is greater than t_H . This will always be the case if E_z^e and H_z^0 satisfy the Meixner edge condition which places a lower limit on the exponent t .

This analysis shows that if the modified surface impedance condition is assumed to hold over the entire wedge face, fields which are in agreement with the analysis of Section II can be found. These fields will be identical with those derived from (44) and (47) for large values of r/δ and the breakdown will occur when H_r^e , given by (48), becomes comparable in magnitude to H_r^0 given by (45). As r/δ approaches zero, moreover, the radial component of the magnetic field will approach zero as shown in Section II.

IV. FINDING APPROXIMATE SOLUTIONS

In Appendix II it is shown that, if H_z^0 is a given wave function which satisfies the Meixner edge condition at the tip of the wedge, then any function E_z which satisfies the tip equation (37) will also satisfy the wave equation for small values of r , and will give rise to fields which are in keeping with the "tip" analysis given in Section II, provided only that none of the resulting field components become independent of the angle ϕ in Fig. 1, as r approaches zero. This condition can usually be satisfied by inspection when looking for approximate solutions. Eq. (37), moreover, can be written in the form,

$$\frac{\partial E_z}{\partial \phi} + (r/b) H_r^0 + O(r^x) = 0, \quad (52)$$

where $b = (j\omega\epsilon/\alpha^2)$, $H_r^0 = -(j\beta/\alpha^2) \partial H_z^0 / \partial r$, and $O(r^x)$ is any function which approaches 0 as r^x where $x > t_H$. Away from the tip region the coupled field can be found by ordinary methods since its value on the faces of the wedge and on other boundaries is a known quantity related to the tangential magnetic field of the perfectly conducting solution to the problem. For large values of r/δ , therefore, E_z is known and has, in the simplest case, the form,

$$E_z = Z_s H_r^0 / P(\phi), \quad (53)$$

where $P(\phi)$ is a well behaved, odd function of the angle ϕ such that $P(\phi_1) = 1$. If (53) is true, then a solution of

$$\frac{\partial E_z}{\partial \phi} - \frac{r}{b Z_s} P(\phi) E_z = -\frac{r}{b} H_r^0 \quad (54)$$

has the following properties:

- 1) For small values of $|r/b Z_s|$ it satisfies (52).
- 2) For large values of $|r/b Z_s|$ it satisfies (53) and therefore approaches its correct value away from the tip region,
- 3) For all values of r it satisfies the surface impedance condition on the faces of the wedge.

Functions which satisfy (54) can be found quite easily; the general solution has the form,

$$E_z = -\exp \left[(r/b Z_s) \int P(\phi) d\phi \right] \times \int \exp \left[(-r/b Z_s) \int P(\phi) d\phi \right] (r/b) H_r^0(r, \phi) d\phi. \quad (55)$$

Using (55) as a guide, it is a simple matter to find an E_z which satisfies the tip equation for small values of r/δ , and which approaches in a continuous manner the "standard" solution given by (53) for large values of r/δ . The condition that none of the field components become independent of ϕ as r approaches 0 can usually be satisfied by inspection. This technique, therefore, enables one, with a minimum amount of guessing, to find

a *continuous* function which satisfies the correct boundary conditions and the wave equation near the tip of the wedge, and which approaches the "standard" coupled mode solution away from the tip. The transition region can be estimated from (49) since it is determined by the distance from the tip of the wedge at which the standard surface impedance condition used in most waveguide problems breaks down.

In the present example, however, E_z^e and H_r^0 do not satisfy (53) and H_r^0 has to be written in the form,

$$\begin{aligned} H_r^0 &= -(j\beta/2\alpha)[J_{t-1}(\alpha r) - J_{t+1}(\alpha r)] \sin(t\phi) \\ &= H_r^A + H_r^B. \end{aligned} \quad (56)$$

In (47), however, E_z^e has the form,

$$E_z^e = E_z^A + E_z^B \quad (57)$$

where

$$E_z^A = \frac{Z_s H_r^A \cos[(t-1)\phi]}{\cos[(t-1)\phi_1] \sin(t\phi)} \quad (58)$$

and

$$E_z^B = \frac{Z_s H_r^B \cos[(t+1)\phi]}{\cos[(t+1)\phi_1] \sin(t\phi)}, \quad (59)$$

both of which are of the form of (53). Both E_z^B and H_r^B vanish instead of becoming infinite at the wedge tip and (59) can be assumed to be valid for all values of r . Eq. (58) represents the dominant fields for small values of r/δ , and H_r^A can be used to replace H_r^0 in (53). A field E_z can then be found as before, using (55) as a guide. This function, of course, approaches E_z^A in (58) for large values of r/δ , but E_z^B as given by (59) can be added to the solution for all values of r without affecting the behavior of the solution near the tip of the wedge since E_z^B vanishes as r^{t+1} . When this is done, the coupled axial electric field in the wedge waveguide is given, on the faces of the wedge, by the simple expression,

$$E_z = \frac{-(\beta\alpha/\omega\epsilon)rJ_t'(\alpha r)[(r/bZ_s) + t \cos(t\phi_1)]}{[(r/bZ_s)^2 + t^2]}, \quad (60)$$

where $b = (j\omega\epsilon/\alpha^2)$. For large values of $|r/bZ_s|$ this is just the surface impedance condition relating E_z to H_r^0 on the wedge surface. For small values of $|r/bZ_s|$, (60) holds for all values of ϕ simply by replacing ϕ_1 by ϕ . When this is done it is a simple matter to show that $H_r^e = -H_r^0$ and $H_\phi^e = -H_\phi^0$ as required by the analysis in Section II.

Since the present theory assumes that (50) holds for all values of r , the total radial magnetic field $H_r = H_r^0 + H_r^e$ is proportional to E_z^e in (60) on the faces of the wedge. This field differs from H_r^0 for small values of r/δ and a plot of H_r in a typical wedge waveguide is given in Fig. 3 for different values of δ/λ_0 , where δ is the skin depth, λ_0 the free-space wavelength, and D the diameter of the waveguide.

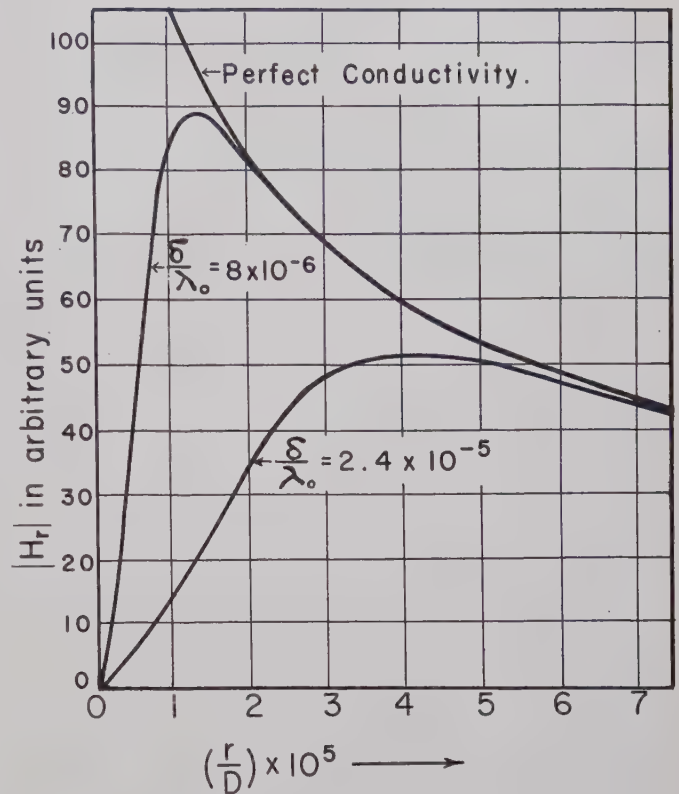


Fig. 3—The variation of the total radial magnetic field with distance from the tip of the wedge in a one-degree wedge waveguide operating in its lowest mode. D is the diameter of the waveguide, λ_0 the free-space wavelength, and δ the skin depth. In this case $\lambda_0/D = 2.0$.

V. OHMIC LOSSES

When (19) to (22) are solved for \bar{L}_1 and \bar{L}_2 , the electric field components *within* the wedge are given, near the tip, by

$$\bar{E}_z = -[j\beta/\sigma \cos(t\pi)](\bar{r})^t \cos(t\bar{\phi}), \quad (61)$$

$$\bar{E}_r = [t/\sigma \cos(t\pi)](\bar{r})^{t-1} \cos(t\bar{\phi}), \quad (62)$$

and

$$\bar{E}_\phi = -[t/\sigma \cos(t\pi)](\bar{r})^{t-1} \sin(t\bar{\phi}), \quad (63)$$

when it is assumed that the axial magnetic field, outside of the wedge, has the form,

$$H_z = (r)^t \sin^-(t\phi), \quad (64)$$

near the tip of the wedge. If $|E|$ is the rms value of the electric field in volts per meter, and if \bar{E} is the complex conjugate of E , the total power loss per unit length within a sector of the wedge bounded by a small radius r_0 , is given by

$$W = \int_0^{r_0} \int_{-\phi_2}^{+\phi_2} \{\sigma E \cdot \bar{E}\} \bar{r} d\bar{r} d\bar{\phi} \text{ watts per meter.} \quad (65)$$

For small values of r_0/δ , this integrates to

$$W = t\phi_0 [2\sigma \cos^2(t\pi)]^{-1} r_0^{2t} \text{ watts per meter.} \quad (66)$$

This is vanishingly small for small values of r_0 , demonstrating that the power dissipated in the tip region is small. As σ becomes infinite, the power dissipated in the tip region approaches zero. The expression is valid for very small values of ϕ_0 , the total wedge angle, the limiting value of ϕ_0 being determined by the breakdown of (33). For vanishingly small values of ϕ_0 , however, the effect of the wedge disappears for any finite value of σ and the minimum value of t approaches unity rather than $\frac{1}{2}$.

A more practical approach to the loss problem is to integrate the real part of the complex Poynting vector S_ϕ^* over the faces of the wedge. In terms of rms field quantities, S_ϕ^* is given by

$$S_\phi^* = E_z \tilde{H}_r - E_r \tilde{H}_z \text{ watts per square meter.} \quad (67)$$

If the value of E_z is given by (60) (or, in general, if E_z is derived by the method outlined in Section IV) the function S_ϕ^* is integrable over the entire wedge face yielding a small flow of power into the tip region which is consistent with (66).

When this method is used to calculate the attenuation constant of a wedge waveguide, the contribution from the region of the wedge surface which is less than one skin depth from the tip is insignificantly small. When the standard, unmodified method is used, however, the contribution from this region dominates the contributions to the attenuation constant from all other regions of the waveguide surface. For an 18° wedge waveguide operating in its lowest mode at a frequency halfway between cutoff and the cutoff frequency of the next lowest mode, the contribution from this "tip region" is equal to the contribution from the rest of the wedge surface. The total attenuation constant found by the unmodified method in this case is 58 per cent larger than that found by the method described in the present paper. For a typical $\frac{1}{2}^\circ$ wedge waveguide, moreover, the unmodified method yields a contribution from the tip region which is 50 times the contribution from the rest of the wedge surface. This yields an attenuation constant which is more than 30 times as large as that found by the method described in the present paper.

Numerical values for the attenuation constants of wedge waveguides have been published elsewhere [11]. These are given as functions of wedge angle, conductivity, and frequency over the usable range of such waveguides. The attenuation constant varies slowly with the wedge angle and approaches a finite value as the wedge angle approaches zero.

VI. CONCLUSIONS

The exact field behavior near the tip of a mathematically sharp, imperfectly conducting wedge has been analyzed and it has been shown that the field components satisfy static boundary conditions in the region of the tip. It has also been shown that the only singularity which can occur in any component of the electric field at the tip of the wedge depends only on the dielec-

tric constant and the conductivity of the wedge. Similarly it has been shown that the only singularity which can occur in any magnetic field component depends only on the permeability of the wedge. This means that highly conducting wedges with a permeability equal to that of the surrounding medium cannot support a singularity in any of the magnetic field components as the perfectly conducting wedge appears to do. The magnetic field components which are perpendicular to the axis of the wedge, however, do in many cases become very large *near* the tip of the wedge but, even if the wedge is perfectly sharp, these field components must reach a maximum value and then vanish at the tip of the wedge. The position of this maximum is established approximately by examining the point at which the coupled radial magnetic field, which occurs as a result of the finite conductivity, becomes comparable in magnitude to the radial magnetic field of the perfectly conducting solution. As the conductivity increases, the curve of H_r vs r approaches the curve of H_r^0 vs r , where H_r^0 is the radial magnetic field near a perfectly conducting wedge. Even though H_r^0 becomes infinite at the tip of the wedge, however, H_r reaches a maximum and decreases to zero at the tip for all finite values of wedge conductivity. This is very similar to the way in which a finite Fourier series approaches a discontinuous function as the number of terms taken becomes infinite.

It has also been shown that the surface impedance condition holds to within a few skin depths of the tip of a metal wedge and that, as long as the tangential magnetic field is not assumed to be that of the perfectly conducting problem, this condition yields results which are in agreement with the exact analysis based on the power series approach, when the condition is assumed to hold over the entire wedge face. Since the axial currents induced in the wedge do not become infinite but rather vanish at the tip, even when the wedge is perfectly sharp, any errors introduced by applying the surface impedance condition to the entire wedge face will be small. The fact that "real" wedges, moreover, are not perfectly sharp does not invalidate their representation by a perfectly sharp mathematical model since the "difference" region does not carry large currents.

In diffraction problems it makes very little difference whether the secondary fields are caused by "Huygen sources" *near* the tip of the wedge, or whether they are caused by conduction currents actually flowing on the wedge. In calculating ohmic losses, however, this difference is extremely important and must be taken into account in such calculations as those involved in determining the attenuation constant of wedge waveguides.

The present investigation is not a mathematically rigorous solution to any particular wedge problem, and further refinements would be needed if it were necessary to determine the fields in the tip region to a very high degree of accuracy. The ideas developed should be looked upon as a second approximation to the problem of boundary conditions on an imperfectly conducting

wedge, the standard surface impedance condition being the first approximation. This approximation does, however, embody some very important features of wedge behavior and gives results for ohmic losses which agree reasonably well with those found in practice.

The radial electric field E_r , on the surface of the wedge, can be made proportional to the axial magnetic field H_z for all values of r without contradicting the Meixner edge condition. This, and conditions on other boundaries, can usually be satisfied by the introduction of additional coupled modes which satisfy known boundary conditions of either the Neumann or the Dirichlet type, and which are vanishingly small in the tip region. The problem of finding such solutions is often very difficult but once the radial magnetic field and the axial electric field are modified as outlined in Section IV, the boundary conditions are admissible in the sense that the resulting fields will satisfy the edge condition. In loss calculations, moreover, the normal component of the Poynting vector is needed only on the faces of the wedge, and the solution developed in Section IV is all that is needed.

APPENDIX I

The Surface Impedance Condition on the Face of a Wedge

Using Green's theorem [10], the axial electric field $\bar{E}_z(r', \phi')$ anywhere within the metal wedge shown in Fig. 4 can be expressed in terms of the normal deriva-

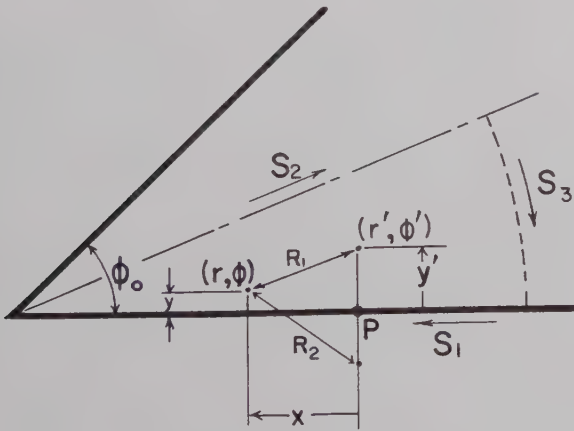


Fig. 4—The coordinate system used to establish the surface impedance condition.

tive of this field on S_1 and in terms of the field and its derivatives on S_2 and S_3 . If the function $G(r, \phi, r', \phi')$ satisfies

$$\nabla^2 G + (\bar{\alpha})^2 G = \delta(r - r')\delta(\phi - \phi') \quad (68)$$

where δ is the Dirac delta function and $\bar{\alpha}$ is defined in Section II following (4), then $\bar{E}_z(r', \phi')$ can be written in the form

$$\bar{E}_z(r', \phi') = \int_{S_1+S_2+S_3} \left\{ \bar{E}_z(r, \phi) \frac{\partial G}{\partial n} - \frac{\partial \bar{E}_z(r, \phi)}{\partial n} G \right\} dS. \quad (69)$$

Eq. (69) can be further simplified by putting

$$G(r, \phi, r', \phi') = j/4 [H_0^{(2)}(\bar{\alpha}R_1) + H_0^{(2)}(\bar{\alpha}R_2)] \quad (70)$$

where R_1 is the distance between (r, ϕ) and (r', ϕ') and R_2 is the distance between (r, ϕ) and the image of (r', ϕ') in the plane S_1 as shown in Fig. 4. $H_0^{(2)}(\bar{\alpha}R)$ is a Hankel function s , of the second kind. In this case $\partial G/\partial n = 0$ on S_1 and, by symmetry for fields which are even function in $\bar{\phi}$ in Fig. 2, $\partial \bar{E}_z/\partial n = 0$ on S_2 . Eq. (69) then becomes

$$\begin{aligned} \bar{E}_z(r', \phi') = & -(j/4) \int_{S_1} \{ H_0^{(2)}(\bar{\alpha}R_1) \\ & + H_0^{(2)}(\bar{\alpha}R_2) \} \frac{\partial \bar{E}_z}{\partial n_1} dS_1 \\ & + (j/4) \int_{S_2} \bar{E}_z \frac{\partial}{\partial n_2} \{ H_0^{(2)}(\bar{\alpha}R_1) \\ & + H_0^{(2)}(\bar{\alpha}R_2) \} dS_2. \end{aligned} \quad (71)$$

Since $(\bar{\alpha})$ has a negative imaginary part, the integration on S_3 can be neglected, provided that S_3 is more than a few skin depths away from (r', ϕ') .

Finally, letting y' approach zero in Fig. 4, R_1 approaches R_2 and (71) becomes

$$\begin{aligned} E_z(P) = & -(j/2) \int_{-\infty}^{r'} H_0^{(2)}(\bar{\alpha} |x|) \frac{\partial \bar{E}_z}{\partial n} dx \\ & + (j/2) \int_{S_2} \bar{E}_z \frac{\partial}{\partial n_2} H_0^{(2)}(\bar{\alpha}R_1) dS_2. \end{aligned} \quad (72)$$

If the constants of the wedge material are given by

$$\bar{\mu} = \mu_0,$$

and

$$\bar{\epsilon} = \epsilon_0 - j\sigma/\omega,$$

then, using (3), it is a simple matter to show that the continuity of H_r across the face of the wedge requires that, when $\phi = \phi_1$ Fig. 1,

$$\frac{\partial \bar{E}_z}{\partial n} = \frac{H_r - (\epsilon_0/\mu\sigma)(1/r)\partial E_z/\partial \phi}{-(j/\omega\mu)(1 + j\omega\epsilon_0/\sigma)}. \quad (73)$$

Substituting (73) into (72) yields

$$\begin{aligned} E_z(P) = & (-j/2) \int_{-\infty}^{r'} \frac{j\omega\mu H_r - (j\omega\epsilon/\sigma)(1/r)\partial E_z/\partial \phi}{(1 + j\omega\epsilon/\sigma)} \\ & \cdot H_0^{(2)}(\bar{\alpha} |x|) dx \\ & + (j/2) \int_{S_2} \bar{E}_z \frac{\partial}{\partial n_2} H_0^{(2)}(\bar{\alpha}R_1) dS_2. \end{aligned} \quad (74)$$

For very good conductors the second term of (74) and the second term within the first integral of (74) can be neglected for all values of r' .

APPENDIX II

THE TIP EQUATION

Theorem: If H_z is a given function of r and ϕ which

- 1) satisfies the two-dimensional Helmholtz equation,
- 2) satisfies the Meixner edge condition, and
- 3) approaches zero as r^t where $t < t_H$, the lowest eigenvalue of a magnetic type solution [see (26) and (27)],

then (37) implies (38) and any E_z satisfying (37) also satisfies the Helmholtz wave equation as r approaches zero, provided that none of the field components become independent of the angle ϕ as r approaches zero.

Eq. (37) can be written in the form,

$$\frac{\partial E_z}{\partial \phi} = \frac{\beta}{\omega \epsilon} r \frac{\partial H_z}{\partial r} + O(r^x), \quad (75)$$

as r approaches 0, where $O(r^x)$ is any function which behaves as r^x for small values of r , and $x > t_H$. Differentiating (75) with respect to r and (4) with respect to ϕ yields

$$\begin{aligned} \frac{\partial H_\phi}{\partial \phi} &= \frac{-j\beta}{\alpha^2} \left[\frac{\partial}{\partial r} \left(r \frac{\partial H_z}{\partial r} \right) + \frac{1}{r} \frac{\partial^2 H_z}{\partial \phi^2} \right] + O(r^{x+1}) \\ &= j\beta r H_z + O(r^{x-1}), \end{aligned} \quad (76)$$

if H_z satisfies (5), the Helmholtz equation. If, moreover, H_z satisfies the Meixner edge condition, then rH_z approaches zero faster than r^{x-1} and therefore the derivative of H_ϕ with respect to ϕ behaves as r^{x-1} . If H_ϕ does not become independent of ϕ as r approaches zero, moreover, then H_ϕ also behaves as r^{x-1} , which is (38).

Differentiating (75) with respect to ϕ yields

$$\frac{\partial^2 E_z}{\partial \phi^2} = \frac{\beta}{\omega \epsilon} r \frac{\partial^2 H_z}{\partial \phi \partial r} + O(r^x). \quad (77)$$

Eq. (4), moreover, implies that as r approaches 0,

$$(-j\beta/\alpha^2 r) \frac{\partial H_z}{\partial \phi} = (j\omega\epsilon/\alpha^2) \frac{\partial E_z}{\partial r} + O(r^{x-1}), \quad (78)$$

since H_ϕ must approach 0 faster than r^{x-1} . Multiplying (78) by r , differentiating with respect to r , and substituting into (77), yields

$$\frac{\partial^2 E_z}{\partial \phi^2} = -r \frac{\partial}{\partial r} \left(r \frac{\partial E_z}{\partial r} \right) + O(r^x). \quad (79)$$

If E_z satisfies (75) and does not become independent of ϕ as r approaches 0, then E_z must approach 0 as r^t if H_z approaches 0 as r^t where $t+1 > t_H-1$. This means that $(\alpha r)^2 E_z$ can be added to (79) without changing its behavior for small values of r and, therefore,

$$\frac{\partial^2 E_z}{\partial \phi^2} + r \frac{\partial}{\partial r} \left(r \frac{\partial E_z}{\partial r} \right) + (\alpha r)^2 E_z = 0 \quad (80)$$

is satisfied by E_z to within a relative error of order r^{t_H-t} .

ACKNOWLEDGMENT

The author wishes to thank Dr. George Sinclair for supervising this research, and Drs. J. L. Yen, V. H. Weston, and R. Mittra for many helpful discussions.

REFERENCES

- [1] J. Meixner, "Die Kantenbedingung in der Theorie der Beugung elektromagnetischer Wellen an vollkommen leitenden ebenen Schirmen," *Ann. Physik*, vol. 6, pp. 2-9; January, 1949.
- [2] L. B. Felsen, "Diffraction by an imperfectly conducting wedge," in "Proceedings of the McGill Symposium on Microwave Optics," U. S. Armed Service Tech. Information Agency, Washington, D. C., No. AD 211500, pp. 287-292; April, 1959.
- [3] T. B. A. Senior, "Diffraction by an Imperfectly Conducting Wedge," University of Michigan, Ann Arbor, Sci. Rept. No. 2; October, 1957.
- [4] J. A. Stratton, "Electromagnetic Theory," McGraw-Hill Book Co., Inc., New York, N. Y., 1st ed., p. 533; 1941.
- [5] E. C. Jordan, "Electromagnetic waves and radiating systems," Prentice-Hall, Inc., New York, N. Y., 1st ed., p. 274; 1950.
- [6] J. Meixner, "The Behavior of Electromagnetic Fields at Edges," New York University, New York, N. Y., Rept. No. E-M 72; 1952.
- [7] W. Magnus and F. Oberhettinger, "Special Functions of Mathematical Physics," Chelsea Press, New York, N. Y., 1st ed., p. 17; 1949.
- [8] *Ibid.*, p. 133.
- [9] J. A. Stratton, *op. cit.*, p. 360.
- [10] *Ibid.*, p. 165.
- [11] R. M. Chisholm, "Attenuation in wedge and septate waveguides," *Proc. URSI Internat. Electromagnetic Theory Symp.*, University of Toronto, Toronto, Can.; June, 1959.

On the Theory of the Ferrite Resonance Isolator*

E. SCHLÖMANN†

Summary—The attenuation constants for both directions of propagation in a rectangular waveguide loaded with a small slab of ferrite are calculated by means of perturbation theory. The maximum attainable ratio of reverse to forward attenuation is found to be inversely proportional to the square of the bandwidth, with a constant of proportionality that is dependent on the shape of the ferrite slab and the proximity of cutoff. The figure of merit is largest for the case of a thin ferrite slab magnetized perpendicular to the plane of the slab. It is shown that a significant increase in the figure of merit can be obtained by proper use of the anisotropy of grain-oriented materials or single crystals.

I. INTRODUCTION

IN this paper the inherent limitations of resonance isolators will be considered. It has been known for some time that the ratio of reverse to forward attenuation cannot exceed a certain optimum value determined by the line width of the ferromagnetic resonance.¹ The bandwidth of resonance isolators has apparently not been considered in any detail up to now. It will be shown that the bandwidth (defined as the frequency range over which the reverse to forward ratio has at least half of its maximum possible value) is proportional to the width of the resonance, with a constant of proportionality that is a rather sensitive function of the shape of the ferrite slab, its magnetization, the frequency, and the cutoff frequency of the waveguide. Under most conditions, the bandwidth is appreciably smaller than the width of the resonance line. It is shown, however, that this situation can be reversed by proper use of magneto-crystalline anisotropy. A device using this effect would require a properly oriented single crystal or grain-oriented polycrystalline material.

We shall consider only the case in which a rectangular waveguide is used. It will be assumed that the cross section of the ferrite slab is very small compared with the cross section of the waveguide, so that a perturbation approach can be used. For simplicity, it is assumed that the unperturbed wave is a TE₁₀ mode. It will also be assumed that the ferrite slab or rod has an ellipsoidal cross section. In practice, this configuration is realized by means of circular rods or, approximately, by means of thin slabs of rectangular cross section.

The performance of resonance isolators that use a thin slab of ferrite magnetized in the plane of the slab and perpendicular to the waveguide axis will be investigated in Section II. The geometry of this case is shown

in Fig. 1(a). In Section III, the results will be generalized to include the case in which the ferrite slab has an elliptical but otherwise arbitrary cross section, in particular the geometry of Fig. 1(b). The generalization to the case in which a grain-oriented material or a single crystal is used is also given in this section. In Section IV, various assumptions made in the development of the theory will be critically evaluated.

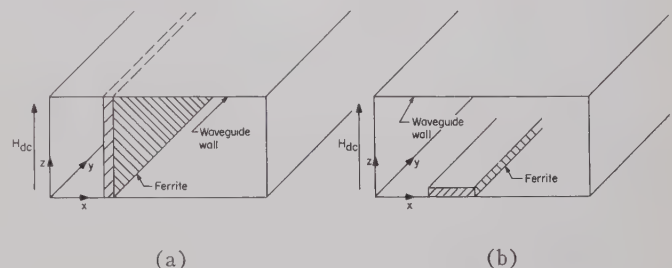


Fig. 1—(a) Ferrite resonance isolator using a thin ferrite slab magnetized in the plane of the slab. (b) Ferrite resonance isolator using a thin ferrite slab magnetized perpendicular to the plane of the slab. The perturbation theory (1) neglects the variation of the microwave field over the ferrite region, and is valid only if the width of the slab is sufficiently small.

II. THEORY

Consider the geometry described in Fig. 1(a). If the cross section of the ferrite slab is much smaller than the cross section of the waveguide, the propagation constant Γ in the presence of the ferrite slab can be calculated by perturbation theory, with the result¹

$$\Gamma + \Gamma_0^* \sim j\vec{h}^* \vec{\chi}_{\text{eff}}^{\leftrightarrow} \vec{h} \quad (1)$$

Here Γ_0 is the propagation constant of the empty waveguide, which is assumed to be lossless (*i.e.*, $\Gamma_0 = j\beta_0$, where β_0 is real). $\vec{\chi}_{\text{eff}}$ is the effective susceptibility, and \vec{h} the RF magnetic field at the site of the ferrite slab. The asterisk denotes the complex conjugate. For a thin slab in the geometry of Fig. 1(a), the effective susceptibility calculated using a Landau-Lifshitz damping term is

$$\vec{\chi}_{\text{eff}}^{\leftrightarrow} = \frac{M}{(\gamma^2 + \lambda^2)H(H + 4\pi M) - \omega^2 + 2j\lambda(H + 2\pi M)\omega} \cdot \begin{pmatrix} (\gamma^2 + \lambda^2)H + j\lambda\omega & j\gamma\omega \\ -j\gamma\omega & (\gamma^2 + \lambda^2)(H + 4\pi M) + j\lambda\omega \end{pmatrix} \quad (2)$$

where the y -direction is the direction of propagation [see Fig. 1(a)], γ is the gyromagnetic ratio and λ a phenomenological loss parameter which is related to the line width $\Delta H = 2\lambda\omega_0/(\gamma^2 + \lambda^2)$. A derivation of (2) is given in Appendix I. The validity of the phenomenological description of losses will be discussed in Section IV.

* Manuscript received by the PGMTT, August 2, 1959; revised manuscript received, November 10, 1959.

† Research Div., Raytheon Co., Waltham, Mass.

¹ B. Lax, "Frequency and loss characteristics of microwave ferrite devices," *Proc. IRE* vol. 44, pp. 1368-1386; October, 1956.

For a TE₁₀ mode, the magnetic field is of the form

$$\begin{aligned} h_x &= j \sqrt{\left(\frac{\omega}{\omega_c}\right)^2 - 1} \sin \phi e^{j\omega t}, \\ h_y &= \cos \phi e^{j\omega t}, \end{aligned} \quad (3)$$

where ω_c is the cutoff frequency, ϕ is determined by the position of the slab in the waveguide, and $\phi=0$ and $\phi=\pi$ correspond to the waveguide walls. In (3) the choice of signs is appropriate for a wave propagating in the $+y$ -direction, if we let $\phi=0$ characterize the left-hand wall. In order to describe a wave propagating in the $-y$ -direction, the sign of the square root has to be reversed. It should be noticed that in the geometry shown and for propagation in the $+y$ -direction, the sense of rotation of the transverse magnetic field forms a right-handed screw with the direction of the field. Thus, the $+y$ -direction is the reverse direction of the isolator.

From (1), (2), and (3) one obtains the complex propagation constant of the ferrite loaded waveguide. The real part of Γ is the attenuation constant α . Since the empty waveguide was assumed lossless, one finds after trivial calculations for the reverse direction

$$\begin{aligned} \alpha_{\text{reverse}} &\sim \frac{M}{[(\gamma^2 + \lambda^2)H(H + 4\pi M) - \omega^2]^2 + [2\lambda(H + 2\pi M)\omega]^2} \\ &\cdot \left\{ (\gamma^2 + \lambda^2)H^2 + \omega^2 \right\} \left[\left(\frac{\omega}{\omega_c}\right)^2 - 1 \right] \sin^2 \phi \\ &+ [(\gamma^2 + \lambda^2)(H + 4\pi M)^2 + \omega^2] \cos^2 \phi \\ &+ 4\gamma(H + 2\pi M)\omega \sqrt{\left(\frac{\omega}{\omega_c}\right)^2 - 1} \sin \phi \cos \phi \}. \end{aligned} \quad (4)$$

The expression inside the braces can be written as

$$\begin{aligned} p \sin^2 \phi + q \cos^2 \phi + 2r \sin \phi \cos \phi \\ = \frac{1}{2}[(p + q) - (p - q) \cos 2\phi + 2r \sin 2\phi] \end{aligned} \quad (5)$$

where the explicit expressions for p , q , and r are obvious from a comparison with (4). Thus, the condition for maximum (or minimum) reverse attenuation is

$$\tan 2\phi_1 = \frac{-2r}{p - q}. \quad (6)$$

Similarly, the condition for minimum (or maximum) forward attenuation is

$$\tan 2\phi_2 = \frac{2r}{p - q}. \quad (7)$$

Fig. 2 demonstrates the relationship between the two positions ϕ_1 and ϕ_2 . It is assumed in this figure that $q > p$. Under these conditions $\phi_1 < \phi_2$. It may be seen from Fig. 2 that the position of the ferrite slab, which maximizes the reverse attenuation, coincides with the position, which minimizes the forward attenuation, only

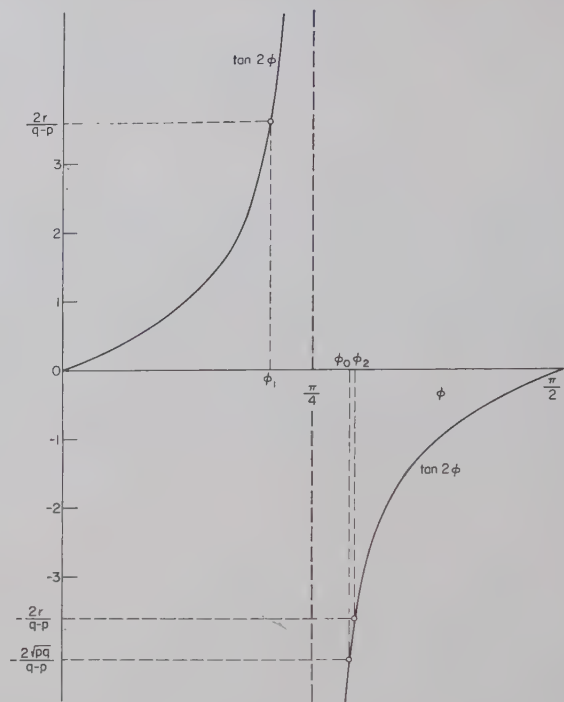


Fig. 2—Graphical determination of the positions of the ferrite slab which maximize the reverse attenuation (ϕ_1), minimize the forward attenuation (ϕ_2), or maximize the reverse to forward ratio (ϕ_0). The full line represents $\tan 2\phi$.

if $p = q$. Then $\phi_1 = \phi_2 = \pi/4$; i.e., the distance between ferrite slab and waveguide wall is one quarter of the width of the waveguide. In general, ϕ_1 and ϕ_2 differ from $\pi/4$ in opposite directions by equal amounts.

Similar results have been obtained by Suhl and Walker,² who have pointed out that the difference between the energy stored at ϕ in the left-handed wave and in the right-handed wave is proportional to $\sin 2\phi$. The difference is largest at $\phi = \pi/4$ and $\phi = 3\pi/4$, so that large nonreciprocal effects may be expected when the ferrite slab is placed in one of these regions.

The ratio of the two attenuation constants is

$$\begin{aligned} R(\phi, \omega) &= \frac{\alpha_{\text{reverse}}}{\alpha_{\text{forward}}} \\ &= \frac{(p + q) - (p - q) \cos 2\phi + 2r \sin 2\phi}{(p + q) - (p - q) \cos 2\phi - 2r \sin 2\phi}. \end{aligned} \quad (8)$$

It can be shown that R assumes a maximum with respect to ϕ at ϕ_0 where

$$\begin{aligned} \cos 2\phi_0 &= \frac{p - q}{p + q}, \\ \sin 2\phi_0 &= \frac{2\sqrt{pq}}{p + q}. \end{aligned} \quad (9)$$

² H. Suhl and L. R. Walker, "Topics in guided wave propagation through gyromagnetic media," *Bell Sys. Tech. J.*, vol. 33, pp. 939-986; July, 1954. See p. 954.

The maximum $R(\omega)$ is thus

$$R_{\max}(\omega) = \frac{\sqrt{pq} + r}{\sqrt{pq} - r} = \frac{\sqrt{[(\gamma^2 + \lambda^2)H^2 + \omega^2][(\gamma^2 + \lambda^2)(H + 4\pi M)^2 + \omega^2]} + 2\gamma(H + 2\pi M)\omega}{\sqrt{[(\gamma^2 + \lambda^2)H^2 + \omega^2][(\gamma^2 + \lambda^2)(H + 4\pi M)^2 + \omega^2]} - 2\lambda(H + 2\pi M)\omega}. \quad (10)$$

Differentiating with respect to ω , one finds that the maximum with respect to ω occurs at $\omega = \omega_0$, where

$$\omega_0^2 = (\gamma^2 + \lambda^2)H(H + 4\pi M). \quad (11)$$

It can be shown from (7) and (9) that at resonance, ϕ_0 is very close to ϕ_2 , the difference being of second order in λ/γ . Fig. 2 illustrates a typical case, where the graphical determination of the various angles for which the two attenuation constants and their ratio are stationary with respect to ϕ .

The maximum reverse to forward ratio is, from (10) and (11),

$$R_{\max}(\omega_0) = \frac{\sqrt{\gamma^2 + \lambda^2} + \gamma}{\sqrt{\gamma^2 + \lambda^2} - \gamma}. \quad (12)$$

In many cases λ is much smaller than γ . Under these conditions, the exact formula (12) can be replaced by the first terms of a power series expansion in $(\lambda/\gamma)^2$

$$R_{\max}(\omega) \approx \frac{4\gamma^2}{\lambda^2} + 2 - \frac{1}{4} \frac{\lambda^2}{\gamma^2} + \dots \quad (13)$$

Consider the frequency dependence of the reverse to forward ratio in the vicinity of the resonance frequency. Assume that the position of the ferrite slab has been chosen in such a way that the maximum R is achieved. From (8) it is possible to obtain, after trivial calculations (described in Appendix II),

$$R(\phi_0, \omega) = \frac{R_{\max}(\omega_0)}{1 + \left[\frac{2(\omega - \omega_0)}{B} \right]^2}. \quad (14)$$

Here $R_{\max}(\omega_0)$ is as given in (12). In the denominator, higher powers of $\omega - \omega_0$ are neglected. According to (14), B is the range of frequencies over which $R(\phi_0, \omega)$ has at least half its maximum value. It will henceforth be called the bandwidth of the isolator. As shown in Appendix II, B to first order in λ/γ is given by

$$B^2 = \frac{2\left(\frac{\lambda}{\gamma}\right)^2 \omega_0^2}{1 + \frac{1}{a^2} + \frac{1}{2a^4} + \left(1 + \frac{1}{a^2}\right) \frac{2\pi M}{\sqrt{(2\pi M)^2 + \left(\frac{\omega_0}{\gamma}\right)^2}}} \quad (15)$$

where a is the ratio of the transverse to the longitudinal component of the magnetic field at the resonance frequency (more precisely, the ratio of the transverse field

at the center to the longitudinal field at the waveguide wall).

$$a = \sqrt{\left(\frac{\omega_0}{\omega_c}\right)^2 - 1}. \quad (16)$$

A comparison of (13) and (15) shows that a large reverse to forward ratio can usually be obtained only at a sacrifice of bandwidth, and vice versa. Therefore, it is reasonable to take this fact into account in the definition of the figure of merit of the isolator. In the existing literature, the reverse to forward ratio itself has sometimes been called the figure of merit. This is a reasonable choice only if the bandwidth of the device is immaterial. We shall adopt a different convention and define the figure of merit as

$$F = R_{\max} \left(\frac{B}{\omega_0} \right)^2. \quad (17)$$

A comparison of (13), (15), and (17) shows that with this definition, the figure of merit is approximately independent of the loss parameter λ . If higher powers of λ/γ are neglected, one obtains

$$F = \frac{8}{1 + \frac{1}{a^2} + \frac{1}{2a^4} + \left(1 + \frac{1}{a^2}\right) \frac{2\pi M}{\sqrt{(2\pi M)^2 + \left(\frac{\omega}{\gamma}\right)^2}}}. \quad (18)$$

Since all terms in the denominator of (18) are positive, the larger a and ω are, and the smaller M is, the greater the figure of merit becomes. If $2\pi M \ll \omega/\gamma$, the last term in the denominator is only a small correction. As a particular example, consider the case where the frequency is 2800 mc and $2\pi M$ is 1000 gauss. For practical purposes, a^2 cannot be made larger than 3. For this particular value, the frequency equals twice the cutoff frequency for TE_{10} modes and is thus equal to the cutoff frequency for TE_{20} modes. The figure of merit for $a^2 = 3$ and for the given values of magnetization and frequency is approximately 3.5.

III. GENERALIZATIONS

The theory presented in the previous section can easily be generalized in such a way that it will apply to situations in which the ferrite slab has an elliptical but otherwise arbitrary cross section and the dc field is applied along an axis of the ellipse. In the latter situation, the transverse demagnetizing field is $4\pi MN$ rather than $4\pi M$ as previously. Here N is the transverse demagnet-

izing factor.³ Similarly, H must now be interpreted as the internal or "demagnetized" field

$$H = H_{\text{app}} - 4\pi MN_z. \quad (19)$$

Here N_z is the longitudinal demagnetizing factor. All significant results derived previously can be taken over immediately if $4\pi M$ is replaced by $4\pi MN$. There are minor exceptions to this rule, namely, the factors M that occur (2), (4), (30), and (31).⁴ It is easily seen, however, that these factors cancel out in all the significant results, such as the positions for minimum or maximum attenuations, maximum reverse to forward ratio, bandwidth, and figure of merit. In particular, one obtains for the figure of merit

$$F = \frac{8}{1 + \frac{1}{a^2} + \frac{1}{2a^4} + \left(1 + \frac{1}{a^2}\right) \sqrt{\frac{2\pi MN}{(2\pi MN)^2 + \left(\frac{\omega_0}{\gamma}\right)^2}}}. \quad (20)$$

Thus, for given a , M , and ω , the best figure of merit is obtained when N is very small. This can be realized in the situation described in Fig. 1(b), in which a thin slab is placed on the bottom of the waveguide and magnetized in a direction which is perpendicular to the plane of the slab. Under these conditions, the figure of merit for $a^2 = 3$ is approximately 5.75; *i.e.*, 65 per cent larger than the figure of merit calculated previously for the geometry of Fig. 1(a).

M. T. Weiss⁵ has reported measurements of the performance characteristics of resonance isolators using rectangular waveguides and ferrite configurations which are similar to those of Fig. 1. For the configuration of Fig. 1(b) ("*H*-plane isolator"), he obtained the following results: $R_{\text{max}} = 75$, $B/\omega_0 = 0.16$. The figure of merit as experimentally determined is thus, according to (17), $F_{\text{exp}} \approx 2$. The theoretical formula (20), on the other hand, leads to $F_{\text{theor}} \approx 3.2$. In this calculation we have used a transverse demagnetizing factor appropriate for a rod of ellipsoidal cross section with an axial ratio equal to that of the rectangular slab used in the device. The parameter a of (20) was deduced from the width of the waveguide (0.9 inch) with the help of (16). Weiss has also reported measurements on "*E*-plane isolators" using configurations similar to Fig. 1(a). In these cases, however, a dielectric slab with a high dielectric constant was placed adjacent to the ferrite slab. The figures of merit as deduced from his data for two such configurations are 0.9 and 0.5, respectively. The theoretical formula (20), on the other hand, predicts figures of merit

of approximately 2.7 and 2.2 in the two cases. It should be remembered, however, that this formula does not take into account the effect of the dielectric slab. For this reason, the lack of agreement between theory and experiment in the *E*-plane geometry is not too serious. It thus appears that (20) is at least qualitatively applicable for typical device configurations even though it was derived on the basis of perturbation theory.

In the *H*-plane geometry of Fig. 1(b), the free precession of the magnetization vector follows a circular cone. In the *E*-plane geometry of Fig. 1(a), however, the circle is distorted by the transverse demagnetizing field into an ellipse which has its major axis lying in the plane of the slab; *i.e.*, in the direction of propagation. Since the figure of merit is larger in the *H*-plane geometry than in the *E*-plane geometry, one may surmise that a further increase in the figure of merit can be obtained by forcing the free precession to follow an ellipsoidal cone with the major axis of the ellipse oriented so that it is perpendicular to the direction of propagation. The calculation presented below shows that this is the case. The ferrite slab must consist of a single crystal or of grain-oriented polycrystalline material. In the presence of crystalline anisotropy, the precessing magnetization generally follows an ellipsoidal cone, unless the dc field is applied along an axis of high symmetry (like the [100] or [111] axes of cubic crystals). The orientation of the single crystal obviously has to be such that through anisotropy forces the magnetization vector is repelled more strongly from the *y*-direction than from the *x*-direction. If the material has hexagonal crystal structure, the desired effect can be obtained if the first-order anisotropy constant is negative (*i.e.*, if the plane perpendicular to the hexagonal axis is energetically preferred over the axis). In this case, the orientation should be such that the hexagonal axis coincides with the waveguide axis (*y*-direction). The desired effect can also be obtained with cubic materials. In this case, the orientation should be such that the field direction (*z*-direction) coincides with a [110] direction. If the first-order cubic anisotropy constant is positive, a [100] direction should be aligned with the waveguide axis; if it is negative, a [110] direction should be aligned with this axis.

We shall consider in detail only the case of a hexagonal material with a preferential plane. The generalization to the cubic case is, however, very straightforward. In the hexagonal case, the anisotropy repels the magnetization only from the *y*-direction and has no effect in the *x*-direction. The additional energy (per unit volume) in this case is

$$E_{\text{anis}} = \frac{M}{2} H_a \alpha_y^2 \quad (21)$$

where $H_a = 2|K_1|/M$ is the anisotropy field and α_y the directional cosine of the magnetization with the *y*-direction. This energy has to be added to the energy given in (30). It is obvious that the energy appropriate for a

³ In the present notation, the sum of the three principal demagnetizing factors equals unity.

⁴ The notation in the present paper is such that M has the factor π in all those cases in which it should be changed to MN . It does not have this factor in all other cases.

⁵ M. T. Weiss, "Improved rectangular waveguide resonance isolators," IRE TRANS. ON MICROWAVE THEORY AND TECHNIQUES, vol. MTT-4, pp. 240-243; October, 1956.

situation in which the ferrite slab has a transverse demagnetizing factor N and the anisotropy is of the form described above, is of essentially the same form as that given in (30). It can be formally obtained from (30) if H is replaced by $H+H_a$ and $4\pi M$ is replaced by $4\pi MN-H_a$. Thus, all the significant results obtained previously can be generalized by applying the same rule. In particular, the figure of merit now becomes

$$F = \frac{8}{1 + \frac{1}{a^2} + \frac{1}{2a^4} - \left(1 + \frac{1}{a^2}\right) \sqrt{\frac{H_a - 4\pi MN}{(H_a - 4\pi MN)^2 + \left(2\frac{\omega_0}{\gamma}\right)^2}}}. \quad (22)$$

A comparison of (20) and (22) shows immediately that a significant increase in the figure of merit can be obtained if $(H_a - 4\pi MN)$ is much larger than $2\omega_0/\gamma$. The ultimate figure of merit according to (22) is

$$F_{\max} = 16a^4.$$

Thus, for $a^2=3$, $F_{\max}=144$; *i.e.*, a factor of 25 better than the previous optimum value. In practice, it will be very difficult to obtain this ultimate figure of merit because the internal magnetic field necessary to produce resonance decreases to zero as the optimum condition is approached. Thus it is eventually not strong enough to magnetize the material. A numerical example that can probably be realized is the following: $4\pi M=2000$ gauss, $N=1/20$, $H_a=2000$ oersteds, $f=2800$ mc, $a^2=3$. The internal magnetic field at resonance is 330 oersteds, and the figure of merit is 17. If $H_a=3000$ oersteds and everything else is unchanged, the internal field at resonance is 210 oersteds, and the figure of merit is 27.5.

IV. DISCUSSION

The theory presented in the preceding sections makes extensive use of a phenomenological description of damping forces. This phenomenological approach cannot be justified on a rigorous basis. It can be shown, however, that a microscopic theory of some of the important loss mechanisms leads to essentially equivalent results. A slight generalization is necessary: the loss parameter λ is, in general, a function of frequency and internal magnetic field.

For a discussion of the resonance isolator, it is important to consider the absorption of radiation which has the negative sense of circular polarization. This absorption, although small, limits the reverse to forward ratio of a resonance isolator. In a previous publication,⁶ the present author has developed a theory of line broadening in polycrystalline ferrites, and has briefly discussed the absorption of radiation with the negative sense of circular polarization. According to this theory, the

susceptibility for circular polarization is essentially given by⁷

$$\chi_+(\omega) = \frac{\gamma M}{\omega_0 - \omega + j(W_p - W_q)}. \quad (23)$$

Here W_p and W_q are functions of frequency and magnetic field which are discussed in an earlier paper.⁶ It can be shown that W_p and W_q are non-negative, that

W_p is nonzero only for $\omega > 0$ (positive sense of circular polarization), and that W_q is nonzero only for $\omega < 0$ (negative sense of circular polarization). For the particular mechanism investigated in the earlier paper,⁶ it can also be shown that $W_p(\omega)$ is approximately equal to $W_q(-\omega)$. The circular susceptibility for the negative sense of polarization is obtained from (23) by inverting the sign of ω and taking the complex conjugate.

On the other hand, the circular susceptibility as calculated from the phenomenological equations is

$$\chi_+(\omega) = \frac{M}{H - \frac{\omega}{\gamma + j\lambda}} = \frac{\frac{\gamma^2 + \lambda^2}{\gamma} M}{\frac{\gamma^2 + \lambda^2}{\gamma} H - \omega + j\omega \frac{\lambda}{\gamma}}. \quad (24)$$

A comparison of (23) and (24) shows immediately that the two results are nearly equivalent if $\lambda/\gamma \ll 1$ and if we allow λ to be dependent on frequency and magnetic field. In this sense, the phenomenological description used in this paper is justified.

It is interesting to compare the bandwidth of the isolator (as defined in Section II) with the width of the ferromagnetic resonance (*i.e.*, the frequency range over which the reverse attenuation has at least half of its maximum value). The width of the resonance can easily be obtained from (4). The numerator of the right-hand side of this equation is relatively insensitive to small changes in frequency around the resonance frequency. The denominator, however, is very sensitive. One finds that to first order in λ/γ , the half width of the resonance for the geometry of Fig. 1(a) is

$$\Delta\omega = 2\lambda(H + 2\pi M) = 2\lambda \sqrt{\left(\frac{\omega_0}{\gamma}\right)^2 + (2\pi M)^2}. \quad (25)$$

An expression appropriate for other geometries is obtained by replacing M by MN . It should be remem-

⁶ E. Schlömann, "Spin-wave analysis of ferromagnetic resonance in polycrystalline ferrites," *J. Phys. Chem. Solids*, vol. 6, no 213, pp. 242-256; 1958.

⁷ *Ibid.*, (42) and (43). The equation given in the present paper is simplified by the assumption of vanishing "intrinsic" loss and neglect of the shift of the resonance frequency.

bered, however, that the phenomenological constant λ is also dependent on the demagnetizing factor. The reason for this is as follows: λ depends primarily on the frequency and the internal (demagnetized) magnetic field. A change in the demagnetizing factor at fixed frequency produces a change in the internal field at resonance. In this way, λ is implicitly dependent on N . The theory described in the earlier work⁶ predicts that λ should be largest for the geometry of Fig. 1(a), smallest for the geometry of Fig. 1(b). A comparison of (25) with (15) shows that for nonoriented polycrystalline material, the bandwidth is at least a factor $\sqrt{2}$ smaller than the width of the resonance.

Consider finally the half width of the resonance determined by varying the magnetic field at constant frequency. From (4) one finds for the geometry of Fig. 1(a) to first order in λ/γ

$$\Delta H = 2 \frac{\lambda \omega_0}{\gamma^2}. \quad (26)$$

The same expression is valid for an arbitrary demagnetizing factor. It is thus also valid for the geometry of Fig. 1(b). Eq. (26) shows that the phenomenological parameter λ appropriate for a given geometry can be obtained experimentally by observing the line width ΔH . The maximum reverse to forward ratio is therefore, from (13) and (26), approximately

$$R_{\max} \approx 16 \left(\frac{\omega_0}{\gamma \Delta H} \right)^2. \quad (27)$$

Here ΔH should be measured at the same frequency and with the same geometry that is actually used in the isolator.

The most significant results of the present investigation are the observation that the bandwidth is usually appreciably smaller than the width of the resonance line, and the prediction that the figure of merit can be appreciably increased by proper use of grain-oriented materials. Since these results are not at all obvious, it is worthwhile to try to understand in a simple way the reasons for this behavior.

In this connection, it is important to realize that the forward attenuation plays a decisive part in determining the reverse to forward ratio. It is easily seen that at resonance the condition for minimum forward attenuation (7) coincides to first order in λ/γ with the condition for maximum reverse to forward ratio (9). It is very possible, therefore, that the bandwidth of the isolator is not the same as the width of the resonance. The phenomenon which primarily determines the bandwidth is the frequency dependence of the ratio of the transverse to the longitudinal components of the magnetic field, because this effect gives rise to a rather strong frequency dependence of the forward attenuation. For this reason the bandwidth is dependent, among other things, on the ratio of the resonance frequency and the cutoff frequency, and vanishes as this ratio approaches unity.

To obtain a better intuitive understanding of the situation, it is advantageous to consider the frequency dependence of ϕ_0 , *i.e.*, the position of the ferrite slab that results in a maximum reverse to forward ratio. For the geometry of Fig. 1(a), one finds from (9) and the remarks at the beginning of Appendix II that ϕ_0 is determined by

$$\tan^2 \phi_0 = \frac{q}{p} = \frac{(\gamma^2 + \lambda^2)(H + 4\pi M)^2 - \omega^2}{[(\gamma^2 + \lambda^2)H^2 - \omega^2] \left[\left(\frac{\omega}{\omega_c} \right)^2 - 1 \right]}. \quad (28)$$

By straightforward differentiation, one obtains the fractional change of $\tan \phi_0$, divided by the fractional change of the frequency taken at resonance.

$$\frac{\omega_0}{\tan \phi_0} \frac{d \tan \phi_0}{d\omega} \bigg|_{\omega=\omega_0} = - \left\{ 1 + \frac{1}{a^2} + \frac{2\pi M}{\sqrt{(2\pi M)^2 + \frac{\omega_0^2}{\gamma^2 + \lambda^2}}} \right\}. \quad (29)$$

This equation can again be generalized to the case of a ferrite slab with an arbitrary transverse demagnetizing factor N and an anisotropy field H_a by replacing $4\pi M$ by $4\pi MN - H_a$. Eq. (29) shows that the frequency dependence of ϕ_0 is weakest for large a and small N . By proper use of grain-oriented materials, the sign of the last term of (29) can effectively be reversed. In the limit as $H_a \gg 2\omega_0/\gamma$ this term approaches -1 . It is thus seen that the frequency dependence of ϕ_0 can be significantly reduced by the use of grain-oriented materials. It is easy to believe, therefore, that the figure of merit of the isolator should be improved in a similar way.

APPENDIX I

EFFECTIVE SUSCEPTIBILITY OF A THIN SLAB

The equation of motion can be derived conveniently from the energy (per unit volume) necessary to pull the magnetization vector out of the z -direction into a direction characterized by the two directional cosines, α_x and α_y . This energy is for a thin slab in the geometry of Fig. 1(a) and for $\alpha_x, \alpha_y \ll 1$.

$$E = \frac{M}{2} \{ (H + 4\pi M)\alpha_x^2 + H\alpha_y^2 \} - M(\alpha_x h_x + \alpha_y h_y). \quad (30)$$

The equations of motion are now

$$\begin{aligned} M\ddot{\alpha}_x &= -\gamma \frac{\partial E}{\partial \alpha_y} - \lambda \frac{\partial E}{\partial \alpha_x} \\ M\ddot{\alpha}_y &= \gamma \frac{\partial E}{\partial \alpha_x} - \lambda \frac{\partial E}{\partial \alpha_y}. \end{aligned} \quad (31)$$

If the driving field has a periodic time dependence ($\sim e^{j\omega t}$), one obtains from (30) and (31)

$$\begin{aligned} [j\omega + \lambda(H + 4\pi M)]\alpha_x + \gamma H\alpha_y &= \gamma h_y + \lambda h_x \\ \gamma(H + 4\pi M)\alpha_x - [j\omega + \lambda H]\alpha_y &= \gamma h_x - \lambda h_y. \end{aligned} \quad (32)$$

By solving (32) for α_x and α_y , it is easy to obtain the effective susceptibility given in (2). The same result can also be derived by converting the "true" susceptibility $\overset{\leftrightarrow}{\chi}$ (as calculated using a Landau-Lifshitz damping term) to the effective susceptibility by using the formula

$$\overset{\leftrightarrow}{\chi}_{\text{eff}} = (1 + 4\pi\overset{\leftrightarrow}{\chi}N)^{-1}\overset{\leftrightarrow}{\chi}. \quad (33)$$

APPENDIX II

ISOLATOR BANDWIDTH

In evaluating the bandwidth, it is convenient to use the left-hand side of (5), thus expressing R in terms of $\cos \phi$ and $\sin \phi$ rather than $\cos 2\phi$ and $\sin 2\phi$. Since (9) is equivalent to

$$\cos \phi_0 = \sqrt{\frac{p}{p+q}} \quad \sin \phi_0 = \sqrt{\frac{q}{p+q}} \quad (34)$$

one obtains from (5) and (8)

$$R(\phi_0, \omega) = \frac{N(\omega)}{D(\omega)} \quad (35)$$

where

$$\begin{aligned} N(\omega) = & [(\gamma^2 + \lambda^2)H^2 + \omega^2][(\gamma^2 + \lambda^2)(H + 4\pi M)^2 + \omega_0^2] \\ & \cdot \left[\left(\frac{\omega}{\omega_c} \right)^2 - 1 \right] \\ & + [(\gamma^2 + \lambda^2)H^2 + \omega_0^2][(\gamma^2 + \lambda^2)(H + 4\pi M)^2 + \omega^2] \\ & \cdot \left[\left(\frac{\omega_0}{\omega_c} \right)^2 - 1 \right] \\ & + 4\gamma(H + 2\pi M)\omega \\ & \cdot \left\{ [(\gamma^2 + \lambda^2)H^2 + \omega_0^2][(\gamma^2 + \lambda^2)(H + 4\pi M)^2 + \omega_0^2] \right. \\ & \cdot \left[\left(\frac{\omega_0}{\omega_c} \right)^2 - 1 \right] \left[\left(\frac{\omega}{\omega_c} \right)^2 - 1 \right] \Big\}^{1/2} \end{aligned} \quad (36)$$

and $D(\omega)$ is obtained from $N(\omega)$ by reversing the sign of γ .

Now let $\omega = \omega_0 + \delta\omega$. Neglecting higher powers of $\delta\omega$, one finds

$$\left[\left(\frac{\omega}{\omega_c} \right)^2 - 1 \right]^{1/2} = a \left\{ 1 + \frac{\omega_0 \delta\omega}{a^2 \omega_c^2} - \frac{(\delta\omega)^2}{2a^4 \omega_c^2} \right\} \quad (37)$$

where

$$a = \sqrt{\left(\frac{\omega_0}{\omega_c} \right)^2 - 1}$$

is the ratio of the amplitudes of the transverse and longitudinal components of the magnetic field. Expanding $N(\omega)$ in powers of $\delta\omega$, one obtains

$$N(\omega) = N_0 + N_1 \delta\omega + N_2 (\delta\omega)^2 + \dots \quad (38)$$

where

$$\begin{aligned} N_0 = & 8(\gamma^2 + \lambda^2)(H + 2\pi M)^2 \omega_0^2 a^2 \left(1 + \frac{\gamma}{\sqrt{\gamma^2 + \lambda^2}} \right) \\ N_1 = & 8(\gamma^2 + \lambda^2)(H + 2\pi M)^2 \omega_0 (2a^2 + 1) \\ & \cdot \left(1 + \frac{\gamma}{\sqrt{\gamma^2 + \lambda^2}} \right) \\ N_2 = & 4(\gamma^2 + \lambda^2)(H + 2\pi M) \\ & \cdot \left\{ (4H + 12\pi M)a^2 + (3H + 10\pi M) \right. \\ & \left. + \frac{\gamma}{\sqrt{\gamma^2 + \lambda^2}} (H + 2\pi M) \left(2a^2 + 1 - \frac{1}{a^2} \right) \right\}. \end{aligned} \quad (39)$$

From (35), (38), and (39) the reverse to forward ratio is

$$R(\phi_0, \omega) = R_{\text{max}}(\omega_0) \frac{1 + \alpha_1 \delta\omega + \alpha_2 (\delta\omega)^2}{1 + \beta_1 \delta\omega + \beta_2 (\delta\omega)^2} \quad (40)$$

where

$$\begin{aligned} \alpha_1 = \beta_1 = & \frac{N_1}{N_0} = \frac{2a^2 + 1}{\omega_0 a^2} \\ \alpha_2 = & \frac{(4H + 12\pi M)a^2 + (3H + 10\pi M) + \frac{\gamma}{\sqrt{\gamma^2 + \lambda^2}} (H + 2\pi M) \left(2a^2 + 1 - \frac{1}{a^2} \right)}{2(H + 2\pi M)\omega_0^2 a^2 \left(1 + \frac{\gamma}{\sqrt{\gamma^2 + \lambda^2}} \right)} \end{aligned} \quad (41)$$

and β_2 is obtained from α_2 by reversing the sign of γ . It is obvious from (41) that β_2 is much larger than α_2 for $\lambda/\gamma \ll 1$. For this reason an expansion of R in powers of $\delta\omega$ converges very slowly, but an expansion of $1/R$ in powers of $\delta\omega$ should converge rapidly. If higher powers of $\delta\omega$ are again neglected, (14) is obtained from (40) and

$$\left(\frac{2}{B}\right)^2 = \beta_2 - \alpha_2. \quad (42)$$

A simple expression for the bandwidth is obtained in the

limit $\lambda/\gamma \ll 1$. The α_2 term of (42) can be neglected if only the lowest order of λ/γ is taken into account. In this approximation

$$B^2 = \frac{4}{\beta_2} = \frac{2(\lambda/\gamma)^2 \omega_0^2}{1 + \frac{1}{a^2} + \frac{1}{2a^4} + \left(1 + \frac{1}{a^2}\right) \frac{2\pi M}{H + 2\pi M}}. \quad (43)$$

Eq. (15) is now obtained by expressing H in terms of the resonance frequency.

Analysis of Microwave Measurement Techniques by Means of Signal Flow Graphs*

J. K. HUNTON†

Summary—Microwave measurement techniques can be analyzed more simply by using signal flow graphs instead of the customary scattering matrices to describe the microwave networks used in the measuring system. This is because the flow graphs of individual networks are simply joined together when the networks are cascaded and the solution for the system can be written down by inspection of the over-all flow graph by application of the nontouching loop rule. This paper reviews the method of setting up flow graphs of microwave networks and the rule for their solution. A single directional-coupler reflectometer system for measuring the reflection coefficient of a load is then analyzed by this method. The analysis shows how auxiliary tuners can be used to cancel residual error terms in the measurement of the magnitude of the reflection coefficient at a particular frequency. The analysis also shows how an additional tuner can be used to measure the phase angle of the reflection coefficient. These reflectometer techniques are particularly useful in the measurement of very small reflections.

INTRODUCTION

THE signal flow graph is a method of writing a set of equations, whereby the variables are represented by points and the interrelations by directed lines giving a direct picture of signal flow. The algebra of flow graphs leading to solutions by direct inspection has been developed by S. J. Mason and others at the Massachusetts Institute of Technology.^{1,2} When microwave network equations are written in scattering matrix form the corresponding flow graph is particularly useful because, in this case, the flow graph of a system of cas-

caded networks is constructed simply by joining together the flow graphs of the individual networks, and the solution is then available directly.

One of the best applications of the flow graph method is in the analysis of measuring techniques and the determination of residual errors. It is the intention here to review the mechanics of the method and to apply it in analyzing the microwave reflectometer system used for measuring the reflection coefficient of a load. This system has been in general use for some time,³ and has been analyzed recently by Engen and Beatty⁴ who showed how tuners could be used to reduce residual errors to a negligible value when measuring the magnitude of the reflection coefficient. Their result will be derived here by the flow graph method. In addition, a technique for measuring the phase angle of the reflection coefficient will be presented.

ONE- AND TWO-PORT NETWORK FLOW GRAPHS

Fig. 1 shows some simple flow graphs used as building blocks. In Fig. 1(a) the general two-port network is shown as specified by its scattering matrix coefficients. Here a_1 and a_2 are the complex entering wave amplitudes, while b_1 and b_2 are the outgoing wave amplitudes at ports 1 and 2 of the network. These are represented in the flow graph as points or "nodes." The nodes are

* Manuscript received by the PGMT, September 14, 1959; revised manuscript received November 25, 1959.

† Hewlett-Packard Co., Palo Alto, Calif.

¹ S. J. Mason, "Feedback theory—some properties of signal flow graphs," *PROC. IRE*, vol. 41, p. 1144-1156; September 1953.

² S. J. Mason, "Feedback theory—further properties of signal flow graphs," *PROC. IRE*, vol. 44, pp. 920-926; July, 1956.

³ J. K. Hunton and N. L. Pappas, "The -hp- microwave reflectometers," *Hewlett-Packard J.*, vol. 6, pp. 1-7; September-October, 1954.

⁴ G. F. Engen and R. W. Beatty, "Microwave reflectometer techniques," *IRE TRANS. ON MICROWAVE THEORY AND TECHNIQUES*, vol. MTT-7, pp. 351-355; July 1959.

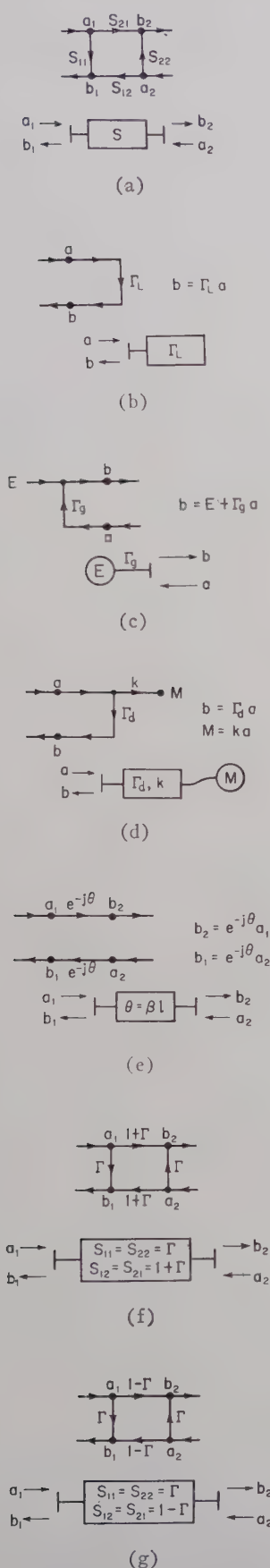


Fig. 1—(a) Two-port network. (b) Load. (c) Generator. (d) Video detector. (e) Lossless line length. (f) Shunt admittance. (g) Series impedance.

related to one another by directed lines (signal flow) marked with appropriate coefficients. These are the scattering coefficients $S_{11}, S_{12}, S_{21}, S_{22}$ and their meaning is derived from

$$b_1 = S_{11}a_1 + S_{12}a_2,$$

$$b_2 = S_{21}a_1 + S_{22}a_2.$$

Here S_{11} is the reflection coefficient b_1/a_1 at port 1 when port 2 is terminated in a matched load (in this case $a_2 = 0$). S_{22} is the reflection coefficient b_2/a_2 at port 2 when port 1 is matched ($a_1 = 0$). S_{12} is the transmission coefficient b_1/a_2 from port 2 to port 1 when port 1 is matched ($a_1 = 0$), and S_{21} is the transmission coefficient b_2/a_1 from port 1 to port 2 when port 2 is matched ($a_2 = 0$). In all reciprocal networks $S_{12} = S_{21}$. The value of each node in the flow graph is the sum of all signals entering it, each signal being the value of the node from which it comes multiplied by its path coefficient. The independent variables a_1 and a_2 in the equations represented by the flow graph are characterized by signal flow directed into the graph.

Fig. 1(b) depicts a termination or load whose reflection coefficient is Γ_L .

Fig. 1(c) shows a mismatched generator. Here E is the wave amplitude at the port when the generator sees a matched load ($a = 0$) and Γ_g is the reflection coefficient looking into the port when E is zero.

Fig. 1(d) shows a video detector (such as a crystal or a barretter mount). Γ_d is the detector reflection coefficient at the port, and k is a scalar conversion efficiency relating the incoming wave amplitude to a meter reading M . It is assumed that this meter is calibrated to take account of the detector law so that k is independent of signal level. It is also assumed that Γ_d is independent of signal level. (Both these conditions are satisfied very nearly with detectors used in reflectometer systems when used in their proper operating range.)

Fig. 1(e) depicts a length of lossless transmission line.

Fig. 1(f) is a shunt discontinuity such as a junction between two lines or a probe which can be considered as a shunt admittance. The coefficient $S_{11} = S_{22} = \Gamma$ is the reflection coefficient which would be measured if the discontinuity were followed by a matched load. The coefficient $S_{12} = S_{21} = 1 + \Gamma$ follows from the fact that the net wave amplitudes on either side of the discontinuity must be equal. The coefficient Γ is related to the normalized shunt admittance Y by

$$\Gamma = -\frac{Y}{Y + 2}.$$

Fig. 1(g) is a lumped series impedance. Here the coefficient Γ is related to the normalized series impedance Z by

$$\Gamma = \frac{Z}{Z + 2}.$$

THE "NONTOUCHING LOOP" RULE

When networks are cascaded it is only necessary to cascade the flow graphs since the outgoing wave from one network is the incoming wave to the next. This is demonstrated in Fig. 2 where a network is placed between a generator and a load. The system now has only one independent variable, the generator amplitude E . The flow graph contains paths and loops. A "path" is a series of directed lines followed in sequence and in the same direction in such a way that no node is touched more than once. The value of the path is the product of all coefficients encountered en route. In the figure there is one path from E to b_2 . It has a value S_{21} . There are two paths from E to b_1 , namely S_{11} and $S_{21}\Gamma_L S_{12}$. A first order "loop" is a series of directed lines coming to a closure when followed in sequence and in the same direction with no node passed more than once. The value of the loop is the product of all coefficients encountered en route. A second-order loop is the product of any two first-order loops which do not touch at any point and a third-order loop is the product of any three first-order loops which do not touch, and so on. In Fig. 2 there are three first-order loops, namely, $\Gamma_\theta S_{11}$, $S_{22}\Gamma_L$, and $\Gamma_\theta S_{21}\Gamma_L S_{12}$ and there is one second-order loop $\Gamma_\theta S_{11} S_{22}\Gamma_L$.

The solution of a flow graph is accomplished by application of the nontouching loop rule,^{5,6} which, written symbolically, is

$$T = \frac{P_1(1 - \sum L(1)^{(1)} + \sum L(2)^{(1)} - \sum L(3)^{(1)} + \dots) + P_2(1 - \sum L(1)^{(2)} + \sum L(2)^{(2)} - \dots) + P_3(1 - \dots)}{1 - \sum L(1) + \sum L(2) - \sum L(3) + \dots}$$

Here $\sum L(1)$ denotes the sum of all first-order loops. $\sum L(2)$ denotes the sum of all second-order loops and so on. P_1, P_2, P_3 , etc., are the values of all the various paths which can be followed from the independent variable node to the node whose value is desired. $\sum L(1)^{(1)}$ denotes the sum of all first-order loops which do not touch path P_1 at any point, and so on. In other words, each path is multiplied by the factor in brackets which involves all the loops of all orders which that path does not touch. T is a general symbol representing the ratio between the dependent variable of interest and the independent variable. This process is repeated for each independent variable of the system and the results are summed.

As examples of the application of the rule, the transmission b_2/E and the reflection coefficient b_1/a_1 are written as follows:

⁵ C. S. Lorens, "A Proof of the Nonintersecting Loop Rule for the Solution of Linear Equations by Flowgraphs," Res. Lab. of Electronics, M.I.T., Cambridge, Mass., Quart. Prog. Rept., pp. 97-102; January, 1956.

⁶ W. W. Happ, "Lecture notes on signal flowgraphs," from "Analysis of Transistor Circuits," Extension Course, University of California, Berkeley, Catalogue No. 834AB.

$$\frac{b_2}{E} = \frac{S_{21}}{1 - \Gamma_\theta S_{11} - S_{22}\Gamma_L - \Gamma_\theta S_{21}\Gamma_L S_{12} + \Gamma_\theta S_{11} S_{22}\Gamma_L},$$

$$\frac{b_1}{a_1} = \frac{S_{11}(1 - S_{22}\Gamma_L) + S_{21}\Gamma_L S_{12}}{1 - S_{22}\Gamma_L}.$$

Note that the generator flow graph is unnecessary when solving for b_1/a_1 , and the loops associated with it are deleted when writing this solution. It is worth mentioning at this point that second- and higher-order loops can quite often be neglected while writing down the solution if one has orders of magnitude for the various coefficients in mind.

THREE-PORT NETWORK

The flow graph of the general three-port network with the third port terminated by a detector is shown in Fig. 3(a). The equations described by the flow graph are

$$b_1 = S_{11}a_1 + S_{12}a_2 + S_{13}a_3,$$

$$b_2 = S_{21}a_1 + S_{22}a_2 + S_{23}a_3,$$

$$b_3 = S_{31}a_1 + S_{32}a_2 + S_{33}a_3,$$

$$a_3 = b_3\Gamma_d,$$

$$M = k_{d3},$$

(note also that $S_{12} = S_{21}$, $S_{13} = S_{31}$, $S_{23} = S_{32}$ for reciprocal networks).

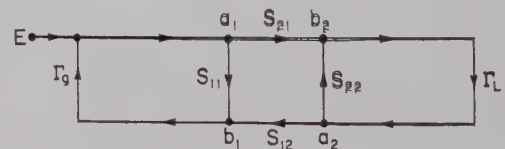
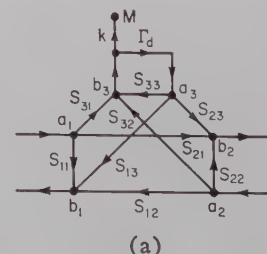
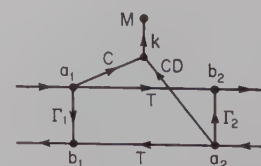


Fig. 2—Cascading of a network between load and generator.



(a)



(b)

Fig. 3—(a) Three-port network with detector. (b) Directional detector.

Since only two RF ports are available with this combination, the flow graph can be simplified considerably. Fig. 3(b) shows this simplification. The symbols for the coefficients are chosen with a directional coupler-detector combination in mind. The directional coupler is assumed to have a built-in termination in one end of its secondary arm, and the other end of the secondary arm is the third port which is terminated by a video detector. The relationships involved are

$$M = \left| CkE' \frac{(D + T\Gamma_{t1}) + \Gamma_L(TT_t^2 - T\Gamma_{t1}\Gamma_{t2} - D\Gamma_{t2})}{(1 - \Gamma_{\theta}'\Gamma_2 - \Gamma_{\theta}'\Gamma_{t1}T^2 - \Gamma_1\Gamma_{t1}) - \Gamma_L(\Gamma_{\theta}'T^2T_t^2 + \Gamma_1T_t^2 + \Gamma_{t2} - \Gamma_{\theta}'T^2\Gamma_{t1}\Gamma_{t2})} \right|.$$

$$b_1 = \Gamma_1 a_1 + T a_2,$$

$$b_2 = \Gamma_2 a_2 + T a_1,$$

$$M = k(Ca_1 + CDa_2),$$

$$\Gamma_1 = S_{11} + \frac{S_{13}^2 \Gamma_d}{1 - S_{33} \Gamma_d},$$

$$\Gamma_2 = S_{22} + \frac{S_{23}^2 \Gamma_d}{1 - S_{33} \Gamma_d},$$

$$T = S_{21} + \frac{S_{13} S_{23} \Gamma_d}{1 - S_{33} \Gamma_d},$$

$$C = \frac{S_{31}}{1 - S_{33} \Gamma_d}, \quad D = \frac{S_{32}}{S_{31}}.$$

These relationships are written directly through application of the nontouching loop rule. Note that the path a_1 to M is the main coupling direction involving an effective coupling coefficient C and the path a_2 to M is the residual coupling direction involving the coupling factor and effective directivity coefficient D . For a directional coupler, the coupling factor as usually defined is $20 \log |1/S_{31}|$ while the directivity is $20 \log |S_{31}/S_{32}|$.

SINGLE COUPLER REFLECTOMETER

A reflectometer system for measuring the reflection coefficient of a load is shown in Fig. 4. In this arrangement a single directional-detector is used in conjunction with two slide-screw tuners, one at each end of the coupler. These tuners are for the purpose of cancelling residual signals which can cause a measurement error. They consist of a probe of adjustable penetration projecting into the line through a slot along which the probe position can be varied. In the flow graph of the system

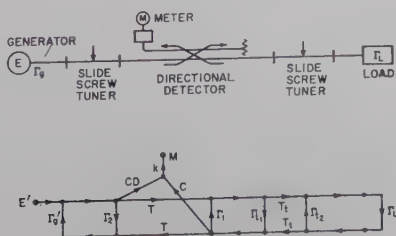


Fig. 4—Single coupler reflectometer.

the generator tuner reflection is lumped together with the generator reflection as Γ_{θ}' and the load tuner is represented as a general two-port network with coefficients Γ_{t1} , Γ_{t2} and T_t . The analysis carried out in Appendix I shows that Γ_{θ}' can be made equal to any arbitrary value by proper adjustment of the generator tuner (although E varies with the adjustment), and Γ_{t1} can be made any arbitrary value by proper adjustment of the load tuner.

The solution for the meter reading M is

This assumes that connector or flange joint reflections are lumped within the tuner networks and the coupler coefficients Γ_1 , Γ_2 , D are small compared to unity. All third- and higher-order loops are negligible and second-order loops involving Γ_1 or Γ_2 are negligible. These approximations are quite valid for practical systems and simplify the algebra considerably. Since the meter reading M is not directly proportional to $|\Gamma_L|$, the reflectometer system as it stands cannot give an accurate result. The procedure for achieving the accurate relationship is as follows:

- 1) Adjust the load tuner: terminate the system with a low-reflection phaseable load. The Γ_L term in the denominator is then negligible by comparison with the constant term, whereas the Γ_L term in the numerator is comparable to the constant term. As the load is moved, the meter reading will vary. By adjusting Γ_{t1} such that no variation occurs, the constant term in the numerator can be brought to zero. This means $\Gamma_{t1} = -D/T$.
- 2) Adjust the generator tuner: the system is now terminated with a phaseable short circuit. As this is moved, the meter reading varies as a result of the beating between the Γ_L term and the constant term in the denominator. By proper adjustment of Γ_{θ}' , the Γ_L term can be made zero. That is

$$\Gamma_{\theta}' = \frac{\Gamma_1 \Gamma_{t2} + \Gamma_{t2}}{T^2 \Gamma_{t1} \Gamma_{t2} - T^2 T_t^2}.$$

With this adjustment no variation in M occurs as the short is moved.

- 3) The meter reading is now directly proportional to $|\Gamma_L|$. That is $M = K|\Gamma_L|$. The meter reading is adjusted to the reference value of unity by adjustment of a gain control. If now an unknown load is connected to the system, the meter will accurately measure the magnitude of its reflection coefficient. In a practical case it may be necessary to apply corrections to the meter readings to take account of small deviations of the detector law from the meter law.

The use of tuners in the magnitude measurement results in a cancellation of residual error signals. In the phase measuring method, the residual error signals are merely depressed since a further probe insertion is required to make the measurement after "flattening" the system. This depression becomes important when the residual reflections in the system are of the same order of magnitude as the reflection to be measured.

APPENDIX I

THE SLIDE-SCREW TUNER

The slide-screw tuner consists of a probe of adjustable penetration projecting into a line through a slot along which its position can be adjusted. The probe itself can be regarded as a purely shunt discontinuity. In addition, there are fixed discontinuities at the ends of the slot and at the connectors or flange joints. It is desirable to lump all the fixed discontinuities at the two ports of the network. To show that this can be done, consider the flow graph of a shunt discontinuity followed by a length of lossless line as in Fig. 6(a).

Here β is the electrical length of the line section and Γ is the reflection coefficient of the discontinuity when backed up with a matched load. The discontinuity can be transferred to the other port as shown in Fig. 6(b).

In either case the scattering coefficients are

$$S_{11} = \Gamma, \quad S_{22} = \Gamma e^{-2j\beta}, \quad S_{12} = S_{21} = (1 + \Gamma)e^{-j\beta}.$$

If a further discontinuity Γ' is present at the right-hand port, the two can be lumped together and described by the flow graph of Fig. 6(c) where,

$$\Gamma_1 = \frac{\Gamma e^{+2j\beta} + \Gamma' + 2\Gamma\Gamma'}{1 - \Gamma\Gamma' e^{-2j\beta}},$$

$$\Gamma_2 = \frac{\Gamma' + \Gamma e^{-2j\beta} + 2\Gamma\Gamma' e^{-2j\beta}}{1 - \Gamma\Gamma' e^{-2j\beta}},$$

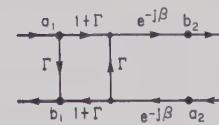
$$T = \frac{e^{-j\beta}(1 + \Gamma)(1 + \Gamma')}{1 - \Gamma\Gamma' e^{-2j\beta}}.$$

For small reflections, the tuner probe is a lossless shunt discontinuity and is equivalent to a shunt capacitive susceptance. The relationship between normalized susceptance B_p and probe reflection coefficient Γ_p is

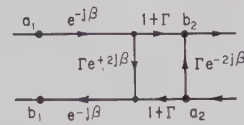
$$\Gamma_p = \frac{-jB_p}{2 + jB_p}.$$

The complete flow graph of a slide-screw tuner is shown in Fig. 6(d) where all the fixed reflections beyond the probe are now lumped at the two ports.

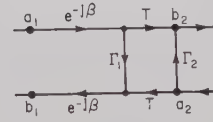
It is desirable to represent the tuner by a two-port flow graph with three coefficients. In order that this be



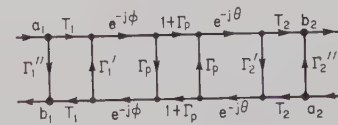
(a)



(b)



(c)



(d)



(e)

Fig. 6—(a) Shunt discontinuity followed by a length of lossless line. (b) Equivalent discontinuity referred to the other port. (c) Additional discontinuity included at the port. (d) Complete flow graph of the slide-screw tuner. (e) Equivalent side-screw tuner flow graph.

useful, however, it is necessary to show that the S_{11} and S_{22} coefficients can be made equal to any arbitrary value by proper adjustment of Γ_p and θ . This can be done in two steps. Consider first the case with no discontinuity at port 1. The S_{11} coefficient is then

$$\frac{\Gamma_p e^{-2j\phi} + \Gamma_2' e^{-2j(\theta+\phi)} + 2\Gamma_p \Gamma_2' e^{-2j(\theta+\phi)}}{1 - \Gamma_p \Gamma_2' e^{-2j\theta}}.$$

Consider the possibility of making this some arbitrary value k . This is a simple problem to solve using a Smith Chart. One would start with a reflection coefficient Γ_2' at port 2 and move toward the generator until reaching a point at which the reflection $\Gamma_2' e^{-2j\theta}$ and the reflection $k e^{+2j\theta}$ were represented on the chart by admittances with the same conductance value. The probe would be inserted at this point until its susceptance equalled the difference between the susceptances at the points representing the two reflections.

Stated analytically these conditions are

$$\begin{aligned}\Gamma_p &= \frac{-jB_p}{2 + jB_p}, \\ ke^{+2j\phi} &= \frac{1 - G - jB_k}{1 + G + jB_k}, \\ \Gamma_2' e^{-2j\theta} &= \frac{1 - G - jB'}{1 + G + jB'}, \\ B_p &= B_k - B' \quad [B_p \text{ positive}].\end{aligned}$$

Substitution of these conditions in the expression for S_{11} above does give the result $S_{11}=k$. Since the S_{11} coefficient can be made equal to any arbitrary value k when the fixed port-1 reflection is absent, it is obvious that the S_{11} coefficient for the complete system can be made

equal to any arbitrary value a . The value is

$$a = \frac{\Gamma_1''(1 - k\Gamma_1') + T_1^2 k}{1 - k\Gamma_1'},$$

or

$$k = \frac{\Gamma_1'' - a}{\Gamma_1''\Gamma_1' - T_1^2 - \Gamma_1'a}.$$

The slide-screw tuner can now be represented as a two-port device with three coefficients as shown in Fig. 6(e), and we can conclude that Γ_1 or Γ_2 can be made any arbitrary value by adjustment of the probe.

ACKNOWLEDGMENT

The author wishes to thank Dr. P. D. Lacy for his many helpful suggestions.

Stepped Transformers for Partially Filled Transmission Lines*

D. J. SULLIVAN† AND D. A. PARKES†

Summary—In recent years, partially-filled transmission lines have been used to improve the characteristics of various ferrite and garnet devices. This paper presents a generalized outline for determining the approximate effective guide wavelength and characteristic impedance of two types of (dielectric-loaded) partially-filled transmission line. The results are used to determine the geometries required for the design of optimum stepped transmission line transformers. The stepped transitions are designed to yield a Tchebycheff-type response for any given bandwidth. The measured results for stepped transitions in partially filled coaxial line and partially filled double-ridge waveguide are presented. The data are found to approximate the theory closely.

I. INTRODUCTION

DIELECTRIC-loading techniques^{1,2} are frequently used to improve the characteristics of certain ferrite and garnet devices. It has been shown that one method of obtaining a nonreciprocal device in conventional coaxial or strip transmission line is to distort the dominant (TEM or Quasi-TEM) mode by use

of a dielectric material.^{3,4} The nonreciprocal characteristics of double-ridge waveguide components are also often improved by supplementing the ferrite or garnet with a dielectric material.⁵ The addition of this dielectric material changes the characteristic impedance of the transmission line, and this in turn introduces the problem of matching. Cohn has shown that for a given number of steps a Tchebycheff stepped transformer design will give the minimum possible VSWR for a specified bandwidth.⁶ Three stepped transitions, in partially filled transmission line, are shown in Fig. 1. The use of a stepped transition will normally 1) substantially reduce the inherent VSWR of a device, 2) enable a specific unit to be made considerably shorter or 3) result in a compromise between the two.

³ B. J. Duncan, L. Swern, K. Tomiyasu, and J. Hannwacker, "Design considerations for broadband ferrite coaxial line isolators," *Proc. IRE*, vol. 45, pp. 483-490; April, 1957.

⁴ D. Fleri and G. Hanley, "Nonreciprocity of dielectric loaded TEM mode transmission lines," *IRE TRANS. ON MICROWAVE THEORY AND TECHNIQUES*, vol. MTT-7, pp. 23-27; January, 1959.

⁵ E. Grimes, D. Bartholomew, D. Scott, and S. Sloan, "Broadband ridge waveguide ferrite devices," presented at the IRE National Symposium on Microwave Theory and Techniques, Harvard University, Cambridge, Mass.; June 1-3, 1959.

⁶ S. B. Cohn, "Optimum design of stepped transmission line transformers," *IRE TRANS. ON MICROWAVE THEORY AND TECHNIQUES*, vol. MTT-3, pp. 16-21; April, 1955.

* Manuscript received by the PGMTT, August 31, 1959; revised manuscript received, December 7, 1959.

† Sperry Microwave Electronics Co., Clearwater, Fla.

¹ P. H. Vartanian, J. L. Melchor, and W. P. Ayres, "Broadbanding ferrite microwave isolators," 1956 IRE NATIONAL CONVENTION RECORD, pt. 5, pp. 79-83.

² E. A. Ohm, "A broadband microwave circulator," *IRE TRANS. ON MICROWAVE THEORY AND TECHNIQUES*, vol. MTT-4, pp. 210-217; October, 1956.

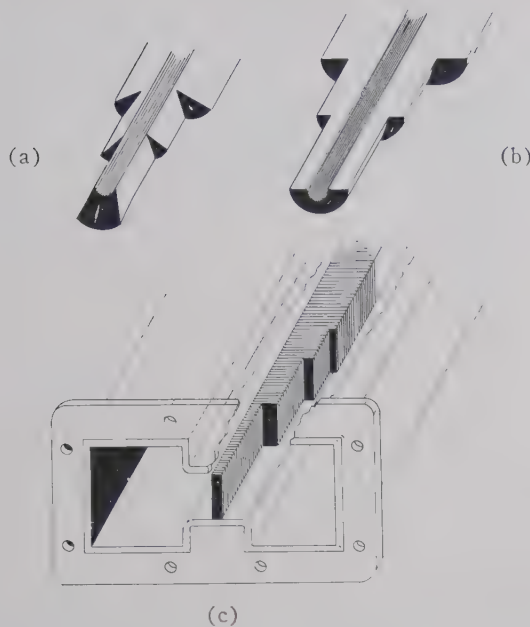


Fig. 1—Step transitions in partially filled transmission line. (a) Coaxial step transition for changing angle, (b) coaxial step transition for changing diameter, (c) double-ridge waveguide step transition.

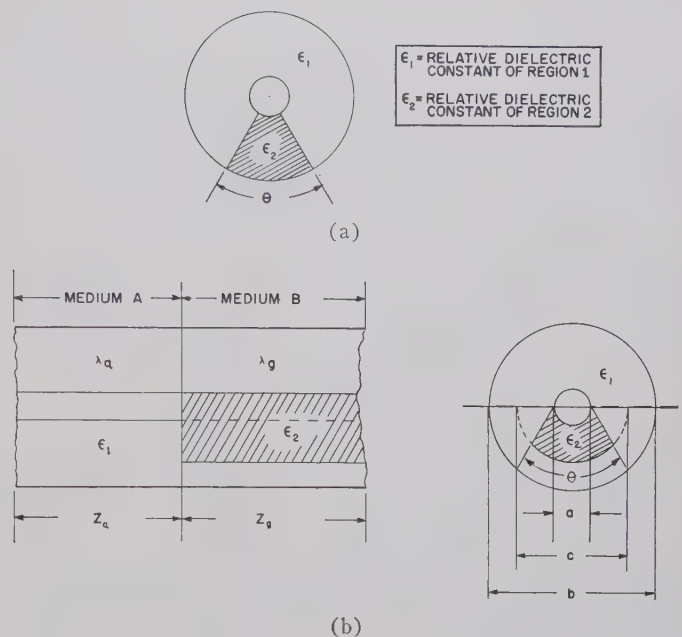


Fig. 2—Cross section of partially filled coaxial transmission lines.

It has been shown that in a partially filled coaxial line, as shown in Fig. 2(a), the guide wavelength may be obtained as a function of the dielectric wedge angle θ .⁷ Normally, it is difficult to machine a dielectric wedge, especially for small angles and small transmission lines. Fig. 2(b) shows another type of partially filled coaxial transmission line.

This paper describes a method for computing the approximate effective guide wavelength and characteristic impedance for the types of partially filled transmission line shown in Fig. 1. It also outlines a generalized procedure for designing step transitions in each type of partially filled transmission line.

II. THEORETICAL DESIGN CONSIDERATIONS

A. Partially Filled Coaxial Transmission Line

1) *Guide Wavelength and Characteristic Impedance:* Fig. 2(b) shows a partially filled coaxial transmission line. Neglecting fringing effects, and under static conditions, the capacitance per unit length for the two cross-sectional areas of medium B may be written as⁸

$$C_1 = \frac{360\epsilon_1}{\ln \frac{b}{a}} - \frac{\theta\epsilon_1}{\ln \frac{b}{a}} \quad \text{and} \quad C_2 = \frac{\theta\epsilon_1\epsilon_2}{\epsilon_1 \ln \frac{c}{a} + \epsilon_2 \ln \frac{b}{c}}$$

⁷ D. J. Angelakos, "A coaxial line filled with two non-concentric dielectrics," IRE TRANS. ON MICROWAVE THEORY AND TECHNIQUES, vol. MTT-2, pp. 39-44; July, 1954.

⁸ J. D. Kraus, "Electromagnetics," McGraw-Hill Book Co., Inc., New York, N. Y., pp. 74-75; 1953.

The total equivalent capacitance is

$$C_e = C_1 + C_2$$

$$= C \left[\frac{\theta}{360} \left(\frac{\epsilon_2 \ln \frac{b}{a}}{\epsilon_1 \ln \frac{c}{a} + \epsilon_2 \ln \frac{b}{c}} - 1 \right) + 1 \right] \quad (1)$$

where

$$C = \frac{360\epsilon_1}{\ln \frac{b}{a}}$$

In medium A, the equivalent phase velocity, V , and propagating wavelength, λ_a , are

$$V = f\lambda_a = \frac{1}{\sqrt{LC}}$$

In medium B, the equivalent phase velocity, V_e , and propagating wavelength, λ_g , are

$$V_e = f\lambda_g = \frac{1}{\sqrt{LC_e}}$$

Thus,

$$V_e = f\lambda_g = \frac{f\lambda_a}{\sqrt{\frac{\theta}{360} \left(\frac{\epsilon_2 \ln \frac{b}{a}}{\epsilon_1 \ln \frac{c}{a} + \epsilon_2 \ln \frac{b}{c}} - 1 \right) + 1}}$$

For coaxial line,

$$\frac{\lambda_g}{\lambda_a} = \frac{Z_g}{Z_a} \quad (2)$$

Therefore,

$$\frac{\lambda_g}{\lambda_a} = \frac{Z_g}{Z_a} = \frac{1}{\frac{\theta}{360} \left[\frac{\epsilon_2 \ln \frac{b}{a}}{\epsilon_1 \ln \frac{c}{a} + \epsilon_2 \ln \frac{b}{c}} - 1 \right] + 1} \quad (3)$$

with the parameters as described in Fig. 2(b). In this equation, λ_g is the effective guide wavelength and Z_g the characteristic impedance of the partially filled coaxial transmission line.

Fig. 3 shows the variation of Z_g/Z_a and λ_g/λ_a as a function of b/c , with $Z_a = 50$ ohms, $\theta = 180^\circ$ and $\epsilon_1 = 1.00$, for various values of the relative dielectric constant ϵ_2 .

2) Step Transition Design Procedure:

a) *Intermediate dielectric radii*: Fig. 4 shows a partially filled coaxial transmission line step transition. The ratio of the two terminating impedances may be defined as

$$C^S = \frac{Z_{n+1}}{Z_1} \quad (4)$$

where

C = a dimensionless constant,

S = the sum of a certain set of a_m constants as outlined by Cohn,⁶ [See Appendix, Sections A and B-1), below],

Z_{n+1} = the highest impedance,

Z_1 = the lowest impedance.

Z_n = the n th impedance.

When the value of C has been determined, the intermediate impedance values are then computed as:

$$\begin{aligned} Z_2 &= Z_1 C^{a_1} \\ Z_3 &= Z_1 C^{a_1+a_2} \\ &\vdots \\ Z_n &= Z_1 C^{a_1+a_2+\dots+a_{n-1}} \end{aligned} \quad (5)$$

where

$$\frac{Z_n}{Z_{n+1}} = \frac{\lambda_n}{\lambda_{n+1}}$$

After the intermediate impedance values have been computed, the values of b/c may be obtained from Fig. 3, in which Z_g/Z_a will correspond to the appropriate individual Z_n/Z_{n+1} ratios. Once each b/c ratio is ascertained, the intermediate c values are known.

b) *Transformer length*: Each transformer length for

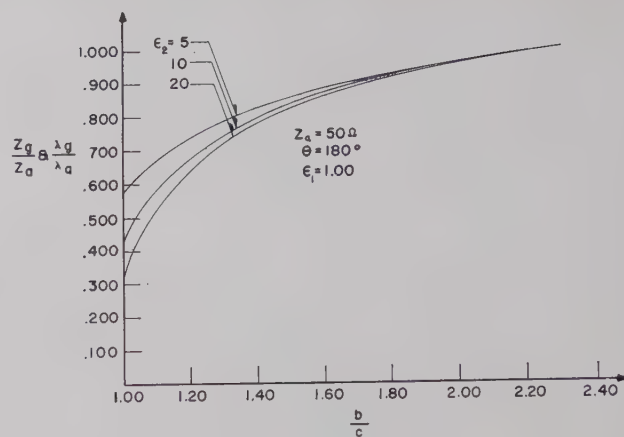


Fig. 3—Normalized guide wavelength and characteristic impedance for partially filled coaxial line.

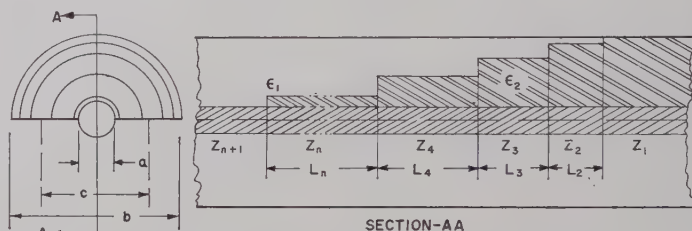


Fig. 4—Partially filled coaxial line step transition.

the partially filled coaxial step transition is given by the following formula:

$$L_n = \frac{\lambda_h \lambda_l}{2(\lambda_h + \lambda_l)} \left(\frac{\lambda_n}{\lambda_{n+1}} \right) \quad (6)$$

where

λ_h = shortest free space wavelength,

λ_l = longest free space wavelength, and

$$\frac{\lambda_n}{\lambda_{n+1}} = \frac{Z_n}{Z_{n+1}}$$

c) *Theoretical VSWR*: The theoretical VSWR⁹ for the partially filled coaxial line stepped transformer is given as

$$\text{VSWR} = 1 + \left[\ln \frac{Z_{n+1}}{Z_1} \right] \left[\frac{\left| T_{n-1} \left(\frac{\cos \phi}{\cos \phi_1} \right) \right|}{T_{n-1} \left(\frac{1}{\cos \phi_1} \right)} \right] \quad (7)$$

where

$T_m(x)$ = the Tchebycheff polynomial of the m th degree,

$\phi_1 = 180/1+p$ = electrical spacing of the steps at the low-frequency edge of the band,

ϕ = electrical spacing of the steps,

p is defined in Section A of the Appendix,

⁹ S. B. Cohn, private communication to D. Sullivan; January 23, 1959.

B. Partially Filled Double Ridge Waveguide

1) *Guide Wavelength and Characteristics Impedance:* Fig. 5(a) shows a cross-sectional view of a double-ridge waveguide in which the effective dielectric constant ϵ_e completely fills the region between the ridges. Neglecting the discontinuity capacitance C_d , the cutoff frequency has been given by¹⁰

$$f_c = \frac{1}{2\pi \sqrt{(C_B) \left(\frac{L_A}{2} \right)}} \quad (8)$$

where

f_c = cutoff frequency,
 C_B = total capacitance between the ridges,
 L_A = total inductance of the side loops.

For Fig. 5(a), (8) may be written as

$$f_c = \frac{1}{2\pi \sqrt{\left(\frac{2d\epsilon_e}{g} \right) \left(\frac{\mu lh}{2} \right)}} \quad (9)$$

where

ϵ_e = effective dielectric constant between the ridges,
 μ = permeability of the loop region,
 and the other parameters are as shown in Fig. 5(a).

Fig. 5(b) shows a double-ridge waveguide partially filled with a dielectric of thickness t . Considering capacitance C_d , but neglecting the capacitance at the dielectric edges, we may write the total capacitance for Fig. 5 as

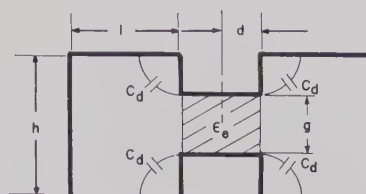
$$\begin{aligned} C_T &= C_d + C_1 + C_2 = C_d + \frac{(2d - t)\epsilon_1}{g} + \frac{t\epsilon_2}{g} \\ &= C_d + \frac{2d\epsilon_1 + t(\epsilon_2 - \epsilon_1)}{g} \end{aligned} \quad (10)$$

When capacitance C_d is taken into account, substitution of (10) for C_B in (8) yields the cutoff frequency for dielectric thickness t as

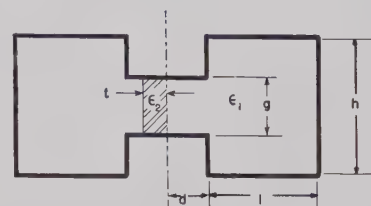
$$f_c = \frac{1}{2\pi \sqrt{\left[C_d + \frac{2d\epsilon_1 + t(\epsilon_2 - \epsilon_1)}{g} \right] \left[\frac{\mu lh}{2} \right]}} \quad (11)$$

An effective dielectric constant ϵ_e can also be computed for Fig. 5(b) using the formula

$$\epsilon_e = \frac{g}{2d} C_d + \epsilon_1 + \frac{t}{2d} (\epsilon_2 - \epsilon_1) \quad (12)$$



(a)



(b)

Fig. 5—Cross section of a partially filled double-ridge waveguide.
 Note: For DR-37 waveguide, $d=0.230$ inch, $g=0.370$ inch, $h=1.120$ inches, $l=0.915$ inch, $C_d=0.222$ $\mu\text{mf/inch}$.

It is known that the guide wavelength is given by the relationship

$$\lambda_g = \frac{\lambda}{\sqrt{\frac{\epsilon_e}{\epsilon_0} - \left(\frac{f_c}{f} \right)^2}} \quad (13)$$

Substitution into the above equation for f_c and ϵ_e from (11) and (12) gives the effective guide wavelength for the partially filled double-ridge waveguide as a function of dielectric thickness. Fig. 6 shows the variation of λ_g as a function of frequency for DR-37 waveguide for various dielectric thicknesses. For Fig. 6, C_d was found to be 0.222 $\mu\text{mf/inch}$; $\epsilon_1=1.00$, and $\epsilon_2=9.60$.

The characteristic impedance for the geometry shown in Fig. 5(b) may be computed through the use of (11) and (13), using the following formula:¹¹

$$Z_0 = Z_{0\infty} \left(\frac{\lambda_g}{\lambda} \right) \quad (14)$$

where

Z_0 = the effective characteristic impedance,
 λ_g = the effective guide wavelength,
 $Z_{0\infty}$ = the characteristic impedance at infinite frequency for the TE_{10} mode.

The impedance $Z_{0\infty}$ may be readily computed as outlined by Cohn.¹¹

2) Step Transition Design Procedure:

a) *Intermediate dielectric thicknesses:* Fig. 7 shows a dielectric step transition in double-ridge waveguide. Experimental results indicate that by using $Z_0/Z_{0\infty}$ values (rather than using either Z_0 or $Z_{0\infty}$) as a basis for the

¹⁰ S. Ramo and J. R. Whinnery, "Fields and Waves in Modern Radio," John Wiley and Sons, Inc., New York, N. Y., 2nd ed., pp. 409-410; 1953.

¹¹ S. B. Cohn, "Properties of ridge waveguide," Proc. IRE, vol. 35, pp. 783-788; August, 1947.

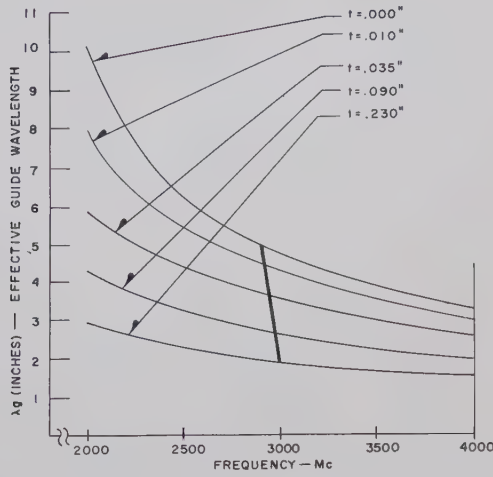


Fig. 6—Effective guide wavelength vs frequency for DR-37 double-ridge waveguide, with $\epsilon_1 = 1.00$ and $\epsilon_2 = 9.60$.

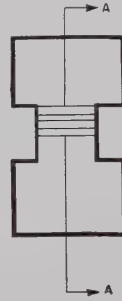
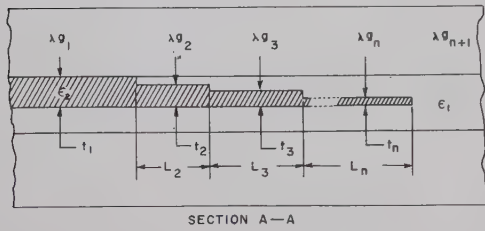


Fig. 7—Partially filled double-ridge waveguide step transition.

design of a step transition, a better over-all response is obtained. It is convenient to define, through the use of (14), the following ratio:

$$C^S = \frac{\lambda_{gn+1}}{\lambda_{g1}} \quad (15)$$

where

C = a dimensionless constant,

S = the sum of a certain set of a_m constants as outlined by Cohn.⁶ [See Appendix, Sections A and B-2), below],

$$\lambda_{gn+1} = \frac{2\lambda_{gl}\lambda_{gh}}{\lambda_{gl} + \lambda_{gh}},$$

where

λ_{gl} = longest guide wavelength at $t = 0$,

λ_{gh} = shortest guide wavelength at $t = 0$,

$$\lambda_{g1} = \frac{2\lambda_{g1h}\lambda_{g1l}}{\lambda_{g1h} + \lambda_{g1l}},$$

where

λ_{g1l} = guide wavelength for the maximum dielectric thickness at the lowest frequency,

λ_{g1h} = guide wavelength for the maximum dielectric thickness at the highest frequency.

As an example in Fig. 6, $\lambda_{gl} = 10.12$ inches, $\lambda_{gh} = 3.24$ inches, $\lambda_{g1l} = 2.93$ inches, and $\lambda_{g1h} = 1.43$ inches.

Upon the solving of (15) for C , the intermediate effective guide wavelengths are computed as

$$\begin{aligned} \lambda_{g2} &= \lambda_{g1} C^{a_1} \\ \lambda_{g3} &= \lambda_{g1} C^{a_1+a_2} \\ &\vdots \\ \lambda_{gn} &= \lambda_{g1} C^{a_1+a_2+\dots+a_{n-1}}. \end{aligned} \quad (16)$$

In Fig. 7, the dielectric thickness, t_n , for each transformer is obtained by use of curves such as those shown in Fig. 6, where $\lambda_{gn+1} = 4.92$ inches and $\lambda_{g1} = 1.92$ inches. When these two points are connected by a straight line, the intersection of this line with the appropriate value of λ_{gn} , from (16), yields the thickness to be used for the n th transformer. For example, if λ_{gn} is computed from (16) to be 3.25 inches, from Fig. 6, the transformer thickness, t_n , is seen to be 0.050 inch.

b) *Transformer length*: Each transformer length for the partially filled double-ridge waveguide is given by

$$L_n = \frac{\lambda_{gn}}{4} \quad (17)$$

where λ_{gn} is as defined in (16).

c) *Theoretical VSWR*: The theoretical VSWR for the stepped transformer has been discussed above [in Section II-A, 1c)]. For the double-ridge waveguide step transition, the theoretical VSWR is obtained by simply replacing

$$\frac{Z_{n+1}}{Z_1} \quad \text{by} \quad \frac{\lambda_{gn+1}}{\lambda_{g1}}$$

in (7).

III. EXPERIMENTAL RESULTS

A. Step Transition for Partially Filled Coaxial Line

Data have been obtained for a four-step coaxial transition, shown in Fig. 8(a), with a design range of 4000 to 7000 mc. A 21.7-ohm end impedance was matched to a standard air-filled, $\frac{3}{8}$ -inch, —50-ohm coaxial line. In this design $\theta = 180^\circ$ and $\epsilon_2 = 9.6$.

The maximum theoretical VSWR is 1.023, while the maximum measured VSWR in the 4000- to 7000-mc design region was 1.033. The band response is shown in Fig. 8(b).

B. Step Transition For Partially Filled Double-Ridge Waveguide

A five-step transition, shown in Fig. 9(a), has been tested for DR-37 double-ridge waveguide. The frequency range covered was 2000 to 4000 mc, which would result in a value of

$$p = \frac{\lambda_{gl}}{\lambda_{gh}} = \frac{10.12}{3.24} = 3.12 \quad (\text{see Fig. 6}).$$

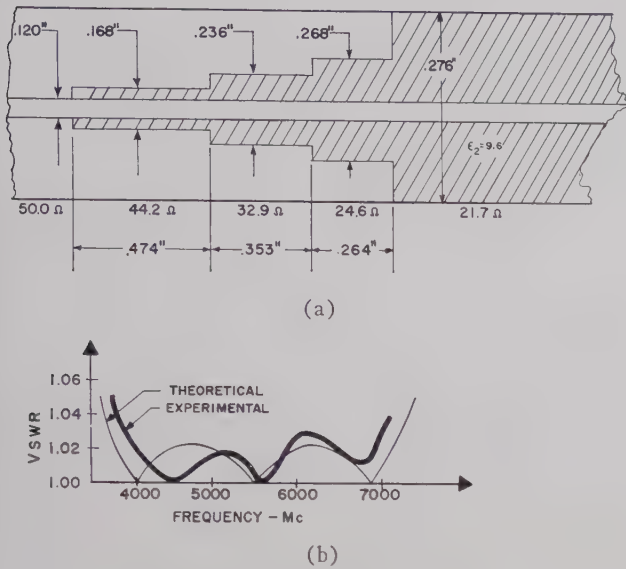


Fig. 8—(a) Design for a partially filled coaxial line, and (b) experimental data.

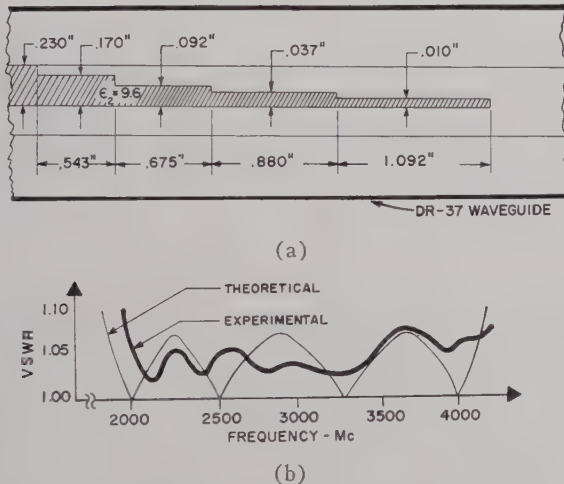


Fig. 9—(a) Design for a partially filled double-ridge waveguide, and (b) experimental data.

However, as an added safety factor, a value of $p = 3.30$ was chosen. The maximum dielectric thickness used was 0.230 inch, with a dielectric constant of 9.6.

The step transition was placed on the input side of a waveguide isolator. The ferromagnetic material did not substantially change the effective characteristics of the partially filled waveguide. For the five-step double-ridge waveguide transition, the maximum theoretical VSWR is 1.081. As can be seen from the band response in Fig. 9(b), the measured VSWR (isolator input VSWR) is less than 1.090 throughout most of the 2000- to 4000-mc band. For a design such as that shown in Fig. 9(b), it should be noted that the thickness of any particularly thin transformer may be increased by simply using a lower dielectric constant material while maintaining the same transformer length.

IV. CONCLUSION

A theoretical analysis has been made of the effective guide wavelength and characteristic impedance of partially filled transmission lines. Although proximity effects have been neglected in this analysis, experimental results are found to closely approximate the theory.

By use of the equations presented, step transitions may be designed for partially filled (dielectric loaded) transmission lines.

APPENDIX

A. Determination of S

In (4) and (15), where $S = \sum a_m = a_1 + a_2 + a_3 + \dots + a_n$, the value of S is determined by 1) the bandwidth p and 2) n , the number of steps used in the step-transition design. A method of computing the a_m values is described by Cohn.⁶ For a five-step transition ($n = 5$) and a bandwidth p equal to 3.30, the value of S would be

$$S = a_1 + a_2 + a_3 + a_4 + a_5.$$

$$S = 1 + 1.787 + 2.194 + 1.787 + 1.000 = 7.768.$$

B. Bandwidth

1) *Partially Filled Coaxial Line*: In the design of partially filled coaxial line step transitions, the bandwidth p is given by the following equation:

$$p = \frac{\lambda_l}{\lambda_h} \quad (18)$$

where

λ_l = longest free-space wavelength,

λ_h = shortest free-space wavelength.

2) *Partially Filled Double-Ridge Waveguide*: In the design of partially filled double-ridge waveguide step transitions, the bandwidth p is given by

$$p \approx \frac{\lambda_{gl}}{\lambda_{gh}} \quad (19)$$

where

λ_{gl} = guide wavelength at the lowest frequency in air-filled double-ridge waveguide,

λ_{gh} = guide wavelength at the highest frequency in air-filled double-ridge waveguide.

The computed value for p in double-ridge waveguide will usually be slightly higher than the precise value required. However, a somewhat still higher value of p is frequently used to provide a small safety factor in the design.

Parametric Diodes in a Maser Phase-Locked Frequency Divider*

M. L. STITCH†, N. O. ROBINSON‡, AND W. SILVEY‡

Summary—The use of an ammonia-beam maser in a portable frequency standard requires a frequency divider which can be transistorized. A divider which uses no microwave tubes and hence one that can be transistorized is described. An ammonia-maser-controlled signal generator used to tune up the divider is also described. It is found that the use of a parametric diode frequency multiplier substantially improves the lock-in performance of the divider. Some data are given for comparing the performance of the maser frequency divider with and without the parametric diode frequency multiplier.

FREQUENCY DIVIDER

IN ORDER TO divide the ammonia-beam maser^{1,2} (hereafter called the maser) frequency down to a useful frequency for standards work, a phase-locked frequency divider has been designed and built. This divider, which does not use any microwave tubes (other than planar triodes), was designed as the first step toward a completely transistorized divider.

The circuit diagram is shown in Fig. 1. The system uses a phase-locked servo loop. A simplified explanation of the operation is as follows: The frequency of the voltage-controlled oscillator, which is approximately 1 mc, is multiplied approximately 24,000 times and beat with the maser output. The resulting IF at a value of several megacycles is fed into a phase-sensitive detector. The reference voltage for this detector is derived from the voltage-controlled oscillator. The error voltage output from the phase-sensitive detector is fed through a suitable integrator and phase-correction circuit to the VCO.

To prevent accidental locks to frequencies derived from the VCO, double heterodyning and frequency division of VCO frequency by a rational fraction are used to secure the phase-detector reference frequency and the translation frequency for the second IF. The VCO is locked with zero error when the frequencies and phases at the two inputs of the phase-sensitive detector are

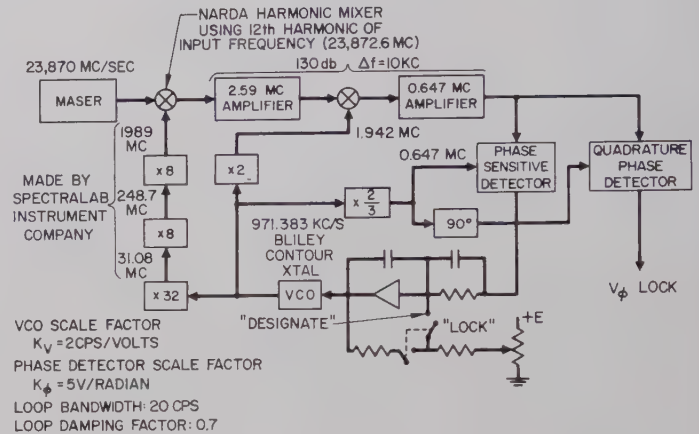


Fig. 1—Block diagram of phase-locked frequency divider.

equal. The frequency condition is then

$$[(Nf_0 - f_m) - Mf_0] = Df_0 \quad (1)$$

where

$$\begin{aligned} f_m &= \text{maser frequency} = 23,870 \text{ mc}, \\ f_0 &= \text{VCO frequency} = 971,383 \text{ kc}, \\ N &= 32 \times 8 \times 8 \times 12 = 24,576, \\ M &= 2, \\ D &= 2/3. \end{aligned}$$

Hence, $f_0 = f_m / (24,573 + 1/3)$. The loop bandwidth is 20 cps; the loop damping factor is 0.7.

MASER-CONTROLLED SIGNAL GENERATOR

Of great utility in "tuning up" the divider for initial lock as well as for optimizing parameters and making the measurements described below is a means of obtaining maser frequency and stability at much greater power than maser signal power. An obvious way of amplifying at frequencies at which stable, high-gain amplifiers are not presently available is by the use of double conversion; *i.e.*, one translates to a frequency where amplification is convenient and then translates back to the desired frequency. This technique uses a common local oscillator for both translations and thus subtracts out to first order the drifts and swings of the local oscillator from the desired amplified signal. In the present case an additional difficulty is encountered because of the extremely low power output of the ammonia

* Manuscript received by the PGM-TT, July 6, 1959; revised manuscript received October 23, 1959.

† Hughes Aircraft Co., Culver City, Calif.

‡ Aeronutronic Systems, Inc., Newport Beach, Calif. Formally of Hughes Aircraft Co., Culver City, Calif.

¹ J. P. Gordon, H. J. Zeiger, and C. H. Townes, "The maser—new type of microwave, frequency standard, and spectrometer," *Phys. Rev.*, vol. 99, p. 1264; August, 1955.

² J. Bonanomi, J. dePrins, J. Hermann, and P. Kartoshoff, "Améliorations d'un maser à NH₃," *Helv. Phys. Acta.*, vol. 30, p. 492; 1952. (In French).

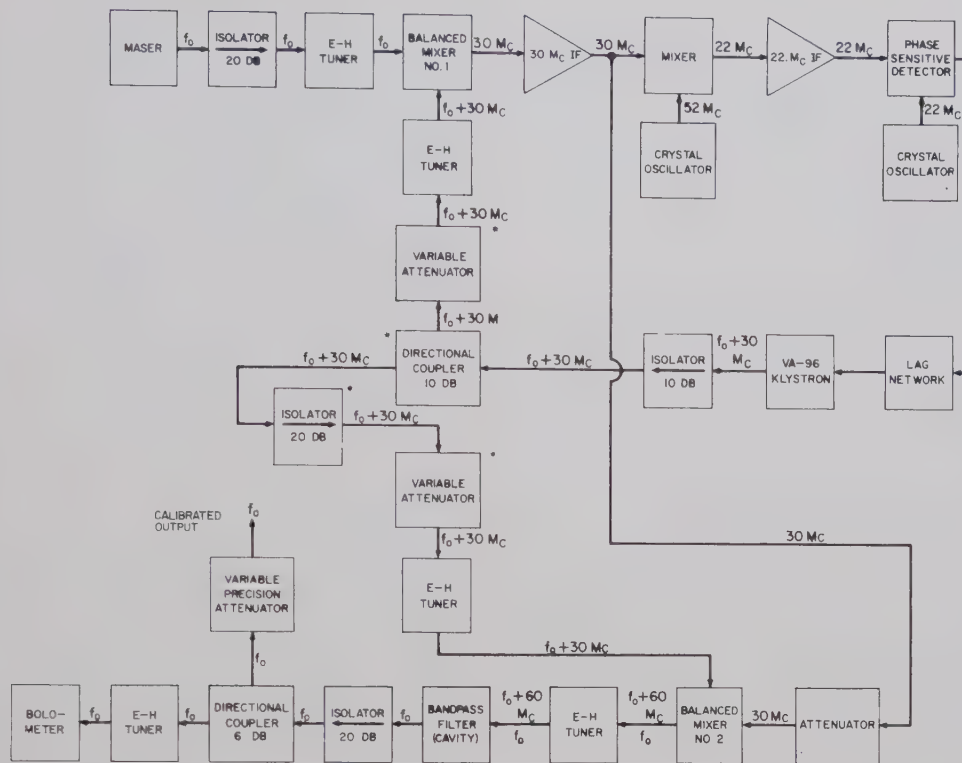


Fig. 2—Maser signal generator. For proper operation, leakage signals at frequency f_0 going from balanced mixer No. 2 to balanced mixer No. 1 must be kept at a lower level than the maser signal. This is accomplished by judicious use of isolators, attenuators, and the directivity of the directional couplers (shown with asterisks).

maser ($\sim 10^{-10}$ watt), the comparatively high conversion loss of K -band mixer diodes (~ 8 db), and the poor stability of K -band klystrons. Amplified power in the milliwatt region requires IF amplification of the order of 90 db. The resulting narrow bandwidth of this high-gain IF amplifier and the consequent rapid phase shift of output with frequency give rise to phase modulation as the local oscillator jitters. This is overcome in the following way. Since it is the maser frequency that we wish to amplify, we can make use of the IF offset phase-locked klystron³ mixed with its IF. In effect, we have substituted the stability of a stable, low-frequency crystal oscillator for that of a klystron as our local oscillator in the double conversion amplifier and have thus eliminated the phase modulation referred to above. The circuit diagram is shown in Fig. 2. Dual conversion from 30 mc to 22 mc is used in the phase-lock loop to alleviate the shielding problem by keeping low-level amplifiers and oscillators at different frequencies. No "ghost locks" were observed. Further comments are contained in the caption for Fig. 2. A power output of approximately 0.2 mw coherent with the maser and at the same frequency has been obtained with this maser signal generator.

LOCKING THE DIVIDER

The frequency divider is connected to the maser signal generator, which is set to supply power several orders of magnitude higher than that of the maser. The divider is put into operation by switching to "Designate" (see Fig. 1) and tuning the VCO into the correct frequency while one watches the beat frequency output of the quadrature phase detector. When the beat frequency decreases to a sufficiently low value, the switch is put on "Lock" and one can observe a further decrease in beat frequency as the VCO frequency drifts and finally comes to a halt at a dc level of quadrature voltage output. It is clear that when the phase-detector output (which is the error signal) is null, the output of the quadrature phase detector is a dc maximum. Further, the value of this dc is, before the onset of saturation, a monotonically increasing function of the input signal, the linearity of which is modified by AGC action in the IF. The AGC acts to compress the range of quadrature phase-detector output. This output can be used as an indicator while the system is being tuned and peaked. As the maser-controlled signal generator power is decreased, the quadrature phase-detector dc output voltage V_q decreases and the increase in gain caused by AGC action increases the noise modulation of V_q . Since this noise is significantly higher in frequency than 20

³ M. Peter and M. W. P. Strandberg, "Phase stabilization of microwave oscillators," *PROC. IRE*, vol. 43, pp. 869-873; July, 1955.

cps, the loop bandwidth frequency, the VCO frequency, is unperturbed. The dc value of V_q remains constant for each value of maser-signal generator power down to very low signal-to-noise ratios. This indicates that the long-term VCO frequency remains a fixed fraction of the maser frequency. The divider can be switched from the maser signal generator directly to the maser.

PARAMETRIC DIODE FREQUENCY MULTIPLIER

Operation at low signal-to-noise ratios does not, as pointed out above, result in decreased stability, but it does increase the probability of an accidental break of lock. As is evident from Fig. 1, the chief cause of poor signal-to-noise ratio is the use of a mixer which must perform two operations: 1) harmonic multiplication (from 1989 mc to its twelfth harmonic at 23,872 mc) and 2) mixing. The result seems to be inefficient operation for both applications. Previous measurements had indicated that a marked improvement in conversion efficiency of the mixer had resulted when the driving frequency for the harmonic mixer was increased to any integral submultiple of 23,872.6 mc. For example, at appropriate frequencies near 1 kmc, 2 kmc, and 3 kmc, the signal-to-noise ratio remained constant providing the driving power was in the ratio of 40 (for 1 kmc) to 8 (for 2 kmc) to 1 (for 3 kmc). With eventual transistorization of the divider in mind, the highest tube frequency used was 1989 mc. There is enough power available at this frequency to degrade the performance of the IN26A mixer diode so that one operates at a rectified current which gives maximum locking. In the typical run cited below, this was at 1 ma, which corresponds to 9.8-mw drive. Even when higher driving frequencies were used, the mixer-diode rectified current was kept constant.

The availability of the new parametric diodes with their possibilities for efficient frequency multiplication^{4,5} raises the question of whether the performance of the divider (in terms of signal-to-noise ratio) will improve if such a diode is inserted in the multiplying circuit between the harmonic mixer and the last multiplying stage. In particular, will the loss in power caused by harmonic-conversion loss be more than offset by the introduction of a higher frequency into the harmonic mixer?

For this purpose, a very crude multiplier was constructed that employed a Hughes Type 2810 parametric diode in a detector mount at the junction of a coaxial T . The system was driven at 1989 mc through a low-pass filter and terminated by a coax-to-waveguide transition

leading to an RG 49/U waveguide, which served as a high-pass filter to the output. The third arm of the T was terminated by a tuner and short, and tuners were inserted at judiciously chosen points. The microwave driving power was adjusted so as to drive the diode beyond its zener point; then the dc bias was set to a value which balanced the dc component of the diode current to zero. Typically, the second harmonic output, which is at 3978 mc, is 7 db down from the input, although, with some critical adjustments, 6 db have been obtained. At these efficiencies, power outputs from 8 to 32 mw have been observed. An attempt was made to measure harmonic outputs higher than the second with the present multiplier. Even the third, at 5967 mc, was more than 15 db down. At these low levels, no attempt was made to determine the relative harmonic content (as between 2, 3, 4, etc.) of the signal driving the harmonic mixer under operating conditions. However, pronounced variations in the sensitivity of the system corresponding to a nearly fixed rectified current from the harmonic mixer diode have been observed when a stub tuner in the line between the diode multiplier and the harmonic mixer was slightly varied. One may infer from this that, since the tuner will vary the relative intensity of harmonic components entering the harmonic mixer, this system is very sensitive to the relative intensity of even extremely low-level harmonic components.

EXPERIMENTAL PROCEDURE

A series of comparative runs was taken both with 1989-mc drive to the harmonic mixer and with the output of the parametric diode frequency multiplier driving the harmonic mixer. The amount of power from the maser signal generator was varied and the dc level of output voltage from the quadrature phase detector, V_q , was noted. The point at which lock-break occurred was also noted. In every case, an attempt was made to obtain optimum conditions of "sensitivity" as evidenced by maximizing V_q . It was found that the IN26A was superior to the IN26 for the harmonic mixer diode. Runs with three IN26A's indicated a wide (approximately 3 to 1) variation in the crystal current giving maximum V_q .

The power available to the harmonic mixer of the frequency divider from the maser signal generator was measured by monitoring the power output of the maser signal generator with a power bridge, tapping some off with a calibrated directional coupler, and then inserting calibrated microwave attenuators. In order to minimize the possibility of obtaining an erroneously high sensitivity figure because of high-level microwave leakage which bypasses the attenuators, readings were obtained by lowering the 30-mc drive into the last mixer of the maser signal generator. This reduced the amount of power at maser frequency which was generated. The new power level was measured with the power bridge,

⁴ A. Uhler, Jr., "The potential of semiconductor diodes in high-frequency communications," *PROC. IRE*, vol. 46, pp. 1099-1115; June, 1958.

⁵ D. B. Leeson and S. Weinreb, "Frequency multiplication with nonlinear capacitors—a circuit analysis," *PROC. IRE*, vol. 47, pp. 2076-2084; December, 1959.

and the microwave attenuation was reduced by the appropriate amount. The resulting V_q agreed with the previous value within the error in reading the power bridge; this indicated that the leakage was negligible. Finally, the direct maser power output was measured by comparison with the output of the calibrated maser signal generator by using V_q as the indicator. At this relatively high drive, it was demonstrated by the technique described above that the error caused by leakage was negligible.

In all subsequent runs the maser alone, with output level controlled by a calibrated attenuator, was used to drive the divider.

CONCLUSION

In Fig. 3, the curves marked (A) and (B) indicate V_q vs attenuation of the maser alone for the frequency divider with 1989-mc drive and with the parametric diode multiplier (3978-mc drive), respectively. These curves were based on a typical run. Curve (C), from a run in which the parametric diode multiplier was used, represents the best performance obtained. The abscissa, which is the attenuation in the maser output, is scaled to the square root of power. This scaling would normally give a straight-line response for a linear detector. Zero db at the right, which is the full maser output, corresponds to -73 dbm. Corresponding values of V_q are obtained at 11 db less maser power with the parametric diode multiplier than with 1989-mc drive. In the respective cases, the power for the harmonic mixer was 3.8 mw with the diode multiplier and 9.8 mw with the 1989-mc drive. The driving powers were obtained by calibrating the harmonic mixer crystal current at 1989 mc, and its second harmonic. Mixer crystal currents were approximately 1 ma for both fundamental and second harmonics. These values gave the best V_q . Lock-break

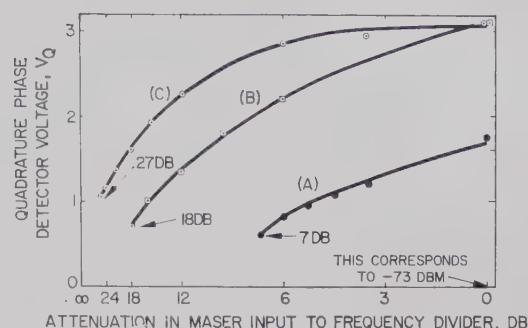


Fig. 3—Response of frequency divider to maser power input. Curve (A) is for 1989-mc drive to harmonic mixer as illustrated in Fig. 1. Curves (B) and (C) are for the case where the Hughes Type 2810 parametric diode is used as a frequency multiplier to drive the harmonic mixer. (Arrows indicate value of maser attenuation at which the divider broke lock.)

occurs at correspondingly lower maser power with the parametric diode multiplier.

It should be noted that whereas the techniques discussed in this paper have enhanced our ability to lock a low-frequency crystal oscillator (the VCO) to a high-frequency reference, conversely, the locking of a high-frequency oscillator to a low-frequency reference can also be enhanced.

ACKNOWLEDGMENT

We are especially grateful to E. V. Phillips of the Airborne Systems Laboratories of Hughes Aircraft Company for his aid and advice, both in the original design of the frequency divider as well as in making available most of the components for its construction. We also wish to thank R. P. Farnsworth of the same organization for the design of the VCO, R. D. Weglein of the Research Laboratories of Hughes Aircraft Company for his aid in assembling a parametric diode frequency multiplier, and E. F. Davis, whose design of the phase detector in the maser signal generator we copied.

Parametric Devices and Masers: An Annotated Bibliography*

E. MOUNT† AND B. BEGG‡

PREFACE

THIS bibliography is restricted to books and periodical articles published prior to October, 1959.

No attempt has been made to include the voluminous material to be found in technical reports, patents or similar sources.

Although the greatest portion of the bibliography has to do with microwave devices, the references do include some devices operating outside of the microwave frequency range, such as the optical, infrared and radio-frequency masers, and the parametrons.

Appreciation is expressed to Drs. M. Arditì and T. B. Warren of ITT Laboratories for their assistance in reviewing the categories into which the references were classified.

TABLE OF CONTENTS

	ITEM NUMBERS
PARAMETRIC DEVICES AND MASERS	
Review Articles.....	1-18
PARAMETRIC DEVICES	
Review Articles.....	19-20
Electron Tube Types.....	21-38
Ferrite Types.....	39-58
Diode Types.....	59-112
Parametron Types.....	113-130
Miscellaneous Items.....	131-151
MASERS	
Review Articles.....	154-180
Oscillators.....	181-207
Amplifiers.....	208-223
Gaseous Types.....	224-255
Solid-State Types.....	256-338
Optical, Radio-Frequency and Infrared Types.....	339-342
Atomic Clocks.....	343-372
Miscellaneous Items.....	373-379
AUTHOR INDEX.....	page 341

BIBLIOGRAPHY

I. PARAMETRIC DEVICES AND MASERS—REVIEW ARTICLES

- [1] Anderson, P. W.
The reaction field and its use in some solid-state amplifiers.
Journal of Applied Physics, 28(9): 1049-1053; September, 1957.
Discussion of phenomena of the radiation reaction field and

* Manuscript received by the PGMTT, May 4, 1959; revised manuscript received, November 12, 1959.

† ITT Laboratories, a Division of International Telephone and Telegraph Corp., Nutley, N. J.

‡ Drexel Institute of Technology, Philadelphia, Pa. Formerly with ITT Labs., Nutley, N. J.

- how it may be used in two solid-state amplifiers (Bloembergen's 3 energy-level type and Suhl's ferromagnetic type).
- [2] Beam, R. E. and Brodwin, M. E.
Report of advances in microwave theory and techniques in U.S.A.—1958.
IRE TRANSACTIONS ON MICROWAVE THEORY AND TECHNIQUES, MTT-7(3): 308-327; July, 1959.
Includes a review of developments in masers and parametric devices, and cites 55 references of the U. S. publications in 1958.
- [3] Damon, R. W.
How the maser operates. Part I—Maser shows promise, some drawbacks. Part II—Maser's potential rests on further work.
Aviation Week, 67(7): 76, 77, 81, 82, 87, 88; August 19, 1957.
67(8): 91, 92, 96, 99, 101, 104; August 26, 1957.
An informative article about the operating principles of the new atomic amplifiers (masers and parametric) with some remarks about their potentialities and limitations.
- [4] Heffner, H.
Masers and parametric amplifiers.
1958 WESCON CONVENTION RECORD, (pt. 3): 3-8.
Reviews principles of both types of devices, then evaluates the progress being made in their development and comments on their relative value.
- [5] Heffner, H.
Masers and parametric amplifiers.
Microwave Journal, 2(3): 33-40; March, 1959.
Discusses the theory and operation of all types of masers and parametric devices. Operational performance figures are given for various experimental models.
- [6] Heffner, H.
Solid state microwave amplifiers.
IRE TRANSACTIONS ON MICROWAVE THEORY AND TECHNIQUES, MTT-7(1): 83-91; January, 1959.
Reviews the operation of both solid-state masers and parametric amplifiers and their performance. Includes a bibliography of 121 items.
- [7] Holahan, J.
Solid state microwave amps (amplifiers) promise milli-micro-watt reception.
Aviation Age, 29(6): 140-149; June, 1958.
A review of solid-state masers and parametric amplifiers.
- [8] Maguire, T.
New microwave systems using low-noise devices.
Electronics, 32(34): 27-30; August 21, 1959.
Reviews the development of masers and parametric amplifiers, particularly use of the latter in military communications systems, as presented in papers at the PGMTT National Symposium held at Harvard University in 1959. Applications of tunable packaged masers are also reviewed.
- [9] Matthei, W. E.
Recent advances in solid state receivers.
Microwave Journal, 2(1): 19-24; January, 1959.
Reviews the state of the art regarding solid-state masers and the diode and ferrite types of parametric amplifiers. Limitations and applications are pointed out.
- [10] Mikaelian, A. L.
The problem of development of ferrite microwave amplifiers (In Russian).
Radiotekhnika i Elektronika, 3(11): 1323-1347; November, 1958.
A general review of the theory and development of solid-state masers and parametric devices.
- [11] Parametrics and masers; questions and answers.
Electronic Industries, 18(3): 238-240, 243; March, 1959.

- Gives brief answers to basic questions about the operation and uses of such devices.
- [12] Rostas, E. and Hulster, F.
Microwave amplification by means of intrinsic negative resistance.
Proceedings of the Institution of Electrical Engineers, 105B (supplement 11): 665-673; May, 1958.
Presents the theory of operation of microwave negative resistance amplifiers, including their bandwidth and noise factor. Points out their connection with parametric devices and masers.
- [13] Salzberg, B.
Masers and reactance amplifiers—basic power relations.
PROCEEDINGS OF THE IRE, 45(11): 1544-1545; November, 1957.
Presents an alternative simple and nonquantum mechanical derivation of the power relations developed by J. M. Manley and H. E. Rowe (see [144]). These relations are of importance in connection with parametric amplifiers.
- [14] Some recent solid state device developments in the U.S.A.
British Communications and Electronics, 6(7): 528-530; July, 1959.
A brief general review, including masers and parametric devices.
- [15] Stevens, K. W. H.
Atomic and molecular generators—introduction.
Proceedings of the Institution of Electrical Engineers, 105b (supplement 11): 674-677; May, 1958.
Explains the principles of operation of both parametric devices and masers and then compares them. A discussion of terminology follows.
- [16] Toth, R. C.
Toward improved missile communications.
Astronautics, 2(1): 54-55, 112-113; August, 1957.
Brief description of work being done by Bell Telephone Laboratories on ferromagnetic and maser amplifiers. Discusses their advantages and disadvantages.
- [17] Von Hippel, A. R.
Molecular Science and Molecular Engineering.
John Wiley and Sons, Inc., New York, N. Y., 446 pp.; 1959.
Includes a chapter, written by J. W. Meyer, on parametric amplifiers and masers. Reviews the theory of the devices, gives examples of typical operational parameters, and discusses requirements for maser materials.
- [18] Wittke, J. P.
New approaches to the amplification of microwaves; masers and the parametric amplifier.
RCA Review, 18(4): 441-457; December, 1957. Also in *Proceedings of the National Electronics Conference*, 13: 610-623; 1957.
Gives a description and discussion of basic principles of operation of the two types of molecular-microwave amplifiers—the maser and the parametric amplifier.

II. PARAMETRIC DEVICES

Review Articles

- [19] "Cathode Ray," pseudonym.
Mavars—another kind of quiet microwave amplifier.
Wireless World, 65(5): 242-246; May, 1959.
Reviews the basic principles of parametric amplifiers, using simple electrical and mechanical analogs to explain their operation. Recent developments are reviewed.
- [20] Weber, S.
The MAVAR: a low noise microwave amplifier.
Electronics, 31(39): 65-71; September 20, 1958.
Recent developments have resulted in three major types of mavar—the ferromagnetic, the variable capacitance, and the electron beam. Descriptions, characteristics, etc., are included for all three types.
- Electron Tube Types*
- [21] Adler, R., Hrbek, G., and Wade, G.
A low-noise electron-beam parametric amplifier.
PROCEEDINGS OF THE IRE, 46(10): 1756-1757; October, 1958.
Reports results of further experimentation on electron tubes using fast-wave parametric amplification by means of a new electrode structure, operating in the 500-mc range.
- [22] Adler, R.
Parametric amplification of the fast electron wave.
PROCEEDINGS OF THE IRE, 46(6): 1300-1301; June, 1958.
Results of an experiment using parametric amplification between two fast-wave beam coupling devices.
- [23] Ashkin, A., Bridges, T. J., Louisell, W. H., and Quate, C. F.
Parametric amplification of space-charge waves.
Proceedings of the Institution of Electrical Engineers, 105B (supplement 11): 649-651; May, 1958.
Describes an amplifier using an electron beam passing through a cavity to implement a traveling-wave parametric amplifier. It provides a method of amplifying the fast space-charge wave rather than the slow space-charge wave.
- [24] Ashkin, A.
Parametric amplification of space charge waves.
Journal of Applied Physics, 29(12): 1646-1651; December, 1958.
Describes the operation of a movable cavity-type device. With the pump frequency twice the signal frequency, an increase of 41 db was observed in the signal over a ten-inch length of beam. With the pump frequency lower than the signal frequency, an increase of the signal by 30 db over a 9.2-inch length of beam was observed.
- [25] Ashkin, A., Bridges, T. J., Louisell, W. H., and Quate, C. F.
Parametric electron beam amplifier.
1958 IRE WESCON CONVENTION RECORD, (pt. 3) 13-22.
Describes the theory and operation of both regenerative type (resonant cavity) and traveling-wave type devices. Experimental results are reported. Gains up to 20 db were achieved with the first type and up to 30 db with the second type.
- [26] Bridges, T. J.
A parametric electron beam amplifier.
PROCEEDINGS OF THE IRE, 46(2): 494-495; February, 1958.
An amplifier using an electron beam instead of the ferrites, as proposed by H. Suhl (see [52]), has been built and some experimental results are reported.
- [27] Buchmiller, L. D. and Wade, G.
Pumping to extend traveling-wave-tube frequency range.
PROCEEDINGS OF THE IRE, 46(7): 1420-1421; July, 1958.
Points out that the effects noted following the pumping with a high-level signal the frequency range of a commercially available traveling-wave tube may be due, at least in part, to the parametric effects available in beams, or it may be due to mixing effects associated with electron beams.
- [28] Clavier, P. A.
Parametric and pseudo-parametric amplifiers.
PROCEEDINGS OF THE IRE, 47(9): 1651; September, 1959.
Develops the theory for a proposed parametric amplifier which would use the transverse oscillations of an electron beam in a time-varied potential-well transverse to the direction of flow. There would be an input and output coupler separated by an interaction. The author declares that the "low-noise electron-beam parametric amplifier" of Adler, Hrbek, and Wade (see [21]) should not be considered a parametric device.
- [29] Cook, J. S. and Louisell, W. H.
Fast longitudinal space charge wave parametric amplifiers.
1959 IRE WESCON CONVENTION RECORD, (pt. 3): 77-85.
First discusses the theory of "active" and "passive" coupling of propagating waves, introducing an "effective coupling" parameter. Principles of traveling-wave parametric amplification are next discussed, followed by a review of problems of fast space charge wave amplifiers and possible solutions.
- [30] Electron-beam parametric amplifier.
Wireless World, 64(11): 555-556; November, 1958.
A brief reference to the Zenith Radio Corporation's device.
- [31] Fast-wave parametric amplifier.
Electrical Engineering, 77(11): 1071-1072; November, 1958.
Gives a brief description of the operating characteristics of Zenith Radio Corporation's vacuum-tube type parametric amplifier. It has a noise figure of about 1 db and a gain up to 30 db.
- [32] Gould, R. W.
Traveling-wave couplers for longitudinal beam-type amplifiers.
PROCEEDINGS OF THE IRE, 47(3): 419-426; March, 1959.

Formulates the expressions governing traveling-wave interaction between an electron beam and a slow-wave circuit. The equations are solved in terms of the mode amplitudes at the output of the traveling-wave coupler and the mode amplitudes at the input. The results are then applied to the design of fast space-charge wave couplers for longitudinal beam type parametric amplifiers.

- [33] Haus, H. A.
The kinetic power theorem for parametric, longitudinal, electron-beam amplifiers.
IRE TRANSACTIONS ON ELECTRON DEVICES, ED-5(4): 225-232; October, 1958.
Develops a generalization of Chu's power theorem, for exploring the limitations on noise performance in such parametric amplifiers. No obstacles appear theoretically to prevent such devices from achieving the ultimate in noise performance.
- [34] Louisell, W. H. and Quate, C. F.
Parametric amplification of space charge waves.
PROCEEDINGS OF THE IRE, 46(4): 707-716; April, 1958. (Bell Monograph 3069.)
Description of a "distributed" parametric amplifier using an electron beam and CW source oscillating at twice the signal frequency for power. Discusses both the fast space charge wave and the slow space charge wave.
- [35] Louisell, W. H.
A three-frequency electron-beam parametric amplifier and frequency converter.
Journal of Electronics and Control, 6(1): 1-25; January, 1959.
Gives conditions for occurrence of a current modulation threshold which must be exceeded to produce growing waves. The Manley-Rowe relations are verified for the parametric beam, and the gain per unit length is found. Expressions are found for the propagation constants and for boundary conditions.
- [36] Someya, I.
Report of advances in microwave theory and techniques in Japan—1958.
IRE TRANSACTIONS ON MICROWAVE THEORY AND TECHNIQUES, MTT-7(3): 331; July, 1959.
Includes one Japanese reference to a parametric amplifier using an electron beam.
- [37] Wade, G. and Heffner, H.
Gain, bandwidth and noise in a cavity type parametric amplifier using an electron beam.
Journal of Electronics and Control, 5(6): 497-509; December, 1958.
Shows that in practice it is almost impossible to cancel completely and simultaneously the two uncorrelated noise sources in the electron beam. The requirements for a large beam current and large plasma wavelength lead to minimum noise figures around 3 db. An actual example is worked out in which the gain is about 15 db and the bandwidth 43 kc.
- [38] Wade, G. and Adler, R.
A new method for pumping a fast space-charge wave.
PROCEEDINGS OF THE IRE, 47(1): 79-80; January, 1959.
Uses the analogy of a pendulum under the influence of a time-varying force field to illustrate the principle of pumping a fast space-charge wave in an electron beam, in parametric amplification.

Ferrite Types

- [39] Amplifier for radio astronomy.
Engineering, 184(4766): 59; July 12, 1957.
A brief description of the Bell Telephone Laboratories ferromagnetic amplifier.
- [40] Berk, A. D., Kleinman, L., and Nelson, C. E.
Modified semi-static ferrite amplifier.
1958 IRE WESCON CONVENTION RECORD, (pt. 3): 9-12.
Describes an operation in which the uniform precession is used as the idling magnetostatic mode. This is compared with a conventional semistatic operation. The theory is checked by an experimental model, and gain was observed in excess of 60 db.
- [41] Ferrite microwave amplifier developed.
Electronics, 31(8): 32-33; February 21, 1958.
Brief description of the Bell Telephone Laboratories solid-state microwave amplifier.
- [42] Haun, R. D. and Osial, T. A.
Gain measurements on a pulsed ferromagnetic microwave amplifier.
PROCEEDINGS OF THE IRE, 47(4): 586-587; April, 1959.
Amplifier has a flattened coaxial resonant line in a rectangular cavity, using polycrystalline yttrium iron garnet. A chart shows power gain as a function of pump power.
- [43] Hogan, C. L., Jepsen, R. L., and Vartanian, P. H.
New type of ferromagnetic amplifier.
Journal of Applied Physics, 29(3): 422-423; March, 1958.
(Presented at Conference on Magnetism and Magnetic Materials, held November 18-21, 1957, at Washington, D. C.)
Simple physical explanation of the device proposed by H. Suhl. (See [52].)
- [44] Microwave device is ferromagnetic.
Electronics, 30(7B): 26; July 20, 1957.
Brief news item of experimental ferromagnetic amplifier being worked on at the Bell Telephone Laboratories.
- [45] Nikolsky, V. V.
On the theory of a microwave ferrite amplifier (In Russian).
Radiotekhnika i Elektronika, 4(4): 726-728; April, 1959.
A theoretical study of the principles of a parametric amplifier of this type.
- [46] Poole, K. M. and Tien, P. K.
A ferromagnetic resonance frequency converter.
PROCEEDINGS OF THE IRE, 46(7): 1387-1396; July, 1958.
Based on the amplifier/oscillator proposal of Suhl, the paper discusses a frequency converter which uses a ferromagnetic material in a cavity which supports three resonant modes. Theory and experimental results were found to agree rather closely.
- [47] Poole, K. M. and Tien, P. K.
Measurements on active microwave ferrite devices.
1957 IRE WESCON CONVENTION RECORD, (pt. 3): 170-174.
To provide a check on the theory of microwave amplification or oscillation in a ferromagnetic resonance system as proposed by H. Suhl, a sample version has been constructed and operated with resulting agreement between experiment and theory.
- [48] Solid state gains new amplifier.
Electronics, 30(8): 24, 26; August 1, 1957. Also in *Bell Laboratories Record*, 35(8): 316-317; August, 1957.
News item about successful operation of a ferromagnetic amplifier in microwave range by Bell Telephone Laboratories.
- [49] Solid-state maser amplifier uses ferrites.
Journal of the Franklin Institute, 264(3): 260-261; September, 1957.
A brief description of the work being done at the Bell Telephone Laboratories on ferromagnetic amplifiers.
- [50] Suhl, H.
Ferromagnetic microwave amplifier.
Physics Today, 11(9): 28-30; September, 1958.
Briefly reviews maser-type devices, then gives basic theory for a ferrite-type parametric amplifier. Also cites related work in this field.
- [51] Suhl, H.
Origin and use of instabilities in ferromagnetic resonance.
Journal of Applied Physics, 29(3): 416-421; March, 1958.
Presents basic theory of the behavior of ferromagnetic materials with application to ferromagnetic amplifiers.
- [52] Suhl, H.
Proposal for a ferromagnetic amplifier in the microwave range.
Physical Review, 106(2): 384-385; April 15, 1957.
Discusses three alternative types of operation (magneto-static, semistatic, and electromagnetic modes) which may be used in the design of a microwave amplifier. In general, it relies on the modulation of the real part of a susceptibility, rather than on the maser principle of altering normal populations of two levels.
- [53] Suhl, H.
Quantum analog of the ferromagnetic microwave amplifier.
Journal of the Physics and Chemistry of Solids, 4(4): 278-282; 1958. (Bell Monograph 2970.)

A quantum mechanical model of a ferromagnetic microwave amplifier has been built to compare modes of operation with a three-level maser. It is found that in a three-level maser it is essential to have a negative temperature for two levels while the analog of the ferromagnetic amplifier depends only on the time-varying part of the density matrix.

- [54] Suhl, H.
Theory of a ferromagnetic microwave amplifier.
Journal of Applied Physics, 28(11): 1225-1236; November, 1957. (Bell Monograph 2926.)
Gives a survey of 3 possible types of operation (electromagnetic, semistatic, and magnetostatic) with general theory included. The three types of operation are also defined as: two electromagnetic cavity modes, two sample modes, and lastly, one sample and one cavity mode. An appendix discusses the gain-bandwidth problem.
- [55] Tien, P. K. and Suhl, H.
A traveling-wave ferromagnetic amplifier.
PROCEEDINGS OF THE IRE, 46(4): 700-706; April, 1958. (Bell Monograph 3043.)
A proposal for a traveling-wave amplifier consisting of two transmission lines embedded in a ferromagnetic medium.
- [56] Weiss, M. T.
Solid-state microwave amplifier and oscillator using ferrite.
Journal of Applied Physics, 29(3): 421; March, 1958. (Presented at Conference on Magnetism and Magnetic Materials, held November 18-21, 1957, in Washington, D. C.)
Brief item on a device built and operated at Bell Telephone Laboratories called the MAVAR (modulating amplifiers, by variable reactance).
- [57] Weiss, M. T.
Solid-state microwave amplifier and oscillator using ferrites.
Physical Review, 107(1): 317; July 1, 1957.
A device based on the proposal of H. Suhl (see [52]) has been built and operated. Results of these experiments are given.
- [58] Whirry, W. L. and Wang, F. B.
Phase dependence of a ferromagnetic microwave amplifier.
PROCEEDINGS OF THE IRE, 46(9): 1657-1658; September, 1958.
Experimental results using a polycrystalline yttrium garnet in a parametric amplifier are described. Photographs show oscilloscope traces of the phase relationship of output pulses, signal input and pump input.

Diode Types

- [59] Bell, C. V. and Wade, G.
Circuit considerations in traveling-wave parametric amplifiers.
1959 IRE WESCON CONVENTION RECORD, (pt. 2): 75-82.
Discusses the circuits appropriate to the wideband operation of a diode-type traveling-wave amplifier. Presents a Brillouin diagram which allows the computation of conditions for high gain, wideband operation and other characteristics.
- [60] Bloom, S. and Chang, K. K. N.
Parametric amplification using low-frequency pumping.
Journal of Applied Physics, 29(3): 594; March, 1958.
Conventional parametric amplifiers use one-pump system. This discusses an amplifier using lower-frequency pumping in which two pumping sources are used.
- [61] Bossard, B. B.
Superregenerative reactance amplifier.
PROCEEDINGS OF THE IRE, 47(7): 1269-1271; July, 1959.
A diode-type parametric amplifier having superregeneration is described. Because of the constant threshold value of the oscillations, this type of amplifier could be used as a threshold device or as a limiter.
- [62] Brand, F. A., Matthei, W. K., and Saad, T.
The Reactatron—a low-noise semiconductor diode, microwave amplifier.
PROCEEDINGS OF THE IRE, 47(1): 42-44; January, 1959.
Uses only semiconductor diodes for its nonlinear reactance. The two p - n junction diodes are in a balanced hybrid system. At a frequency of 2900 mc, power gains in excess of 30 db have been observed, with effective input noise temperatures less than 290°K.
- [63] Breitzer, D. I. and Sard, E. W.
Low frequency prototype backward-wave reactance amplifier.
Microwave Journal, 2(8): 34-37; August, 1959.
Presents the theory and experimental results of amplifiers of this type which use matched pairs of diodes. Numerous parameters are described.
- [64] Chang, K. K. N.
Analysis of a four-terminal parametric amplifier.
RCA Review, 20(2): 205-221; June, 1959.
Describes an amplifier having three cascaded stages—a converter, an amplifier, and a modulator—using germanium junction diodes. It can be operated at linear gains as high as 30 db, with sensitivity at such gains of 120 dbm or better.
- [65] Chang, K. K. N.
Four-terminal parametric amplifier.
PROCEEDINGS OF THE IRE, 47(1): 81-82; January, 1959.
The amplifier uses a lower-frequency pump and has three cascaded stages. It can be operated at linear gains as high as 30 db, with a sensitivity of 120 dbm or better. Noise factors at these gains are around 2.5 db. Germanium junction diodes are used.
- [66] Chang, K. K. N.
Harmonic generation with nonlinear reactances.
RCA Review, 19(3): 455-464; September, 1958.
Following the derivation of the theory of frequency multiplication using nonlinear reactances, results of an experiment using a germanium point-contact diode are given. At high input power levels the efficiency drops below the theoretical value.
- [67] Chang, K. K. N. and Bloom, S.
A parametric amplifier using lower-frequency pumping.
1958 IRE WESCON CONVENTION RECORD, (pt. 3): 23-27.
Experimental work using a special zero-biased semiconductor diode is reported. Two cases are described; one with a signal frequency of 380 mc and a pumping frequency of 300 mc, and the other with a signal frequency of 6.6 kmc and a pump frequency of 4 kmc.
- [68] DeLoach, C. B. and Sharpless, W. M.
An X-band parametric amplifier.
PROCEEDINGS OF THE IRE, 47(9): 1664; September, 1959.
Describes the construction and operation of an amplifier using special point-contact gallium arsenide diodes. It produced a gain of 10 db with a 75-mc bandwidth with 100 mw of pump power.
- [69] Diodes for parametric amplifiers.
Electronic Industries, 18(3): 105, 270; March, 1959.
Reports on the operating characteristic of diodes produced by Hughes Aircraft Co. One type operates below 1000 mc and the other type is for the microwave region. Noise temperatures, cutoff frequencies, gain and bandwidth are described.
- [70] Endler, H., Berk, A. D., and Whirry, W. L.
Relaxation phenomena in diode parametric amplifiers.
PROCEEDINGS OF THE IRE, 47(8): 1375-1376; August, 1959.
Presents a theory to explain relaxation oscillations observed in S-, C-, and X-band parametric amplifiers using CW pump sources and no other signal inputs.
- [71] Englebrecht, R. S.
A low-noise nonlinear reactance traveling wave amplifier.
PROCEEDINGS OF THE IRE, 46(9): 1655; September, 1958.
Gives operating characteristics of an experimental UHF amplifier which uses four diffused-junction silicon diodes having low resistive loss. The noise figure is 3.5 db and the bandwidth 10-20 mc.
- [72] Greene, J. C. and Lombardo, P. P.
Low noise 400-mc reactance amplifiers.
Microwave Journal, 2(5): 28-31; May, 1959.
Gives construction details of three types of parametric amplifiers or for three modes of operation; namely, sum-frequency mode, two-port difference-frequency mode, and one-port difference-frequency mode. Varactor diodes developed by Bell Telephone Laboratories are used.
- [73] Heffner, H. and Kotzebue, K.
Experimental characteristics of a microwave parametric amplifier using a semiconductor diode.
PROCEEDINGS OF THE IRE, 46(6): 1301; June, 1958.
A report on the characteristics of a microwave parametric amplifier using a back-biased germanium junction diode.

- [74] Heffner, H. and Wade, G.
Gain, bandwidth, and noise characteristics of a variable-parameter amplifier.
Journal of Applied Physics, 29(9): 1321-1331; September, 1958.
Discusses the principles of parametric amplifiers, using the two-tank circuit as a model in the analysis. The case of the two-tank circuit for frequency conversion is also included. Noise figures and bandwidth are emphasized throughout. Essentially a revised version of Stanford University Electron Tube Laboratories Technical Report No. 28.
- [75] Heffner, H. and Wade, G.
Minimum noise figure of a parametric amplifier.
Journal of Applied Physics, 29(8): 1262; August, 1958.
Gives a noise figure expression suitable for solid-state parametric amplifiers and contrasts it to the expression for beam types where shot-noise terms are important. The minimum noise figure is found to approach the ratio of the pumping frequency to the idling frequency.
- [76] Heilmeier, G. H.
An analysis of parametric amplification in periodically loaded transmission lines.
RCA Review, 20(3): 442-454; September, 1959.
Gives the theory of traveling-wave parametric amplifiers. A lossless transmission line periodically loaded with nonlinear capacitance (back-biased semiconductor diodes) is the propagating structure. The gain is shown to be a function of the spacing and static capacitance of diodes, frequencies of operation, and impedance of the unloaded line.
- [77] Herrmann, G. F., Uenohara, M., and Uhler, A., Jr.
Noise figure measurements on two types of variable reactance amplifiers using semiconductor diodes.
PROCEEDINGS OF THE IRE, 46(6): 1301-1303; June, 1958.
Results of experiments on low noise amplification at UHF and microwave frequencies by $p-n$ junction diodes.
- [78] Hilibrand, J. and Beam, W. R.
Semiconductor diodes in parametric subharmonic oscillators.
RCA Review, 20(2): 229-253; June, 1959.
Discusses factors affecting the performance of diodes in such oscillators, including effects of stray capacitance, spreading resistance, junction conductance, and capacitance-voltage sensitivity. Minimum rise times and minimum quality factors are stated.
- [79] Jones, E. M. T. and Honda, J. S.
A low noise up-converter parametric amplifier.
1959 IRE WESCON CONVENTION RECORD, (pt. 1): 99-107.
After discussing the relation of gain and noise figures to the diode loss, available capacitance variation and generator and load terminations, the paper describes the construction of an experimental up-converter which uses a back-biased diffused-junction diode. Gains ranged from 12.4 to about 20 db, with noise figures of about 1.0 db.
- [80] Kibler, L. U.
Directional bridge parametric amplifier.
PROCEEDINGS OF THE IRE, 47(4): 583-584; April, 1959.
Gives expressions for the noise figure of a bridge using varactor diodes. Gains up to 25 db were obtained at 530 mc, with the pump frequency 1060 mc. The average of the noise figures was 3.8 db when operating with a 10-db gain and a bandwidth of about 0.6 mc. The device can also be used as a tunable amplifier.
- [81] Kim, C. S.
Four-terminal equivalent circuits of parametric diodes.
1959 IRE WESCON CONVENTION RECORD, (pt. 2): 91-101.
Derives expressions for four-terminal equivalent circuits, including three frequencies, for converters and for amplifiers. These circuits may be used to obtain expressions for gain, bandwidth, and noise figure.
- [82] Knechtli, R. C. and Weglein, R. D.
Low noise parametric amplifier.
PROCEEDINGS OF THE IRE, 47(4): 584-585; April, 1959.
Describes operation of an amplifier using gold-bonded diodes. By cooling with liquid nitrogen the minimum amplifier noise temperature was reduced to 50° K. Operation was in the S band.
- [83] Leenov, D.
Gain and noise figure of a variable-capacitance up-converter.
Bell System Technical Journal, 37(pt. 4): 989-1008; July, 1958.
Discusses the theory of the performance of a $p-n$ junction nonlinear-capacitance diode used as a low-noise amplifying frequency converter in a case in which the output-signal frequency is many times larger than the frequency of the input signal. Gives formulas for maximum gain and for noise figures.
- [84] Lombardo, P. P. and Sard, E. W.
Low-frequency prototype traveling-wave reactance amplifier.
PROCEEDINGS OF THE IRE, 47(5): 995-996; May, 1959.
A junction-diode type amplifier, using commercial diodes, is described and experimental results are given. Frequency responses, power gains and noise are among points covered.
- [85] Lombardo, P. P. and Sard, E. W.
Low noise microwave reactance amplifiers with large gain-bandwidth products.
1959 IRE WESCON CONVENTION RECORD, (pt. 1): 83-98.
Describes the operation of several low-frequency devices using silicon diodes, including amplifiers, up-converters, and demodulators. Both one-part and two-part operation are considered.
- [86] Low-noise amplifier for high frequencies uses new semiconductor diodes.
Bell Laboratories Record, 36(7): 250-251; July, 1958.
Experimental devices, one of a family of parametric amplifiers being developed by Bell Telephone Laboratories, shows great promise and improvement over many types of microwave receivers. It has low noise, greater bandwidth, and operates at ordinary temperatures.
- [87] Low-noise amplifier using semiconductor diodes.
Electronics and Radio Engineer, 35(7): 267; July, 1958. Also in *Journal of the Franklin Institute*, 266(2): 151-152; August, 1958.
Brief description of features of the Bell Telephone Laboratories' parametric amplifiers, including a traveling-wave amplifier configuration which uses arrays of several diodes and has a bandwidth of 100 mc at a 400-mc signal frequency and a pump frequency of 900 mc.
- [88] Microwave amplifiers may improve radar.
Machine Design, 30(12): 14; June 12, 1958.
Brief description of a germanium diode type parametric amplifier developed by RCA Laboratories. It has been tested in the UHF and 6000-mc regions.
- [89] Nergaard, L. S.
Nonlinear-capacitance amplifiers.
RCA Review, 20(1): 3-17; March, 1959.
After briefly reviewing the development of parametric amplifiers, the paper discusses gain mechanism in nonlinear capacitance, diode capacitor amplifiers, and performance characteristics of various types.
- [90] Oguchi, B., Kita, S., Inage, N., and Okajima, T.
Microwave parametric amplifier by means of germanium diode.
PROCEEDINGS OF THE IRE, 47(1): 77-78; January, 1959.
Describes operation of two types of diodes—one, a gold-bonded type, and the other, a silver-bonded type, the latter proving to be superior. A gain of 15-20 db is obtained when the pump frequency is 8100 mc, and a bandwidth of 15-25 mc is observed.
- [91] Olson, F. A., Wang, C. P., and Wade, G.
Parametric devices tested for phase-distortionless limiting.
PROCEEDINGS OF THE IRE, 47(4): 587-588; April, 1959.
Gives results of tests on two diode-type parametric devices, one being an amplifier and the other a frequency converter. Expressions are given to describe the operation of each.
- [92] Parametric amplifier ups scatter range.
Electronics, 31(45): 96; November 7, 1958.
Brief description of a diode-type parametric amplifier developed by ITT Laboratories for use in a 90-mile scatter propagation link. The range is expected to be extended to more than 350 miles under favorable conditions.
- [93] Petrack, P.
Predicts boom for new diode.
Electronics, 32(15): 26; April 10, 1959.
Predicts the sales potential for parametric amplifier diodes, as seen by ITT Components Division managers. The price outlook by 1962 for such diodes is also given.

- [94] Pittman, W. C.
A parametric amplifier in space-probe tracking.
Astronautics, 4(8): 40, 44; August, 1959.
Gives design and operational characteristics of a silicon-diode-type parametric amplifier developed by ITT Laboratories for use in the Army Ballistic Missile Agency tracking station. It allowed tracking of the Pioneer IV satellite to a distance of 200,000 miles on radiated power of 180 mw. It had a noise figure of about 1 db compared to 7.5 db for electron-tube amplifiers.
- [95] Reed, E. D.
The variable capacitance parametric amplifier.
IRE TRANSACTIONS ON ELECTRON DEVICES, ED-6(2): 216-224; April, 1959.
Reviews operation of diode-type devices, and compares noise performance with vacuum-type amplifiers. Written for the nonspecialist.
- [96] Salzberg, B. and Sard, E. W.
Low-noise wide-band reactance amplifier.
PROCEEDINGS OF THE IRE, 46(6): 1303; June, 1958.
Summary of a study of a reactance amplifier operated in a sum-frequency mode indicating that very-low effective input-noise temperatures are possible.
- [97] Seidel, H. and Herrmann, G. E.
Circuit aspects of parametric amplifiers.
1959 IRE WESCON CONVENTION RECORD, (pt. 2): 83-90.
Discusses two cases. In the first, there is only the signal frequency and a lower sideband, as in a lower-sideband amplifier. The second case considers a periodic cascade in which the pump phase varies uniformly.
- [98] Sie, J. and Weisbaum, S.
Noise figure of receiver systems using parametric amplifiers.
1959 IRE NATIONAL CONVENTION RECORD, (pt. 3): 141-157.
Shows that a parametric amplifier used in one of the following three systems can have an over-all-system noise figure of 1 db: 1) circulator coupler (needs only one amplifier); 2) hybrid coupler (needs two amplifiers, no frequency limitation); 3) up-converter (no frequency limitation).
- [99] Siegman, A. E.
Phase-distortion loss limiting by a parametric method.
PROCEEDINGS OF THE IRE, 47(3): 447-448; March, 1959.
Presents the theory of using parametric amplifiers as limiters, with limiting taking place at the threshold point.
- [100] Shunaman, F.
The variable reactance amplifier.
Radio Electronics, 30(2): Cover, 78-80, 82; February, 1959.
Describes in simplified terms the operation of parametric amplifiers of the diode type. Illustrates an amplifier, developed by ITT Laboratories, designed to operate at 900 mc.
- [101] Sterzer, F.
Microwave parametric subharmonic oscillators for digital computing.
PROCEEDINGS OF THE IRE, 47(8): 1317-1324; August, 1959.
Describes a variable-capacitance diode-type subharmonic oscillator having an output frequency of 2000 mc. Pulse-repetition rates of a few hundred megacycles are possible. Applications are discussed for amplifying, scaling and logic functions.
- [102] Stevens, K. W. H.
Circuit analogues of Suhl-type masers.
Journal of Electronics and Control, 4(3): 275-279; March, 1958.
Discusses the theory of operation of two tuned circuits, which use the varying of inductances with time, thereby obtaining amplification under certain conditions. Provides a basis for the theory of parametric amplifiers.
- [103] Torrey, H. C. and Whitmer, C. A.
Crystal Rectifiers.
McGraw-Hill Book Co., Inc., New York, N. Y., 443 pp.; 1948. (M.I.T. Radiation Lab. Series, vol. 15).
Develops the theory of reactance-variation amplification in a form similar to recent theory, and applies the theory to explain their observations of negative conductances in crystal-diode mixers.
- [104] Uhler, A., Jr.
Junction diode amplifiers.
Scientific American, 200(6): 118-120, 123, 124, 126, 127, 129; June, 1959.
Describes the basic principles of parametric diode-type devices, with particular emphasis on the theory and functions of diodes. Recent experimental work is summarized and future applications are mentioned.
- [105] Uhler, A., Jr.
Junction diodes in microwave circuits.
Proceedings of the Institution of Electrical Engineers, 105B (Supplement 11): 661, 672, 673; May, 1958.
Gives only an abstract. States conditions under which diodes can serve as amplifiers, as well as giving suitable diode materials.
- [106] Uhler, A., Jr.
The potential of semiconductor diodes in high-frequency communications.
PROCEEDINGS OF THE IRE, 46(6): 1099-1115; June, 1958.
Describes the function of solid-state diodes in parametric amplifiers and nonlinear frequency converters, as well as related uses. Design data are included with basic theory.
- [107] Uhler, A., Jr.
Shot noise in $p-n$ junction frequency converters.
Bell System Technical Journal, 37(4): 951-988; July, 1958.
Suggests structures for approaching the ideal of theoretically noiseless amplification possible with a $p-n$ junction, having a purely capacitive nonlinear admittance. Experiments with a diffused silicon junction diode are reported. Discusses the low-noise frequency conversion possible with a nonlinear resistance diode used in conjunction with pulsed local-oscillator currents.
- [108] Van der Ziel, A.
On the mixing properties of nonlinear capacitances.
Journal of Applied Physics, 19(11): 999-1006; November, 1948.
Concludes that a variable-reactance amplifier should exhibit very low noise, because of the absence, ideally, of Nyquist-Johnson noise.
- [109] Wade, G. and Heffner, H.
Microwave parametric amplifiers and converters.
Proceedings of the Institution of Electrical Engineers, 105B (supplement 11): 667-679; May, 1958.
Develops expressions for the noise figures and bandwidth for parametric devices.
- [110] Warren, T. B.
Low-noise parametric amplifiers and converters.
1959 IRE NATIONAL CONVENTION RECORD, (pt. 3): 158.
Compares experimental results with theoretical values for various types of variable-capacitance devices as to noise figures, stability and bandwidth, in the 500 to 2000-mc range. Other topics are: fabrication of diffused junction silicon diodes, a system designed to minimize effects of input loading variations, and a stable low-frequency source which produces high-frequency local oscillator power.
- [111] Younger, J. J., Little, A. G., Heffner, H., and Wade, G.
Parametric amplifiers as superregenerative detectors.
PROCEEDINGS OF THE IRE, 47(7): 1271-1272; July, 1959.
Discusses the superregenerative operation of cavity-type parametric amplifiers which use semiconductor diodes. Discusses some of the effects which play a part in the self-quenching process.
- [112] Younger, J. J., Little, A. G., Heffner, H., and Wade, G.
Superregenerative operation of parametric amplifiers.
1959 IRE WESCON CONVENTION RECORD, (pt. 1): 108-111.
Reports on the operation of several diode type cavity amplifiers as both self-quenched and separately-quenched superregenerative devices. In self-quenched superregenerative operation, gains as high as 87 db were observed, compared to 20 db under normal operation. Greatly increased bandwidths and stability were observed without sacrifice in noise figures.

Parametron Types

- [113] Fukui, K., Unose, K., Habara, K., and Kato, M.
Multi-apertured parametrons (In Japanese).
Journal of the Institute of Electrical Communication Engineers of Japan, 41(2): 147-151; February, 1958.
In order to avoid the construction difficulties involved in the small cores used in conventional parametrons, multi-apertured parametrons have been developed having good

- operating characteristics and greater ease of manufacture. Design details are given.
- [114] Goto, E.
On the application of parametrically excited nonlinear resonators (In Japanese).
Journal of the Institute of Electrical Communication Engineers of Japan, 38(10): 770-775; October, 1955.
Shows that oscillations of such resonators can be expressed by a modified form of Mathieu's equation, with a term included to take care of nonlinearity. If parametric excitation is interrupted properly, the resonators are capable of storing binary information with the binary state controlled by means of small signals.
- [115] Goto, E.
The parametron, a digital computing element which utilizes parametric oscillation.
PROCEEDINGS OF THE IRE, 47(8): 1304-1316; August, 1959.
This element consists of a resonant circuit having a nonlinear reactive element (ferrite-core coils) oscillating at one-half the driving frequency. The choice of two stationary phases, π radians apart, is used to represent a binary digit. Circuit design and applications are discussed.
- [116] Hanawa, K. and Kusunoki, K.
Signal converter by magnetic cores for parametron-device (In English).
Electrical Communication Laboratory Reports, Nippon Telegraph & Telephone Public Corporation, 7(2): 25-31; February, 1959.
Discusses core construction and design. Describes a method of converting signals such as from telephone subscribers' lines to parametron signals, using the cores in a matrix arrangement.
- [117] Kamata, K. and Sasaki, F.
Parametron and punched card recorder for standard meson monitor.
Journal of the Scientific Research Institute of Japan, 51: 54; 1957.
Abstract unavailable.
- [118] Muroga, S.
Elementary principle of parametron and its application to digital computers.
Research and Engineering, the Magazine of Datamation, 4(5): 31-34; September-October, 1958.
After reviewing the basic principles of parametrons, the use of such devices in a program-stored binary computer, having fixed point in a parallel system, is discussed. Speed of operation is almost comparable to electron tube types, and maintenance time is negligible.
- [119] Muroga, S. and Takasima, K.
System and logical design of the parametron computer MUSASINO-1 (In Japanese).
Journal of the Institute of Electrical Communication Engineers of Japan, 41(11): 1132; November, 1958.
Abstract not available.
- [120] Nakagome, Y., Kamibayashi, T., and Wada, T.
Parametron Morse to five-unit converter (In Japanese).
Journal of the Institute of Electrical Communication Engineers of Japan, 40(9): 974-980; September, 1957.
Parametrons are used in this automatic code-converter. Experimental results are given as well as a description of its components and circuits.
- [121] Nishiguchi, K.
The misoperation of parametron due to the hysteresis of parametron core (In Japanese).
Journal of the Institute of Electrical Communication Engineers of Japan, 42(2): 151-155; February, 1959.
A signal considerably larger than expected is required in order to overcome the Barkhausen noise. If the control signal is smaller than the read-out signal, the memory of the parametron core which has memorized the phase of the last oscillation is read out, causing a misoperation.
- [122] Oshima, S., Enomoto, H., and Watanabe, S.
Analysis of parametrically excited circuits—parametron and magnetic amplifier (In Japanese).
Journal of the Institute of Electrical Communication Engineers of Japan, 41(10): 971-978; October, 1958.
- Analysis is done by means of conversion matrices in the frequency domain. The parametron is used as an example of a parametrically-excited two-terminal network. The calculated oscillation condition agrees with experimental results.
- [123] Oshima, S., Nakagome, Y., and Inohama, R.
Signal input and output circuits for parametron using transistors and their applications (In Japanese).
Journal of the Institute of Electrical Communication Engineers of Japan, 41(9): 856-861; September, 1958.
Gives circuit designs for signal input and output circuits utilizing parametrons and transistors and describes their application to analog-digital converters, digital-analog converters, and parametron circuit testers.
- [124] Paramistors and computer costs.
Electronic Design, 7(17): 42; August 19, 1959.
A description of their principles of operation and uses, including photographs and a circuit diagram. The cost of a computer using such devices is estimated to be one tenth that of one using semiconductors and cores.
- [125] Terada, H.
Parametron; an amplifying logic element.
Control Engineering, 6(4): 110-115; April, 1959.
Reviews principles of operation, then discusses possible applications, which include logical computing circuits and memory circuits. Speed limitations, imposed by its high-frequency power requirements, constitute the main disadvantage of such devices.
- [126] Zeniti, K., Katsunuma, S., Hanawa, K., Ikeno, N., and Fukuoka, T.
An experimental crossbar telephone exchange system using parametrons (In Japanese).
Journal of the Institute of Electrical Communication Engineers of Japan, 42(3): 225-231; March, 1959.
Describes the operation of an experimental one-hundred-line capacity exchange using about 900 parametrons. After a test of one year, the operation has been good in regard to reliability, compactness, cost, power consumption, etc.
- [127] Zeniti, K., Husimi, K., Hiyama, Y., and Yamanaka, K.
Parametric excitation using selenium rectifier (In Japanese).
Journal of the Institute of Electrical Communication Engineers of Japan, 41(8): 786-791; August, 1958.
Further improvement is necessary for a parametron using a selenium rectifier to achieve faster operating speed and lower power consumption. However, it is satisfactory at low frequencies, uses the same power as a ferrite parametron, and has a capacity-variation rate nearly the same as a germanium junction diode.
- [128] Zeniti, K., Sekiguti, S., and Takasima, M.
Parametric excitation using variable capacitance of ferroelectric materials (In Japanese).
Journal of the Institute of Electrical Communication Engineers of Japan, 41(3): 239-244; March, 1958.
Discusses the use of ferroelectric materials such as barium titanate ceramics in parametron devices. Describes the parametric-excitation ratio, selectivity, power consumption and temperature coefficient.
- [129] Zeniti, K.
Parametron (In Japanese).
Journal of the Institute of Electrical Communication Engineers of Japan, 41(4): 397-403; April, 1958.
Describes and illustrates the design of parametrons—one of a collection of papers on new components and materials.
- [130] Zeniti, K. and Nisiguti, K.
Reading of recorded signals with a low frequency parametron (In English).
Electrical Communication Laboratory Reports, Nippon Telegraph & Telephone Public Corporation, 7(2): 48-53; February, 1959.
Gives a full description of the equipment and operation of the system. In order to increase the memory capacity of the system, various methods of multiplexing, especially time division multiplexing, must be used.

Miscellaneous Items

- [131] Bloom, S. and Chang, K. K. N.
Theory of parametric amplification using nonlinear reactances,

- RCA Review*, 18(4): 578-593; December, 1957.
An analysis of the parametric amplifier in terms of an equivalent circuit using a nonlinear inductance in general enough terms to describe not only linear but nonlinear amplification.
- [132] Cassedy, E. S., Jr.
A surface wave parametric amplifier.
PROCEEDINGS OF THE IRE, 47(8): 1374-1375; August, 1959.
Uses a slab of ferroelectric material to replace the usual dielectric slab, in order to operate at millimeter wavelengths. Theory and operation are described.
- [133] Chang, K. K. N. and Bloom, S.
Parametric amplifier using lower-frequency pumping.
PROCEEDINGS OF THE IRE, 46(7): 1383-1386; July, 1958.
Using a nickel-manganese ferrite core, a nonlinear inductance type parametric amplifier gave a 30 per cent power gain at a signal frequency of 10 mc and a pump frequency of 7 mc. A nonlinear capacitance device using a germanium reversed-bias junction diode achieved a stable net gain of 35 db at 380 mc, having a pumping circuit at 300 mc.
- [134] Chang, K. K. N. and Bloom, S.
A parametric amplifier using lower-frequency pumping.
Proceedings of the Institution of Electrical Engineers, 105B (supplement 11): 680-683; May, 1958.
Describes experiments using first a nickel-manganese ferrite, with a small amount of power gain. Using a germanium junction diode in a second experiment gave much a better result, with a 35-db gain obtained.
- [135] Cohn, S. B.
The noise figure muddle.
Microwave Journal, 2(3): 7, 9, 11; March, 1959.
Points out some of the errors in the common concepts of measurements of noise figures. Discrepancies occur in the measuring of nonlinear networks such as mixers or parametric amplifiers, depending on the use of the noise-source method or the signal-generator method. Proper methods are prescribed.
- [136] Coleman, P. D. and Becker, R. C.
Present state of the millimeter wave generation and technique art—1958.
IRE TRANSACTIONS ON MICROWAVE THEORY AND TECHNIQUES, MTT-7(1): 42-61; January, 1959.
Briefly reviews parametric devices and cites six references representative of major developments.
- [137] Cullen, A. L.
A travelling-wave parametric amplifier.
Nature, 181(4605): 332; February 1, 1958.
Gives expressions for the theoretical amplification possible with a traveling-wave type of parametric amplifier. Requirements for meeting these ideal conditions are briefly mentioned.
- [138] Danielson, W. E.
Low noise in solid state parametric amplifiers at microwave frequencies.
Journal of Applied Physics, 30(1): 8-15; January, 1959.
Uses simple low-frequency network electrical circuits and their mechanical analogs to explain the principles of parametric amplifications; discusses major noise sources; and gives experimental data on four different types of amplifiers (three using semiconductor diodes and one using ferrites).
- [139] Edwards, C. F.
Frequency conversion by means of a nonlinear admittance.
Bell System Technical Journal, 35(6): 1403-1416; November, 1956.
Presents the mathematical analysis of a heterodyne conversion transducer having the nonlinear element made up of a nonlinear resistor and a nonlinear capacitor in parallel. Points out nonlinear capacitor is the preferred element for modulators and a nonlinear resistor alone is preferred for converters.
- [140] Hartley, R. V. L.
Oscillations in systems with nonlinear reactance.
Bell System Technical Journal, 15(3): 424-440; July, 1936.
Studies the properties of a theoretical capacitor having one plate free to vibrate, which is in a circuit containing a generator operating at a frequency higher than the resonant frequency of the plate. Conditions for oscillation are discussed, including conditions for the required generator voltage. Other applications are discussed.
- [141] Haus, H. A.
Power flow relations in nonlinear media.
IRE TRANSACTIONS ON MICROWAVE THEORY AND TECHNIQUES, MTT-6(3): 317-324; July, 1958.
Following the generalizations for nonlinear anisotropic media, and the extension to gyromagnetic media under small-signal excitation at the signal frequency, the author shows under what conditions power gain can be achieved with a three-frequency and a four-frequency excitation of a ferrite. The Manley-Rowe relations (see [144]) are shown to be concerned with coupling coefficients in the operation of a ferrite amplifier.
- [142] Kurokawa, K. and Hamasaki, J.
Mode theory of lossless periodically distributed parametric amplifiers.
IRE TRANSACTIONS ON MICROWAVE THEORY AND TECHNIQUES, MTT-7(3): 360-365; July, 1959.
Introduces an operator useful in analyzing the periodically distributed parametric amplifier. Also, develops an expression for the power gain of the amplifier as an application of the theory.
- [143] Manley, J. M. and Peterson, E.
Negative resistance effects in saturable reactor circuits.
Transactions of the American Institute of Electrical Engineers, 65: 870-881; 1946.
Analyzes sustained oscillators exhibiting many of the properties of free oscillations, as found in saturable reactor circuitry using the work of R. V. L. Hartley (1917). The analysis of the development of negative resistance is expressed simply, and applied to the three classes of oscillations. Experiment data agree with theory.
- [144] Manley, J. M. and Rowe, H. E.
Some general properties of nonlinear elements—part I, general energy relations.
PROCEEDINGS OF THE IRE, 44(7): 904-913; July, 1956.
Derives two independent equations relating the average powers (at different frequencies) in nonlinear inductors and capacitors. The equations are independent of external circuits to which the nonlinear reactor is connected and of the power levels at the various frequencies. These lead to an analysis of gain and stability of nonlinear reactor modulators and demodulators. Special cases are also considered.
- [145] Page, C. H.
Frequency conversion with nonlinear reactances.
Journal of Research of the National Bureau of Standards, 58(5): 227-236; May, 1957.
Develops expressions to show that a lossless nonlinear impedance subject to an almost periodic voltage will absorb power at certain frequencies and supply power at other frequencies. Simple cubic capacitors are found to be sufficient for producing any possible conservative modulation or distortion process.
- [146] Pierce, J. R.
Use of the principle of conservation of energy and momentum in connection with the operation of wave-type parametric amplifiers.
Journal of Applied Physics, 30(9): 1341-1346; September, 1959.
A theoretical discussion based on the terms of the force exerted by traveling-wave discontinuities or reflecting elements on the waves present in wave-type parametric amplifiers. Proposes that for a guided wave the momentum per unit distance is the power divided by the product of the group and phase velocities.
- [147] Roe, G. M. and Boyd, M. R.
Parametric energy conversion in distributed systems.
PROCEEDINGS OF THE IRE, 47(7): 1213-1218; July, 1959.
Discusses the theory of operation of traveling-wave type parametric devices having little or no dispersion. Indicates that pumping will not result in exponential gain of a signal but rather in a conversion of energy to a multiplicity of cross-product frequencies. Discusses two physical models and also the special case of zero dispersion. Use of such systems as frequency converters is pointed out.
- [148] Rowe, H. E.

- Some general properties of nonlinear elements—part II, small signal theory.
 PROCEEDINGS OF THE IRE, 46(5, pt. 1): 850–860; May, 1958.
 Uses the small-signal analysis to study the simplest types of nonlinear capacitor modulators, demodulators and negative-conductance amplifiers. The results give the gain, bandwidth, terminal admittances, and sensitivity of these devices, and show the way in which nonlinearity affects these quantities. In general, the bandwidth of the devices approaches zero as nonlinearity approaches zero.
- [149] Saito, S.
 Parametric amplification of space-charge waves on a thin electron beam (In Japanese).
Journal of the Institute of Electrical Communication Engineers of Japan, 41(11): 1113–1120; November, 1958.
 Discusses the more general cases, assuring a thin longitudinal beam with the modulation large compared to the signal, yet small enough to be general by linear theory. Both the inverting and the noninverting cases are treated.
- [150] Tannenwald, P. E.
 Properties of thin magnetic films for microwave applications. 1959 IRE WESCON CONVENTION RECORD, (pt. 1): 134–141.
 Compares properties of the magnetic films with ferromagnetic insulators. In particular, compares frequency response, electromagnetic wave transmission, relation of thin depth to spin numbers, permeability at microwave frequencies and also a scheme representing a spin parametric amplifier.
- [151] Tien, P. K.
 Parametric amplification and frequency mixing in propagating circuits.
Journal of Applied Physics, 29(9): 1347–1357; September, 1958.
 Develops expressions for the properties of a time-varying reactance in propagating structures, including the case in which parametric amplification is possible, as well as cases for frequency conversion, frequency channel selection, both wide- and narrow-band amplifiers, oscillators and backward-wave devices. Noise figures are also considered.
- [152] Valdes, L. B.
 Circuit conditions for parametric amplification.
Journal of Electronics and Control, 5(2): 129–141; August, 1958.
 Signals in a passive-element circuit can be amplified if there is a nonlinear or time-varying reactance. Paper describes the physical model and the circuit conditions necessary for operation and discusses the difference between parametric amplifiers and mixers or modulators.
- [153] Van der Ziel, A.
 Noise figure of reactance converters and parametric amplifiers.
Journal of Applied Physics, 30(9): 1449; September, 1959.
 Derives the noise figure in a simple fashion, and points out its variation from a formula given by Hoffman and Wade (see [74]).
- ### III. MASERS
- #### Review Articles
- [154] Ancillary equipment: masers.
Civil Aviation Radio News, (28): 65–68; July, 1958.
 History and descriptions of the ammonia and solid-state masers. Includes also information about current developments being made by various groups in England, Canada, and the U.S.A.
- [155] Birnbaum, G.
 Microwave atomic amplifiers and oscillators.
 1957 IRE WESCON CONVENTION RECORD, (pt. 3): 169.
 Reviews developments in the field. Also, gives an explanation of the operations of various devices characterized by a method of obtaining the emissive condition: electrostatic focusing in the ammonia beam maser; optical pumping of rubidium vapor; and microwave pulsing and saturating of paramagnetic solid-state systems.
- [156] Cade, C. M.
 The maser: a new form of microwave oscillator.
Journal of the Television Society, 8(12): 509–511; October–December, 1958.
 Gives a short review of the operational principles of solid-state masers and molecular-beam masers.
- [157] Combrisson, J. and Townes, C. H.
 Production and amplification of microwaves by atomic processes (In French).
Onde Electrique, 36(356): 989–991; November, 1956.
 Brief review describing the principles of the maser, the work being done on the ammonia maser at Columbia University, and the possibility of a solid-state version.
- [158] Culver, W. H.
 Maser; a molecular amplifier for microwave radiation.
Science, 126(3278): 810–814; October 25, 1957.
 A general review of the principles and operations of both gaseous and solid-state masers.
- [159] Gordon, J. P.
 The maser.
Scientific American, 199(6): 42–50; December, 1958.
 Reviews the theory and operation of solid-state and gaseous masers. It is well illustrated and is written for the layman.
- [160] Gordon, J. P.
 A molecular microwave spectrometer, oscillator and amplifier. IRE TRANSACTIONS ON INSTRUMENTATION, PGI-4: 155–159; October, 1955.
 A survey of the principles of a microwave spectrometer and oscillator operating on emission of energy from molecules.
- [161] Goudet, G.
 The production and amplification of radio oscillations using molecular or atomic transitions (In French).
Onde Electrique, 38(379): 671–686; October, 1958.
 Following a discussion of the quantum mechanical principles governing molecular and atomic transitions, the author describes their application to masers and frequency standards of the solid state and of gaseous states. Optical pumping is also described.
- [162] Heineken, F. W.
 De "maser."
Nederlands Tijdschrift voor Naturkunde, 23(6): 164–167; 1957.
 Abstract unavailable.
- [163] Klinger, H. H.
 Molekulare Mikrowellen-Verstärker (maser) (In German).
Elektronische Rundschau, 12(7): 237–239; July, 1958.
 Survey of the electronics of the maser, presenting several basic statements on physical principles. Discusses molecular radiation, negative temperature, light quantum and crystal-type masers, and shows possible applications.
- [164] Kontorovich, V. M. and Prokhorov, A. M.
 Nonlinear effects of the interaction of resonance fields in the molecular generator and amplifier (In English).
Soviet Physics JETP, 33: 1100–1102; June, 1958. Also in *Zhurnal Eksperimentalnoi i Teoreticheskoi Fiziki*, 33(6): 1428–1430; December, 1957 (In Russian).
 An analysis of the polarizability of a quantum system situated in two resonance fields with an auxiliary field. Gives expressions for the possible frequencies of generation and amplification.
- [165] Lequeux, J.
 Une revolution dans le domaine des hyperfréquences: Le "maser" oscillateur et amplification moleculaire (In French).
La Nature, (3272): 470–475; 1957.
 Abstract unavailable.
- [166] Likel, H.
 The Maser: a low-noise microwave amplifier.
Western Union Technical Review, 13(3): 99–100; July, 1959.
 Gives a brief review of the basic principles of the operation of masers.
- [167] Marsh, J. A.
 Survey of communications problems associated with space travel.
 In: *Vistas in Astronautics*, Alperin, Morton, Ed. Pergamon Press, Inc., New York, N. Y., 330 pp.; 1958.
 Pages 85–87 point out the potential use of maser amplifiers in space ships to base communication lines.
- [168] Maser R and D activity now is widespread.
Electronic News, 3(107): 4, 5; September, 22 1958.
 A review of the programs, projects, and progress on masers. Includes list of companies, type of maser, frequency bands and/or wavelengths, and materials being used.
- [169] Shimoda, K., Wang, T. C., and Townes, C. H.

- Further aspects of the theory of the maser.
Physical Review, 102(5): 1308-1321; June 1, 1956.
A more detailed analysis of certain aspects of theory of the maser is given. In particular effects of saturation and of the resonant cavity design are discussed. Various types of noise and frequency shifts of oscillators are examined.
- [170] Shunaman, F.
Revolutionary new oscillator-amplifier.
Radio-Electronics, 26(6): 55-57; June, 1955.
A popular, simplified description of a new device—the maser.
- [171] Singer, J. R.
Masers.
John Wiley and Sons, Inc., New York, N. Y., 147 pp.; 1959.
Treats both solid-state and gaseous masers.
- [172] Souped-up energy at work: meet the maser.
Product Engineering, 29(2): 10; January 13, 1958.
A few brief paragraphs describing gaseous and solid-state masers.
- [173] Townes, C. H.
Masers.
Journal of Applied Physics, 29(3): 238; March, 1958.
Gives an abstract of a review paper on the properties and characteristics of all types of masers.
- [174] Townes, C. H. and Schawlow, A.
Microwave Spectroscopy.
McGraw-Hill Book Co., Inc., New York, N. Y., 698 pp.; 1955.
Description of a device used as a high-resolution spectrometer (the maser) is given on pp. 432-434. Information on the molecular-beam maser is given on pp. 482 and 485.
- [175] Townes, C. H.
A molecular microwave amplifier, oscillator and frequency standard.
1955 IRE CONVENTION RECORD, (pt. 10): 180.
Indications from the tests and analysis of data show that the maser should provide an excellent frequency standard. An abstract of the paper is all that appears.
- [176] Weber, J.
Amplification of microwave radiation by substances not in thermal equilibrium.
IRE TRANSACTIONS ON ELECTRON DEVICES, ED-3(1): 1-4; June, 1953.
Paper based on a presentation made at the IRE Electron Tube Conference in Ottawa, in June, 1952. Gives some of the basic theory and methods for obtaining microwave radiation from crystals and gases.
- [177] Weibel, G. E.
Masers and related quantum-mechanical devices. Part I.
Sylvania Technologist, 10(4): 90-97; October, 1957.
Reviews basic principles: discusses relation to maser operation of quantum-mechanical behavior of single atoms, energy level of isolated microsystems, interaction with electromagnetic field, energy storage and conversion, and, finally, statistical properties of large assemblies.
- [178] Weibel, G. E.
Masers and related quantum-mechanical devices. Part II.
Sylvania Technologist, 11(1): 26-43; January, 1958.
This part consists of a brief review of quantum mechanics fundamentals and of the derivation of the theory of microwave interaction with a two-level system.
- [179] Wittke, J. P.
Molecular amplification and generation of microwaves.
PROCEEDINGS OF THE IRE, 45(3): 291-316; March, 1957.
Reviews the wide variety of devices using molecular systems, including molecular-beam masers, "optically-pumped" amplifiers, etc. Discusses properties such as gain, bandwidth, noise figures. A supplementary note by the author appears in PROCEEDINGS OF THE IRE, 45(7): 1100; March, 1957.
- [180] Wolf, H. C.
The molecular amplifier (In German).
Zeitschrift für Angewandte Physik, 10(10): 480-488; October, 1958.
Reviews the operation of solid-state and ammonia masers.
- Study of the dynamic high-field polarization and the construction of an auto-oscillator of the maser type (In French).
Comptes Rendus de l'Academie des Sciences (Paris), 246(26): 3608-3610; June 30, 1958.
Shows that a nuclear resonance line can be inverted by interaction with the paramagnetic saturated resonance levels of a free radical. An 8-watt magnetron is used to saturate the paramagnetic resonance line. A Q meter is used to detect the oscillation output which is at the proton Larmor-frequency.
- [182] Basov, N. G. and Prokhorov, A. M.
Application of molecular beams to radiospectroscopic study of rotation spectra of molecules (In Russian).
Zhurnal Eksperimentalnoi i Teoreticheskoi Fiziki, 27(10): 431-438; October, 1954.
Narrow spectral lines (width about 7 kc) and rotation spectra of materials in solid state may be obtained by using molecular beams. A theoretical study of rotation transition in CsF molecules at a frequency of 17.7 kmc using a spectroscopy with a waveguide absorption cell and using, also, a cavity-resonator instrument.
- [183] Basov, N. G., Veselago, V. G., and Zhabatinski, M. E.
Increasing the Q factor of the cavity resonator by regeneration (In English).
Soviet Physics JETP, 28: 177-178; July, 1955. Also in *Zhurnal Eksperimentalnoi i Teoreticheskoi Fiziki*, 28(2): 242; February, 1955 (In Russian).
An article on the use of cavity resonator with molecular-beam oscillator, resulting in a Q factor of 5×10^6 for periods of up to 20 minutes.
- [184] Basov, N. G.
Molecular-beam oscillator (In Russian).
Radiotekhnika i Elektronika, 1(6): 752-757; June, 1956.
Description of a 23,870-mc NH_3 beam oscillator.
- [185] Basov, N. G. and Prokhorov, A. M.
Molecular generator and amplifier (In Russian).
Uspekhi Fiziki Nauk, 57: 485-501; 1955.
Applications are mentioned, such as time standards, spectroscopy, etc.
- [186] Basov, N. G.
Molecular generator on a beam of ammonia molecules (part I). Study of the operation of a molecular generator (part II) (In Russian).
Priroda i Tekhnika Eksperimenta, (1): 71-77, 77-82; 1957.
Abstract unavailable.
- [187] Basov, N. G.
On the condition of self-excitation of free-space molecular oscillators (In English).
Radio Engineering and Electronics, 3(2): 427-429; 1958. Also in *Radiotekhnika i Elektronika*, 3(2): 297-298; February, 1958 (In Russian).
Considers the problem of molecular oscillations in free space, in view of its application to obtaining molecular oscillators and amplifiers for millimetric and submillimetric waves. Examples are given for oscillators employing either ammonia beams or paramagnetic crystals.
- [188] Basov, N. G. and Petrov, A. P.
On the relative frequency stability of molecular oscillators (In English).
Radio Engineering and Electronics, 3(2): 431-433; 1958. Also in *Radiotekhnika i Elektronika*, 3(2): 298-299; February, 1958 (In Russian).
Shows the block diagram for comparing the frequencies of two molecular oscillators. The relative stability of frequency was found to be of the order of 10^{-11} over a period of about 16 minutes. The variation of frequency per second was of the order of 10^{-13} to 10^{-14} .
- [189] Basov, N. G. and Prokhorov, A. M.
Possible methods of obtaining active molecules for the molecular generator (In English).
Soviet Physics JETP, 28: 184-185; July, 1955. Also in *Zhurnal Eksperimentalnoi i Teoreticheskoi Fiziki*, 28(2): 249-250; February, 1955 (In Russian).
To obtain resonance transitions between the energy levels in the molecules so as to increase the fraction of active mole-

- cules in the beam, the use of an auxiliary high-frequency field is suggested.
- [190] Basov, N. G. and Prokhorov, A. M.
The theory of a molecular oscillator and a power amplifier. *Discussions of the Faraday Society*, (19): 96-99; 1955.
Gives expressions for the frequency of an oscillator in terms of the transitions among energy levels. Conditions for amplification are given, as well as expressions for the power-amplification ratio.
- [191] Benoit, H., Grivet, P., and Guibe, L.
A maser with purely nuclear magnetic resonance (In French). *Comptes Rendus de l'Academie des Sciences (Paris)*, 246(26): 3608-3610; June 30, 1958.
Uses a current of water with protons oriented, due to a resonance arrangement. The water current passes through a coil tuned to 30 mc. Beats are noticed when the proton resonance frequency is sufficiently near to 30 mc, indicating that oscillations of the maser type are present. Applications are discussed.
- [192] Benoit, H., Grivet, P., and Ottavi, H.
Study of a weak-field maser-type self-oscillator (In French). *Comptes Rendus de l'Academie des Sciences (Paris)*, 248(2): 220-223; January 12, 1959.
Presents the characteristic of the maser discussed in [191].
- [193] Benoit, H., Grivet, P., and Ottavi, H.
Weak-field nuclear-magnetic-resonance maser (In French). *Comptes Rendus de l'Academie des Sciences (Paris)*, 247(22): 1985-1988; December 1, 1958.
Describes an instrument for nuclear-magnetic-resonance studies based on proton spin resonance in circulating benzene. A further description is given in [192].
- [194] Fain, V. M.
On the oscillation equations of a molecular generator (In English). *Soviet Physics JETP*, 33: 726-728; April, 1958. Also in *Zhurnal Eksperimentalnoi i Teoreticheskoi Fiziki*, 33(10): 945-947; October, 1957 (In Russian).
Derivation of equations for both stationary and nonstationary operating conditions of a molecular generator is made using a density matrix in proper approximation.
- [195] Fain, V. M.
Quantum phenomena in the radio range (In Russian). *Uspekhi Fiziki Nauk*, 64(2): 273-313; February, 1958.
Discusses molecular oscillators, quantum effects involved in interactions of selections in resonators with high frequency fields, spontaneous radiation, etc.
- [196] Helmer, J. C.
Maser oscillators.
Journal of Applied Physics, 28(2): 212-215; February, 1957.
Using a second maser as a reference standard, observations have been made of the experimental behavior of a maser under various operating conditions. A comparison of the results is made with the theory from a new analysis which includes the velocity distribution in the beam.
- [197] Helmer, J. C.
Small signal analysis of molecular beam masers.
Journal of Applied Physics, 30(1): 118-120; January, 1959.
Following an expression for the resonance polarization of a molecule in an electric field as a function of time, the author analyzes maser operation having a divergent, univelocity beam; including expressions for the relative beam intensity required to start oscillation and for the molecular Q as a function of cavity length.
- [198] Kemp, J. C.
Theory of maser oscillation.
Journal of Applied Physics, 30(9): 1451-1452; September, 1958.
Derives expressions to account for the amplitude-modulated nature of the signal from an inverted spin system undergoing maser oscillation. Large amplitude nutations of the magnetization are seen to play a major role in the phenomenon.
- [199] Khokhlov, R. V.
On the locking of a molecular oscillator by a small external force (In English). *Radio Engineering and Electronics*, 3(4): 161-166; 1958. Also in *Radiotekhnika i Elektronika*, 3(4): 566-569; April, 1958 (In Russian).
Develops expressions for a theoretical case in which the frequency of the external force is close to that of the oscillator. Results show that the frequency of the external force corresponding to maximum amplitude is somewhat shifted from the oscillation frequency to the side of the frequency of molecular transition.
- [200] Klimontovich, I. L. and Khokhlov, R. V.
Contributions to the theory of the molecular generator (In English). *Soviet Physics JETP*, 32: 937-941; December, 1957. Also in *Zhurnal Eksperimentalnoi i Teoreticheskoi Fiziki*, 32(5): 1150-1155; May, 1957 (In Russian).
Discusses the theory of resonance interactions between an electromagnetic field and a molecular beam in a molecular generator. Velocity spreads are considered, as well as effects of a varying resonator temperature.
- [201] Kontorovich, V. M.
On the use of two auxiliary fields to obtain emission states in quantum-mechanical amplifiers and generators (In English). *Soviet Physics JETP*, 33: 820-821; April, 1958. Also in *Zhurnal Eksperimentalnoi i Teoreticheskoi Fiziki*, 33(4): 1064-1065; October, 1957 (In Russian).
Proposes the use of two fields with frequencies such that the system may be made to generate or amplify at a frequency larger than that of the auxiliary fields. Discusses pulse length of auxiliary fields and its relation to the population of the four levels.
- [202] Oraevsky, A. N.
On the theory of a molecular oscillator (In Russian). *Radiotekhnika i Elektronika*, 4(4): 718-723; April, 1959.
Derives equations to describe the stationary process as a function of time. The molecular oscillator can be considered as an oscillating system with an inertial nonlinearity. Locking-in of the oscillator by an external force is seen to be covered by the expressions.
- [203] Prokhorov, A. M. and Lebedev, P. N.
The effect of the quality of resonator on the frequency of molecular generator (In English). *Radio Engineering and Electronics*, 2(4): 208-209; 1957. Also in *Radiotekhnika i Elektronika*, 2(4): 510; April, 1957 (In Russian).
Gives expressions for the effect of the quality factor of the cavity resonator on the frequency change observed in the molecular oscillator.
- [204] Prokhorov, A. M.
Molecular amplifier and generator for submillimeter waves (In English). *Soviet Physics JETP*, 34: 1140-1141; December, 1958. Also in *Zhurnal Eksperimentalnoi i Teoreticheskoi Fiziki*, 34(6): 1658-1659; June, 1958 (In Russian).
Describes an amplifier using a device in which one horn's radiation crosses a number of molecular beams and reaches a second horn. Produces a maximum power of about $1 \mu\text{w}$.
- [205] Rose-Innes, A. C.
A frequency modulated microwave spectrometer for electron resonance measurements.
Journal of Scientific Instruments, 34(7): 276-278; July, 1957.
Description of an electron resonance spectrometer in the 3-cm microwave band. With frequency modulation method it is possible to use simple equipment to record spectra, and it is suitable for measurements at low temperatures and for recording of wide lines.
- [206] Wells, W. H.
Maser oscillator with one beam through two cavities. *Journal of Applied Physics*, 29(4): 714-717; April, 1958.
A study of the two-cavity beam maser by geometrical representation of the Schrödinger equation. A possible amplifier application is also noted.
- [207] Yariv, A., Singer, J. R., and Kemp, J.
Radiation damping effects in two level maser oscillators. *Journal of Applied Physics*, 30(2): 265; February, 1959.
Derives formulas to show that a nonlinear solution best fits the case for a two-level maser in regards to explaining the spontaneous radiation of an inverted two-level spin system.

Amplifiers

- [208] Arams, F. R. and Krayner, G.
Design considerations for circulator maser systems.
PROCEEDINGS OF THE IRE, 46(5, pt. 1): 912-913; May, 1958.
Maximum-gain bandwidth can be obtained by using a circulator in conjunction with a maser, and receiver noise can be isolated. Reports on the various characteristics and the noise and stability requirements of the system.
- [209] Basov, N. G. and Prokhorov, A. M.
Theory of the molecular generator and molecular power amplifier (In English).
Soviet Physics JETP, 30: 426-429; October, 1956. Also in *Zhurnal Eksperimentalnoi i Teoreticheskoi Fiziki*, 30(3): 560-563; March, 1956. (In Russian).
The theory of a device similar to one described in [236] is presented. Also included are the conditions of self-excitation and the expressions for frequency, amplitude, and maximum power output for the oscillator, as well as the power amplification factor and the condition for linear amplification of the amplifier.
- [210] Brodzinsky, A. and Macphersén, A. C.
Maser sensitivity curves reference sheet.
Electronics, 32(8): 70; February 20, 1959.
Consists of a graph showing the relation between normalized source temperature to over-all-system sensitivity, which is useful in designing super low-noise amplifiers whose noise figures are close to unity.
- [211] Chester, P. F. and Bolef, D. I.
Superregenerative masers.
PROCEEDINGS OF THE IRE, 45(9): 1287-1289; September, 1957.
A comparison is made of the characteristics of a 2-level solid-state maser amplifier operating both intermittently and superregeneratively. A superregenerator maser is found to have the advantage of stability, range of linearity, and stringency of inversion and preparation conditions, especially at high gains.
- [212] Gordon, J. P. and White, L. D.
Noise in maser amplifiers—theory and experiments.
PROCEEDINGS OF THE IRE, 46(9): 1588-1594; September, 1958.
Presents the theory of noise as applied to either reflection or transmission type masers, using the concept of "effective input noise temperature." Experimental studies using an ammonia maser agreed well with the theory. An upper limit of 20°K can be placed on the absolute value of the beam temperature.
- [213] Helmer, J. C. and Muller, M. W.
Calculation and measurement of the noise figure of a maser amplifier.
IRE TRANSACTIONS ON MICROWAVE THEORY AND TECHNIQUES, MTT-6(2): 210-214; April, 1958.
Review of noise performance of regenerative amplifiers. Equations were set up to interpret measurement of noise from an ammonia molecular beam maser amplifier. The measurements were made by using a double heterodyne system with a detuned maser oscillator serving as a second local oscillator.
- [214] Motz, H.
Negative-temperature reservoir amplifiers.
Journal of Electronics, 2(6): 571-578; May, 1957.
Principles of maser operation are discussed theoretically with application to conditions for oscillation in a cavity and for amplification in a transmission line.
- [215] Muller, M. W.
Noise in a molecular amplifier.
Physical Review, 106(1): 8-12; April, 1 1957.
A discussion of the extension of the quantum theory of noise to systems not in thermal equilibrium with application to masers. It predicts a correction to the noise figure usually associated with the spontaneous emission from molecules of the active medium.
- [216] Pound, R. V.
Spontaneous emission and the noise figure of a maser amplifier.
Annals of Physics, 1(1): 24-32; January, 1957.
Points out some factors affecting noise figures in various maser devices and presents the application and use of a wire-circuit model for consideration.
- [217] Shimoda, K., Takahasi, H., and Townes, C. H.
Fluctuations in amplification of quanta with application to maser amplifiers.
Journal of the Physical Society of Japan, 12: 686-700; June, 1957 (In English).
Develops expressions for the probability distribution of quanta for the average values, also for fractional fluctuations and applied to maser-type amplifiers.
- [218] Siegman, A. E.
Gain bandwidth and noise in maser amplifiers.
PROCEEDINGS OF THE IRE, 45(12): 1737-1738; December 1957.
A comparison of two types of masers (circulator and two-port) with respect to gain-bandwidth product and noise figure.
- [219] Smith, W. V.
Microwave amplification by maser techniques.
IBM Journal, 1(3): 232-238; July, 1957.
An elementary analysis has been made of the maser operation with its potentiality for broad-band, short-transit-time amplification.
- [220] Stitch, M. L.
Maser amplifier characteristics for one and two iris cavities.
1957 IRE WESCON CONVENTION RECORD, (pt. 3): 175-181.
Discusses noise figure, gain modulation and bandwidth characteristics of both one- and two-iris cavities in a maser amplifier. Noise temperature is also included.
- [221] Stitch, M. L.
Maser amplifier characteristics for transmission and reflection cavities.
Journal of Applied Physics, 29(5): 782-789; May, 1958.
An analysis and a comparison are made of noise-temperature, bandwidth, and gain-modulation characteristics for a transmission and a reflection maser. It is concluded that the reflection maser is generally superior but is also limited by a lack of good circulators.
- [222] Strandberg, M. W. P.
Quantum-mechanical amplifiers.
PROCEEDINGS OF THE IRE, 45(1): 92-93; January, 1957.
A discussion of possible alternatives to the molecular-beam amplifier such as systems involving interaction between protons or electron spins and magnetic fields. Also, it should be possible to obtain noise-free amplifiers at any frequencies.
- [223] Weber, J.
Maser noise considerations.
Physical Review, 108(3): 537-541; November 1, 1957.
The calculations are given for a noise figure in a three-level maser and are shown to be little affected by the saturation field. Some aspects of spontaneous emission noise are discussed.

Gaseous Types

- [224] Alsop, L. E., Giordmaine, J. A., Townes, C. H., and Wang, T. C.
Measurement of noise in a maser amplifier.
Physical Review, 107(5): 1450-1451; September, 1957.
Results of an experiment using an ammonia beam through a split cavity. A comparison has been made between theory and actual results for several ratios of loaded Q and cavity Q . A footnote gives the early history of maser amplification.
- [225] Atom amplifier demonstrates unilateral gain.
Electrical Manufacturing, 62(2): 11; August, 1958.
News item and photograph of the Philco Corporation's ammonia beam maser. No details of operation are given.
- [226] Atomic amplifier; gas maser.
Journal of the Franklin Institute, 266(2): 153; August, 1958.
Brief report on the Philco Company maser, which uses an ammonia beam and two electrically isolated cavities.
- [227] Bonanomi, J., et al.
Améliorations d'un maser à NH_3 .
Helvetica Physica Acta, 30(6): 492-494; 1957.
Abstract unavailable.
- [228] Bonanomi, J., et al.
Maser à NH_3 ; expériences résultats, applications (In French).
Archives des Sciences, 10: 187-193; 1957.
Abstract unavailable.
- [229] Bonanomi, J., De Prins, J., Herrmann, J., and Kartaschoff, P.
High resolution microwave spectrograph (In German).

- Helvetica Physica Acta*, 30(4): 290–292; August 15, 1957.
Abstract unavailable.
- [230] Bonanomi, J., et al.
Stability of NH_3 frequency standards (In French).
Helvetica Physica Acta, 30(4): 288–290; August 15, 1957.
A report of an experiment to attempt to eliminate the effects of pulling of the molecular oscillator by obtaining a frequency independent of the cavity dimensions.
- [231] Bonanomi, J., Herrmann, J., De Prins, J., and Kartaschoff, P.
Twin cavity for NH_3 masers.
Review of Scientific Instruments, 28(11): 879–881; November, 1957.
A description of a system of two coupled cavities has been given. Using this system it has been found that the curve of oscillator frequency against cavity temperature is a plateau, and the “pulling” effect of the cavity has thus been reduced.
- [232] “Cathode Ray,” pseudonym.
Masers—small scale atomic energy for radio.
Wireless World, 65(4): 197–200; April, 1959.
Presents the basic principles of gaseous masers and atomic clocks.
- [233] Develop portable maser stable to one part in 10^9 .
Machine Design, 30(9): 34–35; May 1, 1958.
Gives a brief description of an ammonia-maser oscillator capable of operating 500 hours without interruption. The ammonia is recirculated to the reservoir after 50 hours of operation, eliminating the need for auxiliary pumping equipment.
- [234] Gordon, J. P. and White, L. D.
Experimental determination of the noise figure of an ammonia maser.
Physical Review, 107(6): 1728–1729; September 15, 1957.
Results of an experiment for noise measurement using two masers have been given and compared with the predicted values.
- [235] Gordon, J. P., Zeiger, H. J., and Townes, C. H.
Maser—new type of microwave amplifier frequency standard and spectrometer.
Physical Review, 99(4): 1264–1274; August 15, 1955.
Experimental results of using a microwave amplifier as a high-resolution microwave spectrometer are compared with the theoretical predictions. The use with ammonia molecules is especially noted. Under certain conditions, an amplifier noise figure of unity should be possible.
- [236] Gordon, J. P., Zeiger, H. J., and Townes, C. H.
Molecular microwave oscillator and new hyperfine structure in the microwave spectrum of NH_3 .
Physical Review, 95(1): 282–284; July 1, 1954.
A microwave amplifier or a stable oscillator has been made which can be used as a high-resolution microwave spectrometer. By directing a focused beam of NH_3 molecules into high- Q oscillating cavity, the molecules within gave up energy. By varying the frequency transmitted through the cavity through the molecular transition frequency, an emission line is seen.
- [237] Helmer, J. C.
Maser noise measurement.
Physical Review, 107(3): 902–903; August 1, 1957.
 3.52 ± 5 db has been found to be the average noise figure of an ammonia-beam-maser amplifier using an ammonia-beam oscillator as a primary frequency standard. Operation was at 24,000 mc.
- [238] Higa, W. H.
Observations of nonlinear maser phenomena.
Review of Scientific Instruments, 28(9): 726–727; September, 1957.
Gives results of an experiment using a double-cavity ammonia maser, in which the cavities produce a beat phenomenon by oscillating individually. It shows that the maser can continue to amplify signals even in the oscillatory state.
- [239] Javan, A. and Wang, T. C.
Two-cavity maser spectrometer.
Bulletin of the American Physical Society, 2(4): 209; April 25, 1957.
Discusses an ammonia-type maser developed for this purpose. Only an abstract is given.
- [240] Johnson, S.
Regulated molecular beam.
Review of Scientific Instruments, 28(7): 575; July, 1957.
A brief description of an apparatus for regulating the beam flux in an ammonia maser.
- [241] King, J. G. and Zacharias, J. R.
Some new applications and techniques of molecular beams.
Advances in Electronics and Electron Physics, 8: 1–88; 1956.
Ammonia masers are discussed briefly on p. 4.
- [242] Maser supports relativity theory.
Electronics, 31(49): 104; December 5, 1958.
Briefly summarizes an experiment using an ammonia-type maser to determine what effect on frequency occurs when the stream of molecules travel in the same direction as the earth in its orbit as compared to traveling in the opposite direction. Einstein's special theory of relativity was confirmed by the work.
- [243] Munster, A. C.
Atomic amplifier; gas maser.
Journal of the Franklin Institute, 266(2): 153; August, 1958.
The ammonia maser developed by the Philco Corporation is briefly described. No details are given.
- [244] Prokhorov, A. M.
Molecular amplifier and generator for submillimeter waves (In English).
Soviet Physics JETP, 34: 1140–1141; December, 1958. Also in *Zhurnal Eksperimentalnoi i Teoreticheskoi Fiziki*, 34(6): 1658–1659; June, 1958 (In Russian).
Gives expressions for the power, and for the conditions of self-excitation, of an ammonia maser for waves shorter than 1 mm.
- [245] “Quantum,” pseudonym.
Molecules and microwaves; maser explained.
Electronic and Radio Engineering, 34(7): 254–257; July, 1957.
A review of the basic principles of the ammonia-type maser.
- [246] Sher, N.
A two-cavity unilateral maser amplifier.
1958 IRE NATIONAL CONVENTION RECORD, (pt. 1): 27–35.
Following a discussion of the physical principles of an ammonia-type maser having two separated resonant cavities, the experimental results obtained are described. Results of gain and noise figure measurements are reported.
- [247] Shimoda, K.
Characteristics of the beam type maser. I (In English).
Journal of the Physical Society of Japan, 12(9): 1006–1016; September, 1957.
Considers causes for velocity distribution of molecules in the maser. Relationship of amplitude to focusing voltage, as well as to frequency characteristics, are in good agreement with theory. Frequency shift caused by the unresolved hyperfine structure is discussed.
- [248] Shimoda, K. and Wang, T. C.
New method for the observation of hyperfine structure of NH_3 in a “maser” oscillator.
Review of Scientific Instruments, 26(12): 1148–1149; December, 1955.
Discusses the use of a maser as a spectrometer to resolve magnetic hyperfine components in NH_3 , using microwave power at frequencies of the satellite lines. An oscilloscope trace shows the structure of the weakest of the satellites.
- [249] Shimoda, K.
Precise frequency of the 3,3 inversion line of ammonia (In English).
Journal of the Physical Society of Japan, 12(5): 558; May, 1957.
Uses a molecular beam maser oscillator to check the frequency measured on an absorption type Stark-Zeeman ammonia clock. The difference between the two frequencies is interpreted in terms of different populations of the quadrupole levels $F_1 = 2, 3, 4$.
- [250] Shimoda, K.
Radio frequency spectroscopy using three level maser action (In English).
Journal of the Physical Society of Japan, 14(7): 954–959; July, 1959.
Following a discussion of the theory involved, a description is given of a three-level radio-frequency spectrometer which was built to observe direct l-type doubling transistors of ICN and OCS. Pumping radiation was supplied by a

- klystron, and the transition was observed by a modified Pound-Knight circuit.
- [251] Shimoda, K.
Three-level maser detector for ultramicrowaves (In English). *Journal of the Physical Society of Japan*, 14(7): 966; July, 1959.
Develops expressions for the absorption of ultramicrowave power by gases. Recommends use of a cavity with a cell volume of ten cubic centimeters, which would allow the detection of 3×10^{-10} watts as compared to the detection of 10^{-6} watts by crystal detectors.
- [252] Singer, J. R.
Proposal for a tunable millimeter wave molecular oscillator and amplifier.
IRE TRANSACTIONS ON MICROWAVE THEORY AND TECHNIQUES, MTT-7(2): 268-276; April, 1959.
Describes a gas-type maser which uses a Stern-Gerlach molecular beam arrangement. The beam has a net magnetic moment. The frequency of operation is determined by the static magnetic field, with an upper limit of about 3 mm.
- [253] Townes, C. H.
Comments on frequency-pulling of maser oscillators.
Journal of Applied Physics, 28(8): 920-921; August, 1957.
Discusses the theory of molecular-velocity distribution as related to the pulling of the oscillator frequency from the molecular resonance frequency. Gives reasons for a lack of observation of increased pulling.
- [254] Troitskii, V. S.
Theory of the maser and maser fluctuations (In English). *Soviet Physics JETP*, 34: 271-273; August, 1958. Also in *Zhurnal Eksperimentalnoi i Teoreticheskoi Fiziki*, 34(2): 390-393; February, 1958 (In Russian).
Presents the maser as an oscillating system with one degree of freedom, using the Basov-Prokhorov equations for steady-state oscillations. There is found to be a "soft" mode and an analog of the "hard" mode following a region of noise generation. It is determined that in an ammonia maser at room temperature the spectral-line width due to thermal noise is 10^{-4} cps.
- [255] Vonbun, F. O.
Proposed method for tuning a maser cavity.
Review of Scientific Instruments, 29(9): 792-793; September, 1958.
Brief description of a method for tuning a cavity by modulating the frequency of the maser output, beating it against the auxiliary oscillator, and multiplying the beat note.
- Solid-State Types*
- [256] Amplifier extends range of radio telescope.
Electrical Engineering, 77(2): 191-192; February, 1958.
An amplifier (three-level solid-state maser), developed by Harvard University scientists, was successfully operated at 21 cm. The article gives a description of the apparatus and explains its application in radio astronomy, including some brief history.
- [257] Arams, F. R.
Low field X-band ruby maser.
PROCEEDINGS OF THE IRE, 47(8): 1373-1375; August, 1959.
Briefly describes operation of a unit at low magnetic fields (350 gauss) with a signal frequency of 9540 mc and pump frequency of 10,850 mc. Pump power was about 50 milliwatts.
- [258] Arams, F. R. and Okwit, S.
Tunable L-band ruby maser.
PROCEEDINGS OF THE IRE, 47(5, pt. 1): 992-993; May, 1959.
Briefly describes the performance of a maser amplifier which operates over a frequency range of at least 850 to 2000 mc, although a tuning range of at least two octaves is believed to be possible.
- [259] Artman, J. O., Bloembergen, N., and Shapiro, S.
Operation of a three-level solid-state maser at 21 cm.
Physical Review, 109(4): 1392-1393; February 15, 1958.
Gives results of the operating of a three-level solid-state maser amplifier and oscillator at 1373 mc at below 2°K .
- [260] Artman, J. O.
The solid state maser.
Proceedings of the Symposium on Role of Solid State Phenomena in Electric Circuits, Polytechnic Institute of Brooklyn, Brooklyn, N. Y., 7: 71-89; 1957.
Reviews the principles of solid-state masers, followed by a review of design problems for reflection cavity masers. Describes the operation of a model under development which is for use in the region around 1400 mc.
- [261] Autler, S. H.
Proposal for a maser-amplifier system without nonreciprocal elements.
PROCEEDINGS OF THE IRE, 46(11): 1880-1881; November, 1958.
Cavity-type solid-state masers without circulators are considered. The system is to use two matched masers and a magic T. Theoretically, the gain, noise and bandwidth would be the same as for a single maser with an ideal circulator. Actual conditions are compared with the ideal.
- [262] Autler, S. H., Kingston, R. H., McWhorter, A. L., and Meyer, J. W.
Solid state maser systems.
1958 IRE WESCON CONVENTION RECORD, (pt. 3): 28.
Gives abstract only, of report on systems operating at 300, 1400, 2800, and 9000 mc. Discusses isolation problems and noise sources.
- [263] Autler, S. H. and McAvoy, N.
21-centimeter solid-state maser.
Physical Review, 110(1): 280-271; April 1, 1958.
Results of operating a three-level solid-state maser as an amplifier at 1382 mc with saturating power supplied at 9070 mc at a power level of 28 milliwatts.
- [264] Basov, N. G., et al.
Molecular generator without using a molecular beam (In Russian).
Uspekhi Fiziki i Nauk, 59(2): 375; 1956.
Abstract unavailable.
- [265] Bergmann, S.
Three-level solid state maser.
Journal of Applied Physics, 30(1): 35-36; January, 1959.
Calculates the maximum values of the real and imaginary components of the paramagnetic susceptibility of a three-level solid-state maser. Gives expressions for the gain and bandwidth of a traveling-wave maser and compares its Q factor with that of a cavity maser.
- [266] Bleaney, B.
A new class of materials for Bloembergen-type masers.
Proceedings of the Physical Society, 73(6): 937-939; June 1, 1959.
Theorizes on the compounds suitable for this use; mentions, as most promising, the following compounds: CaF_2 , CdF_2 , SrF_2 , BaF_2 , SrCl_2 , ThO_2 , and MgO .
- [267] Bloembergen, N.
Electron spin and phonon equilibrium in masers.
Physical Review, 109(6): 2209-2210; March 15, 1958.
Points out that successful operation of $\text{KCo}(\text{Cr})(\text{CN})_8$ salt in a three-level steady-state maser is incompatible with assumption that relaxation rates are not determined by interaction between spins and the lattice vibrations regardless of operating frequencies of the maser.
- [268] Bloembergen, N.
Proposal for a new type solid state maser.
Physical Review, 104(2): 324-327; October 15, 1956.
Negative absorption or stimulated emission at microwave frequencies can be obtained by using the Overhauser effect in the spin multiplet of certain paramagnetic ions. A low-noise microwave amplifier or frequency converter may be achieved through the use of nickel fluosilicate or a low-gadolinium ethyl sulfate at liquid-helium temperature. Some discussion of the operation of a solid-state maser of this type is given.
- [269] Bolef, D. I. and Chester, P. F.
Some techniques of microwave generation and amplification using electron spin states in solids.
IRE TRANSACTIONS ON MICROWAVE THEORY AND TECHNIQUES, MTT-6(1): 47-52; January, 1958.
Describes possible operation of a two-level solid-state maser with the population-inversion techniques used in nuclear magnetic resonance. Discusses continual operation of the maser and its uses as a microwave generator.
- [270] Braunstein, R.

- Proposal for a nuclear quadrupole maser.
Physical Review, 107(4): 1195-1196; August 15, 1957.
- Suggests the use of substances having pure quadrupole spectra (such as the rare earths with atomic numbers above 50) for four-level masers. Discusses tunability, transition probabilities, elimination of external magnetic fields, etc. I_2 and its compounds may be suitable.
- [271] Butcher, P. N.
 Theory of three-level paramagnetic masers.
Proceedings of the Institution of Electrical Engineers, 105B (supplement 11): 684-711, 715; May, 1958.
 Consists of four sections devoted to quantum theory, amplification and oscillation, output noise power spectrum and noise figures. The section on amplification and oscillation contains numerical results, whereas the other sections are primarily theoretical.
- [272] Chang, W. S. C., Cromack, J., and Siegman, A. E.
 Cavity and traveling-wave masers using ruby at S-band.
 1959 IRE WESCON CONVENTION RECORD, (pt. 1): 142-150.
 Describes the operation of several three-level masers using ruby at 3000 mc, using either a high-efficiency cavity or a meander-line slow-traveling-wave circuit with low group velocity over the signal pass band. The traveling-wave type had broader bandwidth, greater stability and built-in non-reciprocity. The cavity gain-bandwidth products are two orders of magnitude larger than were achieved in early maser work.
- [273] Chester, P. F., Wagner, P. E., and Castle, J. G., Jr.
 Two-level solid-state maser.
Physical Review, 110(1): 281-282; April 1, 1958.
 Report of results using a two-level electron-spin system having paramagnetic defects introduced by neutron irradiation in quartz and magnesium oxide.
- [274] Clogston, A. M.
 Susceptibility of the three-level maser.
Journal of the Physics and Chemistry of Solids, 4(4): 271-277; 1958 (Bell Monograph 2977).
 Calculations of the susceptibility by using quantum-mechanical equations of motion, including the effect of off-diagonal components of density matrix, are presented. Effect of the cavity reaction is considered, and it appears that at high levels of pumping field the result is a saturation of susceptibility.
- [275] Combrisson, J., Honig, A., and Townes, C. H.
 Use of electron spin resonance to realize a very high frequency oscillator or amplifier (In French).
Comptes Rendus de l'Academie des Sciences (Paris), 242(20): 2451-2453; May 14, 1956.
 Induced emission in an electron resonance spectrum is used to produce a microwave oscillator or amplifier. Experimenting with silicon, it was found that the ratio of power furnished by electron emission to that required to excite the cavity was $\frac{1}{3}$. In order to obtain free oscillations, experimental details would have to be improved.
- [276] Cross, L. G.
 Silvered ruby maser cavity.
Journal of Applied Physics, 30(9): 1459; September, 1959.
 Describes the techniques of silvering rectangular pieces of ruby which have been cut and ground to the desired cavity dimensions. Advantages are lower preparation costs, greater stability of operation, a less lossy cavity, and freedom of interchange.
- [277] Crystals for masers.
Wireless World, 64(7): 330; July, 1958.
 Brief report on development, at the Royal Radar Establishment (Great Britain), of crystals for a solid-state maser. Gadolinium ethyl sulphate and potassium chromicyanide in a high degree of solution as a solid solution in alum are the chief substances used. Preparation techniques are summarized.
- [278] Davis, C. F., Strandberg, M. W. P., and Kyhl, R. L.
 Solid-state masers and spin-lattice relaxation times.
Bulletin of the American Physical Society, 3(1): 9; January 29, 1958.
 Abstract of a paper given at the annual American Physical Society Meeting, January 29-February 1, 1958. An analysis of operational properties of solid-state masers shows spin-lattice relaxation to have an important part in these devices.
- [279] De Grasse, R. W.
 Slow-wave structures for unilateral solid-state maser amplifiers.
 1958 IRE WESCON CONVENTION RECORD, (pt. 3): 29-35.
 Possible slow-wave propagating structures for traveling-wave masers are discussed, followed by results of using a "comb" type structure. Pink ruby was used for the active maser material and dark ruby for the lossy material. The bandwidth was 25 mc, which could be tuned over a 350-mc range, centered at 5.9 kmc.
- [280] De Grasse, R. W., Schulz-DuBois, E. O., and Scovil, H. E. D.
 The three level solid state traveling wave maser.
Bell System Technical Journal, 38(2): 305-334; March, 1959.
 Develops the theory for this type of maser, then compares its performance with that of cavity-type masers. A traveling-wave maser having a ruby-loaded comb structure was tested, giving a gain of 23 db at 6 kmc with a bandwidth of 25 mc. Performance characteristics of another maser, using gadolinium ethyl sulfate, are given.
- [281] Ditchfield, C. R. and Forrester, P. A.
 Maser action in the region of 60°K.
Physical Review Letters, 1(12): 448-449; December 15, 1958.
 Operational characteristics of a three-level solid-state maser in the range 9280 to 9520 mc. Freedom from use of liquid helium is seen to be likely.
- [282] Fain, V. M.
 Spontaneous radiation of a paramagnetic in a magnetic field (In English).
Soviet Physics JETP, 34: 714-715; 1958. Also in *Zhurnal Eksperimentalnoi i Teoreticheskoi Fiziki*, 34(4): 1032-1033; April, 1958 (In Russian).
 Develops expressions for average power and intensity of radiation from a paramagnetic material at nearly 0°K.
- [283] Foner, S., Momo, L. R., and Mayer, A.
 Multilevel pulsed-field maser for generation of high frequencies.
Physical Review Letters, 3(1): 36-38; July 1, 1959.
 Reports of the operation of a ruby maser, which successfully generates or amplifies at both 12.61 kmc and 19.15 kmc on a pulsed basis, 4.2°K. A peak field of 9.4 kilooersteds was obtained of 1000 volts with a half-period of about three milliseconds.
- [284] Forward, R. L., Goodwin, F. E., and Kiefer, J. E.
 Application of a solid state ruby maser to an X-band radar system.
 1959 IRE WESCON CONVENTION RECORD, (pt. 1): 119-125.
 Special attention is given to a description of a low-loss ferrite TR switch that was developed to reduce leak-through from the transmitted pulse. The combined noise temperature was 65°K for the maser, circulator, mixer and IF amplifier combined, while the figure for the over-all receiver was 173°K. Improvement in the detecting range is considered, as well as antenna noise temperature.
- [285] From, W.
 The maser.
Microwave Journal, 1(3): 18-25; November-December, 1958.
 Traces development of solid-state masers and explains their operation in some detail. Methods of designing such devices are discussed, as well as possible applications.
- [286] Giordmaine, J. A., Alsop, L. E., Mayer, C. H., and Townes, C. H.
 A maser amplifier for radio astronomy at X-band.
 PROCEEDINGS OF THE IRE, 47(6): 1062-1069; June, 1959.
 This radiometer, using a ruby maser, operates with a bandwidth of 5.5 mc at an input noise temperature, including background radiation into the antenna, of approximately 85°K. Sensitivity factors are discussed.
- [287] Giordmaine, J. A., Alsop, L. E., Nash, F. R., and Townes, C. H.
 Paramagnetic relaxation at very low temperatures.
Physical Review, 109(2): 302-311; January 15, 1958.
 A series of experiments using paramagnetic resonance at microwave frequencies and in the 1°-4°K temperature range. Implications of the relaxation process for masers are presented on pp. 310-311.
- [288] Gold, T.
 Range of radio telescopes extended by new amplifier: maser.
Journal of the Franklin Institute, 265(1): 83-84; January, 1958.

Briefly reviews operating features of a solid-state maser developed by Harvard University to be used in their radio telescope. The maser uses a single crystal of potassium cobalticyanide, kept at a temperature of 2°K, and it operates in the 21-cm band.

- [289] Heffner, H.
Maximum efficiency of the solid-state maser.
PROCEEDINGS OF THE IRE, 45(9): 1289; September, 1957.
Gives an estimation of the efficiency of a three-state maser for operation at saturation.
- [290] Herold, E. W.
Future circuit aspects of solid-state phenomena.
Proceedings of the Symposium on the Role of Solid-State Phenomena in Electric Circuits, Polytechnic Institute of Brooklyn, Brooklyn, N. Y., 7: 3-31; 1957. Also in PROCEEDINGS OF THE IRE, 45(11): 1463-1474; November, 1957.
A discussion of superconductivity, molecular amplification, magnetic effects in semiconductors and nonlinear capacitance in junctions. Specific information on solid-state masers is also given.
- [291] Howarth, D. J.
The physics of the solid-state maser.
IRE TRANSACTIONS ON COMPONENT PARTS, CP-6(2): 81-93; June, 1959. (Reprinted from *Royal Radar Establishment Journal*, April, 1958).
Discusses the theory of the three-level solid-state maser, using a quantum mechanical description.
- [292] Itoh, J.
Proposal for a solid state radio-frequency maser (In English).
Journal of the Physical Society of Japan, 12(9): 1053; September, 1957.
The four levels into which a nuclei with spin 3/2 will split in a magnetic field when strong axially symmetrical nuclear quadrupole interaction exists in a single crystal are analyzed for suitability for maser operations at radio frequencies.
- [293] Javan, A.
Description of a Raman type two-level maser.
Bulletin of the American Physical Society, 3(3): 213; May 1 1958.
Abstract of a paper presented at the spring meeting of the American Physical Society, May 1-3, 1958. Treats the case in which two photons are present, having a frequency difference close to the energy separation of the two levels. Amplification at the lower frequency takes place. Noise figures, magnetic susceptibility, and applications to ferrites are also discussed.
- [294] Javan, A.
Theory of a three-level maser.
Physical Review, 107(6): 1579-1589; September 15, 1957.
Develops a theory which covers the discrepancies between a semiclassical treatment based on population differences of various levels and actual effects deduced from a detailed analysis of the subject. Theory covers a gaseous system as well as two cases of paramagnetic materials. Four-level masers are also discussed.
- [295] Kikuchi, C., Lambe, J., Makhov, G., and Terhune, R. W.
Ruby as a maser material.
Journal of Applied Physics, 30(7): 1061-1067; July, 1959.
Outlines the reasons for the original choice of ruby. Gives some measurements of the parameters in the spin Hamiltonian and of spin relaxation times. Discusses the relative advantages of single- and double-pump modes of operation of a four-level maser and gives measurements of the oscillator power.
- [296] Kingston, R. H. K.
A UHF solid-state maser.
PROCEEDINGS OF THE IRE, 46(5, pt. 1): 916; May, 1958.
A new type of maser has been built using a pump-frequency circuit as a resonant cavity and a signal-frequency circuit of the lumped-constant type. This gives independent turning ranges and makes full use of the whole volume of the crystal.
- [297] Kingston, R. H. K.
A UHF solid-state maser.
IRE TRANSACTIONS ON MICROWAVE THEORY AND TECHNIQUES, MTT-7(1): 92-94; January, 1959.
Describes a maser operating in the frequency range of 300 to 500 mc. It uses chromium-doped cobalticyanide, a cavity mode at the pumping frequency, and a tuned loop at the operating frequency, thus avoiding previous design complications.
- [298] Lax, B. and Gatos, H. C.
The remarkable "Maser" story.
Technology Review, 61(7): 360, 374; May, 1959.
Describes briefly the UHF solid-state maser developed by M.I.T. for use in their radar apparatus which contacted the planet Venus. General advantages and future possibilities are mentioned.
- [299] Llewellyn, P. M.
A solid-state paramagnetic-resonance spectrometer.
Journal of Scientific Instruments, 34(6): 236-239; June, 1957.
A description of a sensitive instrument for use in the frequency range 9000-10,000 mc at various temperatures down to 14°K.
- [300] McWhorter, A. L., Meyer, J. W., and Strum, P. D.
Noise figure measurement on a solid state maser.
Proceedings of the National Electronics Conference, 13: 377-384; 1957.
The noise temperature is found not to exceed 2+°K in a three-level solid-state maser using $K_3Cr(CN)_6$ as a paramagnetic salt and amplifying at 2800 mc. Description of materials, apparatus, and amplifier characteristics are given. Figures refer to maser only, not to the entire system.
- [301] McWhorter, A. L., Meyer, J. W., and Strum, P. D.
Noise temperature measurement on a solid state maser.
Physical Review, 108(6): 1642-1644; December 15, 1957.
Noise temperature for a three-level maser with an upper limit of 20°K was measured by comparison with an argon discharge noise tube using a Dicke radiometer method. Results are reported.
- [302] McWhorter, A. L. and Meyer, J. W.
A solid state maser amplifier.
Physical Review, 109(2): 312-318; January, 1958.
Description of operation at 2800 mc using a dual-frequency cavity at 1.25°K. Theory and experimental observations of the maser have been compared as both an amplifier and an oscillator.
- [303] McWhorter, A. L. and Arams, F. R.
System-noise measurement of a solid-state maser.
PROCEEDINGS OF THE IRE, 46(5, pt. 1): 913-914; May, 1958.
An amplifier system has been built with a low-loss S-band circulator and a solid-state maser. The paper discusses the method used to measure noise and the sources of noise in the system.
- [304] Makhov, G., Kikuchi, C., Lambe, J., and Terhune, R. W.
Maser action in ruby.
Physical Review, 109(4): 1399-1400; February 15, 1958.
A brief report of investigations of electron-spin resonance properties of ruby, in a three-level maser operating at 2°K. A net gain of 20 db was observed.
- [305] Malvern maser.
Engineering, 185(4812): 699; May 30, 1958.
A brief description of the Royal Radar Establishment's maser, which uses a paramagnetic salt. Methods used for the growth of crystals are also discussed.
- [306] Maser amplifier brings Venus ten times closer.
Radio Electronics, 29(6): 68; June, 1958.
A brief announcement about the synthetic ruby maser developed by Columbia University for the Naval Research Laboratory radio telescope.
- [307] Maser development offers wider uses.
Aviation Week, 66(18): 37; May 6, 1957.
A news item with description of garnet maser under development by Bell Telephone Laboratories and Harvard University, as created by H. Suhl and C. L. Hogan.
- [308] Maser operates at 2 degrees K for radio telescope.
Electronics, 31(4): 30; January 24, 1958.
Brief report of further development of a maser at Harvard University for use in a radio telescope—a three-level solid-state maser operating at 21 cm.
- [309] Masers probe outer space.
Electronics, 31(1): 12, 14; January 3, 1958.
Report of successful operation of a three-level solid-state maser at Harvard University at 21-cm waveband length

- Points out possible applications and gives a general description of its operation.
- [310] Meyer, J. W.
The solid-state maser—a supercooled amplifier.
Electronics, 31(17): 66–71; April 25, 1958.
A basic article presenting history, description, characteristics, etc., of the two-level molecular maser (gaseous) and the three-level solid-state maser, with a few words about future possibilities.
- [311] Microwave unit may improve radar.
Aviation Week, 66(7): 67; February 18, 1957.
Brief account of a new type of solid-state microwave device (maser) with extremely low noise level that has been developed at Bell Telephone Laboratories.
- [312] Morris, R. J., Kyhl, R. L., and Strandberg, M. W. P.
A tunable maser amplifier with large bandwidth.
PROCEEDINGS OF THE IRE, 47(1): 80–81; January, 1959.
Describes an X-band maser which uses a ruby crystal. It has a 20-mc bandwidth at 10 db gain, and can be tuned from 8400 to 9700 mc.
- [313] New atomic amplifiers developed.
Westinghouse Engineer, 18(5): 146–147; September, 1958.
Brief description and illustration of the Westinghouse Research Laboratories' two-level solid-state maser, which uses a quartz crystal operating at 4.2°K.
- [314] New solid-state oscillator for microwaves.
Bell Laboratories Record, 35(3): 109; March, 1957.
Announcement of successful operation of a new solid-state device which was developed by D. Scovil, G. Feher, and H. Seidel (of the Laboratories). It can be operated as an oscillator as well as an amplifier and is based on the maser principle.
- [315] Range of radio telescope extended by new amplifier.
Journal of the Franklin Institute, 265(1): 83–84; January, 1958.
New (3-level) maser amplifier developed by Harvard University has been successfully operated. Potentialities include certain radar systems as well as radio astronomy.
- [316] Research yields new solid-state oscillator for microwaves.
Industrial Science and Engineering, 4(3): 62, 64, 65; 1957.
Abstract unavailable.
- [317] Rodrigue, G. P.
Microwave properties and applications of garnet materials.
1957 IRE WESCON CONVENTION RECORD, (pt. 3): 182–200.
A summary of known microwave properties of new garnet materials and a comparison with more conventional ferrites is presented. To help explain operation of some of the new devices, recent theories are outlined and possible applications are given.
- [318] Ruby maser.
Journal of the Franklin Institute, 226(5): 423–424; November, 1958.
The University of Michigan's ruby maser is briefly described.
- [319] Ruby maser for new telescope.
Electronics, 31(36): 23; September 5, 1958.
Brief report of advantages afforded the University of Michigan radio telescope by a ruby maser.
- [320] Schulz-DuBois, E. O., Scovil, H. E. D., and DeGrasse, R. W.
Use of active material in three-level solid state masers.
Bell System Technical Journal, 38(2): 335–362; March, 1959.
Presents experimental data for two typical paramagnetic salts used as active materials, which make use of favorable ratios of signal-to-idler relaxation time. Properties of practical isolator materials are surveyed, including high-concentration paramagnetic and polycrystalline ferrimagnetic materials.
- [321] Scovil, H. E. D., Feher, G., and Seidel, H.
Operation of a solid state maser.
Physical Review, 105(2): 762–763; January 15, 1957.
A detailed description of the operation at 9 kmc of a maser oscillator using gadolinium ethyl sulfate at liquid-helium temperature.
- [322] Scovil, H. E. D. and Schulz-DuBois, E. O.
Three-level masers as heat engines.
Physical Review Letters, 2(6): 262–263; March 15, 1959.
Develops expressions for the maser efficiency as a heat engine and shows it to be limited by the same factors as a Carnot engine. Generation of microwaves by thermal excitation at two temperatures seems experimentally probable. Heat is seen excluded as a source of energy for parametric amplification.
- [323] Scovil, H. E. D.
A three-level solid-state maser.
Bell Laboratories Record, 36(7): 242–246; July, 1958.
Presents a brief history of the maser and a description, including characteristics, of low thermal noise and energy levels and giving a mechanical analogy.
- [324] Scovil, H. E. D.
The three-level solid-state maser.
IRE TRANSACTIONS ON MICROWAVE THEORY AND TECHNIQUES, MTT-6(1): 29–38; January, 1958. (Bell Monograph 3001).
An introduction to maser-amplification techniques with the emphasis on the three-level solid-state type. Presents the physical properties of paramagnetic salts, basis of the three-level excitation method, and some design considerations.
- [325] Senitzky, I. R.
Behavior of a two-level solid state maser.
Physical Review Letters, 1(5): 167–168; September 1, 1958.
Explains the amplitude modulation observed in certain masers, such that the behavior can be expressed by a system of coupled equations, one for the spin and one for the field, with energy transfers taking place between the two degrees of freedom. Observations bear out the theory.
- [326] A solid-state maser oscillator.
IRE STUDENT QUARTERLY, 3(4): 22–23; May, 1957.
A news items giving a brief history and a description.
- [327] Solid state oscillator for microwave frequencies.
Engineer, 203(5276): 389; March 8, 1957.
Describes an experimental maser amplifier using gadolinium ethyl sulphate, which is an ionically bound paramagnetic salt, as the active agent.
- [328] Strandberg, M. W. P.
Computation of noise figure for quantum-mechanical amplifiers.
Physical Review, 107(6): 1483–1484; September 15, 1957.
A noise-figure expression is derived in terms of physical quantities describing electromagnetic structure and paramagnetic salts.
- [329] Strandberg, M. W. P.
Gyratron—a new solid-state quantum-mechanical amplifier.
Bulletin of the American Physical Society, 2(1): 36; January 30, 1957.
Abstract of a paper presented at the annual American Physical Society Meeting, January 30–February 2, 1957; describes possible operating characteristics of a new device called the gyratron, and its uses.
- [330] Strandberg, M. W. P.
Inherent noise of quantum-mechanical amplifiers.
Physical Review, 106(4): 617–620; May 15, 1957.
Gives a derivation of noise figure on limiting sensitivity for quantum-mechanical amplifiers of either traveling-wave or resonant-cavity design.
- [331] Strandberg, M. W. P., Davis, C. F., Faughnan, B. W., Kyhl, R. L., and Wolga, G. J.
Operation of a solid-state quantum-mechanical amplifier.
Physical Review, 109(6): 1988–1989; March 15, 1958.
The S-band amplifier was operated at 4.2°K with a computed noise temperature of less than 4.5°K. Comparison is made with a similar device.
- [332] Strandberg, M. W. P.
The Versitron—a new solid-state quantum mechanical amplifier.
Proceedings of the Symposium on the Role of Solid-State Phenomena in Electric Circuits, Polytechnic Institute of Brooklyn, Brooklyn, N. Y., 7: 63–70; 1957.
Discusses basic principles and features of a solid-state maser amplifier. Emphasizes noise figures and noise-temperature properties of the device.
- [333] Tenney, H. D., Roberts, R. W., and Vartanian, P. H.
An S-band traveling wave maser.
1959 IRE WESCON CONVENTION RECORD, (pt. 1): 151–155.
Discusses several slow wave structures of wide-band travel-

ing wave masers, operating at 3 mc. Both garnet and pink ruby were used. Gains in excess of 15 db over a bandwidth of 60 mc were achieved. The garnet slab provided non-reciprocal reverse loss and also smoothed out the gain fluctuation of the maser due to regeneration and degeneration.

- [334] Theissing, H. H., Dieter, F. A., and Caplan, P. J.
Analysis of the emissive phase of a pulsed maser.
Journal of Applied Physics, 29(12): 1673-1678; December, 1958. Also in 1958 IRE NATIONAL CONVENTION RECORD, (pt. 1): 19-26.
A pulsed solid-state maser's operation in the emissive phase is discussed, and it is shown that equations for this phase are amenable to machine computation. Gives numerical results for various values of such variables as relaxation times, input fields and oscillation characteristics. An interpretation is given with regard to both regeneration and superregeneration modes of operation.
- [335] Weber, J.
Masers.
Reviews of Modern Physics, 31(3): 681-710; July, 1959.
Reviews the principles of the solid-state maser, then discusses specific types of masers, including ruby masers. Noise performance is described, followed by a brief discussion of masers at low frequencies and in infrared. There are nine pages of matrix elements and energy levels for ruby.
- [336] Weintraub, S.
A new microwave amplifier.
Nature, 179(4566): 903; May, 1957. Also in *Wireless World*, 63(5): 212; May 4, 1957.
Gives a brief review and description of the first successful operation of a solid-state maser.
- [337] Wessel, G. K.
A UHF ruby maser.
PROCEEDINGS OF THE IRE, 47(4): 590; April, 1959.
A tunable maser operates over the signal frequency range of 380-450 mc. A gain of 15 db and a bandwidth of 100 kc were observed at 1.7°K. Acting as an oscillator, the power output was less than 1 μ w.
- [338] Zverev, G. M., Kornienko, L. S., Manenkov, A. A., and Prokhorov, A. M.
A chromium corundum paramagnetic amplifier and generator (In English).
Soviet Physics JETP, 34: 1141-1142; 1958. Also in *Zhurnal Eksperimentalnoi i Teoreticheskoi Fiziki* 34(6): 1660-1661; June, 1958 (In Russian).
Describes certain basic design criteria for a solid-state maser. At approximately 2°K, the system became self-excited and acted as a generator.

Optical, Radio-Frequency and Infrared Types

- [339] Barker, W. A.
Raser: new solid amplifier reported.
Electronics, 32(18): 25; May 1, 1959.
A brief announcement of the commencement of a project to develop a solid-state quantum-mechanical amplifier operating in the radio-frequency range. It depends upon induced nuclear-spin transitions.
- [340] Javan, A.
Possibility of production of negative temperature in gas discharges.
Physical Review Letters, 3(2): 87-89; July 15, 1959.
Theorizes upon the conditions most suitable for the operation of an optical maser. The differences between pure gases and gas mixtures are developed. Gases considered include neon, helium, and a mixture of krypton and mercury.
- [341] Sanders, J. H.
Optical maser design.
Physical Review Letters, 3(2): 86-87; July 15, 1959.
Discusses the problems involved in an optical maser. Suggests the use of a discharge in the working medium. Recommends the use of a Fabry-Perot etalon for the detection of the maser oscillations.
- [342] Schawlow, A. L. and Townes, C. H.
Infrared and optical masers.
Physical Review, 112(6): 1940-1949; December 15, 1958.
Discusses the application of maser techniques to the optical and infrared regions. Shows that a resonant cavity of centimeter dimensions, and pumping with incoherent light, would result in maser oscillations. Suggests use of both multimode and single-mode cavities. Discusses a system using potassium vapor. The ultraviolet region is considered the shortest usable wavelength.

Atomic Clocks

- [343] Arditi, M. and Carver, T. R.
Atomic clock for space travelers' use.
Electrical Engineering, 77(6): 571; June, 1958.
A summary of a paper presented at the 1958 IRE Convention entitled "Gas cell 'atomic clock' using optical pumping and optical detection." For abstract, see [345].
- [344] Arditi, M. and Carver, T. R.
Frequency shift of the zero-field hyperfine splitting of Cs^{133} produced by various buffer gases.
Physical Review, 112(2): 449; October 15, 1958.
Use optical pumping and optical detection in studying the effects of various noble buffer gases upon the frequency shift in Cs^{133} , using equipment previously described (see [346]), following a suggestion by Dicke for an atomic sodium clock employing buffer gas reduction of the Doppler width.
- [345] Arditi, M. and Carver, T. R.
A gas cell "atomic clock" using optical pumping and optical detection.
1958 IRE NATIONAL CONVENTION RECORD, (pt. 1): 3-9.
Describes the theory and operation of cesium-cell and sodium-cell frequency standards, which use polarized resonance light in order to increase the population difference between the energy levels. A frequency stable to one part in 10^{10} is anticipated.
- [346] Arditi, M. and Carver, T. R.
Optical detection of zero-field hyperfine splitting of Na^{23} .
Physical Review, 109(3): 1012-1013; February 1, 1958.
Describes optical detection system; gives value of the hyperfine splitting of Na^{23} in the ground state, which is slightly lower than the value given by atomic beam measurements. Effects of buffer gas pressure in shifting the hyperfine frequency are described.
- [347] Beck, A. H. W. and Lytollis, J.
Construction of a mobile caesium frequency standard.
Proceedings of the Institution of Electrical Engineers, 105B (supplement 11): 712-715; May, 1958.
(See also [377] below).
The circuitry and illustrations of the frequency standard are coupled with a description of the components of the system, such as the cesium oven, the magnets, paddle tuners, connectors, etc. In the discussion which follows, comments are made on the relation of noise and populations of states in two-level and three-level masers.
- [348] Bell, W. E., Bloom, A., and Williams, R.
A microwave frequency standard employing optically pumped sodium vapor.
IRE TRANSACTIONS ON MICROWAVE THEORY AND TECHNIQUES, MTT-7(1): 95-98; January, 1959.
Describes construction details of the system. Light from a sodium lamp is used to produce population difference between the two quantum levels. Predicts that an accuracy of one part in 10^{10} can be achieved.
- [349] Bonanomi, J. and Herrmann, J.
Ammonia frequency standard.
Helvetica Physica Acta, 29: 224-226; 1956.
Describes equipment which operates at 23,870 mc with a variation of 2×10^{-9} per day. To improve the stability, a maser is introduced.
- [350] Bonanomi, J. and Herrmann, J.
Determination of the inversion frequency of ammonia.
Helvetica Physica Acta, 29: 451-452; 1956.
Uses a maser-type device to arrive at a frequency of 23,870,129.42 \pm 0.05 \pm 0.12 kc.
- [351] Clock produces microwaves direct; varies one second in 300 years.
Chemical and Engineering News, 33(6): 502, 504; February 7, 1955.
A news item describing the ammonia-type clock.

- [352] Dicke, R. H.
Collision reduced Doppler effect. A sodium clock?
1955 IRE CONVENTION RECORD, (pt. 10): 181.
Gives only an abstract of a paper which discussed reduction of the Doppler effect by adding a helium atmosphere to the alkali metal vapor. Optical pumping and techniques for coherent pulse-induced radiations were mentioned in original paper.
- [353] Essen, L.
Atomic clocks.
Journal of the Institution of Electrical Engineers, 4(48): 647-653; December, 1958.
Describes the operation and advantages of a cesium-type atomic clock. Also discusses quartz-clock calibration, variations in mean solar time, and masers. A review is made of the comparison of the British and U. S. atomic frequency standards.
- [354] George, W. D.
Need for a new type frequency and time standard.
PROCEEDINGS OF THE IRE, 42(9): 1349; September, 1954.
Points out the problems in definitions and operational standards currently used for time and frequency. Because, at the present time, the appropriate standard is the period of a molecular, atomic, or nuclear vibration, several atomic clocks should be built and observed in an effort to obtain correlation to at least one part in 10^9 .
- [355] Ince, C. R. S.
Atomic clocks and frequency stabilization.
Journal of Applied Physics, 23(12): 1408-1409; December, 1952.
Some corrections are made for the paper by Townes (see [369]).
- [356] Lewis, F. D.
Frequency and time standards.
PROCEEDINGS OF THE IRE, 43(9): 1046-1068; September, 1955.
Various frequency and time standards are described. Included also is a discussion of atomic and molecular frequency standards such as the ammonia maser.
- [357] Lyons, H.
Atomic clocks.
Scientific American, 196(2): 71-82; February, 1957.
A discussion and general description of the atomic, cesium and maser clocks.
- [358] McCoubrey, A. O.
The Atomichron—an atomic-frequency standard—physical foundation.
1958 IRE NATIONAL CONVENTION RECORD, (pt. 1): 10-13.
Presents the theory of an atomic-frequency standard, particularly the operation of atomic-beam resonance tubes.
- [359] McCoubrey, A. O.
Results of the comparison: Atomichron-British cesium beam standard.
IRE TRANSACTIONS ON INSTRUMENTATION, I-7(3-4): 203-206; December, 1958.
Experiments to compare the British and U. S. standards are described. Final differences amounted to only about 2.2 parts in 10^{10} .
- [360] Mainberger, W. and Orenberg, A.
The Atomichron—an atomic frequency standard—operation and performance.
1958 IRE NATIONAL CONVENTION RECORD, (pt. 1): 14-18.
The operation of a cesium-type frequency standard is explained and circuit diagrams are given. An accuracy of one part in 10^9 is provided. Test results are given.
- [361] Mockler, R. C., Salazar, H., Fey, L., Barnes, J., and Beehler, R.
The ammonia maser as an atomic frequency and time standard.
IRE TRANSACTIONS ON INSTRUMENTATION, I-7(3-4): 201-202; December, 1958.
After various factors affecting such devices are described, there is a discussion of the operation of an experimental type having a frequency stability of 1×10^{-11} or better for short periods.
- [362] Peter, M. and Strandberg, M. W. P.
Efficiency of frequency measurements with an atomic clock.
PROCEEDINGS OF THE IRE, 47(1): 92-93; January, 1959.
Presents the theory of frequency measurements. Concludes that a spectroscope with a sufficiently narrow natural spectral width is required for an atomic clock of optimum efficiency.
- [363] Plotkin, H. H. and Reder, F. H.
Atomic clocks and microwave amplification.
Physics Today, 9(6): 44-46; June, 1956.
Summary of a symposium held February 29th and March 1st, 1956, devoted both to basic ideas and to design criteria.
- [364] Reder, F. H.
Proposed feasibility study of frequency shift in sealed atomic beam frequency standard.
PROCEEDINGS OF THE IRE, 47(9): 1656; September, 1959.
Reports on the comparison of British and U. S. atomic beam frequency standards. Offers possible reasons for the errors observed in a sealed Cs beam frequency standard and suggests ways of determining if a deteriorating vacuum in the beam tube is involved.
- [365] Scheibe, A.
Pendulum, quartz and atomic clocks as time standards (In German).
Zeitschrift für Angewandte Physik, 5(8): 307-317; August, 1953.
Discusses and compares performance of recent forms of standard clocks. Describes the basic principles of the Shortt, Riefler, and Schuler pendulum clocks, the standard quartz clocks at various places in England, France, Germany, and the United States of America, and the NH_3 and Cs atomic clocks. Performance of the quartz clocks indicates they are better than the best astronomical pendulum clocks. It is stated that the " NH_3 clock is inferior to a good quartz clock, but the proposed Cs clock should be superior in performance."
- [366] Shimoda, K.
Atomic clocks and frequency standard on an ammonia line: part 1 (In English).
Journal of the Physical Society of Japan, 9(3): 378-386; May-June, 1954.
Theoretical and experimental examinations are made of the various errors in an atomic clock using the 3-3 line of ammonia. Also given is a brief description of an experimental Stark modulation atomic clock. In order that the fractional error be kept under one part in 10^8 , it is necessary that there be a high degree of frequency-insensitive multiplier output and that the generator and detector be well-matched to the waveguide.
- [367] Shimoda, K.
Atomic clocks and frequency standards on an ammonia-line: parts 2 and 3 (In English).
Journal of the Physical Society of Japan, 9(4): 558-575; July-August, 1954.
In order to eliminate the causes for error in atomic clocks, the use of Zeeman and Faraday effects were observed. A theoretical investigation for accurate atomic-clock design was made of the nonreciprocal transmission characteristics of a waveguide absorption cell in an axial magnetic field. The plan consists of using Stark, source, and Zeeman modulation which is free from errors due to reflections in the microwave line. Preliminary results show accuracy within 10^{-7} possible.
- [368] Shimoda, K.
Characteristics of the beam-type maser; part 2 (In English).
Journal of the Physical Society of Japan, 13(8): 939-947; August, 1958.
Reports on an experimental ammonia-maser frequency standard. Effects of focusing voltages and cavity timing on frequency are compared with theoretical values. Estimates effect of the velocity spread of the molecules.
- [369] Townes, C. H.
"Atomic" clocks and frequency stabilization on microwave spectral lines.
Journal of Applied Physics, 22(11): 1365-1372; November, 1951.
Discusses microwave gas absorption lines and the various types of errors in frequency stabilization due to the nature

- of their lines and to fundamental thermal noise. Accuracy of the order of one part in 10^{12} for a short time are the limits shown for time standards synchronized with microwave absorption in ammonia or resonances in molecular or atomic beams. Smaller fractional errors over longer periods of time will be possible.
- [370] United States sharpens its time standard.
Product Engineering, 28(18): 16; November 4, 1957.
A news item about two types of atomic clock (one is ammonia, the other, cesium) time standards undergoing tests at the National Bureau of Standards.
- [371] Vasniewa, G. A., Grigoriant, V. V., Zhabatinski, M. E., Klyshko, D. N., Sverdlov, I. L., and Sverchkov, E. I.
Molecular frequency standard (In English).
Radio Engineering and Electronics, 3(4): 167-168; 1958. Also in *Radiotekhnika i Elektronika*, 3(4): 569-570; April, 1958 (In Russian).
Describes a circuit for determining the value of the frequency of a quartz oscillator by means of a molecular oscillator, with an error not exceeding 10^{-9} of the nominal value. A telephone receiver is used to tune in conjunction with a cathode ray tube.
- [372] Zacharias, J. R., Yates, J. G., and Haun, R. D. Jr.
An atomic frequency standard.
1955 IRE CONVENTION RECORD, (pt. 10): 180.
Presents abstract of a report. The system uses a cesium beam involving resonant cavities in which either absorption or stimulated emission by the atoms of the beam takes place. An accuracy of one part in $10^{10.5}$ is expected over long periods.
- Miscellaneous Items*
- [373] Alsop, L. E., Giordmaine, J. A., Mayer, C. R., and Townes, C. H.
Observations using a maser radiometer at 3-cm wavelength.
Astronomical Journal, 63: 301; September, 1958.
Abstract unavailable.
- [374] Ewen, H. I.
A thermodynamic analysis of maser systems.
Microwave Journal, 2(3): 41-46; March, 1959.
Points out the role masers have and will have in radio astronomy. A thermodynamic approach to system analysis is introduced. There is a discussion of extraterrestrial noise sources, both celestial and man-made, and their relation to masers.
- [375] Fain, V. M.
Saturation effect in a system with three energy levels (In English).
Soviet Physics JETP, 33: 991-995; May, 1958. Also in *Zhurnal Eksperimentalnoi i Teoreticheskoi Fiziki*, 33: 1290-1294; November, 1957 (In Russian).
The effect of a high-frequency alternating field with given harmonics on a system with three energy levels is analyzed mathematically. Gives expressions, applicable to maser operations, for dielectric constant or permeability.
- [376] Feynman, R. P., Vernon, F. L., Jr., and Hellwarth, R. W.
Geometrical representation of the Schrödinger equation for solving maser problems.
Journal of Applied Physics, 28(1): 49-52; January, 1957.
Resonance behavior of a quantum system using only a pair of energy levels is described in a simple rigorous geometrical picture. With this system it is possible to analyze various maser-type devices.
- [377] Goudet, G.
Report of advance in microwave theory and techniques in Western Europe—1958.
IRE TRANSACTIONS ON MICROWAVE THEORY AND TECHNIQUES, MTT-7(3): 327-330; July, 1959.
Includes references to three French articles on quantum-mechanical amplifiers.
- [378] Siegman, A. E., and Morris, R. J.
Proposal for a "staircase" maser.
Physical Review Letters, 2(7): 302-303; April, 1959.
Proposes using the phenomenon of inversion by adiabatic fast passage of a single electron-spin resonance transition in a multilevel system. Operating points, at which two successive inversions can be performed by the same pump oscillator in a single sweep of the dc magnetic field, can be found in common maser materials.
- [379] Weiss, M. T.
Quantum derivation of energy relations analogous to those for nonlinear reactances.
PROCEEDINGS OF THE IRE, 45(7): 1012-1013; July 1, 1957.
Points out that the Manley-Rowe relations are almost self-evident in a quantum-mechanical system. Energy relations are fully developed on this basis and are shown to be particularly significant in analyzing multilevel solid-state masers.

IV. AUTHOR INDEX

Adler, R.	21, 22, 38	Bleaney, B.	266	Chang, W. S. C.	272
Allais, E.	181	Bloembergen, N.	259, 267, 268	Chester, P. F.	211, 269, 273
Alsop, L. E.	224, 286, 287, 373	Bloom, A.	348	Clavier, P. A.	28
Anderson, P. W.	1	Bloom, S.	60, 67, 131, 133, 134	Clogston, A. M.	274
Arams, F. R.	208, 257, 258, 303	Bolef, D. I.	211, 269	Cohn, S. B.	135
Arditi, M.	343-346	Bonanomi, J.	227-231, 349, 350	Coleman, P. D.	136
Artman, J. O.	259, 260	Bossard, B. B.	61	Combrisson, J.	157, 275
Ashkin, A.	23-25	Boyd, M. R.	147	Cook, J. S.	29
Autler, S. H.	261-263	Brand, F. A.	62	Cromack, J.	272
		Braunstein, R.	270	Cross, L. G.	276
Barker, W. A.	339	Breitzer, D. I.	63	Cullen, A. L.	137
Barnes, J.	361	Bridges, T. J.	23, 25, 26	Culver, W. H.	158
Basov, N. G.	182-190, 209, 264	Brodwin, M. E.	2		
Beam, R. E.	2	Brodzinsky, A.	210	Damon, R. W.	3
Beam, W. R.	78	Buchmiller, L. D.	27	Danielson, W. E.	138
Beck, A. H. W.	347	Butcher, P. N.	271	Davis, C. F.	278, 331
Becker, R. C.	136			DeGrasse, R. W.	279, 280, 320
Beehler, R.	361	Cade, C. M.	156	DeLoach, C. B.	68
Bell, C. V.	59	Caplan, P. J.	334	DePrins, J.	229, 231
Bell, W. E.	348	Carver, T. R.	343-346	Dicke, R. H.	352
Benoit, H.	191-193	Cassedy, E. S., Jr.	132	Dieter, F. A.	334
Bergmann, S.	265	Castle, J. G., Jr.	273	Ditchfield, C. R.	281
Berk, A. D.	40, 70	Chang, K. K. N.	60, 64-67, 131, 133, 134		
Birnbaum, G.	155				

- | | | | | | |
|--------------------|---------------------------------------|---------------------|--------------------|----------------------|--|
| Edwards, C. F. | 139 | Khokhlov, R. V. | 199, 200 | Peter, M. | 362 |
| Endler, H. | 70 | Kibler, L. U. | 80 | Peterson, E. | 143 |
| Englebrecht, R. S. | 71 | Kiefer, J. E. | 284 | Petrack, P. | 93 |
| Enomoto, H. | 122 | Kikuchi, C. | 295, 304 | Petrov, A. P. | 188 |
| Essen, L. | 353 | Kim, C. S. | 81 | Pierce, J. R. | 146 |
| Ewen, H. I. | 374 | King, J. G. | 241 | Pittman, W. C. | 94 |
| | | Kingston, R. H. K. | 262, 296, 297 | Plotkin, H. H. | 363 |
| Fain, V. M. | 194, 195, 282, 375 | Kita, S. | 90 | Poole, K. M. | 46, 47 |
| Faughan, B. W. | 331 | Kleinman, L. | 40 | Pound, R. V. | 216 |
| Feher, G. | 321 | Klimontovich, I. L. | 200 | Prokhorov, A. M. | 164, 182, 185, 189, 190,
203, 204, 209, 244, 338 |
| Fey, L. | 361 | Klinger, H. H. | 163 | | |
| Feynman, R. P. | 376 | Klyshko, D. N. | 371 | Quate, C. F. | 23, 25, 34 |
| Foner, S. | 283 | Knechtli, R. C. | 82 | | |
| Forrester, P. A. | 281 | Kontorovich, V. M. | 164, 201 | Reder, F. H. | 363, 364 |
| Forward, R. L. | 284 | Kornienko, L. S. | 338 | Reed, E. D. | 95 |
| From, W. | 285 | Kotzebue, K. | 73 | Roberts, R. W. | 333 |
| Fukui, K. | 113 | Krayer, G. | 208 | Rodrigue, G. P. | 317 |
| Fukuoka, T. | 126 | Kurokawa, K. | 142 | Roe, G. M. | 147 |
| | | Kusunoki, K. | 116 | Rose-Innes, A. C. | 205 |
| Gatos, H. C. | 298 | Kyhl, R. L. | 278, 312, 331 | Rostas, E. | 12 |
| George, W. D. | 354 | | | Rowe, H. E. | 144, 148 |
| Giordmaine, J. A. | 224, 286, 287, 373 | Lambe, J. | 295, 304 | | |
| Gold, T. | 288 | Lax, B. | 298 | Saad, T. | 62 |
| Goodwin, F. E. | 284 | Lebedev, P. N. | 203 | Saito, S. | 149 |
| Gordon, J. P. | 159, 160, 212, 234-236 | Leenov, D. | 83 | Salzberg, B. | 13, 96 |
| Goto, E. | 114, 115 | Lequeux, J. | 165 | Salazar, H. | 361 |
| Goudet, G. | 161, 377 | Lewis, F. D. | 356 | Sanders, J. H. | 341 |
| Gould, R. W. | 32 | Likel, H. | 166 | Sard, E. W. | 63, 84, 85, 96 |
| Greene, J. C. | 72 | Little, A. G. | 111, 112 | Sasaki, F. | 117 |
| Grigoriants, V. V. | 371 | Llewellyn, P. M. | 299 | Schawlow, A. | 174, 342 |
| Grivet, P. | 191-193 | Lombardo, P. P. | 72, 84, 85 | Scheibe, A. | 365 |
| Guibe, L. | 191 | Louisell, W. H. | 23, 25, 29, 34, 35 | Schulz-DuBois, E. O. | 280, 320, 322 |
| | | Lyons, H. | 357 | Scovil, H. E. D. | 280, 320-324 |
| Habara, K. | 113 | Lytollis, J. | 347 | Seidel, H. | 97, 321 |
| Hamasaki, J. | 142 | | | Sekiguti, S. | 128 |
| Hanawa, K. | 116, 126 | Macpherson, A. C. | 210 | Senitzky, I. R. | 325 |
| Hartley, R. V. L. | 140 | Maguire, T. | 8 | Shapiro, S. | 259 |
| Haun, R. D., Jr. | 42, 372 | Mainberger, W. | 360 | Sharpless, W. M. | 68 |
| Haus, H. A. | 33, 141 | Makhov, G. | 295, 304 | Sher, N. | 246 |
| Heffner, H. | 4-6, 37, 73-75, 109,
111, 112, 289 | Manenkov, A. A. | 338 | Shimoda, K. | 169, 217, 247-251,
366-368 |
| Heilmeyer, G. H. | 76 | Manley, J. M. | 143, 144 | | |
| Heineken, F. W. | 162 | Marsh, J. A. | 167 | Shunaman, F. | 100, 170 |
| Hellwarth, R. W. | 376 | Matthei, W. G. | 9, 62 | Sie, J. | 98 |
| Helmer, J. C. | 196, 197, 213, 237 | Mayer, A. | 283 | Siegmán, A. E. | 99, 218, 272, 378 |
| Herold, E. W. | 290 | Mayer, C. H. | 286, 373 | Singer, J. R. | 171, 207, 252 |
| Herrmann, G. F. | 77, 97 | McAvoy, N. | 263 | Smith, W. V. | 219 |
| Herrmann, J. | 229, 231, 349, 350 | McCoubrey, A. O. | 358, 359 | Someya, I. | 36 |
| Higa, W. H. | 238 | McWhorter, A. L. | 262, 300-303 | Sterzer, F. | 101 |
| Hilibrand, J. | 78 | Meyer, J. W. | 262, 300-302, 310 | Stevens, K. W. H. | 15, 102 |
| Hiyama, Y. | 127 | Mikaelian, A. L. | 10 | Stitch, M. L. | 220, 221 |
| Hogan, C. L. | 43 | Mockler, R. C. | 361 | Strandberg, M. W. P. | 222, 278, 312, 328-332,
362 |
| Holahan, J. | 7 | Momo, L. R. | 283 | Strum, P. D. | 300, 301 |
| Honda, J. S. | 79 | Morris, R. J. | 312, 378 | Suhl, H. | 50-55 |
| Honig, A. | 275 | Motz, H. | 214 | Sverchkov, E. I. | 371 |
| Howarth, D. J. | 291 | Muller, M. W. | 213, 215 | Sverdlov, I. L. | 371 |
| Hrbek, G. | 21 | Munster, A. C. | 243 | | |
| Hulster, F. | 12 | Muroga, S. | 118, 119 | Takahasi, H. | 217 |
| Husimi, K. | 127 | | | Takasima, K. | 119 |
| | | Nakagome, Y. | 120, 123 | Takasima, M. | 128 |
| Ikeno, N. | 126 | Nash, F. R. | 287 | Tannenwald, P. E. | 150 |
| Inage, N. | 90 | Nelson, C. E. | 40 | Tenney, H. D. | 333 |
| Ince, C. R. S. | 355 | Nergaard, L. S. | 89 | Terada, H. | 125 |
| Inohama, R. | 123 | Nikolsky, V. V. | 45 | Terhune, R. W. | 295, 304 |
| Itoh, J. | 292 | Nishiguchi, K. | 121 | Theissing, H. H. | 334 |
| | | Nisiguti, K. | 130 | Tien, P. K. | 46, 47, 55, 151 |
| Javan, A. | 239, 293, 294, 340 | Oguchi, B. | 90 | Torrey, H. C. | 103 |
| Jepsen, R. L. | 43 | Okajima, T. | 90 | Toth, R. C. | 16 |
| Johnson, S. | 240 | Okwit, S. | 258 | Townes, C. H. | 157, 169, 173-175, 217,
224, 235, 236, 253, 275,
286, 287, 342, 369, 373 |
| Jones, E. M. T. | 79 | Olson, F. A. | 91 | Troitskii, V. S. | 254 |
| | | Onose, K. | 113 | | |
| Kamata, K. | 117 | Oraevsky, A. N. | 202 | Uenohara, M. | 77 |
| Kamibayashi, T. | 120 | Orenberg, A. | 360 | Uhler, A., Jr. | 77, 104-107 |
| Kartaschoff, P. | 229, 231 | Oshima, S. | 122, 123 | | |
| Kato, M. | 113 | Osial, T. A. | 42 | | |
| Katsunuma, S. | 126 | Ottavi, H. | 192, 193 | | |
| Kemp, J. C. | 198, 207 | | | | |
| | | Page, C. H. | 145 | | |

Valdes, L. B.	152	Wang, T. C.	169, 224, 239, 248	Williams, R.	348
Van der Ziel, A.	108, 153	Warren, T. B.	110	Wittke, J. P.	18, 179
Vartanian, P. H.	43, 333	Watanabe, S.	122	Wolf, H. C.	180
Vasnieva, G. A.	371	Weber, J.	176, 223, 335	Wolga, G. J.	331
Vernon, F. L., Jr.	376	Weber, S.	20		
Veselago, V. G.	183	Weglein, R. D.	82	Yamanaka, K.	127
Vonbun, F. O.	255	Weibel, G. E.	177, 178	Yariv, A.	207
Von Hippel, A. R.	17	Weintraub, S.	336	Yates, J. G.	372
		Weisbaum, S.	98	Younger, J. J.	111, 112
Wada, T.	120	Weiss, M. T.	56, 57, 379		
Wade, G.	21, 27, 37, 38, 59, 74, 75, 91, 109, 111, 112	Wells, W. H.	206	Zacharias, J. R.	241, 372
Wagner, P. E.	273	Wessel, G. K.	337	Zeiger, H. J.	235, 236
Wang, C. P.	91	Whirry, W. L.	58, 70	Zeniti, K.	126-130
Wang, F. B.	58	White, L. D.	212, 234	Zhabatinski, M. E.	183, 371
		Whitmer, C. A.	103	Zverev, G. M.	338

Correction

Leo Young, the author of "Tables for Cascaded Homogeneous Quarter-Wave Transformers," which appeared on pages 233-237 in the April, 1959 issue of these TRANSACTIONS, has requested that the following revisions be made in his paper.

The values of Z_1 and Z_2 for the four-section ($n=4$) transformers given in Tables IV to XIII are not quite optimum. In computing them, the positive roots of the fourth degree Tchebycheff polynomial were erroneously taken as $\frac{1}{2}(1 \pm 1/\sqrt{2})$ instead of $[\frac{1}{2}(1 \pm 1/\sqrt{2})]^{1/2}$. The effect of this is to reduce the bandwidth by approximately the ratio of the incorrect to the correct outer roots, that is, by a factor $[\frac{1}{2}(1 \pm 1/\sqrt{2})]^{1/2} = 0.924$. At the same time, the match is improved near the center of the band.

Twenty representative four-section transformers were analyzed numerically. The bandwidth reduction appeared to be independent of R , and was about 1/15 below the greatest possible bandwidth for the maximum VSWR specified in Table III. For instance, the stated 60 per cent four-section transformers (Table X) had only 56 per cent bandwidth; and the stated 120 per cent four-section transformers (Table XIII) had only 112 per cent bandwidth, for the VSWR claimed in Table III.

New tables for four-section transformers were computed and are appended. These have been checked out by numerical analysis of representative cases.

Various two- and three-section transformers given in my original tables were also checked by numerical analysis, and found to give the predicted frequency response.

FOUR-SECTION QUARTER-WAVE TRANSFORMERS

Impedance Ratio, R	Maximally Flat		Bandwidth = 0.10		Bandwidth = 0.20		Bandwidth = 0.30	
	Z_1	Z_2	Z_1	Z_2	Z_1	Z_2	Z_1	Z_2
1.00	1.00000	1.00000	1.00000	1.00000	1.00000	1.00000	1.00000	1.00000
1.25	1.01405	1.07223	1.01414	1.07232	1.01440	1.07260	1.01486	1.07306
1.50	1.02570	1.13512	1.02586	1.13530	1.02635	1.13584	1.02719	1.13673
1.75	1.03568	1.19120	1.03591	1.19146	1.03659	1.19224	1.03777	1.19354
2.00	1.04444	1.24206	1.04473	1.24239	1.04558	1.24340	1.04706	1.24508
2.50	1.05933	1.33204	1.05972	1.33252	1.06088	1.33396	1.06287	1.33636
3.00	1.07176	1.41051	1.07223	1.41113	1.07364	1.41296	1.07607	1.41603
4.00	1.09190	1.54417	1.09250	1.54503	1.09435	1.54760	1.09752	1.55190
5.00	1.10801	1.65686	1.10873	1.65794	1.11093	1.66118	1.11472	1.66660
6.00	1.12153	1.75529	1.12235	1.75657	1.12486	1.76043	1.12917	1.76689
8.00	1.14356	1.92323	1.14455	1.92490	1.14758	1.92990	1.15279	1.93828
10.00	1.16129	2.06509	1.16242	2.06710	1.16588	2.07315	1.17184	2.08328
12.50	1.17961	2.21803	1.18090	2.22044	1.18483	2.22770	1.19160	2.23985
15.00	1.19506	2.35186	1.19648	2.35465	1.20082	2.36303	1.20829	2.37706
17.50	1.20847	2.47169	1.21001	2.47483	1.21471	2.48426	1.22281	2.50007
20.00	1.22035	2.58072	1.22200	2.58419	1.22703	2.59463	1.23571	2.61213
25.00	1.24078	2.77447	1.24262	2.77857	1.24824	2.79089	1.25795	2.81154
30.00	1.25803	2.94423	1.26004	2.94891	1.26618	2.96299	1.27679	2.98659
40.00	1.28632	3.23492	1.28862	3.24067	1.29564	3.25798	1.30781	3.28698
50.00	1.30920	3.48136	1.31174	3.48809	1.31953	3.50835	1.33302	3.54228
60.00	1.32853	3.69752	1.33129	3.70517	1.33974	3.72816	1.35440	3.76669
80.00	1.36025	4.06810	1.36338	4.07741	1.37297	4.10544	1.38965	4.15241
100.00	1.38591	4.38263	1.38936	4.39348	1.39992	4.42610	1.41832	4.48078

Impedance Ratio, R	Bandwidth = 0.40		Bandwidth = 0.50		Bandwidth = 0.60		Bandwidth = 0.80	
	Z_1	Z_2	Z_1	Z_2	Z_1	Z_2	Z_1	Z_2
1.00	1.00000	1.00000	1.00000	1.00000	1.00000	1.00000	1.00000	1.00000
1.25	1.01553	1.07371	1.01643	1.07456	1.01761	1.07559	1.02106	1.07830
1.50	1.02842	1.13799	1.03009	1.13961	1.03227	1.14162	1.03866	1.14685
1.75	1.03949	1.19537	1.04182	1.19773	1.04488	1.20065	1.05385	1.20827
2.00	1.04921	1.24745	1.05214	1.25052	1.05598	1.25431	1.06726	1.26420
2.50	1.06577	1.33974	1.06973	1.34412	1.07494	1.34954	1.09026	1.36370
3.00	1.07963	1.42036	1.08448	1.42596	1.09086	1.43290	1.10967	1.45105
4.00	1.10216	1.55795	1.10849	1.56581	1.11685	1.57553	1.14159	1.60102
5.00	1.12026	1.67423	1.12783	1.68414	1.13784	1.69642	1.16759	1.72864
6.00	1.13549	1.77600	1.14415	1.78783	1.15559	1.80248	1.18974	1.84098
8.00	1.16043	1.95009	1.17092	1.96543	1.18482	1.98446	1.22654	2.03453
10.00	1.18060	2.09756	1.19264	2.11613	1.20863	2.13915	1.25683	2.19984
12.50	1.20156	2.25698	1.21527	2.27926	1.23353	2.30691	1.28883	2.37988
15.00	1.21931	2.39686	1.23449	2.42260	1.25475	2.45455	1.31638	2.53898
17.50	1.23478	2.52237	1.25128	2.55137	1.27335	2.58739	1.34074	2.68264
20.00	1.24854	2.63681	1.26625	2.66891	1.28998	2.70880	1.36269	2.81433
25.00	1.27232	2.84069	1.29220	2.87862	1.31891	2.92575	1.40125	3.05065
30.00	1.29251	3.01989	1.31432	3.06324	1.34367	3.11712	1.43467	3.26008
40.00	1.32587	3.32792	1.35100	3.38123	1.38498	3.44754	1.49127	3.62377
50.00	1.35308	3.59021	1.38108	3.65262	1.41905	3.73029	1.53879	3.93704
60.00	1.37624	3.82111	1.40677	3.89200	1.44833	3.98025	1.58022	4.21547
80.00	1.41455	4.21877	1.44952	4.30522	1.49736	4.41293	1.65091	4.70063
100.00	1.44587	4.55802	1.48467	4.65870	1.53798	4.78420	1.71073	5.12003

Impedance Ratio, R	Bandwidth = 1.00		Bandwidth = 1.20	
	Z_1	Z_2	Z_1	Z_2
1.00	1.00000	1.00000	1.00000	1.00000
1.25	1.02662	1.08195	1.03560	1.08683
1.50	1.04898	1.15394	1.06576	1.16342
1.75	1.06838	1.21861	1.09214	1.23248
2.00	1.08559	1.27764	1.11571	1.29572
2.50	1.11531	1.38300	1.15681	1.40907
3.00	1.14059	1.47583	1.19218	1.50943
4.00	1.18259	1.63596	1.25182	1.68360
5.00	1.21721	1.77292	1.30184	1.83358
6.00	1.24702	1.89401	1.34555	1.96694
8.00	1.29722	2.10376	1.42054	2.19954
10.00	1.33920	2.28397	1.48458	2.40096
12.50	1.38421	2.48134	1.55461	2.62317
15.00	1.42350	2.65667	1.61690	2.82190
17.50	1.45869	2.81570	1.67357	3.00321
20.00	1.49074	2.96208	1.72593	3.17095
25.00	1.54791	3.22609	1.82099	3.47548
30.00	1.59831	3.46148	1.90654	3.74905
40.00	1.68552	3.87328	2.05820	4.23198
50.00	1.76055	4.23091	2.19214	4.65555
60.00	1.82732	4.55096	2.31378	5.03760
80.00	1.94412	5.11329	2.53156	5.71502
100.00	2.04579	5.60394	2.72559	6.31175

Correspondence

Analysis of Split Coaxial Line Type Balun*

Since the split coaxial type balun was developed, it has been widely utilized as a microwave radiator with dipole, and a duplexer of television transmitting unit for its superior working capacity. There are several papers¹⁻³ on the analytical theory of this balancing unit. But, strictly speaking, there are still some points remaining to be re-scrutinized, such as the radiator receiving the effect of the split coaxial and its lines from the earth.

We have not thoroughly discussed how the input admittance will change with the balancing of the load and the unequally divided cylinder, or what effects the admittance will have between the outer and split conductors, when it is utilized as a duplexer.

SPLIT COAXIAL TYPE BALUN

We will consider the problem on the split coaxial type balun which is cut in two sections and has a dipole between each segment of the outer cylinder, as shown in Fig. 1. This type of balun has a special character which does not cause any earth current, compared with the other types. But, when it is divided unsymmetrically, the character will not work. In practical use, it is impossible to make it completely symmetrical. Furthermore, if we use it in the arbitrary split, it will be utilized as a matching element because the variable transform ratio is derived. In such a case, the earth effect will be taken into account for the input impedance.

Generally, the antenna load forms the distributed circuit, but we can analyze it by using the simplified theory, replacing it with the equivalent concentric constant. An actual circuit is shown in Fig. 2, where the load is symmetrical, Y is the admittance inserted between terminals 1 and 2 directly, Y_1 and Y_2 are the admittances inserted through the earth, and Y_3 is the admittance existing between the coaxial line and the earth measured from the right boundary surface. Input impedance can be calculated as follows:

$$Y_{in} = \frac{I_1}{V_1} = \frac{1}{\alpha^2} \left\{ Y + Y_s + Y_1(1 - \alpha) + \frac{[Y_2\alpha - Y_1(1 - \alpha)](Y_1 + \alpha Y_3)}{Y_1 + Y_2 + Y_3} \right\}$$

where $Y_s = jY_{s0} \cot \beta l$ and Y_{s0} is the char-

acteristic admittance⁴ of the slot and l is the slot length.

When the voltage between the electrodes 2 and 1, 3 in a body is applied, the current distributed factor α is given by the current on the conductor 1. A numerical calculus is shown as follows:

⁴ H. Kogō and K. Morita, "Electrode capacity of split-coaxial cylinder," *J.I.E.C. of Japan*, vol. 38, pp. 548-552; July, 1955.

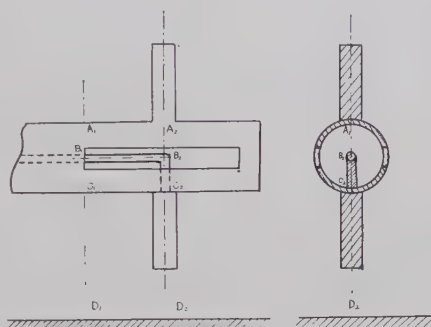


Fig. 1—Split coaxial type balun.

$$Y_{in} = \frac{Y_{in}}{Y_s + Y}, \quad Y_{in0} = \frac{Y_{in0}}{Y + Y_s}$$

Setting

$$Y_1 = Y_0[1 + k(\alpha + \frac{1}{2})], \quad Y_2 = Y_0[1 - k(\alpha - \frac{1}{2})].$$

From the above relations, the numerical results are shown in Figs. 3, 4, and 5.

SPLIT COAXIAL TYPE DUPLEXER WITH OUTER CONDUCTOR

For the purpose of making a branch from the coaxial line A to the other coaxial lines B and C , the split coaxial-type duplexer will

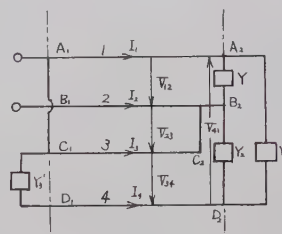


Fig. 2—Equivalent circuit of split coaxial type balun.

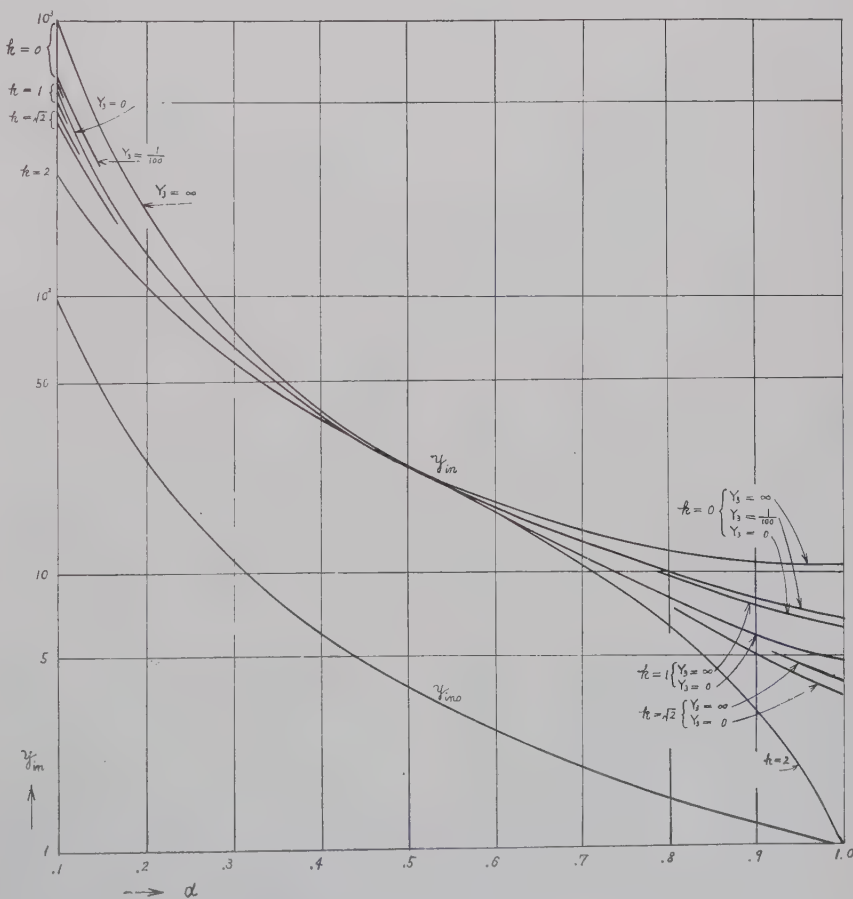


Fig. 3—Relationship between input admittance Y_{in} and current distributed factor α for $Y_s = 1/10$ v, $Y + Y_s = 1/100$ v.

* Received by the PGMTT, February 13, 1959; revised September 22, 1959.

¹ H. Uchida, "Split coaxial balance converter for VHF and UHF," *J.I.E.C. of Japan*, vol. 33, pp. 406-408; August, 1951.

² P. A. T. Bevan, "The 100-kw ERP Sutton cold-field television broadcasting station," *Proc. IRE*, vol. 41, pp. 196-203; February, 1953.

³ H. Kogō and K. Morita, "Antenna impedance transformation by means of split coaxial cylinder-type balun," *J.I.E.C. of Japan*, vol. 38, pp. 359-365; May, 1955.

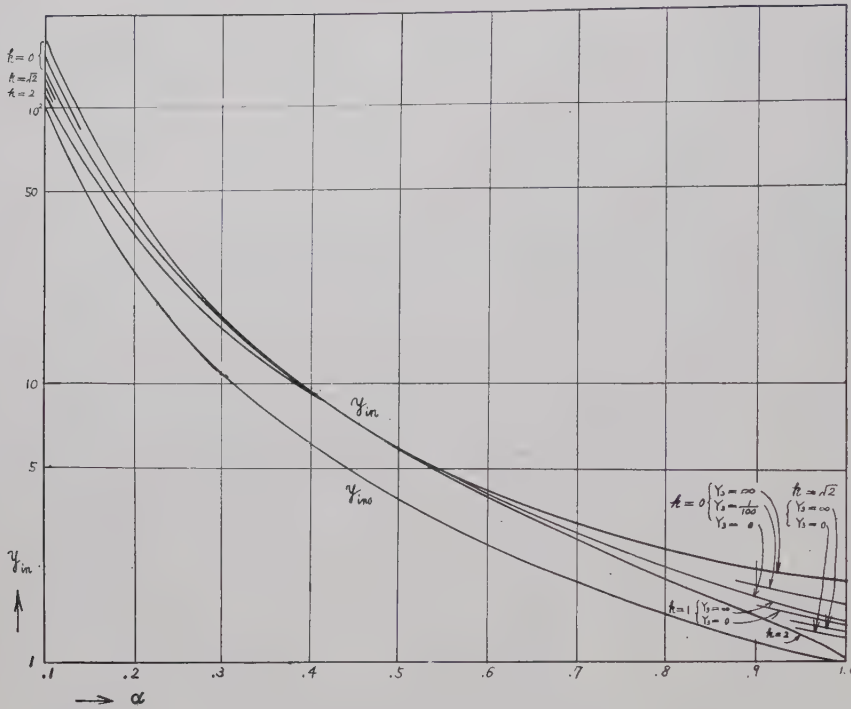


Fig. 4—Relationship between input admittance Y_{in} and current distributed factor α for $Y_0 = 1/100 \text{ ohm}$, $Y + Y_s = 1/100 \text{ ohm}$.

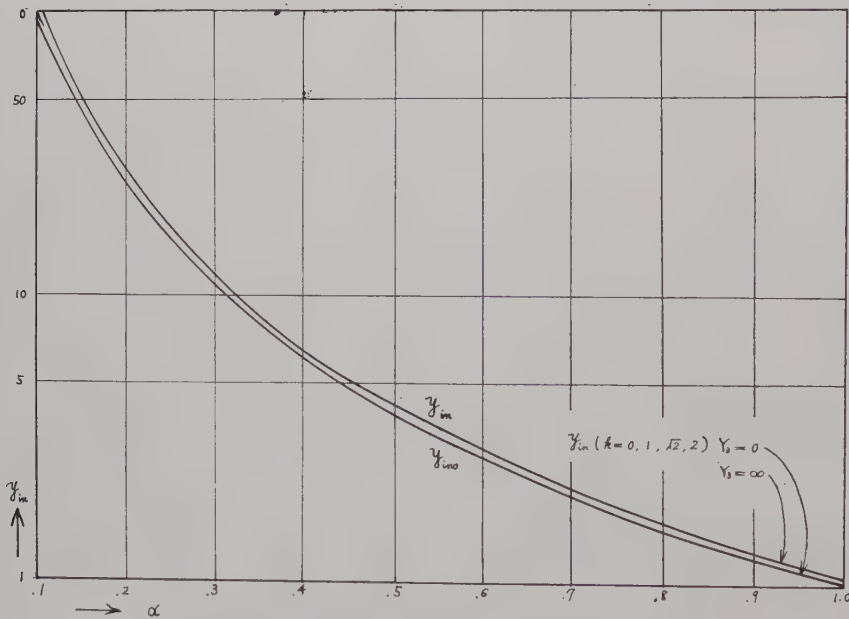


Fig. 5—Relationship between input admittance Y_{in} and current distributed factor α for $Y_0 = 1/1000 \text{ ohm}$, $Y + Y_s = 1/100 \text{ ohm}$.

be used frequently with the outer conductor as shown in Fig. 6. We shall now consider the impedance transform and the power division to the coaxial lines B and C. In Fig. 6 suppose that the unsymmetric duplexer segment 3 and 4 is split by the ratio 1:n and

loaded with Y_{13} , Y_{14} . To simplify it, the slot width shall be made very small and the capacity of each electrode shall be proportionate to the segment area. Equivalent input admittance at the terminal from the coaxial side is as follows:

$$Y_{in} = \frac{i_1}{v_1} = \left(\frac{n+1}{n}\right)^2 Y_2 + \frac{Y_{13}Y_3 - Y_{14}Y_3/n + \frac{n+1}{n^2} Y_{14}Y_3 + \left(\frac{n+1}{n}\right)^2 Y_{13}Y_{14}}{Y_{13} + Y_{14} + Y_3}$$

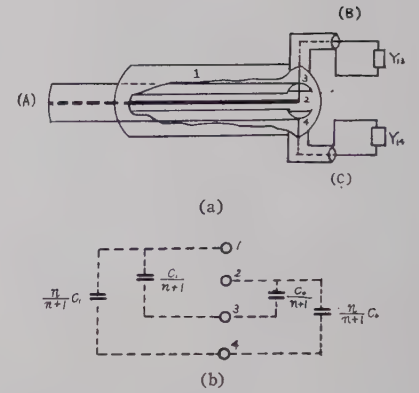


Fig. 6—Split type duplexer with outer conductor; (a) construction, and (b) electrode capacity.

Next, we will consider the power distributed to Y_{13} , Y_{14} and the equivalent input admittance as follows:

1) In the case when $Y_{13} = Y_{14}$:

$$Y_{13} = -\frac{Y_{13} \left(\frac{n+1}{n}\right) + Y_3}{2Y_{13} + Y_3} v_1,$$

$$Y_{14} = -\frac{Y_{13} \left(\frac{n+1}{n}\right) + Y_3/n}{2Y_{13} + Y_3} v_1;$$

the power distributed to each branch is not equal. Equivalent input admittance is as follows:

$$Y_{in} = \left(\frac{n+1}{n}\right)^2 Y_2 + \frac{Y_{13} \left[\left(1 + \frac{1}{n^2}\right) Y_3 + \left(\frac{n+1}{n}\right)^2 Y_{13} \right]}{2Y_{13} + Y_3}$$

where $Y_3 = -i_3/v_3 = jY_{1-2,3,4} \cot \beta l$, and Y_3 is the input admittance at the terminal between 1 and 2, 3, 4 in a body, and $Y_{1-2,3,4}$ is the characteristic admittance.

If $Y = 0$, then,

$$Y_{in} = \left(\frac{n+1}{n}\right)^2 \left(Y_2 + \frac{Y_{13}}{2}\right).$$

2) In the case when $Y_{13} \neq Y_{14}$, $Y_3 = 0$:

$$\frac{Y_{13}}{Y_{14}} = \frac{Y_{14}}{Y_{13}}, \quad Z_{in} = \left(\frac{n}{n+1}\right)^2 (Z_{13} + Z_{14}) \cap Z_2,$$

the voltage division to the ratio of the load impedance.

3) In the case when $Y_{14}/n = Y_{13}$:

$$\frac{Y_{13}}{Y_{14}} = n, \quad Y_{in} = \left(\frac{n+1}{n}\right)^2 Y_2 + \left(\frac{n+1}{n}\right) Y_{13},$$

input admittance is derived independently from Y_3 .

4) In the case when $n = 1$:

$$Y_{in} = 2 \left[\frac{(Y_{14} + Y_{3/2})(Y_{13} - Y_{14})}{Y_{13} + Y_{14} + Y_3} + (Y_{14} + 2Y_2) \right].$$

When the load is symmetrical, $Y_{13} = Y_{14} = 2Y$, $Y_{in} = 2Y_{14} + 4Y_2 = 4(Y + Y_2)$.

Nonreciprocal Attenuation of Ferrite in Single-Ridge Waveguide*

The nonreciprocal transmission characteristics of rectangular and cylindrical waveguides containing ferrites have been extensively studied and utilized in the construction of microwave phase shifters, gyrators, circulators, and isolators.¹⁻³ This note concerns the measurement of the nonreciprocal attenuation produced by ferrite in single-ridge waveguide transmitting dominant mode. In particular, three types of isolators in ridge waveguide are investigated including resonance-absorption isolators, field-displacement isolators,⁴ and isolators operating at low-biasing magnetic fields. Fig. 1 shows the dimensions of the single-ridge waveguide used in the measurement.

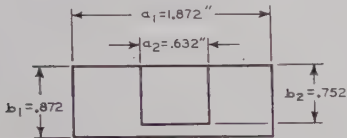


Fig. 1—Geometry of the single-ridge guide.

The cutoff frequencies⁵ for the TE₁₀ and TE₂₀ modes are 1309 and 7008 mc per second, corresponding to cutoff wavelengths of 22.92 and 4.75 cm, respectively. Strong electric intensities exist in the constricted region between the ridge and the bottom guide wall. The two areas on each side of the ridge are inductive regions where the magnetic intensities are strong. However, the exact field distribution in the single-ridge waveguide is difficult to determine analytically.

H-Plane Isolators

Because a small ferrite produces negligible nonreciprocal attenuation and a large slab introduces anomalous modes in the guide, the 0.340×0.100×4-inch Ferramic R-4 slab used in Fig. 2 represents a compromise with regard to ferrite size. The slab is slightly tapered at both ends to give a VSWR below 1.10 over the 2200–4000-mc band. In the measurement, the slab is laid flat with its inner edge directly opposite the edge of the ridge, while the dc magnetic field is varied and the driving frequency is taken as a parameter. At this ferrite position, comparatively high reverse attenuation is produced at 3500 mc per second. However, high ratio of reverse to forward loss is obtained at 2250 mc; this is consistent with the prediction for rectangular guide, where for a ferrite located away from the side wall, the loss ratio becomes better when the frequency is close to the

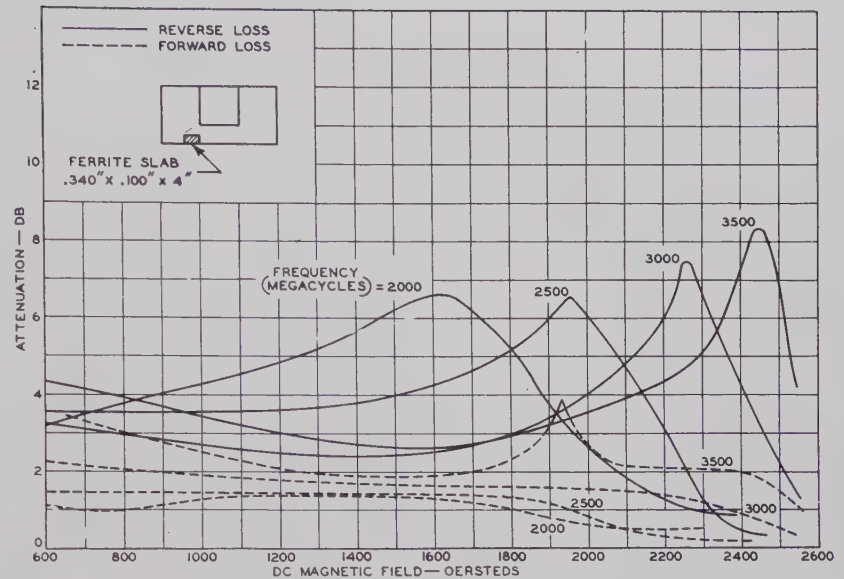


Fig. 2—Performance of H-plane isolator in ridge waveguide.

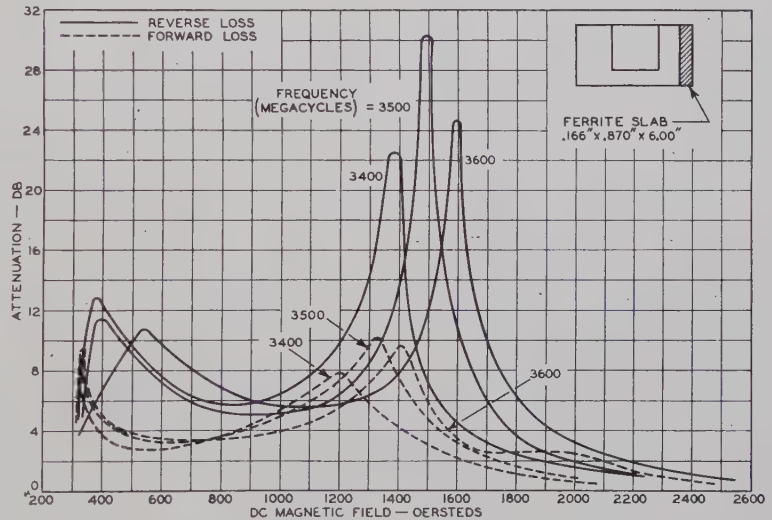


Fig. 3—Attenuation characteristics of E-plane isolator in single-ridge waveguide.

cutoff value than when it is remote from the cutoff.³

When the RF frequency is held constant at 3500 mc, the reverse-to-forward loss ratio gradually increases as the ferrite is displaced from the sidewall toward the ridge. The ratio reaches a maximum value 13.5 when the distance between the sidewall and the center line of the slab is 0.270 inch. If the ferrite is moved further toward the ridge, the peak reverse loss increases moderately, but the maximum forward loss increases in a greater proportion. The resonance magnetic field remains at 2460 oersteds irrespective of the ferrite position.

E-Plane Isolator

In the vicinity of the ridge, higher-order fields exist and the RF magnetic field does not assume a pure positive-circular polarization. Close to the sidewalls, the field distribution bears a strong resemblance to that existing in a rectangular guide. In Fig. 3, the

0.166×0.870×6-inch slab is placed against the sidewall; the ferrite in this position should disturb the field less than if it were placed anywhere else and should result in better heat dissipation.

Measurement reveals the two loss peaks illustrated in Fig. 3 when the dc magnetic strength increases, the frequency being held at 3500 mc. The first peak, having low reverse-to-forward loss ratio, occurs at 400 oersteds. As the magnetic field is increased to 1490 oersteds, the reverse loss reaches 30.6 db and the forward loss 4.4 db, providing a loss ratio of 7. The isolator performance deteriorates if the RF frequency departs from 3500 mc.

The resonant field H_{rez} increases with the driving frequency almost linearly as shown in Fig. 4. The magnetic intensities for producing resonance are lower than those required in H-plane isolators operating at corresponding frequencies. The bandwidth characteristic of this E-plane isolator for a

* Received by the PGMTT, August 10, 1959; revised, October 9, 1959.

¹ G. L. Hogan, "The ferromagnetic Faraday effect at microwave frequencies and its applications," *Bell Sys. Tech. J.*, vol. 31, pp. 1-31; January, 1952.

² F. K. du Pré, "On the microwave Cotton-Mouton effect in ferrocube," *Phillips Res. Repts.*, vol. 10, pp. 1-10; February, 1955.

³ A. G. Fox, F. E. Miller, and M. T. Weiss, "Behavior and applications of ferrites in the microwave region," *Bell Sys. Tech. J.*, vol. 34, pp. 5-103; January, 1955.

⁴ B. Lax and K. J. Button, "New ferrite mode configurations and their applications," *J. Appl. Phys.*, vol. 26, p. 1185; September, 1955.

⁵ S. B. Cohn, "Properties of ridge waveguides," *Proc. IRE*, vol. 35, pp. 783-788; August, 1947.

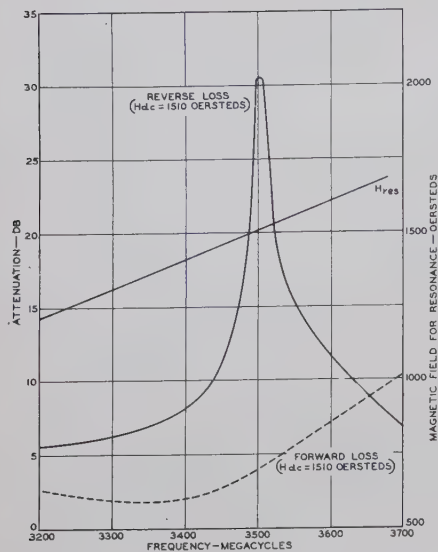


Fig. 4—Resonant magnetic field as a function of frequency, and frequency characteristics of E-plane isolator at fixed biasing magnetic field.

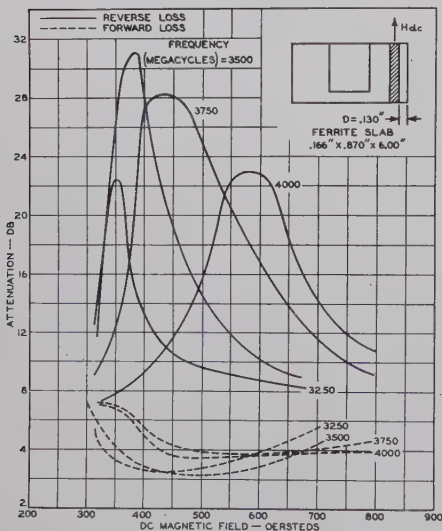


Fig. 6—Nonreciprocal loss of medium-field E-plane isolator as a function of dc magnetic field.

constant field of 1510 oersteds is depicted in Fig. 4. The reverse loss tends to drop abruptly for a slight deviation from 3500 mc; the forward loss begins to increase sharply after this frequency is exceeded.

Medium-Field E-Plane Isolators

If the E-plane isolator in Fig. 3 is separated from the guide wall by 0.07 inch, the reverse loss occurring at medium magnetic field and that caused by resonance absorption assume equal magnitude as shown in Fig. 5. This change constitutes a great enhancement of the medium-field nonreciprocal attenuation. When the ferrite is placed 0.130 inch from the wall, the medium-field loss becoming predominant at 380 oersteds produces a reverse loss of 30 db. The resonance absorption peak takes place at 1940 oersteds where the reverse loss reduces to 16 db. At this position, the medium-field E-plane isolator yields the best performance at 3500 mc. Fig. 6 illustrates the variation of re-

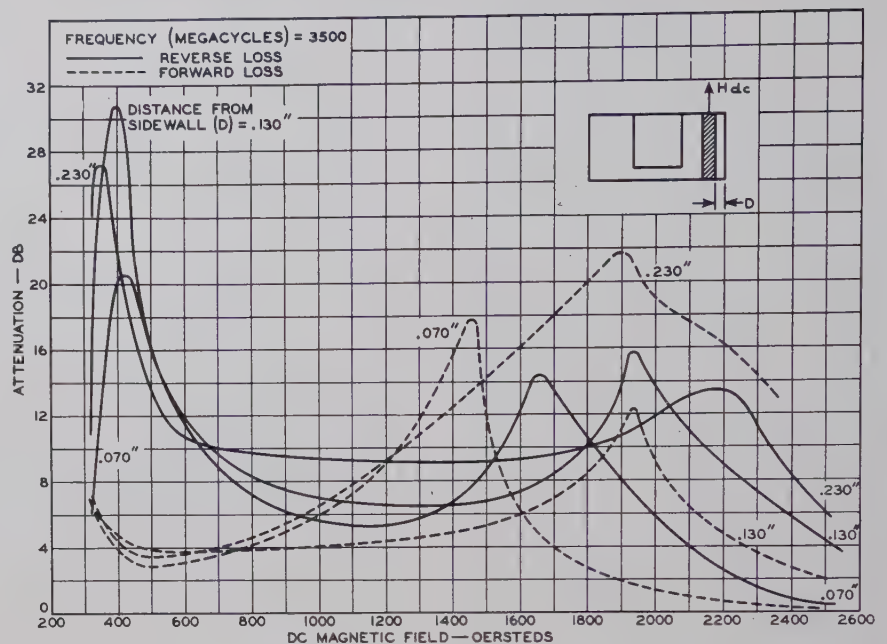


Fig. 5—Performance of medium-field E-plane isolator.

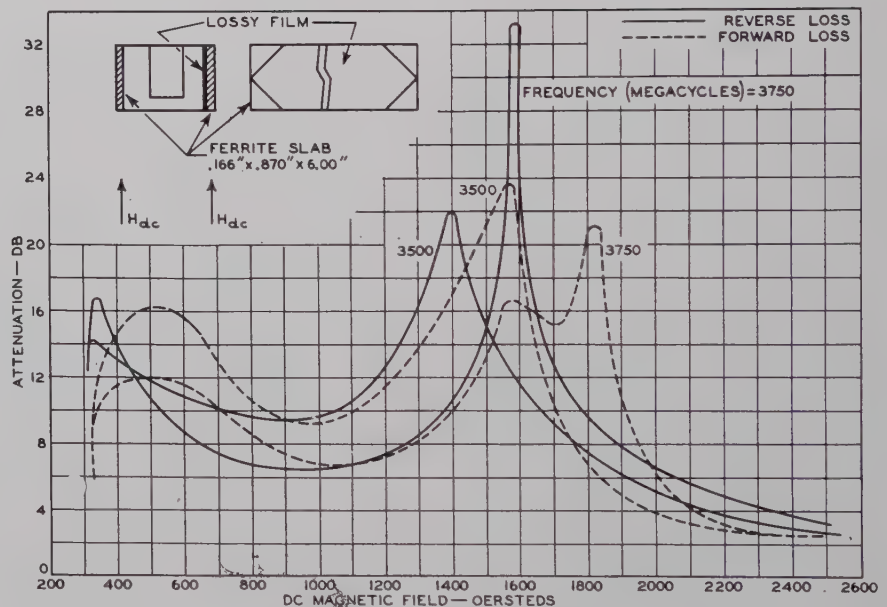


Fig. 7—Loss characteristics of field displacement isolators in ridge waveguide.

verse and forward loss for this isolator at a fixed location as a function of dc magnetic field for four frequencies. Above 3500 mc the maximum reverse loss decreases while the resonant magnetic strength increases. These effects are accompanied by a diminution of the loss ratio and a broadening of the loss curve. A lowering of the driving frequency also produces deleterious effect on the performance.

Field Displacement Isolator

When two $0.166 \times 0.870 \times 6$ -inch ferrites are added to the ridge waveguide as shown in Fig. 7 and a resistive film having tapered ends is deposited on the outer face of one slab, the loss characteristics are measured as a function of the magnetic field at 3500 and

3750 mc. Although two loss peaks are discernible in Fig. 7, the reverse and forward losses are approximately equal, and the nonreciprocal effect is nearly obliterated. Elimination of the resistive film does not reveal any improvement or worsening in the nonreciprocal effect. Both thicker and thinner slabs have been measured for field displacement effect without disclosing significant changes. Thus the differential electric intensity near the outer face of one ferrite caused by the B mode of propagation in rectangular waveguide⁴ is not strong in the single-ridge geometry.

T. S. CHEN
Electron Tube Division
Radio Corporation of America
Harrison, N. J.

ation of the device in question. The substitution method can also be used. A switched ferrite isolator is inserted before the thermistor mount, thus separating the measurement path from reflections and also offering a possibility of zeroing the thermistor bridge.

The VSWR measurement can be made by means of conventional slotted line techniques or by connecting a crystal mount to the fourth port of the first circulator and maintaining a constant power output from the generator. Under such conditions, any indicator connected with the crystal can be scaled in terms of the reflection coefficient. This simple circulator reflectometer was found to be particularly efficient when a large number of measurements were carried out at a fixed frequency; the same restriction was valid for the whole setup given in Fig. 1. In the final stage of measurements, when maximum accuracy was needed, conventional setups were preferred.

The measured ferrite sample was inserted into IK-1M isolator.² A schematic cross section through the main part of this device is given in Fig. 2. Iron flanges and tubing are used for focusing the magnetic field and for forming a special axial distribution of this field, which is flat at the middle part and rapidly decreases to the ends of the circular guide (Fig. 3). In some applications (circulators) the ferrite was placed off the center of symmetry of this distribution (but at the center of the guide) and thus additional tuning was obtained.

The ferrite rod was supported in circular guide by polyfoam or, in final stage of measurements, by polystyrene screws inside a polystyrene sleeve, closely fitting the guide walls.

All measured samples had the shape of a cylinder with 1-inch-long tapers at both ends. Ferrite pieces 2 inches long were ground to the desired length and diameter,

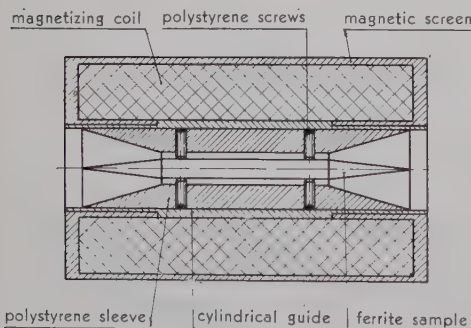


Fig. 2—Schematic cross section through the main part of the IK-1M isolator.

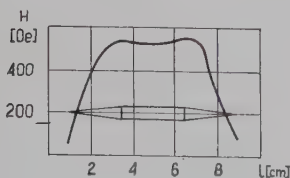


Fig. 3—DC magnetic field distribution on the waveguide axis.

the matching taper was made at one end, and then two such pieces were glued together to obtain the final shape; this procedure reduced the influence of the individual properties of the samples. During the measurements only the length and the diameter of the cylindrical part varied; the length of matching tapers was kept constant. Generous water cooling was provided during grinding.

Choice of the ferrite rod diameter for Faraday rotation devices is extremely difficult. Although the figure of merit F against ferrite diameter was determined,³ this gave little practical information, since F continuously decreases with the increase in the diameter and small diameters are of no use because of great lengths involved.

The following conditions are to be considered in designing ferrite samples for practical Faraday rotation devices:

- 1) the smallest possible losses of the device,
- 2) broadband performance (rotation independent of frequency),
- 3) small dimensions of the device (short ferrite sample—large rotation per unit length; preferably weak magnetic field).

The list conditions may be fulfilled for a given ferrite if proper dimensions (especially the diameter) of the sample are found. The final solution of the problem is in finding a reasonable compromise between the contradictory demands, and the results are, of course, dependent on the kind of ferrite used.

As has been stated before, the figure of merit, generally speaking, decreases with the increase in the ferrite diameter, this effect being caused by a steep increase in the losses, as the specific rotation steadily grows with the diameter (to certain limits). It follows from the above that losses limit the use of large diameters, and the fulfillment of 3) limits the use of small diameters.

In addition to the considerations on the figure of merit, the increase in the ferrite diameter has one more limitation: excitation of higher modes, in particular the hybrid TM_{11} mode (called the HTM_{11} mode throughout this paper), which propagates easily in the structure concerned.

Another problem associated with higher modes propagation in the system is the direct coupling between modes excited by the discontinuities at both ends of the sample. Many spurious effects which have resulted from using short ferrite rods totally vanish after elongating the sample.

The theoretical relation between the rotation and diameter is shown in Fig. 4. The curves were drawn on the basis of calculations made by Waldron.¹ These interesting calculations were not known to the authors at the beginning of this work but the measurements indicated that diameters just below the cutoff value of HTM_{11} should be given special attention. Theoretical confirmation of this conclusion was later found in the paper by Waldron. Optimum ferrite to waveguide diameter ratio was found to be $[d_1/d_0]_{opt} = 0.23$, which is somewhat less than the 0.28 value predicted by Waldron. Samples of this diameter 3 inches long produced 45° rotation at $H = 150$ oersteds with average losses less than 0.3 db (0.2 db was also

frequently observed). The tolerance on the diameter is rather sharp: 1 per cent increase causes an easily detectable increase in the losses of about 0.05 db and 1 per cent decrease produced a rapid increase of the magnetic field (approximately 20 per cent).

Faraday rotation is highly frequency-sensitive and measures must be taken to avoid unfavorable effects in devices like isolators or circulators, where the angle of rotation must be kept constant over a substantial frequency band. Various methods of broadbanding were tried in this laboratory and finally the Rowen³-Ohm⁴ method of dielectric counterbalance was adopted, with some modifications. The effect of reducing the dielectric constant of ferrite by surrounding it by a medium of $\epsilon > 1$ is clearly visible from the curves in Fig. 4. Waldron has observed in his paper that the ferrite di-

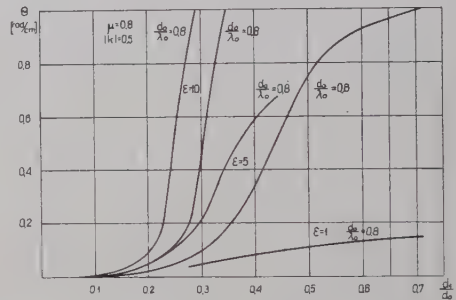


Fig. 4—Faraday rotation per unit length vs ferrite diameter. Influence shown of the surrounding medium and the frequency.

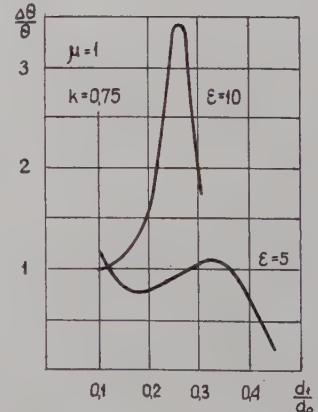


Fig. 5—Relative change in Faraday rotation with frequency ($d_0/\lambda_0 = 0.6 \div 0.8$) vs ferrite diameter.

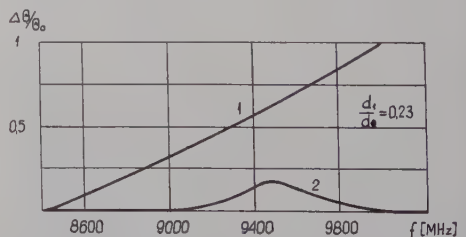


Fig. 6—Relative departures from $\theta = 45^\circ$ as a function of frequency for Ferroxcube B5. Effect of a polystyrene dielectric counterweight demonstrated (curve 2).

² S. Lewandowski, "Szerokopasmowy izolator ferrytowy ze strojeniem magnetycznym," *Przegląd Telekomunikacyjny*, Nr. 8-9, 284-288; September, 1958.

³ J. H. Rowen, "Ferrites in microwave application," *Bell Sys. Tech. J.*, vol. 32, p. 1333; November, 1953.

⁴ E. A. Ohm, "A broad-band microwave circulator," *IRE TRANS. ON MICROWAVE THEORY AND TECHNIQUES*, vol. MTT-4, pp. 210-217; October, 1956.

ameter also has an influence on frequency stability of Faraday rotation (Fig. 5). The combining of these two effects proved to give excellent results experimentally. The main advantage of this method lies in the possibility of using easily accessible and low-loss polystyrene instead of high permittivity dielectrics, and in the fact that the ferrite length has no effect on the broad-band performance. Fig. 6 shows the experimental results for Ferroxcube B5, obtained with a 3-inch-long sample of optimum diameter.

S. J. LEWANDOWSKI

J. KONOPKA

Warsaw Technical University
Dept. of Ultrashort Wave Techniques
Warsaw, Poland

Equivalence of 0 and -1 Space Harmonics in Helical Antenna Operation*

In considering the propagation of electromagnetic waves along helical conductors using the Tape Helix approximation, it is well known¹ that the solution contains an infinite number of space harmonics. The phase constants of these harmonics are related by

$$\beta_m = \beta_0 + \frac{2\pi m}{p},$$

where β_0 is the phase constant of the fundamental, p is the helical pitch and m is any integer including zero. It has been shown by Watkins² that as far as axial propagation is concerned, it is the -1 space harmonic which is responsible for the operation of the helical antenna. If, however, propagation along the conductor is considered, then the correct space harmonic to be considered is the fundamental as used originally by Sensiper.³ It is easy to show that both approaches lead to identical results, the proof being as follows.

Let the phase shift between adjacent turns of the helix be denoted by θ with the subscript 0 or -1; depending on whether the fundamental or the -1 space harmonic is being considered. Then

$$\theta_0 = \frac{L}{\lambda_0} \cdot 2\pi$$

where L is the length of 1 helical turn and λ_0 is the fundamental wavelength. Denoting the axial velocity of the fundamental by v_0 , the conductor phase velocity for the fundamental is $v_0/\sin \psi$, where ψ is the helical pitch angle, so that

$$\theta_0 = \frac{L f}{\left(\frac{v_0}{\sin \psi}\right)} \cdot 2\pi$$

$$= \frac{2\pi p f}{v_0}.$$

Similarly,

$$\theta_{-1} = \frac{2\pi p f}{v_{-1}},$$

where v_{-1} is the axial phase velocity of the -1 space harmonic. This is related to the fundamental axial phase velocity v_0 by

$$\frac{v_{-1}}{v_0} = \frac{\beta_0 a}{\beta_0 a - \cot \psi}$$

so that θ_{-1} eventually simplifies to

$$\theta_{-1} = \frac{2\pi p f}{v_0} - 2\pi,$$

which is identical with the expression for θ_0 except for a difference of 2π which is not significant.

Therefore, it is equally valid to consider either the fundamental or the -1 space harmonic, the first relating to propagation along the conductor, and the second to propagation axially.

As these phase velocities apply to an infinite helix, it is not possible to use them directly for the finite antenna, since it has been found by Kraus⁴ that the phase velocity is also a function of the length of the antenna. Nevertheless, it is known⁵ that the solution for the infinite case may be used as a means of estimating the bandwidth of the antenna for any pitch angle ψ , and it is now shown that both axial and conductor propagation give identical results.

T. S. MACLEAN

Dept. of Engrg.

University of Edinburgh
Edinburgh, Scotland

D. A. WATKINS

Electrical Engrg. Dept.

Stanford University
Stanford, Calif.

* J. D. Kraus, "Antennas," McGraw-Hill Book Co., Inc., New York, N. Y.; 1950.

² T. S. M. Maclean and R. G. Kouyoumjian, "Bandwidth of the Uniform Helical Antenna," presented at URSI Symposium on Electromagnetic Theory, University of Toronto, Toronto, Can.; June, 1959.

Application of Perturbation Theory to the Calculation of ω - β Characteristics for Periodic Structures*

The effect of small periodic changes in the physical dimensions of closed periodic structures can be investigated using the perturbation theory developed by Müller¹ and later by Slater.² From this theory the frac-

tional change in the natural frequency, ω , of a resonant cavity caused by the introduction into the cavity of a small conducting object of volume, τ , is given by

$$\delta\omega/\omega = \frac{1}{2} \frac{\int_{\tau} (\mu_0 H^2 - \epsilon_0 E^2) dV}{\int_v \epsilon_0 E^2 dV}. \quad (1)$$

The integration in the numerator extends only over the volume of the perturbing object, whereas that in the denominator extends over the entire volume of the cavity, and E and H are the amplitudes of the electric and magnetic fields.

A commonly used technique for determining the ω - β characteristic for a closed periodic structure consists of constructing a resonator from an appropriately chosen length of the structure and determining the natural frequencies of the resonator which correspond to the field configurations of interest.³ If the fields within the unperturbed structure are known, (1) may be used to compute the effect of small changes in the physical dimensions on these natural frequencies. This technique has been used by Vanhuyse⁴ in the construction of a linear accelerator using a disk-loaded circular waveguide.

If the perturbations are periodic and if the period of the perturbation is an integral multiple of the fundamental period of the unperturbed structure, the resonant cavity technique may be used to determine the ω - β characteristic for the perturbed structure. For this case (1) may be used to relate the ω - β characteristic for the perturbed structure to that for the unperturbed structure.

As an illustration, let the initial unperturbed structure be a uniform disk-loaded circular waveguide of radius b , and let the perturbed structure comprise cavities alternately of radius b_- and b_+ as shown in Fig. 1.

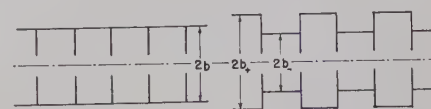


Fig. 1—Uniform and perturbed disk-loaded circular waveguides.

If the average volume per cell is unchanged by the perturbation and if $b_+ - b \ll b$, it is found that the ω - β characteristic for the perturbed structure coincides with that for the uniform structure except when the phase shift per section in the unperturbed structure is $\pi/2$. For this situation (which corresponds to a π phase shift per section in the perturbed structure), two frequencies are found, indicating the presence of a stop band. The width of the stop band is given by the difference between these two frequencies.

* Received by the PGMTT, October 20, 1959.
¹ S. Sensiper, "E.M. wave propagation on helical structures," Proc. IRE, vol. 43, pp. 149-161; February, 1955.

² D. A. Watkins, "Topics in Electromagnetic Theory," John Wiley and Sons, Inc., New York, N. Y.; 1958.

³ S. Sensiper, "E.M. wave propagation on Helical Conductors," M.I.T. Res. Lab. Tech. Rept. No. 194; 1951.

* Received by the PGMTT, November 2, 1959. This work was supported in part by the U. S. Army Signal Engrg. Labs., Fort Monmouth, N. J., under Contract DA 36-039 SC-78254.

¹ J. Müller, "Untersuchung über elektromagnetische hohlräume," Hochfrequenz und Elektroak., vol. 54, p. 157; November, 1939.

² J. C. Slater, "Microwave Electronics," D. Van Nostrand Co., Inc., Princeton, N. J., p. 80; 1950.

³ B. Epsztajn and G. Mourier, "Définition, mesure et caractères des vitesses de phase dans les systèmes à structure périodique," Ann. Radiodélectricité, vol. 10, p. 64; January, 1955.

⁴ V. J. Vanhuyse, "On the proper frequencies of terminated corrugated waveguides with slightly different diameters," Physica, vol. 21, p. 603; July, 1955.

Although calculations of this type do not predict the proper behavior for the ω - β characteristic near stopbands resulting from a periodic perturbation, they do predict the occurrence and width of such stop bands.

MURRAY D. SIRKIS
Microwave Electronics Lab.
Dept. of Electrical Engrg.
Rutgers the State University
New Brunswick, N. J.

Ice as a Bending Medium for Waveguide and Tubing*

Bending waveguide and metal tubing is very often a difficult and time-consuming task. Low melting temperature alloys are at times difficult to remove from waveguide and tubing. The piece to be bent may be filled with water which is then frozen by dry ice, liquid nitrogen, or by a deep freeze. In some applications where the piece to be bent is integral with a larger system, a block of dry ice may be held against it to freeze only the portion of water around the section to be bent. The use of these low temperatures causes not only the water to freeze into quite small crystals (which act like a sand packing), but also prevents the ice from melting because of the pressure of bending.

Several tests were performed on thin walled aluminum tubing and P -band brass waveguide. It was found that in comparison to low melting alloys the bends were identical within the statistical variation of samples. The time required for the operation was considerably shorter.

FRANKLIN S. COALE
Microwave Engrg. Labs., Inc.
Palo Alto, Calif.

* Received by the PGMTT, November 2, 1959.

On Higher-Order Hybrid Modes of Dielectric Cylinders*

In the course of investigations into the properties of various surface wave structures,¹ it became necessary to investigate hybrid modes on dielectric cylinders for modes of order n , where $n > 1$. The case $n = 1$ has received extensive treatment in the literature [1]–[6].

The radial dependence of the axial fields is as $J_n[\rho(p/a)]$ inside the dielectric cylinder and $K_n[q(\rho/a)]$ outside, where ρ is the radial

cylindrical coordinate, a is the radius of the cylinder, p and q are radial eigenvalues, and n is the rank of the mode.

The requirement of continuity of the fields at the boundary leads, in the usual manner, to the characteristic equation involving Bessel functions and their derivatives. This was first given by Schelkunoff [4]. The derivatives of Bessel functions may be eliminated from this equation by the use of identities such as given by Watson [8], to yield the simple form

$$(J^+ + K^+)(\epsilon J^- - K^-) + (J^- - K^-)(\epsilon J^+ + K^+) = 0, \quad (1)$$

where

$$J^- = \frac{J_{n-1}(p)}{pJ_n(p)}, \quad J^+ = \frac{J_{n+1}(p)}{pJ_n(p);}$$

$$K^- = \frac{K_{n-1}(q)}{qK_n(q)}, \quad K^+ = \frac{K_{n+1}(q)}{qK_n(q);}$$

and ϵ is permittivity of dielectric cylinder relative to surrounding medium.

The cutoff values of the parameter p are of great interest; they may be obtained by letting $q \rightarrow 0$ in the characteristic equation. To keep the terms finite requires that the equation be multiplied by an appropriate power of q before the limit is taken. If it is assumed that J^- is finite at cutoff, it is sufficient to multiply the equation by q^2 to obtain a solution for the cutoff values of p ; this was given by Schelkunoff [4]. However, if this assumption is not made, an additional solution may be determined. This will be outlined below.

Multiplying the characteristic equation by $[qpJ_n(p)]^2$ gives

$$(\epsilon^2 J_{n+1} + q^2 K^+ p J_n)(\epsilon J_{n-1} - p J_n K^-) + (J_{n-1} - p J_n K^-)(\epsilon q^2 J_{n+1} + q^2 K^+ p J_n) = 0. \quad (2)$$

Taking the limit as $q \rightarrow 0$ and noting that

$$K^- \rightarrow \frac{1}{2(n-1)}$$

and $q^2 K^+ \rightarrow 2n$ one obtains

$$2n p J_n \left((\epsilon + 1) J_{n-1} - \frac{p J_n}{n-1} \right) = 0. \quad (3)$$

The solutions are, for $n > 1$,

$$\frac{J_{n-1}(p)}{p J_n(p)} = J^- = \frac{1}{(n-1)(\epsilon + 1)}, \quad (4)$$

$$J_n(p) = 0, \quad p \neq 0. \quad (5)$$

Eq. 4 is given by Schelkunoff [4]. The very significant exclusion of the $p = 0$ solution of (5) as a cutoff condition is based on the fact that for $q \rightarrow 0$ and $p \rightarrow 0$, (1) becomes, since

$$J^- \rightarrow \frac{2n}{p^2}, \quad J^+ \rightarrow \frac{1}{2(n+1)},$$

$$\left(\frac{1}{2(n+1)} + \frac{2n}{q^2} \right) \left(\frac{2n\epsilon}{p^2} - \frac{1}{2(n-1)} \right) + \left(\frac{2n}{p^2} - \frac{1}{2(n-1)} \right) \left(\frac{\epsilon}{2(n+1)} + \frac{2n}{q^2} \right) = 0. \quad (6)$$

When the finite terms are neglected in comparison with the infinite terms, it is seen that this is not satisfied at $q = 0$, $p = 0$ for any $n > 1$. However, the $p = q = 0$ solution,

i.e., the condition for "no cutoff," is valid for $n = 1$ [1].

The asymptotes for the p - q curves are of interest. For $q \rightarrow \infty$ the characteristic equation becomes simply $2\epsilon J^- J^+ = 0$, with solutions at $J_{n-1}(p) = 0$ and $J_{n+1}(p) = 0$. It will be seen that the first of these is associated with the modes satisfying the first or Schelkunoff cutoff condition, the second with the alternate cutoff condition given here in (5).

Because of the oscillatory character of $J_n(p)$, the characteristic equation is satisfied by an infinite set of values of p for any given q , in particular also for $q = 0$. These sets of p 's span an infinite set of modes which may propagate along the dielectric rod. It is now seen that the existence of the alternate cutoff condition indicates the existence of an infinite set of modes that interlace the modes that satisfy the cutoff condition of (4). This and other salient characteristics of the doubly infinite set of modes are presented qualitatively in Fig. 1, with the $n = 1$ case treated by Beam [1] included for comparison in Fig. 2. The curve shapes are based upon the detailed numerical solution of (2) obtained with an IBM 650 computer for $n = 2, 6$ for a wide range of ϵ .

The significance of Fig. 1 may be summarized as follows.

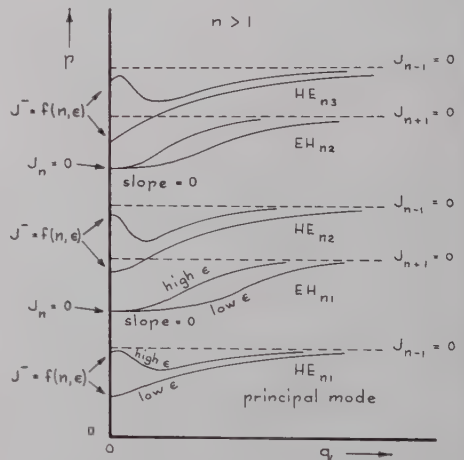


Fig. 1—Loci of solutions of the characteristic equation (1) for $n > 1$.

$$\epsilon(n, \epsilon) = \frac{1}{(n-1)(\epsilon + 1)}.$$

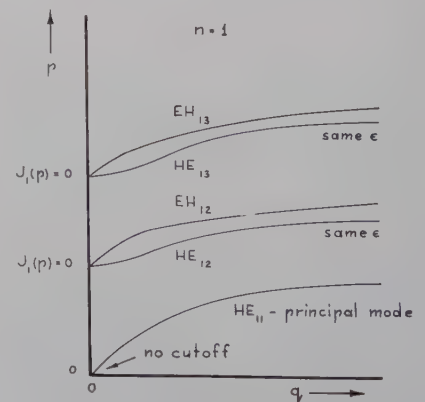


Fig. 2—Curves of p and q for $n = 1$.

* Received by the PGMTT, November 5, 1959. This note is based on studies undertaken pursuant to Contract AF 19(604)3879 with the Air Force Cambridge Research Center.

¹ Report in preparation.

1) There is a set of modes that alternates with those identified with the cutoff condition of Schelkunoff in (4). Their cutoff condition is given by (5).

2) The modes identified with (4) have a cutoff that depends on ϵ , whereas the modes satisfying the alternate condition have a single cutoff value of p for all ϵ .

3) For $n > 1$ all modes have some cutoff value. The principal mode for $n=1$ has no cutoff. There is no "degeneracy" of the modes for $n > 1$ as there is for $n=1$ modes, as described by Beam [1]; that is, each mode has its own distinct cutoff point.

4) There is a unique principal mode for all n .

5) The existence of an additional mode between successive Schelkunoff modes reduces the upper frequency limit at which a pure principal mode may propagate below what the limit would be if only Schelkunoff modes existed, as follows.

The p - q curves may be used to determine the frequency dependence of the mode propagation with the aid of the additional relation

$$b^2 + q^2 = R^2 \quad (7)$$

where $R = (2a/\lambda_0)\pi\sqrt{\epsilon-1}$. This indicates that for a given dielectric rod of radius a , the actual values of p and q may be found at the intersection of the p - q curves with a superimposed circle of radius R corresponding to the frequency of operation for which the free-space wavelength is λ_0 . To insure the propagation of a unique mode, the circle must intersect the p - q curves only once. For the principal mode, this means that the upper limit of R , and hence of frequency, is determined by the requirement that $R < p_0$, where $J_n(p_0) = 0$. The lower limit of frequency is of course determined by the cutoff value of p (see Fig. 3).

It is now seen that there is no degeneracy to impose a notational distinction, so that the modes could be simply numbered successively. In the interest of conforming to

the nomenclature for $n=1$, however, and in order to preserve the distinction between the modes that satisfy the Schelkunoff cutoff condition and those that satisfy the alternate condition, the HE_{nm} , EH_{nm} distinction is retained here, starting with HE_{n1} for the principal mode.

An attempt to verify a possible distinction between H - and E -type modes for the general case of any n , as suggested by Wegener and others [1], [7] for $n=1$, has not been found by the authors to lead to consistent results. The designation here of a mode as HE_{nm} is hence not to be construed as an indication that the mode must be H type.

The existence of the alternate cutoff condition, (5), has been confirmed independently using approximation methods by Snitzer [9] in the course of his investigation into the optical properties of thin fibers.

S. P. SCHLESINGER

P. DIAMANT

A. VIGANTS

Dept. of Electrical Engrg.

Columbia University

New York, N. Y.

BIBLIOGRAPHY

- [1] R. E. Beam, M. M. Astrahan, W. C. Jakes, H. M. Wachowski, and W. L. Firestone, "Dielectric Tube Waveguides," Northwestern University, Evanston, Ill., Rept. ATI 94929, ch 5; 1959.
- [2] D. D. King, "Dielectric image line," *J. Appl. Phys.*, vol. 23, pp. 699-700; June, 1952.
- [3] S. P. Schlesinger, and D. D. King, "Dielectric image lines," *IRE TRANS. ON MICROWAVE THEORY AND TECHNIQUES*, vol. MTT-6, pp. 291-299; July, 1958.
- [4] S. A. Schelkunoff, "Electromagnetic Waves," D. Van Nostrand Co., Inc., New York, N. Y., p. 427; 1943.
- [5] W. M. Elsasser, "Attenuation in a dielectric circular rod," *J. Appl. Phys.*, vol. 20, pp. 1193-1196; December, 1949.
- [6] C. H. Chandler, "An investigation of dielectric rod as waveguide," *J. Appl. Phys.*, vol. 20, pp. 1188-1192; December, 1949.
- [7] H. Wegener, "Ausbreitungsgeschwindigkeit, Wellenwiderstand, und Dämpfung elektromagnetischer Wellen an dielektrischen Zylindern," Forschungsbericht Nr. 2018, Deutsch Luftfahrtforschung, Vierjahresplan, Institut für Schwingungsforschung, Berlin; August 26, 1944. (Document No. ZWB/FB/Re/2018, CADO Wright-Patterson AF Base, Dayton, Ohio.)
- [8] G. N. Watson, "A Treatise on the Theory of Bessel Functions," The Macmillan Co., New York, N. Y.; 1944.
- [9] E. Snitzer, American Optical Co., Southbridge, Mass. Personal communication.

less, relative to the input, this is not an easy fact to observe experimentally. However, if the measured VSWR and isolation of such a hybrid are inconsistent, one may reflect that this must be because of

- 1) experimental error,
- 2) mismatch of terminations or bends introduced for purposes of measurement,
- 3) asymmetry allowed by manufacturing tolerances,
- 4) ohmic loss.

Proof: Let arms 1-3 be the main guide, and arms 2-4 the auxiliary guide. If the hybrid is fully symmetric its scattering matrix will have the form,

$$S = \begin{bmatrix} A & B & C & D \\ B & A & D & C \\ C & D & A & B \\ D & C & B & A \end{bmatrix},$$

where A and B are small, and C and D have approximately equal amplitude. If the hybrid is lossless, S is unitary, which gives us

$$\text{Re}(A\bar{B}) + \text{Re}(C\bar{D}) = 0, \quad (1)$$

$$\text{Re}(A\bar{C}) + \text{Re}(B\bar{D}) = 0, \quad (2)$$

$$\text{Re}(A\bar{D}) + \text{Re}(B\bar{C}) = 0, \quad (3)$$

where the bar denotes the complex conjugate. Let $A = A_1 + jA_2$, and similarly for B and D , and let the reference planes be chosen so that C is real. Then (1) shows that D_1 is a second-order small quantity, leading to the first property that C and D are in quadrature.

Putting $D = jC$, we have from (2) and (3), respectively,

$$A_1 = -B_2,$$

$$A_2 = -B_1.$$

Hence $A = -j\bar{B}$, and A and B have the same amplitude.

I wish to thank T. A. Williams for helpful comments, and the Executive of the AEI Electronic Apparatus Division and the Board of the BTH Company for permission to publish this note.

J. M. SMITH

Military Radar Engrg. Dept.

Electronic Apparatus Div.

Associated Electrical Industries, Ltd.

Trafford Park, Manchester, Eng.

A Property of Symmetric Hybrid Waveguide Junctions*

It is well known that in symmetric hybrid junctions such as the short-slot, branched-guide, and transvar types, the signals in the main and auxiliary guides are in phase quadrature. Another property of fully symmetric lossless hybrids is that if all the arms are matched, the amplitudes of the waves traveling in the reverse direction in the main and auxiliary guides are equal. A proof is given below.

Since in a well-designed hybrid these amplitudes will be of the order of 0.03 or

Attenuation in a Resonant Ring Circuit*

The use of a resonant circuit will permit raising the strength of electromagnetic fields to values considerably higher than that available directly from a transmitter. In the usual resonant cavity, standing waves exist which may raise some doubt as to the usefulness of this method for testing certain

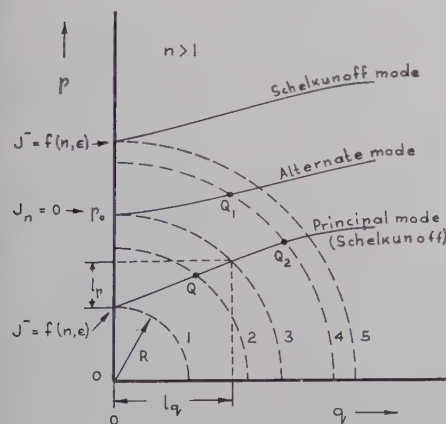


Fig. 3—Determination of operating point Q corresponding to a given frequency by superposition of a circle of radius R on p - q curves.

$$f(n, \epsilon) = \frac{1}{(n-1)(\epsilon+1)}, \quad R = \frac{2a}{\lambda_0} \pi \sqrt{\epsilon-1}.$$

- 1) Lower limit of R .
 - 2) Typical R .
 - 3) Upper limit of R .
 - 4) $R > p_0$.
 - 5) Upper limit of R in absence of alternate modes.
- Q : operating point for typical R . Q_1, Q_2 : two operating points for $R > p_0$: impure mode. l_p, l_q : useful ranges of p, q , for pure principal mode.

* Received by the PGMTT, November 12, 1959.

* Received by the PGMTT, November 13, 1959.

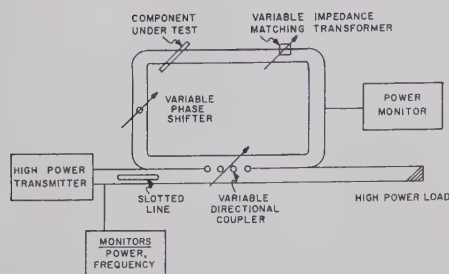


Fig. 1—Resonant ring circuit.

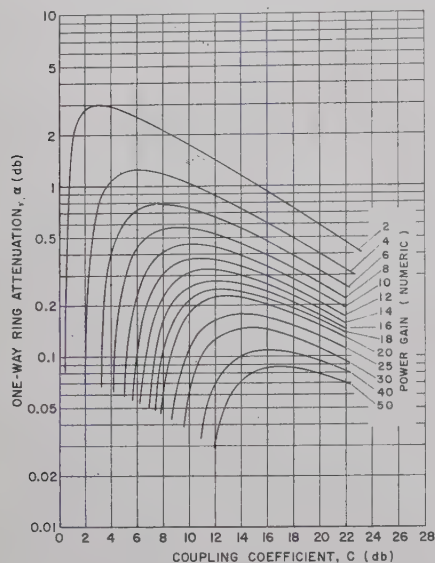


Fig. 2—Resonant ring characteristics with power gain as the parameter.

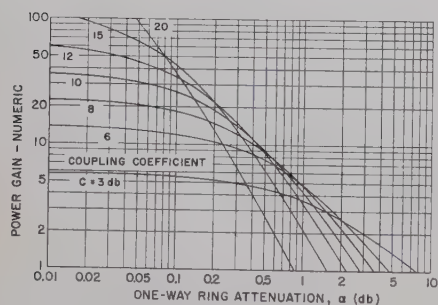


Fig. 3—Resonant ring power gain with coupling coefficient as the parameter.

is very sensitive to the attenuation in the ring circuit.^{2,3} The purpose of this brief paper is to illustrate these dependences in convenient graphical form.

If the ring circuit is properly matched in impedance⁴ and the phase shifter is adjusted for resonance condition, the power "multiplication" or gain PG is given by

$$PG = \left[\frac{C}{1 - k\sqrt{1 - C^2}} \right]^2,$$

where

C = voltage coupling coefficient of the directional coupler, less than unity,
 $k = 10^{-\alpha/20}$, a voltage ratio less than unity, and
 α = one-way attenuation around the ring, in db.

This power gain equation is plotted in Figs. 2 and 3. For example, if a power gain of 20 is desired and the ring circuit attenuation is 0.2 db, either an 11- or 16-db coupler is needed.

K. TOMIYASU

General Electric Microwave Lab.
 Palo Alto, Calif.

⁴ K. Tomiyasu, "Effect of a mismatched ring in a traveling-wave resonant circuit," IRE TRANS. ON MICROWAVE THEORY AND TECHNIQUES, vol. MTT-5, p. 267; October, 1957.

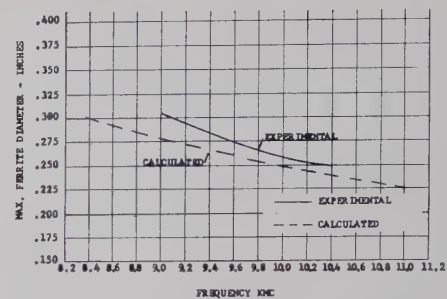


Fig. 1—Calculated and experimental curves of maximum diameter for suppression of higher-order modes as a function of frequency for RG 52/u waveguide. Device uses R-1 ferrite.

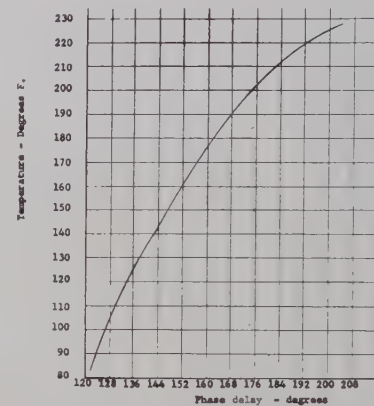


Fig. 2—Change of phase length with temperature using constant bias current of 85-ampere turns. RF frequency, 10.0 kmc. R-1 ferrite 0.250 diameter.

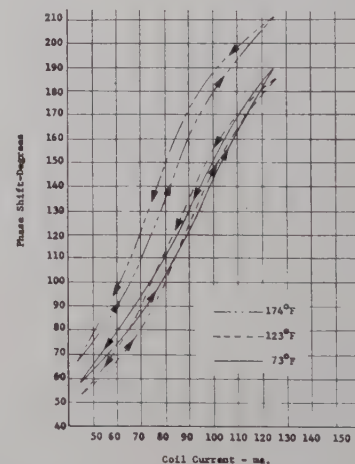
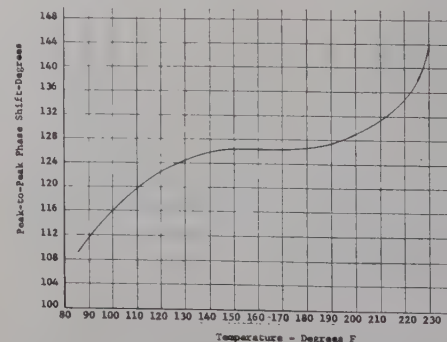


Fig. 3—Phase modulation characteristic of the phase shifter using an 85-ampere turn bias for various temperatures. RF frequency, 10.0 kmc.

Fig. 4—Peak-to-peak phase modulation as a function of temperature with a constant bias of 85 ma, and a modulation current of ± 60 ma at 500 cps.

components. This is because maximum electric fields do not occur at the same location as the maximum magnetic fields. To overcome this doubt, a resonant ring circuit can be employed^{1,2,3} (see Fig. 1). In this circuit, the waves are ideally unidirectional and it is possible to obtain "power-level multiplication" of 10 to 50 times the transmitter output. The amount of multiplication depends on the value of the directional coupler and

Reciprocal Ferrite Phase Shifters* ON HIGHER ORDER MODES

The Reggia-Spencer phase shifter¹ has been the subject of a great deal of investigation²⁻⁴ because of the large amounts of phase shift possible with a relatively simple construction.

Rizzi and Gatlin⁵ have proposed a model which qualitatively explains most of the observed phenomena associated with this type of phase shifter. Their explanation centers about the fact that only large amounts of phase shift are observed when the ferrite exceeds a critical diameter given by

$$d > \frac{C}{1.706f\sqrt{\epsilon}}, \quad (1)$$

* Received by the PGM-TT, November 13, 1959. The research reported herein has been sponsored by the Electronics Research Directorate of the Air Force Cambridge Research Center, Air Research and Development Command, under Contract AF19(604)-3467.

¹ F. Reggia and E. G. Spencer, "A new technique in ferrite phase shifting for beam scanning of microwave antennas," Proc. IRE, vol. 45, pp. 1510-1517; November, 1957.

² A. Clavin, "Reciprocal ferrite phase shifters in rectangular waveguide," IRE TRANS. ON MICROWAVE THEORY AND TECHNIQUES, vol. MTT-6, p. 334; July, 1958.

³ F. E. Goodwin and H. R. Senf, "Volumetric scanning of a radar with ferrite phase shifter," Proc. IRE, vol. 47, pp. 453-454; March, 1959.

⁴ J. A. Weiss, "A phenomenological theory of the Reggia-Spencer phase shifter," Proc. IRE, vol. 47, pp. 1130-1137; June, 1959.

⁵ P. A. Rizzi and B. Gatlin, "Rectangular guide ferrite phase shifters employing longitudinal magnetic fields," Proc. IRE, vol. 47, pp. 1130-1137; June, 1959.

¹ P. J. Sferazza, "Traveling-wave resonator," Tele-Tech., vol. 14, pp. 84-85, 142-143; November, 1955.

² L. Milosevic and R. Vautey, "Traveling-wave resonator," IRE TRANS. ON MICROWAVE THEORY AND TECHNIQUES, vol. MTT-6, pp. 136-143; April, 1958.

³ F. J. Tischer, "Resonance properties of ring circuits," IRE TRANS. ON MICROWAVE THEORY AND TECHNIQUES, vol. MTT-5, pp. 51-56; January, 1957.

where

C = velocity of light,
 f = frequency,
 ϵ = dielectric constant.

It is at this diameter that orthogonal TE_{11} modes can propagate in the ferrite acting as a dielectric waveguide. We have observed an additional phenomena which can also be explained by this dielectric waveguide model. This effect is discussed by Weiss⁴ and is associated with the large amount of periodic loss which occurs as one increases the microwave frequency above a critical value. I believe a simple explanation of this behavior can be attributed to the excitation of the next higher order mode, the TM_{01} . This mode can only propagate in the ferrite region and is not matched to the rectangular waveguide by the transformer that matches the TE_{11} mode. Multiple reflections, therefore, occur between the ferrite ends with periodic losses resulting. In a similar manner to that used by Rizzi and Gatlin, the frequency at which this mode propagates is computed by

$$f > \frac{C}{1.309 d \sqrt{\epsilon}} \quad (2)$$

The dashed curve in Fig. 1 has been calculated using this relationship with $\epsilon=13$. Also presented is an experimental curve obtained with R-1 ferrite. The two curves show a general agreement. Some of the differences in the two curves can be possibly explained by the value of ϵ used as well as the effect of the waveguide height. Since all the microwave energy is not trapped to the ferrite, especially at low applied fields, a reduction in the narrow dimension should raise the frequency at which the TM_{01} mode can propagate. We have experimentally observed the above to be true.

ON TEMPERATURE SENSITIVITY

The temperature sensitivity of the Reggia-Spencer phase shifter has been of concern in those applications which require precise phase control or phase modulation. In applications that require both phase advances and delays, bias currents are required because of the reciprocal nature of

the phase shifter. The phase delay, as a function of temperature at a bias point of 85 ampere-turns for R-1 ferrite 1.4 inches long with 0.6-inch conical tapers, is shown in Fig. 2. It can be observed that over very large temperature ranges as much phase shift can be obtained from this effect as from applied magnetic fields.

The type of phase modulation characteristics obtainable about the 85-ampere-turn bias points as a function of temperature, is shown in Fig. 3. These curves are plotted on a relative basis; *i.e.*, they all use the same zero field phase-shift value. Note that the peak-to-peak phase shift is quite constant. This is illustrated by Fig. 4, which indicates the variation in the peak-to-peak phase shifts as a function of temperature. There is a fairly large range of temperature possible with little change in phase modulation characteristics. Therefore, if one desires to use these devices as phase modulators it is possible to do so with little change in the index of modulation with temperature.

ALVIN CLAVIN
 RANTEC Corporation
 Calabasas, Calif.

Contributors

Barbara A. Begg was born in Boston, Mass. on July 2, 1920. She received the A.B. degree from Boston University, in 1942; a special certificate in aeronautical engineering from New York University, in New York City, in 1944; and in 1956, the masters degree in library science from Carnegie Institute of Technology in Pittsburgh, Pa.

She was employed in the Experimental Flight Test Group at Chance Vought Aircraft, Dallas, Texas; in the Wind Tunnel Computing Section at North American Aviation; and, from 1950 to 1955, in the Aircraft Gas Turbine Division of General Electric Company. In 1956, she joined the ITT Laboratories, Nutley, N. J., as assistant librarian. She became the engineering librarian at Drexel Institute of Technology, Philadelphia, Pa. in July, 1959.



B. A. BEGG

Miss Begg belongs to the AIEE, Special Libraries Association, American Libraries Association, and American Documentation Institute.



Robin M. Chisholm (S'52-A'54) was born in London, Can., in January 11, 1930. He attended Queen's University in Kingston, Ontario, where he received the B.S. degree in engineering physics in 1952. He studied in the graduate school of the University of Toronto where he received the M.A.Sc. degree in electrical engineering in 1954 and the Ph.D. degree in 1958.



R. M. CHISHOLM

Since graduation he has worked during the summers for the National Research Council of Canada at Ottawa, Ontario. In

1956 he joined the staff of the Department of Electrical Engineering at Queen's University, Kingston, Ontario, where he is at present an assistant professor.

He is a member of the Association of Professional Engineers of the Province of Ontario.



John R. Cogdell was born on May 24, 1936 in Quanah, Tex. He received the B.S. degree in electrical engineering in May, 1958, and the M.S. degree in electrical engineering in August, 1959, both from the University of Texas, Austin.



J. R. COGDELL

From June, 1958 to July, 1959 he was research engineer at the Electrical Engineering Research Laboratory at the University of Texas.

Since July, 1959, he has been on the staff of Lincoln Laboratories, Massachusetts Institute of Technology, Cambridge.

Mr. Cogdell is a member of Tau Beta Pi and Eta Kappa Nu.



William Culshaw (SM'57) was born in Lancashire, Eng., on February 5, 1914. He received the B.Sc. degree in physics from the University of Sheffield in 1941, the B.Sc. degree in mathematics from the University of London in 1947, and the Ph.D. degree from the University of London in 1952.



W. CULSHAW

From 1942 to 1954 he was a staff member of the Telecommunications Research Establishment, Malvern, Eng., where he was with the Microwave Receiver and the Millimeter Wave divisions. From 1954 to 1956 he was a member of the Radio Physics Laboratory, Ottawa, Can., where he worked on scattering, and antenna problems. Since 1956, he has been a member of the Microwave Physics Section of the National Bureau of Standards, Boulder Laboratories, Boulder, Colo., where his primary interests are in millimeter wave research and microwave optics.

Dr. Culshaw is a member of the Scientific Research Society of America.



Andrew P. Deam (M'51) was born in Dallas, Tex. on December 10, 1917. He received the B.S. degree in electrical engineering from Texas A & M College, College Station, in 1940, and the M.S. degree in electrical engineering from The University of Texas, Austin, in 1949.



A. P. DEAM

During 1941 and 1942 he was employed by the Dallas Power and Light Company as an assistant engineer.

Since 1942, he has been employed by The University of Texas, both in a teaching and research capacity, and is presently a radio engineer at the Electrical Engineering Research Laboratory, where his work has been primarily related to radio-wave propagation.



James E. Eaton (A'46-M'47) was born in New York, N. Y. on March 27, 1912. He received the B.S. and Ph.D. degrees in 1936 and 1939, respectively, both from Yale University, New Haven, Conn.

He taught at Hofstra College, Hempstead, N. Y., until 1941 where he was associ-

ate professor and chairman of the department of mathematics. He was then appointed to the faculty of Queens College, Flushing, N. Y., where his present rank is associate professor of mathematics. During the latter part of the war, he was a member of the Antenna Group of Radiation Laboratory, Massachusetts Institute of Technology, Cambridge, Mass. He continued his work on micro-



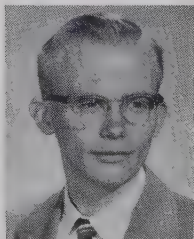
J. E. EATON

wave antennas at the Naval Research Laboratory, Washington, D. C., where he was in residence until 1947, when he returned to Queens College. He remained associated with N.R.L. however, as mathematician and consultant until 1957.

Dr. Eaton is a member of Sigma Xi, the American Mathematical Society, and the Mathematical Association of America.



Charles A. Finnila (S'58) was born in San Francisco, Calif. on January 6, 1937. He is a senior in electrical engineering at the University of California, Berkeley.



C. A. FINNILA

During the summer periods between academic years, he has been employed by Mare Island Naval Shipyard, Vallejo, Calif. (1957); Huggins Laboratories, Inc., Sunnyvale, Calif. (1958); and the Electronics Research Laboratory, University of California, Berkeley, Calif. (1959).

Mr. Finnila is a member of Tau Beta Pi and Eta Kappa Nu. In August, 1959, he received one of the WEMA scholarships awarded each year at WESCON to outstanding engineering students.



Max P. Forrer (A'54-SM'57) was born on October 15, 1925, in St. Gallen, Switzerland. He received the Diploma in electrical engineering from the Swiss Federal Institute of Technology, Zurich, in 1950, and the Ph.D. degree from Stanford University, Stanford, Calif., in 1959.



M. P. FORRER

From 1951 to 1952 he was with the Standard Telephone and Radio Corporation (IT&T) in Zurich, where he was concerned with carrier telephone developments. After coming to the United States in 1952, he joined the Western Electric Com-

pany at Kearny, N. J., working on Microwave Radio Relay systems. Since February, 1955, he has been a member of the technical staff at the General Electric Microwave Laboratory at Palo Alto, Calif., and he also attended Stanford University under the General Electric Honors Cooperative Program. He has been engaged in studies on microwave harmonics suppression, microwave technology for computers, electron multifactor devices and klystron tubes.

Dr. Forrer is a member of Sigma Xi.



J. K. Hunton (SM'57) was born in Montreal, Canada on December 20, 1921. He received the B.A.Sc. degree in engineering physics from the University of Toronto, Canada, in 1943 and served in the Royal Navy as a radar officer until 1946. He attended Massachusetts Institute of Technology, Cambridge, where he was an instructor in electrical engineering and received the S.M. degree in 1948.



J. K. HUNTON

At this time he joined the Hewlett-Packard Company in Palo Alto, Calif. where he is now in charge of the waveguide instruments development group.



E. T. Jaynes (SM'54) was born in Waterloo, Iowa, on July 5, 1922. He attended Cornell College, Mount Vernon, Iowa, and Iowa State University, Iowa City, receiving the B.A. degree in physics from the latter in 1942. He studied in the graduate school of the University of California in Berkeley and at Princeton University, Princeton, N. J., from which he received the M.A. degree in 1948 and



E. T. JAYNES

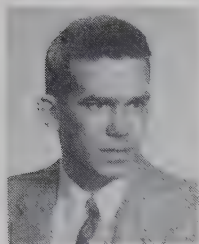
the Ph.D. degree in theoretical physics in 1950.

From 1942 to 1946, he was engaged in microwave research and development as a project engineer at the Sperry Gyroscope Co., Garden City, N. Y., and in the combined research group of the Naval Research Laboratory.

Since 1950, he has been on the faculty of Stanford University, Stanford, Calif., At present he holds the titles of associate professor in the microwave laboratory and lecturer in physics.

Mr. Jaynes is a member of the American Physical Society, the American Association of Physics Teachers, Sigma Xi and the New York Academy of Sciences.

E. M. T. Jones (S'46-A'50-M'55-SM'56) was born in Topeka, Kans., in 1924. He received the B.S. degree in electrical engineering from Swarthmore College, Swarthmore, Pa., in 1944 and the M.S. and Ph.D. degrees in electrical engineering from Stanford University, Stanford, Calif., in 1948 and 1950, respectively. He was a radar maintenance officer in the U. S. Navy from 1944 to 1946. From 1948 to



E. M. T. JONES

1950 he was a research associate at Stanford University, working on the microwave local oscillator project. He joined the staff of Stanford Research Institute, Menlo Park, Calif., in 1950, and in 1957 he became head of the Microwave Group of the Electromagnetics Laboratory.

Dr. Jones is a member of Sigma Tau and RESA.



Howard E. King (A'46-M'55-SM'55) was born in Seattle, Wash., on October 16, 1924. He received the B.S.E.E. degree in 1945 from the University of Washington, Seattle, and the M.S.E.E. degree in 1955 from the University of Illinois, Urbana.



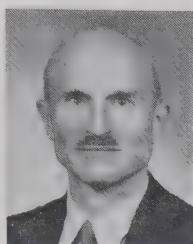
H. E. KING

From 1946 to 1952 he was a member of the broadcast section of the RCA Victor Division, designing FM and television transmitting antennas; he took part in the development of the Empire State Building multiple television antenna system. After a year with the Andrew Corporation, he was appointed as a research assistant of the Antenna Laboratory of the University of Illinois, where he remained until 1955. In 1955, he became a member of the technical staff of the Communications Division of the Ramo-Woolridge Corporation. Here he was engaged in the development of ground and airborne electronic counter measures, antennas, and components. In 1955 he joined the Space Technology Laboratories, Inc., Los Angeles, Calif., where he is presently employed.



Munich (Germany), and Cornell University, Ithaca, N. Y.

He served as teaching and research assistant at the University of Wisconsin in 1932-1934 and as instructor and assistant professor of physics at Lafayette College, Easton, Pa., in 1934-1937. The year 1937-1938 he spent in Germany as a Guggenheim Fellow. In 1938 he joined the faculty of Harvard University,



R. W. P. KING

Cambridge, Mass., where he advanced to the rank of professor in 1946. He is now Gordon McKay Professor of applied physics at Harvard University. In 1958 he studied and traveled abroad as a Guggenheim Fellow. His research has been primarily in the field of antennas, transmission lines, and microwave circuits.

Dr. King is a Fellow of the American Physical Society and the American Academy of Arts and Sciences, a corresponding member of the Bavarian Academy of Sciences, and a member of the American Association of University Professors and the American Association for the Advancement of Science. He is also a member of Phi Beta Kappa and Sigma Xi.



Hiroshi Kogō (M'55) was born on August 16, 1921, in Tokyo, Japan. He received the B.S. degree in electrical engineering in 1944 from the Tokyo Institute of Technology, and the Ph.D. degree in engineering in 1958 from the same institution.



H. KOGŌ

From 1946 to 1947 he was employed by the Nippon Acoustic Co., and from 1947 to 1952 he worked for the Electro-Communication University in Tokyo. Since 1952 he has been an assistant professor in the faculty of engineering, Chiba University, Chiba, Japan.

Dr. Kogō is concerned with the development of microwave circuits, special BALUN, antennas, television receivers and ITV.



Ellis Mount (M'56) was born in Connerville, Indiana, on September 25, 1921. He received the B.S. degree in physics from Principia College, Elsah, Illinois, in 1948, and the M.S. degree in physics from Northwestern University, Evanston, Ill., the following year. In 1950 he received an M.S. degree in Library Science from the University of Illinois.

He served for three years as a communications officer in the Air Force. He was on the staff of the John Crerar Library in Chicago, Illinois, from 1950-1951 and again from 1953-1955. From 1951-1953 he was librarian for the General Electric Company, Aircraft Nuclear Propulsion Project, Cincinnati, Ohio. Since 1955 he has been Chief Librarian for ITT Laboratories, a Division of International Telephone and Telegraph Corporation, Nutley, New Jersey.

Mr. Mount belongs to the Special Libraries Association and the American Documentation Institute.



Gilbert H. Owyang was born in Tientsin, China. He received the B.S. degree in electrical engineering from La Universitato Utopia, Shanghai, China, in 1944, and the S.M. degree in electrical engineering in 1950, and the Ph.D. degree in applied physics in 1959, both from Harvard University, Cambridge, Mass.



G. H. OWYANG

From 1944 to 1949, he worked with the Shanghai Power Company, China, as an engineer. He was on the engineering staff of Devanco, Inc., and Frank L. Capps and Company, both in New York, N. Y., between 1950 and 1954, and from 1955 to 1959, was a research assistant at Gordon McKay Laboratory, Harvard University. Since June 1959, he has been with the Radiation Laboratory of the University of Michigan, Ann Arbor.

Dr. Owyang is a member of Sigma Xi and the Harvard Engineering Society.



D. A. Parkes (S'57-M'58) was born on October 21, 1931, in Jacksonville, Florida. He received the Bachelor of Electrical Engineering degree, in 1958, from the University of Florida, in Gainesville.



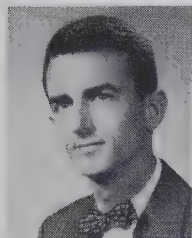
D. A. PARKES

In 1958, he joined the Sperry Microwave Electronics Company, in Clearwater, Florida, a division of the Sperry Rand Corporation. There, he has been engaged in the development of ferrite microwave components and solid-state devices.

H. J. Riblet (A'45-M'55-F'58), for a photograph and biography, please see page 306 of the July, 1959, issue of these TRANSACTIONS.



Lester A. Roberts (S'47-A'50) was born in Los Angeles, Calif., on July 31, 1925. He received the B.S. degree in electrical engineering from Iowa State College, Ames, in 1946, and the M.S. and Ph.D. degrees from Stanford University, Stanford, Calif., in 1947 and 1951, respectively.



L. A. ROBERTS

From 1950 to 1954 he was a research associate at the Electronics Research Laboratory, Stanford University,

engaged primarily in the study and development of traveling-wave tubes and related microwave devices. From 1954 to 1959 he was employed at Huggins Laboratories as chief engineer, where he directed design and development of traveling-wave tubes. In 1959 he joined the Watkins-Johnson Company as a member of the Technical Staff, where he is conducting research and development on microwave electron devices.

Dr. Roberts is a member of Sigma Xi, Tau Beta Pi, and Eta Kappa Nu.



Norman O. Robinson, Jr. (S'54-M'56) was born in Baltimore, Maryland on January 26, 1928. He received the B.S. degree from the University of Maryland, College Park, in 1955 and the M.S. degree from the University of Southern California, Los Angeles, in 1957, both in electrical engineering.



N. O. ROBINSON

He served with the U. S. Marine Corps as a radar technician and as an instructor in an advanced electronics school from 1946 to 1949. Recalled to active duty during the Korean War, he was a member of a team developing an automatic close air support bombing system at Point Mugu, Calif. He worked in the missile division of Sperry Gyroscope Company, Point Mugu, Calif., in 1952, and in the research and development department of Bendix Radio Company, Baltimore, Md., in 1953.

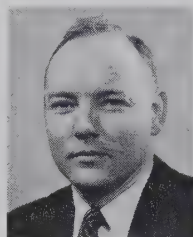
Mr. Robinson joined the technical staff of the Hughes Aircraft Company, Culver City, Calif., in 1955, as a member of the Master of Science fellowship program. He has been involved in the development of circuitry for pulse and pulse doppler radar systems, with emphasis on design of frequency and phase locked loops.

He is a member of Tau Beta Pi.

E. Schlömann, for a photograph and biography, please see page 126 of the January, 1960 issue of these TRANSACTIONS.



C. B. Sharpe (S'46-A'52) was born in Windsor, Ontario, Can., on April 8, 1926. He attended Northwestern University,



C. B. SHARPE

Evanston, Ill., and the University of Michigan, Ann Arbor, Mich., receiving the B.S. degree in electrical engineering from the latter in 1947. He received the S.M. degree from Massachusetts Institute of Technology, Cambridge, Mass., in 1949 and the Ph.D. degree from the University of Michigan in 1953, both in electrical engineering.

From 1953 to 1955 he served as assistant project officer in the guided missile branch of the U. S. Navy Bureau of Ordnance and as a technical aide in the Office of Naval Research.

Since returning to the University of Michigan in 1955, he has done research in microwave circuit theory, microwave measurements of ferroelectrics, and the application of solid-state materials to microwave devices.

He now holds the title of associate professor of electrical engineering at the University and is a faculty consultant to the Electronic Defense Group.

Mr. Sharpe is a member of Tau Beta Pi and Sigma Xi.



William Silvey was born in New York, N. Y. on April 13, 1931. He received the B.S. degree in applied physics in 1956 and the M.S. degree in applied physics in 1959 from the University of California, Los Angeles.



W. SILVEY

From 1956 to 1959, he was a member of the technical staff at Hughes Aircraft Co. Research Laboratories, Culver City, Calif. There Mr. Silvey worked in the Quantum Physics Section and was primarily concerned with microwave spectroscopy and maser research.

Since 1959, when he joined Space Technology Operations of Aeronutronic, a division of Ford Motor Company, Newport Beach, Calif., he has been engaged in the coordination and integration of experiments in Cis-Lunar research vehicles.

Mr. Silvey is a member of the American Physical Society.

Malcolm L. Stitch (SM'58) was born on April 23, 1923 in Elizabeth, N. J. He attended Rensselaer Polytechnic Institute, Troy, N. Y., from 1940-1943. After



M. L. STITCH

military service in the Army, he received the B.S. degree in physics, and the B.A. degree in French literature from Southern Methodist University, Dallas, Texas, in 1957. He entered Columbia University, New York, N. Y., and received the Ph.D. degree in physics in 1953. While at Columbia, he was an instructor in physics at Cooper Union, New York, N. Y., and Sarah Lawrence College, Bronxville, N. Y., and research assistant at the Columbia Radiation Laboratory. His field of interest was high-temperature microwave spectroscopy.

From 1953-1956 he was at the Research Laboratories of Varian Associates, Palo Alto, Calif., where he made contributions in microwave spectroscopy and microwave stabilization by high-Q cavities. He joined the Atomic Physics Department of Hughes Aircraft Company, Culver City, Calif., in 1956 where he has made contributions to the physics and technology of masers. He is currently Head of the Atomic Resonance Group, and senior staff physicist.

Dr. Stitch is a member of Sigma Xi, The New York Academy of Science, RESA, The American Physical Society, American Association of Physics Teachers, AAAS, FAS, Physical Society of Japan and Societa Italiana di Fisica.



Archie W. Straiton (M'47-SM'49-F'53) was born in Arlington, Tex. on August 27, 1907. He received the B.S. degree in electrical engineering, the M.A. degree and the Ph.D. degree, all from the University of Texas, Austin.



A. W. STRAITON

He taught at Texas College of Arts and Industries, Kingsville, from 1931 to 1943. Since 1943 he has been at the University of Texas, where he is now professor of electrical engineering and director of the Electrical Engineering Research Laboratory.

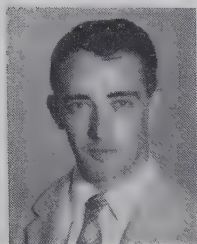
Dr. Straiton is a member of Eta Kappa Nu, Tau Beta Pi, Sigma Xi and American Society for Engineering Education. He is a former member of U. S. A. National Committee and chairman of Commission II of the International Scientific Radio Union.



Donald J. Sullivan (S'51-A'54-M'57) was born on Staten Island, New York, N. Y. on October 19, 1932. He received the B.S.

degree in electrical engineering from Manhattan College, New York, N. Y. in 1954.

After graduation he joined the Sperry Gyroscope Company, Great Neck, N. Y., as an assistant engineer in the Microwave Component Group. In 1957, he moved to Clearwater, Fla., to assist in starting the newly-formed Sperry Microwave Electronics Company.



D. J. SULLIVAN

Since joining the company, he has been engaged in research and development work on high-power and low-frequency solid-state components. He is a senior engineer

and group leader in the Advanced Microwave and Solid-State Devices Group.

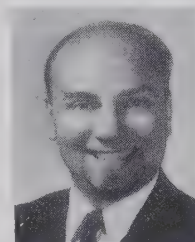


Charles Süsskind (A'47-M'52-SM'53) was born in 1921, in Prague, Czechoslovakia, and received his secondary education in Czechoslovakia and in Great Britain. He graduated from the California Institute of Technology, Pasadena, in 1948, and received the M. Eng. and Ph.D. degrees from Yale University, New Haven, Conn., in 1949 and 1951, respectively.

During the war, he served with the 8th Air Force in Europe as an airborne-radar specialist. From 1951 to 1955, he was a research associate at Stanford University,

where he also acted (after 1953) as lecturer in electrical engineering and assistant to the director of the Microwave Laboratory. In

1955, he joined the electrical engineering faculty of the University of California, Berkeley, where he is now associate professor.



C. SÜSSKIND

Dr. Süsskind is an associate member of the British IRE, and a member of the American Physical Society, the American Society for Engineering Education, the History of Science Society, the History of Technology Society, Sigma Xi, and Tau Beta Pi.

PGMTT National Symposium

HOTEL DEL CORONADO, SAN DIEGO, CALIF., MAY 9-11, 1960

Welcome and Opening Remarks Monday Morning, May 9

D. Proctor, Chairman of the 1960 PGMTT National Symposium.

A. A. Oliner, National Chairman of the PGMTT.

Session 1—Microwave Components and Systems

Chairman: *T. N. Anderson, FXR Inc., Long Island City, N.J.*

"New Developments in Microwave Communications Systems," *C. C. Cutler, Bell Telephone Labs., Holmdel, N. J.*

"Mode Conversion in Helix Waveguide," *H. G. Unger, Bell Telephone Labs., Holmdel, N. J.*

"Some Properties of Dielectric Loaded Slow Wave Structures," *G. B. Walker and C. G. Engelfield, Univ. of British Columbia, Vancouver, B. C., Canada.*

"UHF Strip Transmission Line Hybrid Junction," *I. Tatsughuchi, Bell Telephone Labs., Whippany, N. J.*

"A Variable Slope, Non-Dispersive Microwave Phase Shifter," *G. D. Carey and R. E. Hovda, Autonetics, Div. of North American Aviation, Downey, Calif.*

"A Wide-Band Turnstile Junction and Direction Finding Antenna," *R. C. Honey and J. K. Shimizu, Stanford Res. Inst., Menlo Park, Calif.*

"Microwave Phase Analyser," *K. D. Claborn and R. E. Jones, Bendix Radio, Div. of Bendix Aviation Corp., Baltimore, Md.*

Monday Afternoon

Session 2—Parametric Amplifiers

Chairman: *A. Berk, Research Labs., Hughes Aircraft Co., Culver City, Calif.*

"Gallium Arsenic Point Contact Diodes," *W. M. Sharpless, Bell Telephone Labs., Holmdel, N. J.*

"Characterization of Microwave Variable Capacitance Diodes," *S. T. Eng., Development Lab., Hughes Semiconductor Div., Newport Beach, Calif.*

"A Perturbation Theory for Parametric Amplifiers," *R. H. Kingston and A. L. McWhorter, Lincoln Lab., M.I.T., Lexington, Mass.*

"A Study of the Optimum Design of Wideband Parametric Amplifiers and Up-Converters," *G. L. Matthaei, Stanford Res. Inst., Menlo Park, Calif.*

"A Low-Noise X-Band Parametric Amplifier," *R. D. Weglein, Research Labs., Hughes Aircraft Co., Culver City, Calif., and F. Keywell, Semiconductor Div., Hughes Products, Costa Mesa, Calif.*

"A Four Terminal Low Noise Parametric Microwave Amplifier," *W. Eckhardt and F. Sterzer, RCA, Princeton, N. J.*

"Design and Operation of Four-Frequency Parametric Up-Converters," *J. A. Luksch, E. W. Matthews and G. A. VerWys, RCA, Moorestown, N. J.*

"A Study of the Iterated Traveling-Wave Parametric Amplifier," *C. V. Bell, Walla Walla College, College, Park, Wash.*

Monday Evening

Session 2A—Parametric Amplifiers

Panel Discussion: *A. Berk, Research Labs., Hughes Aircraft Co., Culver City, Calif.; C. J. Carter, Space Technology Labs., Los Angeles, Calif.; J. C. Green, Airborne Instruments Lab., Melville, L.I., N. Y.; E. M. T. Jones, Stanford Res. Inst., Menlo Park, Calif.; N. Uenohara, Bell Telephone Labs., Murray Hill, N. J., G. Wade, Stanford Univ., Stanford, Calif.*

Tuesday Morning, May 10

Session 3—Ferrites

Chairman: *N. Sakiotis, Motorola, Inc., Scottsdale, Ariz.*

"Non-Linear Effects in Ferrites," *M. Weiss, Research Labs., Hughes Aircraft Co., Culver City, Calif.*

"Ferroxplane Type Materials at Microwave Frequencies," *I. Bady, U. S. Army Signal Res. and Dev. Lab., Fort Monmouth, N. J.*

"Antiferromagnetic Materials for Millimeter and Sub-millimeter Devices," *G. S. Heller and J. J. Stickler, Lincoln Lab., M.I.T., Lexington, Mass.*

"Design Problems Associated with Rectangular Waveguide Reciprocal Phase-shifters," *A. Clavin, RANTEC Corp., Calabasas, Calif.*

"Magnetostatic Modes and Ferrites with Conventional Waveguide Geometries," *G. P. Rodrigue, Sperry Microwave Electronics Co., Clearwater, Fla.*

"Wide Band Resonance Isolator," *W. W. Anderson and M. E. Hines, Bell Telephone Labs., Murray Hill, N. J.*

"An Electrically-Variable, Reciprocal Ferrite Phase Shifter," *R. W. Kordos and V. J. McHenry, Research Labs. Div., Bendix Aviation Corp., Detroit, Mich.*

Tuesday Afternoon

Session 4—Millimeter Waves and Diode Applications

Chairman: *P. Vartanian, Melabs, Palo Alto, Calif.*

"Millimeter Wave Generation," *B. Epstein, Microwave Res. Inst., Brooklyn, N. Y. (on leave from Compagnie General TSP, France)*

"Millimeter Wave Generation by Parametric Methods," *G. H. Heilmeier, RCA Labs., David Sarnoff Res. Center, Princeton, N. J.*

"A Pulsed Ferrimagnetic Microwave Generator," *B. J. Elliott, T. Schaug-Petersen and H. J. Shaw, Stanford Univ., Stanford, Calif.*

"Maser Operation at Signal Frequencies Higher Than the Pump Frequency," *F. R. Ames, Airborne Instruments Lab., Melville, L. I., N. Y.*

"Generation of Microwaves by Means of Esaki Diodes," *R. F. Rutz, Research Labs., IBM, Poughkeepsie, N. Y.*

"The Large Signal Behavior of a Cavity Type Parametric Amplifier," *F. A. Olson and G. Wade, Stanford Univ., Stanford, Calif.*

"A Solid State Microwave Source from Reactance Diode Harmonic Generators," *T. M. Hyllin and K. L. Kotzebue, Texas Instruments, Dallas, Tex.*

Wednesday Morning, May 11

Session 5—Microwave Propagation in Plasmas and Solids

Chairman: *L. Goldstein, Univ. of Illinois, Urbana.*

"Propagation of Waves in a Plasma in a Magnetic Field," *W. Allis, Research Lab. of Electronics, M.I.T., Cambridge, Mass.*

"Plasma-Electromagnetic Interaction," *N. Marcuvitz, Microwave Res. Inst., Polytechnic Institute of Brooklyn, Brooklyn, N. Y.*

"Magnetoplasma Effects in Semiconductors," *B. Lax, Lincoln Labs., M.I.T., Lexington, Mass.*

"Coherent Excitation of Plasma Oscillations in Solids," *D. Pines, Univ. of Illinois, Urbana (work done at General Dynamics Corp., San Diego, Calif.)*

Panel Discussion: *O. T. Fundingsland, Raytheon Mfg. Co., Waltham, Mass.; R. Gould, California Institute of Technology, Pasadena; H. Margenau, Yale Univ., New Haven, Conn.; R. F. Whitmer, Sylvania Electronic System, Mountain View, Calif.*

Wednesday Afternoon

Session 6—Filters and Measurements

Chairman: *K. Tomiyasu, General Electric Microwave Lab., Palo Alto, Calif.*

"Lossy Waveguide Resonators," *H. Riblet, Microwave Development Labs., Inc., Wellesley, Mass.*

"Peak Internal Fields in Direct Coupled Cavity Filters," *L. Young, Westinghouse Electric Corp., Baltimore, Md.*

"Strip Transmission Line Directional Filter," *R. L. Steven and P. E. Dorato, Airborne Instruments Lab., L. I., N. Y.*

"Application of the Smith Chart to Problems of Propagation in a Magneto-Ionic Medium," *G. A. Deschamps and W. L. Weeks, Univ. of Illinois, Urbana.*

"Microwave Measurements of Electron Attachment Rates," *V. A. J. van Lint and E. G. Wilkner, General Atomic, Div. of General Dynamics Corp., San Diego, Calif.*

"Fractional Millimicrosecond Electrical Stroboscope," *W. M. Goodall and A. F. Dietrich, Bell Telephone Labs., Holmdel, N. J.*

The banquet speaker at the PGMTT National Symposium will be W. E. Edson of the General Electric Co., Palo Alto, Calif., who will speak on "Microwave Power Sources of the Future."

Roster of PGMTT Members

Listed by IRE Regions and Sections, as of March 1, 1960

Region 1

Binghamton

Drake, J. E.
Fowler, A. K.
Sleeper, G. B., Jr.
Urban, H. E.

Boston

Abate, A.
Abel, Fred
Adams, G. J.
Adams, H. E.
Aitken, W. M.
Alexander, H. C.
Allen, D. C.
Alter, R. S.
Altman, J. L.
Altschuler, E. E.
Amazeen, P. G.
Andreika, J. T.
Angulo, C. M.
Apsokardos, E.
Armstrong, D. G.
Arnum, M.
Astulfi, S. O.
Atchley, D. W., Jr.
Averill, R. J.
Backard, M. J.
Baldwin, T. H.
Barker, H. R., Jr.
Barrett, R. M.
Baumann, A.
Bayliss, R. E.
Bazzy, W.
Beauregard, W. G.
Beckett, H. F.
Belleville, R. L.
Berger, U. S.
Bergmann, S. M.
Bergstad, P. A.
Bibbins, L. L.
Blacksmith, P., Jr.
Blaisdell, A. A.
Blake, C.
Blanchard, R. L.
Blender, M. I.
Bliss, Z. R.
Bloom, L. J.
Bloom, M. I.
Bobroff, D. L.
Bolinder, E. F.
Bonfeld, M. D.
Booth, A. E.
Borghetti, J. C.
Borts, R. B.
Boudreau, J. M. C.
Bougas, A. C.
Bowness, C.
Braden, R. S.
Branche, J. R.
Broderick, D. C.
Brooks, R. O.
Brosnahan, R. E., Jr.
Brown, C. R.
Brown, D. F.
Brown, N. J.
Brunton, R. H., III
Bryant, W. E.
Buckley, E. F.
Burdine, B. H.
Burnham, P. E.
Byck, D. M.
Cahill, T. C.
Caloccia, E. M.
Campbell, B. D.
Cannon, J. H.
Carberry, T. F.
Caron, P. R.
Carr, K. L.
Carson, C. H.
Carter, G. E., Jr.
Carter, L. J.
Cary, T. R., Jr.
Cayer, R. E.
Chacran, J. J.
Charles, R. E.
Chase, D. G.
Child, J. W.
Child, P. J.
Clark, N. F.
Clougherty, J. F.
Cogdell, J. R.
Cohen, A.
Cole, B. R.
Coling, F. L.
Collins, R. M.
Colombo, C. M.
Cook, O. W.
Crandell, P. A.
Cross, H. H.
Crossley, W. P.

Crowley, D. J., Jr.
Cuming, W. R.
DaMocogno, N. G.
Dandreta, W.
Danforth, W. C., Jr.
Day, A. R.
Delacey, E. M. F.
Delaney, W. P.
DeMattos, R. F.
Denman, J. G.
DeTurris, J. M.
Dobson, A. M.
Dodds, W.
Dombrowski, G. E.
Domenichini, C. P.
Dominick, F. J.
Donohue, J. F.
Duffy, J. F.
Duffy, J. M.
Dunbar, E. E.
Duncan, K. W.
Durooss, C. J.
Edelberg, S.
Edwards, L. C.
Eisenstadt, B. M.
Eklund, A. M.
Ellinthorpe, A. W.
Ewen, H. I.
Fafflick, C. E.
Faigen, I. M.
Falconer, S.
Fallows, E. M.
Favaloro, C. J.
Feehan, J. D.
Feldman, E. J.
Fessenden, D. E.
Fischer, R. F.
Fisher, R. S.
Fitzgerald, W. D.
Foley, J. C.
Forderhase, R. S.
Foss, D. W.
Foyt, A. G.
Fried, C.
Friis, R. W.
Fritsch, P. C.
Frohman, E. D.
From, W. H.
Frost, A. D.
Fuller, J. B.
Fulton, D. A.
Fye, D. L.
Galejs, J.
Gallup, G. B.
Gansenberg, V. G.
Gianino, P. D.
Gindberg, J.
Glynn, J. J.
Goldberg, E. B.
Goldman, E. M.
Goldstein, I.
Gordon, R. S.
Gould, L.
Goulder, M. E.
Graham, E. A., Jr.
Graham, J. W.
Grant, R. W.
Grayzel, A. I.
Greenway, T. H.
Gregory, J. G.
Gregory, N.
Gronroos, E.
Grossi, M. D.
Gunn, K. C. C.
Haddad, S. G.
Hadge, E.
Hall, R. T.
Hall, W. M.
Halleran, T. W.
Hamlett, D. W.
Hammond, G. H.
Hanley, J. J.
Hardsog, H. N.
Harris, F. S.
Hart, L. A.
Haus, H. A.
Hawthorne, E. I.
Hayes, C. J.
Hecht, B. P.
Hellenbrand, C. M.
Henderson, C.
Hergenrother, R. M.
Higgins, W. T.
Hoar, G. W.
Holly, S.
Hopkins, C. H.
Horvitz, S.
Houlding, N.
Howe, S. E.
Huang, C.
Hutchinson, D. E.
Ironfield, R., Jr.

Jacavanco, D. J.
Jackson, M. A.
Jacobson, R. E.
Jayne, A. W.
Jenkinson, J. V.
Johnson, E. G.
Johnson, L. F., Jr.
Johnson, S. L.
Jones, R. V.
Jones, W. T., Jr.
Kantor, G.
Karazia, R. J.
Karplus, E.
Kay, A. F.
Kazules, A. J.
Keane, L. M.
Keeping, K. J.
Kelly, J. D.
Kelly, J. W., Jr.
Kelly, P. E.
Kim, Y. S.
King, R. P.
Kingston, R. H.
Kistler, J. F.
Klein, J. A.
Klemm, G. H.
Kline, J.
Kohler, H. M.
Koozekanani, S.
Kostriza, J. A.
Kraetuer, L. D.
Krawiec, J. P.
Kyhli, R. L.
Lanciani, D. A.
Land, H. R.
Landesberg, M. M.
Landry, D. H.
LaPage, B. F.
Lawrence, J. E., Jr.
Lazarkis, P. J.
Leake, B. W.
Leavitt, W. A., Jr.
Lee, G. T.
Lehr, C. G.
Leppanen, K. E.
Lesch, F. A.
Lessin, I.
Lester, D. R.
Lewis, F. D.
Lind, J. N.
Lippincott, S.
Lipsett, M. S.
Loewenthal, M.
Long, R. G.
Lovell, B. W.
Lowe, W. R., Jr.
Lutz, M. W.
Lydiard, C. E.
Lyford, J. C.
Lynnworth, L. C.
Lyon, J. F.
Mack, R. A.
Mack, R. B.
Mackowiak, J. E.
Madore, R. J.
Mailloux, R. J.
Malech, R. G.
Malone, M. H.
Manahan, J. F.
Mann, A. M.
Marshall, J. R.
Matthews, C. M.
Matthewson, A.
Mavroides, W. G.
McCarthy, D. J.
McCarthy, J. G.
McCoubrey, A. O.
McCouch, G. P.
McCoy, A. M., Jr.
McCurley, E. P.
McLeod, W. W., Jr.
Melvin, D. W.
Mercer, W. R.
Meyer, J. W.
Meyer, M. A.
Michelson, M.
Miller, M. S.
Miller, S. J.
Mills, E. D.
Mikolajewski, W.
Milano, U.
Mingins, C. R.
Misek, V. A.
Modestino, J.
Mohr, M. C.
Monell, F. B.
Moulton, W. D.
Moynihan, R. L.
Murray, P. C.
Nelligan, K. P.
Nelson, E. A. A.
Nelson, R. E.

Novello, R. F.
O'Hara, F. J.
Osepchuk, J. M.
Owen, J. O.
Paananen, R. A.
Page, H. M.
Paoli, T. L.
Paquette, N. A.
Parke, N. G., III
Pathe, J. F.
Pease, R. L.
Peeler, G. D. M.
Penfield, P., Jr.
Pengeroth, I. E.
Perloff, G.
Peters, J. D., Jr.
Peterson, D. E.
Pierce, A. W.
Ploussios, G.
Plumb, D. R.
Polk, C.
Pollack, D.
Pomeroy, A. F.
Ponte, A. G.
Postema, G. B.
Pothier, R. G.
Potts, T. J., Jr.
Prasad, S.
Pratt, H. J., Jr.
Priest, W. G.
Pritchard, W. L.
Putnam, H.
Quist, T. M.
Rainville, L. P.
Ramsey, W. H.
Rawlinson, P. E.
Redmond, J. G.
Reed, J.
Reem, G. M., II
Rennick, R. C.
Rev, T. J.
Riblet, H. J.
Ricardi, L. J.
Rice, K. L.
Richter, E.
Rickleby, E. J.
Ripple, E. G.
Rivers, R. A.
Rizzi, P. A.
Roat, W. F.
Robinson, H. P., Jr.
Rodman, A. K.
Rojak, F. A.
Rosato, F. J.
Rosen, S.
Row, R. V.
Rowland, H. J.
Rowlands, E. R.
Rubin, S.
Rudolph, H. W., Jr.
Rummeler, W. D.
Ruta, V. J.
Rutledge, P. D.
Ruze, J.
Ryan, J. W., Jr.
Ryland, B. G.
Saad, T. S.
Sadowski, J. J.
Salomon, L. C.
Salzberg, E.
Sanderson, A. E.
Sandsmark, P. I.
Saunders, J. H.
Scharfman, H.
Schenck, J.
Schmidt, R. A.
Schwab, W. C.
Schwarzkopf, D. B.
Segal, S.
Schafer, C. G.
Shanler, B. H.
Sharp, D. D.
Sheftman, F. I.
Sheingold, L. S.
Sheldon, D. L.
Sherburne, A. E.
Siegel, R. C.
Silverman, E.
Simmons, A. J.
Sims, J. R.
Sinclair, D. B.
Sletten, C. J.
Smith, B. S.
Smith, C. L.
Smith, C. N.
Smith, H. A.
Smith, N. L., III
Smith, P. D.
Smith, R. D.
Smith, R. L.
Smith, R. V.
Smith, W. R.

Smullin, L. D.
Snay, R. J.
Soderman, R. A.
Sommers, D. J.
Soochoo, R. F.
Spiri, G. J.
Stanney, W. J.
Stearns, F. P.
Steen, R. A.
Stewart, R. F.
Stingel, R. E.
Stone, A. P.
Stone, M. L.
Stratoti, A. R.
Street, E. L.
Sweeney, G. C.
Swift, W. H., Jr.
Taft, W. C.
Tahan, E. N.
Teale, J. H.
Teich, W. W.
Tenenboltz, R.
Thomas, A. S.
Thomas, H. J., Jr.
Thomassen, N. E.
Tillman, J. E.
Tillyer, E. D.
Trail, R. S., Jr.
Uhlir, A., Jr.
Ursin, B. E.
Vafiades, B. C.
Vail, W. A.
Vant, L. M.
Versoy, I. R., Jr.
Wade, C. E.
Waldman, A.
Walker, R. M.
Wall, R. B.
Walsh, J. E.
Wang, S. C.
Weiner, M. M.
Wemple, S. H.
Wenzel, J. H.
Westbrook, E. P.
Whelpton, J. P.
White, D. H.
White, W., Jr.
Whiteside, H.
Willenbrock, P. K.
Willey, J. C.
Williston, R. L.
Wilson, W. J.
Wolfe, R. W.
Wolfson, J. A.
Wood, G. D.
Woodward, J. H.
Wundt, R. M.
Yaffe, G.
Yee, T. G.
Young, P. T. K.
Zeender, R. J.
Zettler, W. R.
Zorzy, J.
Zucker, F. J.

Buffalo-Niagara

Bachman, C. G.
Banshak, W. G.
Bartnik, J. C.
Bechtel, M. E., Jr.
Borkowski, C. J.
Burianich, G. F.
Burke, J. J.
DeJoseph, A.
Earl, H. D.
Euler, J. R.
Feinberg, E. J.
Groth, L. H.
Hoffman, K. B.
Horvath, J. O.
Jackman, C. A.
Jocoy, E. H.
Kell, R. E.
Kellerman, R. E.
Klemperper, W. K.
Lampone, D. J.
Leipold, W. H.
Laney, T. F.
Leonard, D. J.
Lewis, F. J.
Maciag, W. J.
Malm, R.
Michalski, R.
Michnik, L.
Newton, D. J., Jr.
Pelton, F. M.
Price, E. L., Jr.
Repski, J. E.
Rupp, R. B.
Sarkees, V. T.
Schlichter, E. S.

Sears, R. A.
Snyder, W. W.
Stengel, C. J., Jr.
Veath, M. S.
Wagner, R. W.
Welch, D. P.
Whyman, E. W.
Wolf, E. H.

Connecticut

Badoyannis, G. M.
Bolus, J. J.
Calvert, T. J.
Capraro, R. R.
Crooks, W. D., Jr.
Edighoffer, E. A.
Elrod, B. D.
Fingerle, W., Jr.
Hall, G. M.
Halloran, V. P.
Hernstadt, W. H.
Hierholzer, F. J., Jr.
Holloway, H. R.
Hunter, T. C., Jr.
Migliaro, B. J.
Ostendorf, B.
Pannullo, F. T.
Penney, A. W.
Pyatt, E.
Rand, P. S.
Reens, L. H.
Reich, H. J.
Sittner, W. R.
Sontheimer, C. G.
Stoker, W. C.
Thayer, D. C.
Thompson, T. W.
Warner, E. J.

Elmira-Corning

Ainey, R. K.
Bamford, A. J.
Barney, W. H., Jr.
Duhl, J. E.
Foreman, R. J.
Gerard, W. A.
Guyer, E. M.
Heostler, C. L.
Keeton, T. G.
Knowles, D. D.
Larson, R. G.
MacDonell, P. A.
Playfoot, K. C.
Scullin, C. H.
Suchanek, R. G.
Washburn, G. W.
White, R. A.

Erie

Olowin, L. J.
Page, R. S.

Ithaca

Blair, W. E.
Bryant, N. H.
Charton, P. W.
Curtice, W. R.
Dysiner, J. H., Jr.
Eastman, L. F.
Farrell, G. F., Jr.
Frey, J.
Kram, W. P.
Mackenzie, L. A.
Maresca, T. J.
Mayer, H. F.
Osofsky, A. J.
Rogers, R. G.
Sackinger, W. M.
Schnurer, F.
Thornton, R. D.
Von Borstel, E. W.
Wheeler, N. D.

Rochester

Baldwin, L. D.
Bendel, S., Jr.
Blum, R. J.
Brock, E. G.
Chesna, J.
Eisaman, L. C.
Geobel, H. K.
Hattersly, T. E., Jr.
Healy, D. W., Jr.
Heise, E. R.
Heit, J. C.
Heurtley, J. C.
Hulse, R. W.
Keim, D. Y.
Morrison, R. F., Jr.
Neugebauer, H. E. J.
Niertit, F.
Price, C. C.
Ramos, A. S.
Raymond, R. S.
Schiff, S.
Smith, D. S. J.
Smoyer, C. B.
Staples, W. D.
Tolliver, P. M.
Williams, R. C.

Rome-Utica

Akerman, S.
Augustine, J. A.
Baldrige, B. H.
Chrestien, C. A.

Cruickshank, J. E.
DeMesme, T. A.
Dover, B. M.
Grimm, R. S.
Harris, R. L.
Ignatz, R. R.
Magyarics, R. F.
Marks, R. L.
Matt, S.
McComb, D. S.
McGuffin, A. L.
Miller, C. R.
Niebuhr, K. E.
Orear, E. R.
Raga, J. F.
Reviere, R. P.
Ring, R. B.
Romanelli, P. A.
Siegel, G. H.
Smith, D. R.
Vaccaro, J.
Vogelman, J. H.
Wallinfeels, W. B.
Warrick, A. C.
Williams, E. E.
Williams, R. L.
Winn, O. H.

Schenectady

Allen, C. C.
Amoth, V. W.
Anderson, J. M.
Babits, V. A.
Beum, W. R.
Blume, M. F.
Bolster, M. R.
Boyd, M. R.
Branch, G. M., Jr.
Chatterton, W. J.
Coffey, W. N.
Curtis, T. P.
Dehn, R. A.
Feiker, G. E., Jr.
Frank, E. M.
Gittinger, N. C.
Glow, A. E., Jr.
Griffin, G. J., Jr.
Grover, F. W.
Hall, R. N.
Hamilton, J. J.
Harges, M. T.
Haskell, R. E.
Hodges, D. J.
Holt, E. H.
Huse, G.
Jensen, A. O.
Keenan, P. P.
Maurer, J. W.
Mayer, C. B.
Mihran, T. G.
Oshima, M.
Owens, O. G.
Peters, P. H., Jr.
Piwnica, W. M.
Quine, J. P.
Raschke, R. R.
Rechnitzer, B. W.
Reppard, D. L.
Speray, M. R.
Stein, H. H.
Teare, W. H.
Thal, H. L., Jr.
Truax, C. J.
Turrentine, R. E.
Vaughan, J. R. M.
Watson, R. P.
Winter, W. H.
Wright, P. H.

Western Massachusetts

Andrews, W. J.
Cetarak, W. K.
Fox, E. D.
Lee, L. T.
Roberts, W. A.

Syracuse

Altes, S. K.
Anderson, A. F.
Anderson, C. T.
Astemborski, T. J.
Bostick, G.
Boyd, C. R.
Burns, D. L.
Caffrey, T. P.
Cape, M. R.
Carson, R. E.
Cheng, D. K.
Conger, W. H.
Coniber, G. A.
Cornacchio, J. V.
Cowburn, F. C.
Doolittle, W. T., Jr.
Drum, J. J.
Duronio, K. B.
Eber, L. O., Jr.
Evans, H. J.
Fitzmorris, S. R.
Gerlack, R. Z.
Gildersleeve, R. E.
Grimm, H. H.
Gruenberg, H.
Gussak, M.
Hall, R. W.
Haussig, L.
Hoffman, J.

Holmes, K. O.
Holonyak, N., Jr.
Hsu, H.
Hu, M. K.
Hu, Y. V. S. H.
Hurley, D. T.
Hwang, V. C.
Johnson, A.
Jones, R. J.
Jordan, J. F.
Keener, M. A.
Kent, G.
Kenyon, S. W.
Kinsey, R. R.
Kirkpatrick, G. M.
Kuhn, D. H.
Lepage, W. R.
Manke, A. G.
Manwarren, T. E.
Martin, H. R.
Mather, D. L.
Mayo, B. R.
McCoy, D. R.
Morelli, A. N.
Morrison, R. H.
Mullen, E. B.
Nester, W. H.
Perreault, D. A.
Place, J. F.
Radford, E. R.
Reale, J. D.
Rothenberg, H. C.
Schwarz, E. G.
Scott, K. J.
Smith, D. L.
Smith, S. L.
Smith, W. F., Jr.
Snitke, J. A.
Sparks, J. E.
Stauffer, J. W.
Stern, E.
Straub, G. H., Jr.
Strawn, R. K.
Tanakaya, S. T.
Totten, H. Q.
Tullman, H. J.
Wanuga, S.
Whistler, W. T.
White, W. C.
Widmann, L. C.
Williamson, J. C.

Region 2

Long Island

Aaron, B. D.
Agree, I.
Aichroth, J. W.
Albanese, V. J.
Amacher, W. E.
Ammirati, S.
Anderson, R. E.
Arams, F. R.
Aull, W.
Basil, A.
Bauer, W. C.
Beamer, F. E.
Becker, J. E.
Berly, E.
Bernstein, G.
Bertan, G. S.
Bertan, L. S.
Biscoe, G. W.
Biss, R. E. P.
Blank, S. J.
Bloom, G. M.
Blum, A. J.
Blyseth, M. C.
Bogner, B. F.
Bogner, R. D.
Bourke, W. A.
Brecht, L. R., Jr.
Breese, M. E.
Brenner, A.
Brenner, M.
Brounstein, A.
Brown, C. A.
Brown, D. A.
Brown, R. H.
Bruch, R.
Brunet, W. J.
Callaghan, E. P.
Campbell, T. A.
Carter, P. S.
Casper, S. D.
Chernak, J.
Chomet, M.
Chybb, E.
Churchill, D. B.
Cohen, A. L.
Cohen, H.
Cohen, Morris
Cohen, Morton
Cohen, S. A.
Coles, W. T.
Collins, K.
Cornes, R. W.
Corwin, A.
Crepeau, P. J.
Crosby, M. G.
Dagavarian, H. O.
D'Agostino, J.
Daly, R. T.
D'Angelo, F.
Daum, A.

Delore, G. E.
Deoul, N.
DeSize, L. K.
DeTroy, B. A.
Dettinger, D.
Deveau, E. J.
DiToro, M. J.
Dolin, M.
Doll, R. E.
Dong, H. L. H.
Dorato, P. E.
Dorne, A.
Doundoulakis, G. J.
Duffy, J. P., Jr.
Eberle, E. E.
Ebert, J. E.
Egan, W. G.
Eisenbach, J.
Elefant, J.
Engle, D. C.
Epstein, I.
Farber, H.
Farkas, Z. D.
Fifer, W. C.
Fisch, J.
Fisher, L. H.
Fleming, P. L.
Fowler, V. J.
Franchina, M. A.
Friedlander, M. O.
Friedman, E. D.
Fubini, E. G.
Fucci, S.
Gallagher, J. H.
Gamble, J. H.
Garretson, C. M.
Gebhardt, J. W.
Geiger, R. H.
Gethin, S. A.
Giba, J. J.
Glass, H. W.
Goldberg, J.
Goldmuntz, L. A.
Goldstein, S.
Goldstone, L. L.
Goodman, D. M.
Goodwin, R. J.
Gordon, J. J.
Gorelick, G.
Gould, R. V.
Grace, M. I.
Gran, R. J.
Granet, A. J.
Grant, F. M.
Grayson, R.
Greene, J. C.
Griemsmann, J. W. E.
Grossman, B. C.
Hall, J. D.
Hana, T. C.
Hanfing, J. D.
Hanley, G. L.
Hannan, P. W.
Hannwacker, J.
Hanover, A. M.
Hanratty, R. J.
Hansard, H. H.
Hanulec, J. D.
Harrison, R. I.
Heacock, W. J., Jr.
Heiss, W. H.
Hellrigel, B. F.
Hendler, A. J.
Hershler, A.
Hinckelmann, O. F.
Hoffman, C.
Hoffman, H. L.
Horowitz, L.
Hronek, R. F.
Hyatt, A. J.
Hyland, J. R.
Iassogna, P. Jr.
Iddings, G. E.
Isaacson, H. B.
Jacobs, F.
Jaffe, D. L.
James, A. V.
Janis, I. R.
Jarecky, J. L.
Jasik, H.
Jaworowski, E. V.
Johnson, A. E., Jr.
Jorge, A.
Kanterman, A.
Kaplan, R. A.
Kaskel, H.
Kearney, J. W.
Keen, H. S.
Keicher, A. J.
Kent, L. I.
Kikta, M. S.
Kinkelin, W., Jr.
Kirschner, D. D.
Kishinsky, L. S.
Klafter, R. D.
Klein, M. M.
Klug, S. H.
Knothe, C. H.
Kofman, I.
Kraemer, E. H.
Kraus, C. P.
Kraus, J.
Kudo, Y.
Kurz, F. A.
LaFleur, M. V.
Lakins, D.

Lamensdorf, C. M.
La Rosa, R.
Learned, V.
Leibowitz, B.
Lepic, R. E.
Lerner, D.
Leshar, A. K.
Levine, H. A.
Levine, S.
Lieberman, S. M.
Liefert, F. R.
Ligori, J.
Lilly, J. L.
Lippke, J. A.
Litton, J., Jr.
Livant, W.
Liverios, D. T.
Lombardo, P. P.
London, M. M.
Lory, J.
Losee, W. B., Jr.
Loss, M. B.
Loth, P. A.
Loughlin, B. D.
Lubell, P. D.
Lyons, J. F., Jr.
Madden, J. L.
Magenheim, B.
Magid, M.
Maher, B.
Malkiewicz, J. F.
Mariotti, P. G.
Marston, R. S.
Martin, C. A.
Martines, L. T.
Marzoli, A.
Maurer, S. J.
Mautner, R. S.
Mazurkiewicz, R. J.
Mazzara, A.
McBee, W. D.
McCrill, J. A.
McInnis, T. F.
McLure, R. E.
Meixner, V. G.
Menaker, D. S.
Michal, R. L.
Mieher, W. W.
Mills, J. J.
Milukas, V. V.
Minkiewicz, M. D. K.
Mohlbrok, D. E.
Mohr, R. J.
Mooney, V. J.
Morrone, T.
Muller, W. M.
Murphy, R. B.
Neiland, A. C.
Newton, A.
Nieminski, W. V.
Noji, T. T.
Nover, E. P.
Novick, L. R.
Novick, M.
O'Donnell, J. R.
O'Dwyer, T. F.
Offutt, W. B.
Okress, E. C.
Okwit, S.
Olah, J.
Oranges, D. F.
Orazio, A. F.
Orford, R. J.
Ortmann, M. W.
Oshiro, F. K.
Ottenberg, E. C.
Packard, K. S., Jr.
Packer, B. S.
Packer, L.
Pariser, B.
Perini, H. R.
Peterson, H. O.
Petrossian, G.
Pizzutiello, R.
Plutchok, H.
Pomeranz, H.
Porter, S. T.
Prew, H. E.
Prude, D. W.
Proctor, D. W.
Puttre, R. E.
Raffier, M.
Rearwin, R. H.
Redlien, H. W., Jr.
Regis, R.
Rehfeld, M. J.
Reinhardt, G.
Renkowitz, D.
Resnick, S.
Reynolds, M. R.
Richer, N., Jr.
Richman, D.
Richter, F. G.
Ries, C. A.
Rinkel, S. A.
Robinson, H. L.
Rosen, B.
Rosenthal, M. M.
Rubin, S. W.
Russell, D. H.
Saks, H. L.
Satre, W. I., Jr.
Scherer, R. L.
Schiffres, P.
Schindler, J. P.
Schmidt, E. R.

Schneider, S.
Schnitkin, H.
Scholer, R. M.
Schwab, C. E.
Segota, A. S.
Sferrazza, P. J.
Shepherd, J. E.
Shilkoff, M.
Shizume, P. K.
Shubel, E. J.
Shulman, I.
Sieminski, E.
Simmonds, J.
Simons, R. F.
Skipper, L. C.
Skwarek, F. J.
Sleven, R. L.
Smith, C. I.
Smook, I. R.
Sonnenschein, A. H.
Soreny, E. V.
Spector, N.
Spencer, N. A.
Spiegelman, S. D.
Sprague, G. J.
Squitieri, A.
Stephenson, J. G.
Stock, D. C.
Strong, J. J., Jr.
Sutkin, S.
Suttenberg, S.
Swain, J. A.
Szabo, J. A.
Tames, J.
Tanenbaum, M.
Taub, J. J.
Teltscher, E. S.
Tenenbaum, F.
Topper, L.
Torgow, E. N.
Trachtenberg, J. M.
Trogdon, W. H.
Tyler, E. M.
Vaher, E.
Valge, J.
Vaupel, G. E.
Viadella, J. W.
Wagner, W. D.
Walker, A. C.
Waller, W. E.
Walters, J. L.
Warren, R. J.
Wasson, I.
Weber, I. J.
Weibel, G. E.
Welch, T. J.
Wengenroth, R. D.
Wexler, H.
Wheeler, H. A.
Whelehan, J. J., Jr.
Whipple, G. D.
Williams, F. H.
Williams, J. H. M.
Wills, A., Jr.
Wilson, L. B.
Wind, M.
Wing, R.
Winzemer, A. M.
Woodward, B. A.
Wright, M. L.
Wrobel, E. J.
Wunderlich, N. E.
Yarnall, W. M.
Young, V. J.
Zanichkowsky, M.
Zeisler, M. D.
Zellers, J. E., Jr.
Zimet, M. R.
Zuzolo, P. R.

New York

Abrams, S. J.
Albanese, A. P.
Alfieri, G. J.
Alloggiamento, A.
Altschuler, H. M.
Angevine, R. A.
Appelman, S.
Arbuthnot, J., Jr.
Arnold, J. W.
Arnold, R. G.
Aslan, E. E.
Baars, R. D.
Bady, I.
Baker, L. C.
Banner, L.
Barash, L. F.
Barber, A. E.
Beck, A. C.
Becker, L.
Beizer, H. H.
Berger, R. M.
Berlin, J.
Bernstein, J. L.
Bevan, R. K.
Bickel, H. J.
Bier, E. J.
Birenbaum, L.
Birnbbaum, J.
Bland, G. F.
Bocharoff, G. M.
Boles, S.
Borck, A.
Brathwaite, A.
Breecher, G. G.
Bresler, A. D.

Brown, D. L.
Bryson, W. B.
Bugnolo, D. S.
Buhl, D.
Byrne, J. J.
Canick, P. M.
Carlin, H. J.
Caruso, A. A.
Cedarholm, J. P.
Chanitz, L.
Chays, S.
Chen, T. S.
Chernoff, D. P.
Cicchetti, J. B.
Clemens, G. J.
Coltun, L.
Connor, J. E.
Cooper, M.
Cooper, N.
Crivello, A. A., Sr.
Dawson, R. W.
De Angelis, D. P.
Defilippis, L. S. M.
Defloria, R. N.
Degazon, D. A.
Del Giorgio, J. A.
De Loach, B. C., Jr.
De Paola, G. E.
Diamant, P.
Dickey, V. F.
Di Fusco, F. J.
Douglas, R. H.
Drosin, A. B.
Dudgeon, D. E.
Elkin, H. C.
Elkord, D. S.
Ellen, N. A.
Epstein, D. J.
Espersen, G.
Ettenberg, M.
Ewen, K.
Faiola, A. R.
Farber, A. S.
Farley, J.
Felsen, L. B.
Ferri, R. I.
Fine, E. M.
Finke, H. A.
Fleisher, H.
Fliegler, E.
Flower, R. A.
Fox, A. G.
Fox, J.
Franco, A. G.
Frankel, S.
Freed, A.
Freibergs, E.
Friedman, C.
Friis, H. T.
Galitzer, S.
Gamertsfelder, G. R.
Gamo, H.
George, D. E.
Gerling, J. E.
Giannattasio, A. R.
Ginsberg, H. E.
Giordano, A. B.
Giordano, P. J.
Glazer, S.
Golden, D.
Goldgewert, D.
Goldie, H.
Goldsmith, A. N.
Goldstone, L. O.
Gonda, T.
Govinsky, W.
Grohner, A.
Guenther, R.
Haase-Dubosc, A. A.
Hambledon, G. E.
Hanft, H.
Harris, L.
Haug, H.
Henderson, P. A.
Hessel, A.
Hirsch, S. A.
Hoffman, J. D.
Hollander, S.
Holtzer, H.
Holzman, G. R.
Honig, A. R.
Honig, W. M.
Kagan, H.
Kahn, W. K.
Kaiser, E. J.
Kaplan, L. J.
Karp, J. R.
Kasper, H. W.
Kerr, S. A.
Kessler, A.
Kibler, L. U.
King, A. P.
Kizilyalli, H. M.
Klein, A.
Klein, M.
Klipper, H.
Korewick, J.
Kowalsky, J.
Krevsky, S.
Kui, W. H.
Kullback, I.
Kurzrok, R. M.
Kusnetz, J.
Lamb, R. U.
Lauricella, J. C.
Lavi, Y.

Lebowitz, R. A.
Lederman, A.
Lee, C. T.
Leibowitz, M. R.
Lesman, E.
Levey, L.
Levine, B. I.
Levine, E.
Li, T.
Lipetz, N.
Litvin, B. T.
Magill, L. M.
Mahar, T. F.
Majean, H. L.
Malloy, E. J.
Mansky, L.
Marcuse, D.
Margolies, D. L.
Marinace, R. G.
Martin, J. E.
Martin, J. F. P.
Martinson, F. L.
Matthei, W. G.
Mazziotti, I. J.
McDermott, J. P.
McLaughlin, N. C.
Meier, P. J.
Meixner, R. P.
Mesorole, W. E.
Meslener, G. J.
Mezei, J. E.
Michtisch, J. J.
Milazzo, S.
Miller, B.
Miller, S. E.
Mitchell, D. C.
Mohr, B. E.
Morel, P.
Newman, H. S.
Ohm, E. A.
Oliner, A. A.
Onder, K.
Orefice, G. T.
Orenstein, N.
Ortolani, F. P.
Ossoff, A.
Oswald, H. J.
Palocz, S.
Parham, S. E.
Parisier, M.
Petrillo, B. J.
Pettai, R.
Pietrzyba, G. J. M.
Plasters, G. T.
Plesset, K.
Plishner, P. J.
Pokorny, G. E.
Pommet, J. A.
Popper, J. N.
Principe, A. J.
Pugliese, L.
Pullman, M.
Rabinowitz, M.
Rabinowitz, S. J.
Reder, F. H.
Reingold, I.
Ren, C. L.
Rickert, H. H.
Rivera, A.
Rofis, J. C.
Rosenthal, S. W.
Rowe, I.
Rudner, B. S.
Rugge, R. A.
Safran, P.
Saltzman, H.
Samaddar, S. N.
Sautner, J.
Sawelson, A. I.
Schafar, J. P.
Schetzen, M.
Schilling, W. A.
Schlesinger, S. P.
Schleiner, K. E.
Schulz, P. R.
Schwartz, L.
Schwering, F. K.
Share, Y.
Share, I.
Sharpless, W. M.
Sheldon, M.
Silverman, L. H.
Silversmith, G. B.
Simon, H.
Skalski, C. A.
Slater, D.
Slevin, R. F.
Slobodin, L.
Smilen, L. I.
Smith, A. W.
Smith, M. G.
Solomon, A. H.
Sonkin, R. M.
Sonsky, S. N.
Speller, J. B.
Stabbe, D. R.
Stalemark, F. R. V.
Standley, R. D.
Stangel, J. J.
Stavis, G.
Steckler, S.
Steigerwalt, G. F.
Stern, K.
Stern, R. M.
Stock, D. J. R.
Sussman, A. I.

Swartz, D. F. X.
Sweet, L. O.
Tamir, T.
Tashjian, A.
Thomas, R. O.
Trimakas, A. K.
Turner, E. H.
Ubbilos, P.
Unger, H. G.
Velardi, L. A.
Victor, H. W.
Vigants, A.
Viola, R. D.
Walton, J. S. V.
Warters, W. D.
Webber, G.
Weber, E.
Weichardt, H. H.
Weinstein, H. M.
Westheimer, M.
Wing, O.
Winkelstein, R. A.
Winkler, A.
Wolfson, R.
Wu, W. I. L.
Zanic, A. P.
Zenchoff, P.
Zucker, M. S.

Northern New Jersey

Aagesen, J.
Abrams, I.
Albrecht, H. W.
Anderson, T. N.
Anick, G.
Arditi, M.
Ashbrook, J. M.
Augenblick, H. A.
Barnett, W. T.
Beeny, L. S.
Benenson, C. A.
Benson, R. K.
Blanchard, R. J.
Blundell, J. W.
Bond, J. E.
Boyd, G. D.
Bozer, R.
Bradbud, E. M.
Brady, L. J.
Brown, A. T., III
Bucklin, K. G.
Canada, C. E.
Carlson, E. S.
Chen, F. S.
Chisholm, D. A.
Cimorelli, J. T.
Clark, J. T., Jr.
Clemens, J. R.
Cocchiaro, M.
Coker, J. A.
Conant, T. W.
Cook, J. S.
Crowell, M. H.
Crump, E. E.
Cuny, J. J.
Danielson, W. E.
De Bell, J. M., Jr.
DeGrasse, R. W.
Dehoney, R. J.
Denton, R. T.
De Rosa, L. A.
Dipple, W. M.
Dishal, M.
DiStadio, D.
Doba, S., Jr.
Donaldson, W. G.
Drexler, J.
Dulac, J. P.
Edwards, R. A.
Egbert, H. F.
Engelmann, H. F.
Evans, N. L., Jr.
Farbanish, R. S.
Fay, C. E.
Fetko, J. F.
Filo, J. P.
Fletcher, R. C.
Foley, R. M.
Forman, L. E., Jr.
French, H. A.
Friedman, D. S.
Fulmer, R. J.
Gaddner, J. L.
Gewartowski, J. W.
Giger, A. J.
Glass, M. S.
Glomb, W. L.
Godley, P. F., Jr.
Goldman, H.
Goldstein, A.
Goldstein, M. I.
Graham, J. S.
Green, M. W.
Greenberg, A. H.
Greenberg, H.
Gunderson, L. C.
Halstead, W. K.
Hammer, H.
Harkless, E. T.
Harvey, J. B.
Helm, G. D.
Heney, J. F.
Henry, T. J.
Hensel, M. L.
Hensperger, E. S.
Hershenov, S.

Hewitt, W. H., Jr.
Hickey, E. J.
Higgins, R. H.
Hines, J. N.
Hines, M. E.
Hodowanec, G.
Holloway, A. L.
Horneck, J. F.
Houghton, E. W.
Ingalls, D.
Jacobs, B. H.
Jacobs, G. W.
Jacobs, I.
Jacobus, W. M.
Johnson, R. E.
Juhas, L. A.
Keller, E. W.
Kessler, J. E.
Kiesling, J. D.
Klein, M. S.
Kluver, B.
Kojima, M.
Kole, W. C.
Kolts, R. C.
Kompfner, R.
Koskos, P.
Kozimor, M.
Kreer, J. G., Jr.
Krogh, R. A.
Kups, E. F.
Kuras, H. F.
Kurokawa, K.
Lamb, J. M.
Lee, T.
Leed, D.
Lenker, J. N.
Lenzing, H. F.
Levin, R. M.
Le Vine, D. J.
Lightcap, E. T.
Lorentzen, R. B.
Lundburg, F. J.
MacVeety, R. C., Jr.
Mattingly, R. L.
McCarter, R. S.
McClelland, W. R.
McCorry, J. R.
McDowell, H. L.
McEnter, J. A., Jr.
McKay, K. G.
McMurrugh, R. W.
Meadows, H. E., Jr.
Merrill, J. L., Jr.
Moltz, A. J.
Moreno, C. N.
Morgan, S. P.
Mottram, E. T.
Mount, E.
Mulligan, J. H., Jr.
Mumford, W. W.
Napoleon, J. J.
Nebel, C. N.
Nielsen, A. H.
Novak, G.
Nowogrodzki, M.
Okean, H. C.
Olin, R. P.
Orlando, A. J.
Osborn, P. H.
Ostermayer, F. W.
Ostlund, E. M.
Panter, P. F.
Patton, B. A.
Peck, J. L.
Pecina, R. G.
Perry, I. D.
Petrich, L. G.
Pfeiffer, G. L.
Pickholtz, R. L.
Pike, N.
Pisani, R. A.
Pravetz, R. M.
Quickel, T. E.
Radin, H. W.
Rapaort, H.
Robertson, J. P.
Rusinow, K.
Saloom, J. A.
Salzer, R. M.
Samson, R. L.
Sansalone, F. J.
Sattam, I.
Schacher, D. L.
Schaefer, R. J.
Scheibner, J. F.
Schmidt, W. M.
Schneider, R. E.
Schneider, W. A.
Schumacher, H. L.
Schwartz, S.
Seidel, H.
Shangraw, C. C.
Shouri, J. C.
Simkovich, J. R.
Simpson, L.
Singer, E.
Skibneski, C. E.
Southworth, G. C.
Spanos, W. M.
Stebbins, M. D.
Stein, V. J.
Steinbrecher, E. E.
Steinhoff, R.
Stillwell, A. L.
Stinehelfer, H. E., Sr.
Sullinger, W. B.

Swall, J. R.
Szekely, Z.
Szentirmai, G.
Tatsuguchi, I.
Trenhaft, M. A.
Tsao, T. C.
Tulchin, H.
Uenohara, M. I.
Vaughan, C. B.
Vignone, E. J.
Vincent, R.
VonAulock, W. H.
Wakefield, P. R.
Walker, H. R.
Wantuch, E.
Weber, S.
Wehrle, A. W.
Welber, I.
Whalen, A. D.
Wheeler, G. W.
White, R. J.
Wickliffe, P. R., Jr.
Williams, N. T.
Wolkstein, H. J.
Woolfson, J. L.
Yariv, A.
Yellen, S.
Yohai, I.
Zach, R. W.
Zayac, F. R.
Zimmerman, A. P.
Zimmerman, G. A.
Zweibel, J.

Princeton

Belohoubek, E. F.
Bennett, S. B.
Braden, R. A.
Brough, J. R.
Caton, W. J.
Churchill, J. N.
Dostis, I.
Engelbrecht, R. S.
Epstein, J.
Ernst, W. P.
Fausel, G. W.
Fich, S.
Fletcher, D. D.
Ginsberg, L. H.
Gross, J.
Hansell, C. W.
Headrick, L. B.
Heim, C. W.
Hilibrand, J.
Hoffman, J. E., Jr.
Houser, B. E.
Keiser, B. E.
Kerbec, M. J.
Klopfenstein, R. W.
Laport, E. A.
Lefrank, F. H.
Levine, S.
Lyon, C. C.
Norman, F. H.
Parker, H.
Pinto, A.
Polgar, M. S., Jr.
Presser, A.
Rankin, J. B.
Rynn, N.
Sabisky, E. S.
Sirkis, M. D.
Snyder, C. L.
Sterzer, F.
Sullivan, B. D.
Vaccaro, F. E.
Vural, B.
Westneat, A. S., Jr.
Woodward, O. M., Jr.

Region 3

Atlanta

Bryant, D. J.
Carnes, H. L., Jr.
Clayton, L., Jr.
Davies, H. S.
Hayes, R. D.
Hildreth, H. J.
Hollis, J. S.
Johnson, R. C.
King, T. R.
Long, M. W.
Moseley, R. E.
Parker, B. A.
Parmer, W. P.
Peace, G. M.
Pittman, N. W.
Skoglund, O. N.
Smith, C. E.
Smith, R. T.
Spencer, J. M., Jr.
Ware, C. L., Jr.
Whitaker, J. L.
Williams, A. B.
Wynn, W. D.

Baltimore

Alexander, R. B.
Ap Rhys, T. L.
Asbed, N. G.
Barthel, D. R.
Barton, J. H.
Bauer, R. J.
Bickart, T. A.

Bishop, F. W.
Blotzer, W. L.
Bolt, C. A., Jr.
Brownell, D. C.
Buehler, G. V.
Carroll, T. J.
Cassedy, E. S., Jr.
Cepoi, J.
Claborn, K. D.
Cohen, A.
Cohn, M.
Cole, E. B., Jr.
Davis, R. J.
De Andrade, W. C.
Dempsey, M. E.
Dickens, L. E.
Dullinger, A. G., Jr.
Eby, J. T.
Evans, G. E.
Fainberg, J.
Farrell, T. W.
Finke, R. S.
Flaherty, J. M.
Fuller, W. C., Jr.
Gessner, U.
Goodman, S. N.
Grauling, C. H., Jr.
Hanks, H. C., Jr.
Hardesty, S. J.
Harris, H. N.
Hendershot, J. H.
Hoffmanner, G. H.
Hom, W. R.
Jackson, H. L.
Johnson, C. M.
Jones, R. E.
Jones, W. R.
Katz, R. E.
King, D. D.
Klein, G. I.
Koether, G. H., Jr.
Kott, M. A.
Kudo, F. M.
La Bree, C. T.
Limansky, I.
Long, P. C., Jr.
Mabry, F. S.
May, H. A.
Meador, A. B., Jr.
McDonough, J. T.
McDonough, R. N.
Molz, K. F.
Moore, R. A.
Mordecai, M. J.
Moskowitz, C.
Mott, O. B.
Munro, J. R.
Nichols, S. C.
Ogg, F. C., Jr.
Packard, R. F.
Pavelka, C. F.
Peters, H. J.
Pipkin, J. E.
Pratt, A.
Ralston, W. P.
Rannelslad, A.
Renwick, W. H., Jr.
Sacks, L. H.
Sanner, G. E.
Sartorio, D. R.
Scanga, W. A.
Schrank, H. E.
Schutz, H.
Sefton, H. B., Jr.
Seman, A. E., Jr.
Shelor, E. G., Jr.
Sichelstiel, B. A.
Silva, F. A.
Skolnik, M. I.
Smith, E. L., Jr.
Smith, R. J.
Spencer, R. C.
Spintman, D. A.
Stephenson, J. O.
Tates, R.
Thompson, J. E.
Tschiegg, M. D.
Tutlington, T. R.
Tyaack, F. H.
Valenzuela, G. R.
Visher, W. A.
Watson, T. E.
Webb, W. R.
Wells, R. W.
Wentworth, F. L.
Wentz, J. L.
Wiesner, J. C.
Willey, R. H.
Wiltse, J. C., Jr.
Young, L.
Youngberg, D. A.
Zimmerman, E. G.

Central Florida

Bivans, R. W.
Clarke, R. L.
Cragger, J. A.
Doughty, S. D.
Ferguson, R. E.
Fletcher, R. C.
McMath, D. C., Jr.
Pelchat, G. M.
Smith, C. E.
Summer, L. E.
Thompson, W. W.
West, K. A.

Williams, L. E.
Wren, A. W., Jr.
Young, L. R.

Florida West Coast

Andrews, J. E.
Aucermann, R. C.
Bellare, D.
Brown, J., Jr.
Coates, J. R.
Dale, C. H., Jr.
Dashiell, E. V.
Day, W. B.
Duncan, B. J.
Eckert, G. F.
Glenn, R.
Gonzalez, R. E.
Greenwood, R. E.
Grimes, E. S., Jr.
Helderman, T. E.
Henning, R. E.
Holt, J. G.
Hoover, J. C.
Horner, G. F.
Hunt, H. W.
Jansen, J. N.
Lampkin, G. F.
Lewis, C. A.
Parkes, D. A.
Phillips, E. N.
Pippin, J. E.
Rodrigue, G. P.
Rosenzweig, J. E.
Ryan, J. J.
Savalli, F. P.
Scott, D. C.
Sloan, S. C., Jr.
Sullivan, D. J.
Taft, D. R.
Uglow, K. M., Jr.
Wells, J. D.
White, E. L.
Willert, A. F.
Wilson, L. K.
Witt, R. E.
Wooten, W. W., Jr.

Gainesville

Akre, R. O.
Beville, R. E.
Bosisio, R. G.
Chambers, R. P.
Eaker, L. C.
Ehster, R. G.
Elder, T. A.
Frerking, H. W.
Garrott, W. L.
Lally, P. M.
Marlow, D. R.
Rhoads, A. S., Jr.
Rich, C. E.
Russ, D. S.
Strauss, R.
Wigle, T. A.
Wing, A. H., Jr.
Yost, N. V.

Huntsville

Creel, J. D.
Gregg, R. W.
Herring, R. A., Jr.
Justus, J. R.
Lowery, H. R.
Parnell, C. C., Jr.
Scheer, A. W., Jr.
Schumann, F.
Scott, W. R.
Smith, C. N.
Valencia, V. I.
Whitehurst, R. N.

Miami

Clark, G. W.
Cook, H. A.
Levin, S. M.
Sneed, J. O.

North Carolina

Balden, J. M.
Barron, J. I.
Beckett, R. R.
Bezera, G.
Brown, F. R.
Carroll, J. C.
Cornett, L. A.
Cronin, H. C.
George, R. T., Jr.
Harris, R. H.
Hinner, J. A.
House, R. O.
Howard, T. E.
Lackey, G. F.
Minor, M. J.
Moore, D. R.
Peake, M. W.
Roberts, J. C.
Rudisill, M. E.
Steuer, W. T.
Ward, D. L.

Northwest Florida

Clifton, C. L.
Crafe, R. W.
Leger, P. F.
Saffer, R. A.
Tomberlin, J. L.

Orlando

Bassett, H. L.
Chasteen, J. W., Jr.
Cutler, M. A.
Gray, A. R.
Horton, W. H.
Houseman, E. O., Jr.
Isaacson, S.
Jaramillo, J. G.
Johnson, R. E.
Painter, P., Jr.
Powers, D. M.
Rhodes, D. R.
Severance, F. D.
Tracy, J. E.
Weaver, H. R.
Webber, H. E.
Webster, R. E.

Philadelphia

Abeyta, I.
Allerton, G. L.
Anderson, W. G.
Arnold, P. H.
Artuso, N. F.
Ausley, J. W.
Avellino, W. R.
Bailey, R. E.
Bargellini, P. L.
Bash, I. F.
Bazan, S. J.
Beardwood, J. T., III
Beatty, P. H.
Beck, M. R.
Benham, T. A.
Benson, S. E.
Berkowitz, R. S.
Bicking, H. P.
Binzer, C.
Bisaga, J. J.
Blasberg, L. A.
Bogush, A. J., Jr.
Bolgiano, L. P., Jr.
Bowman, D. F.
Bradford, C. E.
Bradley, W. E.
Brady, J. A.
Brennecke, N. R.
Brett, G. F.
Brumbaugh, J. M.
Cantaño, L. J.
Carey, G. R.
Cerva, C. H.
Chadwick, P. S.
Chronister, W. M.
Ciletti, V. J.
Clark, F. R.
Clasen, C. P.
Clavier, A. G.
Coburn, J. M.
Colby, N. C.
Combella, E. M.
Cooley, C. C., Jr.
Courtney, J. E.
Cox, A. L.
Crawford, C. F.
Crosby, D. R.
Davis, C. E.
Davis, D. A.
Deaver, D. J.
Doherty, W. E., Jr.
Doviak, R. J.
Dunkel, H. D.
Eberle, H.
Ellis, D. J.
Escriva, C. F.
Everhard, F. U., Jr.
Fast, H.
Faunce, N. P.
Feller, M. S.
Fey, R. C.
Fink, E. A.
Fiore, R. E.
Foley, T. U.
Follensbee, W. R.
Follmer, W. C.
Frank, R. B.
Frederick, R. H.
Fricke, R. H.
Friend, A. W.
Galbraith, J. R.
Gallshaw, J. J.
Gans, J. S.
Gardiner, F. J.
Gazen, L.
Gillette, M. M.
Goldstone, B. J.
Gore, E. M.
Gottschalk, W. M.
Grace, J. W.
Grieco, L.
Grimm, A. O.
Groff, H. A.
Gumacos, C.
Hacking, C.
Haimowitz, B.
Hamm, N. G.
Hammersand, F. G.
Hanemann, H. A., Jr.
Harcar, A. R.
Hayes, D. E.
Heald, M. A.
Heilmeier, G. H.
Heskett, H.
Hewitt, E. C.

Hockeimer, H. E.

Hodge, W. H.
Hoffman, M.
Hoffman, N. N.
Holaday, V. D.
Honda, H.
Hricko, R. M.
Hinnicke, R. L.
Hurst, S. R.
Hyde, G.
Jacobs, E.
Jarecki, S. J.
Jayne, F. B.
Jordan, A. K.
Kall, A. R.
Kampf, R. J.
Kilpatrick, D. G.
King, W. C.
Kinkead, W. K.
Klawnsnik, F.
Klein, M. J. H.
Knapschaefer, D. H.
Koonz, R. F., Jr.
Kos, E. E.
Kozak, M. J.
Kraft, J. E.
Kropp, R. J.
Laurent, G. J.
Lawton, R. S.
Lemberg, B.
Lewis, E. S.
Liston, J.
Lombardini, P. P.
Luciw, W.
Luksch, J. A.
Martin, K. R.
Mathwich, H. R.
Matthews, E. W., Jr.
McCarthy, C. S., Jr.
McCoy, C. T.
McCracken, L. G., Jr.
McGahey, E. W., Jr.
Mittelman, W.
Moule, W. N.
Nash, A. A.
O'Neill, M. J.
Osbahr, B. F.
Paiss, M. H.
Palmer, M., Jr.
Paulsen, J. F.
Peterson, C. E.
Petrilla, A. D.
Podolski, G. A.
Reisener, W. C., Jr.
Richman, R. R.
Rizzetto, D. J.
Roop, R. W.
Rosen, B. H.
Roth, J. H.
Sander, S.
Sayer, T. C.
Schach, S.
Schumacher, R. T.
Schwartz, A. J.
Schwartz, R. F.
Senulis, R. E.
Sheppard, W. H.
Silverstein, E. R.
Simons, K. A.
Smyton, S. A.
Solomon, S.
Spitzer, E. E.
Stahl, P. D.
Stahl, R. A.
Stanton, J. W.
Starks, W. H.
Stokes, P. F.
Story, T. H.
Sumerlin, W. T.
Thompson, J. R.
Thompson, L. E.
Thowless, E. A.
Titefsky, E. J.
Tomei, J. B.
Twist, G. J.
Vaughan, T. J.
Veldhuis, L. A. C.
Venter, D. C.
Ver Wey, G. A.
Vincent, D. G.
Warren, W. L.
Watson, B. W.
Weinberg, A. D.
Wieler, K. E.
Willette, E. L.
Wing, D. H.
Winkler, R. H.
Worst, J. L.
Yaffe, M.
Yingst, T. E.
Young, C. T.

South Carolina

Fellers, R. G.
Hudson, C. A. J.
Jeter, D. G.
Rouffy, F. E., Jr.

Virginia

Baker, W. L.
Blankenship, H. T.
Burlock, J.
Crispin, H. L.
Croswell, W. F.

<p>Fadeley, J. H. Faust, R. P. Forehand, R. R. Fuller, H. P., Jr. Gannett, D. K. Grymes, J. R., Jr. Guth, R. U. Hansen, J. A. Harris, O. R. Harvey, G. L. Hastings, C. E. Herrell, R. W. Jones, T. B., Jr. Keast, P. M. Kluender, E. C. Landes, H. S. Leonard, W. F. Linker, J. B., Jr. Malloy, J. J. Miller, L. S. Mingia, S. L. Muller, E. S., Jr. Poppe, J. R. Purnell, L. S. Ray, K. P. Rose, G. D., Jr. Smith, J. Stermer, R. L., Jr.</p> <p>Washington</p> <p>Alde, R. O. Algor, M. M. Allen, D. A. Allen, P. J. Anderson, R. J. Andrew, R. T. Arnett, H. D. Babcock, J. H. Ballad, J. L. Barnett, J. S. Baylski, M. W. Bateman, R. Bawer, R. Bernstein, B. Bickford, F. H., Jr. Birochak, D. Blankenship, A. C. Boesch, P. W. Bostick, B. E. Bowie, D. M. Briceno, H. D. Bricout, P. A. Brimberg, M. M. Bruns, H. B. Buikhardt, R. H. Callaway, H. D. Carr, L. H. Celderan, B. Chadwick, G. G. Cheston, T. C. Chi, A. R. Chu, Y. Clarke, A. S. Cleckner, D. C. Coleman, H. P. Cook, F. W. Cooper, H. W., III Crenshaw, A. N., Jr. Demaree, G. A. Dent, J. R. Diehl, L. G. Diels, J. C. Distad, M. F. Dropkin, H. A. Dyke, E. Edwards, A. J. Enos, R. M. Facchine, F. B. Feild, S. C., Jr. Fink, C. Fischer, R. L. Fischer, W. Forward, R. L. Frederick, E. W. Friedberg, I. S. Gabriel, W. F. Garner, W. G. Garofalo, N. R. Garrett, W. O. Garver, R. V. Gerlach, H. W. A. Girard, S. H., Jr. Giroux, R. A. Gleason, D. H. Goldberg, H. Gould, W. I., Jr. Grantham, R. E. Green, W. C. Gribbons, J. G. Griffith, K. E. Groff, R. F. Guhne, R. D. Gumina, L. V. Hagaman, B. G. Halligan, F. J. Hanyok, A. Hartle, L. U. Hedrich, A. L. Henry, V. F. Herman, J. Hobokan, A. Hockensmith, R. P. Hocking, L. J. Hooper, E. T. Hornbeck, W. D. Howard, D. D.</p>	<p>Howland, A. R., Jr. Huck, W. J., Jr. Hurlburt, R. W., Jr. Irby, R. F. Jackson, E. H., Jr. James, W. G. Johnson, W. R. Jones, G. R. Jones, S. R. Kaiser, J. A., Jr. Kales, M. L. Katzin, M. Keating, T., Jr. Kefalas, G. P. Kempf, R. F. Kirshner, J. M. Klass, P. J. Kohler, H. W. Krahe, L. R. Krejci, D. W. Kramer, E. Kulesha, K. J. Leahy, C. J. Leavitt, W. E. Lehfeldt, H. J. Lewis, J. E. Liss, F. T. Lockwood, E. H. Luff, F. T. Maestri, A., Jr. Mahoney, F. J., III Marcotte, P. G. Marks, M. M. Marlow, W. C., Jr. Marshall, F. S., Jr. Martin, A. P., Jr. McDonald, K. D. McIntyre, R. T. Mendus, W. M. Miller, J. W. Mills, R. V. Mischler, E. F. Morgan, R. Morrow, C. M. Myers, D. M. Nagy, A. W. Newhouse, A. R. Newman, R. A. Nye, H. A., Jr. Olin, I. D. Ornstein, E. Ould, R. S. Pan, P. M. Parker, C. F., Jr. Parker, M. L., Jr. Peyton, P. B., Jr. Pfund, C. E. Phillips, R. M. Poor, V. D. Popolo, J. V. Portmann, P. A. Ports, D. C. Potter, R. S. Pullara, J. C. Puro, W. O. Quigley, C. E. Quigley, H. D. Randall, C. R. Ranucci, J., Jr. Ravinsky, J. Rayburn, R. A. Read, A. H. Redden, M. S., Jr. Regardh, C. G. B. Reggia, F. Reiser, D. Richardson, D. J. Ringensbach, M. E. Rockwell, P. Roy, L. B. Rueger, L. J. Runyon, C. A. Rutz, E. M. Ryan, W. E. Salisbury, L. L., Jr. Savarese, R. T. Schmid, O. J. Schreyer, S. D. Settersten, R. A. Shamp, D. J. Shapiro, G. Shelton, J. P., Jr. Shimabukuro, K. Silins, A. Simmons, G. C. Singer, C. H. Sloan, R. F. Smith, C. Smith, C. J. Smith, J. V. Smith, S. T. Snead, J. M. Sorger, G. U. Soroko, S. R. Stahl, B. E. Starkey, J. F. Stewart, R. B. Stilwell, D., Jr. Stone, R. O. Swanekamp, J. E. Taylor, R. E. Terauds, J. J. Thompson, J. H. Thwaites, K. W. Tozzi, L. M. Turnage, H. C.</p>	<p>Tuttle, L. P., Jr. Usilton, R. R. Valkenburg, E. P. Vann, W. L. Varela, A. A. Veiel, A. J. Vignali, J. A. Wainwright, R. A. Waldschmitt, J. A. Walsh, D. F. Ward, H. T., Jr. Weinschel, B. O. Weitzel, R. L. White, D. R. J. Wigington, R. L. Wilson, W. H. Withrow, W. E. Wolfe, E. A. Wolfe, J. J. Woo, W. G. Worne, B. E. Wuermsier, E. Yannarell, N. T.</p> <p>Region 4</p> <p>Akron</p> <p>Bohar, J. Bowman, B. M. Brown, D. L. Cherveney, V. J. Chimera, V. J. Cook, E. E. Di Caudo, V. J. Di Feo, V. P. Dorsey, J. P. Gray, C. L. Hakes, T. H. Hazlip, G. M. Houstean, C. M., Jr. Huber, J. C., Jr. Iler, K. R. Ingalls, R. S. Kelly, C. M. Klever, W. O. Mathis, H. F. Naylor, J. T. Pressel, P. I. Strang, J. R. Welch, G. H.</p> <p>Central Pennsylvania</p> <p>Dornecker, J. A. Erdley, R. F. Files, W. D. Geronimo, M. B. Hall, F. T., Jr. Hastert, D. D. Herlt, B. G., Jr. Herman, E. B. Holter, D. H., Jr. Key, J. T., Jr. Krueger, D. Norris, R. S. Obligier, J. T. O'Connor, H. C., Jr. Passow, R. L. Sharp, A. C. Smith, J. P. Thompson, F. C. Willis, P. T. Wolfe, R. E.</p> <p>Cincinnati</p> <p>Bereskin, A. B. Cartei, S. A. Dutton, C. E. Ecker, J. L. Gorker, G. E. Gruser, J. R. Kerber, M. C. Kuecken, J. A. Livingston, E. J. Marshall, D. A. Maxim, R. A., Jr. Sang, W. W. Seward, G. J. Takahashi, E. M. Wallace, T. L. Weaver, C. W. Whittenberger, J. S. Zupansky, M.</p> <p>Cleveland</p> <p>Ackerman, E. K. Bird, J. R. Braschwitz, H. J. Burhans, R. W. Collin, R. E. Davison, B. Eggimann, W. H. Elze, R. P. Gardner, R. A. Hadzoglov, J. Harmon, J. L. Hsu, H. P. Jaralz, E. S. Korman, D. A. Kragle, R. J. Marshall, F. R. Penkowski, L. J. Phillips, W. E., Jr. Plonsey, R. Puskorius, J. Ray, H. A., Jr.</p>	<p>Schunemann, C. F. Scott, E. P. Storey, W. T. Wozniak, A. J.</p> <p>Columbus</p> <p>Baechele, J. R. Blake, R. E. Boehner, C. H. Bulman, W. E. Chang, W. S. C. Chen, S. N. C. Chope, H. R. Chu, T. S. Cosgriff, R. L. Crawford, R. W. Dawirs, H. N. De Vore, R. V. Dobson, D. A. Falkenbach, G. J. Garbacz, R. J. Green, R. B. Habermann, C. L. Hayden, J. R. Jones, E. A. Joost, A. E. Kennaugh, E. M. Kennedy, R. F. Kisha, A. Ko, H. C. Kouyoumjian, R. G. Leonard, J. D. Levis, C. A. Lubnau, D. G. Luke, T. E. Milford, F. J. Pang, T. C. Peake, W. H. Perry, R. C. Peters, L., Jr. Pienkowski, E. C. Plugge, R. J. Potts, B. C. Querido, H. B. Richmond, J. H. Rife, W. E. Rinaldi, A. W. Roland, E. T. Ryan, J. F. Stoutenburg, D. V. Stropki, G. T. Stuart, W. D. Thomas, O. D., Jr. Tice, T. E. Tinkham, H. J. Tischer, F. J. Troyan, J. F. Tsu, R. Wong, K. H. Yaw, D. F.</p> <p>Dayton</p> <p>Benson, M. C. Brumfield, W. T. Crouse, R. J. Garrett, A. F. Hanneman, D. A. Hoeffle, R. R. Klingler, G. McAdory, R. W. Murphy, P. E. Pappas, M. J. Rippin, J. F., Jr. Simopoulos, N. T. Vanderpool, H. D. White, D. A. Wiegert, P. G., Jr.</p> <p>Detroit</p> <p>Adams, A. T. Adams, D. K. Alward, J. L. Bair, M. E. Boers, J. E. Breymaier, R. W. Brown, L. R. Bryant, J. H. Chapman, F. W. Cheal, J. Chute, G. M. Dong, R. P. Earl, K. C. Eidson, J. C. Faram, H. D. Ferris, C. C. Fischl, R. Gunderman, R. J. Haddad, G. I. Haddock, F. T. Hamstra, C. J. Hand, R. F. Heim, D. S. Hiatt, R. E. Hoop, R. E. Jones, H. E. King, J. E. Konrad, G. T. Kordos, R. W. Kuiper, J. W. Larson, R. W. Larson, Ronald W. Lauchner, K. F. Lawrence, B. T. Lyon, J. A. M. Miller, M. H. Nichols, A. D.</p>	<p>Nichols, G. B. Olte, A. O'Neal, R. D. Paul, L. E. Ray, D. C. Raymond, W. W. Ristow, H. E. Rollin, R. A., Jr. Roth, P. F. Rykala, T. P. Schpok, I. L. Sharpe, C. E. Simanyi, A. I. Sklar, J. R. Smith, A. E. Sobel, H. Stone, J. L. Strand, J. Strelzoff, J. A. Szeles, D. M. Taras, S. M. Van Tersch, L. W. Walker, S. H. Walser, R. M. Ward, J. W. Winters, L. C. Wong, A. Wooley, G. J.</p> <p>Emporium</p> <p>Winters, W. J.</p> <p>Pittsburgh</p> <p>Bossart, P. N. Golla, E. F. Hau, R. D., Jr. Hogge, C. R., Jr. Hvatum, H. Kadake, E. Klotzbaugh, G. A. Marusich, E. A. Miller, R. A. O'Shea, R. P. Osial, T. A. Peters, J. E. Reissig, G. W. Rupp, J. A. Schatz, E. R. Sterrett, J. K. Strattan, R. D. Vogley, C. E., Jr. Wood, M. G. Youmans, A. B.</p> <p>Toledo</p> <p>Chipman, R. A. Cooper, D. W. Creighton, G. W. Lavender, J. S., Jr. Wott, H. W.</p> <p>Western Michigan</p> <p>Scott, H. R.</p> <p>Williamsport</p> <p>Eck, J. P. Horrigan, J. B. Sibley, R. C. Simmons, W. J., Jr.</p> <p>Region 5</p> <p>Cedar Rapids</p> <p>Adelson, J. W. Baldwin, L. G. Bellville, W. H. Berry, D. G. Brobst, J. D. Dietrich, F. J. Dowell, R. J. Duhamel, R. H. Duncan, J. W. Emde, J. W. Johnston, D. H., Jr. Lerwick, R. R. Lister, E. C. Minerva, V. P. Ore, F. R. Pavlat, J. R. Post, R. E. Reinhardt, W. E. Ross, R. E. Sawville, E. V. Ulstad, M. S. Ware, L. A.</p> <p>Chicago</p> <p>Aito, I. Allen, C. R. Allen, P. G. Anton, A. J. Arnow, C. L. Baid, J. R. Balmain, K. G. Barrick, W. E. Bauhs, K. C. Beam, R. E. Becker, R. C. Becker, W. R. Beebe, C. W. Beneke, E. H. Berlin, R. E. Bertorello, T. A. Bialecke, E. P. Bliss, G. B.</p>
---	---	--	---	--

Bloomquist, L. A.
Book, E. G.
Branigan, J. T.
Bremigan, R. O.
Brodwin, M. E.
Brown, J. S.
Camillo, C.
Carrel, R. L.
Cassettari, F.
Castor, R. W.
Chapman, R. H.
Chen, F. C.
Chiu, P.
Chow, H. S. C.
Cohn, G. I.
Cohn, S. I.
Cohoon, R. L.
Coleman, P. D.
Crotty, R. E., Jr.
Crumly, C. B.
Dalton, R. C.
Damm, G. J.
Davis, R. H.
Del Vento, J. M.
Dervishian, E.
Deschamps, G. A.
Diers, E. F.
Dougal, A. A.
Druz, W. C.
Durkee, C. E.
Dvorak, J. F.
Dyson, J. D.
Emery, W. L.
Erickson, J. W.
Ernst, E. W.
Evans, K. T.
Findling, M. J.
Flesher, G. T.
Frankart, W. F.
Fuglestad, K. R.
Gaddy, O. L.
Gershon, J. J.
Goldstein, L.
Gorecki, G. S.
Grace, J. W.
Graziano, V.
Green, R. E.
Groberg, L. E.
Haaland, C. M.
Hackbarth, H. R.
Hajek, R. J.
Hakki, B. W.
Hargis, R. N.
Healy, A. M.
Heid, K. K. W.
Hemming, D. H.
Herling, D. L.
Higgs, J. A.
Hubert, J. J.
Ingram, R. W.
Kenyon, R. J.
Kiheri, A.
Kiver, M. S.
Koch, E. N.
Kocsis, L. L.
Kott, W. O.
Kowitz, A. E.
Krakora, J. J., Jr.
Kunchitani, M. S.
Kuniyoshi, S.
Kunz, W. E.
Kvitek, G. L.
Lafrance, J. D.
Lee, C. Q.
Leonard, J. C.
Louie, L. M.
MacAskill, R. B., Jr.
MacPhie, R. H.
Magnuski, H.
Maier, R. H.
Maine, C. P.
Marquand, R. J.
Mast, P. E.
Mathews, C. A., Jr.
Matos, F.
Mayes, P. E.
McClelland, O. L.
McLennan, E. A.
McNamee, R. J.
Miller, C. L.
Miller, D. A.
Mittra, R.
Moore, H. E.
Morgan, R. E.
Mueller, P. H., Jr.
Nagley, R. J.
Nail, J. J.
Pakan, J. J.
Peach, L. C.
Pellock, L. E.
Peterson, J. W.
Pichler, R. H.
Rao, K. V. N.
Robinson, D. E.
Rose, K.
Rosenbaum, F. J.
Sawada, F. H.
Sayles, H. L.
Scheldorf, M. W.
Scherer, P. J.
Schultz, W. J.
Segal, A. A.
Skaperdas, D. O.
Sladek, N. J.
Slawinski, W.
Smoll, A. E.

Soma, R.
Stafford, J. J.
Stastny, G. F.
Stecca, A. J.
Steier, W. H.
Stelzer, D. L.
Sternlight, L.
Stickling, J. E.
Strain, R. J.
Stroik, R. G.
Struck, D. E.
Sumoski, A. W.
Tang, C. H.
Tempka, J. A.
Thomas, C. B.
Thomas, G. E.
Thomas, R. G.
Ulaszek, J. J., Jr.
Verdeyen, J. T.
Watts, C. A.
White, E. S.
White, R. F.
Widugiris, W., Jr.
Woodbury, H. L.
Yang, R. F. H.

Evansville-Owensboro

Finley, R. W.
Quirk, J. B.
Walker, R. J.

Fort Wayne

Dees, J. W.
Di Loreto, C. D.
Fisher, C. C.
Giffin, G. S.
Gough, L. E.
Gramer, E. E., Jr.
Hambrock, H. E.
Hessler, J. Jr.
Jensen, C. W.
Krulic, R. L.
Mast, P. L.
McFadden, J. H.
Snell, J. W.
Terry, C. B.

Indianapolis

Calvert, O. L.
Czarapata, A. H.
Evans, C. M.
George, P. H.
Hayt, W. H., Jr.
Heim, K. E.
Holub, A. J.
Levine, M. W.
Nelson, D. D.
Peralta, E.
Presti, B.
Robbins, A. H.
Schultz, F. V.
Smith, W. A.
Spencer, R. L.
Walter, E. R.

Louisville

Betz, J. D.
Fitzmayer, L. H.
Frederick, R. H.
Haigis, S., Jr.
Koppus, O. G.
Mehling, T. H.
Voyles, R. L.

Milwaukee

Affronti, A. P.
Bloedorn, A. R.
Bucher, R. A.
Cristal, E. G.
Dimmick, R. F.
Ishii, K.
Lemanski, T. J.
Nag, B.
Pepper, J. R.
Scheibe, E. H.
Schickofke, R. C.
Schleicher, F.
Shaver, P. J.
Slowikowski, J. J.
Soref, R. A.
Swift, W. B.
Taus, H. G.
Van Bladel, J. G.

Omaha-Lincoln

Baker, R. L.
Blackmon, O. A.
Bolleson, V. P.
Borcher, E. J.
Cox, D. C.
Doll, C. L.
Doll, R. E.
Elwell, W. G.
Fuchser, T. D.
Gallawa, R. L.
Gishpert, J. F.
Goering, I. G.
Hruby, M. M.
Hyde, C. M.
Jett, C. O.
Kjar, R. A.
Larsen, L. G.
Lasensky, M. M.
Paska, T. M.
Pyle, R. II.
Rader, C. D.

Rood, R. S.
Ross, R. M.
Schaudt, P. D.
Schneider, A. J.
Schrader, K. W.
Sorensen, D. L.
Tyrell, L. A.
Wesner, J. A.

South Bend-Mishawaka

Beazell, H. L.
Cunningham, D. L.
Firner, J. F.
Marshall, R. E.
Modesitt, M. B.
Pilcher, R. M.

Twin Cities

Amoo, L. R.
Armstrong, D. B.
Bergan, K. N.
Boatman, L. R.
Callahan, M. J.
Chen, D.
Coleman, J. R.
Davis, W. W.
Evenson, E. K.
Foster, K. S.
Gahler, W. J.
Grosz, W. S.
Haxby, B. V.
Holte, J. E.
Johnson, R. R.
Kanda, A. F.
Kellough, S. H.
Kerske, J. F.
Lindgren, G. E.
Nordstrom, J. E.
Raabe, H. P.
Rossing, T. D.
Sikorski, J. W.
Spencer, W. H.
Sturges, D. J.
Van Der Ziel, A.

Region 6

Beaumont-Port Arthur

Bean, D. L.
Thompson, A. R.
Walley, J.

Dallas

Anderson, J.
Allen, M. B.
Bailey, R. W.
Bechtel, B.
Blackwell, L. A.
Bondy, M. A.
Bonner, J. H.
Breithaupt, J. J.
Bullock, M. W.
Carr, W. B.
Coats, R. P.
Cuesta, N., Jr.
Davis, C. F., Jr.
Douglas, J. H.
Earhart, C. E.
Forsyth, P. G.
Geia, A. J.
Granberry, D. S.
Grubbs, W. C., Jr.
Hallford, B. R.
Hertel, P. Jr.
Hyltin, T. M.
Jackson, H. J.
Kaiser, R. L.
Kearley, R. I., Jr.
Kettler, E. W., Jr.
Kuehne, W.
Landis, D. W., Jr.
Langston, J. W.
Lee, C. C.
Lovelady, B. W.
Martin, E. E.
Mason, A. E., Jr.
McCord, A. R.
McMillin, J. M., Jr.
Petrasek, A. C.
Petritz, R. L.
Sanford, A. L.
Sharp, F. B., Jr.
Shuffler, R. M.
Stanton, A. N.
Stone, R. M.
Strom, L. D.
Thomas, C. T.
Thompson, W. J.
Vandigriff, J. E.
Vilbig, J. L., Jr.
Vincent, B. T., Jr.
Ware, P. M., Jr.
Warriner, B.
Wetterau, L. C., Jr.
Wilkinson, M. M.
Williams, C. E.
Wunsch, D. E.

Burkepile, J. M.
Bussey, H. E.
Cateroa, J. V.
Culshaw, W.
Dalke, J. L.
Decker, M. T.
Elam, T. W.
Estin, A. J.
Faris, J. J.
Flaherty, C. L.
Foley, W. V.
Green, C. P.
Guiraud, F. O.
Harrington, R. D.
Hedberg, C. A.
Johnson, H. S.
Kelly, G. A.
King, R. J.
Kirby, R. C.
Kopl, W. J.
Lance, H. W.
Larson, R. E.
McGuire, D. W.
Miller, L. W., Jr.
Niesen, E.
Perkins, M. E.
Price, G. W.
Quirk, W. J.
Richardson, J. M.
Rynning, J. L.
Schafer, G. E.
Spano, A. J.
Spillane, L. R.
Stacey, D. S.
Thompson, M. C., Jr.
Wait, J. R.
Wang, C. S.
Wassink, H. W.
Waters, D. M.
Wilber, R. W.
Wiseman, S. D.

El Paso

Bigelow, G. F.
Haas, H. W.
Kerker, R.
Lovitt, S. A.
McCalla, T. M., Jr.
Schaferman, R. L.
Taylor, L. S.
Tipton, R. B.
Welch, C. M.
Wilmot, R. D.

Fort Worth

Bean, F. C.
Brust, M. F.
Bryan, K. W.
Cook, A. B.
Dunlap, K. H.
Gentry, B. F.
Harman, D. G.
Heidt, R. C.
Roy, F. J.
Silvernell, R. B.
Van Hoozer, C. H.
Watkins, O. E.
Willman, J. F.

Houston

Aldridge, J. P., III
Caplan, R. S.
Cox, W. B.
Erath, L. W.
Hays, D. T.
Hudgins, W. T., Jr.

Kansas City

Aco, R. E.
Anderson, R. W.
Boss, G. D.
Brown, T. D.
Chinn, F. T.
Clarke, E. L.
Cummings, A. J.
Dalton, R. C.
Gustafson, G. R.
Hax, D. H.
Hayes, D.
Hodge, R. E.
Jones, P. V.
Long, E. D.
McDowell, J. F., Jr.
Miller, C. V.
Nahman, N. S.
Nowotny, K. E.
Nuckolls, R. G.
Phelps, G. R.
Robertson, A. J. L.
Roszkowski, G. J.
Stout, H. L.
Waite, W. P.
Wilcox, J. V.

Little Rock

Cannon, W. W.
Collins, R. E.
Poularikas, A.

New Orleans

Braquet, L. J., Jr.
Chigoy, W. A.
Crawford, R. M.
Cronvich, J. A.
Davis, P. A., II
Gadsden, C. P.

Tillman, L.
Tunnell, W. A.

Oklahoma City

Herriott, J. K., Jr.
Reynolds, J.
Staley, J. D.
Thomas, D. F.
Wichels, J., Jr.
Wood, G. J.

St. Louis

Abernathy, J. L.
Bennett, D. W.
Brennan, R. D.
Davies, H. W.
Gardner, B. H.
Hirsch, O. C.
Kellerman, R. A.
Kuhlman, E. A.
Lechtreck, L. W.
Mahon, M. J.
McHoney, L. M.
Mohrman, R. F.
Mosley, C. E.
Mueller, T. E.
Netter, H. A.
Reiniger, R. A.
Saxe, R. E.
Schaeperkoetter, L. C.
Troth, B. J.
Verbarg, L. E.
Vicedomine, D. A.
Wood, S.

San Antonio

Coale, C. R., Jr.
Economy, R.
McHugh, E. L.
Simpson, S. H., Jr.
Vivian, R. A.
Wangler, R. B.

Shreveport

Randolph, A. M.
Strickland, E. C.

Wichita

Day, W. R.
Eldridge, C. D.
Flowerday, W. L.
Hutchinson, D. P.
Klatt, W. K.
Kohman, E. J.
Prihar, Z.
Tierney, P. V.

Tulsa

Hill, J. K. H.
Jacobs, G. G.

Region 7

Alamogordo-Holloman

Nicholson, T.

Albuquerque-Los Alamos

Allen, L. J.
Arnot, G. A., Jr.
Brassfield, J. R.
Chia, C.
Cilke, H. J.
Connell, J. C.
Dike, S. H.
Ellis, P. R., Jr.
Fagan, P.
Finch, H. D.
Fossum, D. E.
French, G.
Gelt, P. A.
Glass, R. E.
Hale, L. C.
Hayes, B.
Jones, M. C.
La Fleur, W.
Larison, L. P.
Lincoln, R. A.
Scharer, R. G.
Senter, C. H.
Taylor, C. D.
Weeks, W. L.
Weingarten, D. H.
Widenhofer, N. C.
Yearout, D. K.

Anchorage

Childress, J. C., Jr.
Darrah, G. L.
Grob, L. W.
Hauck, R. A.
Scott, R. C.
Svetc, D. L.
Weatherly, M. R.

China Lake

Creusere, M. C.
Deyoe, D. C.
Hechtel, J. R.
Ruggieri, F. A.

Fort Huachuca

Barkson, J. A.
Lamb, J. J.

Hawaii

Chang, D. C.
Harada, S.

Higa, K.
Jones, R. C.
Miller, R. W.
Teixeira, P. D.

Los Angeles

Abele, R. J.
Adcock, M. D.
Acker, W. W.
Agadoni, C. A.
Ajioka, J. S.
Albrecht, A.
Algeo, J. A.
Alder, J. R.
Allmandinger, E. F.
Alpine, P. E.
Ambrose, J. R.
Anderson, G. R.
Anderson, R. W.
Aron, R. M.
Ashcraft, W. D.
Asmus, J. F.
Ayres, W. P.
Baird, W. H.
Baker, B. W.
Baldwin, R. C.
Barfield, R. O.
Barquist, W. S., Jr.
Batson, D. D.
Bauer, P. W.
Bauman, H. W.
Beavin, R. L.
Beck, A. B.
Becker, J. T.
Bedrosian, E.
Begley, W. W.
Begovich, N. A.
Benbrooks, L. A.
Benson, J.
Bessette, S. V.
Binkey, R. A.
Blackwell, M. B.
Blatchford, D.
Bloom, R. E.
Bobrow, E. N.
Bock, E. L.
Bock, M. J.
Bonebreak, R. L.
Bonney, L. A.
Boreham, J. F.
Bowers, E. O.
Boyd, G. D.
Boyle, S. R.
Bredon, A. D.
Brett, C. F.
Brewer, C. P.
Brown, C. W.
Brown, F. W.
Brown, W. E.
Brunn, K. R.
Buchanan, H. R.
Buckley, J. R.
Buckley, J. W.
Buczek, C. J.
Burnett, E. D.
Burnsweig, J. J.
Campbell, F. L.
Carey, G. D.
Carnegis, G. A.
Carter, C. J.
Carter, J. J.
Cavanagh, J. R.
Chait, H. N.
Chamberlain, W. S.
Chandaket, P.
Chandler, C. W.
Chang, B.
Chang, W. H. K.
Chernin, M. G.
Cheshire, F. C., Jr.
Child, C. H.
Chouinard, R. J.
Christoffers, W. H.
Clapp, R. W.
Clausen, H.
Clavier, P. A.
Clavin, A.
Cochran, E. D.
Coerver, L. E., Jr.
Cohan, L.
Cole, E. J.
Collins, R. F.
Conside, J. M.
Conway, W. H.
Cook, K. R.
Courtier, J. D.
Cowan, C. F.
Cox, H. N.
Craven, W. A., Jr.
Cross, E. F.
Cullen, F. P.
Culver, W. H.
Currie, M. R.
Curtis, C. W.
Dain, H. W.
Dalton, R. A.
Dau, W. K., Jr.
Davis, J. I.
Davis, M. G., Jr.
Deininger, C. F.
Dell-Imagine, R. A.
De Wolf, J. L.
Dexter, G. W.
Diedrichs, R. O.
Dobbertin, W. H.

Doeleman, H.
Dong, P.
Donnelly, J. E.
Dow, D. G.
Downey, E. J., Jr.
Du Fort, E. C.
Dunn, C. E.
Duvall, W. E.
Du Waldt, B. J.
Dvoracek, F. H.
Easton, J. D.
Eatough, C. D.
Edwards, B. N.
Ehrlich, M. J.
Elliott, R. S.
Endler, H. M.
Eng, S. T.
Engle, K. J.
English, D. L.
Erlinger, K. J.
Estes, J. R.
Evendordt, S.
Fahnstock, R. J.
Feeney, J. E.
Fenn, W. H.
Fenton, R. N.
Fisher, M. K.
Fix, O. W.
Fogel, R. L.
Fonda-Bonardi, G.
Fordham, V. C.
Forrester, A. T.
Foster, H. B.
Foster, H. E.
Frame, J. L.
Frank, M. E.
Frankos, D. T.
Fraser, R. H.
Frasure, L. R.
Fredricks, R. W.
Frieburg, H. E.
Fujimoto, Y.
Funk, R. E.
Gage, N. C.
Galindo, V.
Gannaway, R.
George, N., Jr.
Gerber, W. D.
Germer, H. A., Jr.
Ghose, R. N.
Gibbons, T. J.
Gibbs, L. C.
Gillespie, E. S.
Gilliam, D.
Glascock, R. D.
Goldman, R. D.
Goldman, S.
Goldsmith, M. L.
Goodman, F. R.
Goodwin, F. E.
Cooley, T. J.
Gottier, R. L.
Gould, R. W.
Grant, G. W.
Gray, W. W.
Grossfield, S.
Cruder, J. F.
Gullatt, S. P., Jr.
Gustafson, L. A.
Habra, J.
Hadden, F. A.
Hadovsky, F. D.
Hagerty, R. J.
Haigh, W. B.
Hajic, E. J.
Hall, R. B.
Hall, R. D.
Hancock, T. W.
Hand, F. W., Jr.
Hargrove, R. O.
Harper, R. Z.
Harriman, T. J.
Harrington, V. L.
Hata, F. T.
Hautzik, R. M.
Hayman, W. H.
Heath, P. D.
Heimiller, R. C.
Hersberger, W. D.
Hetland, G., Jr.
Hewitt, G. E.
Heyer, F. F.
Higa, W. H.
Highstrete, B. A.
Hile, J. W.
Hitterdal, A. B.
Hodel, J. L.
Holland, J. E.
Holley, A. E.
Holsworth, D. M.
Holt, D.
Holtzman, J. C.
Holzgrafe, H. G.
Hovda, R. E.
Hudspeth, T.
Huffman, J. L.
Hughes, W. A.
Hume, P. D.
Hutcheon, R. S.
Hyneman, R. F.
Inoue, N. S.
Ito, N.
Izzo, A. J.
Jackson, J. A.
Jacques, G. E.
Jahn, R. C.

Jaffe, J. S.
Jamison, R. S.
Jicha, A. J.
Joe, R. H.
Joerger, J. C.
Johnson, H. A., Jr.
Johnson, R. W.
Johnston, J. M.
Jones, L. E.
Joyce, F. J.
Judge, W. J.
Kaprielian, A. Z.
Kasai, G. S.
Katyl, R. H.
Katz, J.
Kaufman, I.
Keiser, J. A.
Kelling, D. G.
Kellner, M.
Kelso, J. M.
Kern, W. W.
Kimmel, R. O.
Kinaga, T.
King, H. E.
Kiser, A. J.
Kitabayashi, T.
Klapper, E.
Klein, R.
Klotz, E. S.
Knechtli, R. C.
Koerner, M. A.
Kooztz, R. H.
Kopp, E. H.
Kopulsky, S.
Koran, A.
Kramer, A. G.
Krausz, R.
Kreinherder, D. E.
Kreismanis, M. V.
Krill, C. K.
Kriz, C. K.
Kudrna, K. L.
Kurashita, J. H.
Kurtz, L. A.
Lader, L. J.
Lance, A. J.
Landis, V., Jr.
Larsen, R. P.
Larter, T. C.
Lees, A. B.
Leng, R. B.
Leon, B. J.
Lew, H. W.
Lieber, M.
Linnes, K. W.
Lloyd, M. S.
Lockhart, C. T.
Lockhart, E. H.
Lockhart, R. M.
Locus, S. S.
Long, J. L.
Long, M. C.
Louapre, M. E.
Louie, W.
Lovick, E., Jr.
Loyet, D. L.
Lucke, M. E.
Lundquist, C. R.
Mackey, R. C.
Maguire, W. W.
Majka, C. J.
Mallinckrodt, A. J.
Mamayek, D. S.
Marchese, T. J.
Margerum, D. L.
Margolin, A. R.
Markin, J.
Martes, G. E.
Martin, D. F.
Martin, D. P.
Martin, D. R.
Martin, D. W.
Martin, W. R.
Masuda, H. B.
Matsun, D. L.
Matsushige, R. H.
Matthews, W. C.
McCaughna, J. R.
McClure, D. H.
McColl, M.
McCone, G. L.
McFarlane, M. D.
McNary, B. D.
McNaughton, J. F.
McQuerry, W. H.
McWilliams, J. D.
Meany, J. E.
Mescall, J.
Messenger, G. C.
Metcalf, D. F.
Metzger, H. W.
Meyer, D. R.
Michaels, E. C.
Mickelson, J. R.
Milham, R. F., Jr.
Miller, C. E.
Miller, G. B.
Millet, M. R.
Moffet, A. T.
Mongan, A. J.
Moore, J. A.
Morris, R. E.
Morris, R. J.
Morrow, J. E.
Morton, W. B., Jr.
Moyer, J. W.

Mueller, G. E.
Mueller, M. C.
Mueller, W. M.
Muhlstein, R. W.
Munushian, J.
Murphy, J. J.
Neben, D. F.
Neelanda, C. H.
Newberg, I. L.
Nielsen, C. L.
Nishimura, R. K.
Norris, K. M.
Notvest, R. A.
Nuttan, D. C.
Ohlmann, G. A.
Okino, T. Y.
Okubo, G. H.
Olson, M. W.
Oltman, H. G., Jr.
Omira, R. Y.
O'Nan, R. L.
Orr, J. A.
Otoshi, T. Y.
Palmerson, P. J.
Papas, C. H.
Parisky, R. N.
Parker, S. E.
Pass, H. R.
Paterno, P. M.
Patin, O. E.
Paul, P. F.
Paulson, E. T.
Pedersen, R. J.
Peringer, P.
Perry, W. C.
Peterson, R. L.
Phillips, G. A.
Pierce, C. C.
Polzin, E. M.
Porter, B. W.
Potter, P. D.
Potts, D. L.
Potwardowski, B.
Poulsen, W. A.
Purdum, L. C.
Randall, G. M.
Rau, J. E.
Reed, R. H.
Roberts, P. S.
Roehl, E. R.
Rohland, A. E.
Rolnik, J. A.
Romeo, D. J.
Rousseau, A. L.
Royal, D. E.
Rudin, M. B.
Rudin, S.
Rumsey, W. E., Jr.
Sabih, D. S.
Saltzman, H.
Samuels, D. N.
Sand, B.
Sato, T.
Savage, R. P.
Sayano, K. F.
Schafer, N. B.
Scharp, G. A.
Schiaivoni, D. W.
Schott, F. W.
Schuster, D.
Scott, A. W.
Seaton, A. F.
Seeley, E. W.
Sensiper, S.
Shahan, O.
Shameson, L.
Shein, S.
Shelton, R. C.
Shestag, L. N.
Shimabukuro, F. I.
Shoulders, H. D.
Siegel, W.
Silberberg, R. W.
Silence, N. C.
Silva, L. M.
Sims, J. L.
Sion, E.
Sission, A. R.
Smith, L. T.
Smith, R. D.
Smith, R. G.
Snyder, W. A.
Sommers, C. E.
Speen, G. B.
Stacey, J. M.
Stark, L.
Steele, E. L.
Stegelmann, E. J.
Stegen, R. J.
Steiger, W.
Steinkolk, R. B.
Stephens, F. M.
Sterling, M. F.
Sternke, E. C.
Stevens, F., Jr.
Stevens, S.
Stitch, B. D.
Stitch, M. L.
Stockhoff, K. C. H.
Stodola, R. A.
Stone, R. E.
Straus, T. M.
Strawn, R. S.
Street, N. C.
Strumwasser, E.
Struve, L. M.

Sur, J.
Swan, R. L.
Swerdfeger, P. M.
Swift, C. W.
Sykora, G. E.
Symonds, R. J.
Taira, W. C.
Tang, R.
Tang, T. T.
Teeter, W. L.
Teragawa, R. T.
Thomas, D. L.
Thomas, R. L.
Todd, B. J.
Tokheim, R. E.
Tondreau, H. J.
Tong, K. C.
Tornheim, H.
Trapp, R. R.
Trembly, B. D.
Troy, P.
Tudor, J. E.
Uebele, G. S.
Underberger, G. M.
Uyetani, B.
Vallar, T. F.
Vannucci, R. P.
Vanous, P. J.
Villeneuve, A. T.
Vuilleumier, R. F.
Wachowski, H. M.
Wada, J. Y.
Wada, R. T.
Walcek, E. J.
Walley, B.
Walsh, B. L.
Wang, F. B.
Wanick, R. W.
Wanselow, R. D.
Ward, B. M., Jr.
Ward, R. C.
Ware, P. H.
Warn, K. L.
Wasmer, W. F.
Waterman, H. B.
Webb, P. S.
Weglein, R. D.
Wehn, S. L.
Wehner, R. S.
Weil, F. M.
Weiss, M. T.
Weiss, W. J., Jr.
Weller, D. B.
Wells, R. E.
Wershoven, G. A.
West, D. B.
Whirry, W. L.
White, R. L.
Whiting, L.
Widell, C. D.
Wierman, E. T.
Wigdahl, E. E.
Wildman, A. J.
Williams, H. M., Jr.
Williams, R. G.
Willis, M. R.
Wills, J. D.
Wilmot, R. D.
Wilson, R. W.
Wilts, C. H.
Winslow, L. M.
Wolking, D. H.
Wong, S. H.
Worthy, N. M.
Wright, P. B.
Wright, T. W.
Wyatt, W. C.
Wylie, J. A.
Yabitsu, C. T.
Yee, D. K.
Young, H. M.
Young, R. A.
Yowell, C. O.
Zamites, C. J.
Zboril, F. R.
Zmuidzinas, J. S.

Phoenix

Aden, A. L.
Black, J. R.
Blixt, R. E.
Cacheris, J. C.
Carter, P. M.
Clar, E. L.
Coppie, M. J.
Echols, R. A.
Elsner, R. W.
Gibson, D. D.
Goodman, R. G.
Gundry, J. C.
Haenichen, J. C.
Ham, N. C.
Jungwirth, J. N.
Knight, W. H.
Lindsay, J. D. G.
Murray, P. W.
Palais, J. C.
Peterson, R. K.
Rabowsky, I.
Robertson, S. D.
Russell, F. D.
Sakiotis, N. G.
Schaffner, G.
Skomal, E. N.
Smith, D. A.

Solem, R. J.
Stearns, W. P.
Steinman, W. L.
Trull, D. L.
Van Druff, J. C.
Voorhaar, F. R., Jr.
West, R. G.
Williams, D. J.

Portland

Baulig, R. H.
Bennett, S. D.
Crenshaw, T. L.
Gibson, C. B., Jr.
Hashizume, G. K.
Lockwood, L. R.
Marihart, D. J.
Miller, F. E.
Mozzini, L. M.
Myers, J. T., III
Porcelli, E.
Richardson, W. E.
Sato, H.
Turnbull, J. L., Jr.

Sacramento

Aldrich, P. S.
Conly, E. R.
Frederick, D. E.
Lane, C. A.
Lebel, A. E.
Levy, M. C.
Sassman, R. W.
Sinkler, C. I.

Salt Lake City

Anderson, D. W.
Bowen, M. J.
Bray, G. L.
Brownell, F. P., Jr.
Buter, B. L.
Davidson, B. G.
Davies, F. A.
Grow, R. W.
Haegle, R. W.
Hansen, C. F.
Hansen, L. L.
McLaughlin, J. W.
Mitchell, L. K.

San Diego

Abbey, K.
Aguios, E. C.
Asato, C. K.
Augustin, E. P.
Babbitz, H. B.
Barnhart, M. A.
Bergant, G. G.
Chazotte, M. M., Jr.
Chesrow, A. F., Jr.
Christensen, N. T.
Delicath, R. C.
Derenthal, R. J.
Dickstein, H. D.
Dobyne, J. C., Jr.
Enslow, P. H., Jr.
Erickson, P. R.
Evey, R. R.
Girismen, M. F.
Gottwald, C. H.
Hendrix, D. L.
Herbert, W. J.
Hively, R. R.
Honer, R. E.
Hopkins, R. U. F.
Ikerd, H. M.
Kluck, J. H.
Martin, L. E.
Matsumoto, T.
Mayer, A.
Medved, D. B.
Moffatt, V. J.
Molnar, S.
Moore, W. E.
Morgan, L. A.
Mulvey, J. X., Jr.
Omiya, C. I.
Proctor, D.
Ratkevich, A. E.
Rayburn, D. A.
Russell, J. D.
Schoonover, M. R.
Senn, J. C.
Siperly, B. H.
Small, B. I.
Smothers, L. A.
Stokely, R. J.
Taylor, W. G.
Thomas, J. J.
Tracy, H. H., Jr.
Trolese, L. G.
Uyehara, M.
Wilson, D.
Wolfe, G. W.
Wood, C. M.
Youngberg, B. E.

San Francisco

Abraham, W. G.
Adam, S. F.
Addleman, L. A.
Adelson, M. B.
Allen, M. A.
Allen, S. E., Jr.
Allen, T. L., Jr.
Allison, J. E.

Alvarez, R.
Anderson, H. E.
Anderson, L. K.
Anderson, R. A.
Andreasen, M. G.
Angelakos, D. J.
Arfin, B.
Arhens, V. R.
Arnold, C. A.
Arnold, D. T.
Ashley, A. C.
August, G.
Auld, B. A.
Austin, G. E.
Ayers, W. R.
Barbano, N.
Barnett, E. F.
Baumgartner, H. E.
Beaver, W. L.
Bell, Ronald L.
Bell, Ross L.
Bennett, C. L.
Benson, S.
Bergman, R. S.
Bevensee, R. M.
Birdsall, C. K.
Bloom, G.
Blumberg, M.
Boilard, D. I.
Booth, R. E.
Borghi, R. P.
Bostwick, W. E.
Bowes, J. D.
Boyer, B. E.
Bradford, C. W.
Bradski, M.
Bridges, W. B.
Brinton, R. L.
Briskin, H. B.
Bristol, T. R.
Brittain, G. H.
Brooks, R. E.
Brown, B. H.
Brunn, J.
Bunn, H. L.
Buss, R. H.
Butterfield, F. E.
Butwell, R. J.
Caddes, D. E.
Carlile, R. N.
Carnahan, C. W.
Carr, J. W.
Carter, P. S., Jr.
Caryotakis, G.
Caswell, D. A.
Chaffee, D. E.
Chan, W. W.
Chang, N. C.
Chenoweth, A. G.
Chodorow, M.
Christie, J. W.
Clapp, F. D.
Clinton, W. R.
Cogshall, P. D.
Cohn, S. B.
Colvin, R. S.
Comstock, R. L.
Connor, T. J.
Contos, P. A.
Cool, L. R.
Craig, R. A.
Crane, M.
Crapuchettes, P. W.
Cromack, J. C.
Cumming, R. C.
Curtis, T. J.
Dalley, D. G.
Damonte, J. B.
Davis, K. S.
Day, H. R.
Dean, D. K.
Debs, R. J.
Detwiler, R. D.
Dimmick, R. R.
Disman, M.
Dodd, C.
Domenico, M. D., Jr.
Dore, B. V.
Dresbach, G. R.
Dunn, D. A.
Dunn, V. E.
Dye, R. E.
Eallionardo, C. M.
Eaves, H. H.
Edberg, E. B.
Edson, W. A.
Eggers, R. E.
Elam, J. M.
Engler, C. G.
Erickson, L. G.
Everhart, T. E.
Fank, F. B.
Ferri, G.
Feuchtwang, T. E.
Fialer, P. A.
Fitzgerald, P. M.
Fitzpatrick, J. P.
Fleig, W. J.
Floyd, W. S., Jr.
Flynn, J. E.
Fong, A.
Fontana, J.
Forrer, M. P.
Fortner, W. D.
Foster, C. P., Jr.
Foster, W. F.

Frankel, S.
Franks, R. E.
Freberg, L.
Froman, J.
Gamara, N. J.
Gan, M.
Gates, W. F.
Gee, W.
Geppert, D. V.
Gerchberg, R. W.
Gerig, J. S.
Getsinger, W. J.
Giddis, A. R.
Gifford, J. T.
Gilden, M.
Gillard, C. W.
Ginzton, E. L.
Gola, A. S.
Goodman, D. H.
Gorman, E. B.
Grace, D. J.
Grande, V. J.
Granger, J. V. N.
Grinich, V. H.
Gross, E. H.
Gunn, T. L.
Guthrie, E. E.
Hadik-Barkoczy, A. B.
Hagopian, J. J.
Halsted, S.
Harker, K. J.
Harman, W. A.
Hartwig, E. C.
Hayes, R. E.
Heffner, H.
Heninger, G. O.
Hennies, S. R.
Henschke, R. A.
Hestand, N. P.
Hiramatsu, Y.
Hlavka, L. F.
Ho, I. T.
Hoag, E. D.
Hockett, S. W.
Holaday, R. E.
Horton, M. C.
Honey, R. C.
Hsu, J.
Huffman, G. A.
Hunter, L. W.
Huntton, J. K.
Hutter, R. G. E.
Inman, R. P.
Jacobus, F. B.
James, B. C.
Jaynes, E. T.
Jepsen, R. L.
Johnson, D. A.
Johnson, D. R.
Johnson, H. R.
Johnson, L. B.
Johnston, R. W.
Jones, E. M. T.
Jory, H. R.
Justice, R.
Kaisel, S. F.
Kannelaud, J.
Katz, J. E.
Katzman, H.
Kavanaugh, J. C.
Keitel, G. H.
Kemanis, G.
Kennedy, P.
Kenny, J. W.
Kidd, T. L.
Kinaman, E. W.
Kino, G. S.
Klamm, C. F., Jr.
Klein, W. F.
Kohl, W. H.
Kootsey, J. M.
Kotzebue, K. L.
Kovalevski, N. N.
Krenz, J. H.
Krivozhavak, G. M.
Kruse, F. W., Jr.
Kuhn, N. J.
Kulke, B.
Kumagai, N.
Kumrage, S.
Kusnezov, N.
Lacy, P. D.
Lagerstrom, R. P.
Lamberty, B. J.
La Rue, A. D.
Latham, R. A.
Leidigh, W. J.
Leifer, M.
Lepoff, J. H.
Lin, C. M.
Linden, D. A.
Lindley, J. P.
Livingston, R. H.
Lo, C. C.
Louie, P. Y.
Lozzarini, R. F.
Luckey, O. E.
Ludovici, B. F.
Luebke, W. R.
Lundstrom, O. C.
Main, W. F., Jr.
Maltzer, I.
Malvino, A. P.
Mao, S.
Markum, J. A., Jr.
Martin, J. A.

Mathers, G. C.
Matthaei, G. L.
Maudens, L. C.
Mawdsley, D. M.
Maxum, B. J.
Mays, A. S.
McCole, J. F.
McConnell, R. A.
McCullough, J. A.
McEuen, A. H.
McKee, L. H.
McMurtry, B. J.
Meares, L. G.
Medina, M. A.
Melchor, J. L.
Menneken, C. E.
Milazzo, C., Jr.
Mizuhara, A.
Moats, R. R.
Mohr, H. J.
Monson, J. E.
Moreno, T.
Morita, T.
Morris, A. J.
Morris, R. J.
Moy, M. S.
Needle, J. S.
Newman, H. L.
Nikonenko, P. V.
Nitz, I. C.
Noon, J. R.
Nordgren, W. E.
Norris, N. J.
Norton, D. E.
Novick, G.
Nye, R. L., Jr.
O'Connor, R. E.
Okamura, C. Y.
Oliver, B. M.
Olson, F. A.
Olson, R. E.
Omori, M.
O'Neal, W. C.
Orrick, G. E.
Orrick, R. L., Jr.
Otsuka, S. P.
Oxner, E. S.
Pantell, R. H.
Patel, C. N.
Pease, M. C., III
Penwell, J. R.
Peterson, C. J.
Pettegrew, J. B.
Phillips, R. M.
Pikarek, K. L.
Pinal, D. G.
Powell, R. M.
Powers, E. J., Jr.
Price, G. W.
Price, V. G.
Price, W. C.
Prickett, R. J.
Proctor, E. K., Jr.
Prommer, A.
Pruefert, H.
Rau, J. H.
Rawlins, R. E.
Reedy, T. M.
Reindel, J.
Rendall, A. H.
Reynolds, W., Jr.
Riley, R. B.
Roberts, L. A.
Robertson, W. H., Jr.
Rodgers, J. L.
Rooney, J. P.
Rosenstein, M. D.
Rosenthal, H. A.
Rothman, H. S.
Rowley, J. J.
Rozak, D. T.
Rudee, E.
Rumfelt, A.
Ruttenberg, R. M.
Ryan, A. H.
Sagawa, S. S.
St. Clair, M. W.
Samuels, A. H.
Santana, G. R.
Sarda, R.
Saunders, C. L.
Savarin, A.
Sayer, W. H., Jr.
Schiffman, B. M.
Schneider, R. F.
Schreiner, R. W.
Schrumph, D. A.
Schubert, R. A.
Schussel, J. H.
Sedin, J. W.
Segerstrom, R. J.
Seiden, P. E.
Serang, A. M.
Shaw, H. J.
Shaw, T. M.
Shelton, W. L.
Shimizu, J. K.
Siegman, A. E.
Silver, S.
Simon, D. H.
Singer, J. R.
Sklar, H.
Sloan, D. H.
Smith, P. G.
Smith, R. G.
Smullin, W. B.

Sonkin, S.
Soohoo, J.
Soref, R. A.
Spangenberg, K.
Stafford, L. E.
Stephenson, J. M.
Sterrett, J. E.
Stevenson, J. C.
Stokes, B. C.
Streleski, T. L.
Strobele, C. H.
Strum, P. D.
Sugimoto, T. T.
Sundberg, V. C.
Sutherland, R. I.
Swanson, W. E.
Szente, P. A.
Tamres, I.
Taylor, E. D.
Taylor, N. J.
Tetenbaum, S. J.
Thompson, A. J.
Thon, W. H.
Thornburg, R. O.
Thornton, D. D.
Todd, L. L.
Tomiyasu, K.
Trainer, R. F.
Tucker, K. C.
Turner, W. R.
Valles, B. V.
Vanderplaats, N. R.
Vane, A. B.
Van Geen, J.
Vartanian, P. H., Jr.
Vehn, R. E.
Veselovsky, L. R.
Vinding, J. P.
Voelker, F., III
Voronoft, G. N.
Wagener, W. G.
Wakabayashi, J.
Waldman, M. D.
Wang, C. P.
Warner, D. B.
Watkins, D. A.
Watson, W. H.
Weaver, J. N.
Weir, W. B.
Wharton, C. B.
Whinnery, J. R.
White, F. M., Jr.
Whitmer, R. F.
Whitten, C. L.
Wholey, W. B.
Wilber, L. E.
Wilds, R. B.
Williams, C. B.
Williams, D. R. W.
Williams, H. A.
Willoughby, D. E.
Wilson, P. B.
Winslow, D. K.
Wood, F. B.
Wood, J. R.
Worley, O. C.
Yadavalli, S. V.
Zitelli, L. T.
Zobel, F. J., Jr.

Seattle

Addington, R. L.
Andermann, A.
Armstrong, C. W.
Asato, U.
Ashbaugh, F. E.
Banack, N. F.
Beals, E. L.
Bernard, G. D.
Biggs, A. W.
Blais, A. H.
Bonstrom, D. B.
Burns, G. A.
Bushby, E. W.
Butler, N. G.
Bystrom, A. Jr.
Charters, R. L.
Coe, R. J.
Currie, W. E.
Dalby, T. G.
Daniel, R. A.
Dobrott, D. R.
Dorratcague, P. E.
Dye, D. L.
Foster, J. H.
Gage, B. P.
Golde, H.
Graybeal, J.
Guy, A. W.
Hasserdjian, G. K.
Held, G.
Helmich, P. F.
Herr, M. D.
Hill, J. L.
Hill, R. V.
Hokenson, H. S.
Holtman, R. F.
Hu, A. Y.
Ishimaru, A.
Kalviste, A.
Kieburz, R. B.
Kiskaddon, W. V.
La Bossiere, P. J.
Larkin, R. S.
Larson, L. A.
Leonard, P. W.

Lillie, W. A.
Lopunch, A. J.
Malik, J. L.
McPherson, E. L.
Metter, R. E.
Oakes, G. K.
O'Hara, R. N.
Patton, D. E.
Pearson, R. E.
Purnell, M. V.
Rao, N. N.
Reynolds, D. K.
Russell, J. S.
Sherrill, G. V.
Siddons, W. J.
Sleeth, J. D.
Smith, J. K.
Spencer, K. E.
Strandrud, H. T.
Tyras, G.
Vanden Bos, L. J.
Winder, D. E.
Yee, J. S.

Tucson

Ashley, F. R.
Eilfr, N.
Ford, J. W.
Gravell, A. J.
Hessemer, R. A., Jr.
Huddleston, R. R.
Koenig, W. A.
Kushnick, A. E.
Lewellyn, J. R.
Marston, E. J.
Noorland, M.
Oliver, J. K., Jr.
Stinson, D. C.
Wasserman, E.

Region 8**Bay of Quinte**

Chambers, R. G.
Chisholm, R. M.
Couves, E. E.
Maki, A. E.
Punchard, J. C. R.
Tanner, R. H.

Hamilton

Ceelen, P. A. J.
Fines, W. W.
Humbert, V. J.
Kubien, S. J.
Lyons, K. C.
Matthies, J. G.
Reesor, C. G.
Ross, R. G.
Stonelake, D. A.
Yachwak, M.

London

Tull, E. H.

Montreal

Adkar, C. K.
Birman, G.
Bonneville, S.
Bousfield, J. A. T.
Buizert, H.
Cadiux, J. P.
Campbell, A. F.
Cox, J. R. G.
Delbridge, W. A.
Dumas, L.
Gamus, A.
Ganapathy, N.
Gentner, R. F.
Germain, C.
Guitian, J. E.
Haeberlin, R. O. W.
Harrison, B. M.
Hryhorijiw, W.
Jackson, K. A.
Jamshedji, J. S.
Kingan, A. J.
Kubina, S. J.
Lapin, A. I.
Le Bell, J.
McNeil, J. E.
Migneault, G. B.
Morris, E. L.
Nadon, L.
Oxley, A. B.
Parent, G. J. C.
Reeves, R.
Schwelb, O.
Scott, P. J.
Tamagi, T. T.
Tatlock, J. F.
Van Manen, S.
Walsh, D.
Wisenden, G. A.

Newfoundland

Louder, J. F.
Tibbett, J. E.

Northern Alberta

Bayer, M. B.
Dewar, D. W.
Lee, J. G. C.
Lipsett, M. S.

Stein, R. A.
Vermeulen, F. E.

Ottawa

Adey, A. W.
Baart, J. G.
Bhattacharyya, B. K.
Cairns, F. V.
Carroll, D. V.
Clark, P. O.
Cole, W. A.
Covington, A. E.
Craven, J. H.
Cumming, W. A.
Deguire, R. A.
Harland, H. B.
Henderson, J. T.
Hurd, R. A.
Kalra, S. N.
Klein, E. J.
McCormick, G. C.
Medd, W. J.
Miller, G. A.
Milroy, J. B.
Nikkel, R. F.
Pulfer, J. K.
Steele, K. A.
Stone, D. G.
Waugh, J. B. S.
White, W. E.
Wightman, B. A.
Wittke, P. H.
Wong, J. Y.

Quebec

Beaubie, J. A.
Blais, R.
Cummins, J. A.
Dion, A.
Guerbilsky, A.
L'Heureux, L. J.
Surtees, W. J.
Vaillancourt, R. M.
Zement, K. H.

Regina

Baxter, K. H.
Thiele, W. F.

Southern Alberta

Davis, A. P.
Johnson, N. P.
Johnston, C. W.
Kerr, W. G.
Nyberg, G. E.
Partin, W.

Toronto

Adams, R. L.
Banner, W. G.
Barclay, A. P. H.
Buckles, F. G.
Bull, T. R.
Bura, P.
Butuk, W.
Byers, H. G.
Cherrington, B. E.
Davey, S. W.
Dennett, L. J.
Der-Young Tang, D.
Dmitrevsky, S.
Dong, W. Y.
Eisen, D. M.
Hackbusch, R. A.
Kelk, G. F.
Maschmann, F. H.
Schmidt, P. J.
Shifman, H.
Sinclair, G.
Smith, E. D.
Swain, H. J.
Swan, C. B.
Sydiaha, R. W.
Tomicio, N.
Vaitkevicius, L. A.
Yachimec, P.
Yen, J. L.

Vancouver

Bohn, E. V.
Buchanan, D. G.
Burns, R. J.
Campbell, J. F.
Caple, C. G.
Cushing, T. D.
Dubnicoff, E.
Fall, S. T.
Green, M. E.
Johnson, T. R.
Karsa, K.
Liang, J. D. S.
Liggins, A.
Marsh, R. A.
McDiarmid, D. R.
Moore, A. D.
Noakes, F.
Panaoti, D.
Pettersen, G. W. E.
Seminoff, A. A.
Sodomsky, K. F.
Vroom, D. R.
Yestadt, R. A.

Winnipeg

Hamilton, W.
Marquart, R. G.

Royno, W.
Shapera, G. H.
Shaver, H. B.

U. S. Possessions**Puerto Rico**

Polachowski, B. A.

Overseas Military

Aulbach, C. E.
Baker, H. O.
Batson, J. A.
Bowley, R. E.
Bowler, J. A.
Carr, B. A.
Cassidy, J. J.
Cranston, R. B.
Dolan, B. A.
Farrar, J. H.
Gilbo, A. W.
Hanrahan, J. A.
Haskell, H. B.
Iwai, K. G.
Jackson, D. A.
Johnson, C. W.
Kelly, P. J.
Kroeckel, C. H.
Laine, R. U.
Pixton, J. R.
Stone, J. H.
Tetrick, C. J.
Williams, R. P.

Foreign Sections**Benelux**

Alma, G. H. P.
Bijl, A.
Bouchier, P.
Buys, W. L.
Gudmansen, P. E.
Heco, Y. V.
Heijboer, R. J.
Hoffmann, J. A. J. L.
Marique, J.
Nijenhuis, W.
Op Den Orth, J. M.
Seger, C. L.
Vanwormhoudt, M. C.
Wouters, H. M.
Zijlstra, P.

Buenos Aires

Pinasco, S. F.

Rep. of Colombia

Errante, E. P.
Gabriunas, K. B.

Egypt

Fahmy, M. N. I.

Israel

Burwin, E.
Porath, N.
Shekel, J.
Weissberg, E.
Zakai, M.

Tokyo

Adachi, S.
Aoi, S.
Aoki, Y.
Azakami, T.
Chiba, J.
Cho, N.
Fujii, T.
Fukata, M.
Fukushi, A.
Harada, N.
Harashima, O.
Hayashi, I.
Hayasi, S.
Ibuka, M.
Ichino, K.
Ida, K.
Imura, N.
Imahata, K.
Imai, H.
Ishikawa, D.
Iwakata, H.
Iwasawa, K.
Kano, T.
Kawano, T.
Kida, A.
Kitsuregawa, T.
Kohno, S.
Konomi, M.
Kumagai, T.
Kuroiwa, Y.
Liu, C. C.
Makimoto, T.
Matsumaru, K.
Matsuyuki, T.
Minozuma, F.
Mita, S.
Mito, S. P.
Miyakoshi, K.
Mizuma, M.
Mizutami, M.

Morimiya, T.
Morita, Kazuyoshi
Morita, Kiyoshi
Morita, M.
Murakami, I.
Mushiake, Y.
Nakagami, M.
Nakahara, F.
Nakatsuka, K.
Namba, S.
Nemoto, T.
Niguchi, K.
Nishida, S.
Nishihara, H.
Nishino, O.
Nishizawa, J. I.
Niwa, Y.
Nojima, S.
Nomura, T.
Ogawa, T.
Oguchi, B.
Okabe, T.
Okada, M.
Okamoto, N.
Okamura, S.
Okochi, J. A. M.
Omori, S.
Ono, S.
Owaki, K.
Owaku, S.
Saito, N.
Saito, S.
Sawada, R.
Shibata, Y.
Someya, I.
Sugawara, S.
Sugi, M.
Suzuki, Michio
Suzuki, Michiya
Takaba, S.
Takada, S.
Takeuchi, Y.
Taki, Y.
Takiyama, K.
Tanabe, Y.
Taniguchi, F.
Tomono, M.
Tomota, M.
Uchida, H.
Uda, S.
Yamashita, K.
Yamazaki, T.
Yasuda, I.
Yasuda, Y.
Yoneyama, T.
Yonezawa, S.
Yoshida, S.
Yoshimura, H.

Foreign Countries**Australia**

Aitchison, R. E.
Honor, W. W.

Austria

Zemanek, H.

Bahamas

Curling, A. E.

Bermuda

Owen Harris, J. H.

Brazil

Annenberg, A.
Chow, Y.
Gregori, I.
Muller, F. R.
Petroni, R.
Rittmeister, H.
Rudiger, H. A.
Sambiasi, L. F. F.
Senise, J. T.
Tai, C. T.

Cuba

Arnaud, J. P.
Collado, R. O.
Montes, J. V.
Pages, E. V.
Pella, A.
Siddall, W. D.

Ceylon

Adikaram, K. B.

Czechoslovakia

Djadjkov, S.

Denmark

Gronlund, M. P. S.
Hansen, G. K. F.
Ingerslev, F. H. B.
Nag, D. S.
Sorensen, E. V.
Stangerup, P.
Toft, S. C.

England

Ash, E. A.
Boden, T. W.
Bowden, B. V.
Bridges, T. J.
Brown, J.

Butler, L. H.
Clout, P. R.
Cullen, A. L.
Dawe, F. W.
Fischbacher, R. E.
Flores, J. P.
Forte, S. S.
Gagne, R. R. J.
Godfrey, R. M.
Halsey, J. E.
Harris, K. E.
Hills, W. J.
Jackson, W.
Jurkus, A. P.
Karp, A.
Kelliher, M. G.
Laverick, E.
Macnee, D. H.
Mayo, R. F.
McCall, D. R.
Muir, L. M.
Parker, J. D.
Parsons, A. N.
Potok, M. H. N.
Preece, K. E.
Rantzen, H. B.
Rastorgoueff, V.
Roberts, D. A. E.
Rouse, F. W. D.
Rzymowski, E.
Savard, J. Y.
Shefer, J. O.
Voyner, Z. F.
Warren, K. A. J.
Wilson, A. G.
Wood, J.

Ethiopia

Mehta, B. B.

Finland

Ivars, R. E.

Formosa

Ong, H. Y.
Wang, C. C.

France

Angot, A. M.
Baron, J.
Berline, S. D.
Boudouris, G.
Calon, A. E.
Christensen, P. E.
Comte, G. N.
Deschamps, J. D.
Eltassen, K. E.
Ferrier, P. A.
Fuchs, A.
Ghertman, J.
Guyot, L. F.
Labin, E.
Leblond, A. F.
Mandel, P.
Mourier, G.
Musson-Genon, R. P. A.
Prache, P. M.
Robieux, J. H.
Sirel, M.
Voge, J. P.
Warnecke, R. R.
Weill, H.
Weissfloth, A. J.
Zwobada, R. L.

Germany

Borgnis, F. E.
Bruck, L.
Bruckmann, H. P.
Busch, C. W.
De Vos, J. M.
Grasselt, K. H.
Kleen, W. J.
Meyer, E. W.
Peters, J. F.
Rohe, L.
Ruger, J. F.
Schupp, P.
Severin, H. K. F.
Tauf, F. F.
Ulbricht, G.
Von Trentini, G.
Zinke, O.

Greece

Karlambas, N.

India

Agarwala, S. S. S.
Chatterjee, A. K.
Daruvula, D. J.
Peterson, P. R.
Raman, S.
Rao, K. L.
Shenoy, R. P.

Ireland

McBride, J. M. W.
Williams, K. F.

Italy

Banfi, A.
Bardelli, F.
Barzilai, G.
Blondi, E.
Bonetti, T.

Bruno, A.
Dalla Volta, E. M.
D'Auria, G.
Derossi, A. D.
De Vito, G. R.
Egidi, C.
Fagnoni, E.
Floriani, V.
Gerosa, G.
Koch, R.
Lombardi, M.
Monti-Guarnieri, G.
Palandri, G. L.
Reggiani, M.
Schiaffino, P.
Teofilato, A. V.
Vergani, A.

Jordan

Shaweesh, H. M.

Korea

Hwang, I. Y.
Lee, Y. H.

Malaya

Dhillon, G. S.

Mexico

Diaz, J. S.
Higuera-Mota, H. R.
Joaquin, D. S.
Mendez, E. D.
Rodrigues, E.
Wenzel, P. H.

Nicaragua

Guerrero, M. A.

Norway

Bostad, J.
Gaudernack, L. F.
Hiis, P. T.
Jaeger, T. C.
Wessel-Berg, T.

Poland

Litwin, R.
Smolinski, A. K.

Russia

Akulin, M. S.
Efimov, E. A.

Pokrovski, A. G.
Sorokin, A. A.

Singapore

Ho, L. H.
Hock, T. C.

Scotland

Campbell, C. K.

South Africa

Phillips, W. E.
Zawels, J.

Spain

Colino, A.
Gomez, J. H.

Sweden

Andersson, K. N.
Aurell, C. G. P.
Ejewall, L. A.
Elfving, A. L.
Fagerlind, S. V.
Granqvist, C. E.
Holm, L.
Johansson, B. O.

Josephson, B. A. S.
Joste, S. V.
Karlstedt, L.
Lofgren, E. O.
Nerhag, O.
Nilsson, B. N. A.
Olving, S.
Perers, O. F.
Persson, N. I. E.
Richter, H. F.
Roll, A.
Scheftelowitz, H.
Sivers, C. H. V.
Snaar, B. S. A.
Tengblad, R. G.
Viggh, M. E.
Westerhult, B. C. O.
Yngvesson, Y. K. O.

Switzerland

Baumgartner, R. H.
Bonanomi, J. A.
Braun, A. F.
Epprecht, G. W.
Furrer, F. E.
Gayer, J. H.
Guanella, G.

Hagger, H. J.
Lang, G. J.
Lapostolle, P. M.
Nalos, E. J.
Schneider, M. V.
Schoeberlein, W.
Tank, F.
Walder, E.

Venezuela

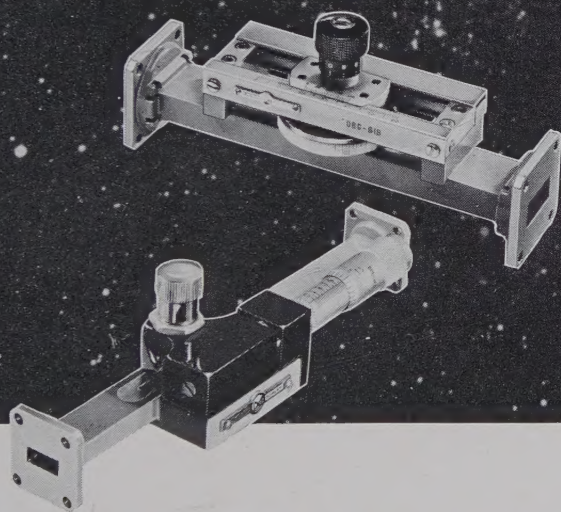
Alamo-Segovia, J. A.
Arreaza, R. G.
Carter, Jack
Guia-Monasterio, A. E.
Huerta, A. F.
Hussein, N. A.
Kroll, W. H. O.
McBain, H. F.
McClead, D. A.
Mireles, A.
Rios, E. E.
Stapulionis, A.
Yaselli, P.

Vietnam

Fozdar, J. K.



what is the frequency standard for the U.S.A.?



ANSWER: By act of Congress, the U.S. Bureau of Standards determines the primary standard, based on the revolution of the earth. All DeMornay-Bonardi microwave instruments are calibrated at frequencies which are verified by our secondary standard, which, in turn, is periodically calibrated, point for point, by the U.S. Bureau of Standards.

One way to properly match a microwave transmission line is by using a D-B Stub Tuner to reduce mismatch losses and utilize the total energy available.

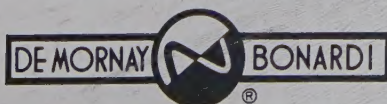
D-B stub tuners in the 2.6 to 18 KMC range have a new scale and vernier that gives precise resettability in longitudinal travel. A new micrometer scale on the probe meas-

ures penetration with very high accuracy.

Probe wobble is eliminated, and no resonances can occur under any conditions. You can correct VSWR as high as 20:1 with amazing accuracy (1.02). You can tune with precision...reset to original settings with certainty that phase and magnitude have been duplicated.

Ditto for higher frequencies. D-B tuners in the 18 to 90 KMC range are not simply scaled-down units—they're engineered for ultramicrowave® use. All the above features are available, plus micrometer positioning which provides readability to .0001".

Write for data sheets—they detail all features, applications, dimensions, sizes. Bulletin DB-919.



780 SOUTH ARROYO PARKWAY • PASADENA, CALIFORNIA

INSTITUTIONAL LISTINGS

The IRE Professional Group on Microwave Theory and Techniques is grateful for the assistance given by the firms listed below, and invites application for Institutional Listing from other firms interested in the Microwave field.

AIRTRON, INC., A Division of Litton Industries, 200 East Hanover Ave., Morris Plains, N.J.
Designers and Producers of Complete Line of Microwave Electronic and Aircraft Components

COLLINS RADIO CO., Texas Division, Dallas, Tex.
Complete Microwave and Transhorizon Communication Systems

ITT LABORATORIES, 500 Washington Ave., Nutley 10, N.J.
Line-of-Sight and Over-the-Horizon Microwave Systems; Test Equipment and Components

LITTON INDUSTRIES, Electron Tube Div., 960 Industrial Rd., San Carlos, Calif.
Magnetron, Klystrons, Carcinotrons, TWT's, Backward Wave Oscillators, Gas Discharge Tubes, Noise Sources

MICROWAVE DEVELOPMENT LABS., INC., 92 Broad St., Babson Park 57, Mass.
Designers, Developers and Producers of Microwave Components and Assemblies, 400 mc to 70 kmc

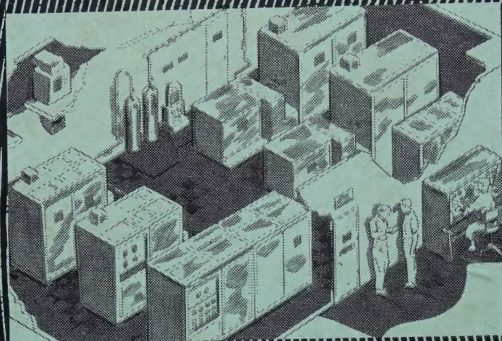
WHEELER LABORATORIES, INC., Great Neck, N.Y.; Antenna Lab., Smithtown, N.Y.
Consulting Services, Research & Development, Microwave Antennas & Waveguide Components

The charge for an Institutional Listing is \$50.00 per issue or \$140.00 for four consecutive issues. Applications for Institutional Listings and checks (made out to the Institute of Radio Engineers) should be sent to Tore N. Anderson, PGMTT Advertising Editor, 1539 Deer Path, Mountainside, N.J.

NOTICE TO ADVERTISERS

Effective immediately the IRE TRANSACTIONS ON MICROWAVE THEORY AND TECHNIQUES will accept display advertising. For full details contact Tore N. Anderson, Advertising Editor, PGMTT TRANSACTIONS, 1539 Deer Path, Mountainside, N. J.

FXR's ENGINEERING KNOW-HOW!



Control room of a 50 million watt transmitter created to better man's understanding of the atmosphere and ionosphere—The complete transmitter developed and manufactured by FXR.

FXR's precision microwave equipment, high-power pulse modulators and high-voltage power supplies have prominent roles in such leading scientific programs as this 50 million watt transmitter, thermonuclear control research, communication and ballistic missiles systems and similar astronautical, aeronautical and electronic developments.

50-MILLION-WATTS!



FXR, Inc.

Design • Manufacture • Development

26-12 Borough Place • RA • 1-9000
Woodside 77, N. Y. • N.Y. 43745

PRECISION MICROWAVE EQUIPMENT • HIGH-POWER PULSE MODULATORS • HIGH-VOLTAGE POWER SUPPLIES • ELECTRONIC TEST EQUIPMENT